GEOCHEMICAL STUDIES ON THE SCOURIAN COMPLEX, N.W. SCOTLAND

HUGH R. ROLLINSON

Thesis submitted for the degree of Doctor of Philosophy

Department of Geology

University of Leicester

December 1978

ABSTRACT

The gabbro-tonalite-trondhjemite-granodiorite-granite suite of the Scourian complex of northwest Scotland was studied at Scourie, Gruinard Bay and Torridon and represents highly deformed and metamorphosed plutonic igneous rocks, whose formation ca. 2900 Ma. ago represents the generation of new continental crust.

Amphibolites, found predominantly in amphibolite facies gneisses at Gruinard Bay may be metavolcanic and are chemically similar to present-day island arc tholeiites; they are complementary to the layered cumulitic gabbro-anorthosite complexes in granulite facies gneisses and together they represent the remnants of an early basic volcanic-plutonic suite. Tonalite was generated by the partial melting of amphibolite, similar in chemistry to that found at Gruinard Bay. Trondhjemite, granodiorite and granite evolved from tonalite by the fractional crystallisation of plagioclase and hornblende at depths of less than 60 km. Granulite facies metamorphism at Scourie depleted originally wet tonalitic and trondhjemitic magmas in LIL elements but not potassium. Relatively dry granitic magmas were not depleted during granulite facies metamorphism. There is a change in the principal magma-type from Scourie in the north (tonalite) through Gruinard Bay (trondhjemite) to Torridon in the south (granodiorite) reflecting a southerly increase in K_2O across the complex. Granulite facies gneisses at Scourie show a continuum of rock types between ultramafic and granitic, but amphibolite facies gneisses show a distinct bimodality.

Igneous temperatures of 1000°C to 1150°C were obtained from feldspar and ilmenite-magnetite thermometry. The peak of the granulite facies metamorphism was at 820°C and 10 kb. and was determined using plagioclase-scapolite and garnet-pyroxene equilibria. Many mineral pairs equilibrated at lower temperatures and reflect the cooling history of the complex. Water was introduced into granite sheets during cooling at about 600°C. The Archaean crust at Scourie was originally 60 km thick and the thermal history of the area suggests that the crust was magmatically thickened.

The plutonic igneous and metamorphic history of these rocks invite comparison with modern Cordilleran batholiths and suggest that the Scourian complex formed in an analogous tectonic setting.

I am indebted to my wife Patricia for the help, encouragement and patience she has shown during the course of this work and this thesis is dedicated to her with love.

CONTENTS

FIGURES AND TABLES

Introduction

INTRODUCTION

Progress in science is often made when research workers use a model as a basis for their studies. The research then has direction and significance and the results of research can be used to test, and discard or modify the working hypothesis.

The working model behind this study stems from the suggestion of Windley and Smith (1976) and Tarney (1976) that Archaean high-grade granulite-gneiss belts may be the ancient analogues of modern Cordilleran batholiths. This suggestion was supported in general by Moorbath (1977) and Bowes (1978) and more specifically by Davies (1974, 1976, 1977) who showed from field mapping that the Scourian complex of N.W. Scotland comprises gabbro, tonalites, trondhjemites, granodiorites and granites which can be interpreted as the remnants of a highly deformed and metamorphosed igneous plutonic complex.

The first aim of this study, therefore, was to examine the Scourian complex, the oldest portion of the Lewisian complex of N.W. Scotland, from an igneous point of view and study the geochemistry of the quartzofeldspathic gneisses. The field work of Davies (1974, 1976, 1977, 1978) showed that the geological relationships between the different rock types in these highly deformed areas can only be deciphered in zones of low strain. The logical extension of this conclusion is that the geochemistry of these rocks can also be best understood in low deformation areas where a convincing chronology can be established on the basis of intrusive relationships and where the original rock types are least deformed. For this reason small areas of low strain were selected in different parts of the Scourian complex and mapped in detail to show the relative age relations as a basis for interpreting the rock geochemistry.

The second aim of this study was to examine the mineral chemistry of the Scourian rocks; in view of the great number of

man-years invested in the study of the Lewisian complex it is surprising that there are so few data on the mineral chemistry of the major rock types. The suggestion of O'Hara (1977) that preliminary geothermometry and barometry indicated very high temperatures (ca. 1200°C) and pressures (15 kb) of formation of the granulites at Scourie led to a detailed examination of this problem in that area and data are presented for a variety of mineral assemblages which are useful in estimates of P - T conditions. This work compliments the first part of this study, for in order to fully test an igneous plutonic model it is important to have estimates of the geothermal gradient and crustal thickness during its evolution.

This thesis therefore is divided into two parts. The first three chapters aim to establish a magmatic origin for the Scourian complex and discuss the processes which operated at three slightly different levels in the lower part of the continental crust. Chapter 1 discusses the granulite facies rocks at Scourie (Fig. 1) and their possible magmatic origin and the effects of the granulite facies metamorphism on their chemistry. Chapter 2 looks at identical rocks metamorphosed to amphibolite facies grade at Gruinard Bay (Fig. 1) and a petrological model is presented for their evolution. Chapter 3 is a preliminary study of amphibolite facies gneisses from the Torridon area (Fig. 1) which, in view of their more potassic chemistry, may reflect a slightly higher level in the crust than the Gruinard Bay rocks.

The last five chapters are concerned with the different ways of estimating pressure and temperature in the granulite facies gneisses around Scourie. Chapter 4 is a detailed study of the cooling history of ilmenite-magnetite intergrowths in trondhjemites using the experimental data of Buddington and Lindsley (1964).

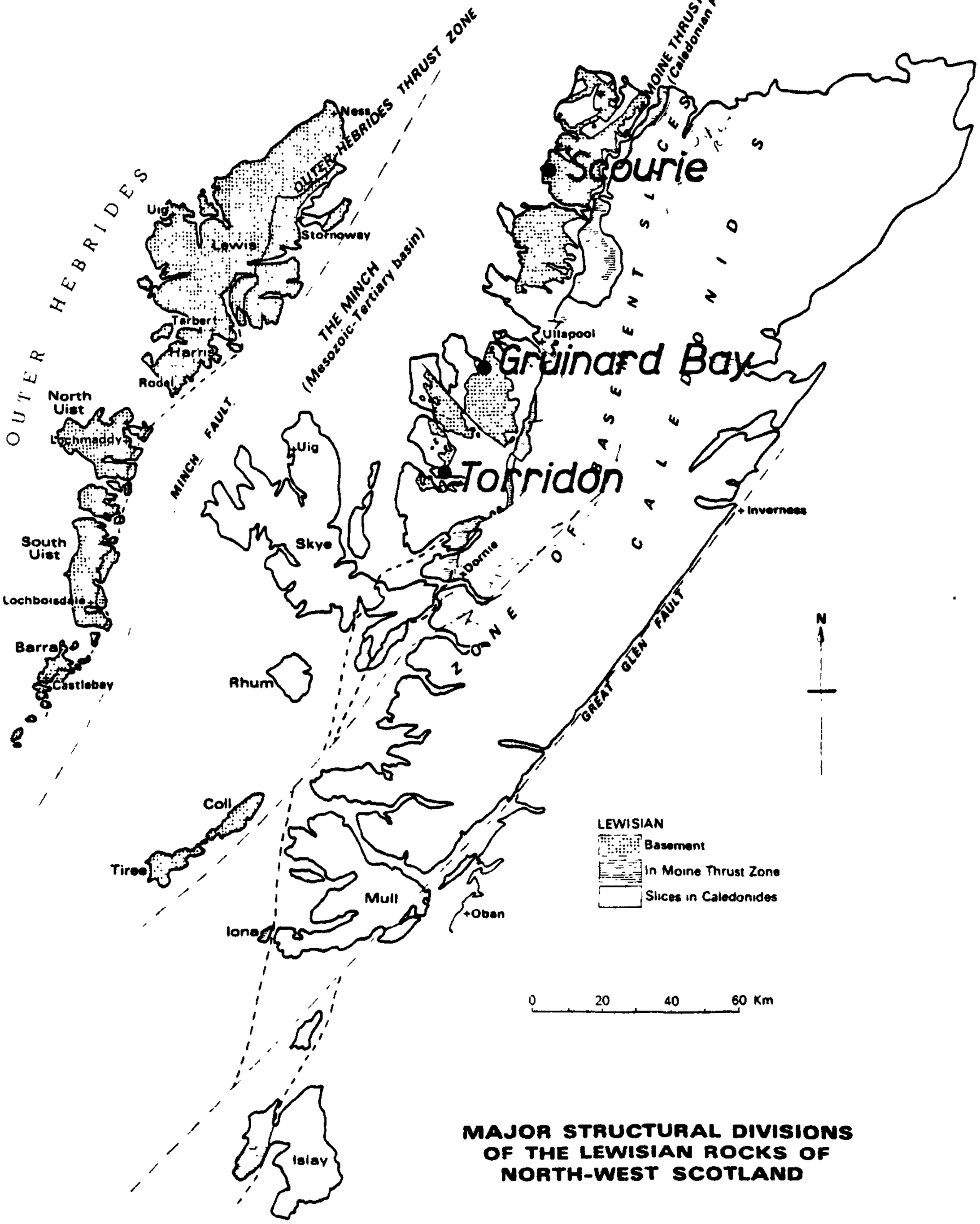

MAJOR STRUCTURAL DIVISIONS OF THE LEWISIAN ROCKS OF NORTH-WEST SCOTLAND

FIGURE 1. The areas examined in this study in relation to the outcrop of the Lewisian complex in northwest Scotland.

Chapter 5 examines the feldspars in granite sheets and compares their cooling history with iron titanium oxides in the same rocks. Chapter 6 is a minor digression into the controls on the distribution of Mn into and between ilmenite and magnetite during magmatism and slow cooling. In chapter 7 the mineral chemistry of a scapolite-bearing calc-silicate rock is used to set constraints on the pressure and temperature of the granulite facies metamorphism and Chapter 8 tests some of the current geothermometric and barometric models which use garnet and pyroxenes and it presents a preferred P - T estimate for the granulite facies metamorphism.

There is a voluminous literature on the Lewisian complex which extends over nearly one hundred years, the first phase of which culminates in the North West Highlands memoir, published by the Geological Survey of Great Britain (Peach et al., 1907). Another landmark is the 1951 paper by Sutton and Watson on the chronological classification of the Lewisian Complex in which they showed that it formed as a result of two major gneiss-forming cycles, an early Scourian cycle and a later Laxfordian cycle which were separated by a period of intrusion of basic dykes (Scourie dykes). A detailed summary of Lewisian geology was published by Watson in 1975.

One of the most important problems of Lewisian geology is the extent to which the two gneiss forming cycles identified by Sutton and Watson represent the addition of new material to preexisting crust, or the reworking of older crustal material. This study discusses this problem in relation to the Scourian cycle; geochronological studies by Moorbath et al. (1975) and field studies by Davies and Watson (1977) suggest that the Laxfordian events represent the reworking of older (Scourian) rocks and that substantial amounts of new material were not added to the crust at this time.

Geochronological studies by Giletti et al. (1961) and Moorbath et al. (1969) confirmed the chronology proposed by Sutton and Watson in 1951 and indicated an Archaean age for the Scourian rocks and a Proterozoic age for Laxfordian events. Recent geochronological studies, using the revised decay constants of Steiger and Jager (1977) indicate an age of between 2600 and 2700 Ma. for the Scourian metamorphism (Moorbath et al., 1975; Chapman and Moorbath, 1977). Hamilton et al. (in press) reported a Sm-Nd age* of 2920 ± 50 Ma. on granulites from the Assynt area, which in view of the immobility of the rare earth elements during granulite facies metamorphism, they interpreted as the age of emplacement of the igneous precursors to the granulites. This new data is in good agreement with earlier suggestions by Moorbath et al. (1975) and Chapman and Moorbath (1977) who argued that the Scourian gneisses are not reworked old continental crust and that the precursors of the Scourie gneisses separated from their source region not more than 200 Ma. before the measured Rb/Sr and Pb/Pb ages of 2600 - 2700 Ma. In contrast to other parts of the North Atlantic craton, therefore, gneisses with measured ages of greater than ca. 2900 Ma. are not known from the Scourian complex.

Acknowledgements

I wish to thank Dr. Brian Windley for interesting me in the problems of Lewisian geology and for guidance and encouragement during the course of this work. Dr. Brian Davies is thanked for making available unpublished field data and for guiding me to the areas best suited for this study. Rob Wilson introduced me to the mysteries of the microprobe and without his highly efficient technical assistance much of this work would not have been possible. I am

---

* Using a decay constant of 6.45×10^{-12} .yr^{-1} for ^{147}Sm

also indebted to Dr. Graham Hendry of the University of Birmingham for several hundred X.R.F. analyses, and Dr. Norman Charnley of Cambridge University and Dr. Phil Potts of the Open University for electron 'probe facilities. Sue Cunningham is thanked for typing the manuscript and the receipt of a postgraduate studentship from the Natural Environment Research Council is gratefully acknowledged. Final thanks go to my wife Patricia for her support and encouragement over the last three years and not least for producing the diagrams for this thesis.

TABLE 1. List of abbreviations of mineral names used in this thesis.

antip	antiperthitic plagioclase
ap	apatite
bi	biotite
cc	calcite
cht	chlorite
cpx	clinopyroxene
epid	epidote
gt	garnet
hbl	hornblende
hyp	hypersthene
ilm	ilmenite
magt	magnetite
micr	microcline
msp	mesoperthite
musc	muscovite
olv	olivine
opq	opaque oxides
opx	orthopyroxene
plag	plagioclase
qz	quartz
sph	sphene
spin	spinel
sulph	sulphide minerals
trem	tremolite
zn	zircon

Chapter 1

THE GEOCHEMISTRY AND ORIGIN OF TONALITES, TRONDHJEMITES, GRANODIORITES AND GRANITES FROM SCOURIE, N.W. SCOTLAND.

SUMMARY

The Lewisian complex of the Scourie-Badcall area is composed predominantly of banded tonalitic gneiss, which intrudes layered gabbro-ultramafic rock complexes. Intrusive into both gabbro and tonalitic gneiss are homogeneous acid sheets which are trondhjemitic to granitic in composition.

Smooth, continuous trends on chemical variation diagrams suggest that the evolution of these rocks was dominated by fractional crystallisation. A scheme is proposed whereby a tonalitic melt is parental to trondhjemite and granite. Variation within tonalites is a function of the fractional crystallisation of hornblende and plagioclase and trondhjemite is derived from tonalite by the fractional crystallisation of hornblende and/or plagioclase. Granite and granodiorite represent residual liquids which evolved along the quartz-feldspar cotectic surface at high pressure and low pH_2O; they were derived by the fractional crystallisation of plagioclase from a trondhjemite liquid. Some trondhjemitic looking sheets are quartz-plagioclase residues from which a granitic melt was removed.

The associated gabbros and ultramafic rocks are not directly related to the proposed fractional crystallisation scheme and are not crystal residues removed from the tonalitic melt.

Tonalites are probably derived from a basaltic source by partial melting or fractional crystallisation with either hornblende and/or granite as residual phases.

Depletion in LIL during granulite facies metamorphism was controlled by mineralogy; K-feldspar bearing granites and granodiorites are not depleted with respect to Rb but tonalites

and trondhjemites are strongly depleted. There is no evidence to suggest that depletion of K has occurred and K concentrations are consistent with two primary trends, one a trondhjemitic and the other granitic.

1. INTRODUCTION

An igneous origin for the Lewisian complex was first proposed by J.J.H. Teall of the Geological Survey in the classic memoir by Peach et al. (1907). Sutton and Watson (1951), however, in their re-examination of these rocks concluded that they had formed predominantly from sediments. Subsequent workers (e.g. Sheraton, 1970; Bowes, 1971; Sheraton et al., 1973) using geochemical arguments have returned to the idea of an igneous origin for the bulk of the Lewisian complex.

The main disagreement in recent years has been over whether the complex is of plutonic as originally proposed by Teall, or volcanic origin. Several workers have argued that the Scourian complex originated as a volcanic assemblage of basalts, andesites, dacites and rhyolites because (a) their bulk chemistry and low concentrations of K, Rb, Th and Y and the high K/Rb ratio are similar to a calc alkaline volcanic supracrustal series (Sheraton, 1970), (b) the $Na_2O + K_2O$, FeO and MgO content of the gneisses defines a calc alkaline trend on an A-F-M diagram (Sheraton et al., 1973; Bowes et al., 1971) and (c) plots of major and trace elements against modified Larsen values are consistent with an igneous origin (Bowes, 1971). A plutonic origin was proposed by Holland and Lambert (1975) who suggested that Scourian granulites are mantle differentiates which crystallised at depth underplating pre-existing crust. Windley and Smith (1976) pointed out similarities between Archaean high grade areas, such as the Scourian complex, and the deep seated batholiths located along the West coast of North and South America and suggested that they formed by similar processes.

A number of earlier studies (Sheraton, 1970; Sheraton et al., 1973; Holland and Lambert, 1973) were based on a large number of

samples collected on a grid pattern over a large area of the Scourian complex and the authors emphasised the bulk chemistry of the complex and outlined in a broad way its geochemical evolution.

This approach, however, neglects the fact that there are different gneiss types (e.g. gabbro - anorthosite complexes, tonalitic gneiss intrusive trondhjemite - granite sheets) with slightly different ages. This is important because it is impossible to fully understand the evolution of a suite of rocks until the relative ages of the different rock types are known.

The purpose of this study is to present new chemical data for gabbros, tonalites, trondhjemites and granodiorites whose relative ages can be demonstrated in the field and this is used to support a plutonic igneous origin for these rocks and set limits on how they may have evolved.

GEOLOGICAL SETTING

Two small areas were mapped in detail in the Scourie - Badcall region which show the range of lithological types in the Scourian complex (Figs. 1 and 2).

(a) Gabbros and Tonalitic gneisses

The Lewisian complex in the Scourie - Badcall area is composed predominantly of banded, tonalitic, quartzofeldspathic gneiss, metamorphosed to granulite facies. Enclosed within the tonalitic gneiss are blocks and lenses of gabbro and ultramafic rocks ranging in size from a few cm to about 200m wide and up to 2 km long (see Davies and Watson, 1977, fig. 1).

Two gabbro bodies have been mapped; one on Scourie More, an ultramafic - garnet gabbro (Fig. 1) and the other from upper Badcall a slightly more leucocratic association of gabbro and mafic gabbro with no ultramafic rocks and cut by metre-wide coarse grained anorthosite sheets (nomenclature after Windley et al., 1973)

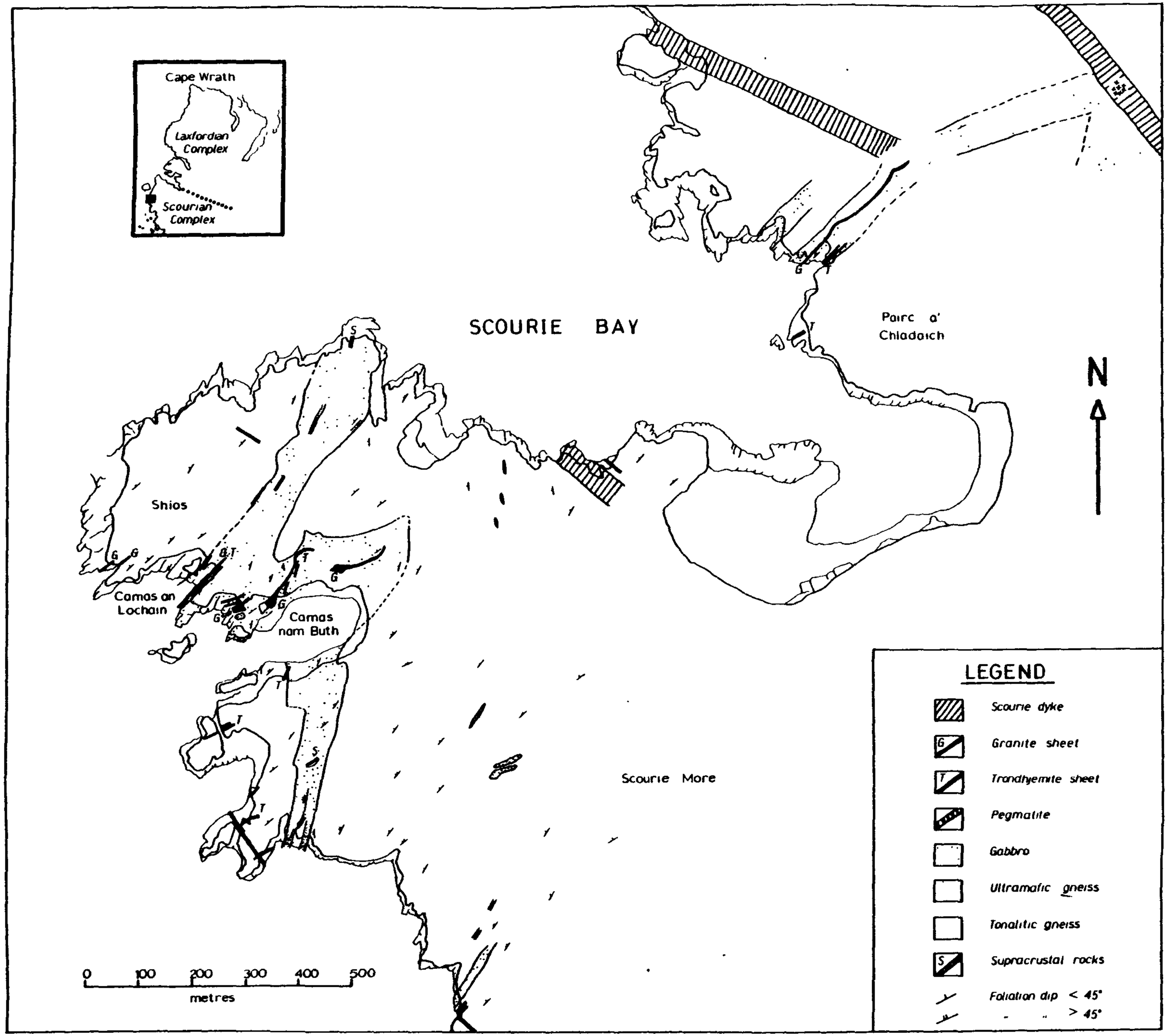

FIGURE 1. The geology of the area around Scourie, showing the different rock types which make up the granulite facies Scourie gneisses.

(see Fig. 2).

The gabbro bodies have well developed mineralogical layering and are tightly folded about NE-SW trending axial surfaces ascribed by Davies, 1976, to the early Scourian.

Ultramafic horizons occur predominantly at the margins, possibly the base of, the Scourie More body. The Badcall gabbro contains an 8m band of homogeneous gabbro sandwiched between horizons of layered gabbro and it contains highly irregular, flattened and boudinaged ultramafic dykes. Often associated with gabbro are lenses of what may be supracrustal gneiss with the mineral assemblage garnet + plagioclase + orthopyroxene/biotite + pyrite $\pm$ quartz.

The relationship between tonalitic gneiss and gabbro is generally unclear since gabbro is concordant with the banding in the gneiss. At Geodh' nan Sgadan, Upper Badcall, layering in the gabbro is truncated by tonalitic gneiss (Fig. 2) indicating that the gabbro and associated metasediments are the oldest rocks in the Scourian complex.

Davies (1975) suggested that older quartzofeldspathic gneiss predates the gabbro, however Chapman and Moorbath (1977) have shown on isotopic grounds that there is no great age difference between the proposed older gneiss of Davies (1975) and the bulk of the Scourie gneisses in this area.

(b) Intrusive Acid Sheets in the Scourie - Badcall area

Intrusive into both gabbro and tonalitic gneiss are homogeneous acid sheets trondhjemitic to granitic in composition (Figs. 1 and 2) they are a few metres wide and several hundred metres long, possess a strong tectonic fabric and have granulite facies mineralogy. Undeformed Scourie dykes are chilled against intrusive acid sheets indicating that these rocks have not been greatly altered since

FIGURE 2. Scourian gneisses at Geodh' nan Sgadan (Upper Badcall Bay); (grid reference : NC 147416).

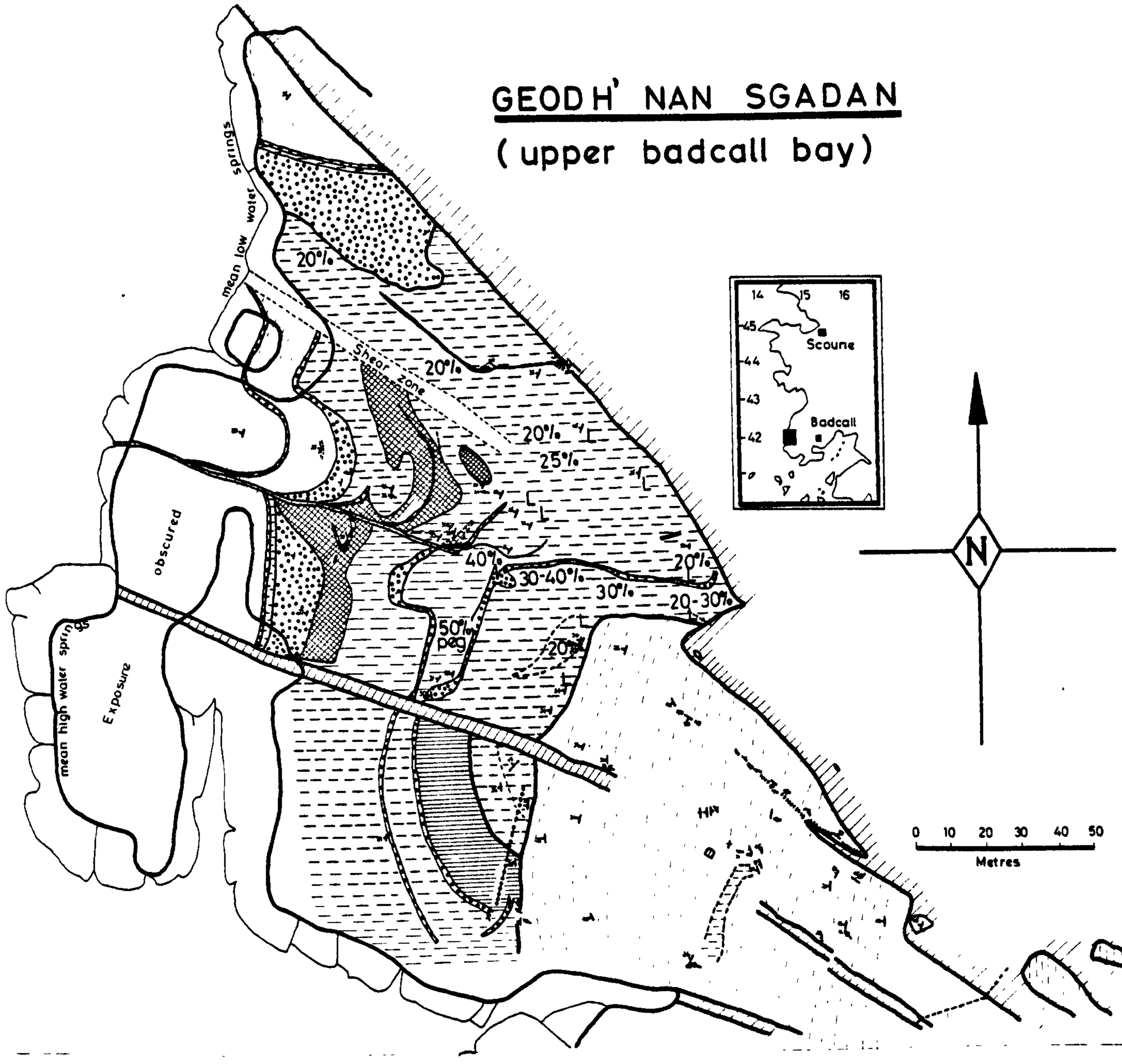

LEGEND

- Dip and strike of banding
- Fold axis / lineation
- Shear zone
- Dip of dyke wall
- Scourie dyke
- Intrusive trondhjemite
- L — Leopard spotted anorthosite
- Gabbro
- Leuco gabbro
- Rusty weathering sulphide band
- Homogeneous gabbro. with ultramafic dykes
- Pegmatite
- Banded leucogneiss with ultramafic pods
- 30% — % intrusive phase in gabbro

FIGURE 3.

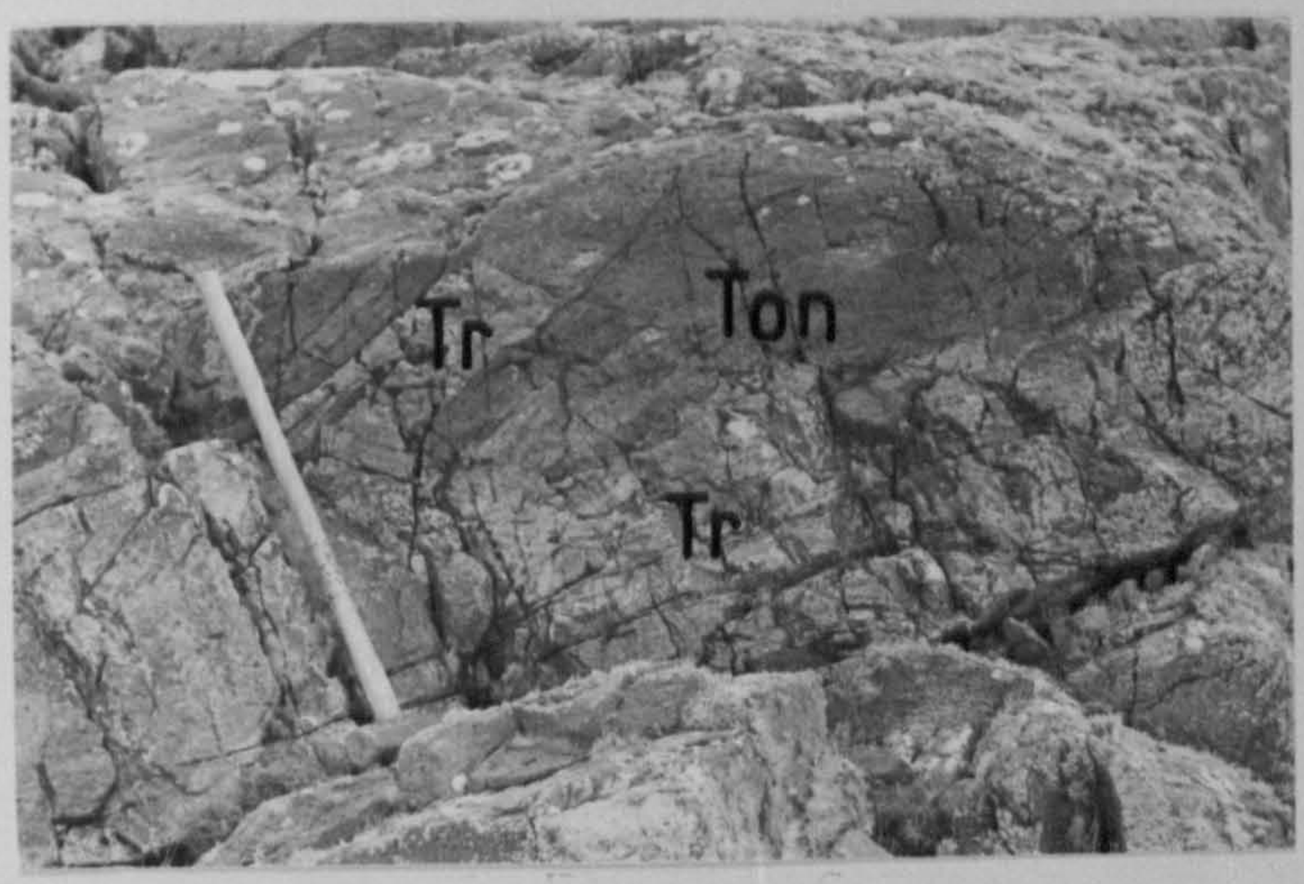

(A).Trondhjemite sheet (Tr) cutting tonalitic gneiss (Ton), Cleit Mhor, Scourie More.

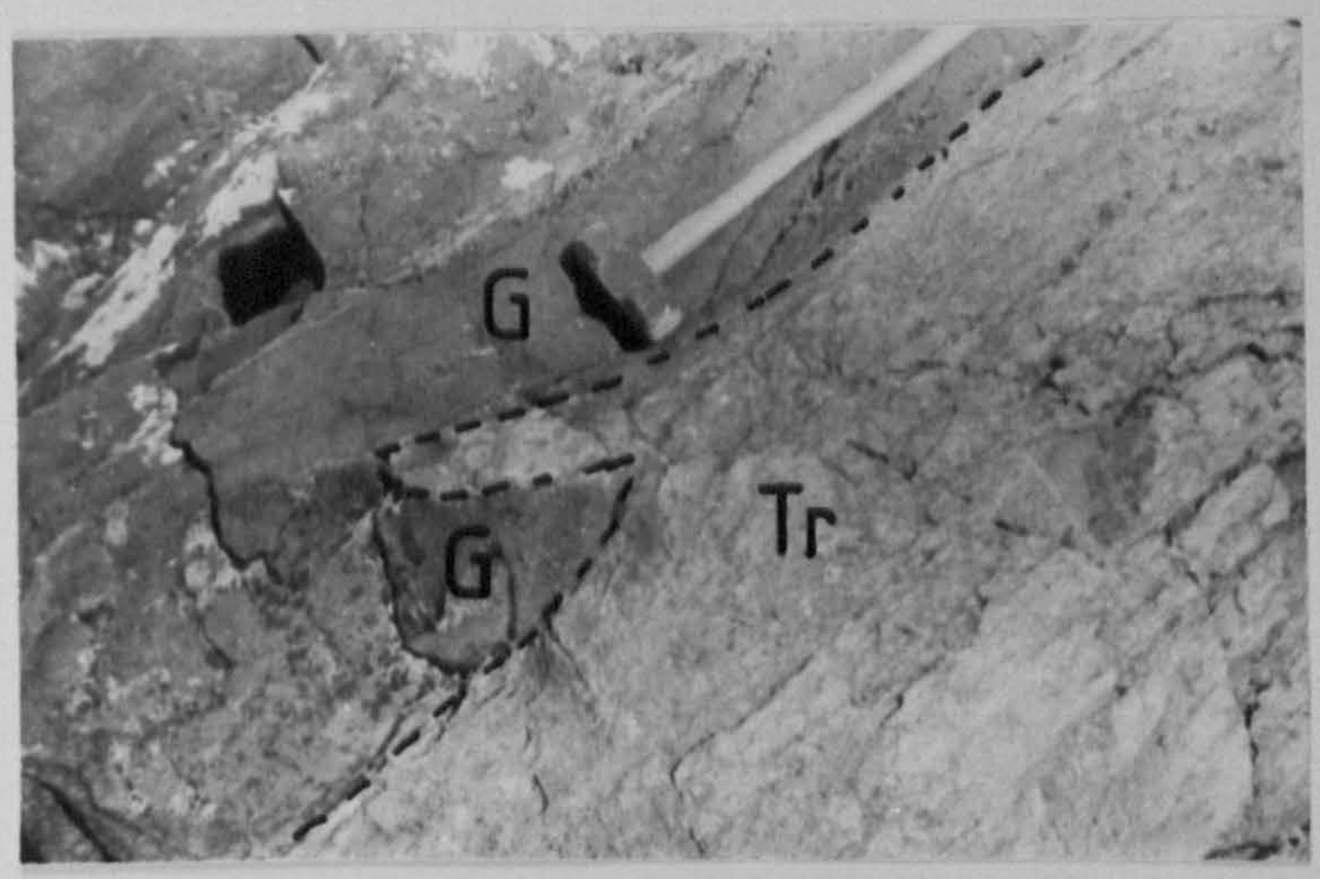

(B). Granulite facies trondhjemite sheet (Tr) cutting gabbro (G), west of Pairc a' Chladaich.

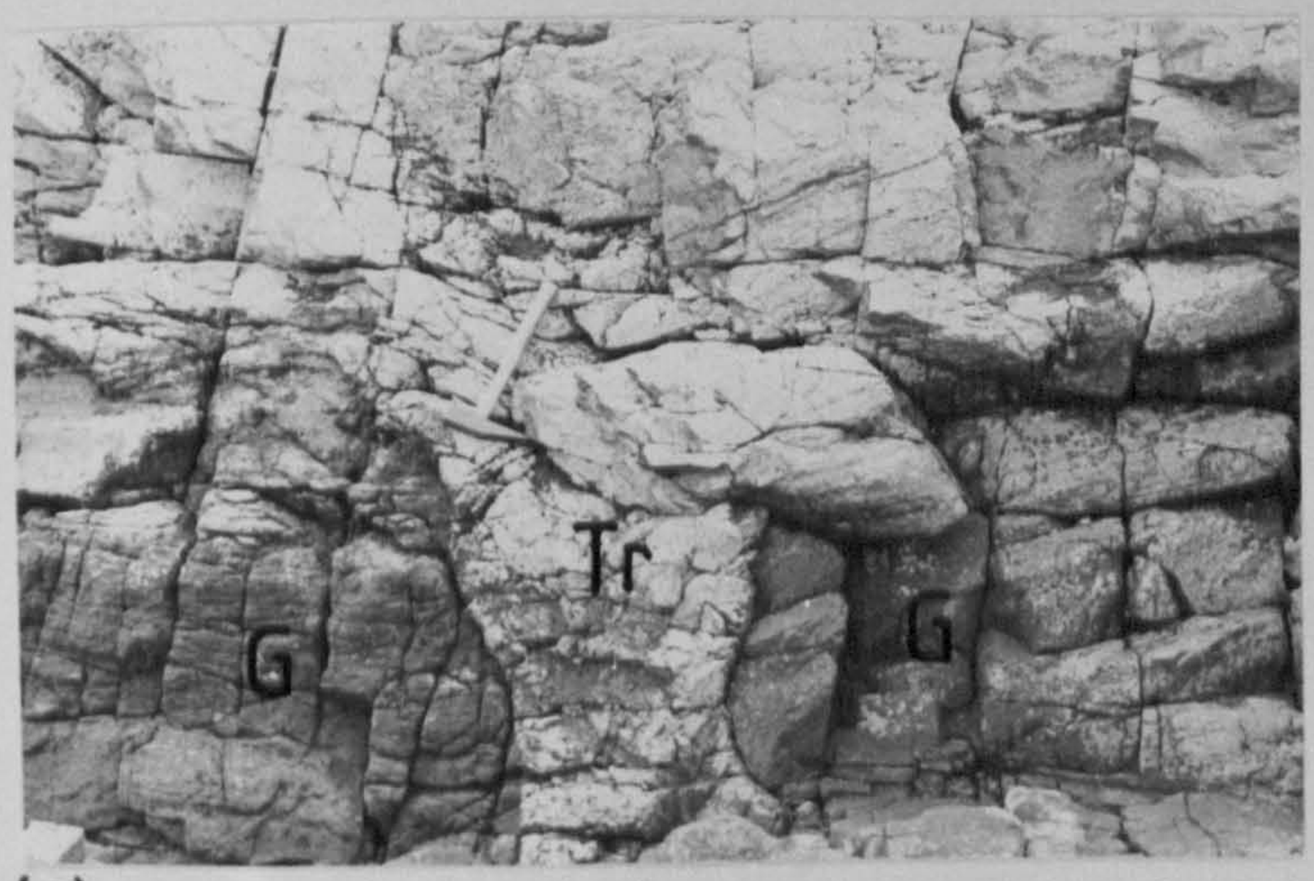

(C). Trondhjemite (Tr) cutting gabbro (G), east of Camas an Lochain, Scourie More.

FIGURE 4.

(A). Trondhjemite (Tr) interleaved with gabbro (G) and folded during late-Scourian folding. Glac an Fheadair.

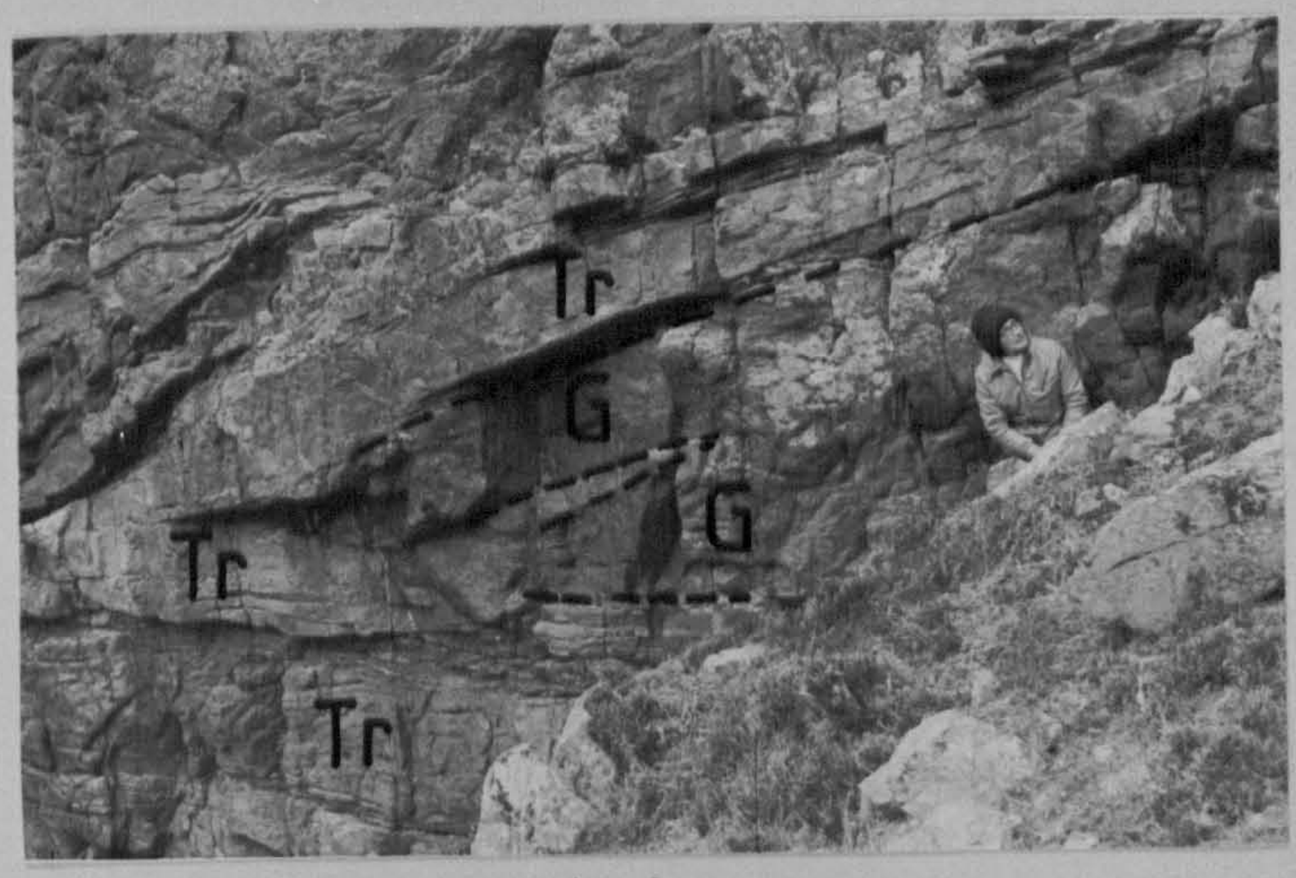

(B). Trondhjemite (Tr) interleaved with gabbro (G). Glac an Fheadair.

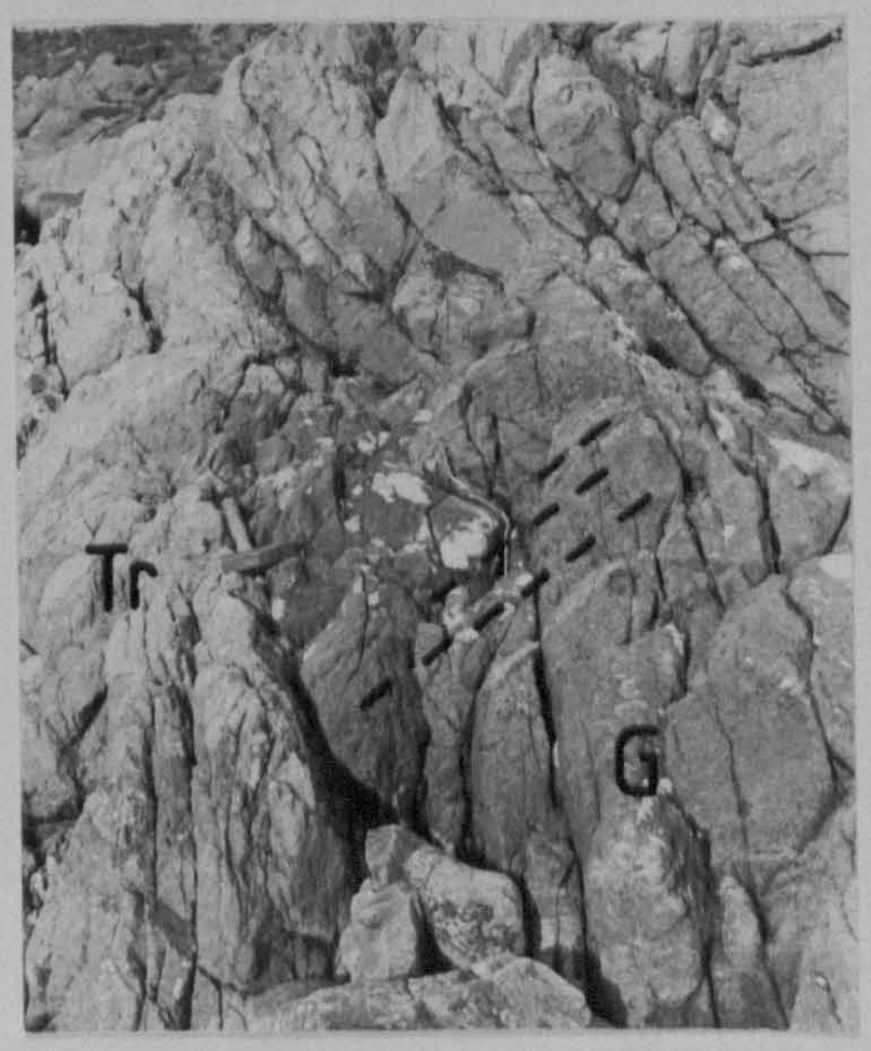

(C). Granulite facies trondhjemite (Tr) with a fabric parallel to its margin cuts banded gabbro (G); dashed line indicates banding in gabbro.

the Archaean (Figs. 2, 8a).

Intrusive contacts between acid sheets and tonalitic gneiss and gabbro are seen at the following localities:

west of Pairc a' Chladaich (NC 152 453) Fig. 3b.

east of Camas an Lochain (NC 146 441); at the base of the sheet trondhjemite passes into a discordant pegmatitic dyke (Fig. 3c).

Glac an Fheadair (NC 152 429); pink trondhjemitic sheets bifurcate and send minor apophyses into gabbro (Figs. 4a,b).

south of Camas nam Buth (NC 143 445) trondhjemite with a mineral fabric parallel to its margin cuts at a high angle the banding in the gabbro (Fig. 4c).

west of Loch an Daimh Mhor (NC 157 434); trondhjemite with a pegmatitic margin cuts banded gabbro.

Geodh' nan Sgadan (NC 147 416); there is a low angle discordance between trondhjemite and gabbro (Fig. 2).

the Shios peninsula (NC 138 447); a two metre wide sheet cuts banded tonalitic gneiss containing trains of ultramafic pods (Fig. 5).

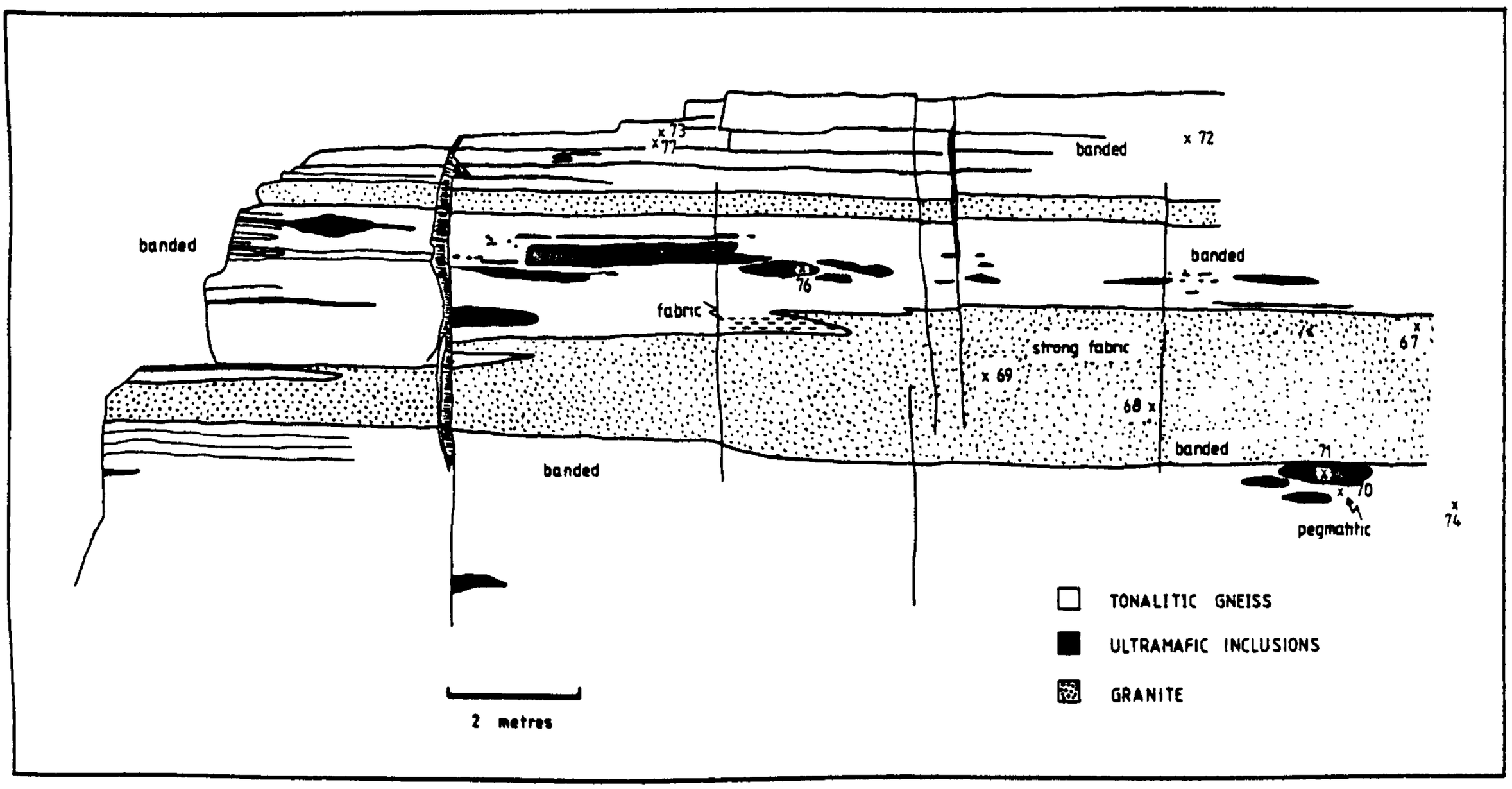

Fig. 5 Sketch of an outcrop on the Shios peninsula, Scourie more, showing intrusive granitic sheets in tonalitic gneiss.

For the most part, however, granitic and trondhjemitic sheets are concordant with the banding in the enclosing gneiss and show a strong mineral fabric, emphasised by flattened quartz grains and mafic schlieren (Fig. 6a). In the granitic sheets west of Pairc a' Chladaich (NC 153 454) and on Torran nan Clach Boga (NC 156 424) quartz grains are elongated (ca. 10mm by 0.5mm) parallel to the strike of the sheet, but (Fig. 6) normal to the strike, the grains are much less flattened and are remniscent of a graphic, igneous texture, (Fig. 6b) implying that the foliation tends towards an L-fabric and that the original texture is preserved in a direction normal to the maximum elongation. Lenses of chlorite after garnet are also oriented parallel to this lineation. The granite sheet at the end of Loch an Daimh Mhor (NC 159 435) is coarse grained and foliated at its margin and yet at the centre has a fine grained (less than 0.5mm), sugary texture; microcline is the main K-feldspar (uncommon in most sheets) and the fine grained texture may be due to recrystallisation.

At Glac an Fheadair (NC 152 429) thin trondhjemite sheets intruded into gabbro are tightly folded into recumbent folds with highly attenuated limbs and an amplitude of about 10m (Fig. 7a,b). The fabric in the trondhjemite is folded around the nose of the isoclines, implying that this folding is late and is probably related to a late Scourian shear zone which truncates an early Scourian fold to the south. Folded mafic lenses in trondhjemite sheets at Rhuba Clach an Eorna and Glac an Fheadair, Scourie More, represent an earlier phase of folding (Fig. 7b, c).

A granulite facies mineralogy (clinopyroxene - dark grey antiperthitic feldspar - bluish quartz $\pm$ garnet) is only present in some trondhjemites, noteably west of Paric a' Chladaich (NC 152 453), south of Camas nam Buth (NC 143 445) and east of Camas an Lochain (NC 146 441). At this last locality a large

FIGURE 6.

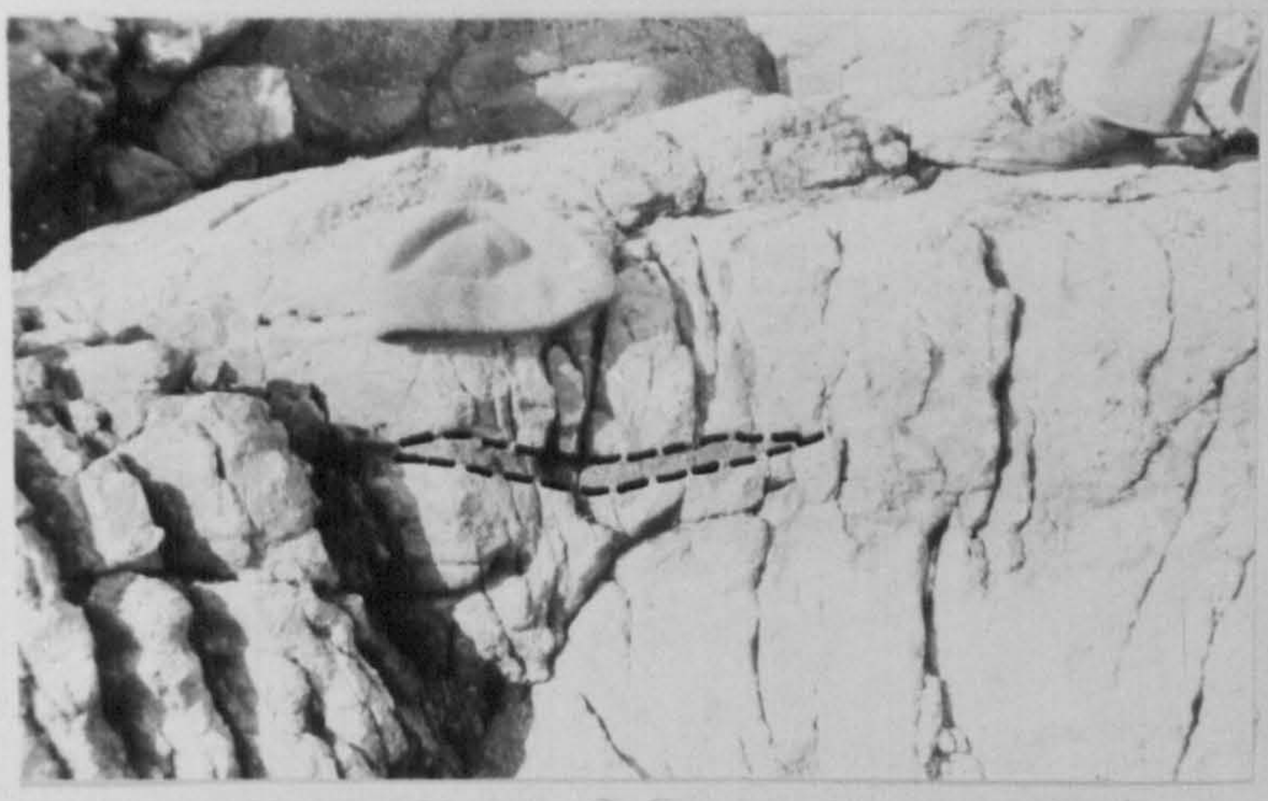

(A). Flattened gabbroic schlieren in trondhjemite, west of Pairc a' Chladaich.

(B)

(C)

(B) & (C). Relict igneous texture preserved normal to the main stretching direction (C) and intensely flattened parallel to the strike (B) in granite sheet west of Pairc a' Chladaich.

FIGURE 7.

(A). Late Scourian folds in trondhjemite (Tr) and gabbro (G). A biotite fabric in trondhjemite is folded around the nose of the recumbent fold in the centre of the photograph. Glac an Fheadair.

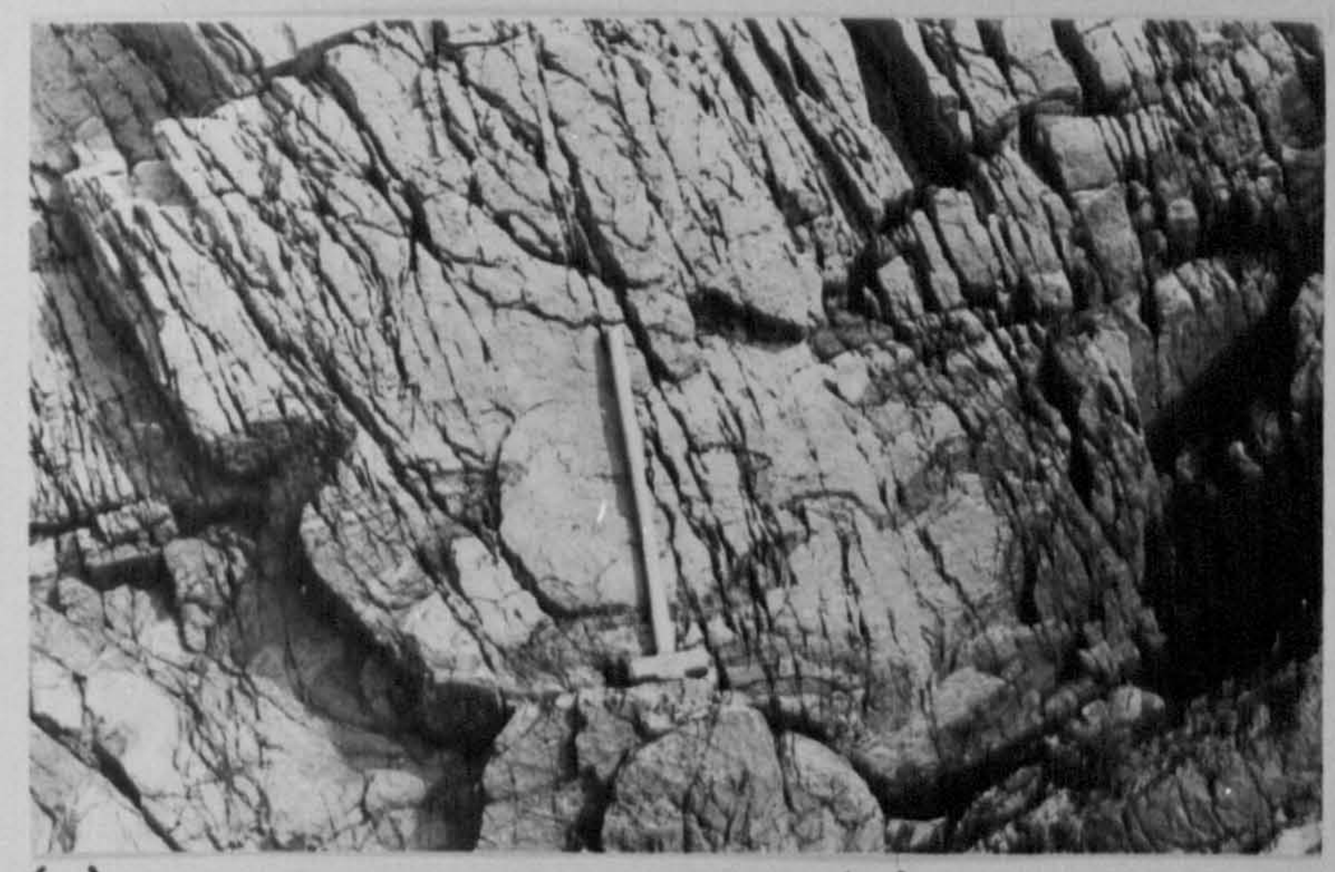

(B). Early Scourian folds (?) in trondhjemite; Rhuba clach an Eorna.

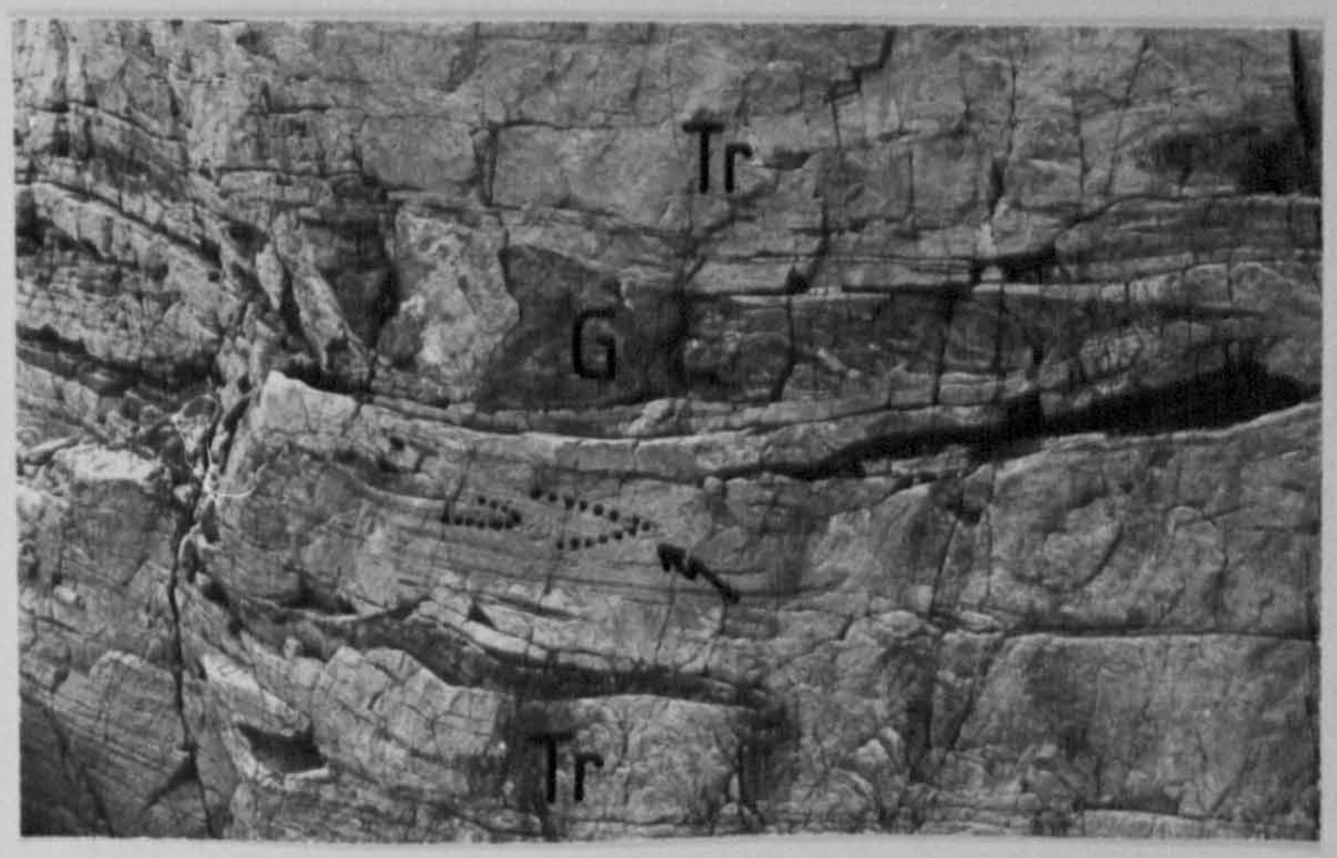

(C). Gabbroic lenses in trondhjemite (Tr); Glac an Fheadair. Note the fold closure in the trondhjemite.

FIGURE 8.

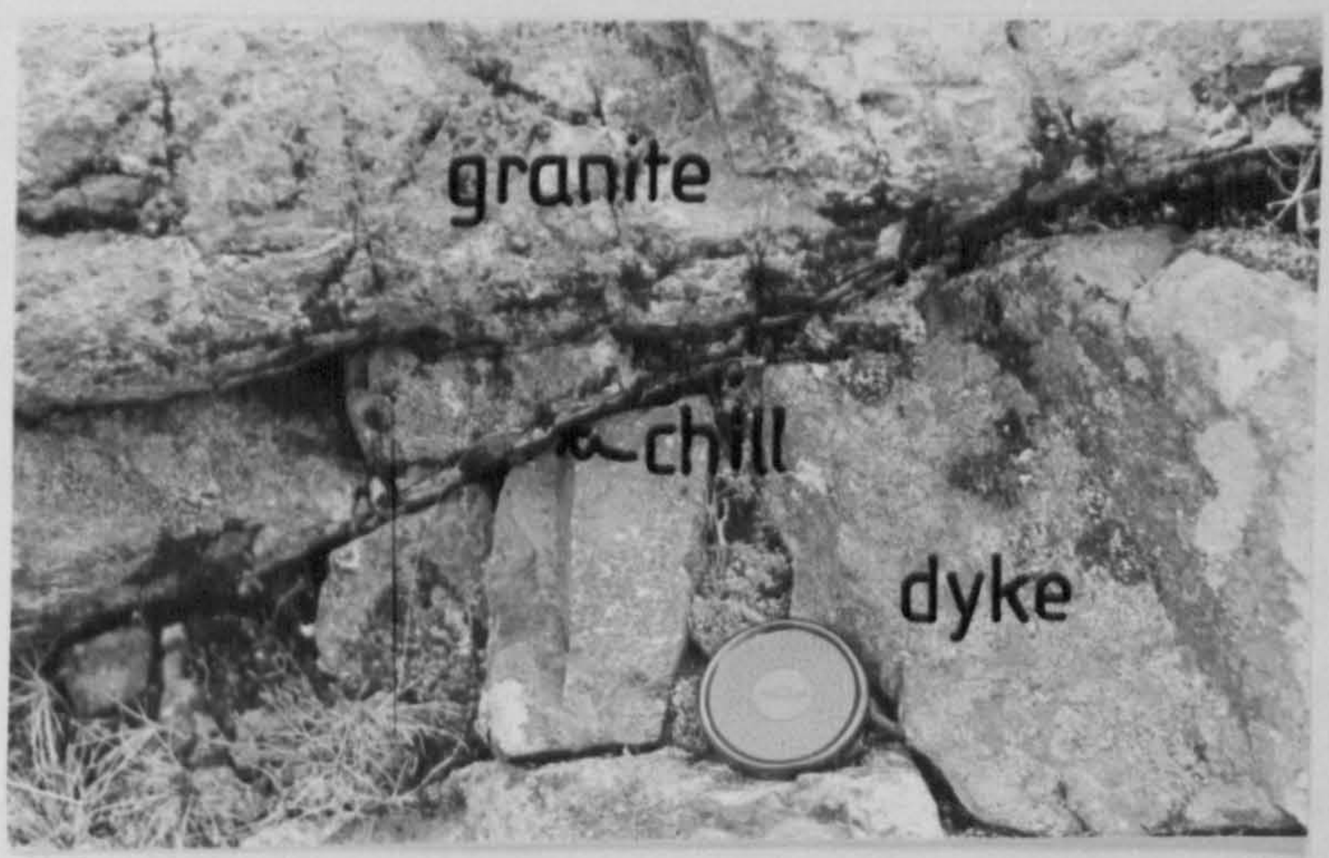

(A). Offshoot from Scourie dyke chilled against granite sheet, west of Pairc a' Chladaich.

(B). Concordant composite sheet with inclusions of ultramafic rock. See fig. 9. Camas an Lochain.

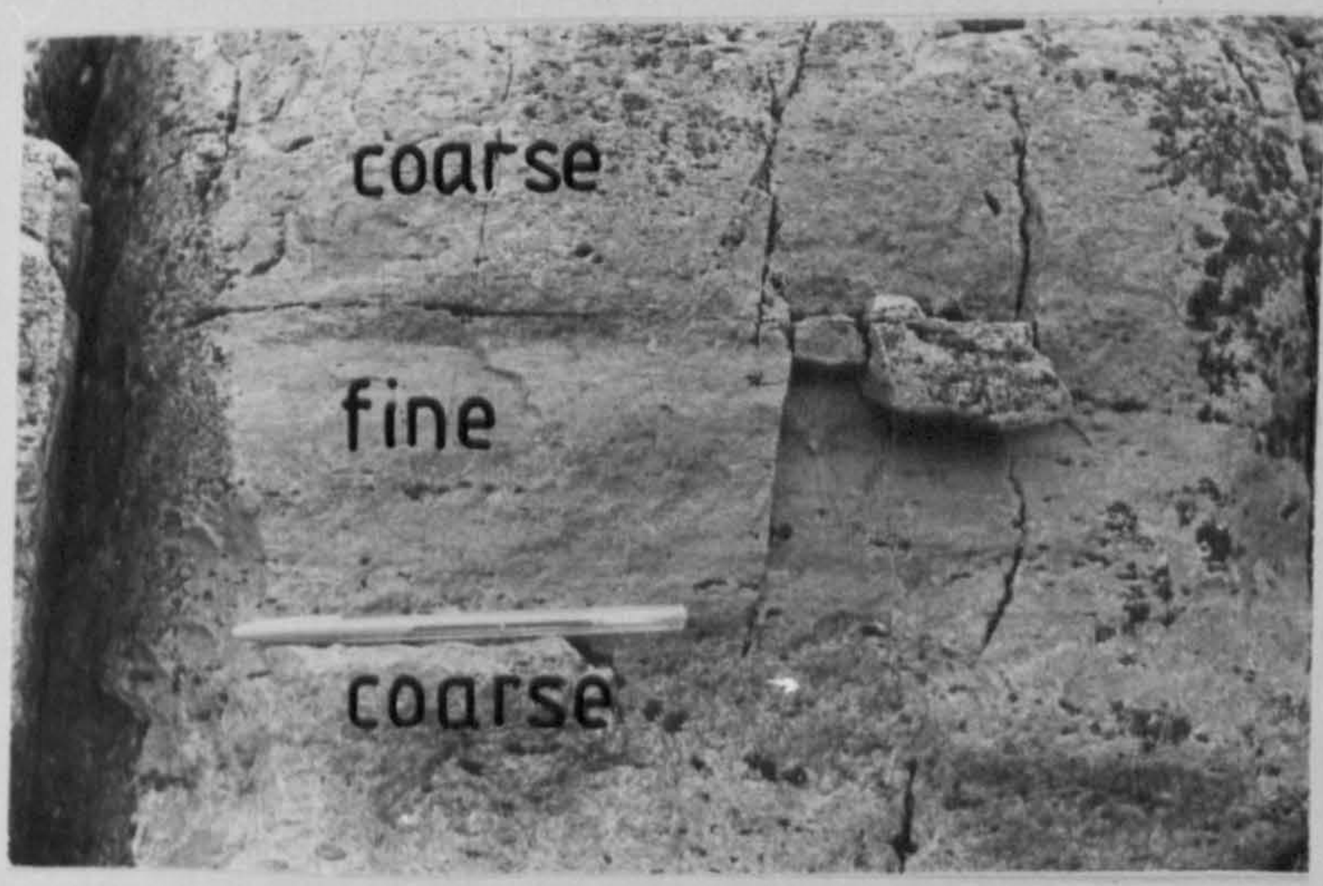

(C). Coarse and fine grained facies of trondhjemite in composite sheet, Camas an Lochain.

garnet overgrows the margin of a trondhjemite apophysis into gabbro, indicating that the granulite facies metamorphism post-dates the intrusion of the trondhjemite. The presence of bluish quartz, almandine garnet and pseudomorphs after orthopyroxene in the granite sheets implies that they also have been through granulite facies metamorphism. The white appearance of many of the trondhjemite sheets and the presence of hornblende, chlorite and biotite suggests that there has been extensive recrystallisation aided by the presence of H_2O following the granulite facies metamorphism.

Some trondhjemite - granite sheets are composite; e.g. east of Camas an Lochain (NC 146 441) there is an acid sheet which varies from trondhjemite at the top to anorthosite at the base (Fig. 9) and at one point is a hypersolvus granite being composed of quartz and mesoperthite and has a trace of graphic texture. On the shore west of Camas nam Buth (NC 142 446) there is a granite sheet which becomes a trondhjemite 100 metres inland.

Age of the Acid Sheets Davies (1974, 1975, 1976) described the structure of the Laxford front and suggested a chronology for Archaean events which is applicable to the Scourie - Badcall area:

6) Late Scourian Folds. amplitude up to 1 km at the Laxford front, become weaker and more open southwards; possibly synchronous with shear zones in the Scourie - Badcall area; main trend NW-SE.

5) NW trending dislocation along Laxford front.

4) End of granulite facies metamorphism. dated ca. 2,700 Ma.

3) Early Scourian folding. outlined by basic sheets; recumbent in style; axial traces trend NE-SW; axial planar fabric.

2) Thrusting. only evident at the Laxford front.

1) Early plutonic complex. migmatisation - intrusion of layered

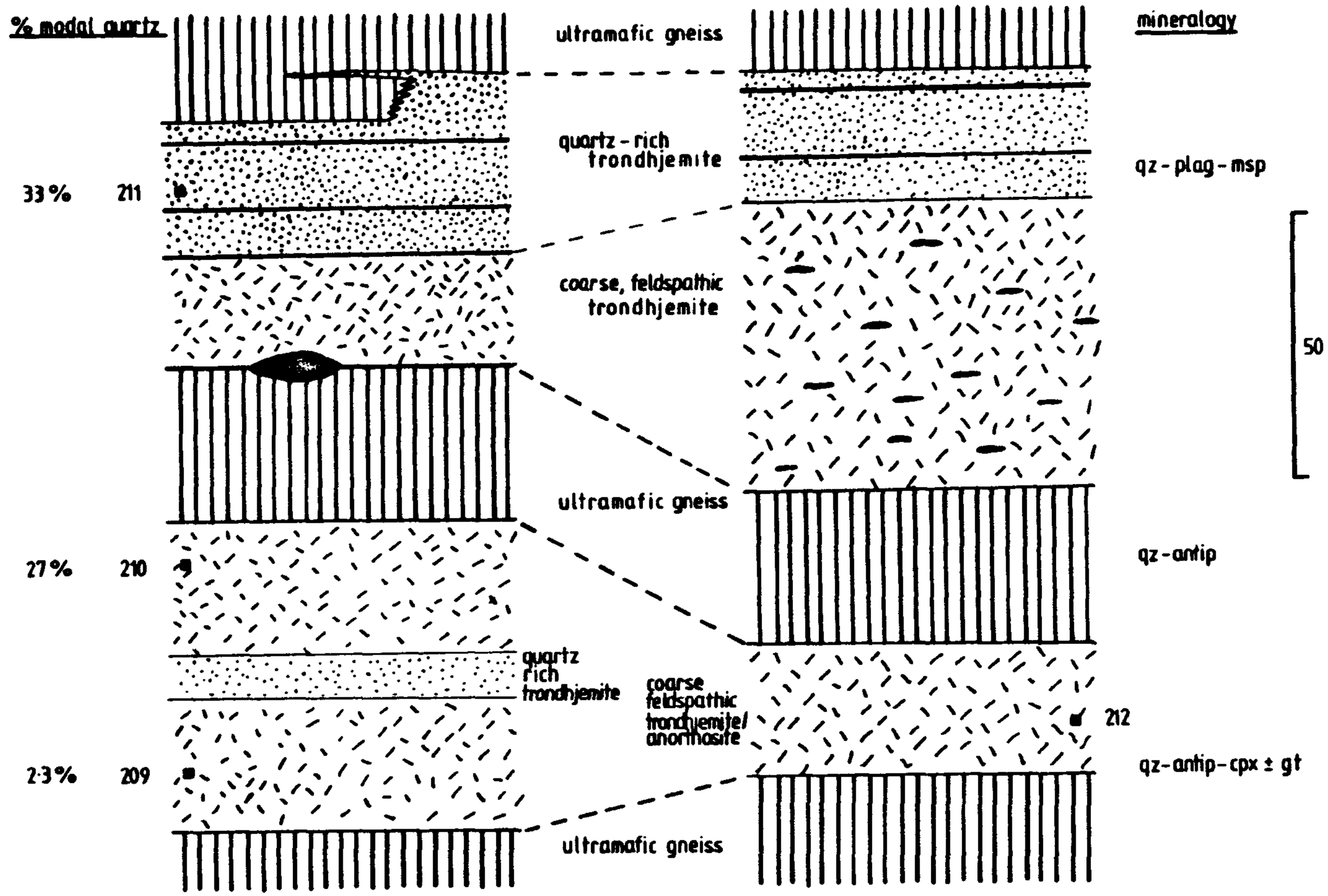

FIGURE 9. Composite trondhjemite-anorthosite sheet, E. of Camas an Lochain, depicted in Figs. 8(b) & 8(c). The northerly extension of this acid sheet is granitic. The numbers adjacent to the filled squares are sample numbers for specimens from this locality.

basic rocks - intrusion of granodiorite - deposition of supracrustal - earliest quartzo-feldspathic rocks.

The presence of granulite facies mineral assemblages means that the acid sheets were emplaced before the end of the granulite facies metamorphism (4) at ca. 2,700 Ma and a strong mineral fabric implies that the sheets were emplaced before the end of the early Scourian folding (event 3). The effect of late Scourian folding in this region was to fold an earlier fabric rather than to produce a new one.

2. PETROGRAPHY

Primary mineral assemblages are given in Table 1 and modal proportions of quartz, plagioclase and alkali feldspar plotted in Figure 10 after Streckeisen, 1973.

(a) Tonalitic gneiss

Tonalitic gneiss varies from diorite to tonalite according to the nomenclature of Streckeisen (1973) (Fig. 10). There is a granular texture, preserved by plagioclase grains when pyroxene is altered. Plagioclase (An_{32-36}) sometimes contains antiperthitic blobs of orthoclase in several orientations and sometimes rounded inclusions of quartz. Clinopyroxene is sometimes rimmed by hornblende or completely altered to the assemblage green hornblende, quartz and opaque oxides pseudomorphing after the original grain. Orthopyroxene alters to uralite and green hornblende; biotite overgrows hornblende and opaque oxides.

TABLE 1

Representative mineral assemblages from granulite facies rocks at Scourie

Ultrabasic rock

opx - cpx - hbl

olv - cpx - spin - mgt

Garnet gabbro

opx - cpx - gt - plag - magt/ilm ± grn hbl

Gabbro

opx - cpx - plag - hbl ± bi ± mgt

opx - cpx - plag (An40-50) ± spin ± hbl (grn & brn) ± cc

Homogeneous gabbro

opx - cpx - plag - ap

Tonalitic Gneiss

opx - cpx - plag (An32-36) - mgt/ilm ± qz - hbl (grn) - ap - zn ± bi

Trondhjemite - granulite facies

plag (An23-34, antiperthite) - qz - cpx ± hyp ± gt

Trondhjemite - amphibolite facies

plag - qz - bi - hbl - ilm/mgt - ap - zn

Granodiorite and granite

qz - plag (An21-31) - mesoperthite - opx - ilm/mgt

qz - mesoperthite - opx

qz - mesoperthite - plag - gt - ilm/mgt

qz - plag - micr - gt

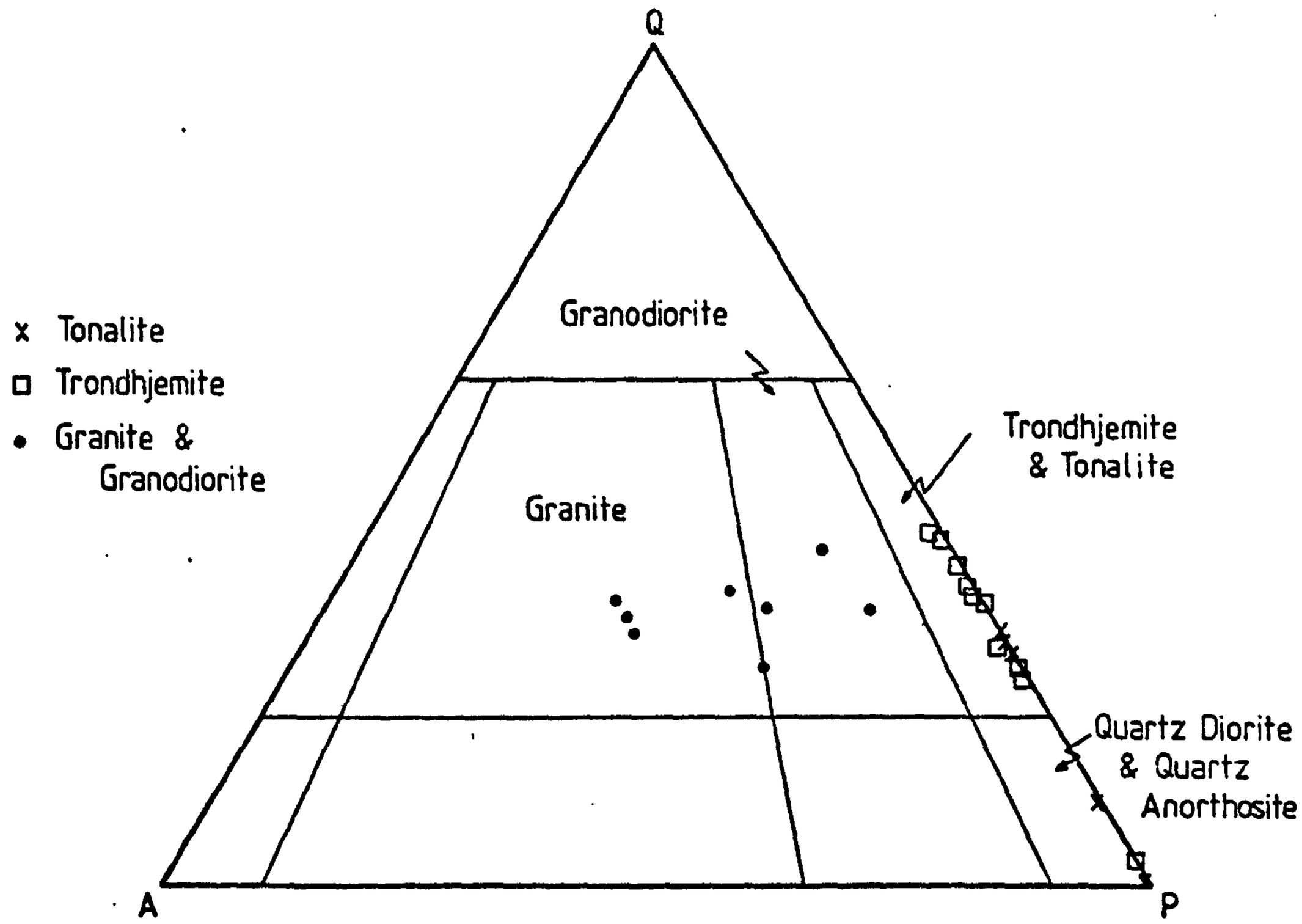

Fig. 10. Modal proportions of quartz (Q) - plagioclase (P) - alkali feldspar (A) in rocks from the Scourie - Badcall area. Nomenclature after Streckeisen, 1973.

(b) Trondhjemite

Intrusive trondhjemite sheets in the Scourie - Badcall area show either granulite facies or amphibolite facies mineralogy.

Granulite facies sheets are dark, medium to coarse grained (up to 5mm) with an equigranular texture. Plagioclase originally contained a high proportion of the orthoclase molecule in solid solution which has now exsolved as lamellae in four different orientations. Some of these lamellae have subsequently been altered to muscovite. Diopside may be rimmed by hornblende or completely altered to chlorite, calcite, epidote and magnetite. Hypersthene is often altered to green-brown uralite which is overgrown by hornblende, quartz and magnetite. At the base of one sheet the rock contains about 95% plagioclase and is an

andesine anorthosite; a few large almandine garnets are present.

Amphibolite facies trondhjemite sheets are white in colour, medium-grained (grain size ca. 1mm) and contain some bluish quartz indicating that they are the retrogressed equivalents of the granulite facies sheets. They have a granoblastic texture, although the minerals are of variable grain size. Plagioclase generally forms large, subidiomorphic grains and has irregular, lobate grain boundaries; it may be replaced along grain boundaries by microcline; rounded inclusions of quartz are common in plagioclase. Quartz occurs as large grains with undulose extinction and granulated margins or more commonly as finer grained polygonal aggregates; it contains trains, rods and rarely hexagonal negative crystals of red-brown rutile, a characteristic feature of quartz in granulite facies rocks. Laths of brown biotite overgrow hornblende and iron titanium oxides; they may be altered along cleavage planes to epidote or chlorite. A green biotite with higher Al, lower Ti and a higher Fe/Mg ratio than brown biotite is present together with brown biotite in some samples; it may represent a mixed layer silicate intermediate between chlorite and biotite. Magnetite and ilmenite form complex intergrowths and in some rocks they are altered to the assemblages sphene + magnetite and rutile + magnetite + haematite-ilmenite solid solution; sphene also overgrows rutile. Iron pyrites is a common accessory and is usually altered to haematite and/or limonite. Plagioclase is altered to chlorite, muscovite and calcite.

(c) Granite and Granodiorite

Quartzofeldspathic rocks containing plagioclase and alkali feldspar are grouped together as granites and granodiorites; this is not strictly according to the nomenclature of Streckeisen (1973), which is difficult to apply to these rocks because they contain unusually calcic alkali feldspars, now replaced by mesoperthitic

intergrowths of orthoclase and plagioclase. Microcline is only present in a few samples. Two examples of a one feldspar hypersolvus granite with feldspars ca. $An_{10}Ab_{45}Or_{35}$ represent an unusual liquid composition.

Orthopyroxene is altered to uralite and garnet to green biotite and chlorite. Opaque oxides form simple and complex intergrowths of ilmenite and magnetite.

3. MAJOR ELEMENT CHEMISTRY

Total alkalis - FeO - MgO

The variation of $Na_2O + K_2O$ vs. FeO_{total} vs. MgO in ultramafic rocks, gabbros, trondhjemites, granodiorites and granites is shown in Fig. 11. Gabbros and ultramafic rocks scatter about a tholeiitic

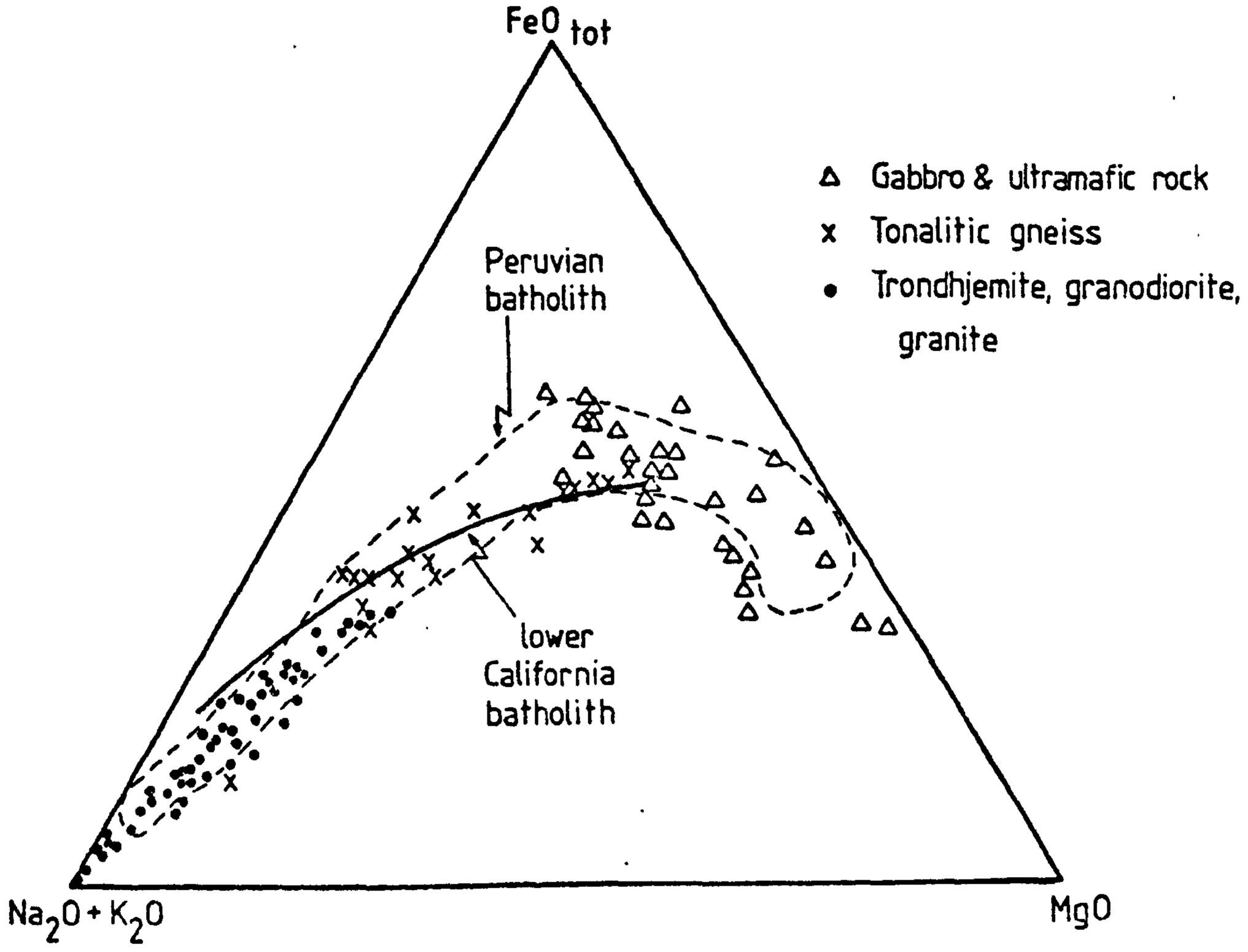

Fig. 11. Plot of total alkalis vs. FeO vs. MgO for rocks from the Scourie - Badcall area compared with the trend from the Lower California Batholith (Carmichael et al., 1974) and the field of gabbros and granitoids from the Peruvian batholith (Pitcher, 1978).

trend and tonalites, trondhjemites and granites follow a calc-alkaline trend. A calc-alkaline trend was identified in the Scourian gneisses of the Assynt area by Sheraton et al. (1973) and they suggested that this was probably partially original but may be in part metasomatic and in part tectonic (i.e. as a result of a change in rock composition during deformation due to the interleaving of different rock types or the development of layered gneiss from an originally homogeneous rock). Amphibolite facies gneisses from Gruinard Bay differ from the granulite facies gneisses of the Scourie area in that they show a bimodal distribution on an A-F-M diagram.

The samples in this study are from areas of low deformation where a change in rock composition during deformation is minimal. It is proposed, therefore, that (a) both the calc alkaline and tholeiitic trends apparent in acid and basic rocks at Scourie are original and (b) the difference between the trends in granulite facies and amphibolite facies terrains is real.

The majority of analyses in Fig. 11 fall within the field defined by gabbros - granitoids from the Peruvian coastal batholith (Pitcher, 1978) and they also show a trend similar to, although lower in alkalis than, the rocks of the lower California batholith (data in Carmichael et al., 1974). This lends support to the ideas of Windley and Smith (1976) who suggested that the Scourian complex formed by processes similar to those which give rise to the Mesozoic-Cenozoic batholiths emplaced along active continental margins.

The calc-alkaline trend is commonly interpreted (e.g. Barker et al., 1976) to be the result of crystal fractionation; if the tonalite to granite series at Scourie has evolved by crystal fractionation the majority of gabbros and ultramafic rocks cannot be the crystal residue extracted from the more siliceous rocks because they are too magnesian.

Silica Variation diagrams

The granulite facies gneisses of the Scourie area show a continuum of silica contents from 45 - 78 wt % SiO_2, which is in marked contrast to the bimodal distribution of amphibolite facies Scourian gneisses. Silica variation diagrams are plotted in Figs. 12 and 13 for all major and some minor and trace elements for gabbros, tonalites trondhjemites and granites. There is a marked change in slope at 50 - 52 % SiO_2 for the elements Ti, P, Na, Ce, Y, Pb, Al which marks the boundary between gabbro and tonalite. In the tonalites, trondhjemites, granodiorites and granites Ti, Ca, Mg, Y, Zn and Fe fall on a straight line showing decreasing concentrations of the element with increasing SiO_2, which suggests that these rocks may represent liquids which are related by crystal fractionation with a phase or phases fractionating which are low in SiO_2 and rich in the elements depleted.

The elements Ti, Al, Y and Ce increase in concentration in the gabbros with increasing SiO_2 and decrease in concentration in the tonalite to granite sequence; if these elements have been removed from the more leucocratic members by fractional crystallisation the gabbros cannot represent the residue (i.e. the crystal fraction removed) because they themselves are depleted rather than enriched in these elements. Similarly Fe and Zn concentrations scatter around the tonalite end of a fractionation line and yet the residues from crystal fractionation would be much richer in iron.

P and Zr form parabolic curves with a peak in the tonalite gneiss compositions; since in silicic rocks P and Zr are restricted almost entirely to the minerals apatite and zircon, depletion in these elements from tonalites to granites implies that zircon and apatite were removed from the liquids by fractionation. Since gabbros and ultramafic rock in the Scourie area are low in P and Zr they cannot represent the apatite - zircon bearing cumulates which

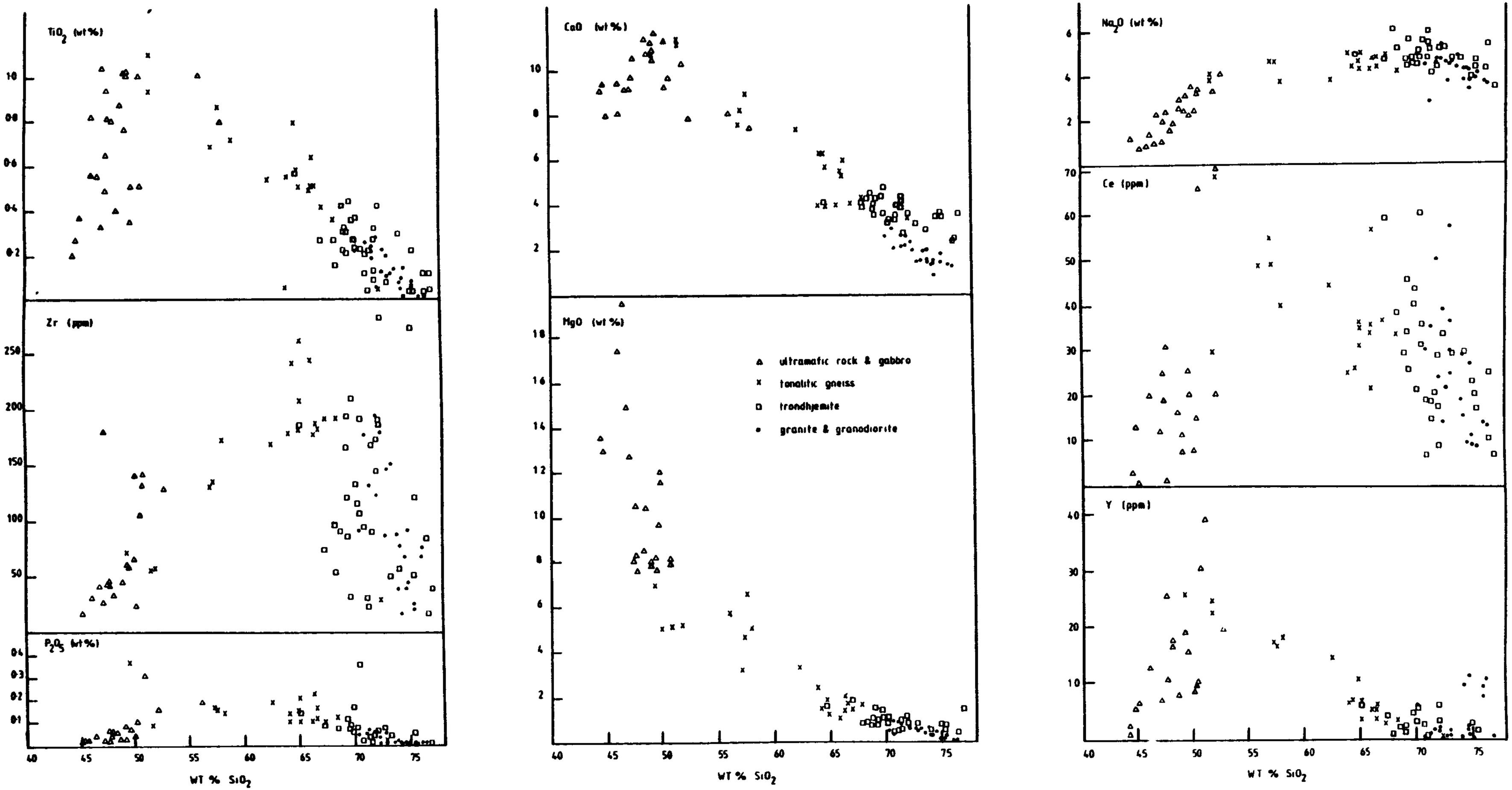

FIGURE 12. Silica variation diagrams for major and minor elements in ultramafic rock, gabbro, tonalite, trondhjemite, granodiorite and granite from Scourie. Chemical analyses are presented in table 3 at the end of this chapter.

FIGURE 13. Silica variation diagrams for major and minor elements in ultramafic rock, tonalite, trondhjemite, granodiorite and granite from Scourie. Chemical analyses are presented in table 3 at the end of this chapter.

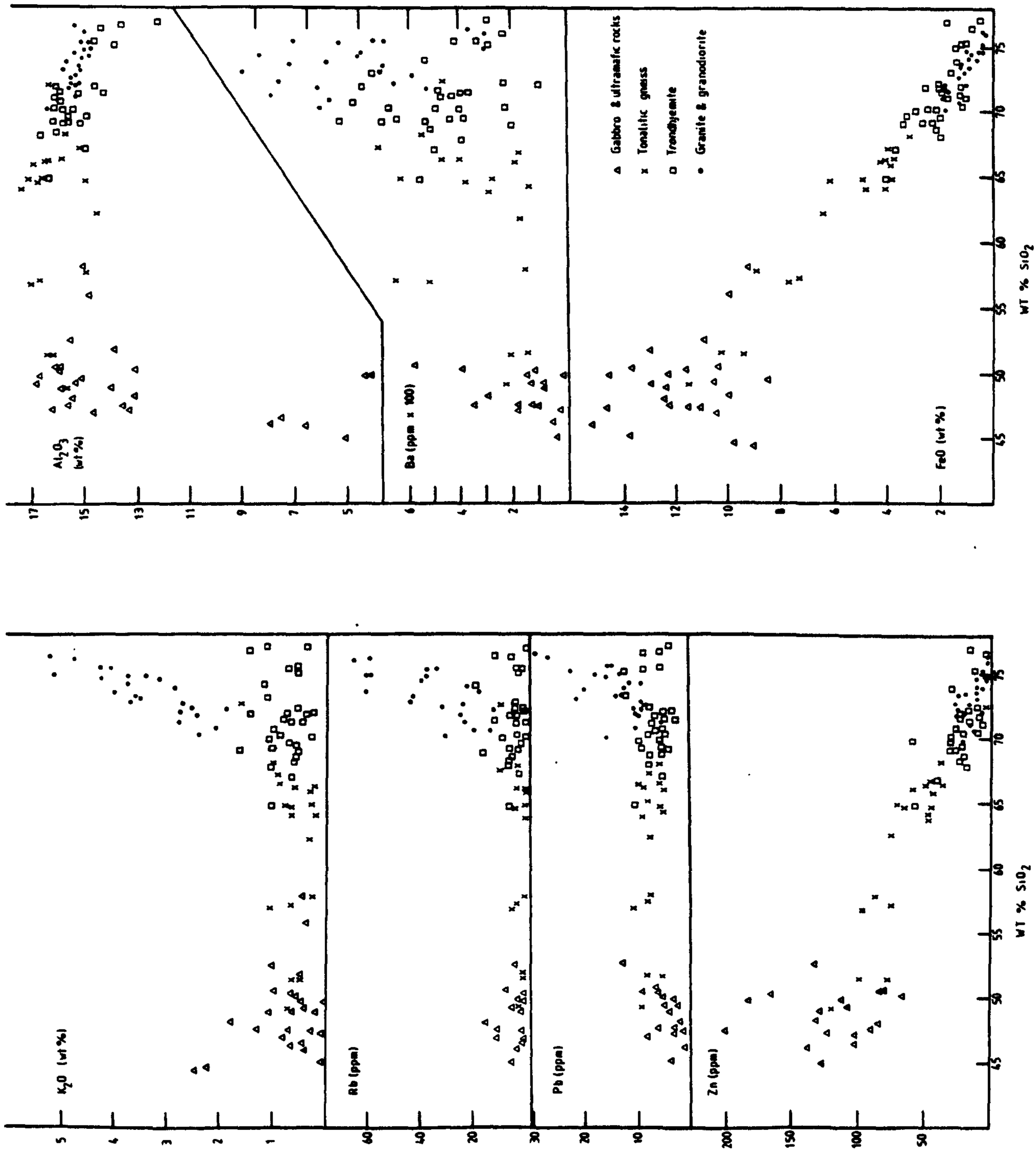

are the residues from the tonalitic to granitic rocks.

K, Rb and to a lesser extent Pb and Ba show two trends: there is a flat, trondhjemite trend which shows a maximum of 1.5 wt % K_2O and 20 ppm Rb with increasing SiO_2 and a granitic trend which shows a marked increase in K, Rb, Ba and Pb with increasing SiO_2 in the range 70 - 80 % SiO_2. Barker and Arth (1976) showed that the trondhjemite trend on an A-F-M diagram is similar to a calc-alkaline trend, but the two trends may be identified on a K_2O - SiO_2 diagram. It is important to note, however, that the increase in K_2O with SiO_2 in the Scourie granites is not the same as in a calc-alkaline sequence where there is a regular increase in K_2O with SiO_2 over the range 50 - 80 % SiO_2; it is probable therefore that if these chemical variations are produced by crystal fractionation that a phase such as hornblende which can accept K into its structure is involved.

Sheraton et al. (1973) discussed K_2O and Rb vs. SiO_2 relations in Scourian gneisses from Assynt but failed to notice that there are two trends; they suggested that K and Rb are depleted in the Assynt gneisses. Evidence from the granite - granodiorite sheets at Scourie, which were emplaced before the granulite facies metamorphism argues strongly against a universal metamorphic depletion.

Ce and Y, monitoring the light and heavy rare earth elements (REE) respectively, increase with increasing silica content in the gabbros; a similar trend is described by Arth et al. (1978) in Proterozoic gabbros from S.W. Finland; the opposite trend is present in tonalite gneiss. Ce in tonalite, trondhjemite and granite does not follow the usual pattern of strict variation with SiO_2 indicating that Ce in tonalite, trondhjemite and granite is controlled by different processes.

Relations in the system Qz-Ab-Or-An-H_2O

The normative compositions of tonalitic gneiss, trondhjemite and granite form a continuum when plotted in the tetrahedron Qz-Ab-Or-An (Fig. 14) implying a genetic relationship between these rocks, known to be related in space and time. There are two trends (Fig. 14):

a) tonalite gneiss and trondhjemite lie on a line of decreasing Ab+An and increasing quartz, while orthoclase remains constant,

b) trondhjemite and granite lie on a line of decreasing Ab+An with increasing orthoclase, while quartz remains constant.

From the trends outlined in Qz-Ab-Or-An space several inferences may be made:

(i) the line of liquid descent in the evolution of these rocks could have been controlled by crystal fractionation

(ii) tonalites could be parental to trondhjemites

(iii) trondhjemites could be parental to granites, which have crystallised along the quartz feldspar cotectic.

Drury (1972; 1978) described a trondhjemite-granite suite from the Scourian of Coll and Tiree, which is very similar in field relations and major element chemistry and which shows identical trends in the tetrahedron Qz-Ab-Or-An.

A study of the mineral chemistry of adjacent gabbros suggests that garnet - orthopyroxene pairs equilibrated in the pressure range 10 - 11 kb; ilmenite-magnetite pairs yield temperatures of at least 1010°C in trondhjemites and an An-rich alkali feldspar in a hypersolvus granite suggests possible magmatic temperatures of greater than 1100°C and a maximum H_2O content in the magma of 2%, which means it was highly undersaturated, compared with 14% H_2O measured in a water saturated granite magma at 10 kb (Huang and Wyllie, 1975). These data are used in Fig. 15 to place limits on

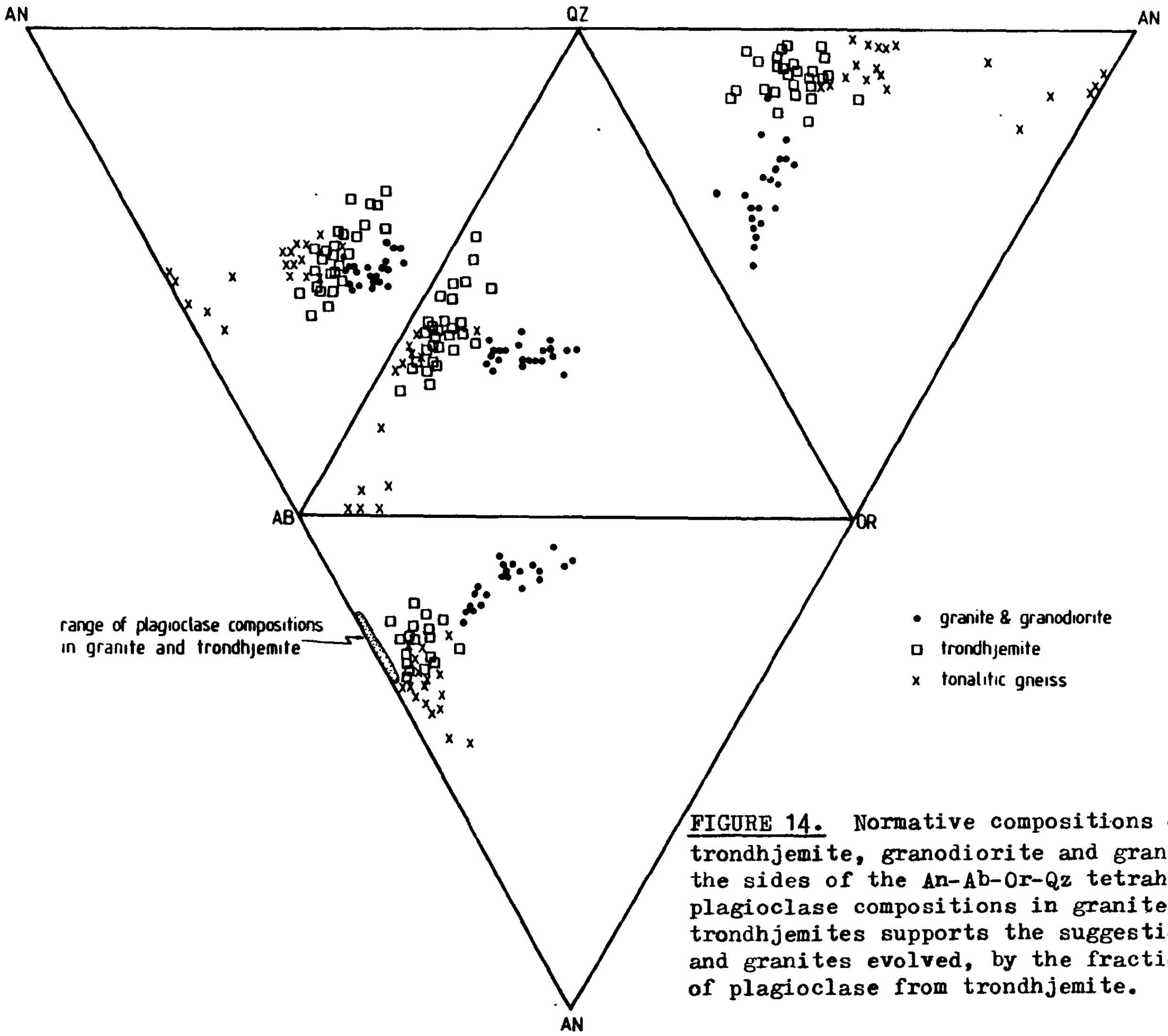

FIGURE 14. Normative compositions of tonalitic gneiss, trondhjemite, granodiorite and granite projected onto the sides of the An-Ab-Or-Qz tetrahedron. The range of plagioclase compositions in granites, granodiorites and trondhjemites supports the suggestion that granodiorites and granites evolved, by the fractional crystallisation of plagioclase from trondhjemite.

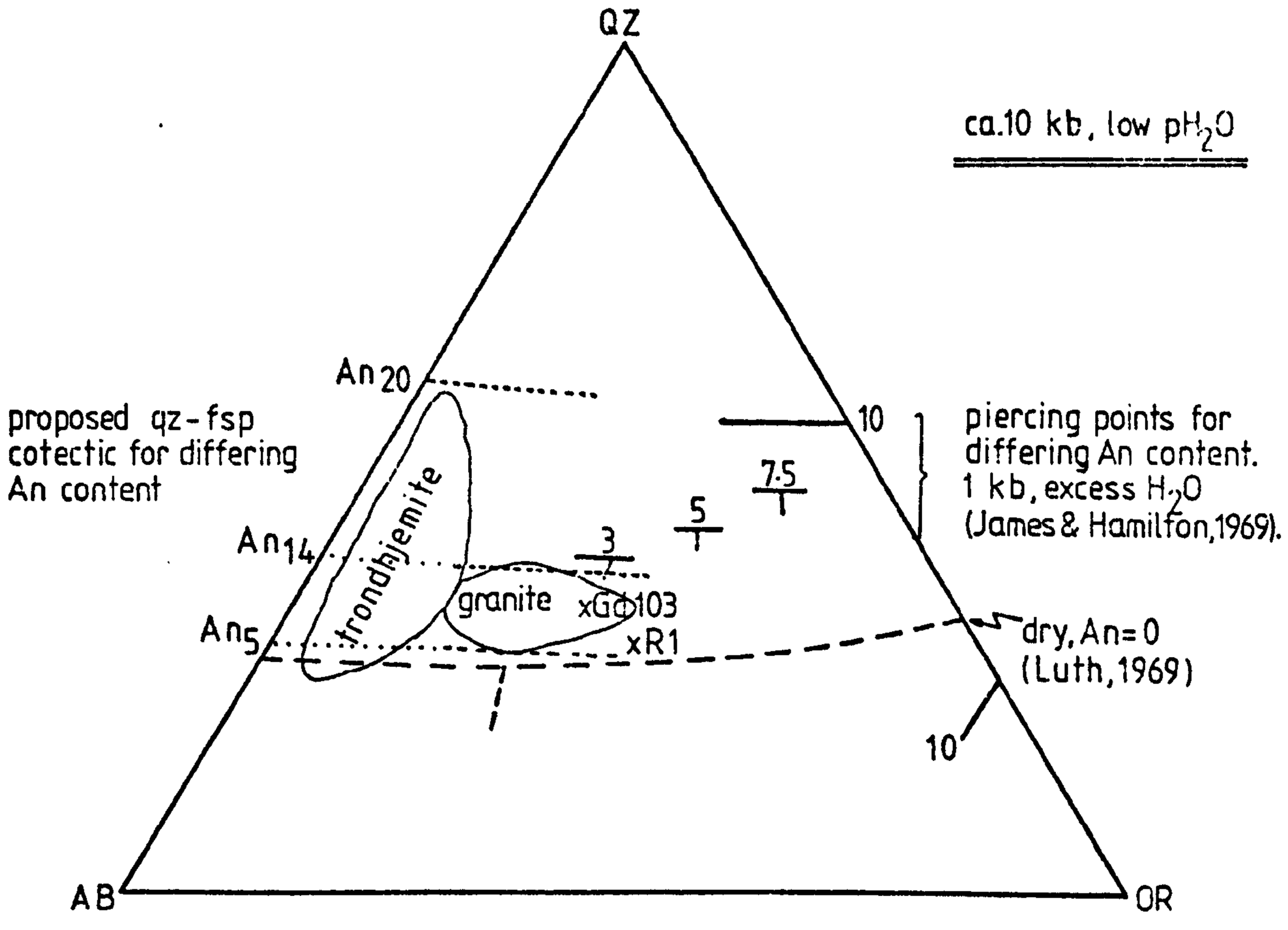

Fig. 15 Probable position of the quartz-feldspar cotectic for varying An content (short broken lines) in the projection Qz-Ab-Or at ca. 10 kb and pH_2O much less than ptotal, estimated from the composition of Scourian trondhjemites and granites. For comparison the piercing points from the study of James and Hamilton (1969) for differing An contents at 1 kb pH_2O (solid lines) and the position of the quartz-feldspar cotectic at 10 kb pressure, dry, in the system Qz-Ab-Or (Luth, 1969) are shown (long broken lines). The compositions of Granodiorite 103 (Piwinskii, 1973) and granite R 1 (Whitney, 1975) are also plotted for comparison.

phase boundaries in the system Qz-Ab-Or-An-H_2O for high pressures (ca. 10 kb) and low water contents, a part of the haplo-granodiorite system which has not been experimentally determined. The quartz-feldspar cotectic for 10 kb, low pH_2O and An_{20} (the highest An content of the trondhjemites) lies on the quartz side of the field of trondhjemites, whilst the cotectic for An_{5-14}, the An content of the granites, is defined by the field of granites (Fig. 15). There is only a small amount of experimental evidence to back up this

proposition: the granite R1 used by Whitney (1975) has an An content of 7.5% and this composition defines the Ab-Or boundary at 6% H_2O at 8 kb; the granodiorite 103 studied by Piwinskii (1973) with an An content of 16% was predicted by Wyllie (1977, see his Fig. 13) to lie on the quartz feldspar cotectic at 10 kb and 2% H_2O, but this was only an informed guess. The data from this study suggest that in the Qz-Ab-Or projection:

(i) the quartz field expands at the expense of alkali feldspar at high pressure and low pH_2O in a similar way to water saturated systems at high pressure (cp. Tuttle and Bowen, 1958; Luth and Tuttle, 1964; Huang and Wyllie, 1975).

(ii) the quartz field contracts with increasing An as was found by James and Hamilton (1969) at 1 kb pH_2O

(iii) the quartz field contracts more rapidly with increasing An content (cp. James and Hamilton, op. cit.)

Possible changes in bulk composition during metamorphism and retrogression

Some trondhjemites show a granulite facies mineralogy and others have been retrogressed to amphibolite facies. When plotted on a Qz-Ab-Or projection they define a broad trend between $Ab_{25}Qz_{75}$ and $Ab_{42}Qz_{58}$. Both amphibolite facies and granulite facies trondhjemites show a spread of compositions and the two groups overlap (Fig. 16). This scatter is interpreted as primary and is thought to be related to the igneous origin of the sheets rather than the redistribution of elements during metamorphism and retrogression for the following reasons; a) if amphibolite facies sheets are chemically altered granulite facies trondhjemites a spread would be seen in only amphibolite facies compositions, and this is not found; b) metasomatism usually produces a variation in K content and yet there is little variation in orthoclase content

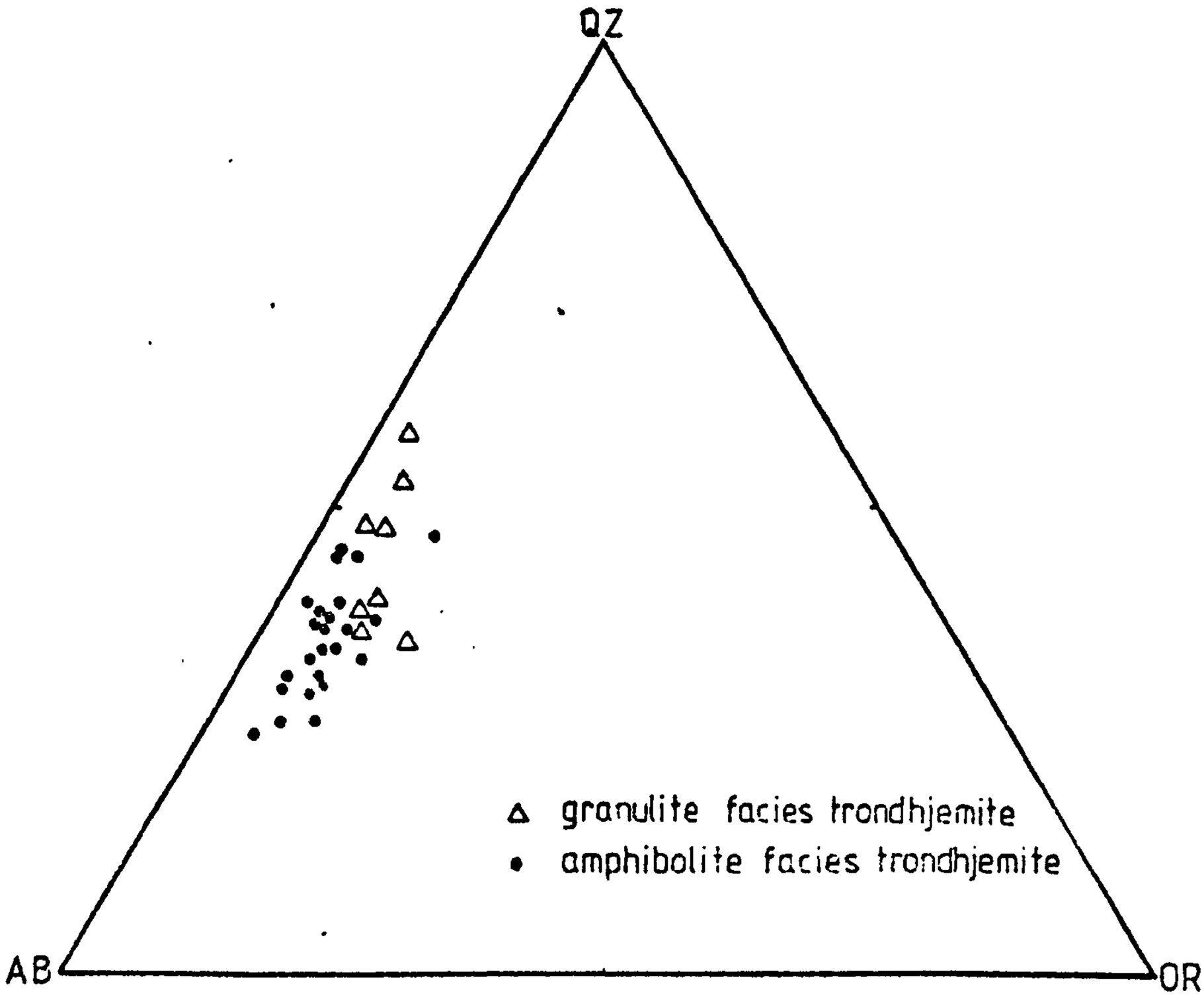

Fig. 16 Granulite facies trondhjemite and amphibolite facies trondhjemite plotted in the projection normative Qz-Ab-Or; both groups show a spread of compositions which overlap. This is a primary feature and is not due to the redistribution of elements during granulite facies metamorphism (see text).

compared with the difference in albite and quartz between the two groups of rocks; c) the average amphibolite facies trondhjemite is lower in K than the average granulite facies trondhjemite by about 30% (Table 2). This argues against K depletion during granulite facies metamorphism. The absolute amount of K difference is small, and does not affect the position of the amphibolite facies points in An-Qz-Or space. Table 2 gives the average composition of granulite facies and amphibolite facies trondhjemites; there are differences but

the standard deviation is also large for several elements.

Trace element studies on granite sheets (see below) show that Rb and Ba may have moved during the recrystallisation of alkali feldspar but K (mainly in alkali feldspar) and Sr (in plagioclase) have not moved on the same scale, so that the major element chemistry is believed to represent their original pre-metamorphic composition.

It is possible that the sheets were emplaced into hot, dry crust approaching granulite facies conditions, (cp. the Raftsund Mangerite, Griffin et al., 1974) in which case there is no reason to expect that any but the most volatile elements were mobile.

4. RARE EARTH ELEMENT (REE) CHEMISTRY

All trace elements in this study were determined by XRF analysis, a technique which is capable of determining only the light REE (La, Ce, Y). Since there is some imprecision in the La values, Ce is used to monitor the light REE and Y, with the same charge and ionic radius as Holmium (Whittaker and Muntus, 1970), is used to monitor the heavy REE and for comparative purposes is plotted in the Erbium position, since Ho is not always measured. Towell et al. (1965) have plotted Y for Er in otherwise full REE determinations (excluding Gd) for a gabbro-tonalite-granodiorite-quartz monzonite suite from the Southern California Batholith and found that a chondrite-normalised value for Y in the Er position was consistent with the other heavy REE. Drake and Weill (1975) showed in their determination of partition coefficients between plagioclase and basaltic and andesitic liquids that Y behaves as a super-heavy REE.

The REE are particularly useful in understanding the premetamorphic history of a high grade rock because they are thought to be immobile during metamorphism (O'Nions and Pankhurst, 1974;

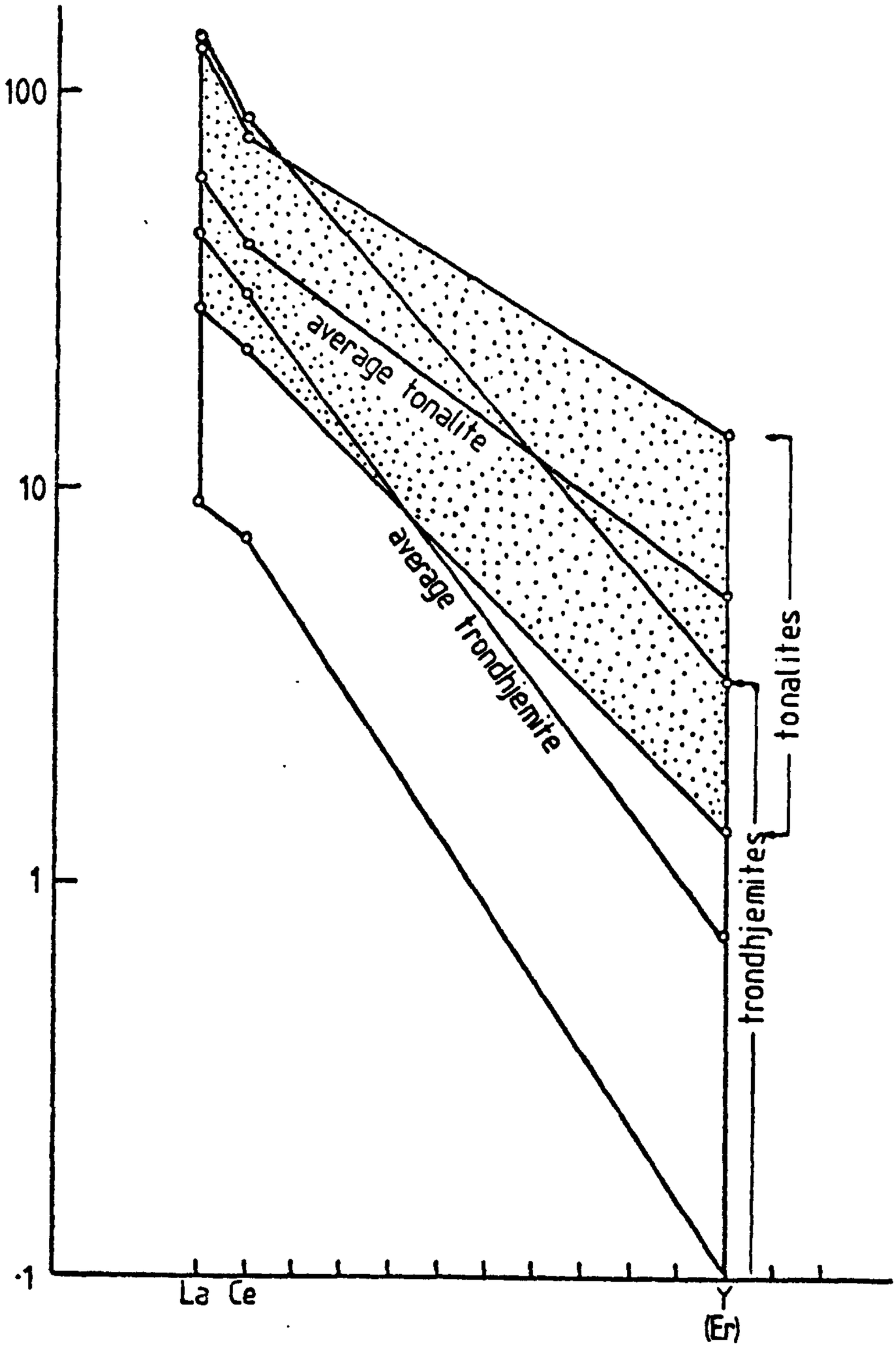

FIGURE 17. Chondrite normalised values for La, Ce and Y (after Er) for trondhjemites and tonalites, using the chondrite values of Herrman (1974). Note the wide range of values in the trondhjemites and the extreme depletion in Y.

Green et al., 1972; Herrmann et al., (1974). La, Ce and Y are used to construct simulated REE patterns (Fig. 17) and chondrite normalised Ce/Y ratios are plotted against normalised Y values (Fig. 18) and show the relative degree of enrichment and slope of the REE pattern

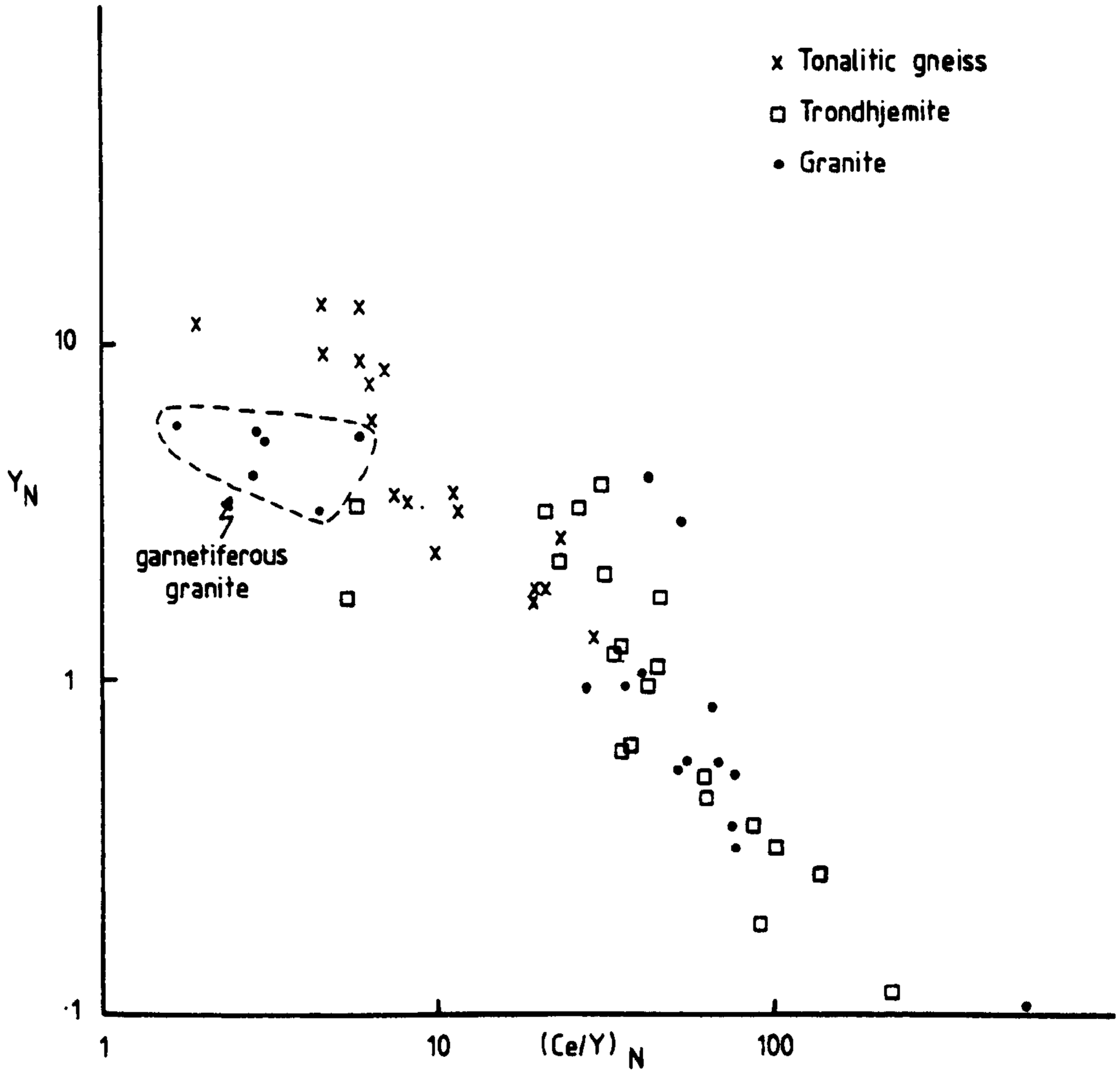

Fig. 18 *Chondrite normalised values for Y plotted against the normalised Ce/Y ratio. Note the continuum between tonalite and trondhjemite and the high (Ce/Y) ratios in some trondhjemites. Garnetiferous granite is anomalous due to the retention of Y in garnet.

---

* REE were normalised using the following values for chondritic meteorites: Y, 1.96 ppm; La 0.32 ppm; Ce, 0.94 ppm; from the compilation of Herrmann (1974).

in the tonalite - granite suite. Trondhjemites are more strongly fractionated than the tonalites and show a large range in $(Ce/Y)_n$ ratios from 5.0 to greater than 200; they are strongly depleted in Y and many samples contain less than 1 ppm Y. Tarney et al. (in press) identified two groups of trondhjemites on the basis of their REE patterns in the Lewisian of the Inner Hebrides; there is a group with low $(Ce/Y)_n$ ratios (ca. 5 - 29) and a group with high $(Ce/Y)_n$ ratios (ca. 140). It is probable that both these groups and intermediate types are represented in the Scourie area. Granites and granodiorites also show highly fractionated REE patterns although the range in $(Ce/Y)_n$ ratios (27 - 80) is not so great; granites containing garnet have high Y and low $(Ce/Y)_n$ ratios (1 to 6) due to the retention of Y in garnet.

5. A FRACTIONAL CRYSTALLISATION MODEL FOR THE ORIGIN OF SCOURIAN GRANITES

Fig. 14 shows the compositions of the Scourian Granite sheets in the system Qz-Ab-Or-An. Relationships in the Qz-Ab-An projection suggest that the granitic liquids have evolved along the quartz feldspar cotectic and were derived from a trondhjemite parent. In the projection An-Ab-Or granitic liquids, trondhjemites and analysed feldspars from granites, and trondhjemites lie on the same straight line implying that the removal of plagioclase from a trondhjemite liquid will produce a successively more granitic liquid.

If it is assumed that plagioclase and quartz are the two main phases crystallising in trondhjemites, it is possible to test a fractional crystallisation model using the concentration of trace elements which are preferentially accommodated or rejected by plagioclase. The elements Rb, K, Ba, Sr were selected because there are experimentally-determined distribution coefficients between

plagioclase and granitic liquids for these elements. Trace element concentrations for the elements Rb, K, Ba and Sr for granite sheets have been divided by the concentration in the assumed trondhjemite parental liquid in order to derive an enrichment factor ($X_{tr}^{granite}$ / $X_{Tr}^{trondhjemite}$) which is plotted against Or/Ab, a measure of differentiation in the trondhjemite-granite suite (Fig. 19). Trace element concentrations for the assumed parental trondhjemite liquid were taken from the average of the granulite facies trondhjemites because (1) they are not over enriched in normative Ab and therefore probably are not plagioclase-rich cumulates and (2) any redistribution of trace elements during retrogression will be minimal.

Enrichment factors greater than 1.0 imply a distribution coefficient of less than 1.0 for the element concerned between the fractionating phase(s) and the granitic melt, and an enrichment factor of less than 1.0 implies that the element is preferentially concentrated in the fractionating phase. Fig. 19 shows that the trace elements have the following pattern of enrichment Rb > K > Ba > 1.0 > Sr which means that the distribution coefficients for the fractionating phases(s) are Sr > 1.0 > Ba > K > Rb. Measured distribution coefficients for plagioclase, anorthoclase, orthoclase, biotite, hornblende, clinopyroxene, orthopyroxene and garnet for dacitic and rhyolitic rocks are quoted in Table 2 of Hanson (1978) and show that plagioclase is the only mineral with distribution coefficients in the order Sr > 1.0 > Ba > K > Rb. A 'kink' in the curve for Ba (and possibly Rb) indicates a change in the liquid composition at about Or/Ab = 0.7. Fig. 19 also shows that the curves for K and Sr are well defined but the data for Rb and Ba show a scatter implying that these elements have moved during post-magmatic recrystallisation on the scale of tens of cm. A detailed textural study of the alkali feldspars shows that they have recrystallised in the temperature range 500 - 600^{o}C in the presence of an aqueous fluid

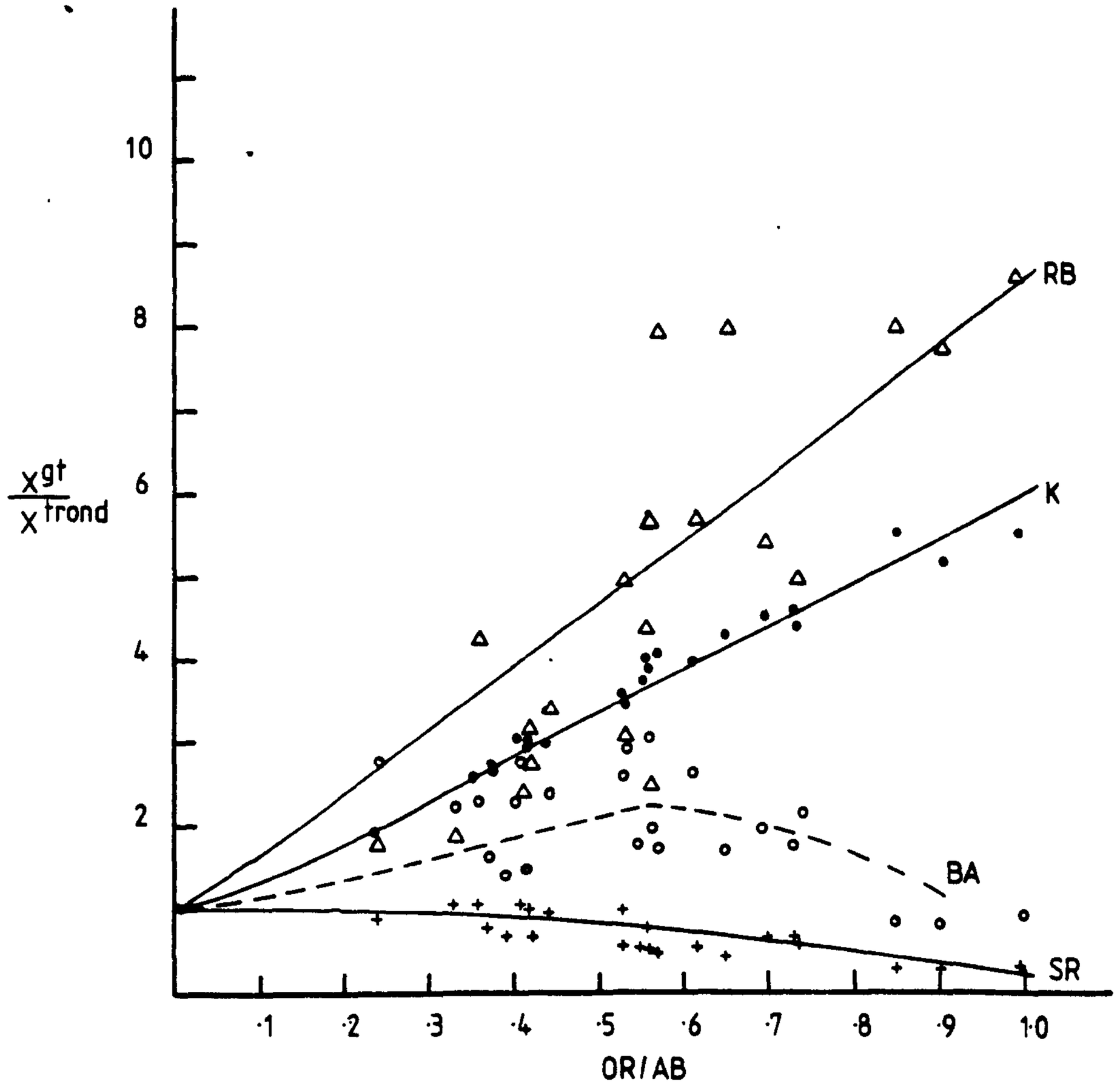

FIGURE 19. The concentration of the trace elements Rb (triangles), K (filled circles), Ba (open circles) and Sr (crosses) in Scourian granite sheets relative to their concentrations in the parental trondhjemite increase with increasing normative Or/Ab ratio in a manner that is consistent with plagioclase fractionation. The scatter in the Rb and Ba data indicate that these elements were redistributed on the scale of tens of centimetres during retrogression.

phase and since Rb and Ba are concentrated in alkali feldspar they probably moved during this late recrystallisation rather than during granulite facies metamorphism (see below). Pb is also concentrated in alkali feldspar which has important implications for the interpretation of both Pb/Pb and Rb/Sr isotopic studies on these sheets (cf. Chapman, 1978, and see below).

Simulated rare earth patterns for trondhjemites and granites are comparable (Figs. 17 and 18); this is consistant with a fractional crystallisation origin for the granitic liquids because the distribution coefficients for Ce and Er (after Y) are both much less than 1.0 between plagioclase and rhyolitic and dacitic liquids and therefore Ce and Y will remain in the liquid in proportions similar to the parental trondhjemite, and although the concentrations may be enriched slightly the slope will not be significantly different. Full REE patterns, however, are expected to show a depletion in europium in the granites relative to the trondhjemites. This is partly supported by recent REE determinations by Tarney et al. (in press) on Scourian trondhjemites and granites from Coll and Tiree.

It is difficult to calculate precisely the amount of fractional crystallisation necessary to produce the observed trends in Fig. 19 because the distribution coefficients are strongly dependant upon temperature and the composition of the melt (Drake and Weill, 1975); however, the extreme concentration of K and Rb indicated that the most potassic granite liquids represent a small fraction (ca. 10%) of the original trondhjemite liquid.

In view of the large amount of crystal fractionation necessary to produce some of the granitic liquids and the difficulty in separating the liquids from the crystal residue it is probable that separation occurred during deformation, by filter press action. There is good field evidence to support the view that granitic and

trondhjemitic liquids are related by plagioclase fractionation. In the sheet East of Camas an Lochain both granite and trondhjemite are present and at the base of the sheet there is an andesine anorthosite with only 3% modal quartz, which could represent a plagioclase rich residue (Fig. 9). Other sheets show a close association between granite and trondhjemite.

Plagioclase fractionation explains some of the scatter of trondhjemite analyses in the tetrahedron An-Ab-Or-Qz (Fig. 14) because some of the trondhjemites are plagioclase rich residues.

There is a progressive change in ferromagnesian mineralogy related to changes in composition of the host rock; trondhjemites contain clinopyroxene (or amphibole after clinopyroxene), granites with more than 10% An in the Or-An-Ab projection are orthopyroxene-bearing, and granites with lower concentrations of An in the norm contain garnet (almandine rich) as the dominant ferromagnesian mineral.

An important corollary to the above argument is that if the granites and granodiorites are derived by the fractional crystallisation of plagioclase from trondhjemite some trondhjemite-looking sheets are in fact plagioclase and quartz residues. Recent REE determinations by Tarney et al. (1978) support this view; they found that trondhjemite sheets from the Lewisian of the Inner Hebridees (where there are also granite sheets (Drury 1972)) can be classified into two groups: (a) trondhjemites which are depleted in all REE, with low $(Ce/Y)_n$ ratios and prominent Eu anomolies and (b) trondhjemites with more fractionated REE patterns and with higher concentrations of light REE and no Eu anomaly. They suggest that the REE patterns of group (a) trondhjemites resemble those of feldspathic cumulates and are similar to those in Proterozoic anorthosites. Trondhjemite sheets at Scourie show a range of $(Ce/Y)_n$ ratios from 5.0 to greater than 200 and could represent primary trondhjemitic liquids, plagioclase and quartz rich residues and all the stages inbetween.

6. THE EVOLUTION OF THE TONALITES AND TRONDHJEMITES

The low initial $^{86}Sr/^{87}Sr$ ratio in Scourian tonalites (Moorbath et al., 1975; Chapman, 1978) indicates that these rocks were derived from a source with a low Rb/Sr ratio ca. 2700Ma. ago; this source may be the mantle, basic volcanic rocks or immature sediments derived from basic volcanic rocks (O'Nions and Pankhurst, 1978), but it cannot be quartzofeldspathic material older than ca. 3000Ma. (Moorbath et al., 1975).

There are four possible models for the generation of tonalite - trondhjemite magmas with low initial $^{87}Sr/^{86}Sr$ ratios: (i) a low degree of partial melting of the mantle (Holland and Lambert, 1975) (ii) the partial melting of a basaltic composition with amphibolitic or quartz eclogite mineralogy (Arth and Hanson, 1972; 1975; Barker and Arth, 1976; Barker et al., 1976); (iii) fractional crystallisation of wet basaltic magma (Arth et al., 1978); (iv) partial melting of tonalite gneiss to form trondhjemite.

The fourth model was suggested by Chapman (1978) and C. Pride (pers. comm.), to account for the origin of the trondhjemites and associated acid sheets at Scourie. However, both field and laboratory evidence argue against this: trondhjemites show sharp intrusive contacts against the tonalite gneiss and there is no evidence that tonalite gneiss melted in the Scourie area; partial melting of tonalite with a high water content (greater than 3% H_2O) produces a granitic or granodioritic liquid (Brown and Bowden, 1973); partial melting at lower water contents cannot generate the trace element concentrations in trondhjemite because plagioclase is the last phase to melt and yet the similar Sr content of average tonalite and average trondhjemite would imply that all the plagioclase melted i.e. 100% melting (Wyllie, 1977).

Evidence for the derivation of trondhjemite and tonalite by fractional crystallisation

The continuum of rock types over a range of SiO_2 contents from 45 - 78 wt per cent and the smooth trends on A-F-M and Harker variation diagrams suggests that these rocks may be related by crystal fractionation and argues against their derivation by partial melting. A fractional crystallisation model is also consistent with the relative ages of the rocks in this suite, which become more silicic with time. The smooth variation in Ce and Y which increases in the basic rocks and decreases in tonalites and trondhjemite is similar to the variation in REE in the Proterozoic gabbro-trondhjemite suite of S.W. Finland which Arth et al. (1978) have interpreted as due to fractional crystallisation.

The significance of the gabbros and ultramafic rocks in the Scourie sequence, however, is difficult to evaluate. The evidence presented above from variation diagrams indicates that they cannot be crystal residues derived from the tonalites; this agrees with their small volume, relative to the tonalites and the field relationships which indicate that they are earlier than the tonalites. Their frequent occurrence in high grade areas, however, indicates that the association is more than fortuitous, but it is concluded that there is no direct genetic link between tonalites and gabbros.

It is probable therefore that tonalites, trondhjemites and granites are related by fractional crystallisation, but there is no obvious source in the Scourie area for the large volume of tonalite which forms the greatest part of the Scourie gneisses.

Tonalites and trondhjemites lie on the same common trends on:

(i) an A-F-M diagram - they define a calc-alkaline trend; (Fig. 11)

(ii) silica variation diagrams - they show a decrease in Fe, Mg, Ca, Ti, Zn and Y with increasing SiO_2; (Fig. 12 & 13)

(iii) a (Ce/Y) vs. Y plot - they show an increasing fractionation of REE and a depletion in Y; (Fig. 18)

(iv) a normative Qz-Ab-An-Or diagram - they show decreasing (Ab+An) with increasing Qz (Fig. 14).

It is possible to understand the variations in Qz-Ab-Or-An space by using the Qz/Ab ratio as a measure of differentiation for tonalites and trondhjémites (Fig. 20). Ti and Y decrease with increasing Qz/Ab in tonalite but not in trondhjemite, Al_2O_3 decreases in trondhjemite and Sr shows two trends; (a) a trend of decreasing Sr in some trondhjemites and (b) constant Sr in tonalites and trondhjemites. The dissimilarity between tonalite and trondhjemite on Qz/Ab diagrams indicates that the variation in Qz/Ab ratio in tonalites and trondhjemites is caused by different processes.

Barker et al. (1976) and Barker and Arth (1976) suggested that there are high alumina trondhjemites (greater than 15% wt Al_2O_3) generated by the fractional crystallisation of hornblende gabbro, and low-alumina trondhjemites (less than 15% wt Al_2O_3) generated by the partial melting of basalt with plagioclase in the source. The variability of Al_2O_3 between 12 and 17 % wt in the Scourie trondhjemites makes this classification meaningless in view of the close spatial relationships between these trondhjemites which points to a common origin.

In summary, therefore, the chemical variation in tonalites and trondhjemites is a function of crystal fractionation of a phase or combination of phases which depleted the melt in Fe, Mg, Ca, Ti, Y and Zn and enriched it in Ce and SiO_2. Qz/Ab diagrams show that there are differences between the fractionating phases in tonalites and trondhjemites.

A mechanism for the fractionation of Scourie tonalites and trondhjemites

Hornblende and garnet are the only phases which can deplete a tonalite - trondhjemite melt in Y; garnet, however, is incapable of depleting a melt in Ti (Cawthorn and Brown, 1978) implying that the fractionating phases were either garnet accompanied by a Ti-bearing phase or hornblende, which is capable of removing both Ti and Y. The removal of hornblende er garnet will increase the amount of Sr in the melt, therefore plagioclase must also have been a fractionating phase in order to produce the trend of constant Sr with increasing Qz/Ab (Fig. 20). The steep Sr vs. Qz/Ab trend is produced by hornblende fractionation or by the accumulation of plagioclase (Sr enrichment) and removal of plagioclase (Sr depletion), Garnet and plagioclase tend to be mutually exclusive in tonalitic melts (Wyllie, 1977) suggesting that hornblende and plagioclase were the main fractionating phases.

There are three main implications of this conclusion: (1) the magmas evolved at less than 60 km depth for hornblende to be stable, and less than 45 km for plagioclase to be stable (Arth et al., 1978). (ii) there was a high water content in the melt (greater than 10% H_2O at 10 kb) in order for hornblende to be the primary ferromagnesian phase on the liquidus, otherwise it was accompanied by clinopyroxene (Wyllie, 1977). (iii) water was lost during granulite facies metamorphism.

7. THE ORIGIN OF THE SCOURIE TONALITES

Constraints on the origin of the Scourie tonalites are:

(i) the low initial strontium isotope ratio

(ii) the relatively high concentrations of Sr and Ba

(iii) the fractionated REE

(iv) the low concentrations of K and Rb and the high K/Rb ratio.

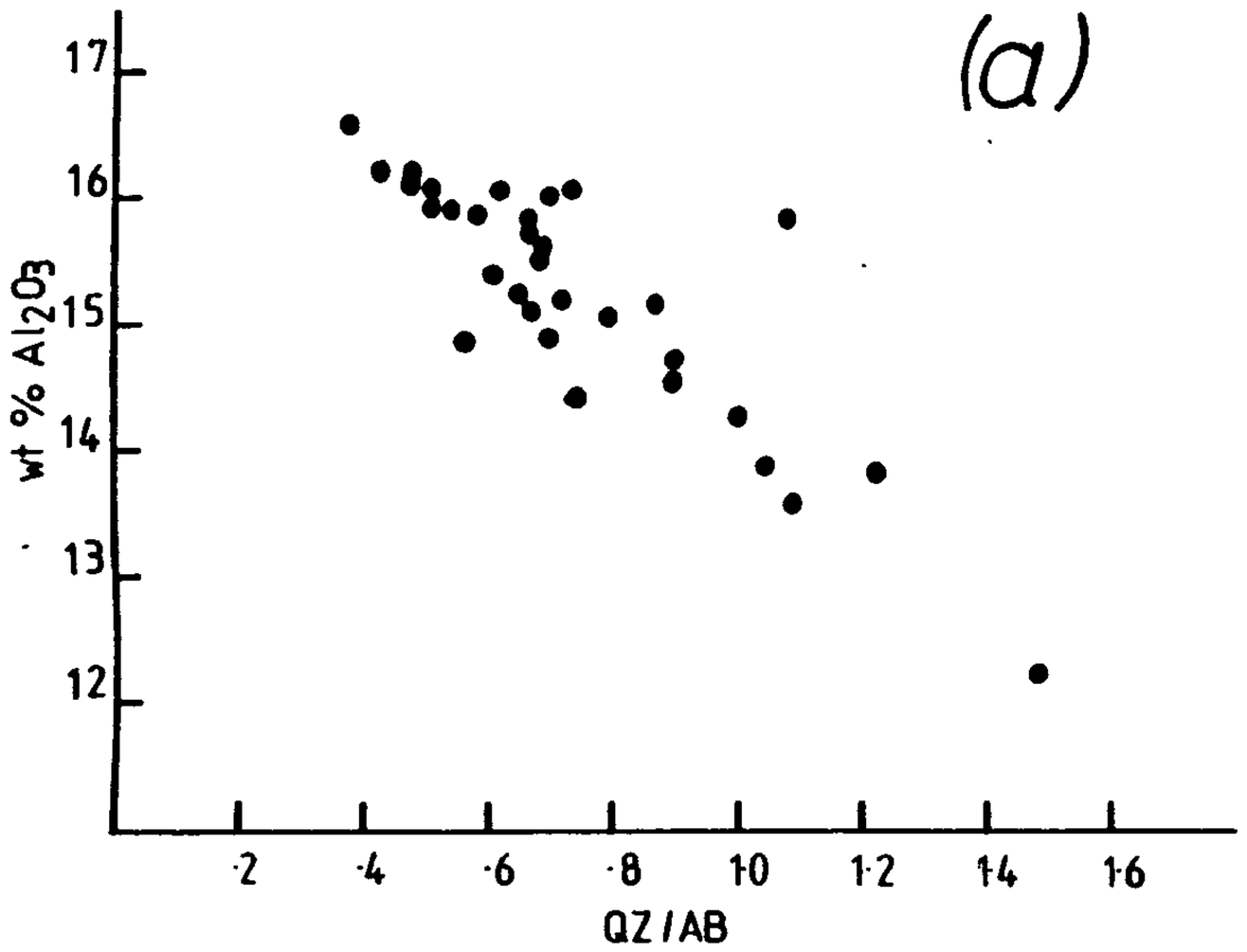

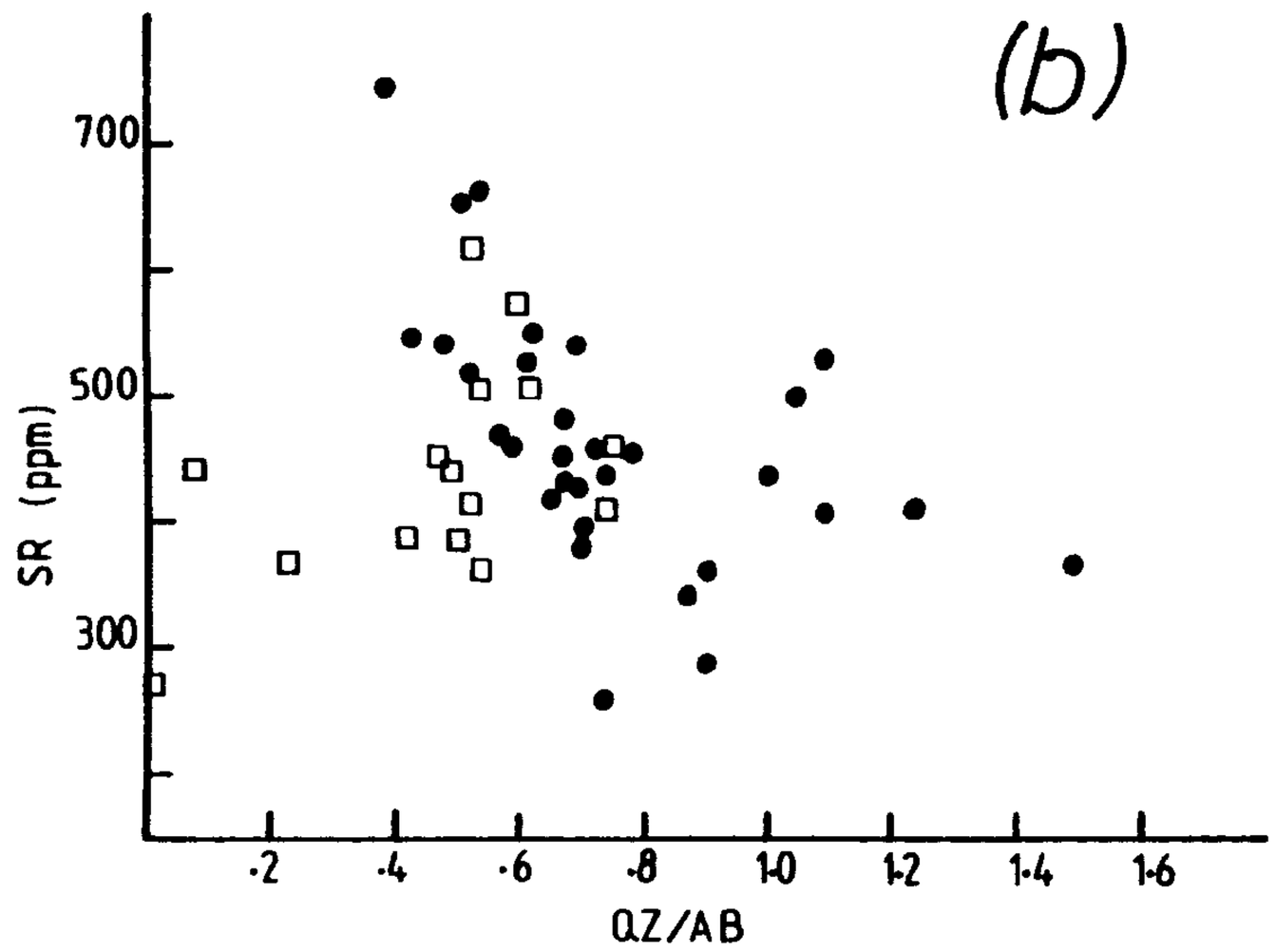

FIGURE 20. Plots of Al_2O_3, Sr, TiO_2 and Y against normative Qz/Ab; open squares are tonalitic gneiss filled circles are trondhjemite.

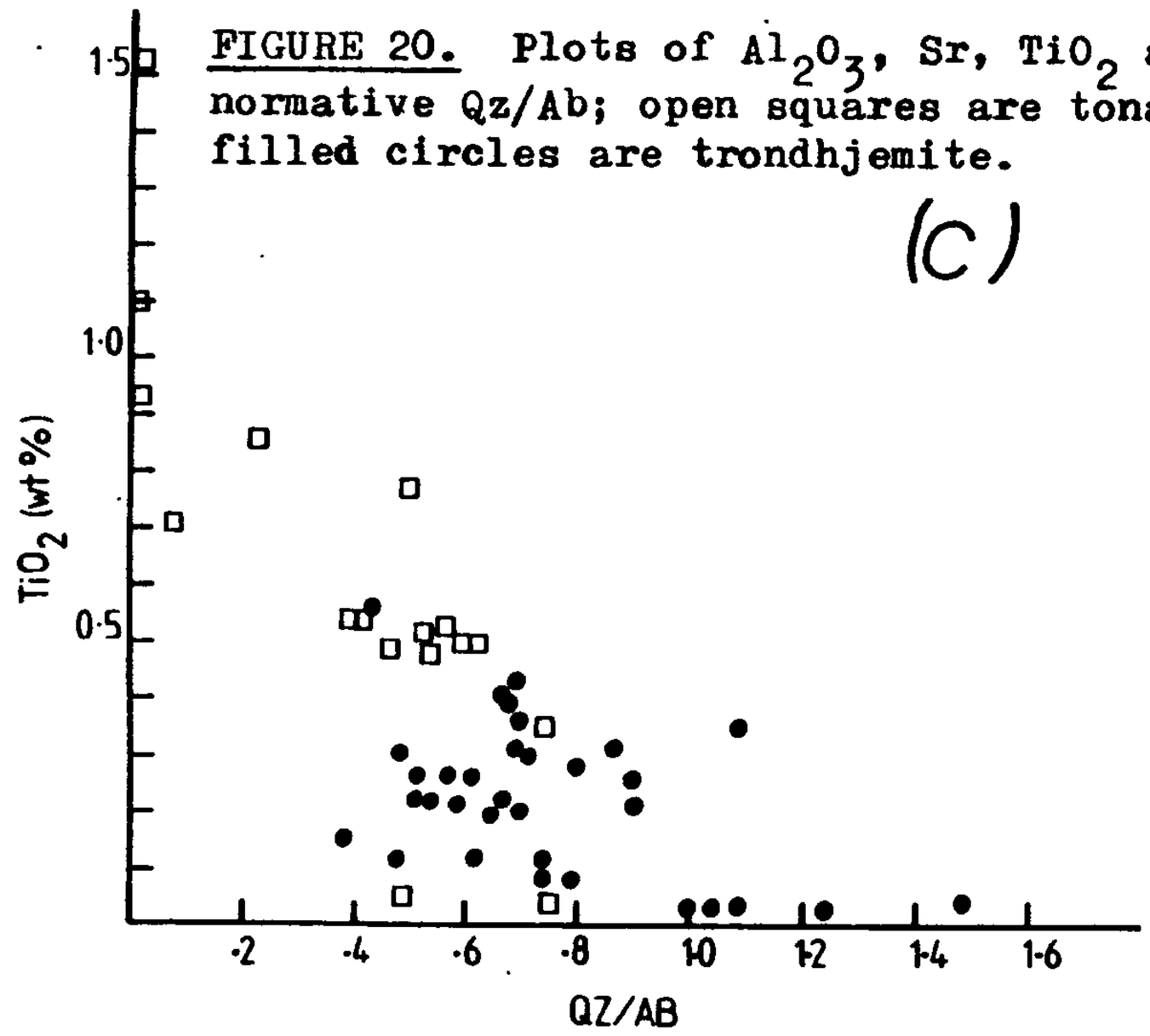

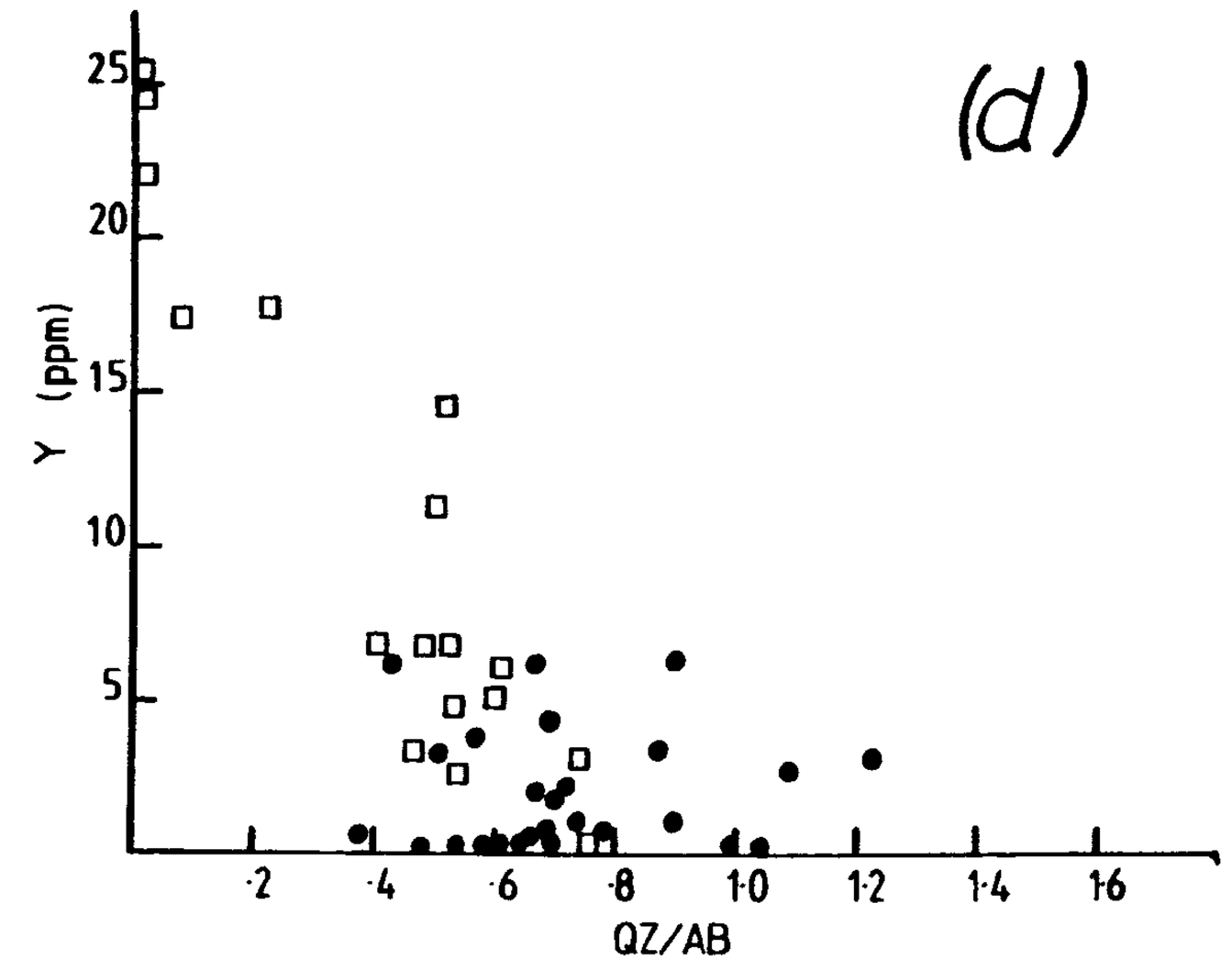

In view of the low initial strontium isotope ratio a basaltic or mantle source is the most favourable for the generation of large volumes of tonalitic magma (Arth and Hanson, 1972, 1975; Barker and Arth, 1976; Barker et al., 1976). There are problems with a mantle source because of the low degrees of partial melting necessary and the difficulty in extracting small amounts of melt (O'Nions and Pankhurst, 1978; Tarney et al., in press; Arndt, 1977); it is also difficult to see how this process can produce the large volume of tonalite which forms the Scourian rocks in this area. Because of the high K/Rb ratio in the tonalites and the difficulty in increasing the K/Rb ratio by magmatic processes a source with a high K/Rb ratio such as an ocean tholeiite (K/Rb ca. 1000) seems probable; weathered oceanic tholeiite can have even higher K/Rb ratios but these are unlikely to form a substantial thickness of the oceanic crust. Nevertheless it is very difficult to derive a tonalite with a K/Rb ratio of ca. 1900 from a tholeiitic source by either partial melting or fractional crystallisation. The depletion in heavy REE in the tonalites indicates that garnet or hornblende is a major fractionating phase if a fractional crystallisation model is applicable and yet neither garnet nor hornblende fractionation can increase the K/Rb ratio of the melt sufficiently. A low degree of partial melting of a basaltic composition with clinopyroxene and garnet in the residue can increase the K/Rb ratio but it is also necessary to have some plagioclase and phlogopite in the residue in order to reduce the absolute concentrations of K, Sr, Rb, and Ba in the melt. The amount of phlogopite necessary is constrained by the amount of K in the source and it is unlikely to be high enough to reduce the K levels in the melt. The only way in which the high K/Rb ratios can be produced in tonalitic melts from a basaltic source is by a two-stage process which involves (i) the production of the melt and (ii) the depletion

of Rb relative to K.

It has been argued above that the gabbros and tonalites in the Scourie area cannot be related by fractional crystallisation which means that there is no obvious source for the large volume of tonalites in this area. The low initial strontium isotope ratio suggests an original basaltic source as discussed above and trace element concentrations are consistent with a derivation from a basaltic source by either the fractional crystallisation of garnet or the partial melting with garnet and/or hornblende in the residue. It is not possible to resolve the origin of the tonalites further with the available data.

8. DEPLETION IN THE SCOURIAN GRANULITES

Two of the most difficult features to understand in the granulites of the Scourie area are the low abundances of large ion lithophile elements (LIL) K, Rb, U, Th, Cs, and the high K/Rb ratio. In gabbro cumulates, where these elements are incompatible, this is to be expected but LIL depletion is also found in tonalites and trondhjemites. The K/Rb ratio is a useful indicator of this depletion; granulite grade tonalites and trondhjemites at Scourie have mean K/Rb ratios of 1900 and 1180 respectively compared with 309 and 470 for amphibolite facies Scourian tonalites and trondhjemites at Gruinard Bay (Fig. 21) and with Shaw's (1968) K/Rb ratio of 254 for igneous rocks with 1.0% K.

Heier (1973) has discussed depletion in relation to granulite facies rocks throughout the world and regards it as characteristic of medium to high pressure granulites. Tarney (1976) has summarised the hypotheses which have attempted to account for the depleted chemistry of granulites:

(a) depletion is a primary feature of the rocks themselves (Holland and Lambert, 1973).

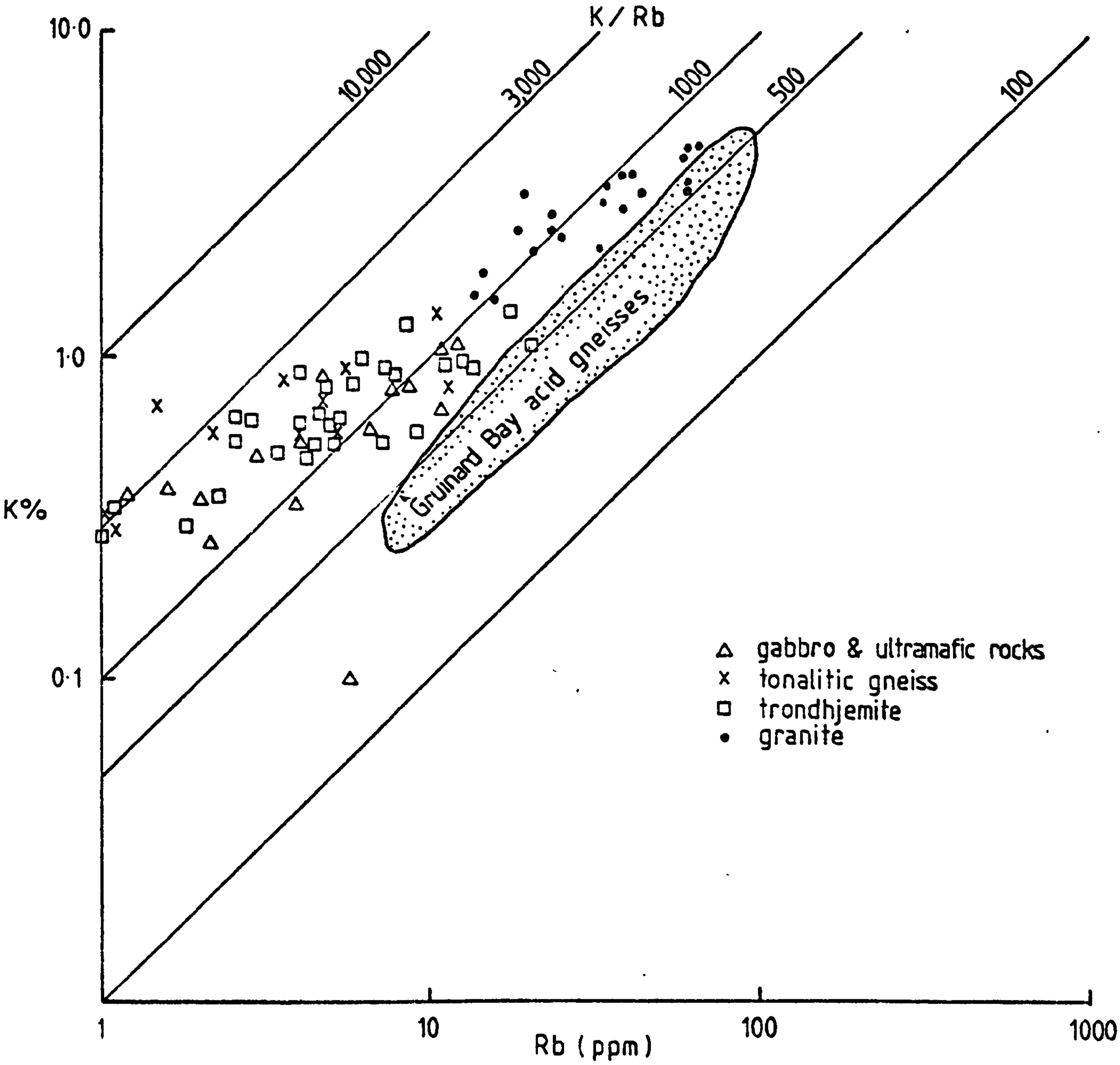

FIGURE 21. K/Rb ratios for Scourie granulites compared with amphibolite facies acid gneisses (tonalitic to trondhjemitic) from Gruinard Bay. Note the scatter in the data for ultramafic to trondhjemitic rocks in contrast to the grouping and consistently lower K/Rb ratios in granites (and granodiorites).

(b) granulites represent a residuum from which a granitic melt has been removed into which all the LIL have been partitioned (Fyfe, 1973; O'Hara, 1978).

(c) the development of a high pressure mineral assemblage excludes LIL elements which are removed along with any water in the system (Lambert and Heier, 1969; Heier, 1973).

(d) it is a specifically Precambrian process whereby LIL are removed by mantle degassing (Tarney et al., 1972; Sheraton et al., 1973).

(e) Tarney and Windley (1977) suggested another mechanism - the removal of LIL in a CO_2-rich fluid phase.

Tarney and Windley (op.cit.) also pointed out that high K/Rb ratios are not always found in high pressure granulite terrains, neither are they restricted to granulites because they occur in rocks of lower metamorphic grades. Gray (1977) has described granulites from Central Australia which are undepleted in LIL except for uranium and which have normal K/Rb ratios (200 - 1750). Field and Clough (1976) present a diagram which shows a range of K/Rb ratios (1000 - 200) for both amphibolite facies and granulite facies metabasites which suggests that the K/Rb is controlled by something other than a granulite facies metamorphic process.

There are three main arguments which suggest that the K/Rb ratios in the Scourie granulites are not original and that they were depleted in Rb relative to K during granulite facies metamorphism:

1. The K/Rb ratio is much higher than (a) other Archaean tonalites (see, for example, Arth and Hanson (1975) and this study, Chapter 2) (b) Mesozoic-Cenozoic tonalites (although values for K/Rb between 550 and 1000 are reported for tonalites in Japan (Ishizaka and Yanagi, 1977) and Fiji (Gill, 1970)) and (c) Shaw's average K/Rb ratio for igneous rocks containing ca. 1% K.

2. Shaw (1968) showed that K/Rb typically decreases during magmatic evolution; this is not found. K/Rb ratios for gabbros and trondhjemite are scattered between 450 and 3000 irrespective of rock type suggesting that there has been mobility of K and/or Rb.

3. It is not possible to derive the Scourie tonalites from a source with a lower K/Rb ratio by any simple petrological process and it is difficult to find a source with a higher K/Rb than the tonalites, implying that the high K/Rb ratios are not an original magmatic feature of these rocks.

Even though there is a strong case for the depletion of the Scourie granulites there is evidence which suggests that the nature and extent of the depletion must be qualified.

1. Depletion in K. A plot of K_2O vs. SiO_2 in granulite facies rocks from Scourie shows two trends (Fig.22); one of marked K_2O enrichment between 70 and 80% SiO_2 (the granite-granodiorite trend) and the other marked by low K_2O over the range 45 - 78% SiO_2 (the gabbro - trondhjemite trend). Sheraton et al. (1973) and Tarney (1976) argued that since K_2O enrichment with increasing SiO_2 is a common feature of calc alkaline rocks over the range SiO_2 45 - 80% SiO_2 the lack of such a trend indicates that these rocks were depleted in K during granulite facies metamorphism. The presence of two trends, one showing K_2O enrichment makes the ideas of Sheraton et al. (1973) and Tarney (1976) less tenable. Furthermore identical K_2O vs. SiO_2 relations are seen in amphibolite facies Scourian tonalites to granodiorites from Gruinard Bay and Torridon (Fig. 22) suggesting that both trends are a function of magmatic rather than metamorphic processes.

Additional evidence for the non depletion of K during granulite facies metamorphism is the greater K_2O content of granulite facies trondhjemites from Scourie (mean K_2O 0.94 wt %) compared with their retrogressed amphibolite facies equivalent from the same area (mean K_2O

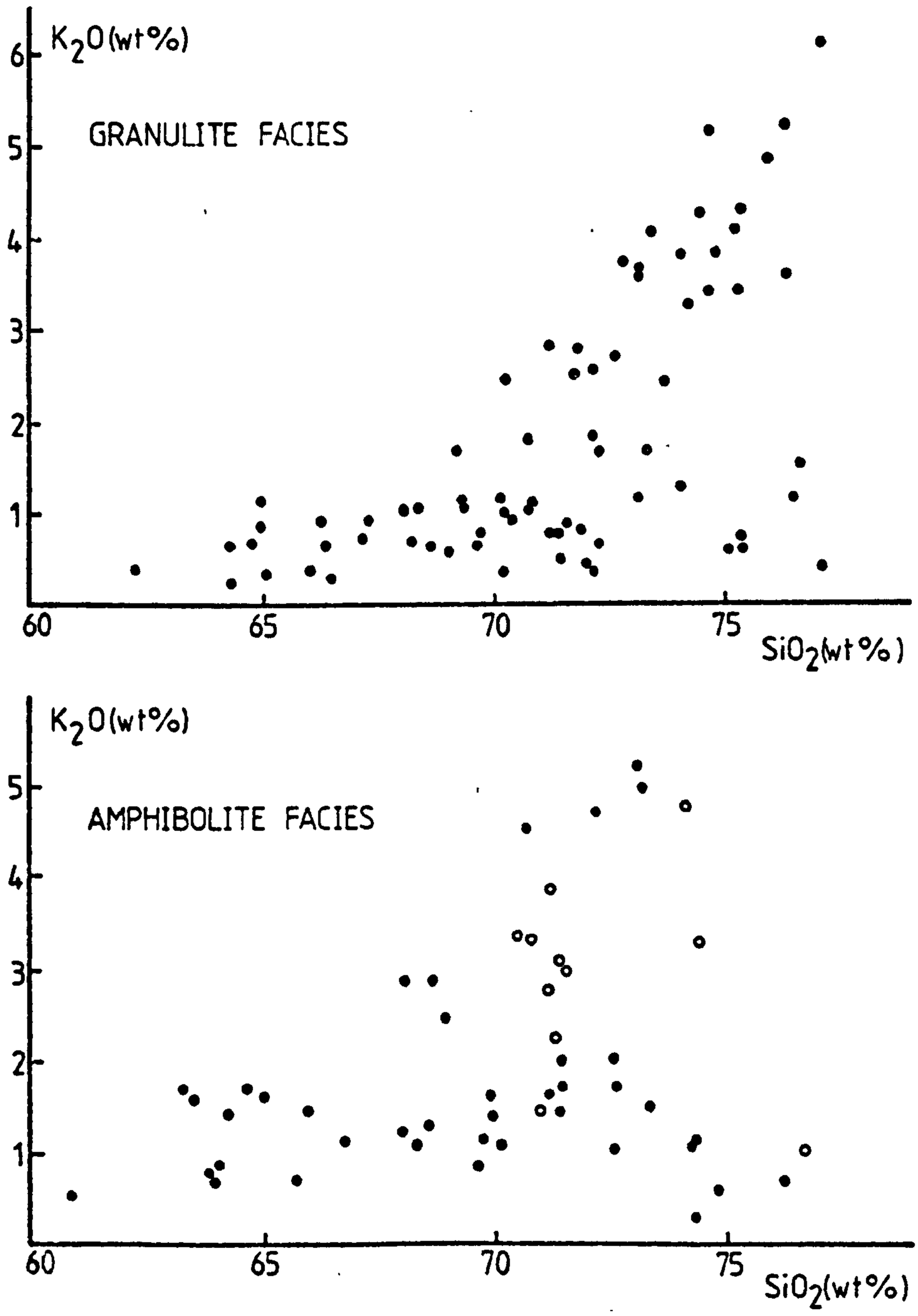

Fig. 22. Plot of K_2O vs. SiO_2 for granulite facies tonalites to granites from Scourie and amphibolite facies tonalites to granites from Gruinard Bay (filled circles) and Torridon (open circles).

0.64 wt %) indicating that any depletion in K in the Scourie are occurred during retrogression rather than granulite facies metamorphism.

2. Depletion in Rb relative to K. Intrusive granite-granodiorite sheets predate the granulite facies metamorphism; the trace elements Sr, Rb and Ba show smooth trends with increasing Or/Ab, which are

consistent with the previously proposed fractional crystallisation of plagioclase from trondhjemite. It is unlikely that these trends would survive granulite facies depletion. Potassium in these sheets is contained in plagioclase mesoperthites, whose textural relationships are entirely consistent with an origin by exsolution from an original homogeneous alkali feldspar, and thus it is unlikely that potassium has been added to the sheets.

Furthermore Rb increases with SiO_2 in the granodiorite-granite suite (Fig. 13) suggesting that it is not depleted in these rocks.

K/Rb ratios in the granodiorite-granite suite are lower than in gabbros to trondhjemites and do not show the same scatter, implying that they are controlled by a different process.

Evidence from the granite-granodiorite sheets in the Scourie area therefore suggests that they have an igneous chemistry which has not reequilibrated during granulite facies metamorphism. If this is true for rocks of granitic to granodioritic composition, which were metamorphosed to granulite facies it should be true for trondhjemites and tonalites because they were also metamorphosed to granulite grade.

Additional evidence for the non-depletion of high pressure granulites comes from two examples of granulite sensu-stricto; these are from the Granulitgebirge, Saxony and from Tovqussap, W. Greenland (see Appendix 1). Both examples contain the mineral assemblage quartz - plagioclase - alkali feldspar - garnet - aluminosilicate which can be used to fix both pressure and temperature of equilibration using the equations of Ghent (1976) for the high pressure breakdown of plagioclase and the two-feldspar thermometer of Powell and Powell (1977a). The Saxony granulite ss. equilibrated at high pressures (10 $\pm$ 1.5 kb and 760°C $\pm$ 90°C) and has K/Rb ratios in the range 117 - 176 which are lower than Shaw's

(1968) main trend. Similar high pressure granulites from Poland show consistently low K/Rb ratios in the range 250 - 500 irrespective of rock type (Tarney and Windley, 1977). Granulite ss. from Tovqussap, W. Greenland equilibrated in the range 6.4 ± 0.8 kb and 675°C ± 50°C and has K/Rb ratios in the range 280 - 550. It is interesting to note that the high pressure granulites from Saxony have higher K/Rb ratios than the lower pressure granulites from W. Greenland supporting the idea that K/Rb ratio and associated LIL depletion is not simply a function of high pressure granulite facies metamorphism.

Discussion

The low abundances of LIL in the granulite facies Scourie tonalites are regarded by several workers (e.g. Sheraton et al., 1973; Tarney, 1976) to represent depletion during granulite facies metamorphism. Further confirmation of this view comes from this attempt to model the derivation of the tonalites by the partial melting or fractional crystallisation of a basaltic source; and yet there is evidence from granite-granodiorite sheets, which have also been metamorphosed to granulite facies that they retained their original igneous chemistry with respect to K and Rb, and this has not been disturbed by granulite facies metamorphism. This apparent paradox can be resolved by considering the mineral phases in which K and Rb reside.

Evidence was presented above to suggest that the Scourie tonalites were derived from a wet tonalitic melt by fractional crystallisation of hornblende. The present mineral assemblages are extremely dry (two pyroxenes and minor amphibole) suggesting that a large amount of water has been lost during granulite facies metamorphism. The transport of this water provides a means of

removing LIL and the recrystallisation of hornblende to pyroxene constitutes a reason for the expulsion of elements such as Rb. Granitic sheets on the other hand contain alkali feldspar which holds most of the K and Rb; this may be igneous in origin and there is evidence to suggest that these rocks crystallised from a relatively dry melt at high temperature (see Chapter 5) and did not recrystallise during granulite facies metamorphism.

Depletion in granulites therefore is not simply a function of high pressure metamorphism, as originally suggested by Lambert and Heier (1968) and Heier (1973) but depends upon the original composition of the rocks and also their mineralogy. The principal depletion in the Scourie area is of Rb with respect to K and this is primarily controlled by the mineralogy of the rocks, as outlined above. This is consistent with the wide range of K/Rb ratios in tonalites and trondhjemites and the lack of a decrease in the K/Rb ratio from gabbro to trondhjemite, a feature which is normally observed in a fractionating igneous system. There is no necessity to invoke K depletion for these rocks and this was never proposed by Heier (1973) and Lambert and Heier (1968) in their earlier studies of granulite facies depletion; this means that the two trends on a K_2O vs, SiO_2 diagram are original and represent a trondhjemite trend and a granodiorite-granite trend and does not imply depletion of K as suggested by Sheraton et al. (1973) and Tarney (1976).

Mineralogical control of depletion is also consistent with the low K/Rb ratio in the mesoperthite-bearing granulites ss. from Saxony and W. Greenland (see Appendix 1), but does not fully explain the low K/Rb ratios irrespective of rock type in the Polish granulites of Tarney and Windley (1977). It is possible, therefore, that, as suggested by the last two authors the nature of the fluid phase is also an important factor in controlling depletion in granulite facies rocks.

9. CONCLUSIONS

1. A plutonic igneous origin is favoured for the tonalitic gneiss, trondhjemite granite and granodiorite at Scourie.

2. The smooth continuous trends on chemical variation diagrams suggest that the petrological evolution of these rocks was dominated by fractional crystallisation. A scheme is proposed whereby tonalitic melt is parental to trondhjemites and granites. Trondhjemite is derived from tonalite by the fractional crystallisation of hornblende and plagioclase. Granite and granodiorite represent liquids which evolved along the quartz-feldspar cotectic surface due to the fractional crystallisation of plagioclase from a trondhjemite liquid. Some trondhjemites are quartz plagioclase residues from which a granitic liquid has been removed.

3. Tonalites are probably derived from a basaltic source by either fractional crystallisation or partial melting with hornblende or garnet in the residue.

4. Associated gabbros are not directly related to the tonalites and do not represent crystal residues from fractional crystallisation.

5. Depletion of LIL during granulite facies metamorphism was controlled by the mineralogy of the rocks; K-feldspar bearing granites and granodiorites are not depleted with Rb with respect to K because they crystallised from a dry, high temperature melt and did not recrystallise during granulite facies metamorphism; tonalites and trondhjemites, however, were depleted and this is primarily a function of the loss of H_2O during the crystallisation of pyroxene from hornblende during granulite facies metamorphism.. K concentrations are original and reflect two magmatic trends, a trondhjemite trend and a granitic trend. Depletion in granulite facies terrains is therefore a complex function of (i) the magmatic processes operating (ii) high pressure metamorphism (iii) the mineralogy of the

rocks (iv) the composition of the associated fluid phase.

10. A REINTERPRETATION OF THE ISOTOPE DATA OF CHAPMAN (1978) AND THE AGE OF THE SCOURIE ACID SHEETS

Chapman (1978) carried out Rb/Sr and preliminary Pb/Pb isotope studies on samples of trondhjemite and granite from the Scourie Badcall area, some of which have been used in this study. Her results are as follows:

	Locality	no. of samples	age (Ma.)	$^{87}Sr/^{86}Sr$ init. ratio
1.	Amphibolite facies trondhjemite sheets, Geod'nan Sgadan	9	2810 ± 300	0.7072 ± 2
2.	Trondhjemite/ granite sheet, N. side Scourie Bay	3	2535 ± 115	0.7022 ± 2
3.	Granite sheet, Loch an Daimh Mor	4	2500 ± 90	0.7011 ± 12
4.	Granite/trondhem-ite sheet, Scourie more Camas an lochain	3	2625 ± 140	0.7044 ± 4
5.	Granite sheet, Scourie more	6	2510 ± 425	0.7024 ± 13
6.	Data points from 2, 3, 5 with initial ratios within error	13	2420 ± 30	0.7023 ± 2

These results were interpreted as showing two different ages of emplacement for the trondhjemite and granite sheets and that they were derived by partial melting of earlier Lewisian crust with a slightly lower $^{87}Sr/^{86}Sr$ initial ratio (0.7019). Preliminary

Pb/Pb data for the granite sheets give a best fit regression line of 2810 $\pm^{240}_{310}$ Ma.

Field evidence suggests that the acid sheets are all of the same age and that they predate the Scourian granulite facies metamorphism generally agreed to be ca. 2700 Ma. (Chapman and Moorbath,1977). Major element and trace element data indicate that the granite sheets were derived by fractional crystallisation from a trondhjemite parental liquid. The elements K, Rb, Ba, Sr show enrichment patterns consistent with plagioclase fractionation. Rb and Ba show some scatter about a mean trend (Fig. 19) implying that they have moved since the igneous fractionation. K does not appear to have moved and so the redistribution of Rb and Ba is interpreted as a local redistribution of the elements, possibly aided by a fluid phase during retrogression rather than large scale removal during granulite facies metamorphism (see discussion above).

Evidence from the mineral chemistry of composite ilmenite-magnetite grains indicates that a fluid phase was introduced into the rock during cooling at about 500 - 600°C (see Chapter 5). Mesoperthitic alkali feldspars also show equilibration temperatures between host and lamellae in this range. These feldspars contain very broad (30μm) orthoclase lamellae in an albite-rich host, whose growth took place by exsolution aided by the presence of a fluid phase. Since Rb and Ba (and probably Pb) occur predominantly in alkali feldspar, it is probable that Ba and Rb moved during this recrystallisation.

It is proposed, therefore, that the mean Rb/Sr age of 2420 ± 30 Ma. for the granite sheets of the Scourie-Badcall area dates the closure of the system to the redistribution of Rb at ca. 500 - 600°C; this is also the time at which alkali feldspar (the main host of Rb) stopped exchanging Rb. Preliminary Pb/Pb data on granite sheets and Rb/Sr data on trondhjemite sheets (with no alkali feldspar)

yield an age of emplacement or metamorphism of ca. 2810 ± 300 Ma. This is consistent with their intrusion prior to the granulite facies metamorphism and the intial ratio for the trondhjemite (0.7027 ± 2) is in keeping with a mantle origin ca. 2900 Ma. ago.

Table 2. Average analyses of tonalite and trondhjemites from Scourie area.

	Av. Tonalite		Av. Trondhjemite		Av. Trondhjemite (amph facies)		Av. Trondhjemite (gran facies)	
	mean	s.d.	mean	s.d.	mean	s.d.	mean	s.d.
SiO_2	62·32	6·1	71·38	2·8	70·62	1·8	73·54	3·1
TiO_2	·61	·3	·22	·1	·29	·1	·14	·1
Al_2O_3	16·09	·8	15·25	·9	15·58	·6	14·31	1·1
Fe_2O_3	5·89	2·7	2·15	·8	2·55	·6	1·75	·6
MnO	·09	·1	·03	·0	·04	·0	·02	·0
MgO	2.80	1·9	·93	·3	1·05	·3	·87	·3
CaO	6·68	2·3	3·78	·6	4·20	·4	3·48	·6
Na_2O	4·38	·5	4·87	·6	4·66	·3	4·39	·6
K_2O	·69	·4	·85	·3	·64	·2	·94	·4
P_2O_5	·19	·2	·06	·1	·10	·1	·03	·0
TOTAL	99·74		99·52		99·73		99·47	
Y	10·5	8·0	1·4	1·8	2·1	1·9	·5	1·2
Sr	436·	101·	480·	114·	444·	119·	448·	149·
Rb	3·0	3·3	6·0	4·6	4·5	3·0	7·8	7·7
Th	·9	·9	·9	1·3	1·1	1·1	1·2	2·5
Pb	7·6	1·7	7·4	2·6	6·9	1·8	8·8	3·8
Ga	22·4	1·8	20·5	3·9	20·4	1·4	17·5	5·7
Zn	63·0	26·0	22·5	12·9	27·0	10·4	14·6	8·8
Ba	365·	182·	518·	315·	337·5	152·7	393·7	123·6
Ni	46·3	39·6	7·9	7·7	6·6	5·3	12·6	14·7
Cr+V	83·8	73·3	11·4	8·6	11·3	6·2	12·2	12·5
Ce	38·6	13·5	28·2	22·2	31·4	12·2	17·8	8·7
La	19·4	6·8	15·6	9·6	16·4	7·0	8·2	5·1
Zr	158·	64·	117·	68·	147·2	64·	103·8	85·1
Nb	4·2	2·2	1·8	2·0	3·1	1·7	1·8	1·7
K/Rb	1903·		1176·		1180·		1000·	
No. Anals.	19		33		16		8	

s.d. = standard deviation

		SiO2	TiO2	Al2O3	FeO	MnO	MgO	CaO	Na2O	K2O	P2O5	TOTAL
GABBRO	HR4	45.21	.37	5.14	12.4[illegible]	.24	27.[illegible]2	7.06	.75	.12	.01	100.[illegible]6
GABBRO	HR12	46.14	.56	6.6[illegible]	13.68	.27	17.42	9.47	.91	.42	.04	95.59
GABBRO	HR5	47.3[illegible]	.[illegible]4	13.42	13.29	.25	7.9[illegible]	13.05	1.9[illegible]	.16	.06	[illegible]8.55
GABBRO	HR14	49.35	1.[illegible]3	15.35	11.63	.17	9.17	[illegible].9[illegible]	2.45	.44	.[illegible]7	99.56
GABBRO	HR[illegible]1	5[illegible].37	.51	15.[illegible]4	[illegible].46	.2[illegible]	7.77	11.31	2.52	.6[illegible]	.02	99.7[illegible]
GABBRO	HR55	5[illegible].46	2.[illegible]2	13.13	12.32	.22	6.79	9.24	3.15	.68	.37	99.94
GABBRO	HR53	5[illegible].7[illegible]	2.[illegible]9	15.56	[illegible].0[illegible]	.15	5.[illegible]9	7.[illegible]	4.13	1.[illegible]7	.34	99.[illegible]2
GABBRO	HR39	47.13	.33	14.67	9.41	.16	12.72	9.23	2.26	.84	.[illegible]1	97.37
GABBRO	HR54	49.5[illegible]	.76	16.73	9.6[illegible]	.16	7.[illegible]2	1[illegible].53	3.13	.71	.[illegible]6	98.5[illegible]
GABBRO	HR62	47.[illegible]6	.65	15.66	[illegible].[illegible]4	.2[illegible]	7.55	13.60	2.[illegible]2	1.37	.[illegible]5	98.[illegible]9
GABBRO	HR43	47.55	.49	6.1[illegible]	1[illegible].46	.14	22.[illegible]0	9.74	1.[illegible]0	.32	.[illegible]1	99.42
GABBRO	1[illegible]6	5[illegible].45	2.[illegible]4	15.[illegible]1	1[illegible].[illegible]6	.17	5.46	7.[illegible]3	3.77	.74	.34	99.7[illegible]
GABBRO	1[illegible]7	5[illegible].1[illegible]	.37	16.62	[illegible].7[illegible]	.16	7.[illegible]7	11.5[illegible]	2.[illegible]6	1.30	.[illegible]5	99.[illegible]2
GABBRO	1[illegible]8	5[illegible].63	1.19	16.42	10.32	.2[illegible]	6.36	10.30	3.27	.52	.14	99.45
GABBRO	1[illegible]9	5[illegible].33	1.[illegible]8	15.57	11.57	.24	5.23	1[illegible].61	3.62	.44	.2[illegible]	99.[illegible]9
GABBRO	2[illegible]4	52.[illegible]3	1.61	14.55	[illegible].[illegible]9	.44	4.[illegible]4	[illegible].91	3.[illegible]9	.31	.17	1[illegible].16
GABBRO	237	49.[illegible]7	1.[illegible]2	14.[illegible]6	[illegible].1[illegible]	[illegible].0[illegible]	7.7[illegible]	12.26	2.5[illegible]	.24	.[illegible]8	99.[illegible]
GABBRO	2[illegible]6	49.76	.35	15.12	7.76	[illegible].0[illegible]	9.[illegible]7	13.[illegible]9	2.24	.42	.03	99.34
GABBRO	23[illegible]	47.73	.[illegible]4	[illegible]3.55	11.[illegible]4	[illegible].0[illegible]	1[illegible].49	1[illegible].5[illegible]	1.97	.75	.[illegible]4	97.42
GABBRO	24[illegible]	[illegible]8.4[illegible]	.[illegible].	13.22	[illegible].[illegible]3	[illegible].0[illegible]	1[illegible].4[illegible]	13.[illegible]7	1.[illegible]6	1.14	.[illegible]2	97.[illegible]4
GABBRO	24[illegible]	44.[illegible]3	.[illegible]7	[illegible]7.[illegible]2	[illegible].[illegible]9	[illegible].0[illegible]	13.[illegible]4	[illegible].41	1.[illegible]9	2.33	.[illegible]2	97.[illegible]1
GABBRO	24[illegible]	44.54	.[illegible]0	[illegible]7.73	[illegible].[illegible]0	[illegible].0[illegible]	13.[illegible]2	[illegible].[illegible]1	1.[illegible]6	2.56	.01	98.55
GABBRO	25[illegible]	51.[illegible]7	1.[illegible]6	13.91	[illegible]2.52	[illegible].0[illegible]	5.19	1[illegible].37	3.26	.52	.15	99.57
AMPHIBOLITE	24[illegible]	[illegible].[illegible]3	.[illegible]3	[illegible]5.[illegible]5	[illegible].46	[illegible].0[illegible]	5.11	7.41	4.[illegible]	.49	.14	99.[illegible]0
AMPHIBOLITE	244	50.14	1.[illegible]0	14.79	[illegible].12	[illegible].0[illegible]	5.[illegible]8	[illegible].1[illegible]	3.[illegible]	.41	.18	99.[illegible]2
U.MAFIC DYKE	42A	[illegible]9.[illegible]7	.51	4.12	[illegible]3.10	.3[illegible]	[illegible]2.[illegible]2	16.5[illegible]	.[illegible]8	.[illegible]5	1.37	9[illegible].7[illegible]
U.MAFIC DYKE	42B	[illegible]9.[illegible]1	.51	4.41	13.[illegible]9	.2[illegible]	11.[illegible]4	16.45	.77	.[illegible]7	1.[illegible]6	9[illegible].23

TABLE 3a (i) Major element analyses for basic rocks from the Scourie area.

		Y	SR	RB	TH	PB	W	GA	ZN	BA	NI	CR+V	CE	LA	ZR	NB
GABBRO	HR4	6.8	37	6	4	4	0	8	126	36	1353	3055	0	8	19	2
GABBRO	HR12	13.2	36	4	3	2	0	11	138	56	742	2860	20	18	32	5
GABBRO	HR5	24.0	70	4	0	1	0	15	122	19	95	275	12	7	24	3
GABBRO	HR14	13.2	113	2	2	5	0	19	131	98	64	305	12	5	59	7
GABBRO	HR41	10.7	155	3	0	6	0	18	67	122	58	6	8	5	24	4
GABBRO	HR55	30.9	342	1	0	9	0	23	168	394	106	150	67	33	105	16
GABBRO	HR63	26.1	778	5	0	13	0	24	134	740	79	132	69	46	128	16
GABBRO	HR34	7.5	194	11	0	6	0	17	103	192	345	310	25	10	179	3
GABBRO	HR40	16.3	304	7	0	2	0	20	100	130	99	361	26	12	57	5
GABBRO	HR62	16.6	566	10	0	3	0	18	201	359	166	390	19	12	46	3
GABBRO	HR43	11.5	57	2	0	5	0	11	87	103	1153	3110	2	9	44	2
GABBRO	196	29.0	308	3	0	6	0	23	139	357	51	109	67	40	350	17
GABBRO	197	7.8	313	2	0	3	0	16	69	680	36	42	15	6	34	1
GABBRO	198	21.0	220	2	0	7	0	25	130	135	74	241	34	19	92	7
GABBRO	199	30.0	217	1	0	7	0	23	127	161	65	144	32	26	102	8
GABBRO	200	35.0	251	1	0	5	0	20	99	148	78	76	24	23	91	7
GABBRO	237	19.2	205	1	0	4	0	15	119	61	97	110	21	8	42	5
GABBRO	238	9.3	154	2	0	4	0	16	116	63	100	60	19	8	25	7
GABBRO	239	16.4	175	19	2	4	0	16	116	125	390	432	31	4	63	0
GABBRO	240	8.2	154	10	0	4	0	17	116	212	84	2	17	8	41	0
GABBRO	241	6.2	108	35	2	6	0	14	114	444	485	464	14	8	22	0
GABBRO	242	3.1	93	34	0	5	0	13	113	593	440	459	3	8	4	0
GABBRO	255	39.1	159	4	0	7	0	22	122	175	96	120	36	4	96	6
AMPHIBOLITE	243	28.3	396	5	0	12	0	25	125	202	90	187	42	12	107	15
AMPHIBOLITE	244	23.9	466	2	0	5	0	21	121	172	78	152	46	10	149	11
U.MAFIC DYKE	42A	94.5	30	0	1	6	0	13	113	0	250	220	136	59	140	2
U.MAFIC DYKE	42B	62.4	34	1	3	4	0	15	115	3	282	211	116	48	139	2

TABLE 3a (ii) Trace element analyses for basic rocks from the Scourie area.

			SIO2	TIO2	AL2O3	FEO	MNO	MGO	CAO	NA2O	K2O	P2O5	TOTAL
TONALITE		23	57.13	.65	16.58	7.03	.14	3.32	7.62	4.62	1.14	.16	98.35
TONALITE		25	60.23	.35	15.67	2.37	.04	1.56	4.31	4.22	1.05	.12	99.47
TONALITE		26	51.68	.83	16.16	9.61	.17	6.49	11.25	3.79	.49	.08	100.65
TONALITE		71	51.7_	1.13	16.48	8.55	.16	5.11	11.05	4.12	.68	.09	99.77
TONALITE		72	66.28	.50	16.52	3.91	.07	1.66	5.56	4.29	.91	.23	99.53
TONALITE		73	65.33	.57	16.62	4.55	.08	1.88	5.71	4.34	.85	.21	99.76
TONALITE		74	72.36	.04	16.30	.93	.02	.09	3.36	4.65	1.68	.02	100.36
TONALITE		80	64.33	.65	15.66	4.31	.07	2.28	6.36	4.37	.69	.14	98.33
TONALITE		84A	62.33	.53	14.47	5.96	.11	3.33	7.42	3.84	.37	.19	98.65
TONALITE		84B	66.47	.51	15.83	3.88	.06	1.53	6.00	4.38	.27	.16	99.48
TONALITE		85	49.34	1.54	15.71	10.42	.18	6.92	10.68	3.14	.75	.37	99.04
TONALITE		183	57.07	.86	14.83	8.10	.13	5.64	8.36	3.73	.46	.14	99.62
TONALITE		184	66.07	.48	16.90	3.57	.05	1.61	5.45	4.61	.35	.16	99.79
TONALITE		190	64.27	.54	17.32	3.77	.06	1.39	5.73	5.15	.26	.16	98.42
TONALITE		191	65.07	.49	17.12	3.56	.06	1.24	5.41	4.96	.33	.10	98.34
TONALITE		192	64.71	.70	14.87	5.64	.09	1.75	4.69	4.63	.73	.15	98.29
TONALITE		193	67.32	.40	15.23	3.73	.06	1.52	4.13	4.85	.97	.16	98.28
TONALITE		265	66.41	.63	16.41	3.44	0.00	1.48	5.28	4.79	.65	.11	99.56
TONALITE		266	57.35	.68	16.69	6.67	0.00	4.55	8.28	4.64	.76	.15	100.46
TRONDHJEMITE	GF	175	76.85	.03	13.30	1.42	.03	.04	3.45	3.92	.61	.01	99.17
TRONDHJEMITE	GF	176	77.88	.04	12.25	1.71	.03	1.44	3.59	3.51	.41	0.00	100.06
TRONDHJEMITE	GF	177	71.52	.03	14.25	1.28	.02	.08	4.05	4.18	.51	0.00	96.62
TRONDHJEMITE	GF	179	75.41	.03	13.86	1.12	.01	.76	3.54	4.34	.77	.01	99.86
TRONDHJEMITE	GF	200	60.52	.05	21.17	1.09	.02	.64	5.13	6.86	1.75	.09	97.32
TRONDHJEMITE	GF	215	69.25	.36	15.28	2.54	0.00	1.17	3.82	4.35	1.68	.07	98.26
TRONDHJEMITE	GF	216	69.39	.31	15.63	2.22	0.00	.93	4.65	4.66	1.10	.09	98.47
TRONDHJEMITE	GF	13	74.13	.28	15.03	1.48	.02	.65	2.97	4.83	1.28	.01	100.64
TRONDHJEMITE	GF	20	76.43	.11	14.45	.85	.02	.38	2.34	5.43	1.17	.02	101.25
TRONDHJEMITE	AF	46	69.76	.21	14.88	1.98	.03	.95	4.30	4.79	.66	.06	97.81
TRONDHJEMITE	AF	47	71.34	.19	15.26	1.76	.03	.68	3.58	5.20	.78	.03	99.05
TRONDHJEMITE	AF	48	71.95	.08	16.08	1.68	.04	1.14	3.81	4.77	.79	.05	100.59
TRONDHJEMITE	AF	49	75.41	.21	14.69	1.19	.03	.62	3.57	4.76	.64	.05	101.17
TRONDHJEMITE	AF	50	70.99	.35	15.83	2.65	.04	1.11	4.38	4.50	1.16	.08	100.19
TRONDHJEMITE	AF	52	72.36	.41	15.19	2.05	.03	.82	3.69	5.21	.64	.07	100.47
TRONDHJEMITE	AF	53	72.02	.26	14.56	2.39	.03	.91	4.18	4.39	.43	.06	99.18
TRONDHJEMITE	AF	56	69.80	.43	15.56	3.06	.06	1.48	4.30	4.61	.77	.17	100.24
TRONDHJEMITE	AF	57	70.33	.22	15.80	2.31	.05	1.16	4.39	4.79	.96	.36	100.42
TRONDHJEMITE	AF	58	70.25	.36	16.11	2.72	.04	1.19	4.67	4.75	.34	.10	100.53
TRONDHJEMITE	AF	59	69.14	.41	15.75	3.13	.05	1.52	4.54	4.68	.58	.12	99.69
TRONDHJEMITE	AF	86	72.53	.31	15.14	1.98	.03	.69	4.28	4.54	.36	.04	99.51
TRONDHJEMITE	AF	172	64.95	.26	16.23	3.71	.06	1.57	4.07	5.02	1.13	.14	97.44
TRONDHJEMITE	AF	180	76.66	.03	13.59	.54	.01	.50	2.48	4.66	1.53	0.00	99.54
TRONDHJEMITE	AF	195	68.72	.22	15.99	1.92	0.00	.71	4.20	5.55	.65	.07	98.03
TRONDHJEMITE	AF	194	68.28	.15	16.63	1.67	0.00	.61	4.11	6.09	.69	.06	98.69
TRONDHJEMITE	AF	205	70.84	.29	15.13	2.22	.03	1.06	3.92	4.58	1.18	.05	99.26

TABLE 3b (i) Major element analyses for tonalites and trondhjemites from the Scourie area.
AF amphibolite facies trondhjemite; GF granulite facies trondhjemite.

			Y	SR	RB	TH	PB	W	GA	ZN	BA	NI	CR+V	CE	LA	ZR	NB
TONALITE		23	17.3	442	6	[illegible]	11	[illegible]	24	99	525	69	172	49	26	130	4
TONALITE		25	3.6	4[illegible]9	4	2	6	[illegible]	22	39	547	13	26	34	19	169	3
TONALITE		26	22.1	1[illegible]30	1	2	5	[illegible]	16	99	153	95	304	21	16	56	3
TONALITE		70	24.6	432	1	2	[illegible]	[illegible]	24	77	214	151	131	72	33	57	5
TONALITE		72	[illegible].0	576	5	1	[illegible]	[illegible]	23	[illegible]4	485	42	[illegible]6	57	33	176	5
TONALITE		73	6.3	61[illegible]	2	[illegible]	8	[illegible]	26	71	626	24	83	37	21	206	5
TONALITE		74	[illegible]	456	11	1	9	[illegible]	22	3	482	5	13	[illegible]3	14	31	1
TONALITE		6[illegible]	6.6	438	2	[illegible]	[illegible]	[illegible]	21	49	3[illegible]3	36	[illegible]9	25	15	138	4
TONALITE		84A	14.5	415	[illegible]	2	8	[illegible]	21	77	1[illegible]8	55	153	45	22	164	4
TONALITE		84B	6.[illegible]	5[illegible]5	[illegible]	[illegible]	6	[illegible]	23	50	1[illegible]0	29	37	34	16	183	5
TONALITE		85	25.6	268	3	2	8	[illegible]	26	126	229	79	122	56	30	71	8
TONALITE		1[illegible]	17.[illegible]	365	1	[illegible]	7	[illegible]	23	[illegible]6	167	82	141	40	17	173	4
TONALITE		189	4.6	361	1	2	5	[illegible]	22	43	221	10	16	22	9	242	4
TONALITE		19[illegible]	[illegible].4	385	[illegible]	[illegible]	5	1	21	47	143	10	10	26	10	239	5
TONALITE		191	3.4	45[illegible]	[illegible]	[illegible]	8	1	22	47	284	6	19	31	13	26[illegible]	6
TONALITE		192	11.3	3[illegible]5	5	[illegible]	6	[illegible]	22	65	385	47	42	35	18	179	9
TONALITE		193	2.[illegible]	5[illegible]6	11	1	8	[illegible]	21	46	712	31	73	37	15	191	4
TONALITE		265	3.6	5[illegible]7	1	1	10	[illegible]	21	39	413	5	6	36	22	183	0
TONALITE		266	16.3	570	4	2	8	[illegible]	24	76	648	92	118	55	19	136	0
TRONDHJEMITE	GF	175	3.3	415	4	[illegible]	13	2	13	9	296	38	10	23	8	271	1
TRONDHJEMITE	GF	176	[illegible]	3[illegible]8	[illegible]	[illegible]	4	[illegible]	12	17	3[illegible]4	26	37	7	4	34	0
TRONDHJEMITE	GF	177	[illegible]	440	1	[illegible]	5	[illegible]	13	15	37[illegible]	15	2[illegible]	7	4	165	0
TRONDHJEMITE	GF	179	[illegible]	5[illegible]3	3	[illegible]	6	[illegible]	15	16	428	7	[illegible]	17	4	57	1
TRONDHJEMITE	GF	209	[illegible].4	742	12	[illegible]	14	[illegible]	28	1[illegible]	569	[illegible]	7	16	[illegible]	56	2
TRONDHJEMITE	GF	215	[illegible].1	45[illegible]	18	1	[illegible]	[illegible]	21	29	857	[illegible]	2[illegible]	46	31	192	[illegible]
TRONDHJEMITE	GF	216	[illegible].8	542	4	2	5	[illegible]	22	33	69[illegible]	4	2	26	16	[illegible]3	[illegible]
TRONDHJEMITE	GF	18	[illegible]	4[illegible]6	21	7	1[illegible]	[illegible]	21	31	53[illegible]	1	4	29	17	59	5
TRONDHJEMITE	GF	20	[illegible]	2[illegible]1	13	1	9	[illegible]	19	3	251	2	1	26	12	[illegible]5	2
TRONDHJEMITE	AF	46	[illegible]	3[illegible]3	3	1	6	1	13	21	45[illegible]	3	11	22	10	34	1
TRONDHJEMITE	AF	47	[illegible]	42[illegible]	5	2	5	2	19	17	412	7	10	19	9	32	3
TRONDHJEMITE	AF	48	1.[illegible]	437	5	[illegible]	7	[illegible]	21	25	492	4	10	29	15	172	[illegible]
TRONDHJEMITE	AF	49	1.2	364	5	2	[illegible]	[illegible]	19	14	336	2	11	21	6	116	2
TRONDHJEMITE	AF	50	2.7	4[illegible]3	11	1	9	[illegible]	21	31	413	5	13	41	23	133	4
TRONDHJEMITE	AF	52	[illegible].5	431	5	3	[illegible]	[illegible]	19	18	246	5	5	34	20	281	6
TRONDHJEMITE	AF	53	6.2	2[illegible]4	2	[illegible]	6	[illegible]	19	24	113	25	18	17	[illegible]	19[illegible]	2
TRONDHJEMITE	AF	56	4.3	43[illegible]	3	3	10	[illegible]	23	60	399	3	4	48	24	20[illegible]	7
TRONDHJEMITE	AF	57	[illegible].2	453	5	2	[illegible]	[illegible]	23	33	49[illegible]	9	27	61	27	105	3
TRONDHJEMITE	AF	58	1.[illegible]	39[illegible]	1	[illegible]	5	[illegible]	22	32	225	[illegible]	2	37	23	191	3
TRONDHJEMITE	AF	59	2.[illegible]	453	4	3	6	[illegible]	19	33	215	[illegible]	13	34	19	162	4
TRONDHJEMITE	AF	66	3.3	342	2	[illegible]	4	[illegible]	21	24	108	4	6	9	1	185	3
TRONDHJEMITE	AF	172	[illegible].2	545	7	[illegible]	11	[illegible]	22	59	561	13	29	[illegible]0	43	184	6
TRONDHJEMITE	AF	180	[illegible]	530	6	[illegible]	[illegible]	[illegible]	11	5	15[illegible]6	6	7	11	4	19	1
TRONDHJEMITE	AF	195	[illegible].3	655	7	[illegible]	[illegible]	2	20	20	[illegible]58	3	16	34	16	91	3
TRONDHJEMITE	AF	194	0.7	744	[illegible]	[illegible]	[illegible]	[illegible]	21	20	395	3	16	3[illegible]	15	99	3
TRONDHJEMITE	AF	205	1.2	5[illegible]4	4	[illegible]	[illegible]	[illegible]	22	32	777	6	26	22	9	177	1

TABLE 3b (ii) Trace element analyses for tonalites and trondhjemites from the Scourie area.
AF amphibolite facies trondhjemite; GF granulite facies trondhjemite.

		SiO2	TiO2	Al2O3	FeO	MnO	MgO	CaO	Na2O	K2O	P2O5	TOTAL
TRONDHJEMITE AF	208	73.39	.05	15.76	.80	.01	.29	2.78	4.99	1.67	.01	99.75
TRONDHJEMITE AF	272	72.63	.12	16.03	1.12	0.00	.71	2.74	5.30	1.54	.01	100.37
TRONDHJEMITE AF	274	71.21	.11	16.15	.98	0.00	.51	3.42	6.05	.74	.04	99.21
TRONDHJEMITE AF	264	70.87	.22	15.93	1.25	0.00	.51	3.40	5.56	1.11	.02	98.87
TRONDHJEMITE AF	251	68.42	.26	16.02	2.16	0.00	.52	3.96	5.22	1.06	.07	98.09
TRONDHJEMITE AF	249	73.15	.07	15.05	1.56	0.00	.66	3.22	4.73	1.20	.04	99.80
TRONDHJEMITE AF	253	71.33	.26	15.43	2.04	0.00	.83	3.65	5.13	.97	.02	98.66
TRONDHJEMITE AF	254	67.28	.26	14.87	3.39	0.00	1.83	4.89	4.73	.72	.08	97.96
TRONDHJEMITE AF	256	69.42	.30	16.23	2.13	0.00	.71	3.61	5.50	1.10	.03	99.16
TRONDHJEMITE AF	257	71.62	.21	15.85	1.51	0.00	.58	3.39	5.46	.87	.05	99.54
GRANITE	3	73.10	.10	15.79	1.16	.02	.57	1.50	4.58	3.66	.04	100.62
GRANITE	6	75.48	.05	15.14	.53	.01	.32	1.45	4.11	4.32	.01	101.31
GRANITE	11	74.53	.09	15.39	.63	.01	.47	1.39	4.30	4.26	.01	101.30
GRANITE	13	73.49	.11	15.22	.94	.01	.35	1.53	4.37	4.05	.01	100.08
GRANITE	19	73.[illegible]	.13	15.10	1.25	.02	.53	1.61	4.50	3.57	.02	99.88
GRANITE	67	72.10	.27	15.52	1.75	.04	.73	2.67	4.76	2.55	.03	100.46
GRANITE	68	71.91	.21	15.24	1.77	.03	.97	2.23	4.47	2.82	.06	99.95
GRANITE	69	71.79	.18	15.56	1.61	.03	.70	2.69	4.62	2.50	.06	99.74
GRANITE	81	73.77	.13	15.69	1.17	.02	.66	1.99	4.94	2.88	.02	101.23
GRANITE	82	74.86	.23	15.48	1.15	.03	.90	2.96	4.58	2.14	.05	98.39
GRANITE	83	72.73	.12	15.46	1.24	.02	.56	2.44	4.61	2.76	.05	100.01
GRANITE	87	75.[illegible]	.01	15.02	.35	.03	.47	1.44	3.76	4.67	.01	101.54
GRANITE	88	74.76	.11	14.70	.43	.05	.16	.93	4.25	5.21	.01	100.48
GRANITE	89	76.27	.01	15.38	.41	.03	.18	1.26	3.68	5.23	.01	102.36
GRANITE	173	71.34	.21	16.36	1.68	.03	.56	2.64	4.96	2.46	.04	99.22
GRANITE	201	77.03	.02	13.91	.39	.01	.21	.87	2.76	6.21	.01	101.47
GRANITE	204	76.42	.01	15.05	.31	.02	.15	2.36	3.66	3.56	.01	101.44
GRANITE	210	73.51	.02	14.96	.79	.02	.56	2.01	5.16	1.25	0.30	99.15
GRANITE	211	72.2[illegible]	.05	15.15	.95	.03	.61	2.19	5.40	1.84	0.00	98.42
GRANITE	213	75.34	.05	14.76	.43	.01	.18	1.78	3.69	4.10	0.00	100.54
GRANITE	214	74.10	.04	14.80	.61	.12	.28	.98	4.27	3.24	0.00	99.50
GRANITE	245	72.77	.22	15.28	1.29	0.03	.43	2.02	4.27	3.76	.01	100.12
GRANITE	246	74.78	.13	14.81	1.03	0.00	.25	1.62	4.43	3.38	.01	100.36
GRANITE	262	74.08	.07	15.04	.68	0.00	.24	1.47	4.70	3.78	.02	100.28
GRANITE	263	74.74	.07	14.96	.56	0.00	.13	1.44	4.71	3.63	.01	100.47
GRANITE	271	71.22	.25	15.33	1.34	0.00	.87	2.23	4.68	2.66	.07	99.47

TABLE 3c (i) Major element analyses for trondhjemites and granites from the Scourie area.

			Y	SR	RB	TH	PB	W	GA	ZN	BA	NI	CR+V	CE	LA	ZR	NB
TRONDHJEMITE	AF	243		765	7	2	11	0	16	8	1648	2	9	13	4	38	1
TRONDHJEMITE	AF	272		552	9	0	5	0	20	10	781	2	3	17	13	143	0
TRONDHJEMITE	AF	274		533	5	0	6	0	20	7	481	7	0	15	10	25	0
TRONDHJEMITE	AF	264		664	14	0	5	0	21	12	841	4	2	19	13	95	2
TRONDHJEMITE	AF	251	2.	518	0	0	6	0	24	24	526	10	2	38	29	57	0
TRONDHJEMITE	AF	249	0.	458	6	0	12	0	20	12	736	6	4	30	25	56	0
TRONDHJEMITE	AF	253		522	6	0	7	0	25	22	673	8	13	31	26	115	0
TRONDHJEMITE	AF	254	3.	467	4	0	6	0	28	42	498	21	21	59	33	75	0
TRONDHJEMITE	AF	256		455	8	0	4	0	26	24	536	4	9	29	17	120	0
TRONDHJEMITE	AF	257		459	0	1	3	0	28	19	437	4	5	21	13	98	0
GRANITE		3	.7	355	44	0	13	0	21	14	1216	1	1	25	7	149	1
GRANITE		8	0	389	39	0	15	0	19	7	693	1	2	13	9	67	1
GRANITE		11		333	42	0	6	0	21	4	776	1	3	9	9	68	2
GRANITE		13	1.	211	62	0	20	0	22	20	665	0	3	37	25	67	1
GRANITE		19	1.1	250	34	2	14	0	23	25	708	1	6	30	19	117	3
GRANITE		67	2.0	354	33	1	12	0	22	26	667	1	5	39	20	178	3
GRANITE		68	1.6	444	25	0	14	0	21	20	928	2	6	51	27	194	3
GRANITE		69	1.8	314	21	1	10	2	20	29	532	2	5	24	13	121	1
GRANITE		81	0	513	19	0	13	0	21	13	904	0	0	19	13	69	1
GRANITE		82	.1	499	15	0	11	0	21	15	961	4	7	31	10	177	3
GRANITE		83	.6	319	25	0	9	0	21	19	586	1	1	22	11	83	3
GRANITE		87	.8	319	60	3	27	0	15	3	320	0	4	14	4	77	0
GRANITE		88	10.3	161	62	6	23	1	15	3	321	0	2	9	4	43	0
GRANITE		89	10.4	177	67	7	29	0	16	4	388	1	2	14	5	60	1
GRANITE		173	5.6	497	33	5	16	1	21	22	927	5	4	143	64	92	6
GRANITE		201	.1	209	87	2	26	1	10	5	817	1	7	5	2	19	0
GRANITE		204	7.7	141	43	3	16	0	16	3	630	0	7	10	0	78	0
GRANITE		210	0	516	8	1	8	0	17	6	1270	1	7	16	15	66	2
GRANITE		211		418	4	0	9	0	15	7	1093	1	1	15	9	26	1
GRANITE		213		264	35	0	16	0	17	5	865	2	5	10	6	12	1
GRANITE		214		401	24	0	12	1	17	9	1160	4	6	17	8	18	3
GRANITE		245	.2	259	45	0	22	0	28	29	1047	7	0	58	35	146	0
GRANITE		246	.6	257	39	0	14	0	21	13	1027	4	0	27	15	93	0
GRANITE		262	1.3	229	28	0	9	25	25	12	790	1	0	28	10	45	0
GRANITE		263	1.0	224	62	0	13	50	25	7	734	0	1	24	6	4	1
GRANITE		271	1.1	459	24	0	5	31	22	19	1100	2	0	36	19	132	0

TABLE 3c (ii) Trace element analyses for trondhjemites and granites from the Scourie area.

Chapter 2

THE GEOCHEMISTRY OF THE ARCHAEAN AMPHIBOLITE - TRONDHJEMITE SUITE AT GRUINARD BAY, N.W. SCOTLAND.

SUMMARY

Archaean rocks at Gruinard Bay form a bimodal assemblage of amphibolites and tonalites to granodiorites; amphibolite is enclosed in tonalitic gneiss, and homogeneous trondhjemite and granodiorite intrude both tonalitic gneiss and amphibolite.

Amphibolites represent basalts or unfractionated gabbros whose composition is similar to tholeiitic basalt found in present day island arcs and some marginal basins; some amphibolites are similar in composition to tholeiitic komatiites.

A model is presented, based on new chemical data, for major elements and K/Rb, Sr/Ba and Ce/Y ratios, whereby tonalites are generated by the partial melting of amphibolite similar in composition to the amphibolites found as rafts in acid gneiss; feldspar and hornblende remain in the residue. Trondhjemites and granodiorites are derived from a tonalitic melt by the fractional crystallisation of plagioclase and hornblende. This model is consistent with magma generation at a depth of less than 60 km at the base of a thick lava pile or more probably, in a subduction zone. The magma types, the sequence of magmas and mode of generation invite comparison with deep seated 'granite' batholiths located on active continental margins.

There is a north - south variation in principal magma-type across the Scourian complex, which shows a southwards increase in K_2O; this is interpreted as a function of the level of exposure.

1. INTRODUCTION

The importance of trondhjemitic rocks in the Archaean was recently emphasised by Barker et al. (1976) and Arth and Barker (1976) who pointed out that they form an important part of many Archaean gneiss terrains and suggest that their generation may have been a critical step in the development of the continents.

The rocks at Gruinard Bay are dominantly trondhjemitic in composition which is in marked contrast to the Scourie area (see above) and the major part of the Scourian complex (Tarney et al., in press) which is tonalitic. Trondhjemite forms about 75% of the surface area of the present complex and amphibolite about 20% and there are only minor amounts of ultramafic rock, tonalite, granodiorite and metasediment. There is a distinct bimodality about the suite which is emphasised on an A - F - M diagram and

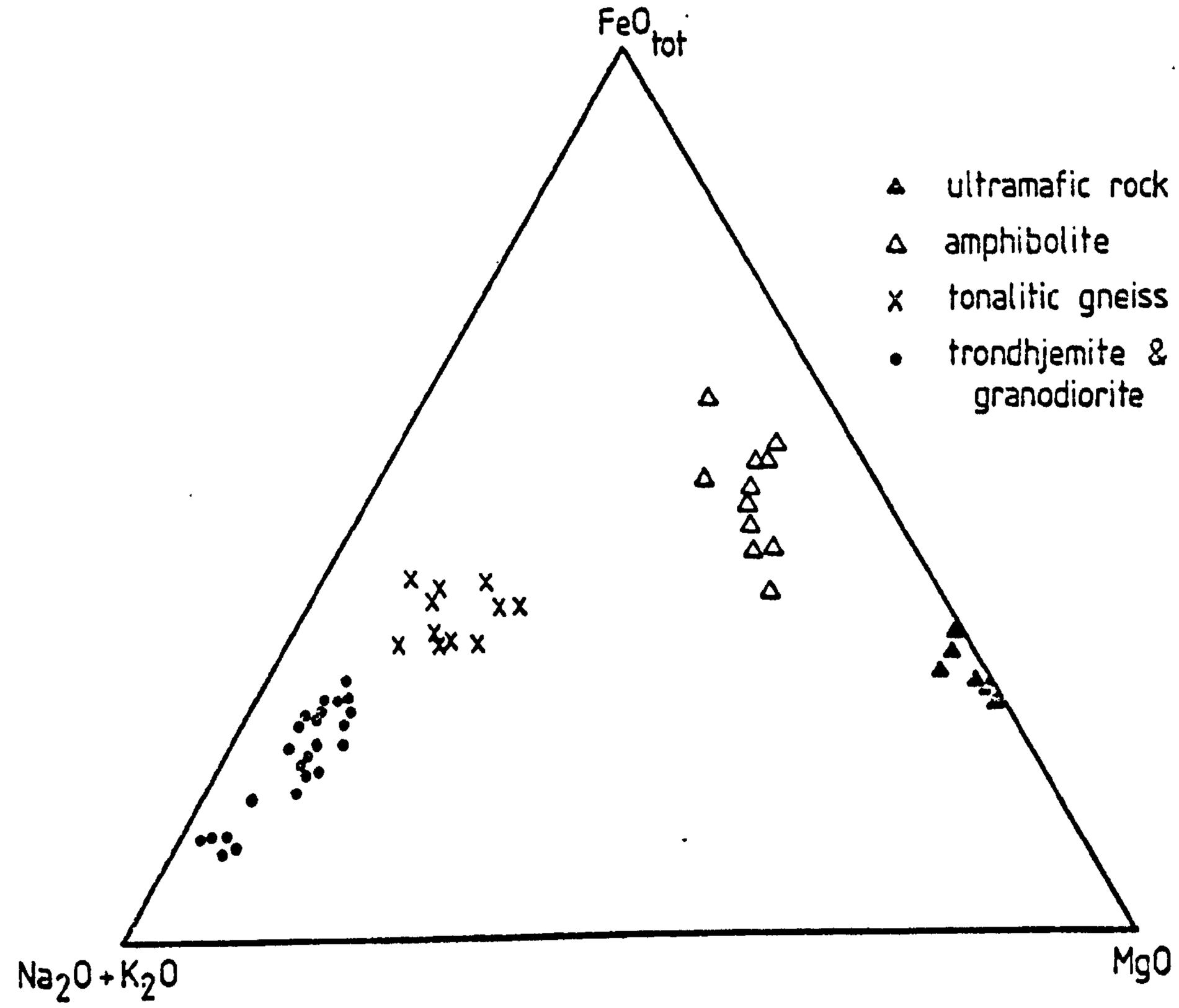

FIG. 1. A - F - M diagram showing bimodality between amphibolite and ultramafic rock and tonalites and trondhjemites from Gruinard Bay.

shows that intermediate compositions (with silica contents between 52% and 61%) are absent (Fig. 1). This contrasts with the pronounced calc-alkaline trend shown by Scourian gneisses from the Scourie area (see above) and Assynt (Sheraton et al., 1973).

In this study new chemical data are presented for amphibolites, tonalites, trondhjemites and granodiorites (Tables 6 and 7) and are used to place limits on the origin and tectonic setting of these rocks.

2. FIELD RELATIONSHIPS

The geology of the area was first described by Peach et al., (1907) and more recently by Davies (1977) who showed that Laxfordian deformation in the area is minimal and that most features of the complex are directly attributable to Scourian events. Davies (op. cit.) proposed that these rocks evolved as part of a plutonic igneous complex in Scourian times.

Samples for this study were collected from four small areas where the field relationships are known in detail:

1) Lochan an Daimh; agmatitic gneiss cut by a Scourie dyke (Fig. 2).
2) Carn nan con Easan; agmatitic gneiss.
3) Loch an Fhamair; tonalitic gneiss and blocks of amphibolite and ultrabasic rock veined with trondhjemite and pegmatite.
4) Cnoc Bad nan Cuileag; homogeneous trondhjemite cut by Scourie dyke.

The oldest rocks are amphibolites (Fig. 3) and ultrabasic rocks which occur as agmatitic blocks up to 300m long in acid gneiss. Ultrabasic rocks are banded and cut by amphibole-rich veins (Lochan an Daimh) and are similar to the more extensive

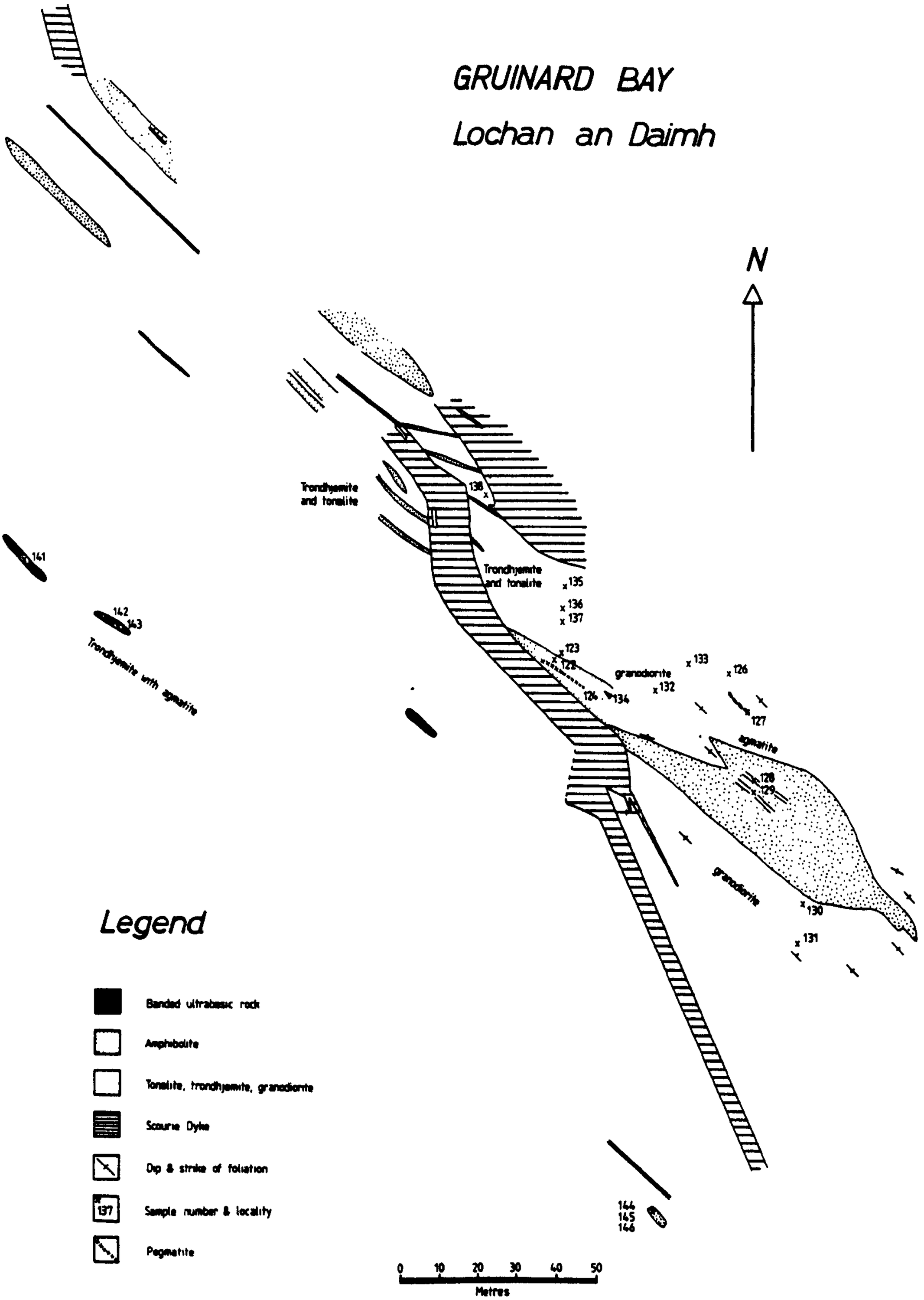

FIGURE 2. Map of Scourian amphibolites and tonalitic to granodioritic gneisses at Lochan Daimh, Gruinard Bay. The irregular form of the Scourie dyke is thought to be original and not due to deformation. The relationship between tonalitic gneiss and trondhjemite is illustrated in Fig. 3B. X indicates a sampling locality; sample numbers refer to analyses in Tables 6 & 7 at the end of this chapter.

FIGURE 3. Amphibolites trondhjemites and tonalites at Lochan an Daimh, Gruinard Bay.

(A) Amphibolitic inclusions (a) in banded tonalitic gneiss.

(B) Tonalitic gneiss (t) intruded by trondhjemite (tr).

(C) Discordant trondhjemite (tr) veins in weakly banded amphibolite.

layered gabbro - ultramafic rock sequences in the Scourie area. Amphibolites are fine grained and often banded; they alter to epidote-rich rocks. Tonalitic gneiss (Lochan an Daimh and Loch an Fhamhair) contains small inclusions of amphibolite and ultrabasic rock (Fig. 3) and is always banded in contrast to the more homogeneous veins of trondhjemite and granodiorite which intrude it; banding in tonalitic gneiss implies an early Scourian, pre-trondhjemite deformation.

Trondhjemite and associated granodiorite are the most common rock types which are intrusive into amphibolite, ultramafic rock and tonalitic gneiss; they form veins 2 to 30 cm wide (Fig. 3) and also thick homogeneous sheets. At Cnoc bad nan Cuileag inclusions of amphibolite, leucogabbro and ultramafic rock are enclosed in undeformed homogeneous trondhjemite which has only a trace of a fabric. Late pegmatities cut trondhjemites and granodiorites.

Scourie dykes intrude agmatitic gneiss (Lochan an Daimh) and homogeneous trondhjemite (Cnoc bad nan Cuileag); at Lochan an Daimh the main Scourie dyke is amost undeformed; it varies in strike from 350° to 315° and width from 0.5 m to 12.0 m. The thinnest parts of the dyke are chilled and small apophyses are preserved (Fig. 2). This suggests that there was minimal Laxfordian deformation in the area.

Comparison with the Scourie Area

Although similar lithologies with identical age relationships are present in both the Gruinard Bay and Scourie areas there are a number of important differences:

(1) the metamorphic grade at Gruinard Bay is amphibolite facies in contrast to the granulite facies grade at Scourie.

(2) the major part of the Scourie area consists of banded tonalitic gneiss, and trondhjemites form minor intrusive sheets; at Gruinard Bay banded tonalitic gneiss is a minor rock type and trondhjemite is predominant.

(3) layered gabbro complexes at Gruinard Bay are much more fragmented by intrusive trondhjemite than their equivalents in the Scourie area. The trondhjemite is homogeneous and relatively undeformed suggesting differing modes of intrusion in the two areas (Davies, 1977).

(4) there is a distinct bimodality in the Gruinard Bay rocks between amphibolites and tonalites to trondhjemites which contrasts with the continuum of rock types in the Scourie area.

3. PETROGRAPHY

Representative mineral assemblages are presented in Table 1. The quartzo-feldspathic rocks are classified according to the nomenclature of Streckeisen (1973) and modal analyses are plotted on a Q - A - P diagram (Fig. 4). At least 1500 points were counted on each thin section.

Amphibolite

Some amphibolites contain recrystallised laths of feldspar which resemble a relict ophitic texture, but most are fine grained and equigranular. Amphibole varies in composition from deep green hornblende to pale green magnesian amphibole; green hornblende contains opaque oxides exsolved along the cleavage planes and is sometimes recrystallised to fine grained hornblende and quartz. In sample 109 hornblende overgrows clinopyroxene; this rock contains the lowest concentrations of K and Rb of the amphibolites and is probably the least chemically altered. Plagioclase forms irregular, zoned grains, altered to sericite and small euhedral

TABLE 1

Representative mineral assemblages from the Scourian rocks of Gruinard Bay

Ultrabasic rock

Olv - opx - spin - mgt - hbl (pargasitic)

Hbl - mgt - sph - cc

Trem - bi - mgt

Amphibolite

Hbl (green) - plag - epid - qz ± sph ± mgt

Hbl (green) - plag - epid ± sph ± mgt

Hbl (pale green) - plag - epid - qz ± white mica

Hbl (pale green) - plag - epid ± white mica

Tonalite

Qz - plag - bi - epid - musc

Qz - plag - bi - epid - hbl

Qz - plag - bi - epid

Trondhjemite

Qz - plag - epid - bi - hbl - micr (accessory: ap - sph - cht - mgt - zn - cc)

Qz - plag - epid - bi - hbl

Qz - plag - epid - hbl

Qz - plag - epid - bi - musc - micr

Qz - plag - epid - bi - musc

Granodiorite

Qz - plag - micr - bi - epid - musc (accessory: ap - sph - cht - mgt - zn - cc)

Qz - plag - micr - bi - epid

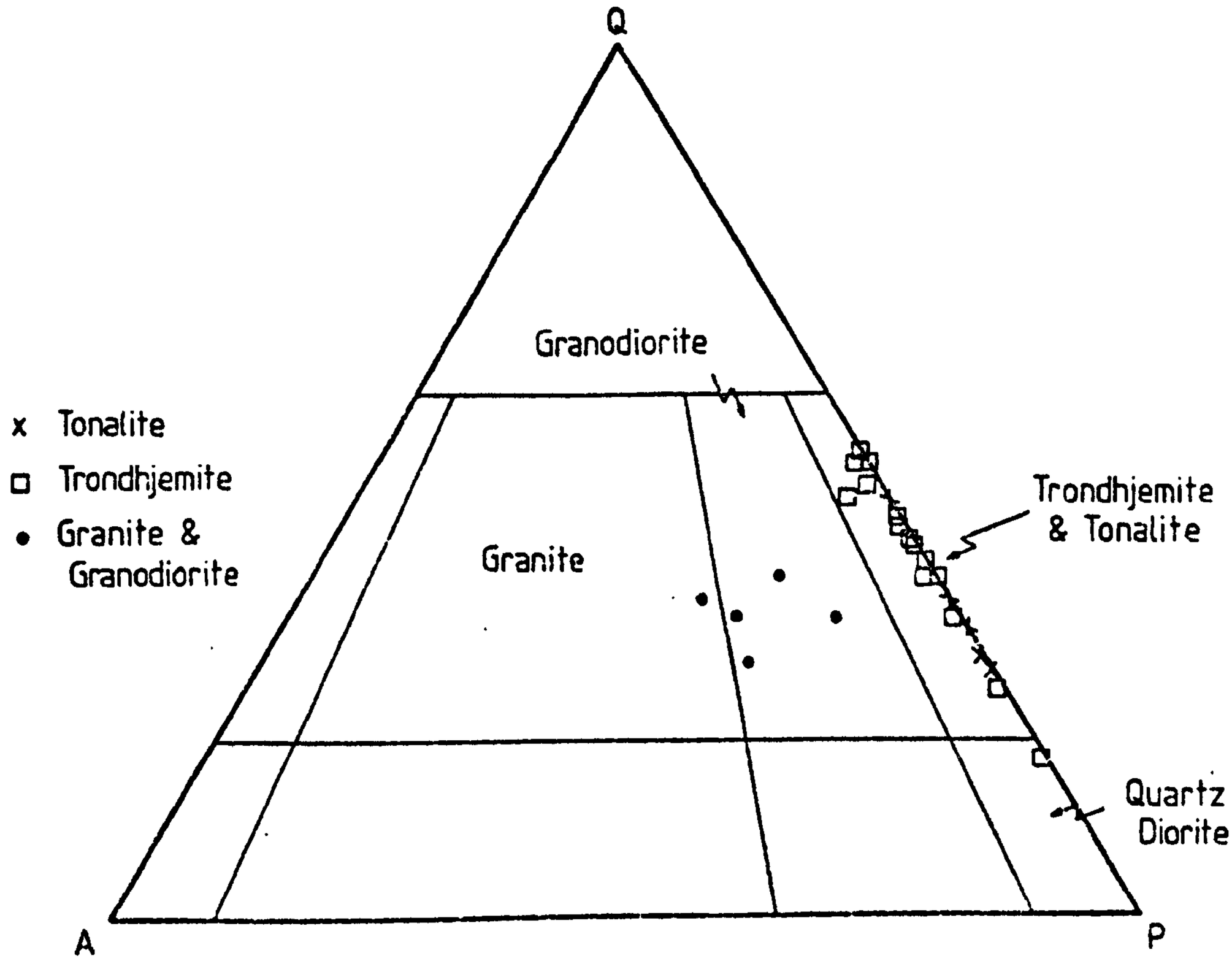

Fig. 4. Quartz (Q) - Alkali feldspar (A) - plagioclase (P) concentrations in tonalites, trondhjemites and granodiorites from Gruinard Bay, based on modal analyses. (After Streckeisen, 1973).

grains of epidote. Sphene forms coronas around opaque oxides.

Tonalitic Gneiss

Tonalite is defined according to the nomenclature of Streckeisen (1973) (quartz, less than 60% but greater than 20%; alkali feldspar less than 5%; ferromagnesian minerals, greater than 10%) and differs from trondhjemite only in the greater proportion of ferromagnesian minerals.

Tonalitic gneiss is medium grained (grain size less than 3 mm) and is well banded. Plagioclase (ca. An_{26}) forms subhedral grains with slightly curved to very irregular grain boundaries; it is altered to euhedral and subhedral grains of epidote and is replaced by sericite and a low birefringence mica (which is probably hydromuscovite). Rounded inclusions of quartz are common in plagioclase. Large quartz grains have recrystallised into a fine grained mosaic between plagioclase grains. Biotite is the main ferromagnesian mineral and overgrows plagioclase, hornblende, opaque oxides and sphene; it contains small rounded inclusions of zircon and is altered along its cleavage planes to chlorite and epidote. Hornblende is sieved with quartz inclusions and is altered to chlorite. There are fine needle-like inclusions of rutile oriented in several different planes in both biotite and hornblende in sample 149; these probably represent the exsolution of excess TiO_2 from hornblende and biotite with falling pressure and temperature. Sphene forms coronas around rutile or opaque oxides and epidote overgrows allanite and sphene.

Trondhjemite and granodiorite

There is no sharp division between trondhjemite and granodiorite the only difference being arbitrarily based on the amount of modal microcline. Both form medium to coarse grained homogeneous veins in amphibolite and tonalitic gneiss and extensive areas of homogeneous gneiss (Fig. 2). Their homogeneity is in marked contrast to the strong banding in tonalitic gneiss. Plagioclase (ca. An_{26} in trondhjemite, ca. An_{21} in granodiorite) forms large embayed grains in a matrix of recrystallised quartz and is slightly zoned. It is replaced by sericite and small, euhedral grains of epidote and contains inclusions of quartz zircon and apatite. There are small lamellae of microcline in

plagioclase which are altered to muscovite and less regular patches of microcline with no regular crystallographic orientation. Some plagioclase grains are sieved with quartz inclusions which make up 30% of the grain and resemble 'chess-board' oligoclase figured in Smith (1974). Biotite is late and overgrows plagioclase, hornblende sphene and zircon and is altered along its cleavage planes to chlorite and epidote; some grains contain small vermiform inclusions of quartz. Hornblende is intergrown with quartz and is altered to chlorite and muscovite. Muscovite is a late mineral replacing hornblende, biotite and plagioclase. Hornblende and muscovite are mutually exclusive in all but one rock, where muscovite replaces hornblende; hornblende is only found in acid veins in amphibolite, whereas muscovite is only found in areas of homogeneous gneiss. The pH_2O in amphibolite may buffer the pH_2O of intrusive trondhjemite veins and a low pH_2O may prevent muscovite growth, due to the restricted mobility of elements such as K. Microcline replaces plagioclase in trondhjemite but forms large subhedral grains in granodiorite; it is perthitic with plagioclase lamellae in two different orientations. Microcline grain boundaries are granulated and myrmekite is common between plagioclase and microcline. Amorphous sphene is a common accessory and forms coronas on rutile and opaque oxides.

4. MINERAL CHEMISTRY

Feldspars

Plagioclase (Ab_{79}) enclosed in perthitic microcline (Ab_{11}) in granodiorite 132 yields equilibration temperatures of 530°C at 5kb. and 585°C at 10 kb, using the two-feldspar thermometer of Whitney and Stormer (1977) and Powell and Powell (1977a) modified for the microcline - low albite solvus (see above). Lamellae of

plagioclase in microcline indicate that it was originally richer in the albite component and therefore these are minimum equilibration temperatures.

Muscovite

Muscovite is a late mineral replacing biotite, plagioclase and hornblende. Most rocks containing muscovite are not peraluminous and the muscovite is not related to the igneous history but has formed by the reaction:

plagioclase + biotite → muscovite + epidote + sphene

An upper stability limit for the assemblage muscovite - albite - quartz in the absence of an aluminosilicate of 705°C at 7kb, 660°C at 5kb and 580°C at 2kb has been calculated from the reaction:

$$\text{muscovite}_{ss} + \text{albite}_{ss} + \text{quartz} \rightarrow \text{K-feldspar} + \text{aluminosilicate} + H_2O$$

by Chatterjee and Froese (1975).

Muscovite in trondhjemite 171 is phengitic (ca. 7% Mg and 14% Fe in the octahedral site) but low in paragonite (4% Na in the interlayer site). Velde (1967) proposed that Si^{4+} in muscovite, a function of the phengitic component, is related to pressure and temperature but not to rock composition. A temperature estimate based on Velde's (1967) data of 620°C at 8kb, 550°C at 5kb is in general agreement with other temperature estimates in these rocks, although this method only strictly applies to Mg-Al micas where pH_2O = ptotal.

The assemblage muscovite - calcite - quartz - microcline - plagioclase - epidote - vapour in granodiorite 167 represents an invariant point in the system K_2O - Na_2O - CaO - SiO_2 - Al_2O_3 - CO_2 - H_2O, which is at ca. 510°C when plagioclase is An_{40} and the mole fraction of CO_2 in the vapour phase is 0.06 (Hewitt, 1973). In this rock plagioclase is An_{21} so that the temperature and XCO_2 will be slightly lower than for more calcic plagioclase; the effect of Fe on the system is unknown.

Biotite and Hornblende

Biotites from trondhjemites and one tonalite vary in TiO_2 content and FeO/MgO ratio; this can be directly attributed to the composition of the host rock (Fig. 5). Coexisting hornblende shows a similar variation in composition but this is not simply related to the rock chemistry. FeO and MgO in hornblende show an antipathetic relationship whereas in biotite FeO and MgO vary in different grains in the same thin section and there is no clear antipathetic relationship. Ti varies antipathetically with Mg/Fe in biotite. There is no simple correlation of FeO/MgO between biotite and hornblende (Fig. 5). These data suggest that biotite chemistry is controlled by the host rock and hornblende chemistry is not; variable FeO/MgO in hornblende therefore is probably related to variations in P, T and fO_2 during magmatism and cooling. This is consistent with the petrographic evidence that hornblende is primary and biotite is late.

Sphene

Coronas of sphene around ilmenite and rutile formed by the reaction

$$\text{anorthite} + \text{K-feldspar} + \frac{\text{rutile}}{\text{ilmenite}} + H_2O \rightarrow$$

$$\text{muscovite} + \text{sphene} + \text{quartz}$$

(reaction 7, Hunt & Kerrick, 1977)

which they place at 570°C at 5kb although since none of the phases is pure this is only an approximate temperature estimate.

Discussion of mineral chemistry

If a pressure of 5kb is assumed, the mineral assemblages in trondhjemites and granodiorites from Gruinard Bay equilibrated between 500°C and 600°C. These temperatures do not necessarily represent the peak of metamorphism but the closure of exchange reactions between the minerals. In this temperature interval CO_2

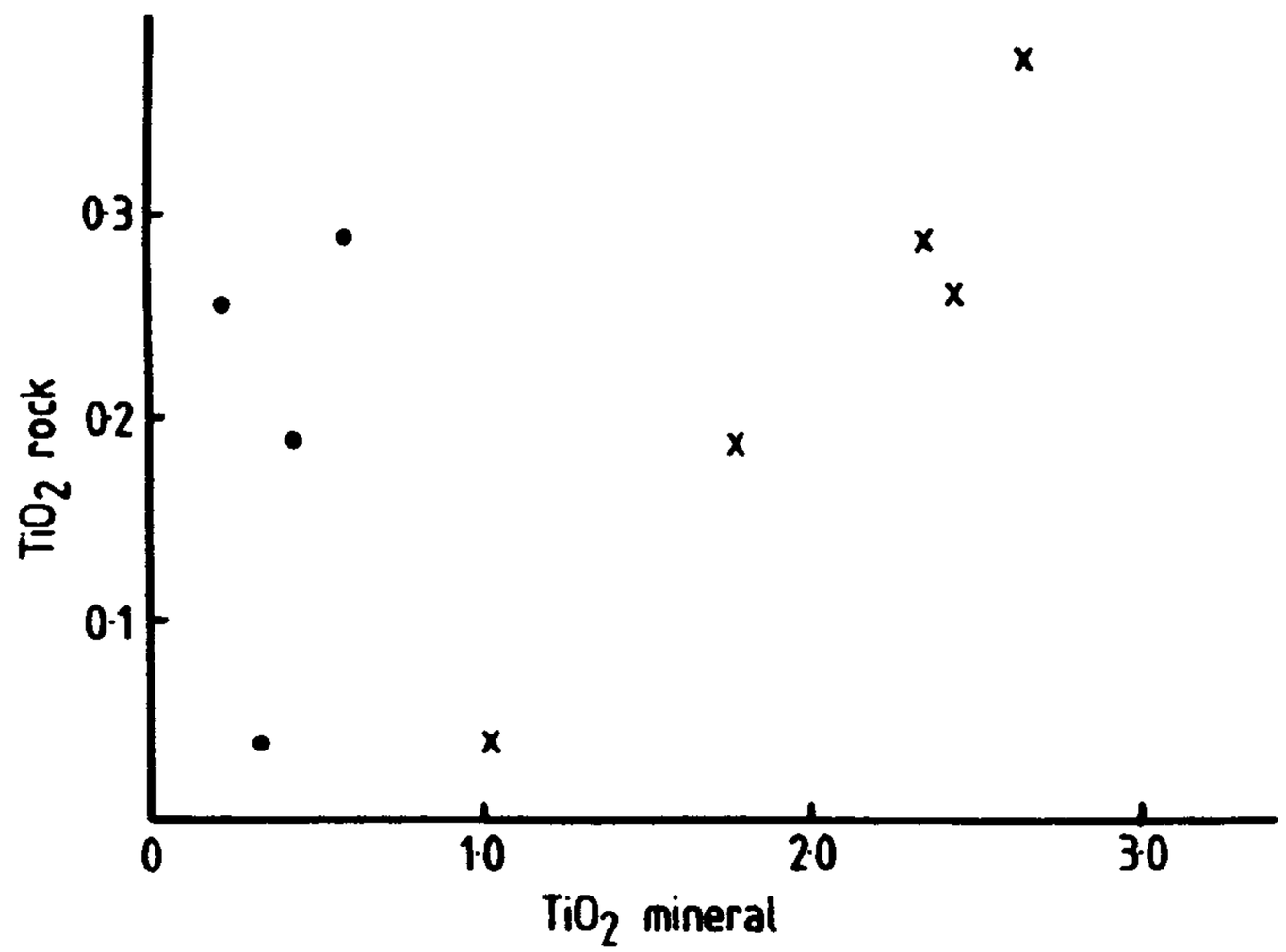

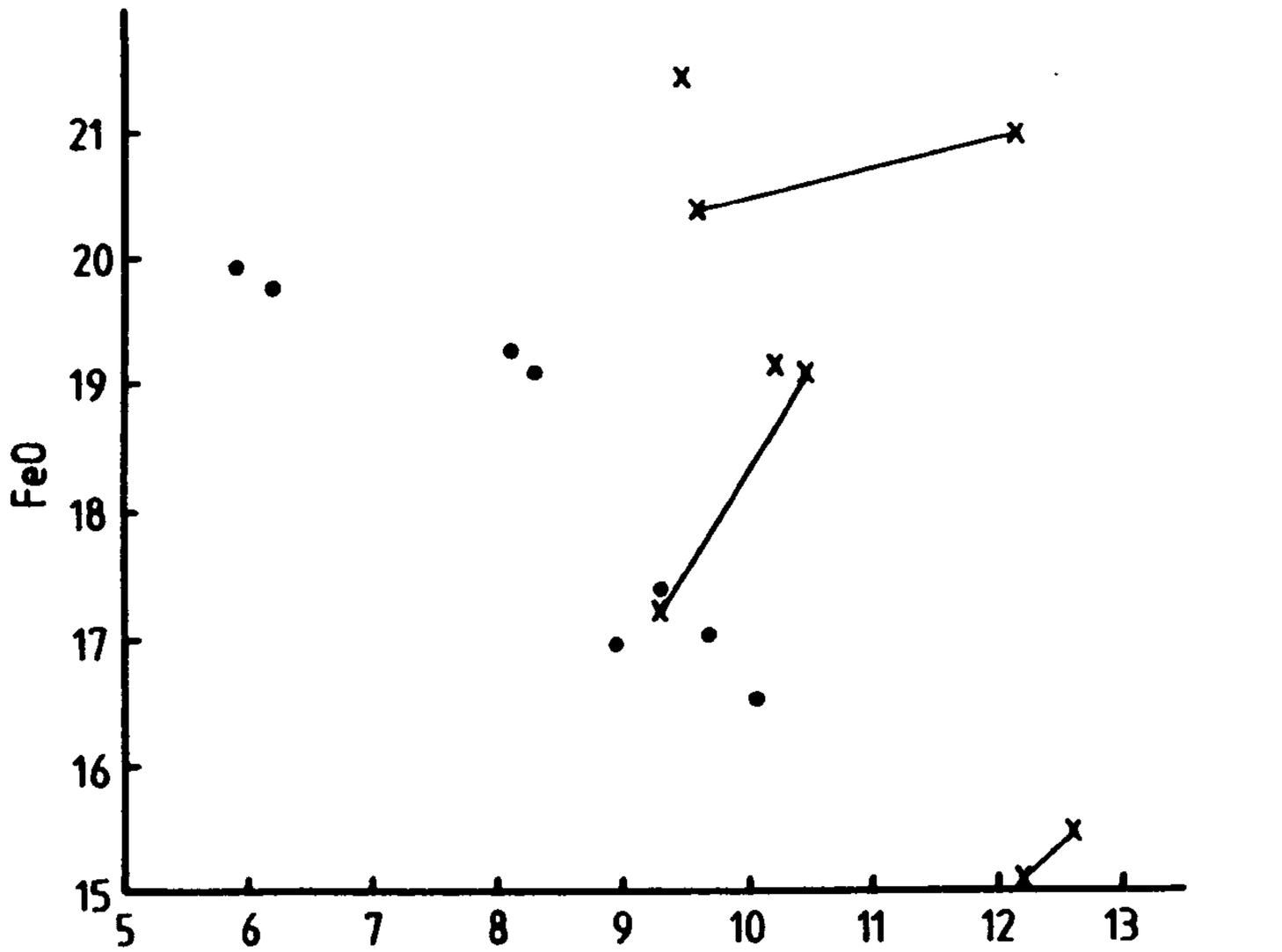

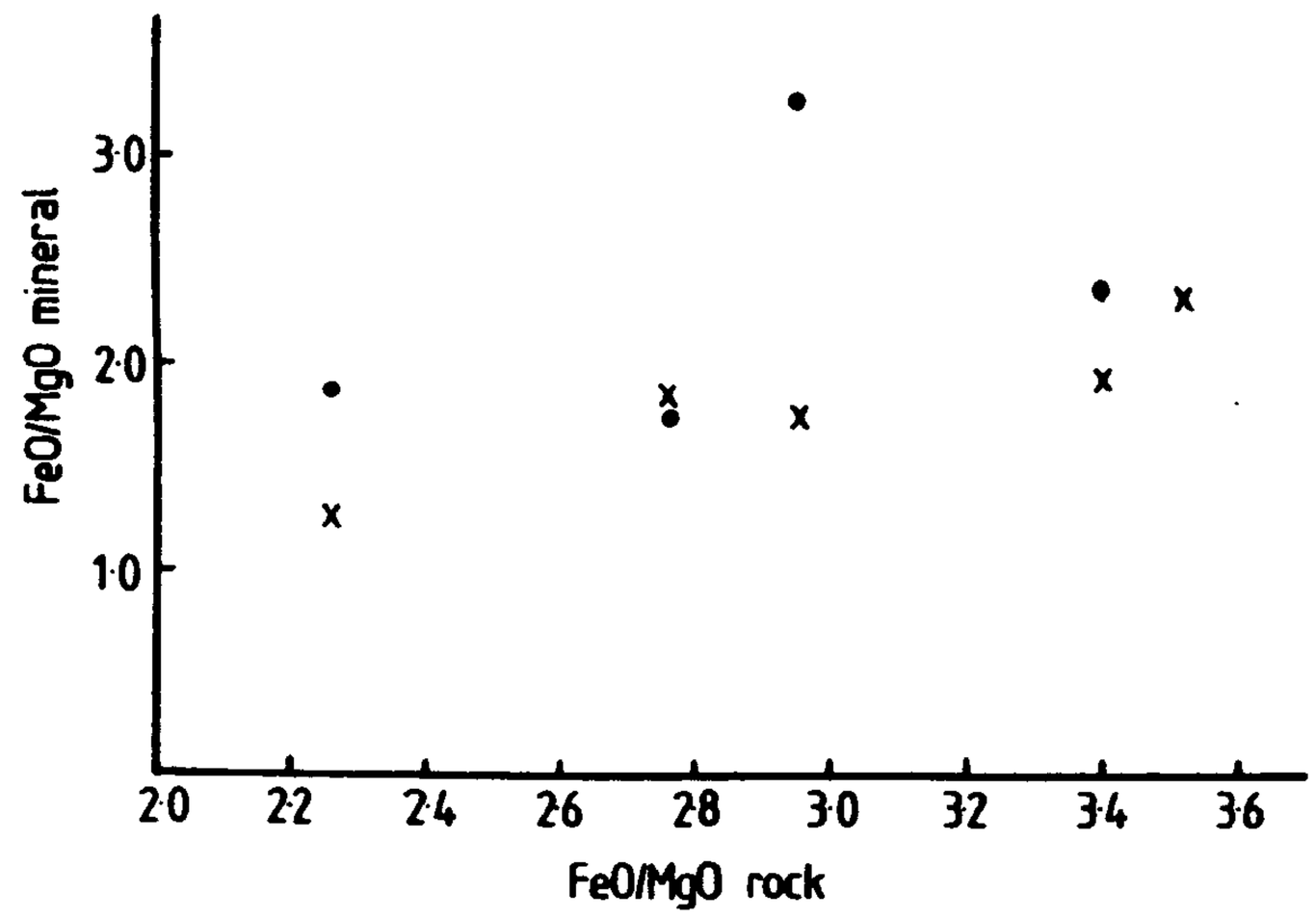

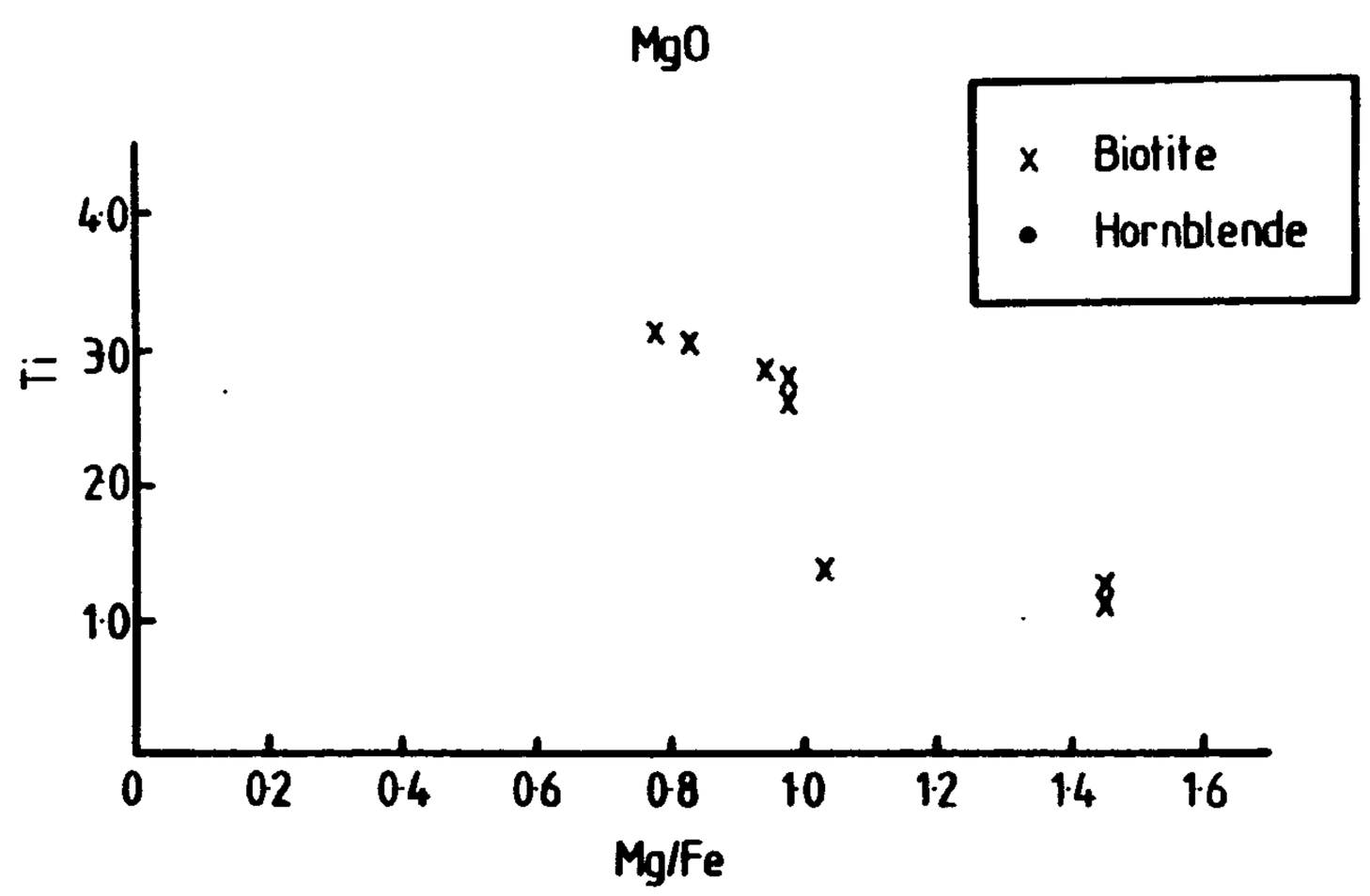

FIGURE 5. Chemical data for coexisting hornblende and biotite in Gruinard Bay tonalites and amphibolites. Tie-lines indicate minerals in the same thin section.

never exceeded 6% (mol) of the vapour phase (see discussion under muscovite above).

5. THE ORIGIN OF THE AMPHIBOLITES

Analyses of 12 amphibolites from six different agmatitic blocks in three separate localities are given in Table 6.

Two features indicate that the Gruinard Bay amphibolites are igneous in origin (i) their close association in the field with ultramafic blocks containing olivine, spinel and orthopyroxene (ii) they define an igneous trend on the niggli mg - c - (al + alk) diagram of Leake (1964) and plot outside the field of sediments (shale + carbonate) and with a different trend on a Cr - niggli mg diagram (Van der Kemp, 1969) (Figs. 6a, b).

The mobility of elements in altered amphibolites and basalts

The elements Y, Zr, Nb, Ti and the rare earth elements (REE) are unaffected by the submarine weathering of basalt (Cann, 1970; Philpotts et al., 1969; Herman et al., 1974); Sr and P_2O_5 are slightly affected and K, Rb, Cs, Ba and the K/Rb ratio are substantially altered (Hart, 1969; 1970; Hart et al., 1974; Philpotts et al., 1969; Cann, 1970). During low grade metamorphism (zeolite and green schist facies) Y, Zr, Ti, Nb, (some authors include P, Cr, V, Ni and Hf) are stable (Smith et al., 1976; Humphris et al., 1978; Wood et al., 1976). Vallance (1974) reports that Ti is the least mobile element during spilitisation, whilst Cann (1969) considers Y, Zr, Cr, V and Ni also immobile.

At high metamorphic grades Elliot (1973) and Field and Elliott (1974) found that during the retrogression of gabbro to amphibolite TiO_2, MgO, MnO, Na_2O, Ni, Ga, Y and possibly Al_2O_3 are immobile and that K_2O, P_2O_5, Rb and to a small extent Zr are enriched in amphibolite. Engel and Engel (1962) in a study of progressive

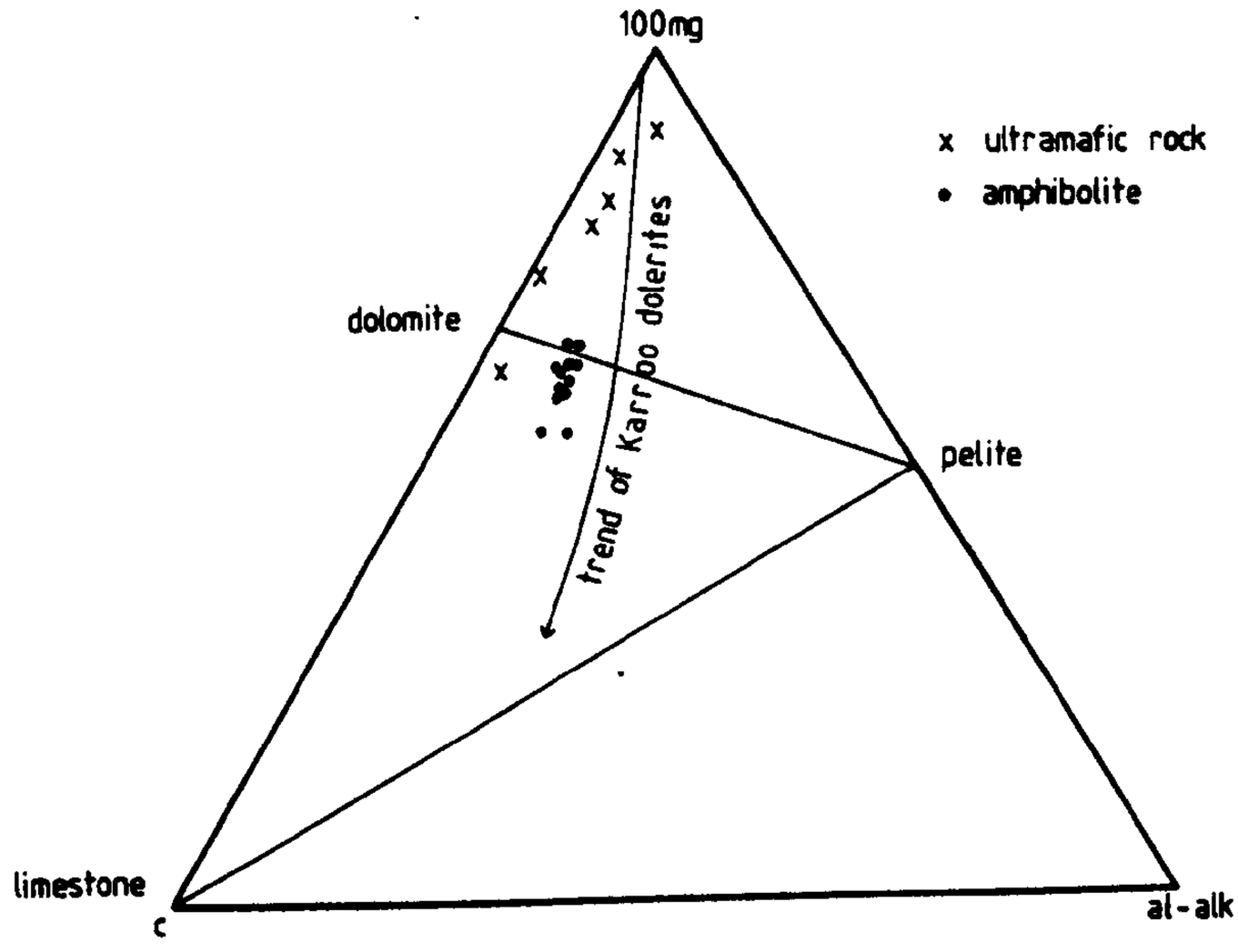

FIGURE 6(a). Gruinard Bay amphibolites and ultramafic rocks plotted on a mg-c-al-alk diagram (after Leake, 1964). The amphibolites plot parallel to the igneous trend and at right angles to the sedimentary trend.

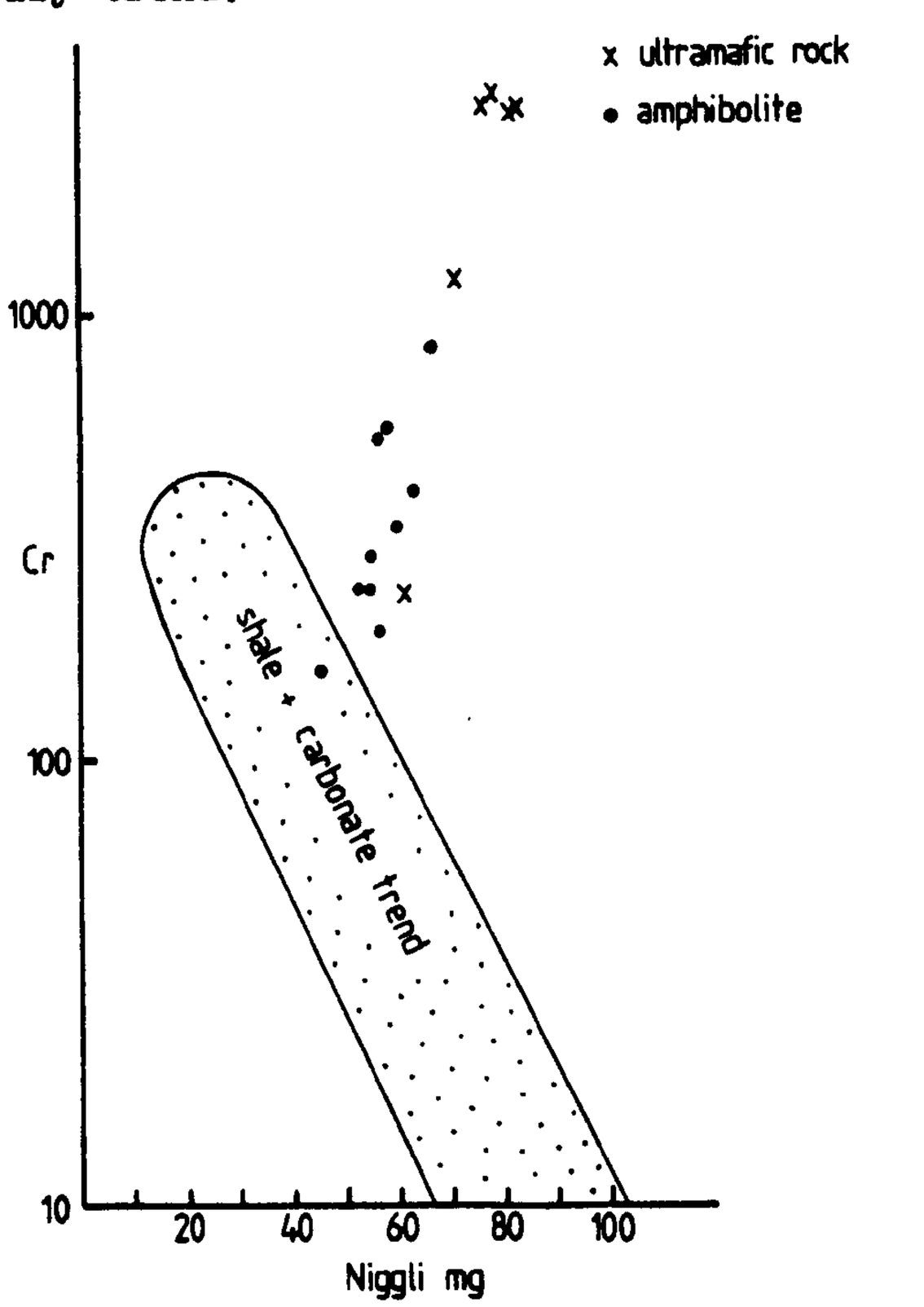

FIGURE 6(b). Gruinard Bay amphibolites and ultramafic rocks plotted on a niggli mg - Cr diagram (after Van der Kemp, 1969). The amphibolites plot outside the field of sediments.

metamorphism in amphibolites found that K, TiO_2 and P_2O_5 decrease in concentration with increasing temperature. Seidel (1974) regards Ti and Zr immobile in basalts under glaucophane schist facies conditions.

A comparison between the chemistry of the Gruinard amphibolites and gabbro from the Scourie - Badcall area

Davies (1977) suggested that the amphibolites and ultramafic rocks in agmatite trains at Gruinard Bay are fragmented layered gabbro complexes analogous to those found in granulite facies gneisses around Scourie. The immobile elements Ti, Y, Zr and Cr are used to test this hypothesis by comparing gabbros from the Scourie - Badcall area (SiO_2 44.5 to 53.5 %, MgO + CaO 13 to 24%) with the amphibolites from Gruinard Bay (SiO_2 45.7 to 52.2%, MgO + CaO 16.5 to 22%). There is a positive correlation between Ti and Zr, Ti and Y, Zr and Y, (Figs. 7 and 8) and a negative correlation between Ti and Cr + V and Zr and Cr + V (Fig. 9) in both the gabbros and amphibolites. Gabbros lie on the same trends as the amphibolites but generally show a greater scatter and intercept the TiO_2 axis and the origin, whilst amphibolites intercept the Y axis. On the ternary plots Ti-Zr-Y and Ti-Zr-Sr (Fig. 10) gabbros show a much greater scatter than amphibolites. There is a broad similarity in the concentration of the elements Ti, Cr, Y, and Cr in the gabbros and amphibolites which suggests that they may have originated from basic liquids of similar composition. Well developed mineralogical layering in the gabbros at Scourie and Badcall has probably developed by crystal fractionation and accounts for their greater compositional range and the scattering of the data on Figs. 7 to 10. The lack of pronounced mineralogical banding and the greater homogeneity in the amphibolites indicates that their parent gabbro or basalt did not undergo extensive

fractionation.

The variation in the concentrations of immobile elements is governed by crystal - melt equilibria in the parental liquid. Some constraints can be set upon residual and/or fractionating phases by considering distribution coefficients for minerals in tholeiitic melts (Pearce, 1978; Irving, 1978). A summary of observed and expected correlations between trace elements, whose concentrations are governed by known distribution coefficients and major elements whose concentrations are governed by crystal-chemical constraints is given in Table 2. Some of the correlations are plotted in Figs. 7 to 9, and 11; all other correlations were plotted and the data is presented in Table 6. These data are used to eliminate and set limits upon residual phases in equilibrium with the melt from which the basic rocks crystallised. Some correlations are produced by more than one mineral but by using several expected correlations for a mineral whose role is equivocal it is possible to single out residual phases. Inspection of Table 2 shows that the observed major and trace element data is consistent with magnesian orthopyroxene as a residual phase. It is probable that orthopyroxene fractionated during the crystallisation of the parent to the amphibolites. The Scourie - Badcall gabbros are more complex and both magnesian orthopyroxene and plagioclase were fractionating phases during cooling.

Mobile elements in Scourian basic rocks

Cann (1970) found that in unaltered basalts the immobile elements Y and Zr correlated with the more mobile elements K and Rb, but this correlation was not found in altered samples. There is no correlation between K and Y or Zr in the Gruinard Bay amphibolites suggesting that their K content has changed. Similarly Erlank and Kable (1976) found a correlation between Zr/Nb

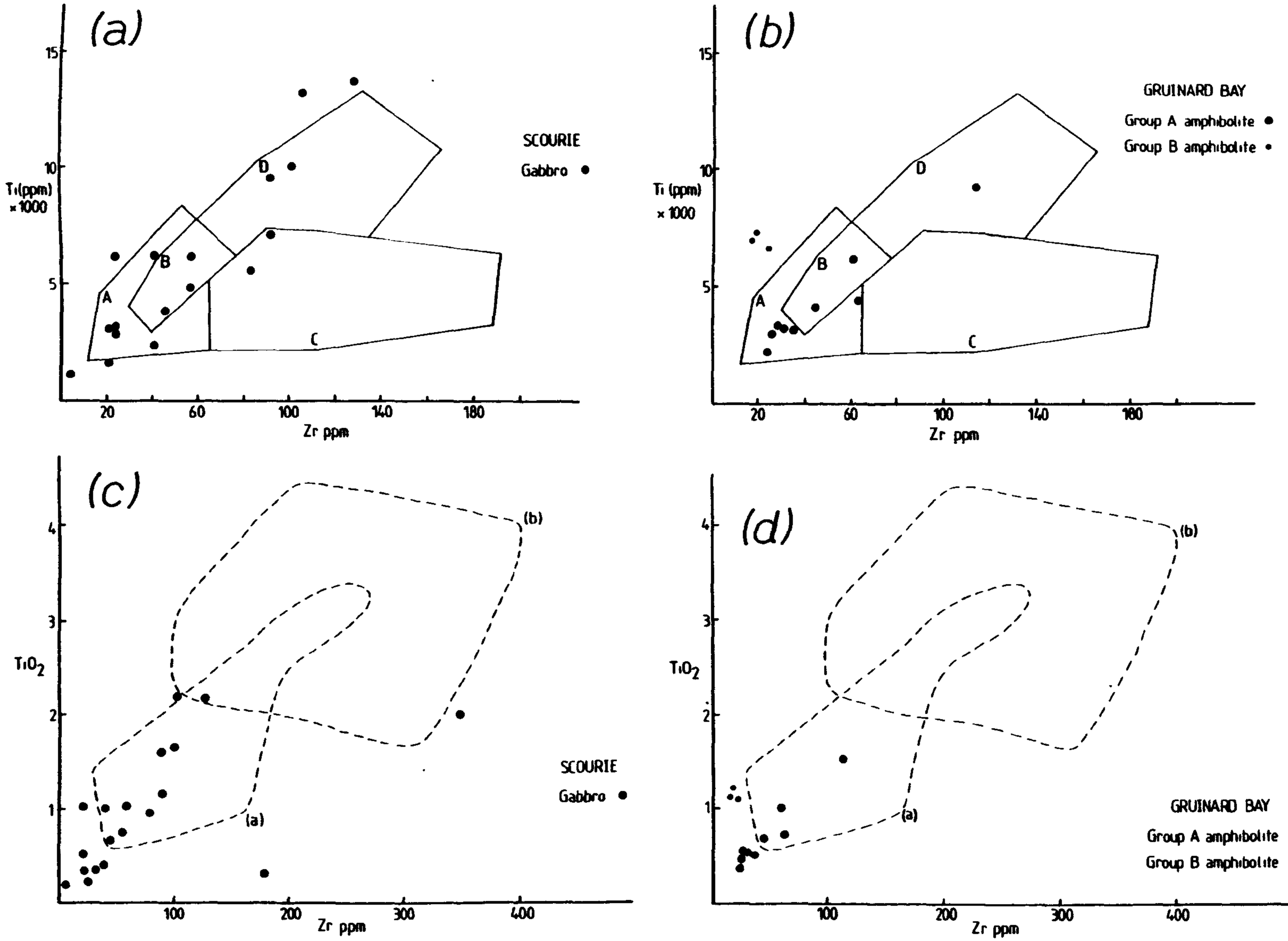

FIGURE 7. (A & B) Ti vs Zr for Scourie gabbros and Gruinard Bay amphibolites; ocean floor basalts plot in fields D and B, low-potassium tholeiites in fields A and B and calc alkali basalts in fields C and B. The Gruinard Bay amphibolites plot as low-K tholeiites. (C & D) TiO_2 vs Zr for Scourie gabbros and Gruinard Bay amphibolites; oceanic tholeiites plot in field (a), continental tholeiites plot in field (b). The Gruinard Bay amphibolites plot in the field of oceanic tholeiites. (A & B) after Pearce and Cann (1973), (C & D) after Floyd and Winchester (1975).

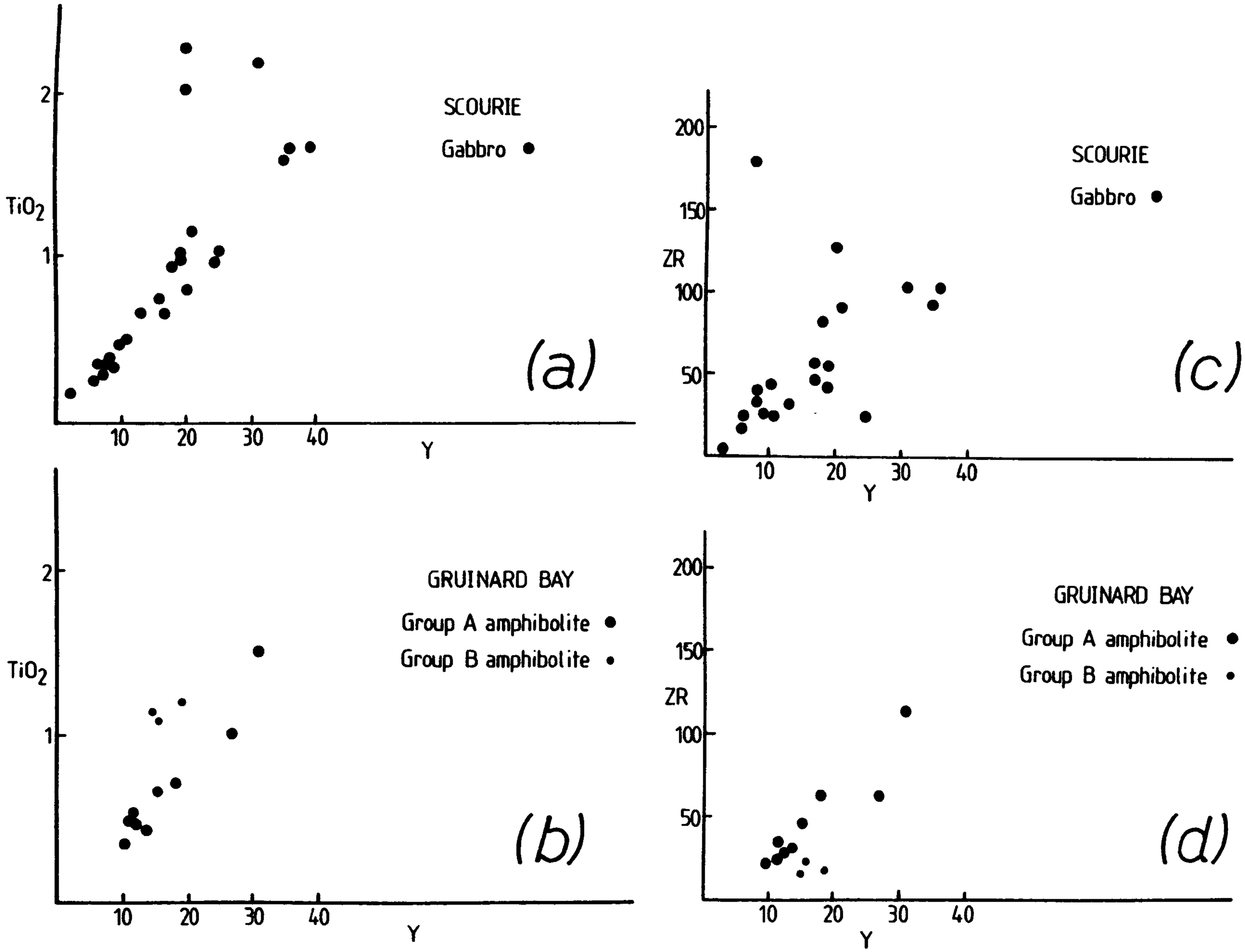

FIGURE 8. Plots of TiO_2 vs Y (a & b) and Zr vs Y (c & d) for Scourie gabbros and Gruinard Bay amphibolites. Note the different intercepts with the axes for the two groups of rocks.

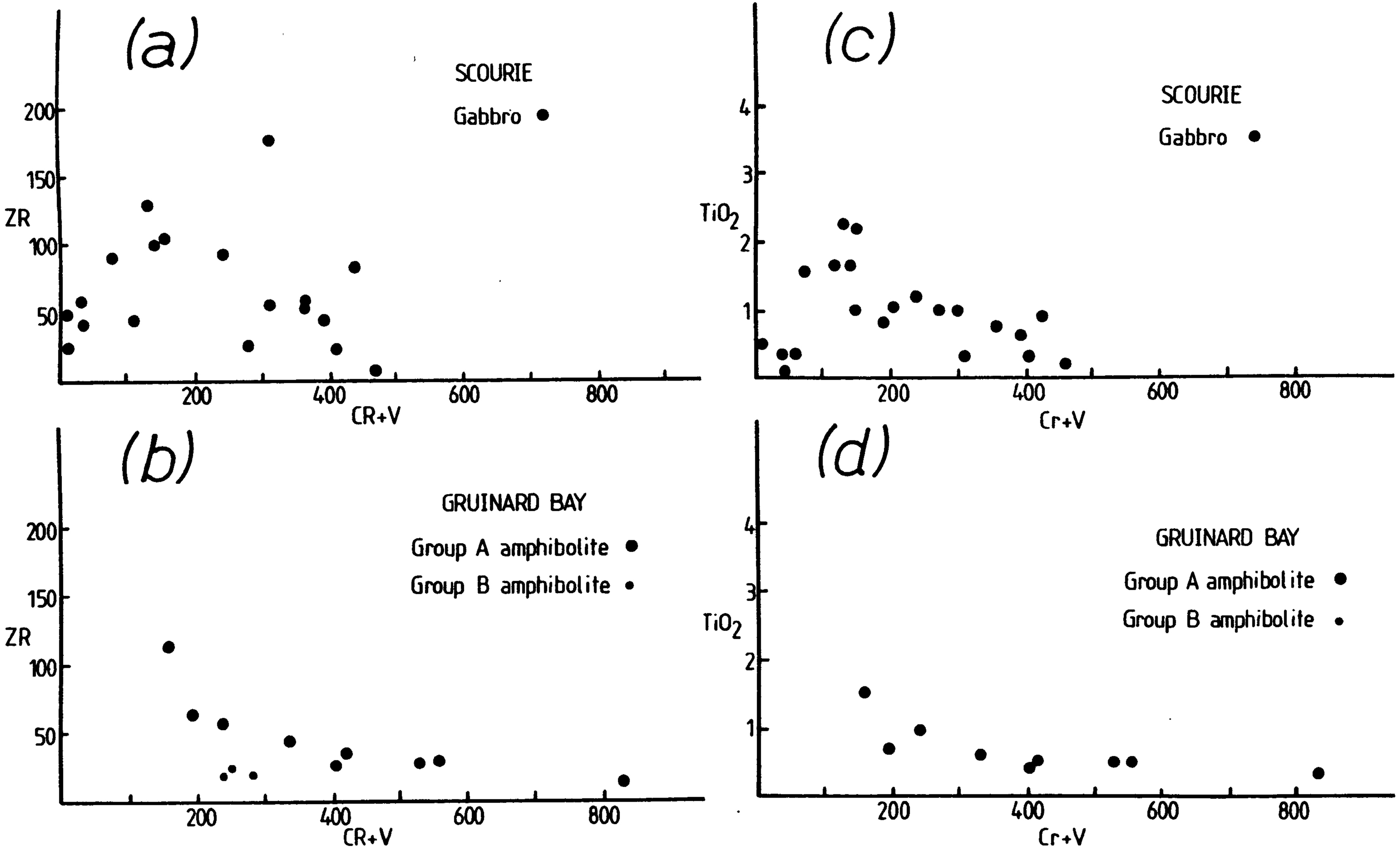

FIGURE 9. Plots of Zr vs Cr+V (a & b) and TiO_2 vs Cr+V (c & d) for Scourie gabbros and Gruinard Bay amphibolites. Similar trends are apparent in the two groups of rocks although there is greater scatter in the data from Scourie.

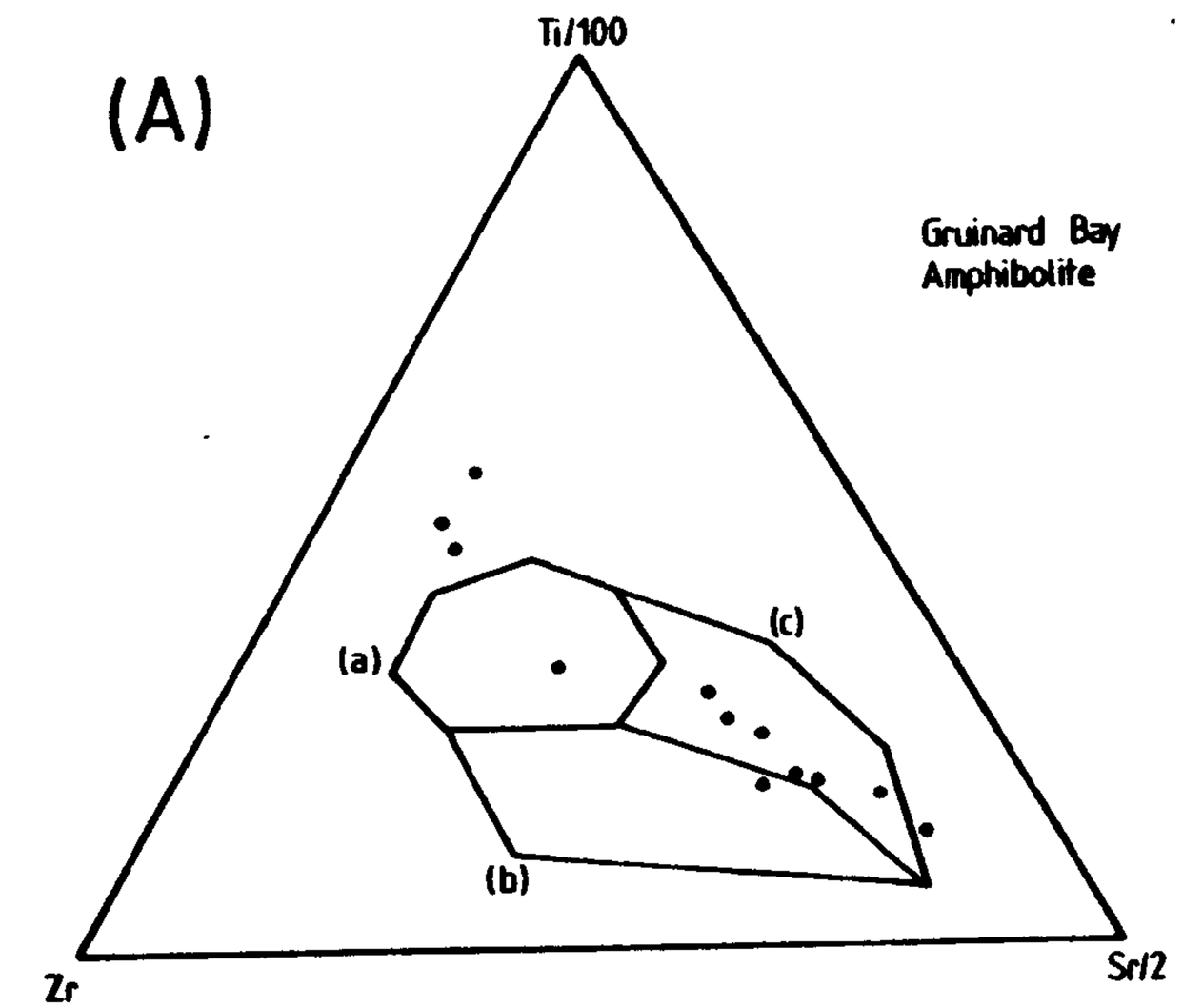

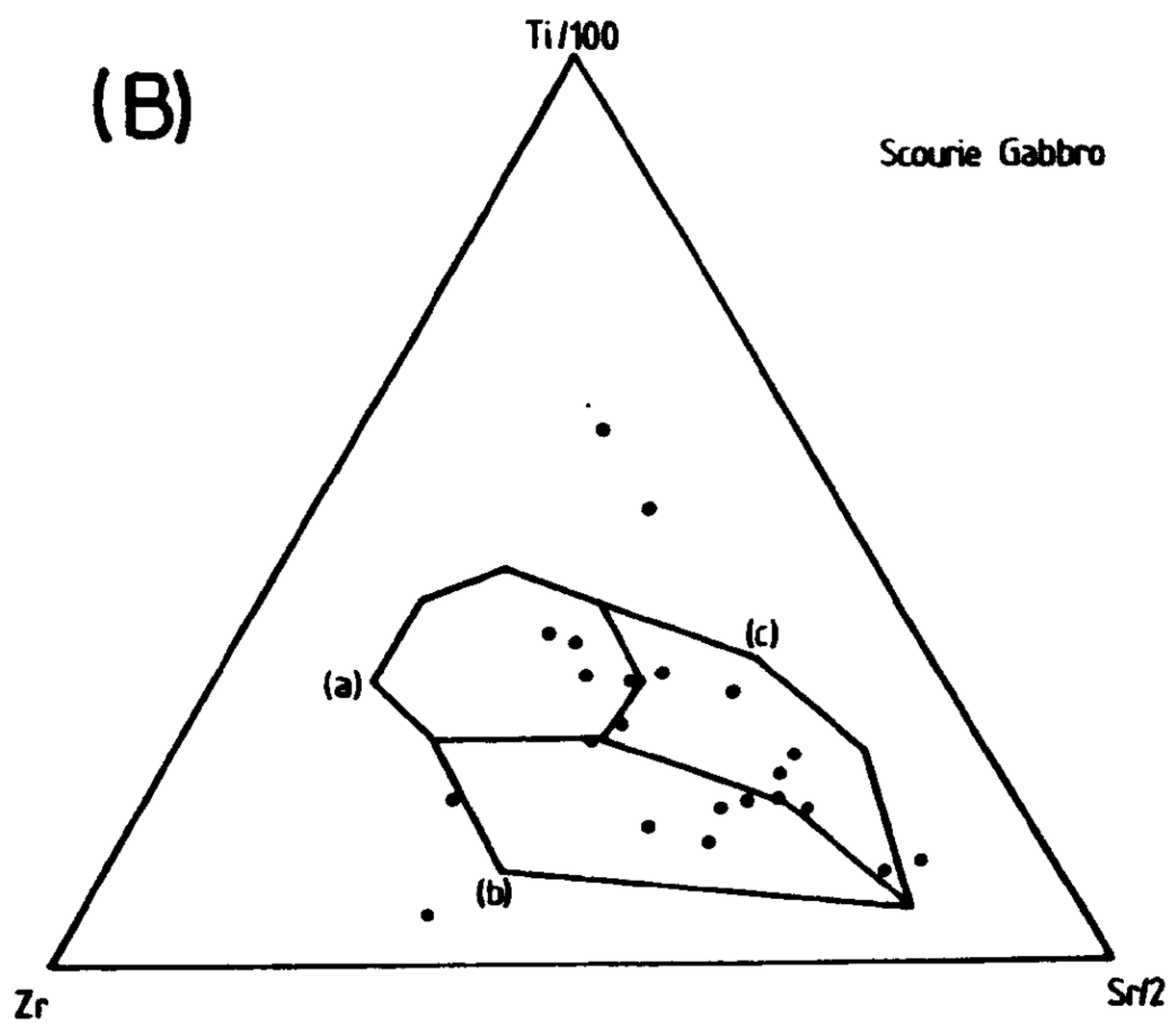

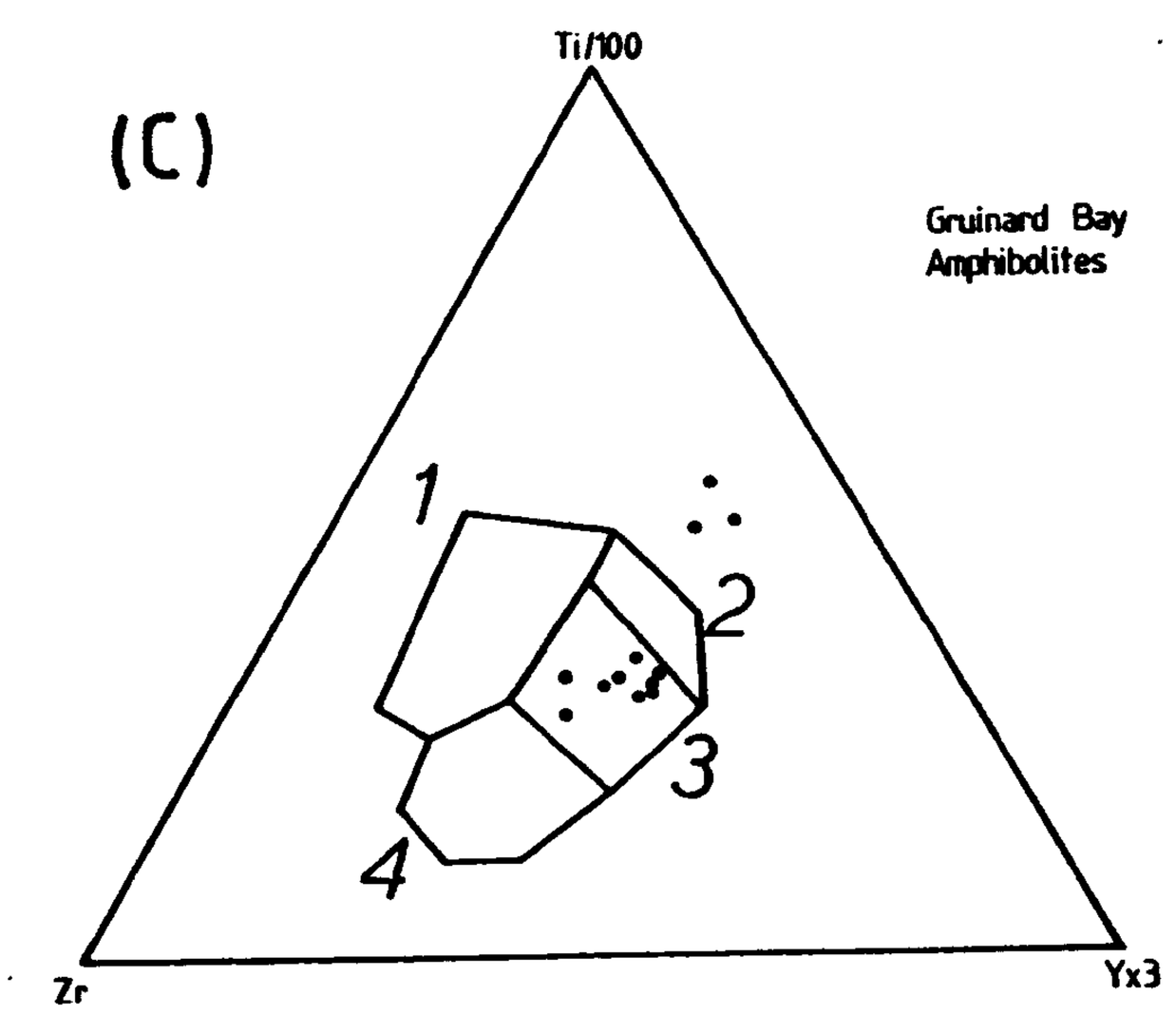

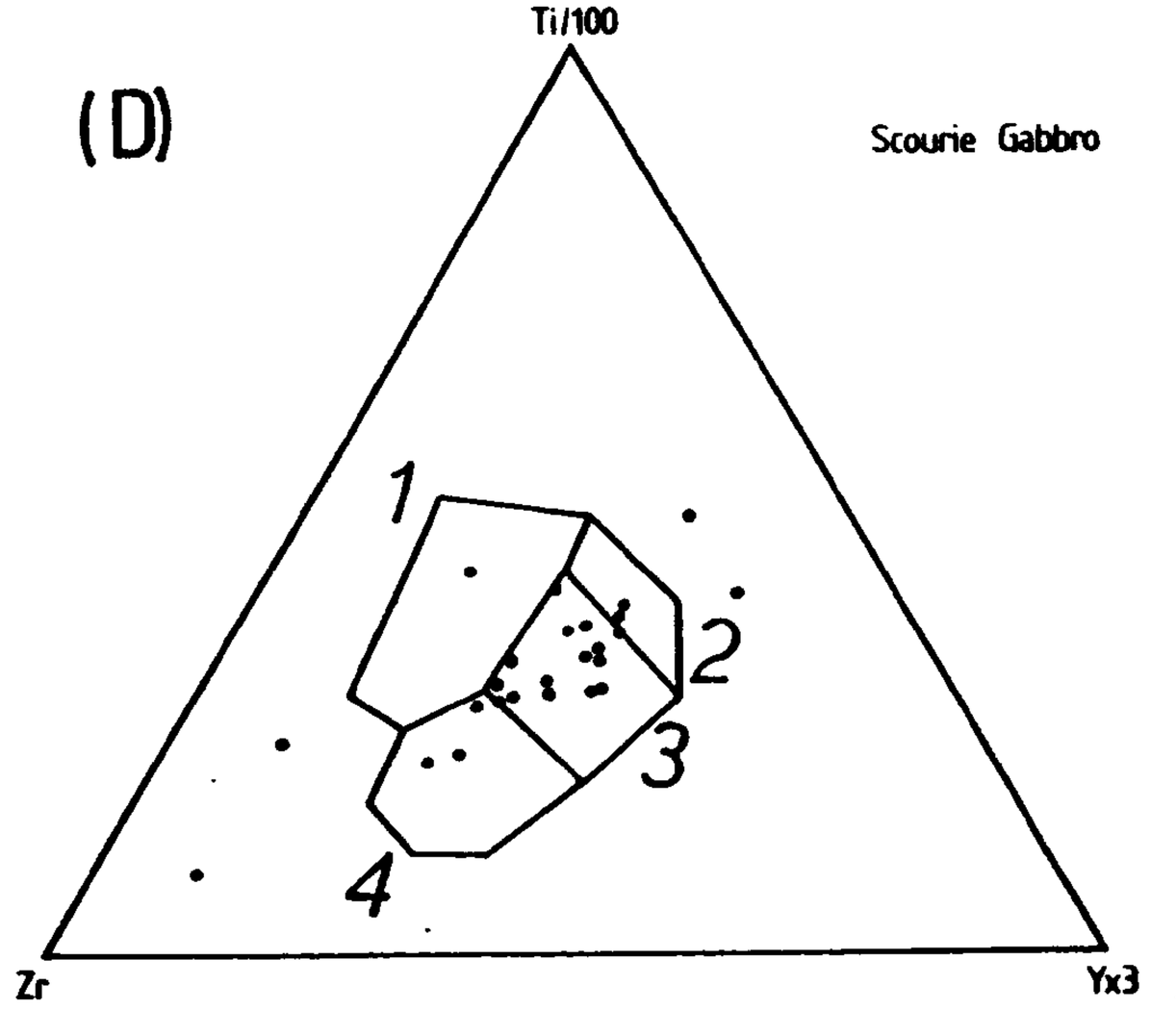

FIGURE 10. (A & B) Ti-Sr-Zr plot for Gruinard Bay amphibolite and Scourie gabbros.Ocean floor basalts plot in field (a) calc alkaline basalts in field (b) and low-potassium tholeiites in field (c). Gruinard Bay amphibolites define two groups but most analyses scatter away from the Sr apex in the field of low-K tholeiites. The Scourie gabbros show no consistent pattern.
(C & D) Ti-Zr-Y plot for Gruinard Bay amphibolites and Scourie gabbros. Ocean island and continental basalts plot in field 1, ocean floor basalts in field 3, low-K tholeiites in fields 2 and 3 and calc alkali basalts in fields 3 and 4. The Gruinard Bay amphibolites define two groups but most analyses fall in the field defined by low-K tholeiites and calc alkali basalts. The Scourie gabbros scatter away from the Zr apex and show no consistent grouping.

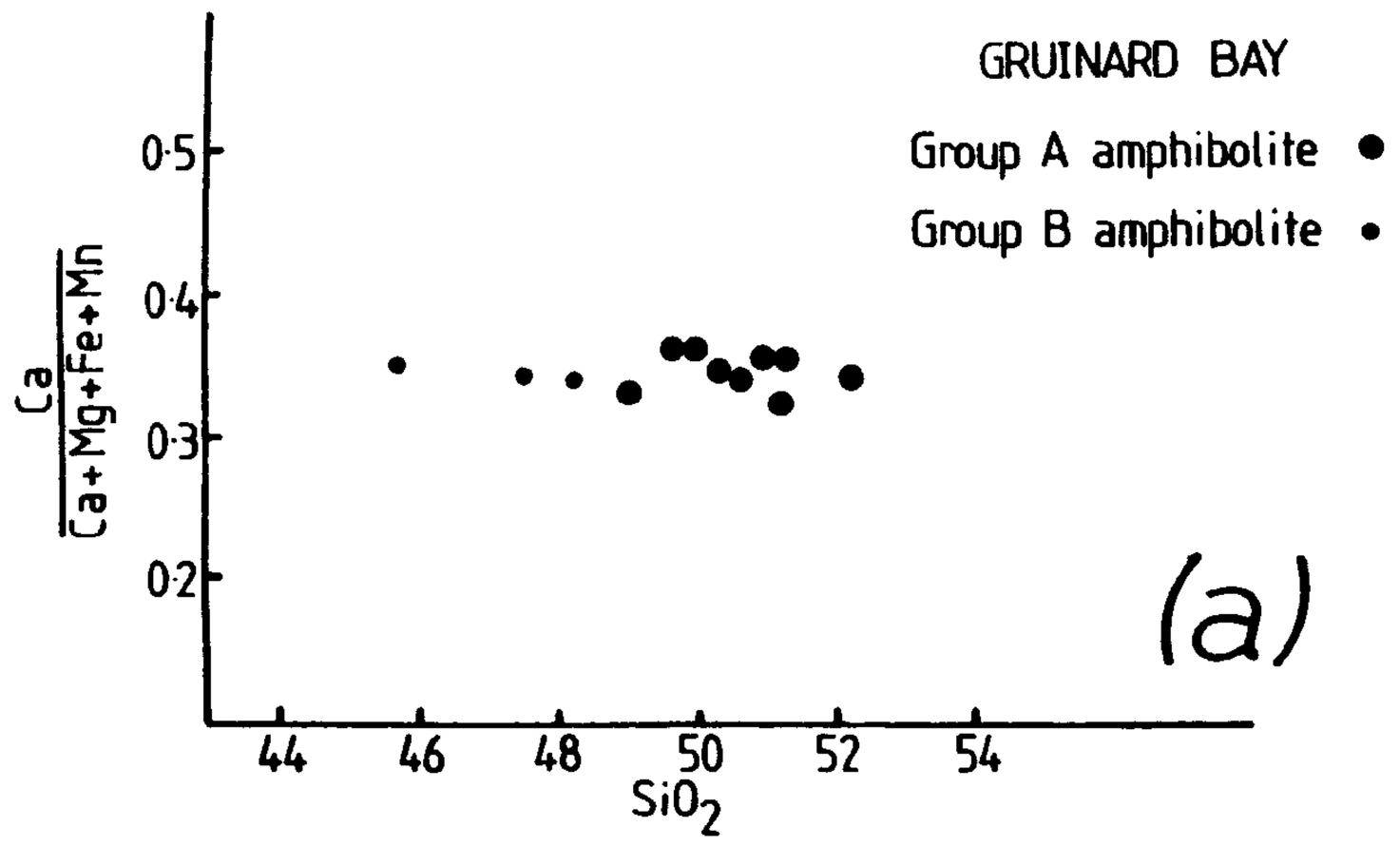

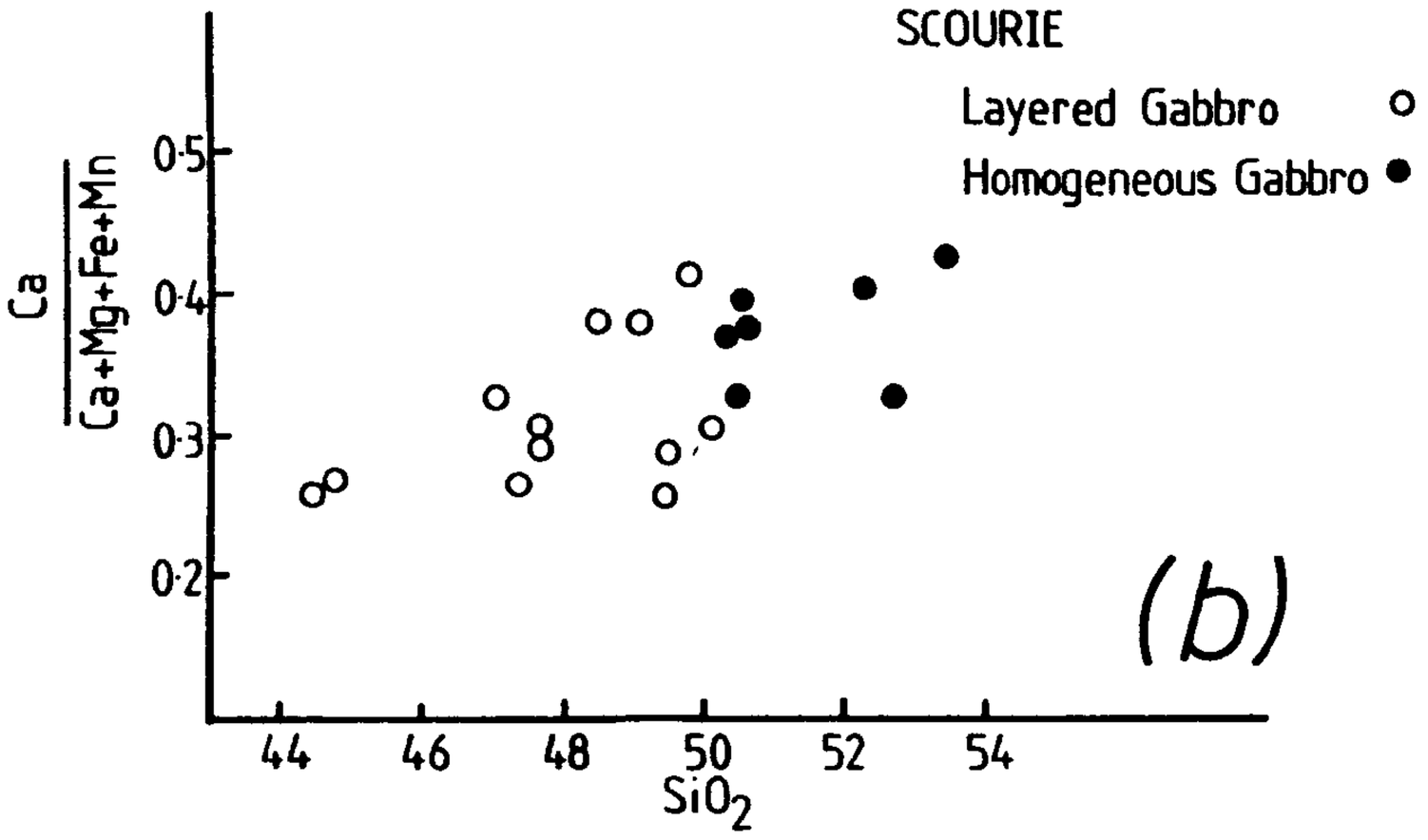

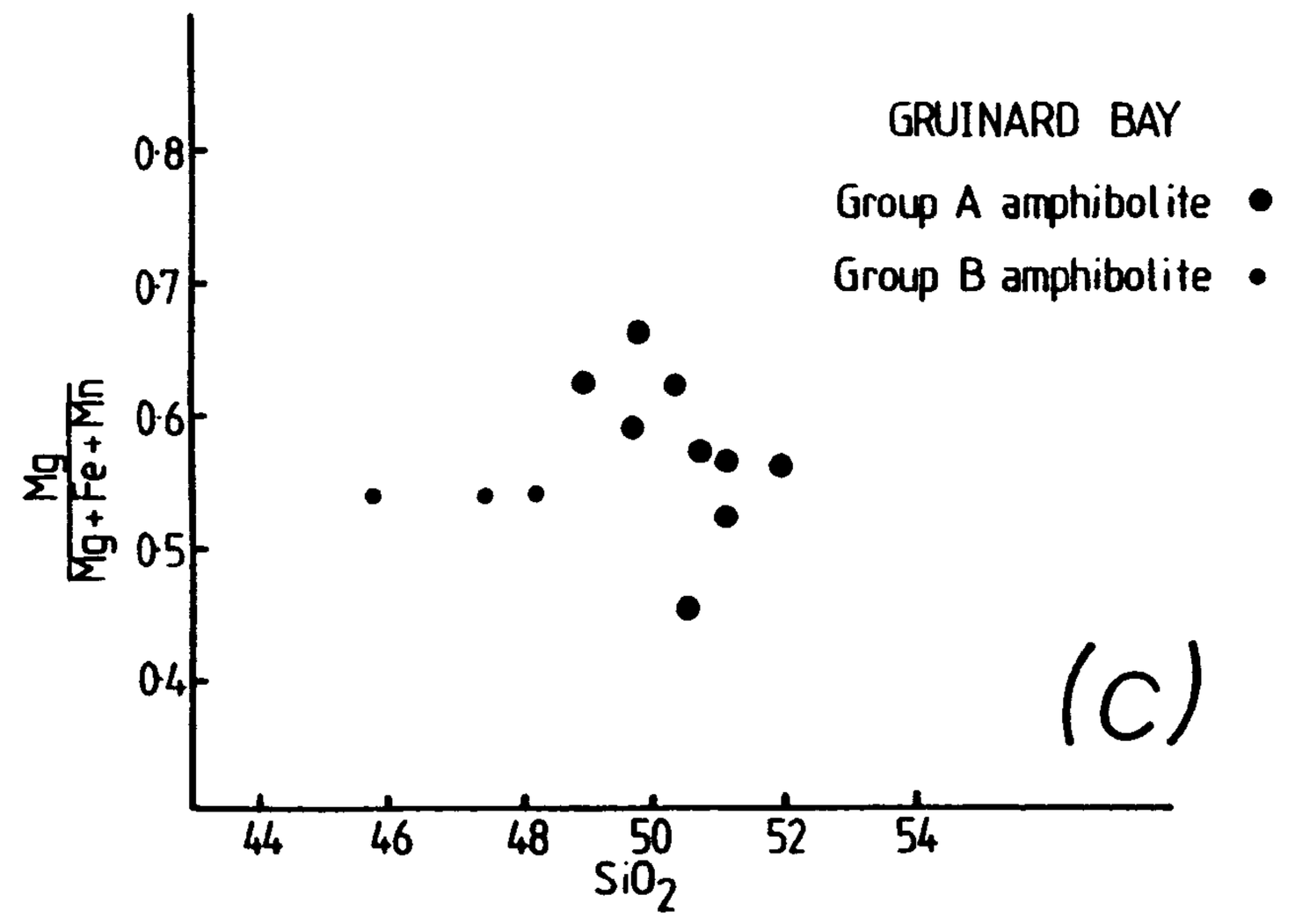

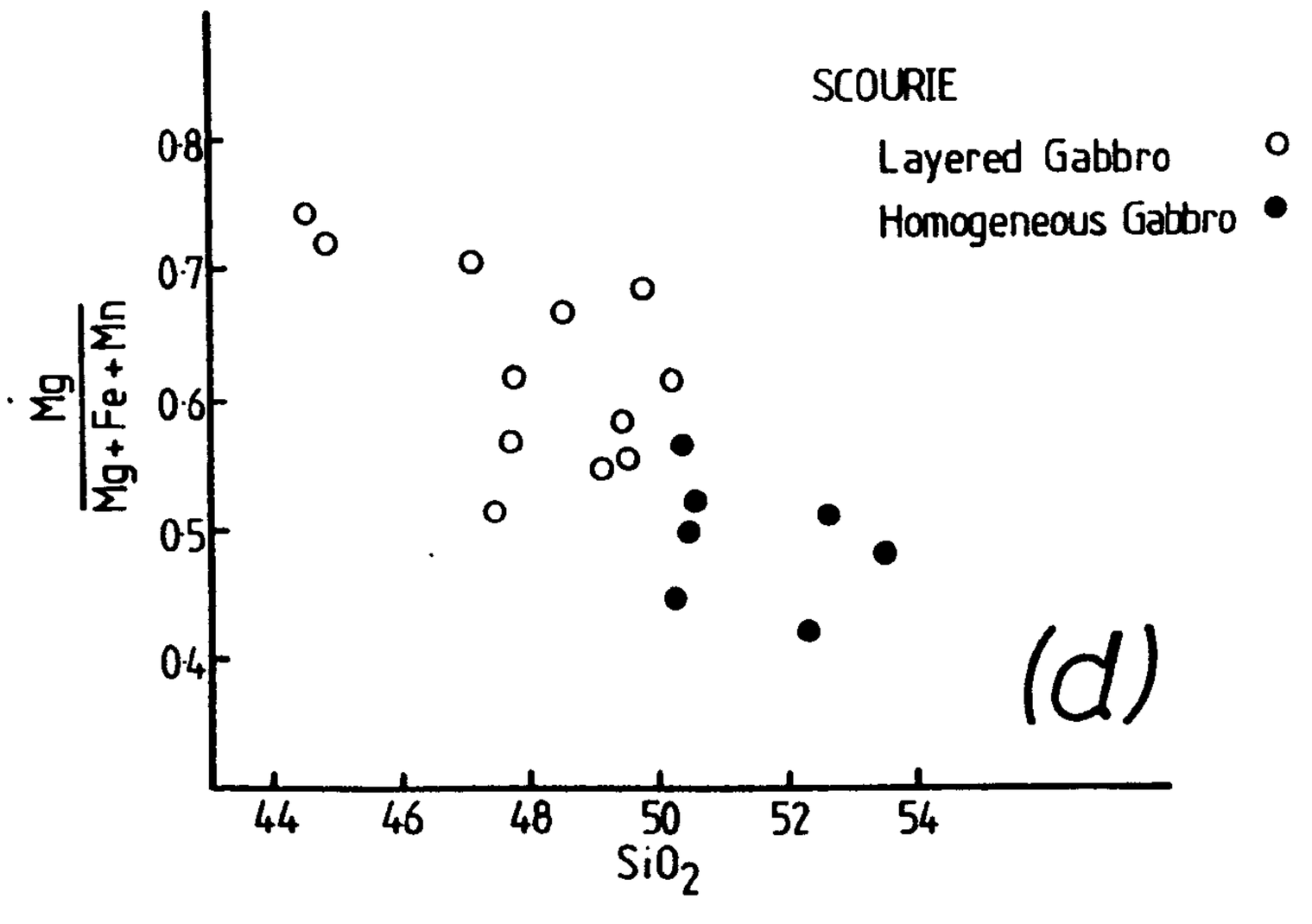

FIGURE 11. (A & B) variation in Ca/Ca + Mg + Mn + Fe(tot) with SiO_2 in amphibolites from Gruinard Bay and gabbros from Scourie. The amphibolites show no variation indicating that chemical variations are not due to the fractionation of a calcic phase. (C & D) variation in Mg/Mg + Mn + Fe(tot) with SiO_2 in amphibolites from Gruinard Bay and gabbros from Scourie. Both data sets indicate that a magnesian phase has fractionated.

TABLE 2 A Summary of expected and observed inter-element correlations for residual phases in equilibrium with basaltic melts with the composition of the Gruinard Bay amphibolites and the scourie gabbros

Major residual phase	Correlation expected in melt		Amphibolite	Gabbro
Garnet	Y - Zr	negative	No < 20%	No
	Y - Ti			
Olivine	Ni - Mg	positive	No < 10%	No
	Ti - (Cr+V)	positive	No	No
	Zr - (Cr+V)			
Plagioclase	Ti - (Cr+V)	positive	No	Some
	Zr - (Cr+V)			
Ilmenite	Fe - Ti	positive	Yes	
	Ti-Cr	positive	No	
	Ti - Nb	negative	No	No
	Ti - Zr			
Spinel	Mg - Al	positive	No	
Magnetite	Fe - Ti	positive	Yes	
	Ti - Cr	positive	No	
Hornblende	Ti - (Cr+V)		< 25%	
Clinopyroxene	Zr - (Cr+V)	negative	Yes < 33%	Yes
Orthopyroxene			< 67%	
Hornblende Clinopyroxene	Ca/Ca+Mg+Fe+Mn - SiO_2	positive	No	Possible
Orthopyroxene	Mg/Mg+Fe+Mn - SiO_2	positive	Yes	Yes
	Mg - Ti	negative	Yes	

and K/Rb in unaltered basalts from the mid Atlantic ridge and they proposed that the ratio Zr/Nb may be as useful in characterising a mantle source region as the K/Rb ratio. Gabbros from Scourie and Badcall and amphibolites from Gruinard Bay have a wide range of K/Rb ratios (400 - 1000) and a restricted range of Zr/Nb ratios (gabbros 5 - 25, and one at 60; amphibolites 8 - 23 and one at 44) suggesting that they may be from a similar source but that K and Rb have changed during metamorphism.

Amphibolites at Gruinard Bay are enclosed in rocks which are relatively rich in K and Rb; these two elements are very mobile under amphibolite facies conditions and are likely to have migrated into amphibolite. It is suggested that this accounts for the range in K/Rb ratios and the scatter of points towards K_2O in the TiO_2-P_2O_5-K_2O diagram (after T.H. Pearce, 1975) (Fig. 12).

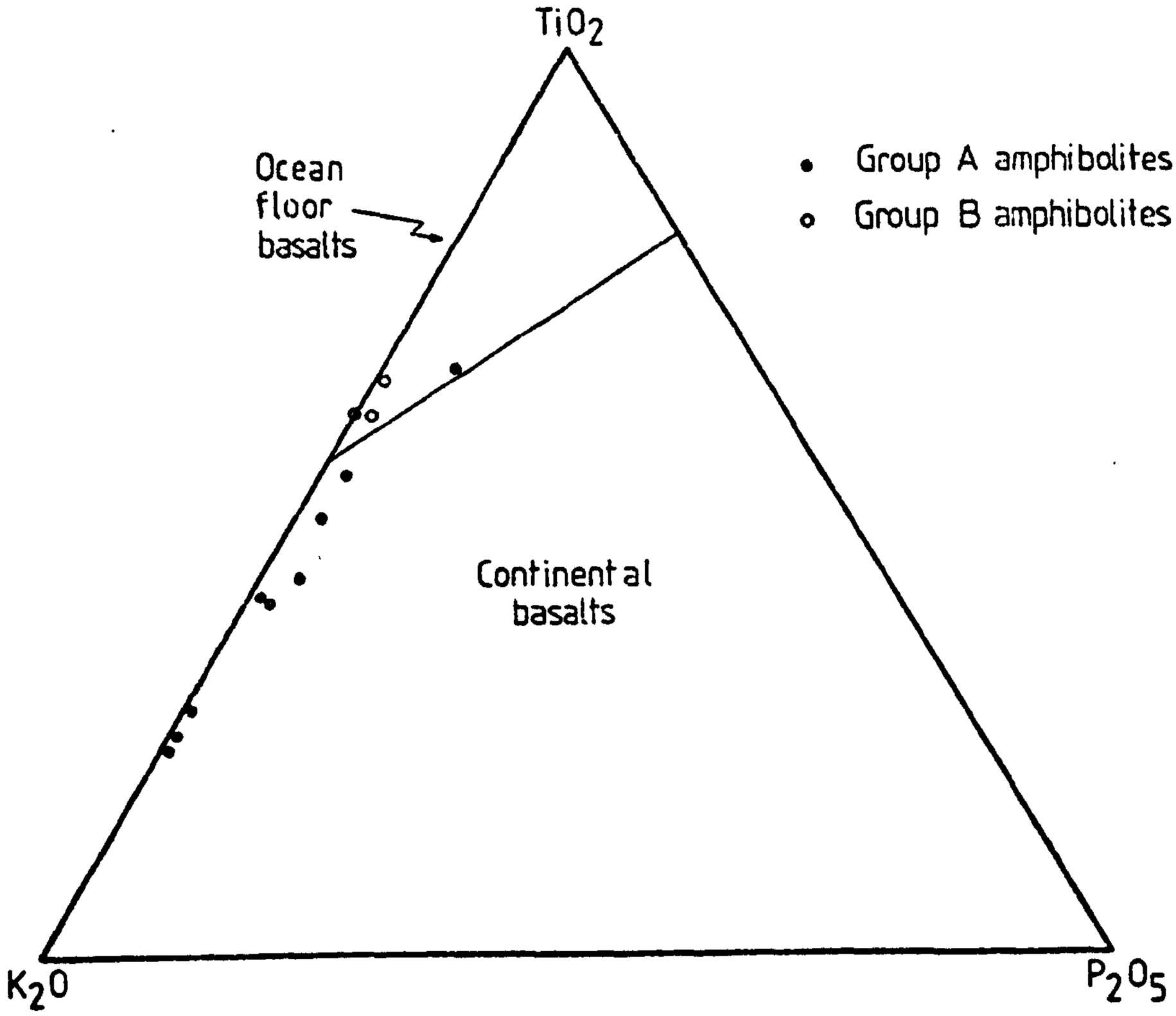

Fig. 12. Variation in TiO_2, K_2O and P_2O_5 in Gruinard Bay amphibolites, showing the wide range in K_2O content produced by the migration of K into the amphibolites during metamorphism.

(After T.H. Pearce et al., 1975)

Sample 109 with the lowest observed K and Rb and the highest K/Rb is the only amphibolite to contain relict pyroxene and occurs as a large raft 300m long and 100m wide veined with trondhjemite and is regarded as the least altered with respect to K and Rb. The scatter of points towards Sr in the plot Ti - Zr - Sr (Fig. 10) suggests that Sr was also mobile in the amphibolites.

The tectonic setting of basic rocks using immobile element ratios

Several classifications relating basic volcanics to their magma type and tectonic setting by means of 'immobile' trace element concentrations have been proposed. Pearce and Cann (1971, 1973) suggested a scheme based on Ti, Zr and Y and for less altered rocks Ti, Sr and Zr. T.H. Pearce et al., (1975) distinguished between oceanic and non oceanic basalts using TiO_2, K_2O and P_2O_5. Floyd and Winchester (1975) proposed a scheme based on Ti, Nb, Y, P and Zr to discriminate between tholeiitic and alkali basalts. Bloxham and Lewis (1972) used Ti, Cr and Zr to discriminate between ocean tholeiite, island arc tholeiite, calc alkali basalt and alkali basalt. More recently J. Pearce (1976) and T.H. Pearce (1977) developed classifications based on major elements.

The application of discrimination diagrams to identify tectonic setting can be criticised on several grounds:

(1) the empirical nature of the method; although partition coefficients are now available for immobile elements between basaltic liquid and mantle minerals and it is possible to derive a theoretical basis for discrimination diagrams (Pearce, 1978).

(2) their restricted application to relatively unaltered basaltic compositions ($12\% < CaO + MgO < 20\%$); when they

are applied to amphibolites and gabbros and dolerites (which may be highly fractionated) (i.e. indiscriminate discriminant analysis) there are large uncertainties.

(3) the method does not always work; Morrison (1978) found that basalts from the British Tertiary volcanic province plot in the fields of low alkali tholeiites, within plate basalts and calc alkali basalts; Deitrich et al., (1978) found that basalts from the Marianas trench plot in the fields of ocean floor basalts, within plate basalts and calc alkali basalts.

Nevertheless, these schemes have given geologically sensible answers when applied to both Phanerozoic orogenic belts (Bickel and Nesbit, 1972; Floyd et al., 1976; Pearce, 1975) and Archaean greenstone belts (Hallberg and Williams, 1972; Winchester and Floyd, 1976; T.H. Pearce et al., 1975) and in order to further test the applicability of this method amphibolites from Gruinard Bay are plotted on a series of immobile element variation diagrams. Morrison (1978) pointed out that the discriminant approach is useful even if it only identifies separate magma types and does not correctly classify them according to tectonic setting.

The tectonic setting of the Gruinard Bay amphibolites

The Ti-Zr-Y, Ti-Zr-Sr, Ti-Zr and Nb/Y-Zr/P_2O_5 diagrams of Pearce and Cann (1973) and Floyd and Winchester (1975) demonstrate that there are two types of amphibolite at Gruinard Bay (Figs. 7, 10, 13).

Group A amphibolites. Analyses cluster in the field which includes ocean floor basalts and volcanic arc basalts on the Ti-Zr-Y diagram and lie on a trend away from the Sr apex on a Ti-Zr-Sr diagram in the field of low - K tholeiites. They plot in the field of low-K tholeiites on a Ti-Zr diagram and in the field

of tholeiitic basalts on an $Na_2O + K_2O - SiO_2$ diagram (Fig. 13c) and in the field of oceanic tholeiites on Zr/P_2O_5 - Nb/Y, TiO_2-Y/Nb and TiO_2-Zr diagrams (Figs. 13a, b, 7).

Group B amphibolites. Three samples from an amphibolite raft in trondhjemite 10m long and 2m wide which is more strongly banded than other amphibolites cluster separately on most diagrams. These rocks have komatiitic affinities (CaO/Al_2O_3>1.0, MgO≈9.0, K_2O<0.9; Brooks and Hart, 1974); they are depleted in K, Rb, Sr, Zr, Na and Ce and enriched in TiO_2 relative to Group A amphibolites and they have higher K/Rb and La/Ce ratios and a lower $(Ce/Y)_n$ ratio. Although they are slightly altered (biotite and epidote in thin section) the low concentrations of K and Rb argue against extensive alteration. In several respects Group B amphibolites resemble sample 109 from group A which has the lowest concentration of K and Rb and Sr, the highest K/Rb ratio a high La/Ce ratio and a low $(Ce/Y)_n$ ratio and is probably the least altered of the group A amphibolites (see Table 3). Group B amphibolites lie in the field of ocean floor basalts on a TiO_2-K_2O-P_2O_5 diagram and Group A amphibolites define a K-enrichment trend away from these points into the field of continental basalts (Fig. 12); clearly the mobility of K in these rocks renders this classification meaningless.

If the absolute abundances of elements are considered (Table 4), group A and B amphibolites closely resemble island arc tholeiites, although Ni is higher than the quoted values. The Ce/Y ratios for the two groups of amphibolites are closer to the quoted values for marginal basin basalts than mid-ocean ridge basalts (Fig. 14), Tarney and Windley (1977) but have slightly lower Y. Tarney and Saunders (1978) report basalts from the Scotia Sea with low abundances of Ti, Zr, Nb and Y and higher K, Rb, Ba and Sr than mid-ocean ridge

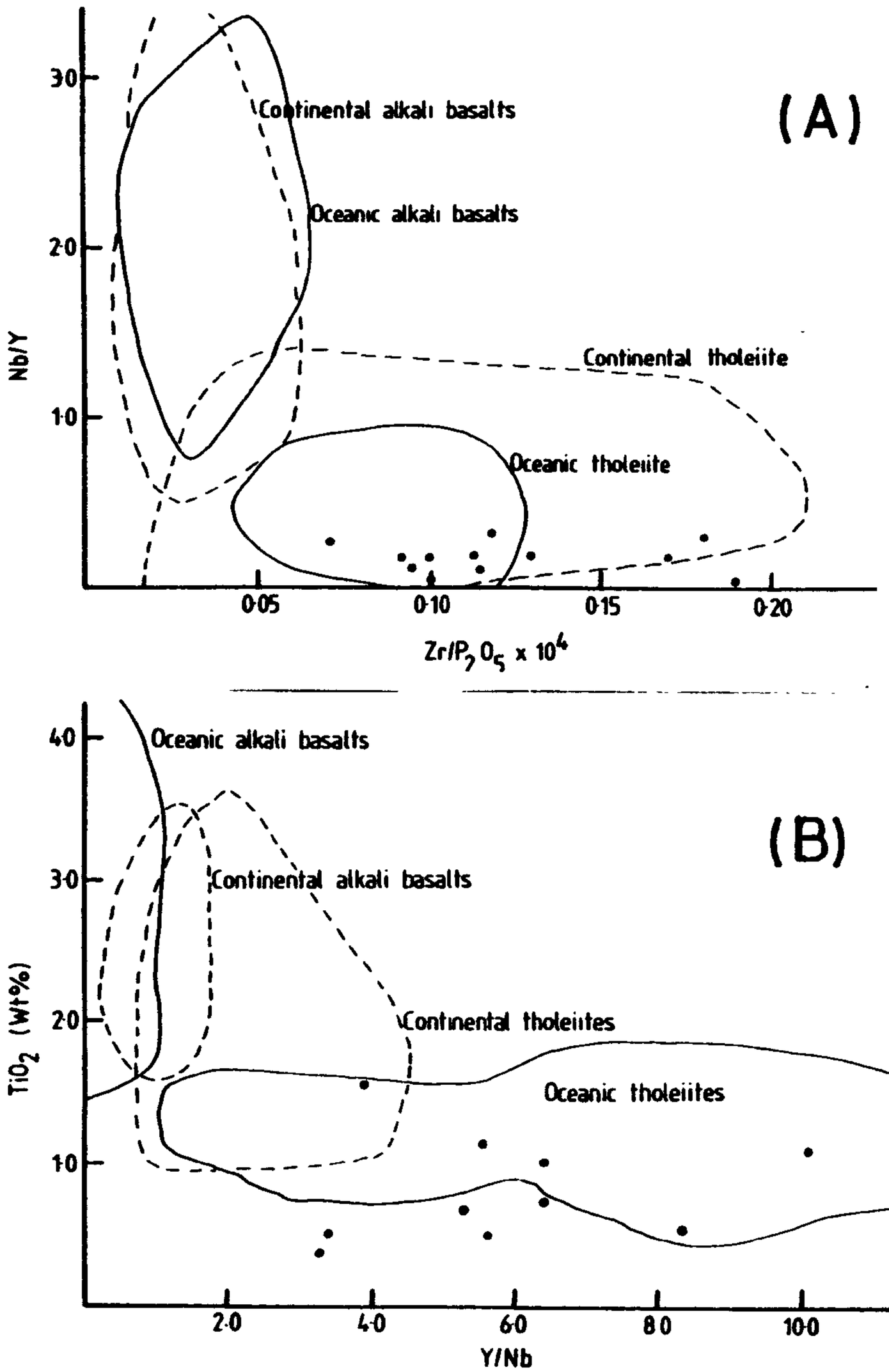

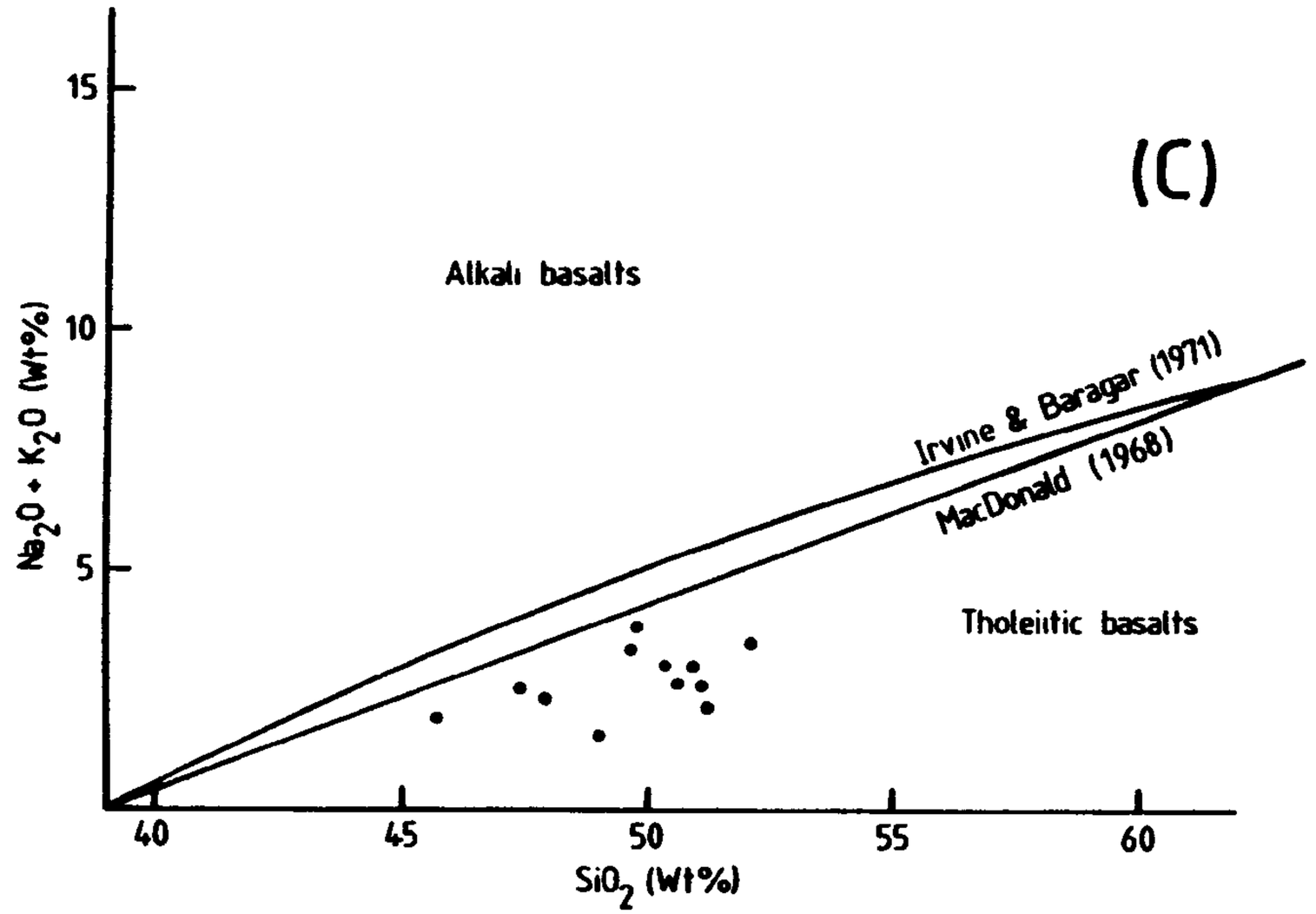

FIGURE 13. (A & B) Nb/Y vs Zr/P_2O_5 and TiO_2 vs Y/Nb diagrams after Floyd and Winchester (1975) showing the fields of continental and oceanic tholeiitic and alkali basalts. Gruinard Bay amphibolites plot as oceanic tholeiites. (C) $Na_2O + K_2O$ vs SiO_2 diagram showing the fields of alkali and tholeiitic basalts after Irvine and Baragar (1971) and MacDonald (1968). Gruinard Bay amphibolites plot as tholeiitic basalts.

TABLE 3 Gruinard Bay amphibolites

	Group A (mean)	109 (Group A)	Group B (mean)
No. of analyses	9	1	3
TiO_2	0.72	0.55	1.16
Y	16.7	11.7	17
Sr	220	110	108
K	8400	4600	6000
Rb	15	4.5	3.5
Ni	106	146	133
Ce	18	4.8	6.2
La	9.7	10.1	7.3
Zr	47.7	28.5	19.7
Nb	3.17	1.4	1.5
K/Rb	560	1022	1731
La/Ce	0.53	2.10	1.18
$(Ce/Y)_N$	2.34	0.86	0.76
Zr/Nb	15	20	13

TABLE 4. A comparison between the trace element chemistry of the Gruinard Bay amphibolites and present-day basalts.

Locality	K(ppm)	Rb	Sr	Y	Zr	Nb	Ti(ppm)	Ni	Ref.
GRUINARD BAY									
Group A	8400	15	220	17	48	3·2	4316	106	
109	4600	4·5	110	12	29	1·4	3297	146	
Group B	6000	3·5	108	17	20	1·5	6954	133	
ISLAND ARC THOLEIITE									
	–	–	207	19	52	1·5	5150	–	1.
	3652	5	200	19	70	–	4766	30	7.
S.Sandwich Is.	2241	6·5	128	–	–	–	5246	38	4.
MARGINAL BASIN									
Scotia Sea	–	5	220	29	–	–	–	180	2·
Marianas	3547	4	208	–	–	–	8933	69	6.
W. Marianas	1577	11	108	36	94	3·5	10029	98	8.
" metagabbro	374	11	82	19	24	10	3145	201	8.
Sarmiento ophiolite	–	2	236	27	–	–	–	118	2.
CALC ALKALI BASALT									
	–	–	375	23	106	2·5	5400	–	1.
OCEAN ISLAND THOLEIITE									
	–	–	438	29	215	32	16250	–	1.
CONTINENTAL THOLEIITE									
	–	–	460	29	215	20	15150	–	1·
OCEAN RIDGE BASALT									
	–	–	131	30	92	5	8350	–	1.
	–	1·1	135	43	–	–	–	110	2.
	1079	–	–	24	49	6·9	6020	204	3.
ARCHAEAN BASALTS									
E. Goldfields	1494	9	105	–	61	–	5664	170	5.
mean	–	6·4	153	18	–	–	–	120	2.

References.

1. Pearce & Cann, 1973.
2. Tarney et al., 1976.
3. Langmuir et al., 1977.
4. Hawksworth et al., 1978.
5. Hallberg & Williams, 1972.
6. Hart et al., 1972.
7. Jakes & White, 1972.
8. Dietrich et al., 1978.

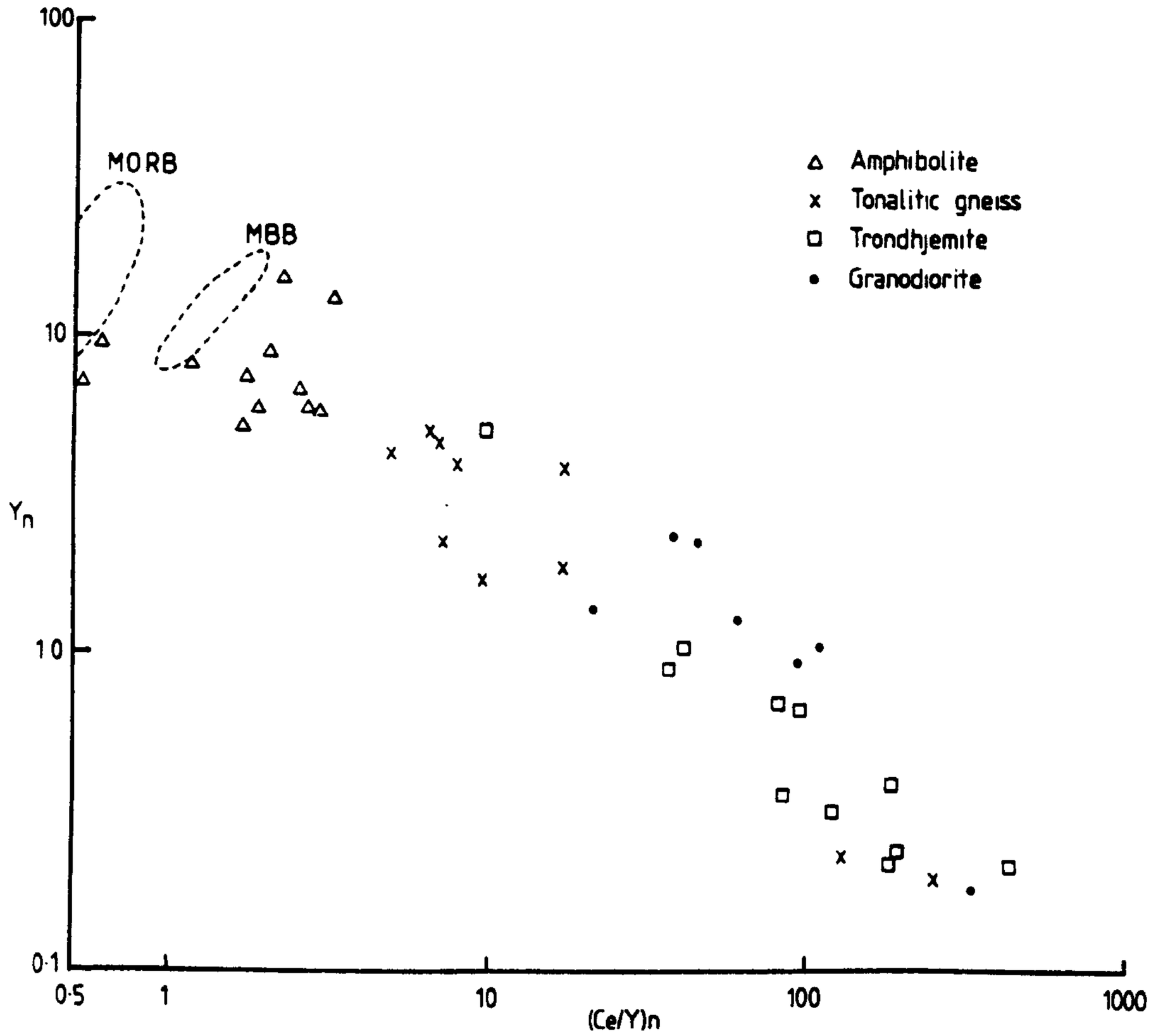

FIGURE 14. Y vs Ce/Y for amphibolites, tonalites, trondhjemites and granodiorites from Gruinard Bay; all values are chondrite normalised using the data of Herrmann (1974). MORB mid ocean ridge basalt, MBB marginal basin basalt.

basalts and $(Ce/Y)_n$ ratios in the range 0.9 to 1.43 which are higher than mid-ocean ridge basalts; these basalts are also chemically similar to the Gruinard Bay amphibolites.

In summary therefore, it is not clear whether the Gruinard Bay amphibolites were originally gabbros or basalts, nevertheless the liquid from which they were derived has not fractionated greatly in situ, in contrast to similar rocks in the Scourie area, and has a composition that is similar to tholeiitic basalts found in present day island arcs and some marginal basins. This conclusion is broadly consistent with the discriminant approach of Pearce and Cann (1971) and Floyd and Winchester (1975) based on immobile trace element ratios.

6. THE GEOCHEMISTRY OF THE ACID GNEISSES

Relations in the system Qz-Ab-Or-An-H_2O

The high proportion of normative quartz, albite, orthoclase and anorthite in the acid gneisses means that they can be described in the system Qz-Ab-An-Or-H_2O; the sum of the normative components Qz-Ab-An-Or in tonalitic gneiss is greater than 75% (mean 84%), in trondhjemites greater than 80% (mean 93%) and in granodiorites greater than 92% (mean 94%). It is not possible, however, to relate directly the composition of these rocks to experimentally determined phase boundaries in the system Qz-Ab-An-Or-H_2O, since the water content and equilibration pressure of the melts from which they crystallised are not known.

The normative proportions of Qz-Ab-Or-An in tonalites, trondhjemites and granodiorites are plotted in Fig. 15; the main features of this diagram are:

(i) trondhjemite and tonalite define a trend parallel to the Qz-Ab side of the Qz-Ab-Or projection

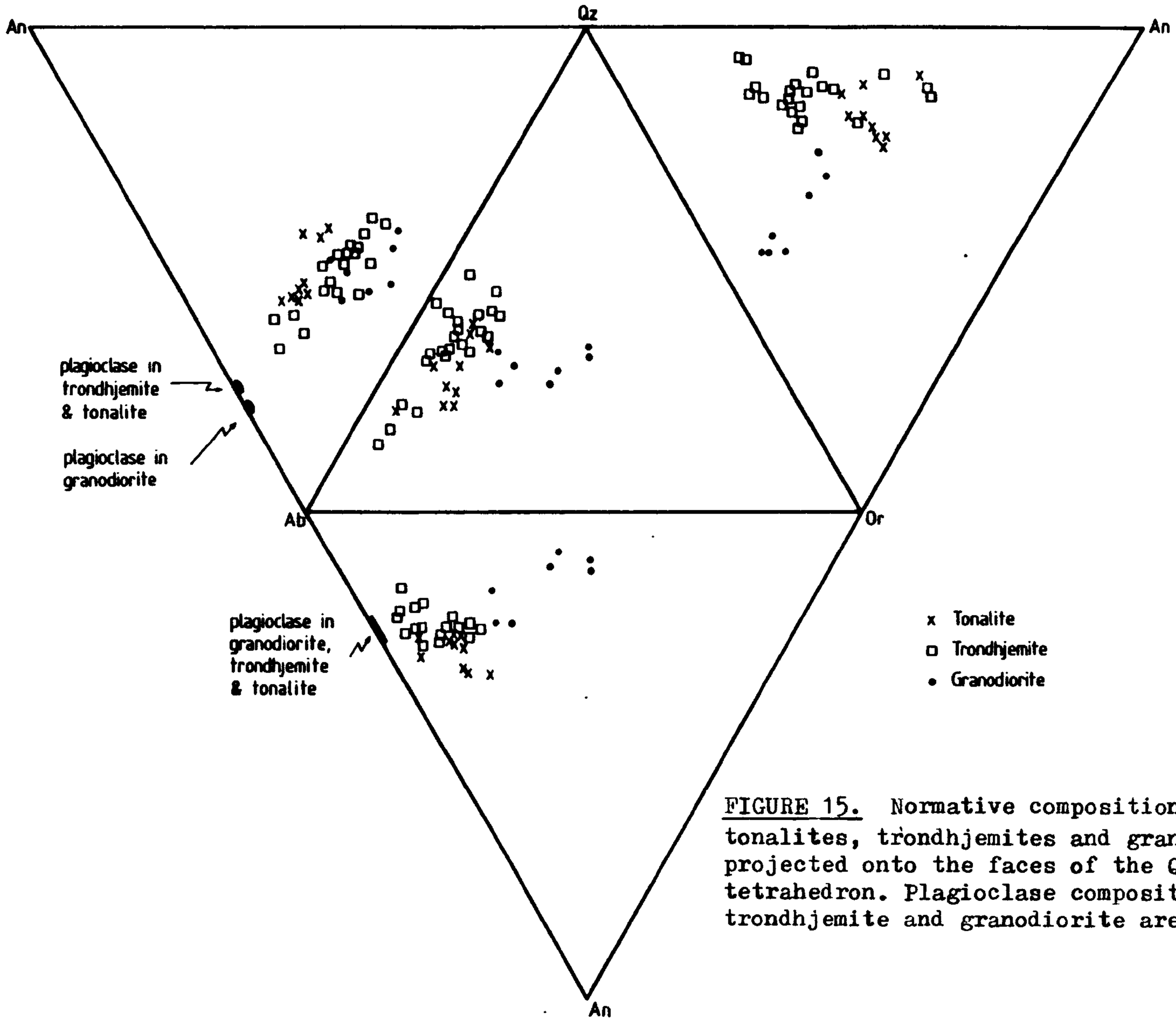

FIGURE 15. Normative composition of Gruinard Bay tonalites, trondhjemites and granodiorites projected onto the faces of the Qz - Ab - Or - An tetrahedron. Plagioclase compositions in tonalite trondhjemite and granodiorite are also shown.

(ii) tonalite is more anorthite rich than the trondhjemite

(iii) granodiorite defines a trend close to the quartz feldspar cotectic at high pH_2O in the Qz-Ab-Or projection.

It is possible to estimate which phases are responsible for the variation in Qz-Ab-An-Or by plotting major and trace element concentrations against Qz/Ab for trondhjemite and tonalite and Or/Ab for granodiorites (Figs. 16, 17). The results are summarised as follows:

a) although tonalite and trondhemite show parallel trends in the projection Qz-Ab-Or there are a number of important differences when major and minor elements are plotted against Qz/Ab (Fig. 16) indicating that the two trends represent different processes.

b) with an increase in Qz/Ab tonalites decrease in FeO, Cr+V, TiO_2, Ni, (Al_2O_3), and possibly Rb and increase in Sr. The Rb trend (mirrored by K and Ba) is equivocal; because these elements are incorporated into biotite, a late mineral in these rocks, these elements may reflect a post-magmatic process. Y decreases (poorly defined trend) with decreasing Qz/Ab indicating that the main variation in these rocks is caused by the fractional crystallisation of hornblende or various degrees of partial melting of a hornblende rich source.

c) trondhjemites decrease in Al_2O_3, and Sr and increase in Rb with increasing Qz/Ab. As has been discussed above, the variation in Al_2O_3 means that these trondhjemites defy the classification of trondhjemites proposed by Barker et al., (1976) based on high Al_2O_3 (greater than 15% Al_2O_3) and low Al_2O_3 (less than 15% Al_2O_3). The interpretation of these trends will be discussed below.

FIGURE 16. Plots of major and minor elements against normative Qz/Ab for trondhjemites (filled circles) and tonalites (crosses) from Gruinard Bay.

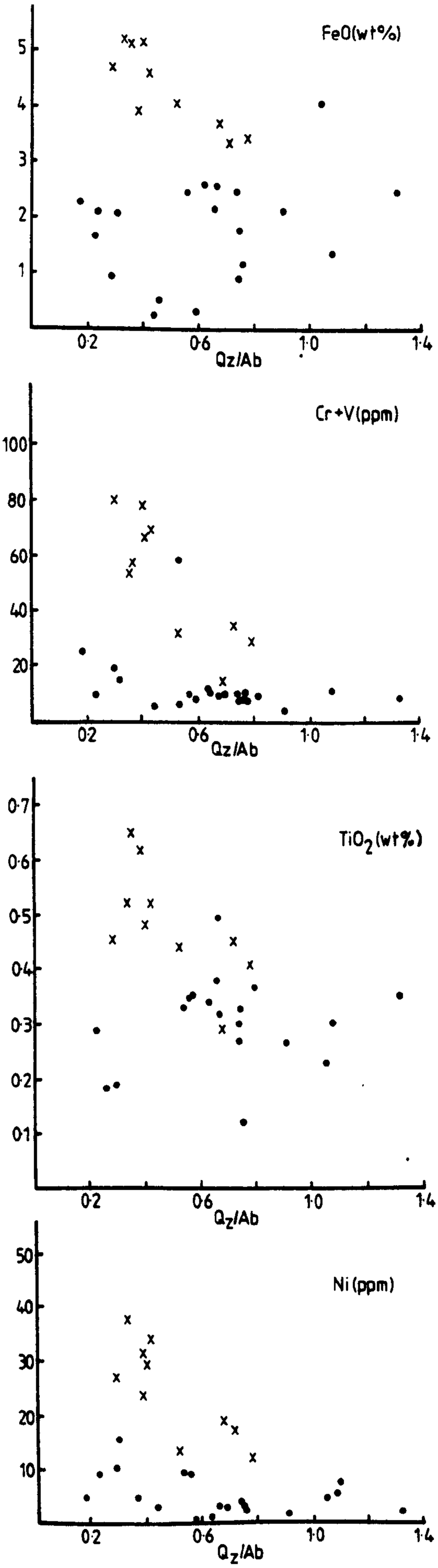

FIGURE 17. Plots of major and minor elements against normative Or/Ab for trondhjemites (filled circles) and granodiorites (open circles) from Gruinard Bay.

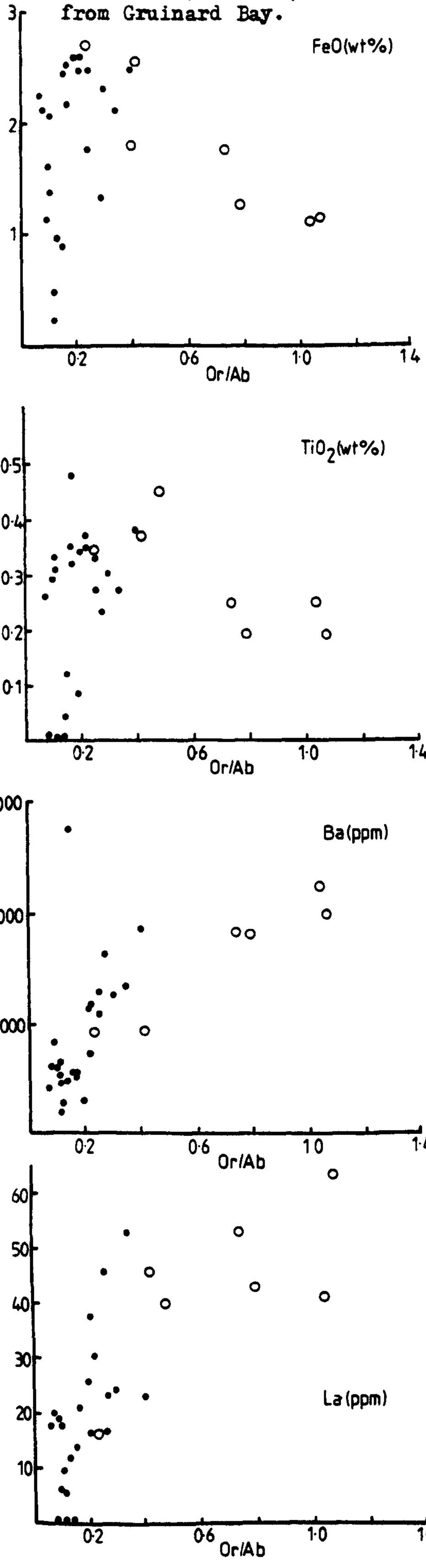

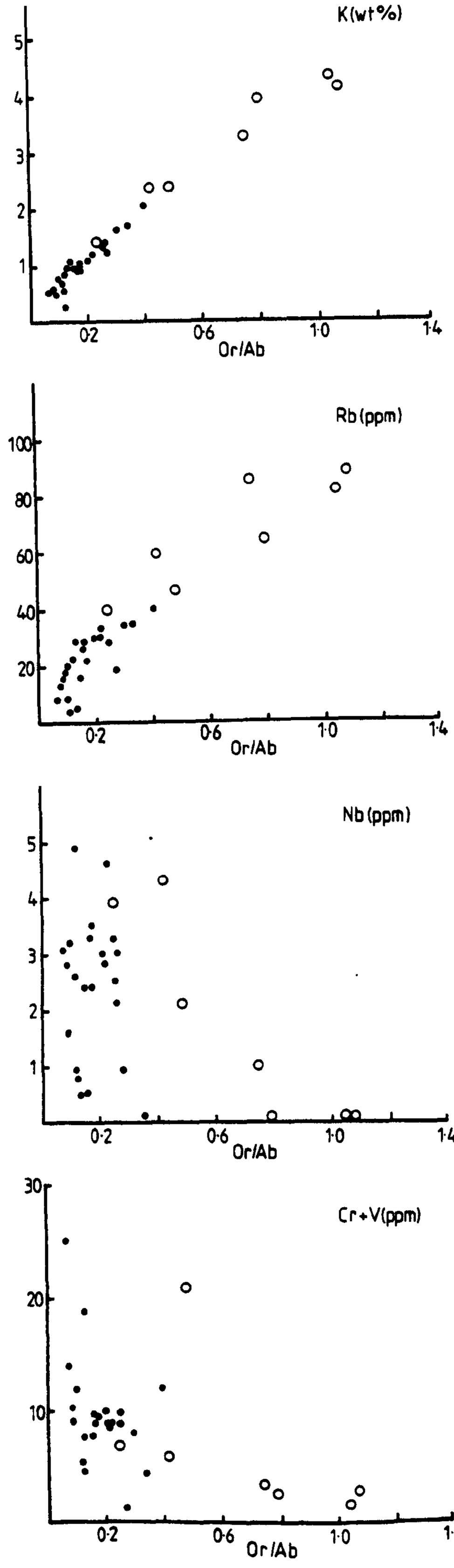

d) granodiorites decrease in FeO, TiO_2, Nb, Cr+V with increasing Or/Ab and increase in K (predictably!), Rb, Ba and La. Al_2O_3 is constant and Sr shows no trend. These data are consistent with the fractional crystallisation of hornblende, plagioclase and quartz from a trondhjemitic source.

Rare Earth Elements

The elements La and Ce are used to monitor the light REE and Y with the same charge and ionic radius as Ho to monitor the heavy REE. Tonalitic gneiss shows two types of REE fractionation (Fig. 14); the majority of samples are only moderately fractionated with $(Ce/Y)_n$ ratios in the range 5 - 17 but two samples contain a low birefringence white mica (possibly hydromuscovite) and are highly fractionated ($(Ce/Y)_n$ 130 and 250). White mica replaces hornblende, the main source of Y, in some trondhjemites and so the highly fractionated REE patterns may be a function of alteration during retrogression. Ba follows the REE in most tonalites and behaves as a super-light REE, but it does not always follow the light REE which may indicate that it has been altered in some rocks.

Trondhjemites are highly fractionated with $(Ce/Y)_n$ ratios in the range 10 to 400 (mean 240). Granodiorites are also highly fractionated with $(Ce/Y)_n$ in the range 21 to 110 (and one at 330) which are intermediate between tonalite and trondhjemite; the granodiorites are enriched in the light REE and Ba relative to trondhjemite and are slightly enriched in Y. Tonalites and trondhjemites show the same range of heavy REE depletion as the tonalite group in the Amitsoq gneisses of O'Nions and Pankhurst (1978) but are more strongly enriched in the light REE.

7. THE ORIGIN OF TONALITES AND TRONDHJEMITES AT GRUINARD BAY

Rubidium - strontium and lead isotope studies on tonalites and trondhjemites from the Scourian complex indicate that they

were derived from a low Rb/Sr source about 2.8 Ma ago (Moorbath et al., 1969; 1975; Chapman, 1978). This source could be the mantle, basic volcanic rocks or immature sediments derived from basic volcanic rocks (O'Nions and Pankhurst, 1978); the isotopic evidence however is incompatible with a derivation from quartzo-feldspathic rocks older than 3.0 Ma. It is unlikely that the large volume of trondhjemite can be derived by partial melting of short lived graywacke sediments as proposed by Arth Hanson (1978) for the quartz monzonite of Minnesota. There are three possible models for tonalites and trondhjemites whose origin is ultimately the mantle: (1) crystal fractionation of less siliceous, more mafic liquids under dry or relatively wet conditions (Arth et al., 1978); (2) partial melting of the basaltic parent of eclogitic, amphibolitic or gabbroic rock types (Arth and Hanson, 1972; 1975; Barker and Arth, 1976; Barker et al., 1976; Condie and Hunter, 1976; O'Nions and Pankhurst, 1978); (3) a low degree of partial melting of the mantle. Since tonalites and trondhjemites are probably polygenetic, it is important to elucidate which model or combination of models most satisfactorily explains the geochemical and field evidence from the Scourian complex. Possible models are constrained by the results of melting experiments and the theoretical modelling of the behaviour of trace elements during melting using experimentally determined partition coefficients. Additional constraints stem from the field relationships between tonalites and trondhjemites. At Scourie, Guinard Bay and in the Inner Hebrides (Drury, 1972) trondhjemite always intrudes tonalite which is consistent with a fractional crystallisation model in which the more siliceous liquids are later than intermediate compositions. On the other hand at Gruinard Bay there is not a continuum of rock types between acid and basic implying that the tonalites and trondhjemites are not fractionated from a basic source.

Any attempt to compare analysed rocks with measured liquid compositions assumes that the rocks represent liquid compositions. This may not be so and the evidence presented above suggests that the variation in chemistry within similar rock types is best explained by crystal fractionation. Rocks which are cumulates or residual liquids must be screened out before rock and liquid compositions can be directly compared.

The following discussion is based on the concentrations of the elements Rb, Sr, Ba, K, Ce, Y, Ni and Cr+V in amphibolites, tonalites and trondhjemites. As discussed above, Rb, Ba, Sr and K may have migrated into amphibolite from the enclosing trondhjemite and so values for an average amphibolite are selected with care from the least altered samples (Table 3). Arth et al., (1978) found a correlation between δO^{18} values and Sr, Ba and Rb but not Ce and Yb in their study of Finnish tonalites and trondhjemites and argued that these elements were transported by a water rich fluid which originated in the country rock into which the magmas were intruded. They suggest that the elements Sr, Ba and Rb should not be used to obtain precise genetic information about the origin of such magmas. In an earlier study, however, Barker et al., (1976) found that a small variation of Rb with δO^{18} in trondhjemite from Colorado was within the range of unaltered and unmetamorphosed trondhjemite bodies. In the rocks from Gruinard Bay the elements Rb, Sr and Ba show meaningful trends when plotted against Qz/Ab or Or/Ab (Figs.16,17) which suggests that the elements are still useful to obtain some genetic information. It is possible that tonalite enclosed in trondhjemite may have taken up K, Rb, Ba and possibly Sr from a fluid phase during the growth of late minerals such as biotite. For this reason arguments based on the distribution of the less mobile elements Ce, Y, Ni, Cr+V and possibly K are to

be preferred to arguments based solely on the distribution of mobile elements.

Trace element modelling

In order to test fractional crystallisation or partial melting models it is possible to calculate the trace element concentrations of a melt in equilibrium with a crystal residue given the phases which constitute the residue and the degree of fractional crystallisation or partial melting. Hanson (1978) showed that the trace element concentration of a liquid produced by partial melting is controlled by the bulk distribution coefficient of the residual phases in equilibrium with the melt when it was removed. This is an elegant way of taking account of non-modal melting.

The success of trace element modelling depends upon (1) knowing the composition of the parental rock; at Gruinard Bay amphibolites are a possible source of the acid rocks and their composition is known; (2) the accuracy of the partition coefficients used in the calculations. There are five main areas of uncertainty in our knowledge of partition coefficients which are briefly outlined:

(i) they are strongly dependant upon the structure of the melt which in turn is dependant upon its composition and the dissolved fluid phases

(ii) they can vary with pressure, temperature and fO_2

(iii) they do not always obey Henry's Law especially at low concentrations (few ppm) and the upper limit for which Henry's Law applies is not well known

(iv) trace elements may be preferentially partitioned into a vapour phase coexisting with a melt; partition coefficients between solid and vapour and melt and vapour are largely unknown.

(v) they are, to date, mostly measured on phenocryst/matrix pairs, which, whilst being applicable to natural rocks, means that P, T and fO_2 at equilibration are unknown.

The partition coefficients which have been used in this study are from compilations in Arth and Hanson (1975), Gill (1978) and Arth and Barker (1976). Partition coefficients for Y have been taken from the data for Er in view of the similarity between measured partition coefficients for Y and Er in basic rocks (Pearce, 1978; Arth and Hanson, 1975).

A mantle origin for tonalites and trondhjemites

Experimental studies by Kushiro et al. (1972) and Mysen and Kushiro (1974) led them to postulate that dacitic and andesitic liquids are generated by the partial melting of hydrous spinel-lherzolite at high pressures. They found that up to 20% partial melting of spinel lherzolite yielded highly siliceous liquids (60 - 68% SiO_2) with high Al_2O_3 (16 - 20%), high CaO (10%) and low K_2O (0.03 - 0.3%) between the pressures of 7.5 to 26kb. Both these studies depend upon the microprobe analysis of quenched glasses to determine the liquid composition and this is open to a number of uncertainties as discussed below. More recently Mysen (1977) proposed that andesitic liquids are produced by the partial melting of garnet peridotite followed by the fractional crystallisation of spinel or an immiscible sulphide saturated melt.

If Scourian tonalites and trondhjemites are partial melts of the mantle, the highly fractionated REE patterns in the trondhjemites stipulate that the source contained garnet; the incompatible elements K, Rb, Sr and Ce set limits on the amount of partial melting permissible (O'Nions and Pankhurst, 1978; Tarney et al., in press). Using the estimate of O'Nions and

Pankhurst (1978) for the composition of the Archaean mantle the concentrations of incompatible elements in the tonalites indicate that the maximum amount of partial melting that could have taken place is K 3%, Rb 2%, Sr 6%, and Ce 8%; similarly the maximum amount of partial melting necessary to produce trondhjemite is K 2%, Rb 3%, Sr 6% and Ce 5%. Arndt (1977) recently showed that a melt of less than 5% is unable, under its own buoyancy, to escape from a peridotite source and that low degrees of partial melting can only be extracted when the source is stressed. It is unlikely that (a) the small amount of melt necessary to explain the concentrations of incompatible elements in Scourian tonalites and trondhjemites could escape from the mantle and (b) a significant amount of siliceous liquid can be obtained in this way. It is interesting to note that, if Ringwood's (1975) pyrolite model for the composition mantle is accepted, Scourian tonalites plot outside the field of permitted melts of mantle pyrolite with respect to their FeO and MgO contents, according to the recent model proposed by Hanson and Langmuir (1978). This further confirms the trace element evidence which suggests that these rocks are not primary melts of the mantle.

The derivation of tonalites and trondhjemites by the partial melting of a basaltic source

(1) Evidence from experimental petrology. Experimental studies by Stern (1974) and Peto and Hamilton (1976) show that it is possible to produce aluminous, quartzo-feldspathic liquids by the partial melting of a variety of basaltic and andesitic compositions. Peto and Hamilton (1976) melted both quartz saturated and undersaturated basalts with excess water and undersaturated with water at 10kb in the temperature range 810°C to 1010°C; the water saturated melts (15 to 45% of the volume of the parent) are in the equilibrium with amphibole and clinopyroxene and the

water undersaturated melts (5 to 25% of the volume of the parent) are in equilibrium with plagioclase clinopyroxene, olivine, orthopyroxene and amphibole. The hydrated glasses resemble calcic trondhjemites and tonalites and plot near the Qz - Ab side of the Qz-Ab-Or projection in a similar position to the analysed tonalites and trondhjemites from Gruinard Bay in Fig. 15. More femic, less silicic melts are produced in water under-saturated experiments. The main problem with this study is that glass compositions (analysed by microprobe) are assumed to represent liquid compositions in equilibrium with the residual phases, but Cawthorn et al. (1973) and Cawthorn (1976) pointed out that this assumption must be tested rigorously because quenched phases can change the glass composition; nevertheless the study of Peto and Hamilton (1976) shows that quartzofeldspathic liquids can be obtained by moderate degrees of partial melting of basaltic compositions. The water content of the glasses was estimated from the data of Burnham and Davies (1974); this method gives reliable totals for the analyses.

Stern (1974) avoided the problems associated with analysing quenched glasses by calculating liquid compositions from measured and calculated compositions of residual phases and an estimate of their proportions. Stern studied olivine basalt and andesite at 30kb with 5% H_2O and the melts were in equilibrium with clinopyroxenes and garnet. He showed that the liquids produced by the partial melting of a basalt and andesite are more calcic than liquids on the calc alkaline trend and suggested that magmas produced by the partial melting of subducted ocean crust must undergo fractionation at shallower depths to bring them on to the calc alkaline trend. The same conclusion can be drawn from Peto and Hamilton's (1976) lower pressure study as their melt

compositions for olivine tholeiite, quartz tholeiite and andesite all plot to the calcic side of a calc alkaline trend. It is not possible to obtain temperatures of 1000°C at 35 km depth (ca. 10kb pressure) in the present oceanic lithosphere, even though there is evidence of higher geothermal gradients in the Archaean (O'Hara, 1977; Tarney and Windley, 1977).

(2) Evidence from trace elements. It is possible to test partial melting models using trace element ratios; for the more mobile elements such as K, Rb, Ba and Sr elemental ratios are less sensitive to alteration than the absolute abundances. The K/Rb ratio is most useful in identifying hornblende and to a lesser extent plagioclase as a fractionating or residual phase; similarly the Sr/Ba ratio is sensitive to residual plagioclase and to a lesser extent hornblende and the Ce/Y ratio is a useful guide to the presence of residual hornblende and/or garnet.

Sr - Ba diagram: A plot of Sr against Ba shows several important features (Fig. 18a).

1) there are two groups of trondhjemites; one group has high Ba and low Sr, the other has higher Sr and low Ba.

2) granodiorites define a trend parallel to the high Ba trondhjemites

3) amphibolites, tonalites and some trondhjemites have the same Sr/Ba ratio of about 1.0.

4) some tonalites show increasing Ba with no change in Sr.

The high Ba trondhjemites are (i) relatively rich in quartz, do not show a great variation in Qz/Ab ratio and cluster about the trondhejmite end of the quartz feldspar cotectic; (ii) have higher Y values than the high Sr trondhjemites. The high Sr trondhjemites show a greater range of Qz/Ab ratios and have lower Y.

There are two possible interpretations of these trends:

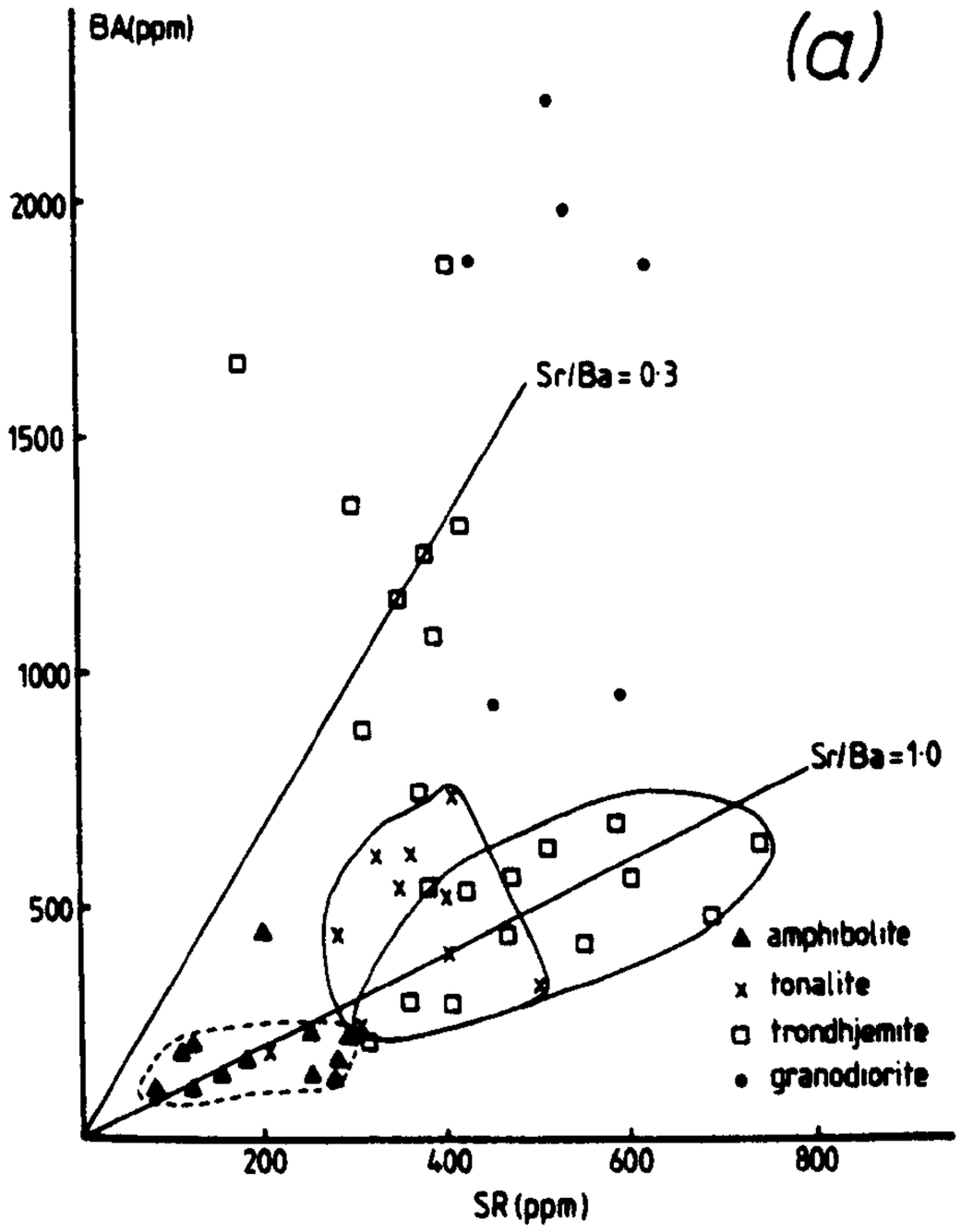

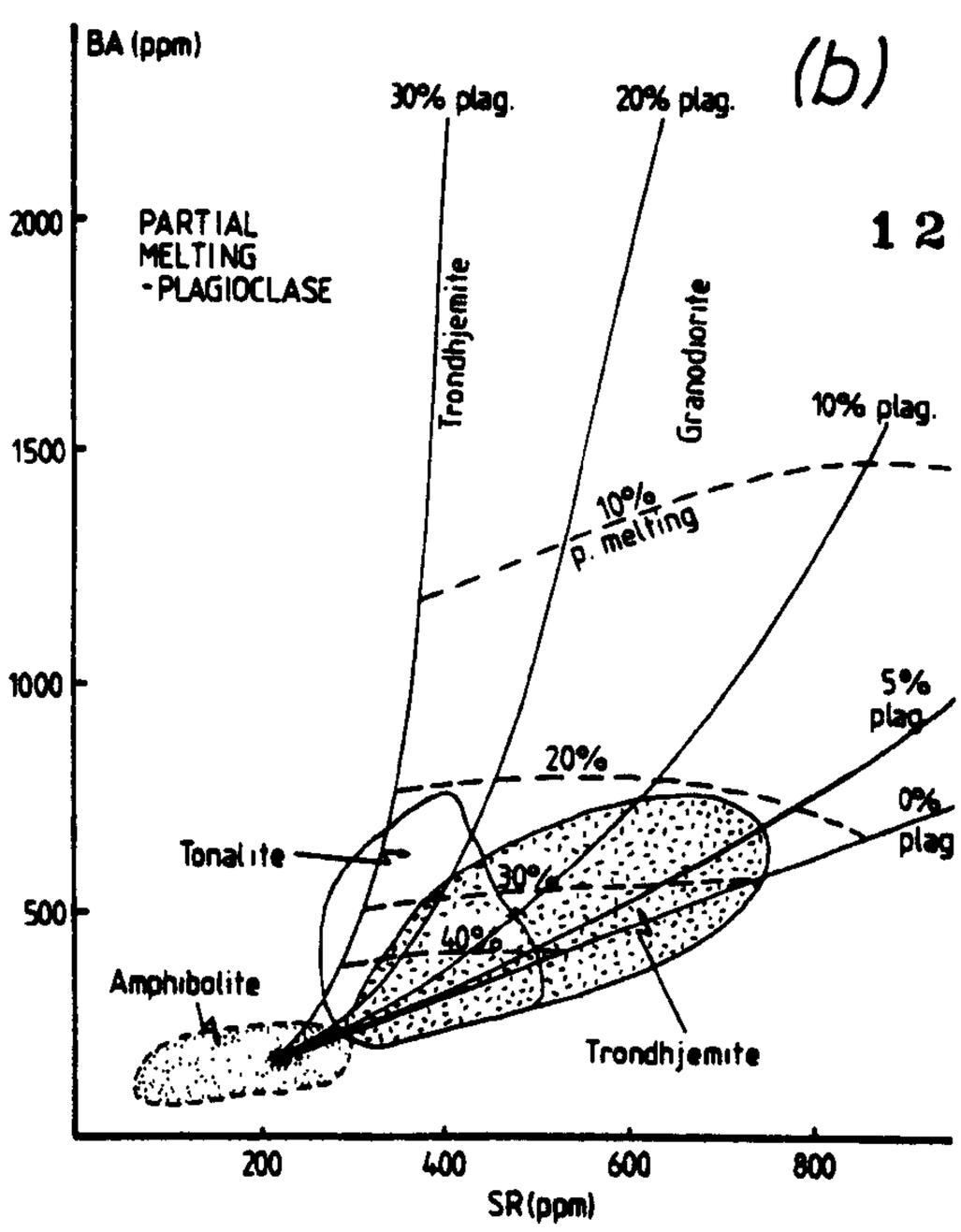

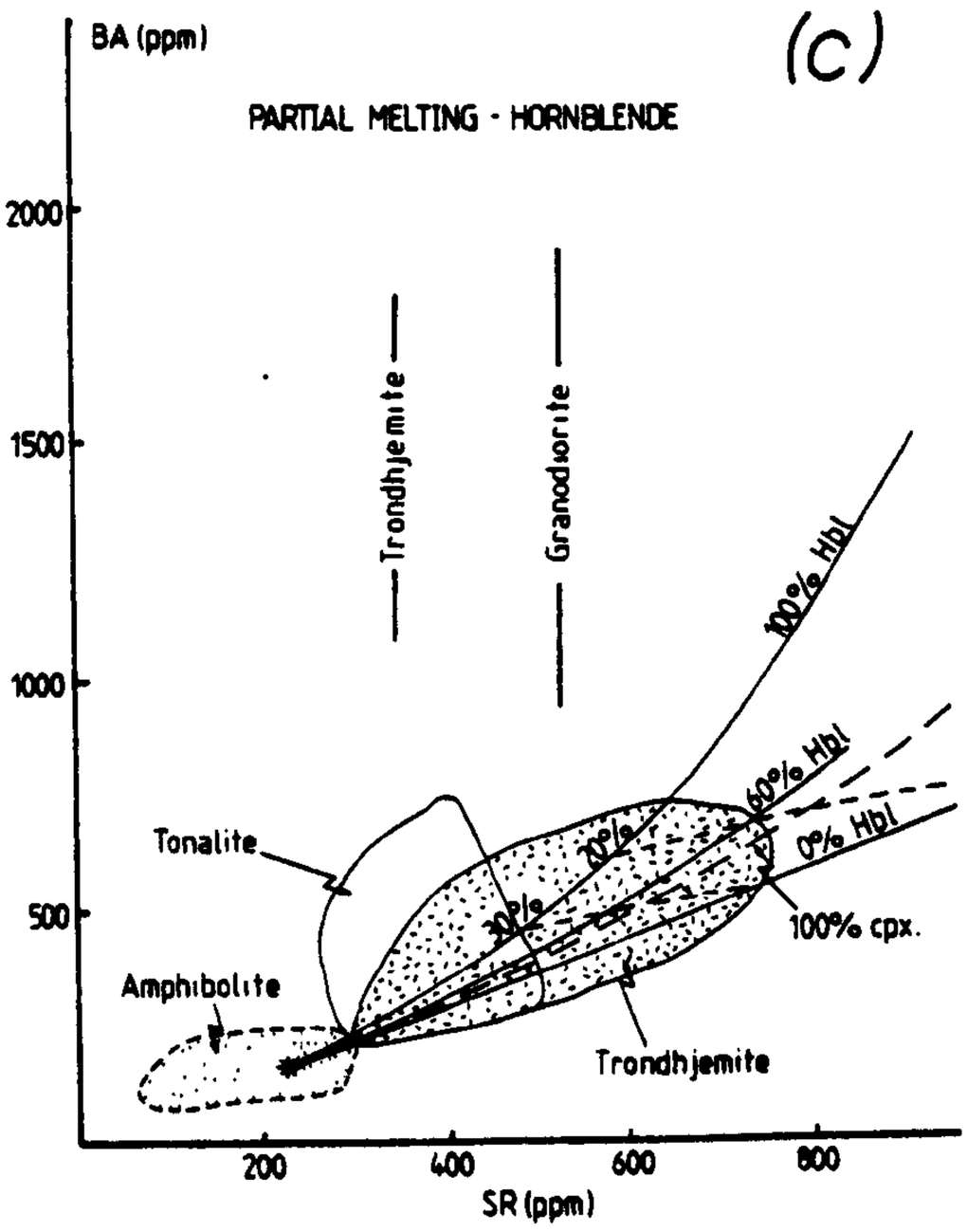

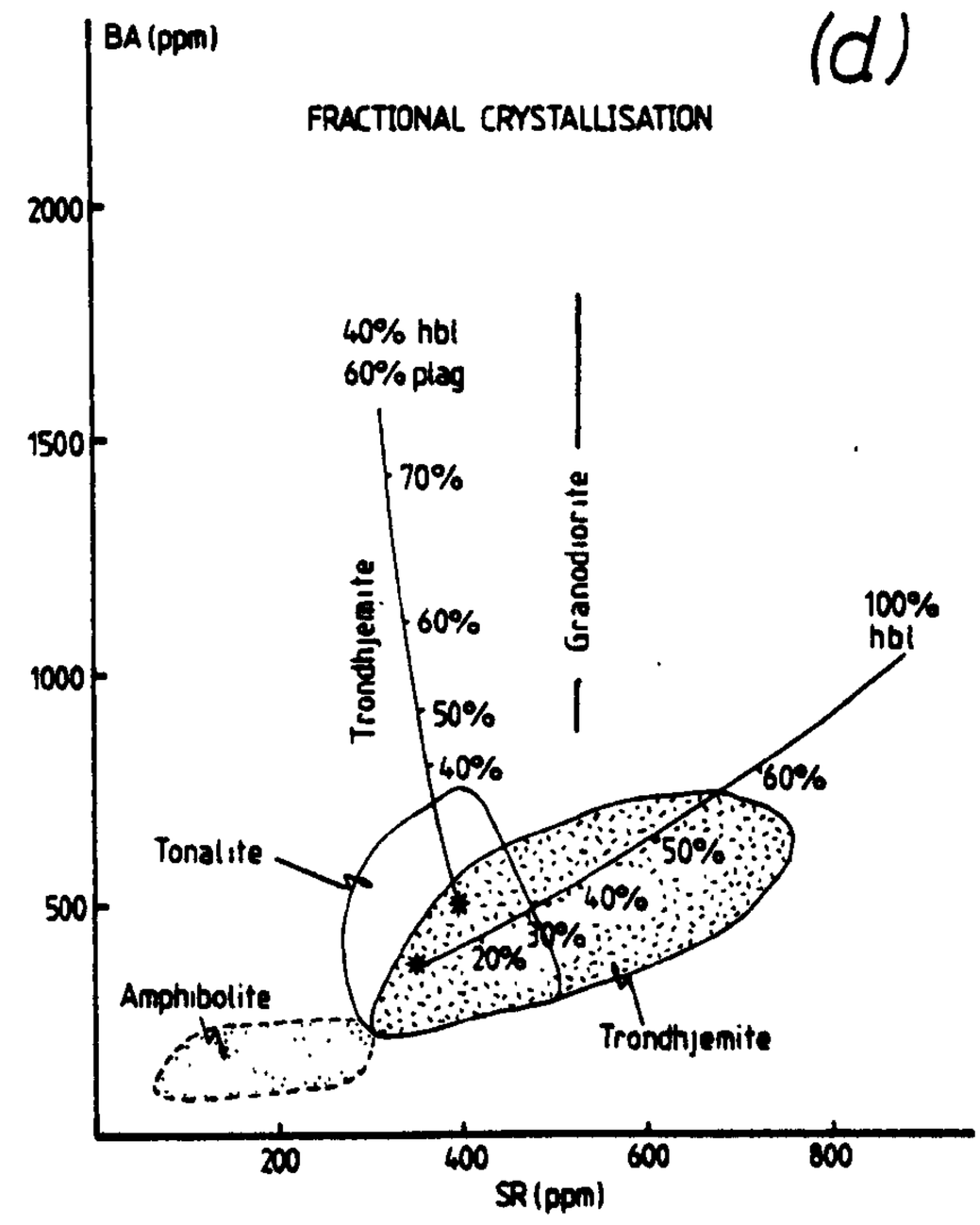

FIGURE 18. (a) Ba vs Sr for amphibolites, tonalites, trondhjemites and granodiorites at Gruinard Bay. (b) Sr and Ba content of liquids formed by the partial melting of a basaltic source (star) with between 0% and 30% plagioclase in the residue, contoured for the degree of partial melting. The fields of the Gruinard Bay amphibolites, tonalites, trondhjemites and granodiorites are indicated. (c) Sr and Ba content of liquids formed by the partial melting of a basaltic source (star) with between 0% and 100% hornblende in the residue, contoured for the degree of partial melting. The fields of the Gruinard Bay amphibolites tonalites, trondhjemites and granodiorites are indicated. (d) Sr and Ba content of liquids formed by the fractional crystallisation of hornblende and hornblende + plagioclase from a tonalitic source (stars) The fields of the Gruinard Bay amphibolites, tonalites, trondhjemites and granodiorites are indicated.

(i) It is possible to draw contour lines for the degree of partial melting and the amount of plagioclase in the source for liquids produced by the partial melting of a basaltic source with a composition similar to the amphibolites at Gruinard Bay (Fig. 18b). From these contour lines a plot of Ba and Sr in trondhjemites and tonalites suggests that the high Ba trondhjemites are produced by 5 - 40% partial melting of a basaltic source with 30% plagioclase in the residue and that the tonalites and high Sr trondhjemites are produced by 20 - 50% partial melting of a source with o - 10% plagioclase. Since the two types of trondhjemite are associated in the same area it is unlikely that both these possibilities are correct. Similarly the high Sr trondhjemites can be produced by the partial melting of a source rich in hornblende (Fig. 18c), although it is not possible to produce the high Ba trondhhemites in this way. A source rich in clinopyroxene is unlikely as a pure clinopyroxene source is capable of reproducing the Sr/Ba ratios of only a few of the high Sr trondhjemites and none of the high Ba trondhjemites.

(ii) On the other hand the two trends can be produced by the fractional crystallisation of plagioclase and hornblende (60% and 40% respectively) (high Ba trondhjemite) and pure hornblende (the high Sr trondhjemite) (Fig. 18d).

<u>K - Rb diagram</u>: this also shows two trends (Fig. 19a) although they are not as well defined as the trends on the Sr - Ba diagram;

1) amphibolites, tonalites and some trondhjemites define a trend with a relatively low K/Rb (analogous to the high Sr trend)

2) some trondhjemites and granodiorites define a trend with higher K/Rb ratios (analogous to the high Ba trend).

If this diagram is contoured for the percentage residual hornblende in equilibrium with a melt derived from a source similar in composition to the Gruinard Bay amphibolites, and for the degree of partial

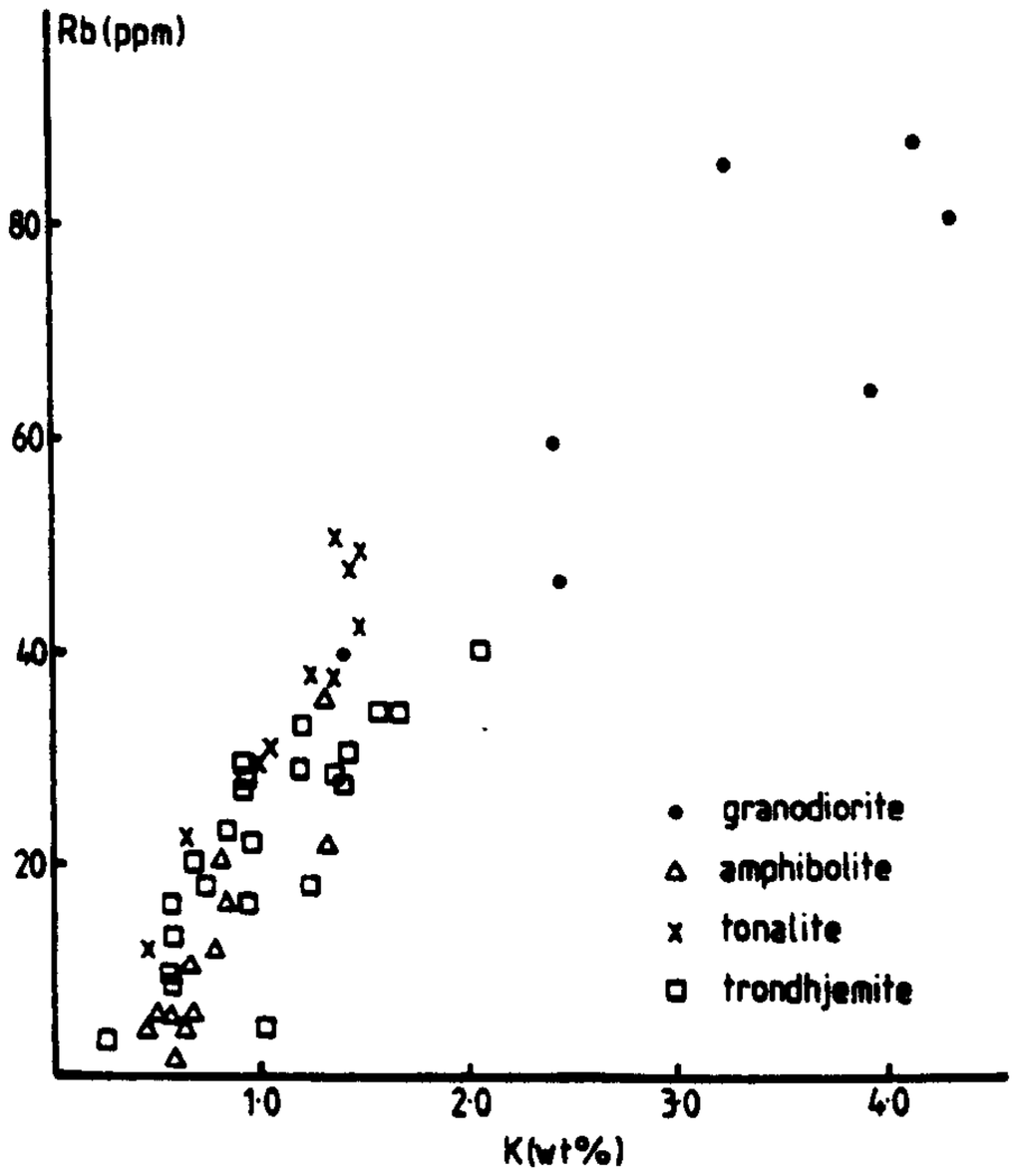

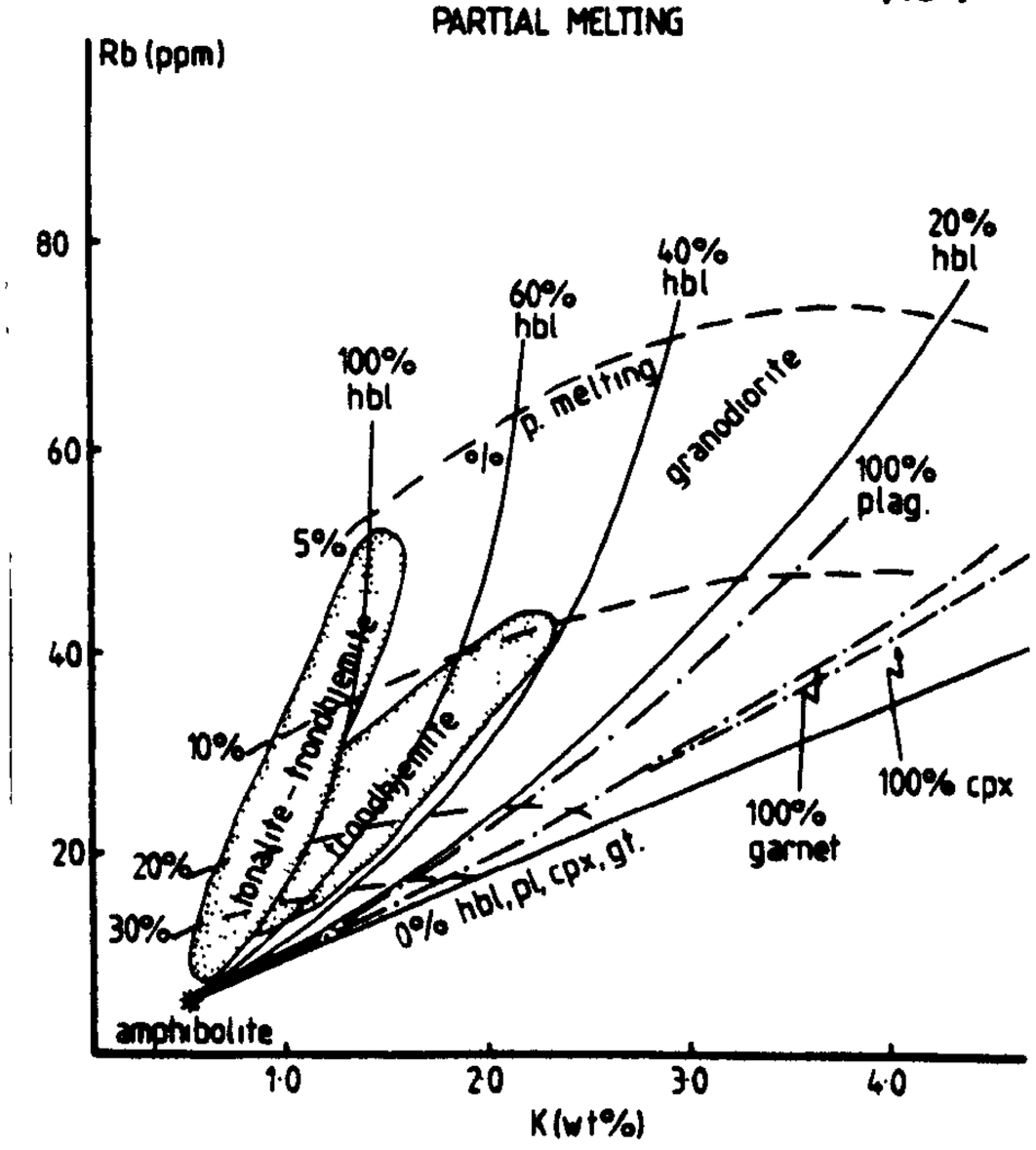

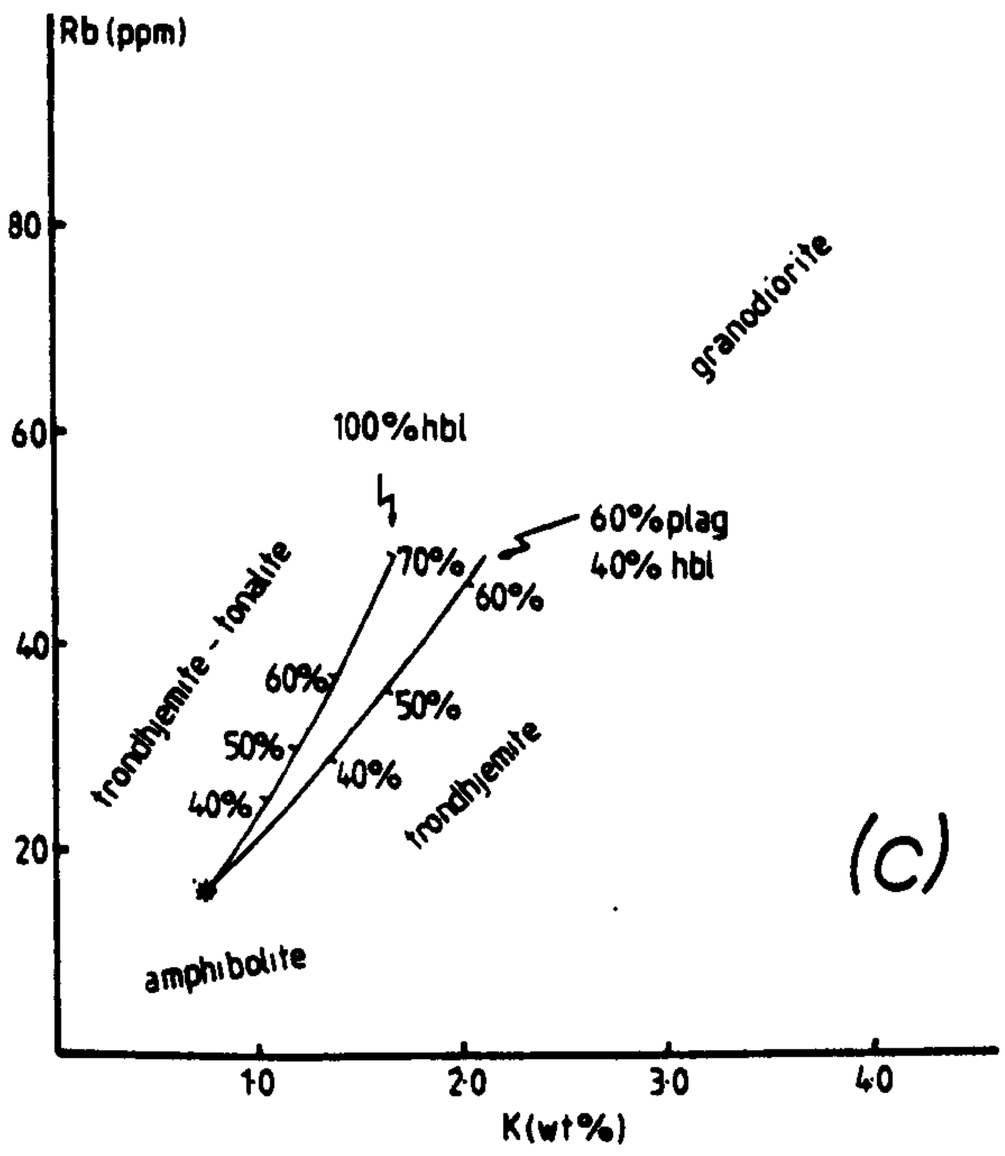

FIGURE 19. (a) Rb vs K for Gruinard Bay amphibolites, tonalites, trondhjemites and granodiorites. There are two trends: amphibolites, tonalites and trondhjemites define a steep, low K/Rb trend and the granodiorites and some trondhjemites define a high K/Rb trend. (b) Rb and K content of liquids formed by the partial melting of a basaltic source (star) with between 0% and 100% hornblende in the residue, contoured for the degree of partial melting. The limiting curves for residues composed entirely of plagioclase, garnet or clinopyroxene in equilibrium with the same basaltic source are also shown. The fields of the Gruinard Bay amphibolites, tonalites, trondhjemites and granodiorites are indicated. (c) K and Rb content of liquids formed by the fractional crystallisation of hornblende and hornblende + plagioclase from a tonalitic source (star). The fields of the Gruinard Bay amphibolites, tonalites, trondhjemites and granodiorites are indicated.

melting, it can be seen that both groups of rocks wiht the high and low K/Rb ratios must represent liquids in equilibrium with a hornblende rich source produced by 5 - 40% partial melting (Fig. 19b). The K/Rb ratios in these rocks are not consistent with a source rich in garnet, plagioclase or clinopyroxene (Fig. 19b). (This diagram also shows that if the granodiorites are produced by partial melting they represent less than 5% melting, which is unlikely).

It is also possible to reproduce the two trends by a fractional crystallisation process in which pure hornblende (reproducing the low K/Rb trend) and plagioclase and hornblende (reproducing the high K/Rb trend) are extracted. The evidence from Ba-Sr and K-Rb diagrams are in themselves not conclusive and so it is necessary to consider all possible explanations of the data. In the light of Ce/Y ratios, however, it is possible to eliminate some of these possibilities.

Ce/Y ratios: The extreme depletion in Y in these rocks relative to a basaltic source (with about 10 times chondritic values) and the wide range of Ce/Y ratios in the tonalites and trondhjemites (Fig. 14) indicate that garnet or hornblende is present as a residual phase in the evolution of these rocks (i.e. in the source during partial melting or as a fractionating phase). It is very difficult to reproduce the extreme range of Ce/Y ratios assuming a partial melting model with substantial amounts of garnet or hornblende in the source. The most efficient way of producing the extreme depletion of Y is by the fractional crystallisation of hornblende or garnet.

In view of the bimodal nature of this complex it is unlikely that the tonalites are the product of fractional crystallisation of hornblende from a basaltic or gabbroic source (cp. Arth, 1978).

It is proposed therefore that the tonalites and possibly some trondhjemites are generated by the 30 - 40% partial melting of a basaltic source similar in composition to the amphibolites at Gruinard Bay (Fig. 20a), leaving a residue rich in hornblende and low in plagioclase and possibly a small amount of garnet, although it is not essential to this model. This is consistent with the Ce/Y ratio (Fig. 20a), the Sr/Ba ratio and the K/Rb ratio in the tonalites and the melting experiments of Stern (1974) and Peto and Hamilton (1976). The majority of trondhjemites and granodiorites, however, are generated by the fractional crystallisation of hornblende or hornblende and plagioclase from a tonalitic liquid; garnet fractionation could accomplish the necessary depletion in Y more efficiently than hornblende, but it is probable that a liquid formerly in equilibrium with a hornblende rich source is more likely to crystallise hornblende than garnet. The high Sr trondhjemites are generated by the fractional crystallisation of up to 60% hornblende from tonalite (Fig. 20b); this is in keeping with their very low Y (zero ppm in some rocks). The high Ba trondhjemites are produced by the fractional crystallisation of plagioclase and hornblende from tonalite and this is consistent with the slightly higher Y in the samples and the low Sr. Granodiorite is the product of plagioclase and hornblende fractionation from a more evolved (trondhjemitic) source.

In summary, the partial melting of basalt produced a tonalite magma and a hornblende and plagioclase residue, which is not seen because it sank, due to its high density. Hornblende fractionation from the tonalite magma accompanied by plagioclase at a shallower depth can account for generation of the trondhjemites and granodiorites (Fig. 21).

FIGURE 20 (a). Calculated Ce/Y ratios, normalised to chondritic values for liquids produced by the partial melting of a basaltic source in equilibrium with a hornblende rich residue. These calculations show that the Gruinard Bay tonalites could be generated by the partial melting of a source similar in composition to the amphibolites.

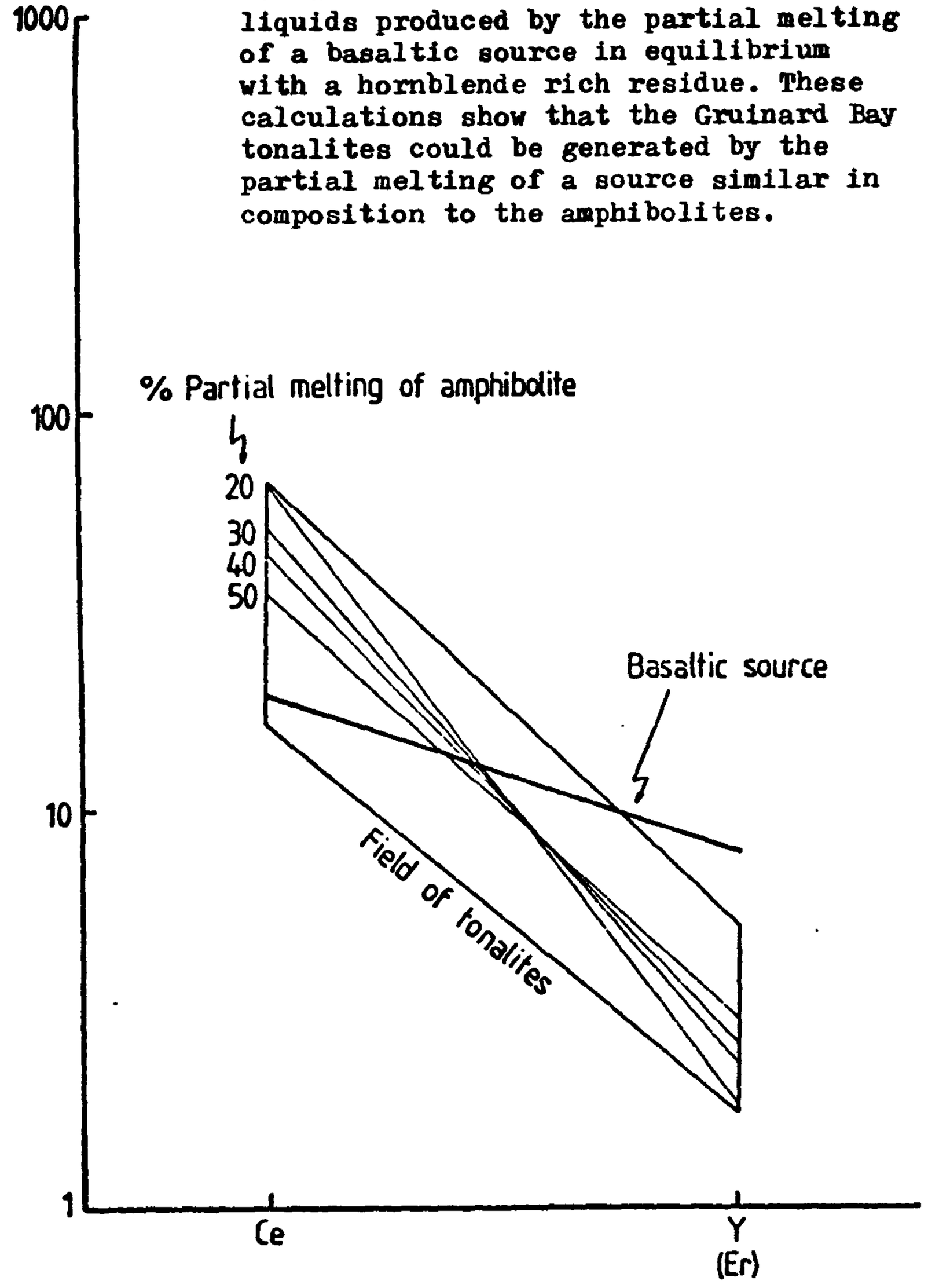

FIGURE 20 (b). Calculated Ce/Y ratios, normalised to chondritic values for liquids produced by the fractional crystallisation of hornblende from a tonalitic liquid. These calculations show that the Gruinard Bay trondhjemites could represent between 5% and 50 % fractional crystallisation of hornblende from a tonalitic liquid.

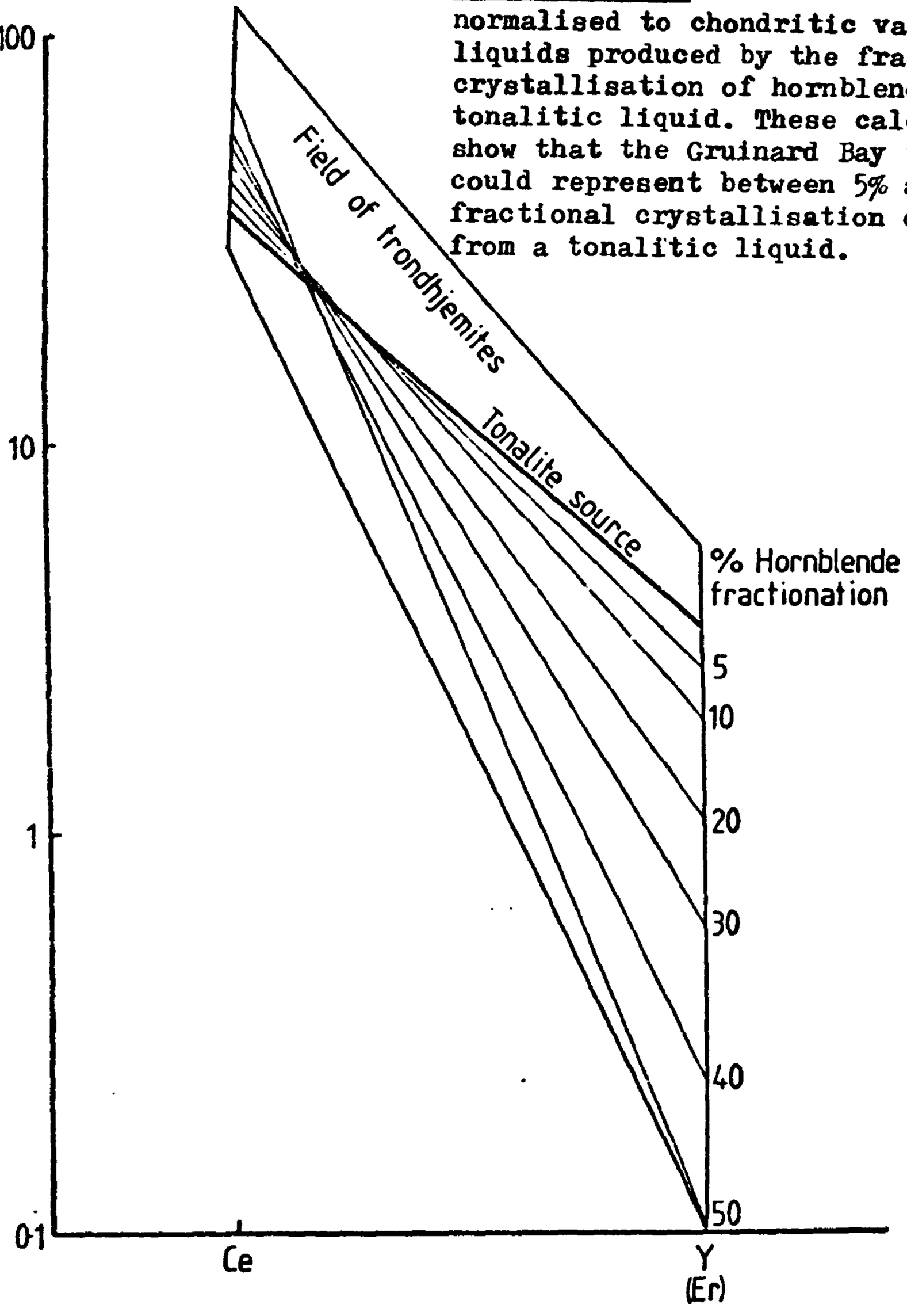

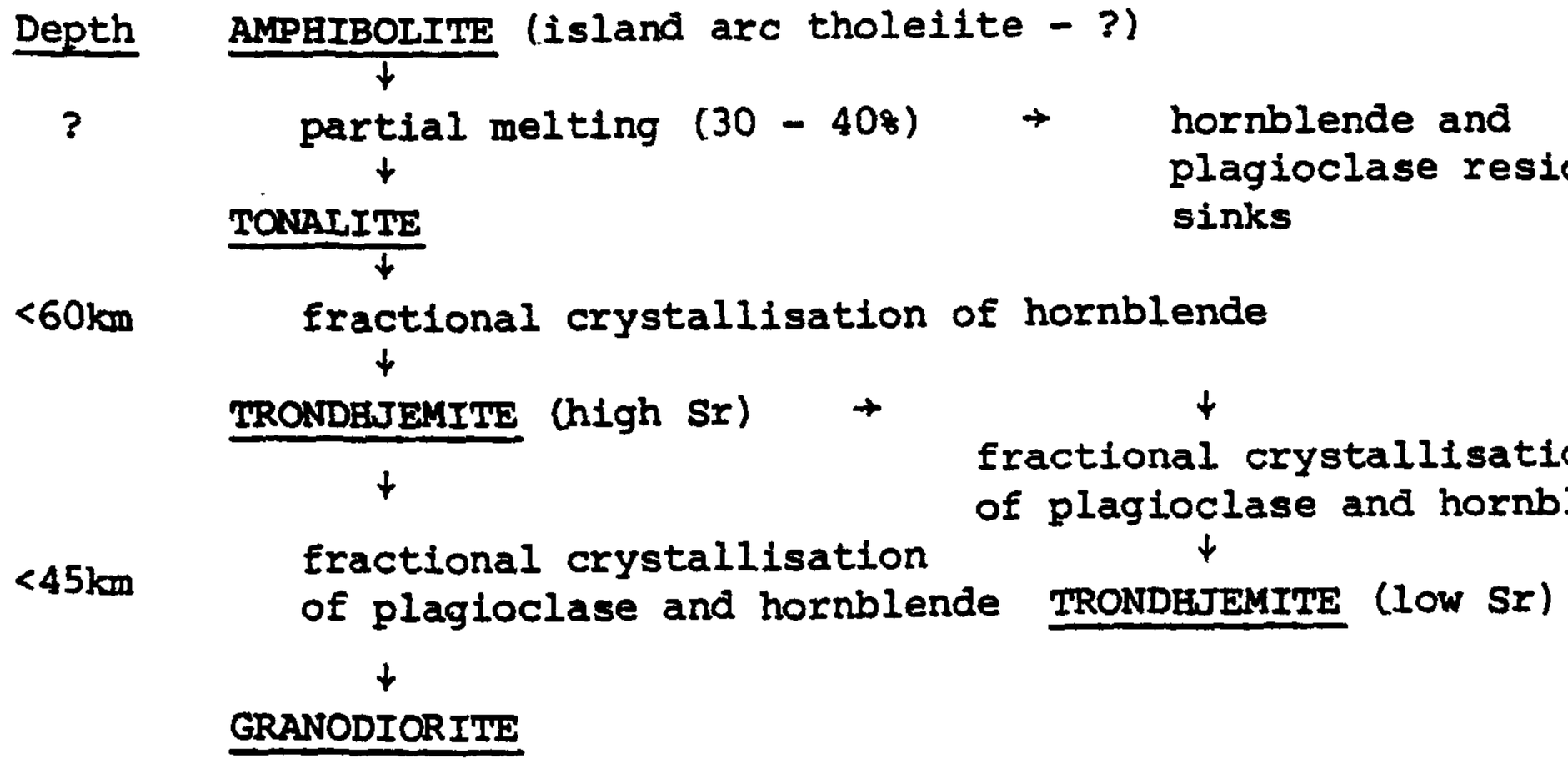

Fig. 21. Flow diagram showing the suggested evolution of magmas in the Scourian gneisses of Gruinard Bay.

The model proposed above is consistent with the following features of the Scourian gneisses at Gruinard Bay:

1) their bimodal nature

2) the relative ages of the gneisses (amphibolite older than tonalite older than trondhjemite)

3) a smooth variation from tonalite to granodiorite on A-F-M, Or-Ab-An and Ce/Y diagrams

4) the results of experimental petrology which show that calc alkaline liquids can be produced from basalts by partial melting followed by fractional crystallisation

5) the trace element ratios Sr/Ba and K/Rb and the REE Ce and Y

6) Ni and Cr+V which are very low in trondhjemites (removed by hornblende fractionation).

Discussion

Previous workers (e.g. Arth and Hanson, 1972; 1975; Condie and Hunter, 1976; O'Nions and Pankhurst, 1978) proposed models in which Archaean tonalites are produced by the partial melting of quartz eclogite; an amphibolite model, however, is more consistent with the data presented above for Scourian gneisses at

Gruinard Bay.

The partial melting of amphibolite and subsequent hornblende fractionation indicate that:

(i) partial melting took place at relatively shallow depths (compared with an eclogite model); this is not improbable in view of the higher geothermal gradient in the Archaean;

(ii) the early tonalitic melts had a high water content. Tarney et al. (in press) proposed that large amounts of water can be introduced into a system in which basalt melts by the serpentinisation of high Mg - basalt, common in the Archaean. Late stage granites at Scourie (see above) appear to have low water contents (less than 2% H_2O) and have orthopyroxene and garnet as liquidus phases; it is possible that as hornblende fractionated from the melt, the residual liquids became drier than the parental liquid.

(iii) fractional crystallisation took place at less than 60 km depth in the case of hornblende and at less than 45 km depth in the case of plagioclase. Arth and Barker (1976) and Arth et al. (1978) suggested on the basis of experimental work by Lambert and Wyllie (1974) that amphibole is not stable in a water saturated tonalite melt at pressures greater than 20kb and that plagioclase is not stable at pressures greater than 15kb. Biotite becomes a liquidus phase before plagioclase in a water saturated tonalitic melt at high pressures and may in part be responsible for the low Ba trondhjemite trend. On the other hand tonalites produced by the partial melting of basalt are unlikely to be water saturated at high pressure since a water saturated tonalite contains more than 20% H_2O at 20kb and so biotite may not be present. The experimental evidence suggests that hornblende fractionation is likely to dominate tonalite melts at deep levels (i.e. lower crust and upper mantle) and plagioclase joins hornblende on the liquidus as the pluton rises and the temperature falls. This could explain

why tonalite is the dominant rock type in deep crustal levels (e.g. the granulite facies terrain of the Scourie area) whereas trondhjemite and granodiorite whose genesis is controlled by plagioclase fractionation are present at higher crustal levels (e.g. the amphibolite facies terrain of Gruinard Bay and Torridon).

8. A MODEL FOR THE EVOLUTION OF THE SCOURIAN COMPLEX

The two main conclusions of this study are:

(i) amphibolites at Gruinard Bay represent fragments of island arc (?) tholeiite and komatiitic(?) tholeiite.

(ii) tonalites at Gruinard Bay are derived by the partial melting of amphibolite similar in composition to the amphibolites found as rafts in the acid gneisses, and trondhjemites and granodiorites are derived from a tonalite melt by the fractional crystallisation of plagioclase and hornblende.

Partial melting of amphibolite could have taken place (a) at the base of a thick lava pile in a young island arc or (b) in a subduction zone. A subduction zone is probably the more efficient mechanism for producing large volumes of tonalitic magma.

Table 5 shows a comparison between the Scourian gneisses at Scourie, Gruinard Bay and Torridon (for details see below). There are a number of striking contrasts between these three areas; granulite facies gneisses are predominantly tonalitic and contain relatively large layered gabbro - ultramafic rock complexes and trondhjemite forms thin intrusive sheets of minor importance; amphibolite facies gneisses at Gruinard Bay and Torridon are predominantly trondhjemitic and granodioritic and contain amphibolite and small highly fragmented remnants of layered gabbro - ultramafic rock complexes; tonalite is not a major rock type in the area. A comparison across the Scourian

TABLE 5

A comparison of Scourian gneisses from north to south across the complex

	NORTH		SOUTH
OLDEST	Scourie	Gruinard Bay	Torridon
	sediments	sediments	
		amphibolite	amphibolite
	layered gabbro	layered gabbro	
	tonalite	tonalite (minor)	
	trondhjemite to granite (minor)	trondhjemite to granite	granodiorite
YOUNGEST	granulite facies metamorphism	amphibolite facies metamorphism	amphibolite facies metamorphism

complex is important because it highlights the fact that:

(i) the same lithologies are present in both amphibolite facies and granulite facies areas showing the same relative ages;

(ii) the proportions of the main rock types are very different in granulite and amphibolite facies areas

(iii) there is a N - S change in the major quartzo-feldspathic component of the gneisses; at Scourie (N) tonalite is dominant, at Gruinard Bay (central) trondhjemite is dominant and at Torridon (S) granodiorite is the predominant rock type indicating a southerly increase in K_2O.

Windley and Smith (1976) showed that there are a number of important comparisons between the pattern of magmatism found in Archaean rocks in high grade areas and the deep-seated granitic batholiths located on the western margin of North and South America. If this observation is applied to the Scourian complex the following comparisons can be made:

1) tonalite, trondhjemite and granodiorite are the dominant quartzofeldspathic rocks; true granite is rare. (cp. the Peruvian batholith, Pitcher (1978); the Coast Plutonic complex, British Columbia, Roddick and Hutchinson (1974); the South California batholith, Gastil et al. (1974) and Heitenan (1973)).

2) tonalites are early, trondhjemite and granodiorite are later (cp. the Peruvian batholith, Pitcher (1978))

3) quartzofeldspathic magmas intrude amphibolites wiht a chemistry similar to modern tholeiites and layered cumulitic gabbro complexes (cp. Peruvian batholith, Pitcher (1978))

4) the acid magmas define a calc alkaline trend and the basic magmas a tholeiitic trend (cp. Peruvian batholith, Pitcher (1978); the Coast Plutonic complex, British Columbia, Roddick and Hutchinson (1974))

5) from petrological considerations the Scourian complex may have formed in an analogous tectonic setting to a modern batholith.

The major difference between modern batholiths and Archaean high grade gneiss terrains is the absence of andesites (Barker and Arth, 1976); these are preserved as the roof over high level sections of a batholith as in the Peruvian example, but they are uncommon in the Archaean. This may be a function of the level of exposure preserved or it may be a function of the processes operating.

Variation across the Scourian complex is largely due to the different crustal levels exposed. Granulite facies gneiss containing fragments of layered gabbro (possibly part of the ocean floor layer three) represents a lower level in a pluton than amphibolite facies gneiss with less layered gabbro and possible volcanic material. Bridgwater et al. (1974) proposed that Archean tectonics were dominated by horizontal movements rather than vertical and that magmas were intruded as nappe-like sheets; this explains the presence of metasediments in the deepest levels of the complex. The variation in magma-type with crustal level may be due to a combination of factors including the fractionation of plagioclase and/or hornblende at different depths and the density and viscosity of the magmas. It is unwise to interpret the variation in K_2O across the Scourian complex as analogous to modern batholiths in view of the small crustal segment available for study in northwest Scotland; it is more likely that this variation is fortuitous and indicated that the Scourian complex is made up of several different plutons with their own characteristics seen at different levels of exposure.

			SIO2	TIO2	AL2O3	FEO	MNO	MGO	CAO	NA2O	K2O	P2O5	TOTAL
ULTRAMAFIC	ROCK	HR134	[illegible]	[illegible]	4.60	[illegible]	.42	31.41	1.07	.05	.01	.01	99.73
ULTRAMAFIC	ROCK	HR141	45.72	.35	5.[illegible]	[illegible]	.[illegible]	28.02	8.46	.47	.11	.03	101.46
ULTRAMAFIC	ROCK	HR142	[illegible]	.31	[illegible]	[illegible]	.25	32.09	0.31	.39	.10	.01	101.[illegible]
ULTRAMAFIC	ROCK	HR143	46.77	.43	5.72	[illegible]	.21	24.03	9.41	.94	.24	.03	100.63
ULTRAMAFIC	ROCK	HR148	55.13	.[illegible]	[illegible]	[illegible]	.25	21.42	12.80	.41	.11	.01	100.77
ULTRAMAFIC	ROCK	HR150	43.28	1.40	4.23	[illegible]	.27	11.62	15.83	.63	.46	.10	95.76
AMPHIBOLITE	A	[illegible]	[illegible]	.37	[illegible]	[illegible]	.16	9.[illegible]	11.60	2.[illegible]	.99	.02	96.95
AMPHIBOLITE	A	[illegible]	[illegible]	1.55	[illegible]	13.29	.22	6.33	11.17	2.04	.68	.06	96.55
AMPHIBOLITE	A	[illegible]	[illegible]	.55	[illegible]	[illegible]	.24	6.53	11.10	2.57	.56	.03	96.93
AMPHIBOLITE	A	[illegible]	[illegible]	.54	[illegible]	[illegible]	.24	8.[illegible]	10.55	2.25	.01	.03	96.79
AMPHIBOLITE	A	[illegible]	[illegible]	.43	[illegible]	[illegible]	.21	9.76	11.40	1.68	1.03	.02	96.91
AMPHIBOLITE	A	[illegible]	[illegible]	.51	[illegible]	[illegible]	.21	10.14	11.66	2.[illegible]	1.58	.02	96.45
AMPHIBOLITE	A	[illegible]	[illegible]	.73	[illegible]	[illegible]	.21	8.14	10.32	2.74	.95	.07	97.54
AMPHIBOLITE	A	[illegible]	[illegible]	.68	[illegible]	[illegible]	.21	6.[illegible]	11.70	2.39	1.02	.14	97.14
AMPHIBOLITE	A	[illegible]	[illegible]	.[illegible]3	[illegible]	[illegible]	.21	7.15	[illegible].16	2.[illegible]	.04	.[illegible]6	30.64
AMPHIBOLITE	A	[illegible]	[illegible]	[illegible].16	[illegible]	[illegible]	.43	9.13	12.48	1.23	.77	.11	94.40
AMPHIBOLITE	B	[illegible]	[illegible]	[illegible].21	[illegible]	[illegible]	.22	8.03	11.03	1.93	.72	.02	95.64
AMPHIBOLITE	B	[illegible]	47.48	[illegible].21	[illegible].37	[illegible].37	.24	5.59	11.58	1.66	.66	.01	95.97

			Y	SR	RB	TH	PB	W	GA	ZN	BA	NI	CR+V	CE	LA	ZR	NB
ULTRAMAFIC	ROCK	HR134	9.8	1	0	0	3	0	11	142	9	1099	2957	0	6	11	2
ULTRAMAFIC	ROCK	HR141	7.3	37	0	3	5	0	8	70	15	1347	2770	0	2	18	1
ULTRAMAFIC	ROCK	HR142	3.9	20	1	0	8	0	6	71	12	1662	2762	0	1	14	2
ULTRAMAFIC	ROCK	HR143	8.3	36	2	2	6	0	8	74	24	906	3090	0	1	19	1
ULTRAMAFIC	ROCK	HR148	8.6	9	2	0	1	0	5	16[illegible]	45	1006	1203	0	0	3	3
ULTRAMAFIC	ROCK	HR150	14.6	46	3	1	3	0	14	168	34	358	240	32	22	70	9
AMPHIBOLITE	A	HR103	[illegible].1	273	21	0	6	0	13	69	130	104	663	8	3	24	3
AMPHIBOLITE	A	HR104	3[illegible].[illegible]	104	6	1	2	0	21	114	174	61	161	32	18	114	8
AMPHIBOLITE	A	HR109	11.7	[illegible]6	5	1	7	0	13	82	196	146	563	5	10	29	1
AMPHIBOLITE	A	HR113	1097	149	6	3	5	0	13	120	138	114	529	17	5	31	1
AMPHIBOLITE	A	HR115	11.9	246	23	0	9	0	15	117	229	82	402	15	8	26	2
AMPHIBOLITE	A	HR122	11.5	203	36	4	6	0	16	98	456	105	416	16	9	56	3
AMPHIBOLITE	A	HR127	17.[illegible]	293	12	[illegible]	7	0	18	127	230	75	196	17	8	64	3
AMPHIBOLITE	A	HR147	15.5	277	17	[illegible]	7	0	16	112	167	154	333	12	5	45	3
AMPHIBOLITE	A	HR151	26.9	247	10	1	10	0	17	122	139	86	236	41	19	61	4
AMPHIBOLITE	B	HR144	15.[illegible]	80	4	[illegible]	10	0	14	138	104	153	243	4	6	17	3
AMPHIBOLITE	B	HR145	16.2	121	2	1	13	0	17	142	119	136	249	9	9	23	2
AMPHIBOLITE	B	HR146	19.7	123	5	0	11	0	17	106	204	110	285	6	7	19	0

TABLE 6. Chemical analyses of ultramafic rocks and amphibolites (groups A and B) from Gruinard Bay.

		SIO2	TIO2	AL2O3	FEO	MNO	MGO	CAO	NA2O	K2O	P2O5	TOTAL
TONALITE	123	68.14	.41	15.65	3.41	.05	1.47	4.54	3.99	1.23	.08	98.27
TONALITE	135	65.46	.79	15.61	3.72	.05	2.16	6.51	3.58	1.64	.04	98.04
TONALITE	135	66.83	.45	15.38	3.36	.05	1.58	4.87	4.01	1.21	.08	97.82
TONALITE	143	63.25	.48	14.77	5.14	.06	2.13	5.51	4.05	.77	.10	97.66
TONALITE	153	66.48	.52	15.15	5.19	.06	1.66	4.10	4.93	1.58	.06	97.69
TONALITE	154	65.21	.44	15.66	4.01	.06	1.66	4.30	4.54	1.49	.08	98.27
TONALITE	159	64.23	.52	15.04	4.66	.09	1.58	4.76	4.69	1.47	.09	97.55
TONALITE	167	66.35	.45	15.16	4.73	.11	2.73	7.50	4.75	.56	.09	96.67
TONALITE	173	64.75	.62	16.72	3.03	.05	1.31	3.96	4.95	1.72	.01	97.92
TONALITE	179	65.6	.05	16.26	5.14	.07	1.17	4.22	4.31	1.73	.11	97.56
TRONDHJEMITE	115	69.74	.33	15.64	2.11	.03	.59	3.77	5.45	.83	.14	98.80
TRONDHJEMITE	116	74.43	.12	14.66	.80	.02	.46	2.49	5.22	1.14	.00	99.41
TRONDHJEMITE	117	64.43	.29	19.17	1.80	.03	.85	4.77	6.24	.88	.00	97.96
TRONDHJEMITE	118	73.30	.23	13.42	4.05	.11	.47	2.05	3.09	1.49	.00	99.90
TRONDHJEMITE	122	69.54	.14	17.34	.95	.02	.42	4.41	6.60	1.28	.00	100.20
TRONDHJEMITE	127	65.65	.19	17.87	2.11	.02	.43	4.65	6.19	.69	.03	98.23
TRONDHJEMITE	133	68.99	.05	16.59	2.29	.03	.03	4.56	6.06	.68	.01	98.13
TRONDHJEMITE	135	76.29	.32	13.35	1.35	.06	.02	3.26	4.39	.66	.00	100.01
TRONDHJEMITE	139	69.62	.43	15.42	2.17	.05	.03	3.76	4.80	1.18	.08	98.73
TRONDHJEMITE	144	71.75	.33	15.44	1.75	.07	.02	3.24	4.66	1.69	.17	99.62
TRONDHJEMITE	153	69.33	.35	15.69	2.45	.03	.98	4.71	4.91	1.11	.09	98.05
TRONDHJEMITE	159	72.6	.12	15.54	.47	.01	.13	3.19	6.11	1.04	.01	100.12
TRONDHJEMITE	167	74.32	.04	15.05	.29	.01	.15	2.26	6.05	1.11	.00	99.46
TRONDHJEMITE	174	74.05	.12	14.11	1.13	.02	.23	2.85	5.33	.65	.01	99.20
TRONDHJEMITE	182	74.43	.04	15.55	.21	.01	.02	3.95	5.23	.31	.00	99.81
TRONDHJEMITE	184	71.25	.27	15.38	2.48	.03	.63	3.31	4.57	1.65	.07	99.34
TRONDHJEMITE	192	72.3	.02	15.31	2.55	.03	.82	3.07	4.76	1.15	.10	98.90
TRONDHJEMITE	195	72.58	.27	14.45	2.09	.02	.52	3.13	4.16	2.63	.15	99.29
TRONDHJEMITE	197	71.53	.37	14.48	2.66	.03	.72	3.58	4.45	1.43	.06	99.26
TRONDHJEMITE	198	74.63	.35	14.31	2.47	.03	.79	3.29	4.23	1.76	.06	99.77
TRONDHJEMITE	199	72.48	.34	15.18	2.03	.02	.65	3.57	4.92	1.42	.08	98.80
TRONDHJEMITE	171	71.53	.31	15.22	2.33	.02	.69	3.20	4.53	1.92	.05	99.78
TRONDHJEMITE	172	69.97	.38	15.62	2.56	.03	.71	3.33	4.36	2.49	.13	98.52
GRANODIORITE	114	69.64	.45	16.06	1.92	1.05	.63	3.43	4.27	2.93	.03	98.21
GRANODIORITE	125	70.92	.19	14.82	1.14	.02	.39	1.69	3.36	5.00	.04	99.69
GRANODIORITE	131	69.73	.37	15.38	2.03	.04	.05	2.51	4.96	2.92	.14	98.49
GRANODIORITE	132	72.17	.25	15.28	1.76	.03	.61	1.66	4.33	4.55	.09	99.25
GRANODIORITE	135	72.24	.19	14.36	1.26	.02	.27	1.15	4.18	4.75	.04	98.96
GRANODIORITE	138	73.13	.25	15.18	1.42	.02	.25	1.49	3.52	5.25	.14	100.15
GRANODIORITE	139	69.94	.34	15.14	2.73	.03	.74	3.30	4.66	1.66	.09	98.70
PEGMATITE	111	72.89	.09	15.87	.67	.02	.31	2.76	5.76	1.36	.01	99.55
PEGMATITE	124	74.22	.01	15.15	.12	.01	.03	.50	1.97	8.97	.00	100.96
PEGMATITE	136	74.00	.02	14.98	.16	.01	.05	1.64	4.07	4.18	.00	99.09
PEGMATITE	162	77.35	.04	13.73	.96	.01	.19	2.26	6.62	.33	.01	100.52
PEGMATITE	163	68.34	.24	13.65	4.05	.07	2.38	4.72	4.76	.82	.17	97.80

TABLE 7(i). Major element analyses for tonalites, trondhjemites, granodiorites and pegmatites from Gruinard Bay.

		Y	SR	RB	TH	PB	W	GA	ZN	BA	NI	CR+V	CE	LA	ZR	NB
TONALITE	123	0.5	403	31	1	8	0	21	35	733	12	29	28	14	92	4
TONALITE	135	4.5	333	38	1	8	0	20	38	504	19	15	15	6	75	5
TONALITE	136	3.4	398	29	0	10	1	20	32	400	18	35	16	5	105	7
TONALITE	149	0.3	297	22	4	10	0	23	57	243	30	67	32	15	129	5
TONALITE	153	3.8	322	51	3	10	0	24	54	605	38	54	30	13	132	5
TONALITE	154	7.9	401	38	4	10	0	23	40	522	13	32	30	13	118	5
TONALITE	156	0.4	203	42	2	8	0	15	8	439	34	69	32	15	115	6
TONALITE	157	8.5	203	12	4	9	0	23	54	187	27	80	20	6	114	2
TONALITE	158	0.4	353	48	4	11	0	25	54	534	23	78	47	33	259	5
TONALITE	159	7.6	363	49	15	13	2	25	52	616	31	57	63	41	186	7
TRONDHJEMITE	105	0.0	505	20	0	15	0	20	19	622	10	59	32	18	149	5
TRONDHJEMITE	106	0.0	381	16	0	16	0	13	14	2751	4	8	6	0	86	1
TRONDHJEMITE	107	0.0	737	16	0	9	1	24	23	623	10	4	28	19	157	3
TRONDHJEMITE	108	10.1	140	18	3	11	2	18	34	1658	5	1	48	24	636	1
TRONDHJEMITE	111	0.0	635	5	0	13	0	21	22	461	11	19	21	12	231	2
TRONDHJEMITE	112	0.0	589	13	2	9	0	23	18	625	16	14	30	20	144	3
TRONDHJEMITE	117	0.0	559	8	1	18	0	24	25	407	5	25	28	18	252	3
TRONDHJEMITE	118	0.0	382	8	1	21	1	15	23	519	6	12	17	6	572	3
TRONDHJEMITE	119	0.6	466	22	2	9	0	20	27	562	3	9	36	22	245	3
TRONDHJEMITE	120	0.8	333	27	6	13	0	26	21	1081	3	9	67	46	223	2
TRONDHJEMITE	128	0.7	569	27	2	10	0	20	32	551	10	10	29	14	146	3
TRONDHJEMITE	129	0.0	466	23	2	10	1	17	19	437	4	5	19	10	35	1
TRONDHJEMITE	137	0.0	416	29	0	13	0	13	10	281	1	8	4	0	41	1
TRONDHJEMITE	138	0.0	314	16	0	4	1	15	7	875	1	10	6	0	91	2
TRONDHJEMITE	152	0.0	311	3	0	6	3	17	3	197	3	4	15	6	50	1
TRONDHJEMITE	161	1.8	417	28	0	7	0	21	20	1307	4	10	32	17	190	3
TRONDHJEMITE	162	0.4	420	28	0	9	0	23	31	512	3	10	38	21	213	2
TRONDHJEMITE	166	0.4	300	34	22	8	1	18	20	1357	2	4	88	53	218	0
TRONDHJEMITE	167	1.4	373	33	4	9	2	21	35	733	1	9	55	30	204	5
TRONDHJEMITE	168	1.4	355	30	9	7	0	19	20	1154	3	9	65	39	177	3
TRONDHJEMITE	169	0.5	356	29	3	6	0	21	31	293	2	10	43	26	66	3
TRONDHJEMITE	170	0.5	380	34	1	11	0	21	27	1262	2	8	42	25	212	3
TRONDHJEMITE	171	2.1	436	40	1	9	0	21	32	1870	3	12	42	24	142	3
GRANODIORITE	114	0.4	674	47	5	20	3	19	26	3524	8	21	56	40	338	2
GRANODIORITE	126	2.1	527	86	38	29	0	17	37	1998	1	4	112	64	201	0
GRANODIORITE	130	4.7	590	60	10	14	2	22	32	958	3	6	86	46	180	4
GRANODIORITE	131	4.5	623	86	21	22	0	19	27	1857	1	4	99	53	193	1
GRANODIORITE	132	2.5	431	64	22	14	0	23	16	1043	0	3	75	43	166	0
GRANODIORITE	133	1.3	520	82	19	29	0	19	27	2259	0	2	72	41	166	0
GRANODIORITE	164	2.3	454	40	0	9	0	22	33	925	2	7	28	16	139	4
PEGMATITE	110	10.0	176	16	3	11	2	18	34	1670	5	1	48	31	637	1
PEGMATITE	124	1.8	324	166	8	25	0	14	12	1275	0	6	8	5	34	2
PEGMATITE	155	0.2	267	80	0	10	0	14	8	1715	1	6	11	11	24	0
PEGMATITE	165	4.9	286	8	12	13	0	19	9	158	0	6	4	2	98	12
PEGMATITE	160	7.3	374	23	0	11	0	23	42	272	60	119	43	26	76	3

TABLE 7(ii). Trace element analyses for tonalites, trondhjemites, granodiorites and pegmatites from Gruinard Bay.

TABLE 8. Mineral analyses from tonalites and trondhjemites at Gruinard Bay.

HORNBLENDE

	111/1	111/2	112/1	112/2	156/1	156/2	117/1	117/2
SiO_2	44·55	43·35	43·73	42·13	41·51	40·82	43·24	43·03
TiO_2	·55	·35	·45	·43	·65	·54	·22	·22
Al_2O_3	12·57	12·66	12·84	13·15	13·42	14·93	12·76	12·73
FeO	16·51	16·95	19·12	19·29	19·79	19·96	17·39	17·02
MnO	·32	·31	·26	·31	·45	·42	·34	·32
MgO	10·04	8·98	8·29	8·12	6·21	5·91	9·35	9·70
CaO	13·25	11·62	11·94	11·82	11·95	11·88	11·79	11·66
Na_2O	1·57	1·78	1·57	1·75	1·74	1·76	1·75	1·81
K_2O	·60	·61	1·14	1·19	1·22	1·12	·98	·85
TOTAL	99·96	96·61	98·34	98·19	96·94	96·74	97·82	97·34

BIOTITE

	111/1	111/2	112/1	112/2	156/1	156/2	156/3	171/1
SiO_2	35·20	35·09	33·31	34·54	35·93	36·09	35·30	35·43
TiO_2	1·03	·96	1·21	2·57	2·26	2·45	2·44	2·66
Al_2O_3	18·37	18·60	17·27	17·22	17·12	18·19	16·76	17·01
FeO	15·06	15·46	21·00	20·40	19·05	17·19	19·14	21·43
MnO	·14	·14	·23	·18	·28	·22	·20	·73
MgO	12·22	12·62	12·15	9·58	10·47	9·33	10·23	9·51
CaO	·06	·09	·09	·09	·03	·03	·01	nd
Na_2O	·48	·17	·09	·15	·21	·18	·25	·09
K_2O	6·53	5·82	6·66	8·31	9·57	9·65	9·34	9·84
TOTAL	89·09	88·95	92·01	93·04	94·92	93·33	93·67	96·70

nd not determined

Chapter 3

A PRELIMINARY GEOCHEMICAL STUDY OF SCOURIAN GRANODIORITIC GNEISSES FROM TORRIDON

SUMMARY

Scourian gneisses at Torridon are predominantly granodioritic in composition. They form banded and homogeneous gneisses which enclose lenses of amphibolite and are intruded by Scourie dykes. Coarse-grained granodioritic sheets low in mafic minerals intrude amphibolite lenses.

Banded and homogeneous gneisses evolved by the fractional crystallisation of plagioclase and hornblende or garnet from a trondhjemitic parent. Intrusive granodiorite sheets in amphibolite have an unusual chemistry; they are low in Sr and Ce and have low $(Ce/Y)_n$ ratios and probably represent late-stage liquids which evolved in equilibrium with plagioclase and apatite and may be derived from the adjacent gneisses.

1. FIELD RELATIONSHIPS

The Lewisian rocks around Loch Torridon were first described by the Geological Survey in Peach et al. (1907) and were subsequently the subject of a major study by J.H. Sutton (in Sutton and Watson, 1951). Sutton (op. cit.) proposed that a sedimentary pile, intruded by basic and ultrabasic rocks was metamorphosed to form the gneiss complex which was subsequently intruded by basic Scourie dykes, metamorphosed again (with the addition of microcline to the acid gneisses) and sheared. Recent unpublished field work by Windley and Davies (pers. comm.) has shown that the structure of the area can be interpreted as a major NNW trending shear belt in which relatively undeformed lacunae of gneiss are enclosed in highly deformed gneiss, intruded by Scourie dykes.

The samples collected for this study are from a low strain lacuna, 1000 metres long and 300 metres wide, SE of Loch Diabaigas Airde, in which banded amphibolite (300m x 100m) is enclosed in and intruded by granodioritic gneiss (Fig. 1).

The rocks can be divided into three minor suites on the basis of their field relationships:

(i) mottled and banded granodioritic gneiss cut by pegmatites up to 10cm wide (samples 277 - 280).

(ii) Coarse white granodioritic sheets with a very low mafic mineral content about 1m wide cutting amphibolite (samples 281 - 283) (282 contains large microcline megacrysts).

(iii) homogeneous granodioritic gneiss cut by a Scourie dyke; (samples 284-287).

The intrusive nature of the acid sheets in the amphibolite suggests an igneous origin.

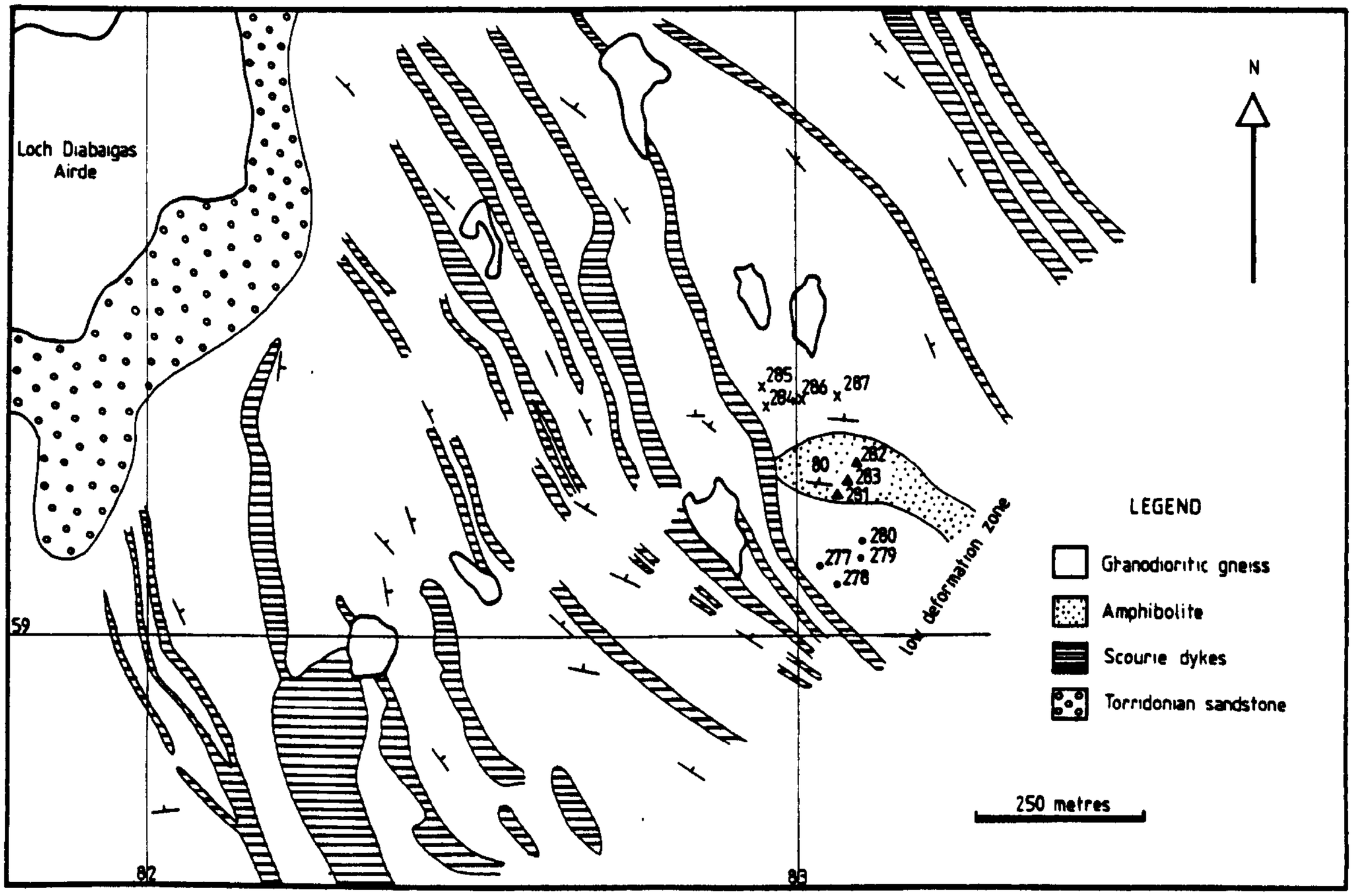

Fig. 1. Geological sketch map of the area S.E. of Loch Diabaigas Airde, after unpublished field work of Windley and Davis, showing location of samples. The symbols used for the samples in this diagram are repeated on subsequent diagrams in this chapter.

2. PETROGRAPHY

Quartzo-feldspathic gneiss from the Torridon area varies in composition from granodiorite to trondhjemite, using the nomenclature of Streckeisen (1973), but in contrast to the Scourie area and Gruinard Bay (see Chapters 1 and 2) the majority of the rocks in this area are granodiorite (Fig. 2) and for convenience they will all be referred to as granodiorites.

The granodiorites are inequigranular in texture with large plagioclase and quartz grains and fine-grained irregular grains of muscovite, biotite and epidote, replacing plagioclase; microcline forms large irregular grains and granular and interstitial

FIGURE 2. (A) and (B) White granodiorite sheets intruding amphibolite, S.E. of Loch Diabaigas Airde, Torridon.
(C) Detail of granodiorite sheet in amphibolite showing large microcline megacrysts.

(A)

(B)

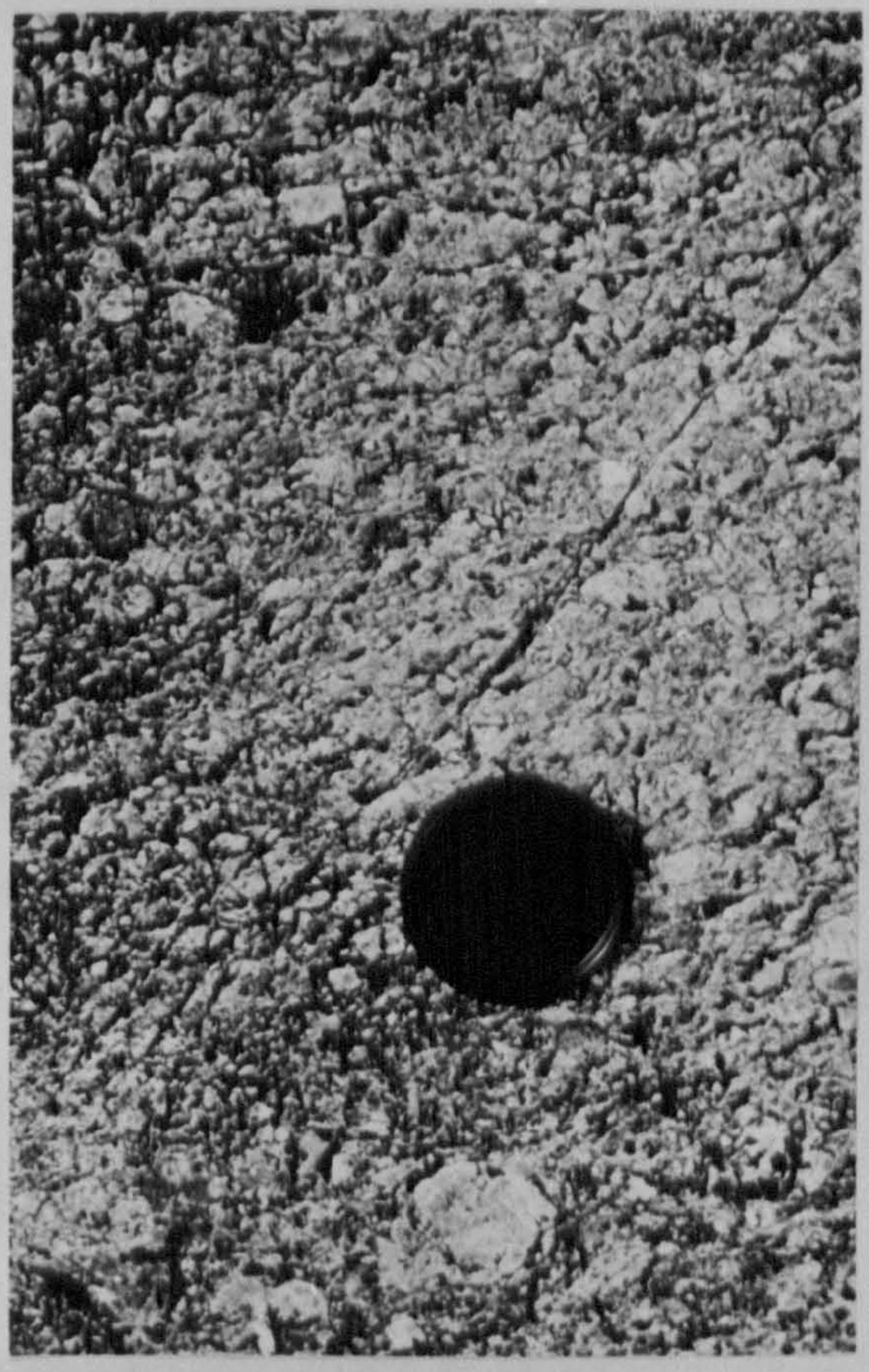

(C)

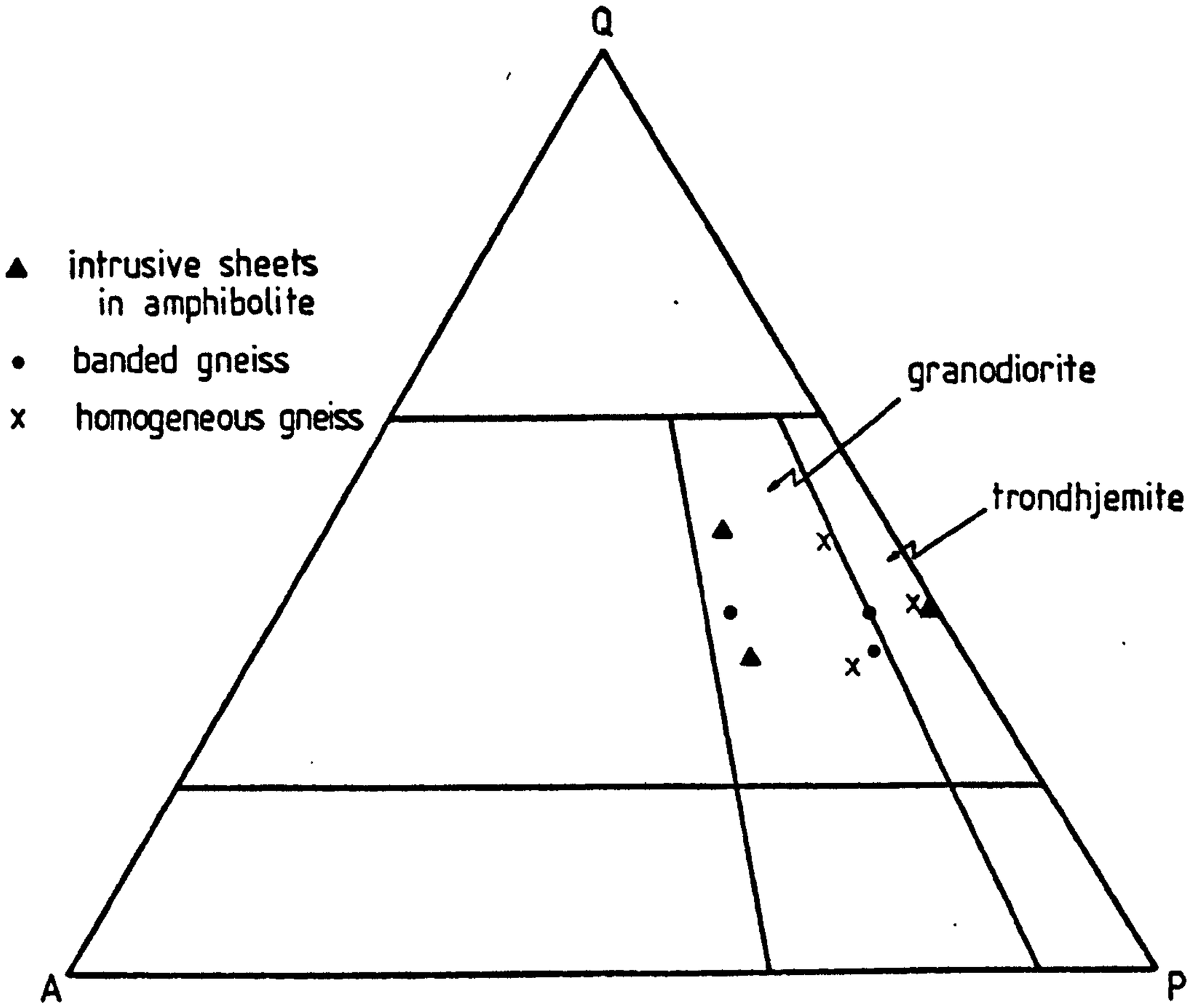

Fig. 3. Modal proportions of Quartz (Q), plagioclase (P) and alkali feldspar (A) in rocks from the Torridon area (after Streckeisen, 1973).

intergrowths. The white granodiorite sheets in amphibolite contain granulated plagioclase, altered to muscovite and epidote. Plagioclase (An_{21}) is zoned, contains rounded inclusions of quartz and myrmekite is developed at grain boundaries with microcline; microcline is perthitic and contains inclusions of plagioclase. A two-feldspar equilibration temperature from Whitney and Stormer (1977) of 440°C at 5 kb on sample 284 indicates a minimum temperature in view of the exsolved albite in microcline. Microcline contains measurable Ba (0.60 wt % BaO). Biotite contains inclusions of apatite, zircon and sphene and is altered to chlorite and epidote; muscovite often forms symplectitic intergrowths with quartz.

3. GEOCHEMISTRY

Granodioritic to trondhjemitic rocks from the Torridon area are of two types:

(a) high Sr (430 - 535 ppm) trondhjemites and granodiorites with highly fractionated REE; this group is represented by the banded and homogeneous gneiss which encloses amphibolite.

(b) low Sr (220 - 250 ppm), light REE depleted trondhjemites and granodiorites with relatively unfractionated REE; this group is represented by the intrusive sheets in amphibolite.

Homogeneous and banded Gneisses

These rocks define a trend parallel to the quartz feldspar cotectic for 5 kb pH_2O in the projection Qz-Ab-Or (Fig. 4). which

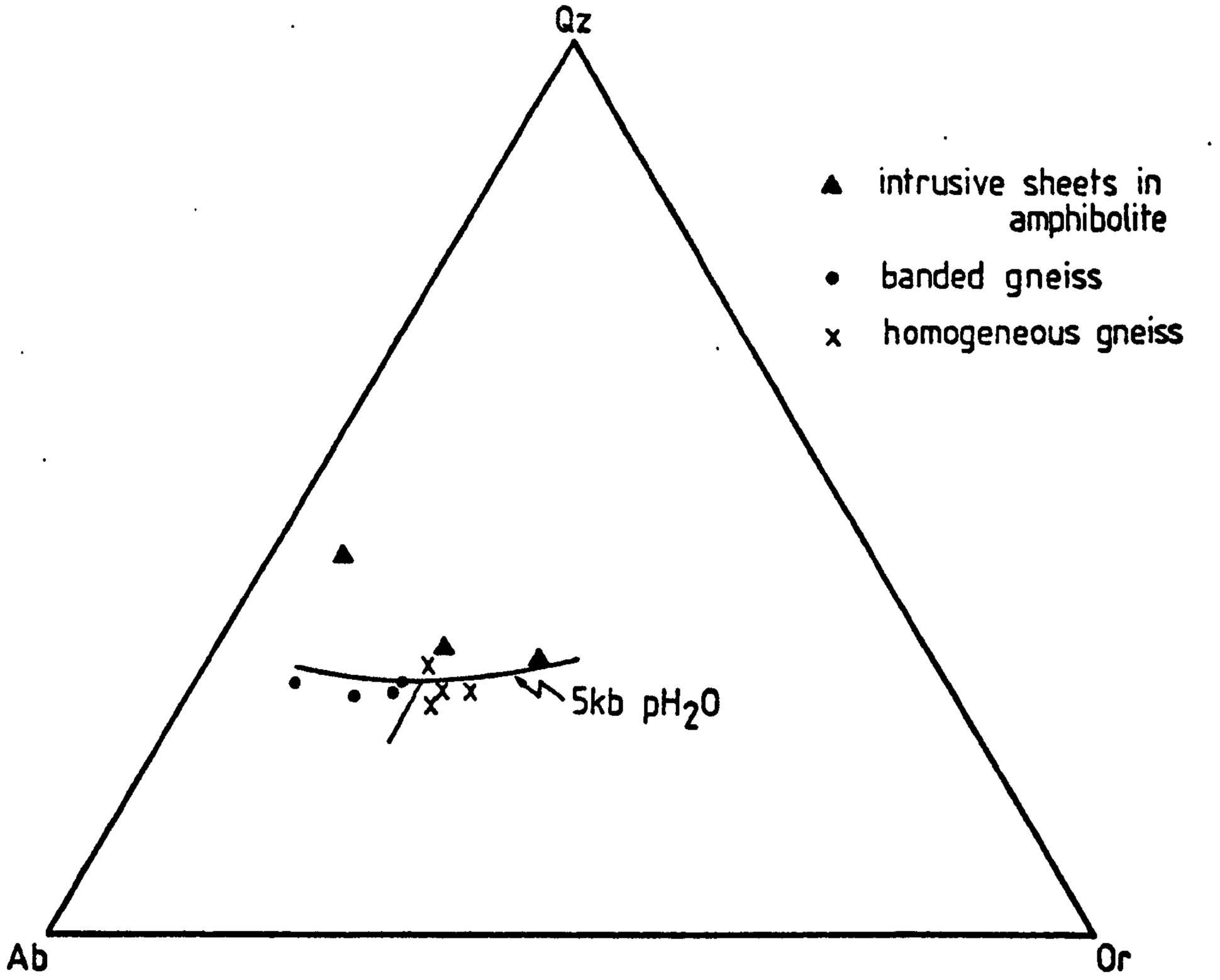

Fig. 4. Normative composition of Torridon gneisses plotted in the projection Qz-Ab-Or. These rocks also contain between 7% and 13% normative An.

could reflect the cotectic crystallisation of plagioclase and quartz from a trondhjemitic melt. There is a correlation between increasing Rb and decreasing Sr with an increase in the normative Or/Ab ratio, which is consistent with the fractional crystallisation of plagioclase. There is an increase in $(Ce/Y)_n$ from 2.8 to 55, with increasing normative Or/Ab which is not explicable purely in terms of plagioclase fractionation and indicates that hornblende or garnet was also a fractionating phase. The REE are highly fractionated; $(Ce/Y)_n$ ratios vary from 2.8 to 55 (Fig. 6) but these rocks are not

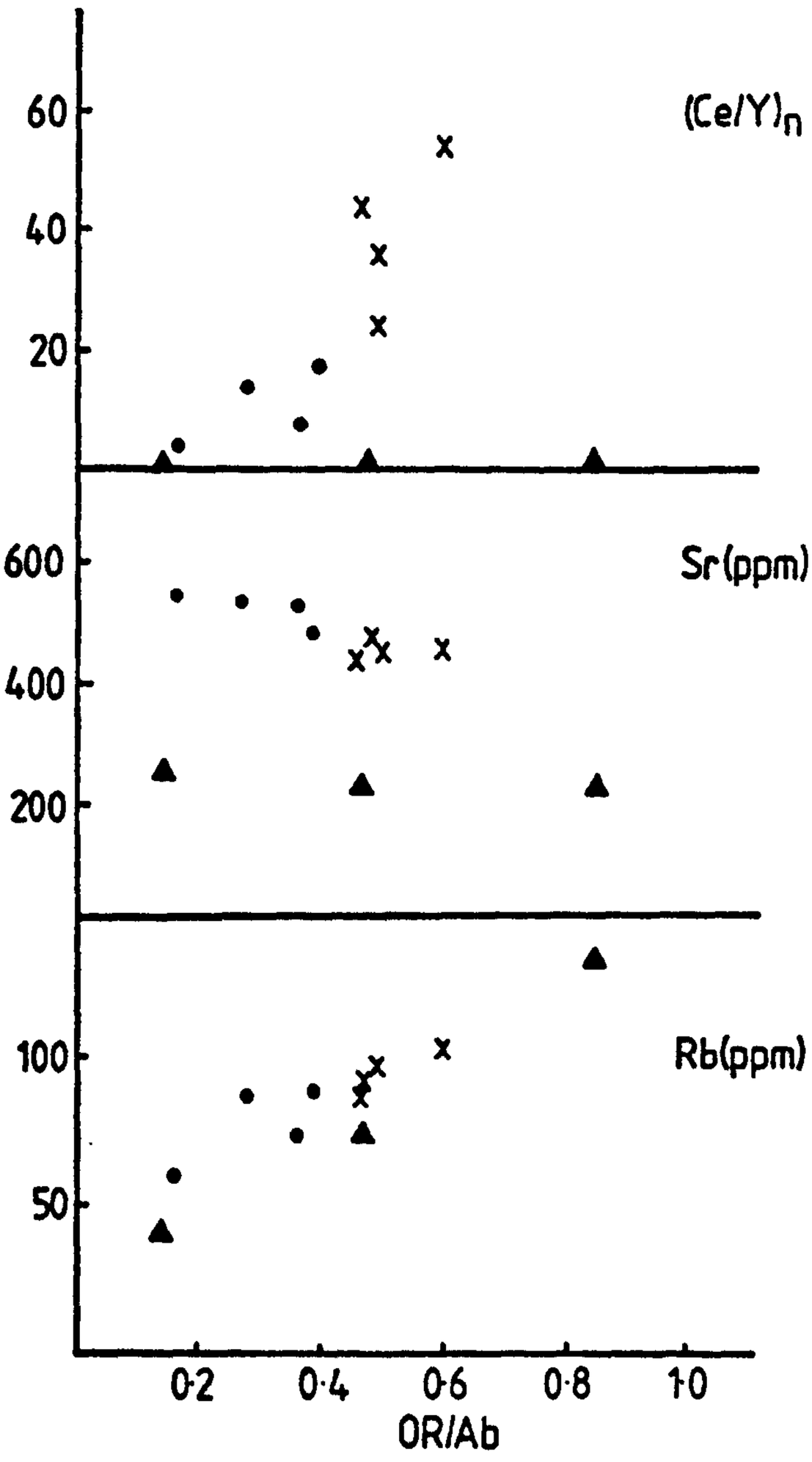

Fig. 5. $(Ce/Y)_n$, Rb and Sr plotted against normative Or/Ab for trondhjemitic-granodioritic rocks from Torridon

as highly depleted in Y as the trondhjemites at Gruinard Bay (the lowest Y recorded at Torridon is 2 ppm, at Gruinard Bay zero Y is common). Fig. 6 also shows that the banded gneiss is not as highly fractionated as the homogeneous gneiss (Y less than 6 ppm); homogeneous gneiss also plots closer to the centre of the Qz-Ab-Or projection (Fig. 4).

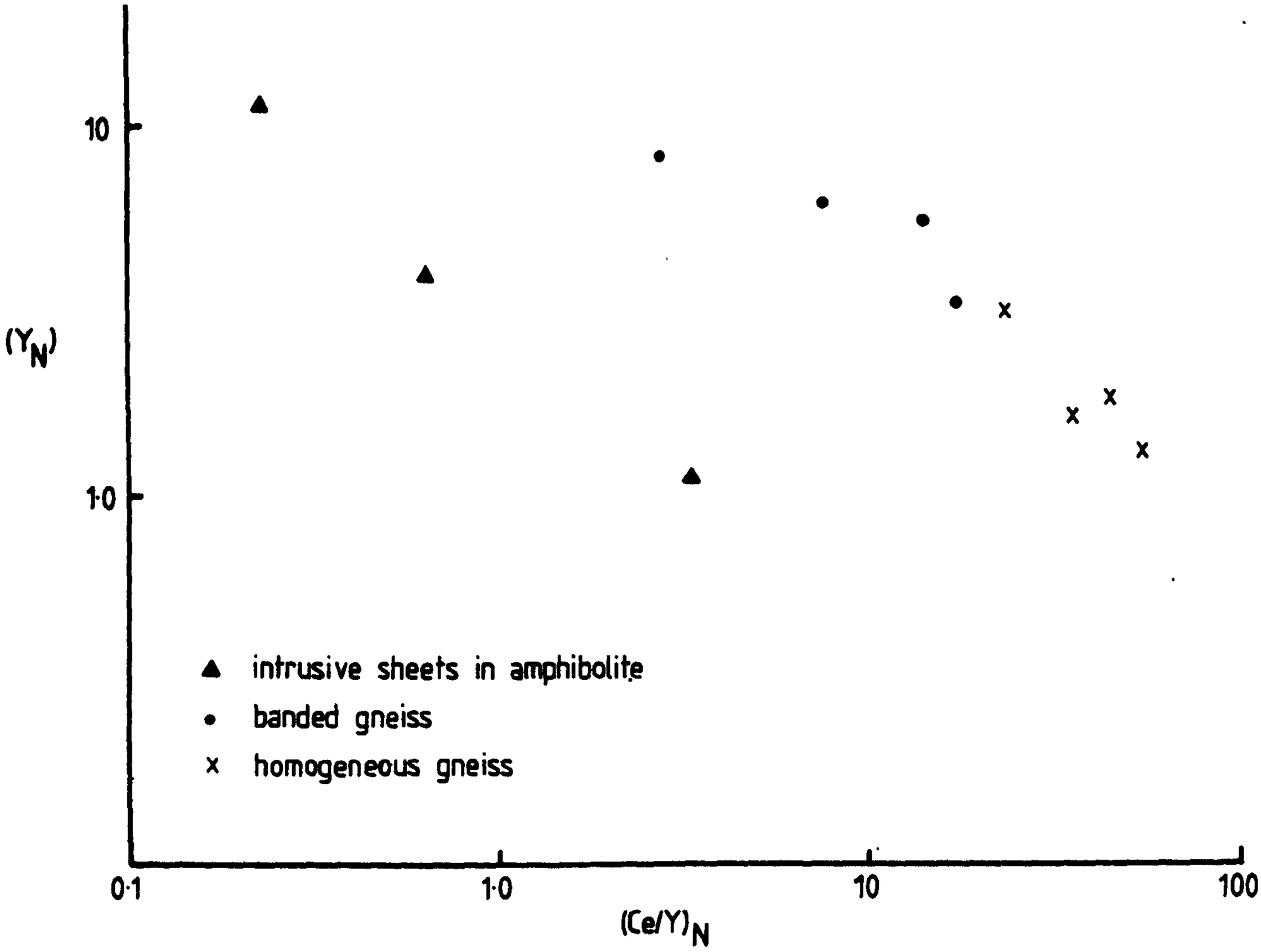

Fig. 6. Y vs. Ce/y normalised to chondritic values using the averaged chondrite of Herrmann (1974) for trondhjemitic to granodioritic rocks from Torridon.

Intrusive sheets in amphibolite

The granodiorites which form intrusive sheets in amphibolite lie on a trend close to the quartz-feldspar cotectic in Qz-Ab-Or space (Fig. 4) although they have evolved from a more quartz-rich trondhjemite than the banded and homogeneous gneiss. There is a slight decrease in Sr and a marked increase in Rb with increasing normative Or/Ab, but the concentrations of Sr are much lower than in

the gneisses. There are also very low concentrations of the light REE Ce and La (Ce 2 to 4 ppm) and Y varies from 2 to 23 ppm; $(Ce/Y)_n$ ratios vary from 0.23 to 3.4; low $(Ce/Y)_n$ ratios are not normally associated with 'granitic' rocks and are more typical of basalts. Intrusive sheets define a different trend on a Y_n vs. $(Ce/Y)_n$ plot from the banded and homogeneous gneiss suggesting that they are derived from a different source.

Discussion

Banded and homogeneous granodioritic gneiss forms the major part of the Scourian gneisses at Torridon and has major and trace element characteristics which are very similar to the amphibolite facies trondhjemite-granodioritic rocks at Gruinard Bay. The variation in Sr and Rb with increasing Or/Ab suggests that the rock compositions reflect liquid compositions which evolved on the quartz-feldspar cotectic surface in the system An-Ab-Or-Qz by the removal of plagioclase and quartz. The increase in the $(Ce/Y)_n$ ratio with increasing normative Or/Ab, however, indicates that hornblende or garnet was also a fractionating phase; this means that it is not possible to fully represent the evolution of these rocks in the simple system Qz-Ab-Or-An.

Homogeneous granodioritic sheets in amphibolite with low Sr and low $(Ce/Y)_n$ ratios are similar in chemistry to Scourian pegmatites at Scourie. Pegmatites at Scourie vary in mineralogy from microcline-rich to plagioclase-rich but have low Sr (100 - 160 ppm) and Ce (1 - 13 ppm) irrespective of mineralogy, indicating that Sr was retained in a phase in equilibrium with the liquid; this phase was probably plagioclase. The low concentrations of Ce are more difficult to explain. Tarney et al. (in press) describe trondhjemites from the Scourian complex with highly depleted REE patterns which they consider are feldspathic cumulates. This

cannot be the case in the Torridon area because of the intrusive nature of these sheets and their low concentrations of Sr. In view of the low concentrations of P in these sheets, relative to the adjacent gneisses, it is possible that Ce is retained in apatite; apatite, however, depletes a melt in all REE and particularly the middle REE and so this idea can be tested by obtaining a full REE pattern which is expected to be depleted and concave upwards.

The intrusive sheets in amphibolite are late stage residual liquids, possibly related to the adjacent gneiss, which evolved in equilibrium with residual plagioclase and apatite.

		SIO2	TIO2	AL2O3	FEO	MNO	MGO	CAO	NA2O	K2O	P2O5	TOTAL
GRANODIORITE	277	71.30	.22	15.49	1.62	0.00	.43	2.14	5.69	2.27	.05	99.19
GRANODIORITE	278A	71.24	.23	15.41	1.65	0.00	.42	1.99	5.37	2.82	.06	99.19
GRANODIORITE	279	71.55	.15	15.56	1.16	0.00	.46	1.99	5.26	2.98	.05	99.16
GRANODIORITE	280	71.01	.18	15.90	1.30	0.00	.41	2.71	6.10	1.44	.04	99.09
GRANODIORITE	281	74.42	.01	15.13	.34	0.00	.13	1.69	4.94	3.32	0.00	99.98
GRANODIORITE	282	74.10	.04	15.52	.46	0.00	.24	1.58	3.97	4.63	0.00	100.72
GRANODIORITE	283	76.78	0.00	14.91	.25	0.00	.10	2.57	5.09	1.05	0.00	100.74
GRANODIORITE	284	71.17	.26	15.26	1.77	0.00	.54	1.90	4.59	3.94	.06	99.51
GRANODIORITE	285	70.40	.27	15.60	1.82	0.00	.58	2.21	4.94	3.43	.08	99.33
GRANODIORITE	286	71.38	.29	14.93	2.00	0.00	.61	2.04	4.77	3.18	.09	99.29
GRANODIORITE	287	70.61	.24	15.31	1.78	0.00	.56	2.06	4.88	3.44	.07	99.15

		Y	SR	RB	TH	PB	W	GA	ZN	BA	NI	CR+V	CE	LA	ZR	NB
GRANODIORITE	277	12.0	520	74	4	20	36	27	35	748	1	0	45	26	146	6
GRANODIORITE	278A	12.7	533	86	11	21	13	24	34	966	0	0	88	60	157	0
GRANODIORITE	279	9.5	480	69	13	23	21	23	23	913	3	0	55	31	107	1
GRANODIORITE	280	16.3	535	60	11	0	42	22	21	373	1	1	22	10	123	1
GRANODIORITE	281	22.6	222	71	7	0	31	12	1	825	1	0	2	4	56	0
GRANODIORITE	282	2.2	223	134	10	1	22	15	5	1084	2	0	4	3	34	1
GRANODIORITE	283	7.9	247	44	0	1	53	14	2	132	0	2	2	3	62	1
GRANODIORITE	284	2.6	453	103	4	8	24	26	32	1093	2	5	69	51	140	0
GRANODIORITE	285	6.2	469	92	13	18	24	24	36	882	2	3	70	46	144	0
GRANODIORITE	286	3.8	427	38	7	11	45	25	39	792	2	4	78	51	169	0
GRANODIORITE	287	3.3	452	97	6	15	32	25	34	898	2	4	57	47	113	2

TABLE 1. Chemical analyses of granodiorites from Torridon.

Chapter 4

Ilmenite - Magnetite geothermometry in trondhjemites from the Scourian complex of N.W. Scotland.

Hugh R. Rollinson

Department of Geology, University of Leicester, Leicester LE1 7RH.

Summary.

Ilmenite-magnetite intergrowths from intrusive trondhjemites in the Scourian complex, N.W. Scotland were analysed with the electron probe and their equilibration temperatures and oxygen fugacities determined from the experimental work of Buddington and Lindsley (1964). Temperatures range from 1000°C (possible magmatic) down to 400°C; different parts of single grains became closed systems at different temperatures and different grains in the same rock show differing cooling histories. The oxygen fugacity of the magma was buffered by ilmenite, magnetite and possibly pyroxene slightly above the Ni-NiO buffer for 8kb; on cooling the oxygen fugacity fell below the QFM buffer curve for 8kb. and this is consistent with the loss of H_2O from the system into hydrous silicates.

Manuscript in press with

Mineralogical Magazine.

1. Introduction.

The crystallisation history of four trondhjemite samples from the Scourian complex, N.W. Scotland has been investigated using composite ilmenite-magnetite grains. A variety of compositions are present both as large and small scale exsolution lamellae, which can be used to unravel the complex cooling history of these rocks.

The samples were collected from Geodh'nan Sgadan bay near the village of Upper Badcall, Sutherland, where intrusive trondhjemite sheets one to two metres thick are seen to cut banded and homogeneous gabbro; the geology of the area has been described recently by Davies (1976). The samples were collected from three different sheets about 8 metres apart separated by gabbro. A Scourian age is assumed for the trondhjemites and gabbros because they are cut by undeformed, en echelon, Scourie dykes with chilled margins. The trondhjemites were intruded into the gabbro synchronous with or prior to granulite facies metamorphism. Quartzo-feldspathic gneisses adjacent to the gabbro, although in part retrogressed contain two pyroxenes. Two pyroxene assemblages in the gabbro show equilibration temperatures between 600°C - 680°C using the Nehru - Wyllie equation (1974) and between 820°C - 870°C using the Wood - Banno (1973) model. An estimate of the pressure of equilibration can be obtained from the method of Wood (1974); garnet-orthopyroxene pairs in adjacent gabbros show equilibration pressures in the range 8-12kb. and a figure of 8kb. has therefore been adopted as a conservative estimate in the recalculation of the oxygen buffer curves. The trondhjemites contain no pyroxene and the earliest minerals that can be recognised are plagioclase (An_{30}), bluish-grey quartz, hornblende and biotite. Some hornblende grains are poikiloblastic and seived with small grains of quartz; others occur as small grains in a matrix of fine grained granular quartz suggesting that they have grown from a pyroxene. Similar granodiorite sheets on Scourie More 3 km. to the north contain orthopyroxene as their main ferromagnesian

phase. Later minerals include green biotite, chlorite, carbonate, epidote and sphene. Retrogression is localised and patchy.

The trondhjemites of Upper Badcall Bay have a complex history which includes the following stages: (i) magmatic (ii) granulite facies metamorphism (iii) hydration and retrogression to amphibolite facies (iv) slow cooling with uplift.

Fig. 1

Sketches of the grains analysed are presented in fig. 1.

Ilmenite-magnetite grains in samples HR.49,53,86 display a complex exsolution pattern (Fig.2A). An original titanomagnetite exsolved into large scale (up to 50 μm wide) ilmenite-magnetite lamellae from which have subsequently exsolved small scale lamellae (ca 2 μm wide) parallel to the earlier lamellae. The ilmenite-magnetite pairs form subhedral grains in a granoblastic aggregate of plagioclase and quartz. A small amount of biotite overgrows some oxide grains. Ilmenite-magnetite grains in sample HR.56 are composed of broad zoned lamellae (Fig.2B); small scale exsolution lamellae are not present. Silicate grain boundaries are most irregular and lower temperature minerals (chlorite and carbonate) are more common.

Fig. 2

2. Analytical Procedure.

Analyses were made on polished thin sections using a Cambridge Microscan V electron probe in the Department of Geology, at the University of Leicester. Operating conditions were 15kv and a specimen current of 0.02 μamps. A spot size of less than 1 μm diameter was used. Iron and titanium were usually determined simultaneously. Points were relocated using X - Y coordinates. Full ZAF and dead time corrections were applied

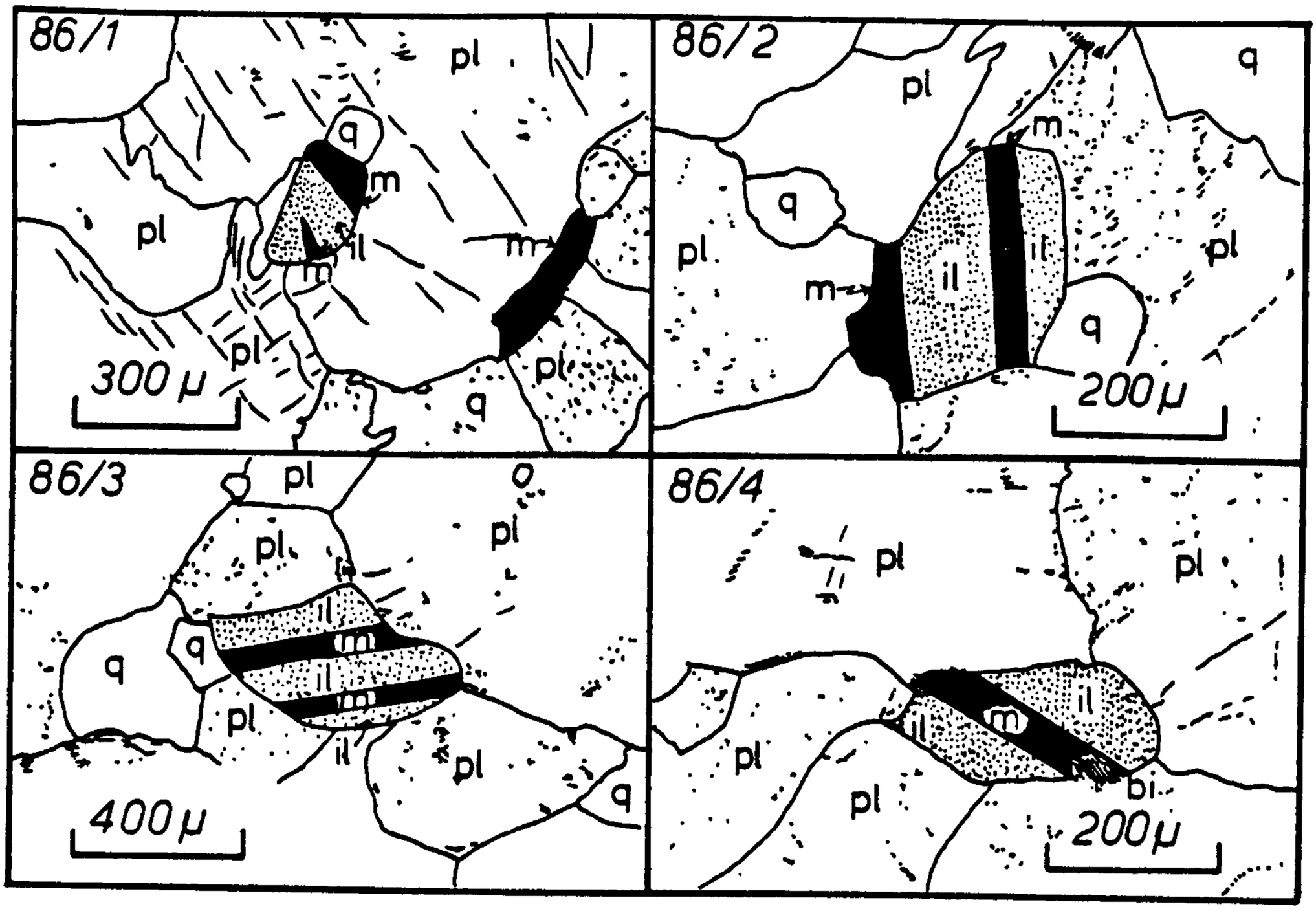

(a)

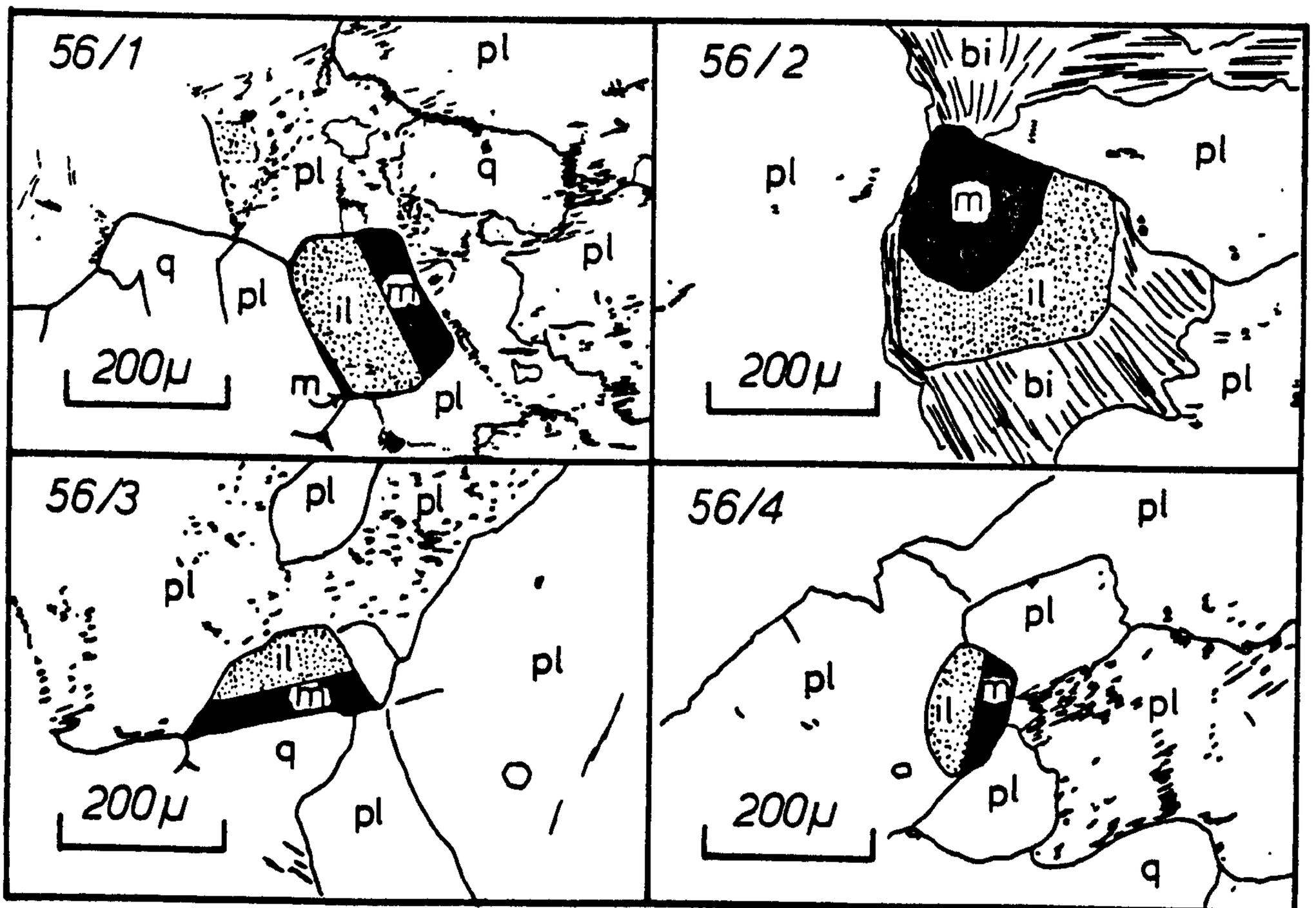

(b)

Figure 1: a,b,c, sketches of oxide grains analysed showing only the large ilmenite and magnetite lamellae; M, Magnetite; il, ilmenite; pl, plagioclase; bi, biotite; q, quartz; the density of the stipple on the plagioclase indicates the degree of sericitisation.

(C)

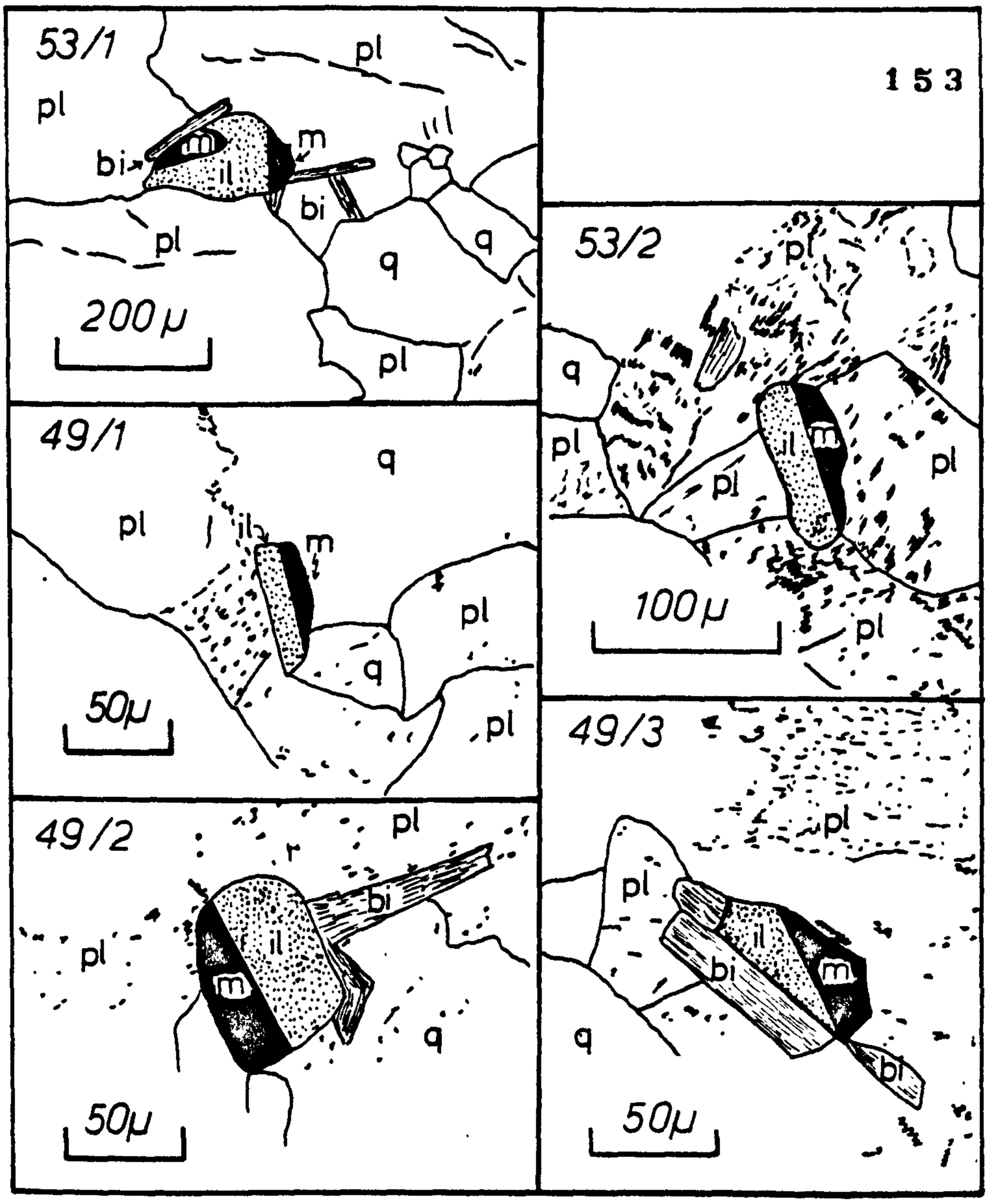

Figure 1 (continued).

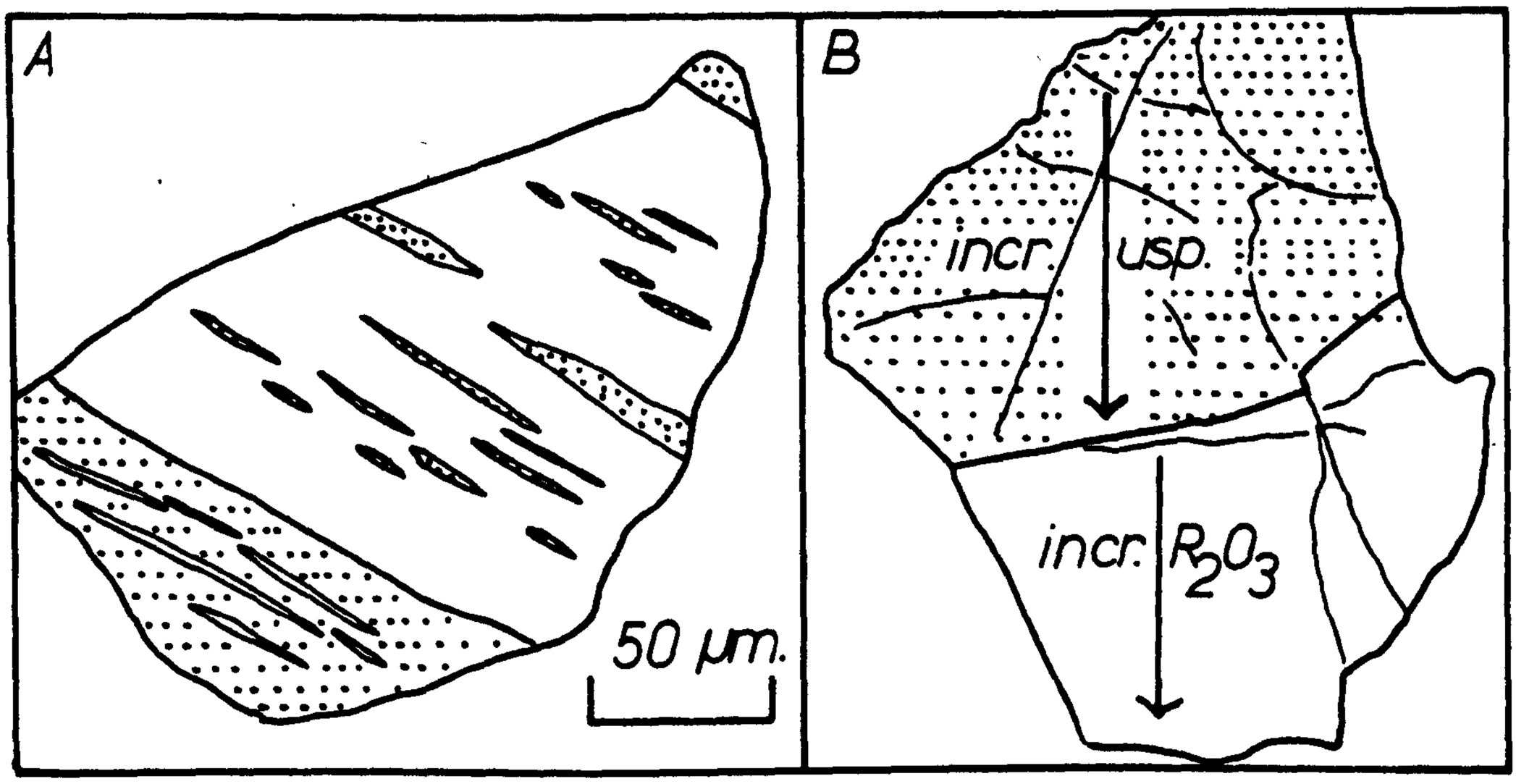

Figure 2: (A) A complex ilmenite magnetite grain with late exsolution lamellae; the magnetite is stippled. (B) A low temperature ilmenite magnetite grain showing the direction of zoning; the magnetite is stippled.

using the computer program Magic IV of Colby (1971) modified by R.N.Wilson.

Standards used were synthetic Fe_3O_4 for Fe (this gave good agreement with Fe metal, but was 3% lower than Fe determined using natural ilmenite; a similar discrepancy is found using the computer program of Mason, Frost and Reed, 1969), Ti, natural ilmenite (Ti 29.73, Fe 36.87, Mn 0.66, Mg 0.66, Al 0.02); Cr, pure chromium metal; Mn, natural rhodonite (Si 21.83, Al 0.09, Fe 2.80, Mn 31.58, Mg 0.34, Ca 5.59); Mg, synthetic MgO; Al, natural jadeite (Si 27.80, Al 13.30, Fe 0.10 Na 11.20). Minimum detection limits are Fe, 140 ppm., Ti, 60 ppm., and for minor elements from 100 ppm., to 240 ppm.

In order to obtain an average analysis of a grain which contains minute exsolution lamellae of ilmenite or magnetite both a defocused beam (diameter ca. 20μm) and a scanning beam over an area of up to 30 x 45 μm., free from surface irregularities on a stationary specimen were used; this gives the pre-exsolution composition of the grain as regards total cations.

Low totals in magnetites are thought to indicate that they are not stoichiometric due to late stage alteration towards γ-maghemite. Since total iron is determined as FeO it is necessary to calculate the mole fraction of ulvospinel in titanomagnatite on the basis of the TiO_2 content which does not change with oxidation; the remaining Fe is made into magnetite. It is therefore possible to use these analyses to study events prior to late oxidation. An average analysis of a magnetite grain containing lamellae of ilmenite will also have a low total, since the method used to recast the analysis as $Mgt\text{-}Usp_{ss}$ does not take into account subsequent oxidation of Fe^{2+} to Fe^{3+} during the exsolution of ilmenite lamellae (Powell & Powell 1977). For a grain with the composition $Usp_{45}Mgt_{55}$ exsolving into $Usp_{26}Mgt_{74}$ and $Ilm_{65}R_2O_{3\ 35}$ in the proportion 3:1 an average grain analysis will be ca. 1.0% too low.

Iron was allocated to Fe^{2+} and Fe^{3+} on the basis of mineral stoichiometry and the mole fractions of ulvospinel and R_2O_3 (Fe_2O_3 + Al_2O_3 + Cr_2O_3) were calculated using the method of Carmichael 1967.

3. Thermometry and oxygen barometry.

The experimental results of Buddington and Lindsley (1964) allow the equilibration temperature and oxygen fugacity of coexisting ilmenite and magnetite to be determined from their chemical composition. Subsequent workers have shown that it is possible to determine liquidus temperatures and oxygen fugacity for volcanic rocks (Carmichael, 1967; Anderson, 1968a); slowly cooled igneous and metamorphic rocks, however, have continued to equilibrate below their solidus and show a range of temperatures and oxygen fugacity conditions (Anderson, 1968b; Duchesne, 1972; Oliver, 1978 Recent work by Bowles shows that the equilibration temperature and oxygen fugacity estimated from compositions of ilmenite-magnetite grains in slowly cooled gabbros may be a function of the silicate environment, that different rocks from the same igneous complex may show different cooling histories and that complex ilmenite-magnetite grains may show a complex cooling history. (Bowles, 1976, 1977).

In the Scourian complex, O'Hara (1977) reports ilmenite-magnetite compositions which suggest low equilibration temperatures (below 500°C) and oxygen fugacities of less than $10^{-23.5}$ bars, in acid, basic and metasedimentary rocks.

This paper presents 42 new pairs of analyses from 13 composite ilmenite-magnetite grains (Fig.1, Table 1). Mole percent ulvospinel and R_2O_3 values have been used to determine temperature and oxygen fugacity at equilibration, from the experimental data of Buddington and Lindsley (1964). These have been plotted on $-\log_{10} fo_2$ vs. T°C. diagrams with haematite-magnetite, NiO-Ni, and quartz-fayalite-magnetite oxygen buffers calculated for 8 kb.

total pressure from the data of Eugster and Wones (1962) for reference (Figs. 3, 6-8).

4. Treatment of minor elements.

Since the experiments of Buddington and Lindsley (1964) were confined to the pure $FeO-Fe_2O_3-TiO_2$ system, their application to natural Fe-Ti oxides is limited by the presence of impurities. Several methods for recalculating analyses to minimise these effects have been proposed and are reviewed by Bowles (1977b). For the purposes of recalculating an analysis divalent elements are grouped together as RO, trivalent elements as R_2O_3 and tetravalent elements as TO_2: $RTO_3-R_2O_3$ and $R_2TO_4-R_3O_4$ stoichiometry is assumed. There are two types of recalculation; firstly the method which assumes that the minor elements form analogues of ulvospinel, magnetite, ilmenite and haematite and such solid solutions behave as the pure Fe-Ti end-members (Carmichael 1967); secondly the method which assumes that the minor elements are inert and so are discarded (Anderson, 1968b, Buddington and Lindsley, 1964). This latter method arbitrarily groups together and discards RO and R_2O_3 as spinel and RO and SiO_2 as silicate.

In this study the method of Carmichael has been adopted. The only minor element of any significance is Mn in ilmenite, which rises to 4.6 wt% MnO. Using the recalculation procedure of Anderson (1968b) (the least favourable alternative) ulvospinel in coexisting titanomagnetite differs by 0.18% Usp. and Fe_2O_3 differs by 0.71% Fe_2O_3. These values make no material difference to T and fO_2 derived from the Buddington and Lindsley graph.

A plot of FeO vs MnO for ilmenite in acid and basic rocks from the Scourian complex shows that Mn correlates inversely with Fe^{2+} in acid rocks and positively with Fe^{2+} in basic rocks (Rollinson in prep.). This suggests that Mn behaves differently in acid from basic rocks and that in acid rocks Mn behaves as Fe^{2+}, favouring the recalculation procedure of Carmichael (1967).

5. Equilibration of early broad lamellae.

By using a scanning electron beam it is possible to obtain the average composition of a broad lamella which contains smaller exsolution lamellae in order to estimate its composition prior to exsolution. A plot of lamellae whose original composition has been determined in this way shows that they lie on a curve slightly above the Ni-NiO buffer between 1010°C and 850°C (fig.3). Temperatures of the order of 1000°C are probably magmatic temperatures since they are higher than is normally recorded for granulite facies metamorphism; 850°C is interpreted as the blocking temperature, below which diffusion was unable to occur to form large scale lamellae.

Fig. 3.

The interpretation of the log fO_2 - T curve defined by these earliest phases is difficult. Carmichael and Nicholls (1967) have pointed out that the oxygen fugacity of a melt may be externally controlled by a volatile phase or the surroundings of the melt or, internally buffered by crystal liquid equilibria, provided the mass of the solid phases is sufficiently great compared with the mass of the gas. Hornblende is the earliest ferromagnesian mineral seen that is likely to have coexisted with Fe-Ti oxides, but it may not be primary. If a comparison is made with the curves determined by Carmichael (1967) (fig.3) for oxygen fugacity in acid lavas coexisting with different phenocryst phases and an adjustment is made for the difference in bulk composition and pressure** between these and the Scourian rocks some correspondence between the analysed points and the curve for hydrous silicates would be expected if equilibria involving hornblende had been controlling the oxygen fugacity. This is not found implying that amphibole did not control the oxygen fugacity either because it was not the main Fe bearing phase at magmatic temperatures or because the oxygen fugacity was externally controlled.

** The lower alkaline content of the trondhjemite will lower the curves, whilst increased pressure will raise them by about 1 log unit (assuming fO_2 is controlled by a reaction involving solid phases; if H_2O is involved in the reaction, as in the case of hydrous silicates the curve will be raised by a greater amount depending upon pH_2O); the net effect will be that the position of the curves will be unchanged except for the hydrous silicates which will be slightly raised.

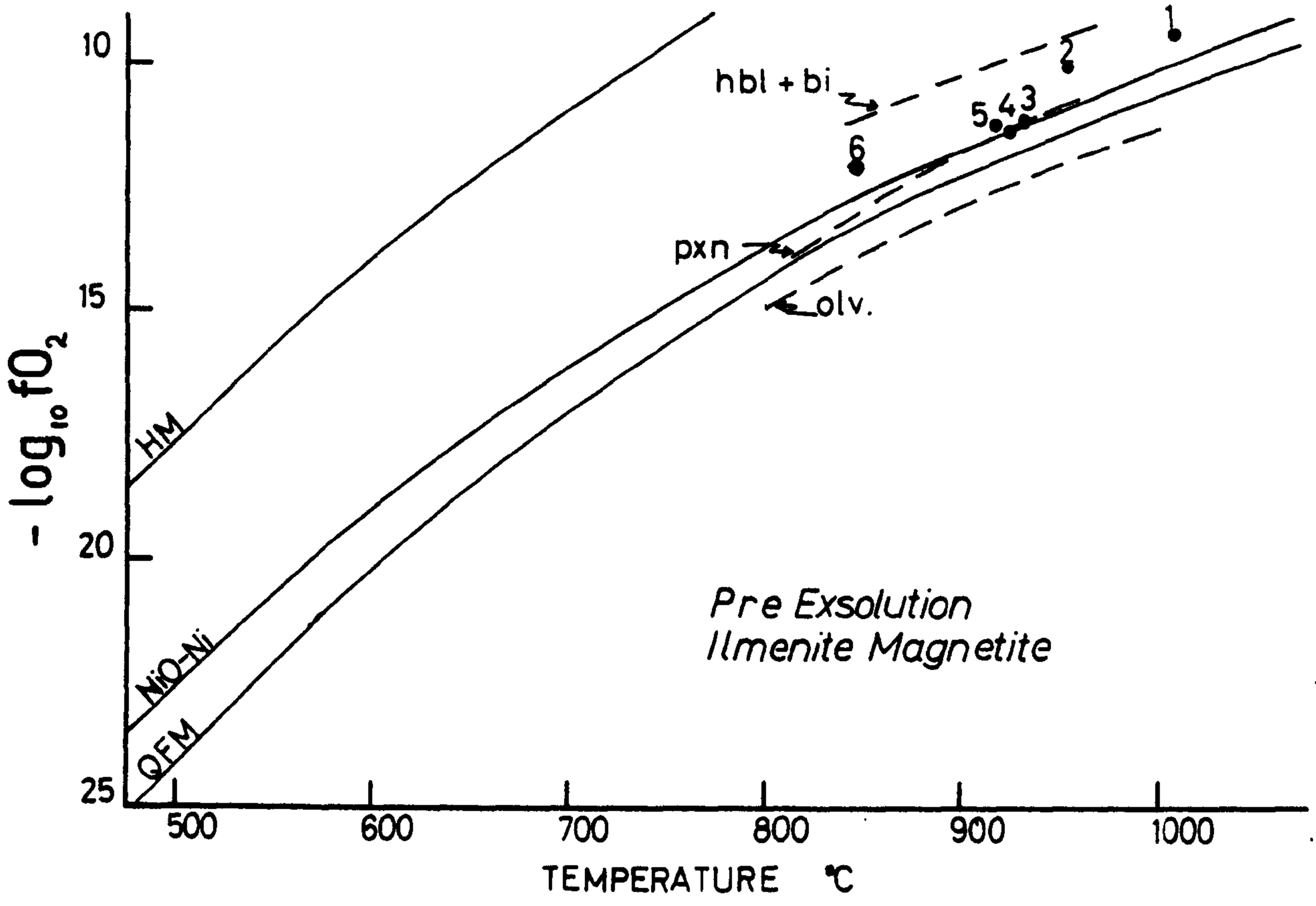

Figure 3: Plots of $-\log_{10} fO_2$ (in atmos.) versus temperature for coexisting ilmenite magnetite grains prior to exsolution. Also shown are buffer curves for sialic magmas in equilibrium with ilmenite and magnetite and olivine, pyroxene or hornblende and biotite at 1 atmos. pressure (after Carmichael 1967). Buffer curves are calculated to 8kb. after Eugster and Wones (1962). HM haematite-magnetite, Ni-NiO Nickel-Nickel oxide, QFM quartz-fayalite-magnetite.

Fig. 4

6. Equilibration of small scale lamellae.

After the formation of broad high temperature lamellae Ti diffusion continued on a smaller scale (2-3 μm) so that the lower temperature history of these grains can be considered in terms of many independent microsystems (Fig.4). Limited diffusion continued across the boundaries of and within early magnetite and ilmenite lamellae. The compositions of small scale exsolution lamellae in ilmenite and magnetite hosts have been determined and the results plotted in figs. 5 and 6. For HR 86/1 lamellae of ilmenite plot between 765°C and 730°C along a buffer curve close to the Ni-NiO buffer. Similar lamellae in HR.53 and 86/2 plot between 1005°C and 950°C along a buffer curve parallel to the Ni-NiO buffer but at a higher fO_2 than that for the equilibration of the high temperature lamellae. Lamellae of magnetite in ilmenite plot at lower temperatures below the QFM buffer curve in HR 86/1 and HR 52/2. Both groups of points show decreasing oxygen fugacity with decreasing temperature although they equilibrated at different temperatures.

Figs. 5, 6.

Individual microsystems have equilibrated at different temperatures and oxygen fugacities within the same grain and yet similar microsystems in different grains have equilibrated at different temperatures and oxygen fugacities suggesting that the rock itself has become a series of independent closed systems. Similar findings have been made in the gabbros of the Freetown complex, Sierra Leone (Bowles 1976, 1977).

In the case of magnetite lamellae in an ilmenite host it is possible that the smaller lamellae (i.e. of the order of 2 μm wide) show an excess of TiO_2 in the analysis. This is because a small (less than 1 μm) electron

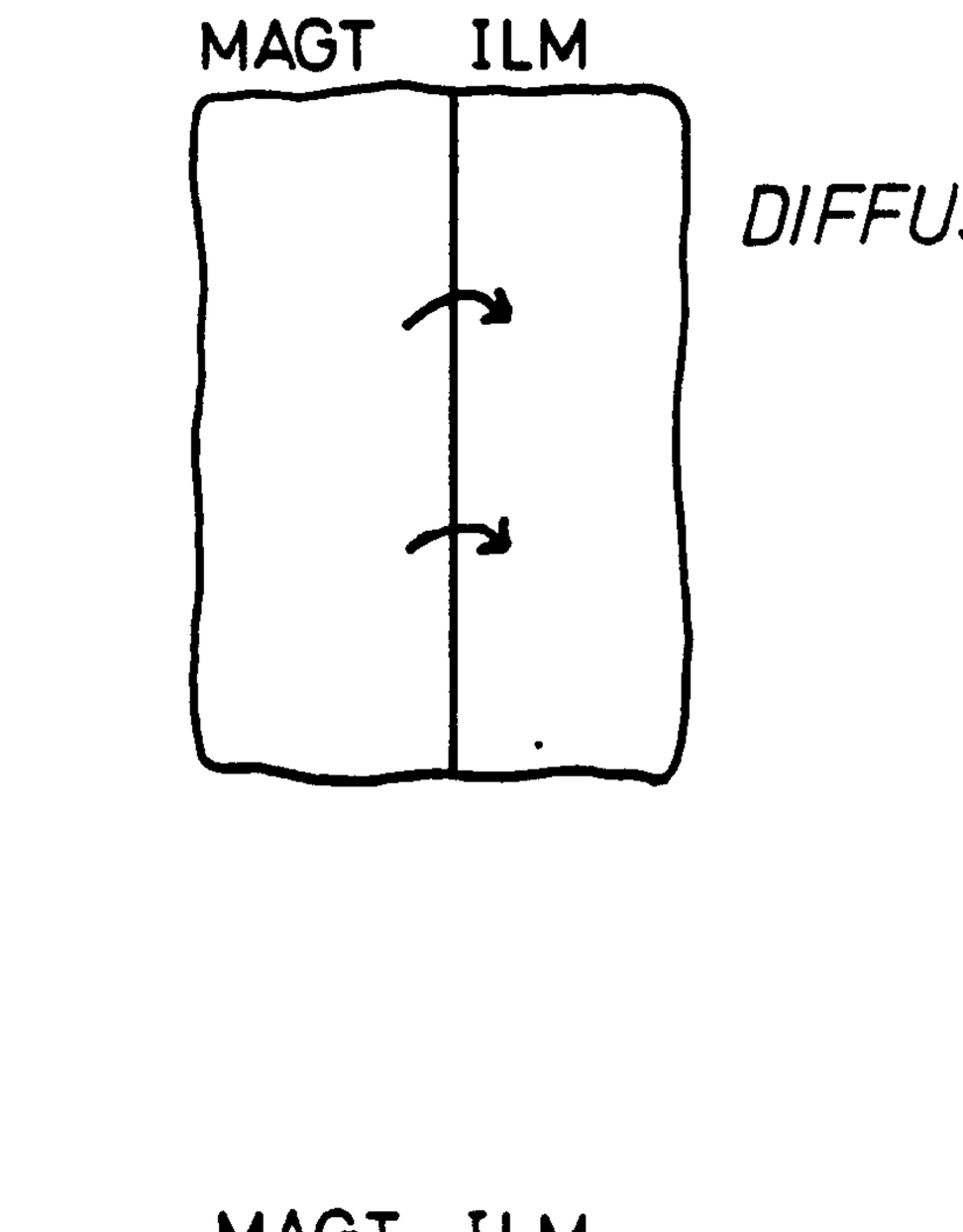

Figure 4: Model for diffusion in composite ilmenite magnetite grains at high and low temperatures. Stage 1: the formation of ilmenite lamellae from an originally homogeneous titanmagnetite. Stage 2: at lower temperatures microsystems A (ilmenite and a rim of magnetite), B (magnetite and ilmenite at the boundary of high temperature lamellae), and C (magnetite and a rim of ilmenite) are the only systems that can be in equilibrium.

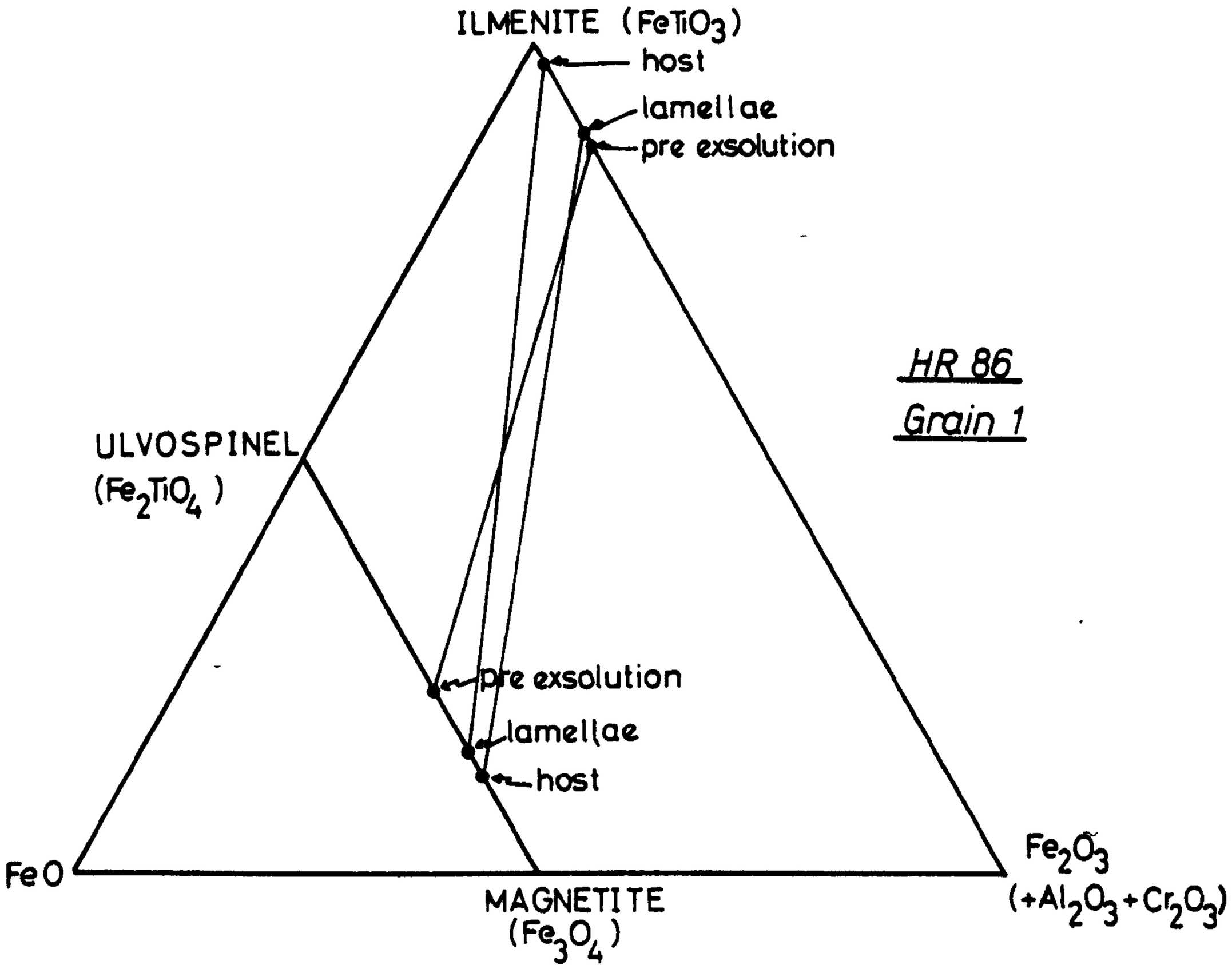

Figure 5: Composition of phases plotted as mole percent in the system $FeO-R_2O_3$ - $FeTiO_3$. The tie lines indicate coexisting phases.

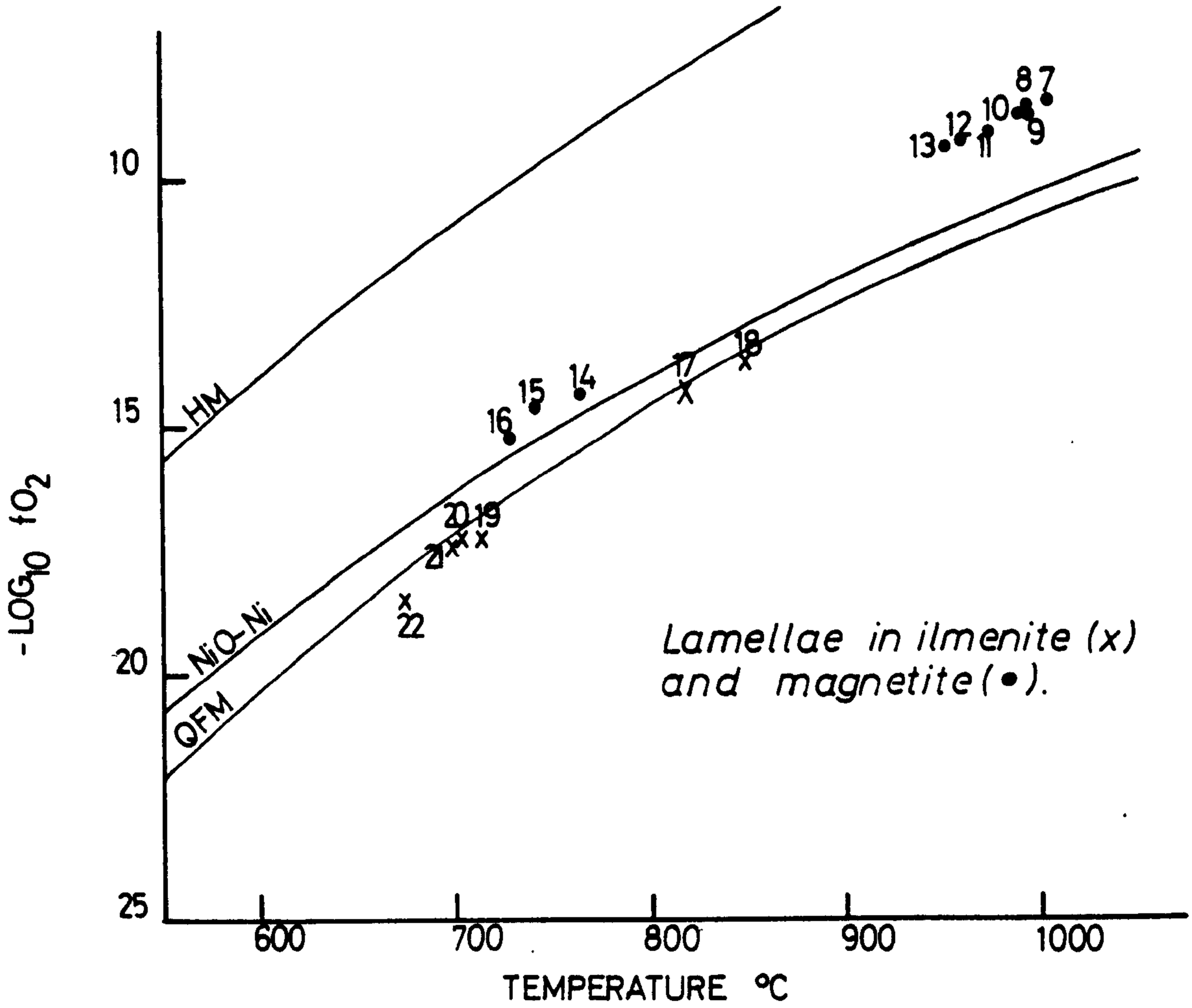

Figure 6: Plots of $-\log_{10} fO_2$ (in atmos.) versus temperature for coexisting ilmenite magnetite pairs occurring as lamellae and host in high temperature lamellae (systems A and C, fig.3). 14-16, 19-22 (HR 86 grain 1), 7-10 (HR 86 grain 2), 11,13,18 (HR 53 grain 1), 12,17 (HR 53 grain 2). Buffer curves as in fig.2.

beam excites an area of up to 10 μm wide below the surface of the specimen. In the case of magnetite in ilmenite Fe in the magnetite will fluoresce Ti in the enclosing ilmenite. It is possible to apply an extra fluorescence correction making some assumptions about the orientation of the lamellae. Given a lamella 2 μm. wide with vertical sides and apparently 10.0 wt% TiO_2 the maximum TiO_2 due to fluorescence of the ilmenite is 2.5 wt % TiO_2 (S.J.B. Reed pers comm.). This has the effect of changing the equilibration temperature from 714°C to 670°C and logfO_2 from -17.2 to -18.0. There is therefore some uncertainty over the position of points 17 to 22 on fig.6, although their positions relative to the QFM buffer curve remain unchanged. This does not affect the main conclusions of this section which suggests that individual microsystems within ilmenite-magnetite grains have behaved differently.

7. Later diffusion across boundaries between early lamellae.

The composition of phases either side of early high temperature lamellae boundaries have been measured and the results plotted in figs. 7 and 8. Analyses from HR.49 & 53 lie on the QFM buffer curve in the temperature range 765°C to 610°C, whilst those for HR.86 plot in the same temperature range at a lower fO_2 (Fig.8). Equilibration temperatures for HR.86/1 are the same as those for the equilibration of magnetite lamellae in ilmenite. Separate buffer curves for different rocks were described by Bowles (1976) who has pointed out that whilst there is a real difference between two sets of analyses their exact position in $\log_{10} fO_2$ - T space is subject to the limits of experimental error quoted by Buddington and Lindsley (1964). Consequently since there is a real difference in the analyses of samples HR49 & 53 and HR56 the separate buffer curves are regarded as meaningful. Grains 49/3 and 86/4 have exsolved into broad high temperature lamellae but are zoned and contain no small scale exsolution lamellae. The sense of the zoning is such that R_2O_3 in ilmenite decreases as it approaches magnetite.

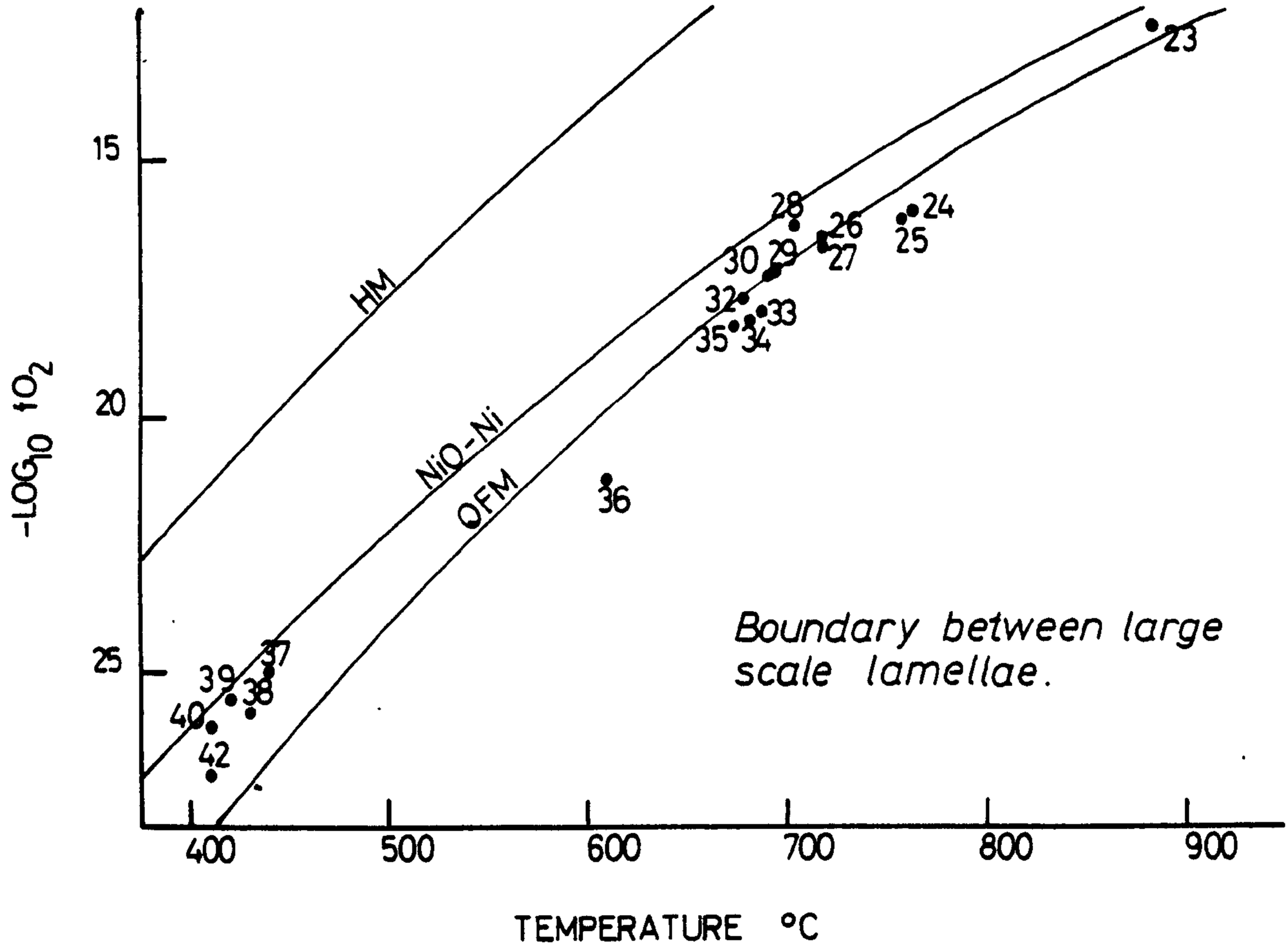

Figure 7: Plots of $-\log_{10} fO_2$ (in atmos.) versus temperatures for coexisting ilmenite magnetite pairs, measured close to the grain boundary between high temperature lamellae (system B in fig.3). Buffer curves as in fig.2.

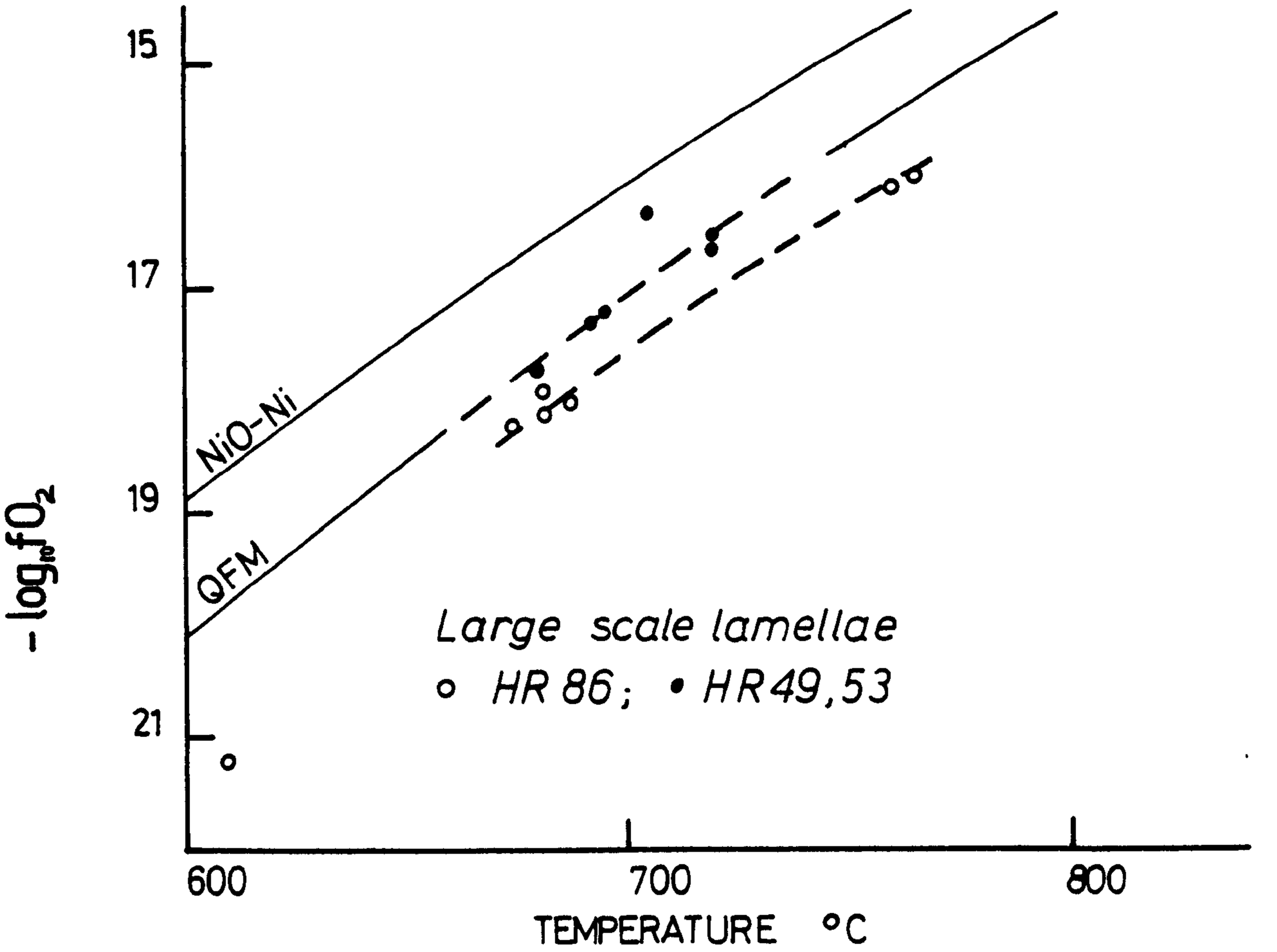

Figure 8: Plots of $-\log_{10} fO_2$ (in atmos.) versus temperature for coexisting ilmenite magnetite pairs, measured close to the grain boundary between high temperature lamellae in samples HR 86, 53 and 49.

The equilibration temperature and fO_2 at the grain boundary varies from the centre of the grain (fig.6 points 24 & 25) to a higher temperature and fO_2 at the edge of the grain (fig.6 point 23).

Figs. 7, 8

8. Low temperature grains.

In HR 56 ilmenite-magnetite grains show bread zoned lamellae with no late, small, exsolution lamellae. The sense of zoning is such that magnetite grains increase in ulvospinel content towards ilmenite and ilmenite decreases in R_2O_3 towards magnetite. Even though the grains are in disequilibrium it is assumed that equilibrium was at least established close to the boundary between lamellae. Equilibration temperatures thus obtained are between 410°C and 430°C at an fO_2 between the NiO-Ni and QFM buffers. Ilmenite-magnetite grains in HR 56 coexist with a biotite richer in Ti and a hornblende depleted in Fe relative to those in samples HR.49, 53 & 86, suggesting that there was continuous Fe-Ti exchange between oxides and silicates as well as between ilmenite and magnetite.

9. Conclusions and discussion.

The present study shows that: (i) ilmenite-magnetite thermometry for intrusive trondhjemites in the Scourian complex yields reasonable magmatic temperatures. (ii) ilmenite-magnetite oxygen barometry suggests that the trondhjemites crystallised in equilibrium with pyroxene. (iii) the ilmenite-magnetite geothermometry is best interpreted in terms of the cooling history of the rock rather than separate metamorphic events. (iv) different parts of the same oxide grain become closed systems at different times (v) different grains in the same rock show different cooling histories (vi) different samples of similar rocks from the same locality may show greatly differing equilibration temperatures.

1. Discussion of equilibration temperatures. These may be read as blocking temperatures below which diffusion of Ti can no longer take place at the scale in question. Buddington and Lindsley (1964) suggest that the blocking temperature is a function of (a) the diffusion rate (i.e. the temperature of the system), (b) the amount of the guest phase present, and (c) the cooling rate (probably not very important in these slowly cooled rocks), (d) the presence of a fluid phase as catalyst.

The blocking temperature for the large lamellae, which formed first, was determined principally by factors (a) and (b); on cooling, given that a certain amount of guest phase had exsolved a threshold is reached which prevents further diffusion on this scale, although it continues to take place on a smaller scale.

Factors determining the blocking temperature of the small-scale lamellae must include (a) and (b) but also in the case of ilmenite exsolving from magnetite the availability of oxygen (i.e. its mobility within magnetite and its availability within the system), since it is consumed in the reaction. This is not the case in the exsolution of small magnetite lamellae an ilmenite host, and may be why they equilibrate at a lower temperature at a lower temperature (Fig.6).

The low temperatures obtained from HR.56 probably indicate the presence of a fluid phase which aided the diffusion of Fe and Ti between ilmenite, magnetite, biotite and hornblende.

2. Discussion of Oxygen Buffers. As the trondhjemite magma cooled the oxygen fugacity was probably controlled by the magma and crystallised phases. With further cooling possible oxygen buffers are: (i) water, (ii) the water-rock system, and (iii) the oxides themselves, since the production of ilmenite lamellae in magnetite involves a reaction which consumes oxygen and the production of titaniferous magnetite from ilmenite produces oxygen.

The difference in fO_2 and cooling history of HR.86/1 from HR.86/2 and HR.53 (fig.6) is problematical. Bowles (1976) has shown that ilmenite-magnetite grains in different silicate environments in the same rock have different cooling histories. In these rocks however the silicate environment is identical. This would suggest the importance of a fluid phase in determining the history of these grains and indicates that early in the history of the rock fluids became isolated microsystems in equilibrium with their particular local environment. In the case of HR.86 the microsystems may have been of the order of 1 cm. or less in average dimension.

If the only water in the system was that dissolved in the original magma and the trondhjemites have remained a closed system during cooling it is possible to show, using the model outlined in Buddington and Lindsley (1964), that the observed decrease in oxygen fugacity, across oxygen buffers, with falling temperature represents the loss of H_2O in the system to hydrous silicates.

Acknowledgements: This work was carried out during the tenure of an N.E.R.C. Studentship at the University of Leicester. I am grateful to Dr. B.F. Windley for his encouragement and advice and to R.N. Wilson for his abundant help with electronprobe micro analysis. Professor E.A. Vincent and Dr. J.F.W. Bowles are thanked for their constructive comments on the manuscript.

TABLE 1. CHEMICAL ANALYSES OF COEXISTING ILMENITE AND MAGNETITE.

ILMENITE

	Average grains						Magnetite host										Ilmenite host				
	1.	2.	3.	4.	5.	6.	7.	8.	9.	10.	11.	12.	13.	14.	15.	16.	17.	18.	19.	20.	21.
Rock/grain Anal. No.	HR 86/3 915/5	HR 53/1 925/17	HR 86/2 914/14	HR 53/2 925/12	HR 86/1 977/1	HR 49/2 924/13	HR 86/2 914/9	HR 86/2 914/6	HR 86/2 914/18	HR 86/2 914/2	HR 53/1 924/26	HR 53/2 925/15	HR 53/1 924/28	HR 86/1 977/21	HR 86/1 977/16	HR 86/1 977/20	HR 53/2 925/7	HR 53/1 924/30	HR 86/1 978/5	HR 86/1 978/2	HR 86/1 978/7
TiO_2	43.44	43.76	46.85	46.25	45.54	43.19	24.73	27.77	28.38	30.92	32.04	32.40	33.10	45.48	45.10	45.69	48.36	49.16	49.67	49.52	49.30
Al_2O_3	.37	.05	-	.02	.02	.01	-	-	-	-	.03	.04	.04	.03	.03	.03	.02	.02	.03	.03	.02
Cr_2O_3	-	.08	-	.03	.11	.00	-	-	-	-	.10	.20	.10	.15	.17	.16	.04	.00	.06	.03	.05
'FeO'	53.14	51.90	52.71	51.08	50.72	49.78	68.96	64.09	67.47	63.39	60.57	62.40	59.90	49.52	49.94	48.95	48.36	47.31	47.08	47.29	47.23
MnO	1.29	1.31	-	1.59	1.05	3.02	-	-	-	-	.86	.94	1.01	.98	.93	.93	1.73	1.48	1.17	1.17	1.12
MgO	-	.00	-	.00	.17	.04	-	-	-	-	.08	.00	.07	.19	.22	.23	.00	.11	.22	.22	.23
Total	98.25	97.11	99.56	98.97	97.59	96.04	93.70	91.86	95.84	94.31	93.67	95.97	94.21	96.33	96.38	95.99	96.19	98.07	98.23	98.25	97.95
FeO	37.76	38.02	42.13	39.98	39.59	35.71	22.24	24.97	25.52	27.80	27.80	28.18	28.62	39.57	39.22	39.37	41.74	42.51	43.09	42.95	42.79
Fe_2O_3	17.10	15.42	11.76	12.34	12.37	15.64	51.92	43.47	46.62	39.55	36.49	38.03	34.77	11.06	11.91	10.24	4.78	5.33	4.44	4.82	4.94
TOTAL	99.95	98.64	100.74	100.21	98.85	97.61	98.89	96.22	100.52	98.27	97.33	99.72	97.70	97.46	97.58	97.02	96.69	98.61	98.67	98.74	98.44
R_2O_3	16.91	15.12	11.16	11.83	12.09	15.35	51.23	43.92	45.11	39.02	36.35	37.16	34.56	11.03	11.87	10.27	4.78	5.18	4.38	4.71	4.85

MAGNETITE

Anal. No.	915/13	924/25	914/15	925/20	977/5	924/12	914/8	914/5	914/17	914/3	924/27	925/16	924/19	977/29	977/15	977/19	925/10	924/4	978/6	978/1	978/8
TiO_2	15.98	15.35	15.99	15.30	14.77	11.15	8.68	8.73	9.10	9.10	8.44	7.55	8.14	8.91	8.16	7.92	15.59	17.84	10.38	9.60	9.08
Al_2O_3	.14	.05	-	.07	.11	.12	-	-	-	-	.05	.08	.05	.12	.12	.11	.04	.05	.07	.06	.10
Cr_2O_3	-	.14	-	.21	.35	.12	-	-	-	-	.18	.30	.16	.32	.35	.31	.23	.20	.34	.28	.35
FeO'	74.96	77.97	75.74	74.57	75.32	82.77	82.44	80.85	82.65	81.18	81.10	80.10	81.36	79.72	80.18	80.63	73.30	74.01	79.31	79.89	79.44
MnO	.32	.31	-	.24	.22	.73	-	-	-	-	.06	.08	.17	.06	.05	.10	.27	.41	.16	.23	.04
MgO	-	.02	-	.00	.04	.03	-	-	-	-	.02	.00	.02	.01	.00	.02	.00	.00	.01	.02	.00
Total	91.41	93.85	93.52	90.39	90.81	94.92	91.13	89.58	91.75	90.28	89.85	88.19	89.91	89.14	89.49	89.08	89.42	92.51	90.26	90.09	89.02
FeO	44.00	44.23	45.01	43.14	42.78	40.52	37.89	37.42	38.46	37.97	37.14	35.83	36.82	37.36	36.85	36.43	43.63	45.87	38.90	38.08	37.50
Fe_2O_3	34.41	37.50	36.13	34.93	36.16	46.95	49.51	48.27	49.11	48.02	48.75	49.20	49.50	47.08	48.85	49.12	33.64	31.27	44.91	46.47	46.61
TOTAL	94.85	97.60	97.13	93.89	94.43	99.62	96.08	94.42	96.67	95.09	94.63	93.04	94.86	93.86	94.38	94.01	92.80	95.64	94.77	94.74	93.68
Usp.	47.98	44.85	46.90	46.45	44.58	32.04	25.95	26.55	27.03	27.47	25.60	22.31	24.64	27.37	24.82	24.19	47.87	53.05	31.38	29.05	27.80
ToC	1010	980	935	930	922	850	1005	995	995	990	975	960	952	765	742	730	820	850	714	705	700
$-\log_{10} fO_2$	9.4	10.1	11.2	11.4	11.3	12.1	8.4	8.5	8.6	8.6	9.0	9.2	9.3	14.3	14.6	15.2	14.4	13.7	17.2	17.02	17.4

'FeO' total iron determined as FeO

TABLE 1 (Continued)

ILMENITE

		Grain Boundary Pairs																			
Rock/grain Anal. No.	22 HR 86/1 978/4	23 HR 86/4 915/23	24 HR 86/4 915/21	25 HR 86/4 913/19	26 HR 49/3 924/17	27 HR 49/3 924/19	28 HR 49/2 925/7	29 HR 49/1 924/1	30 HR 53/31 924/30	31 HR 49/1 924/4	32 HR 53/2 925/9	33 HR 86/1 977/10	34 HR 86/1 977/12	35 HR 86/1 977/14	36 HR 86/2 914/21	37 HR 56/4 916/24	38 HR 56/3 916/17	39 HR 56/1 916/2	40 HR 56/2 916/13	41 HR 56/2 916/13	42 HR 56/1 916/1
TiO_2	49.81	46.03	46.96	49.57	47.94	48.05	47.57	47.41	49.16	47.62	48.55	49.89	50.01	49.65	51.24	50.06	50.42	49.66	48.87	48.87	50.38
Al_2O_3	.02	.06	.03	.04	.01	.01	.01	.01	.02	.02	.00	.02	.01	.01	-	.03	.04	.03	.21	.21	.09
Cr_2O_3	.04	-	-	-	.04	.00	.00	.00	.00	.02	.04	.02	.03	.01	-	-	-	-	-	-	-
'FeO'	46.72	46.86	44.65	46.99	46.46	46.25	46.92	43.74	47.31	43.74	46.98	47.22	47.32	47.21	48.23	47.61	45.59	49.30	44.09	44.09	48.31
MnO	1.16	1.06	1.71	1.29	2.05	2.13	3.15	4.60	1.48	4.45	1.64	1.06	1.10	1.12	-	1.75	3.15	1.45	4.42	4.42	1.48
MgO	.23	-	-	-	.07	.06	.04	.01	.11	.05	.00	.22	.23	.26	-	-	-	-	-	-	-
Total	97.98	94.97	93.35	97.89	96.57	96.51	97.70	95.78	98.07	95.96	97.21	98.44	98.70	98.25	99.47	99.45	99.10	100.44	98.10	98.10	100.26
FeO	43.21	40.32	40.50	43.27	40.91	40.94	39.52	37.96	42.51	38.29	42.00	43.40	43.45	43.05	46.08	43.24	42.15	43.19	39.49	39.49	43.81
Fe_2O_3	3.90	8.34	4.59	4.14	6.17	5.90	8.23	6.43	5.33	6.06	5.54	4.25	4.30	4.62	2.39	4.85	3.71	6.79	5.13	5.13	5.01
Total	98.37	95.81	93.79	98.30	97.19	97.09	98.51	96.41	98.61	96.58	97.76	98.86	99.13	98.72	99.71	99.94	99.47	101.12	98.10	98.10	100.76
R_2O_3	3.84	8.39	4.71	4.06	6.10	5.80	7.98	6.37	5.18	6.02	5.44	4.13	4.17	4.48	2.28	4.85	3.61	6.45	5.30	5.30	9.86

MAGNETITE

Anal. No.	978/3	915/24	915/20	915/20	924/16	924/16	925/8	924/2	924/27	924/3	925/16	977/9	977/11	977/13	914/17	916/25	916/18	916/5	916/9	916/10	916/6
TiO_2	9.58	15.20	15.15	15.15	9.45	9.45	8.69	7.69	8.44	7.78	7.55	9.33	8.96	8.30	9.10	.93	.87	.72	.47	.59	.56
Al_2O_3	.08	.22	.07	.07	.04	.04	.05	.05	.05	.05	.08	.09	.11	.09	-	.32	.32	.28	.11	.16	.36
Cr_2O_3	.31	-	-	-	.16	.16	.13	.09	.18	.11	.30	.39	.36	.34	-	-	-	-	-	-	-
'FeO'	80.23	73.27	75.47	75.47	79.79	79.79	83.85	80.49	81.10	80.62	80.10	79.19	80.33	81.07	82.65	91.04	89.95	92.80	90.74	91.20	93.10
MnO	.28	.38	.25	.25	.06	.06	.13	.09	.06	.09	.08	.03	.11	.06	-	.07	.12	.10	.11	.16	.06
MgO	.06	-	-	-	.03	.03	.03	.04	.02	.01	.00	.01	.03	.00	-	-	-	-	-	-	-
Total	90.54	89.07	90.95	90.95	89.55	89.55	92.88	88.44	89.85	88.65	88.19	89.02	89.89	89.87	91.75	91.36	91.26	93.91	91.41	92.03	94.09
FeO	38.10	42.49	43.19	43.19	37.92	37.92	38.31	35.99	37.14	36.19	35.83	37.72	37.57	37.08	38.46	31.56	31.10	31.86	30.80	31.13	31.83
Fe_2O_3	46.82	34.20	35.88	35.88	46.53	46.53	50.61	49.45	48.75	49.38	49.20	46.09	47.52	48.88	49.11	66.10	65.41	67.72	66.61	66.76	68.09
TOTAL	95.23	92.50	94.53	94.53	94.19	94.19	97.95	93.40	94.63	93.61	93.04	93.66	94.66	94.76	96.67	98.98	97.81	100.69	98.80	98.72	100.90
Usp.	28.83	46.79	45.69	45.69	28.77	28.77	25.47	23.65	25.60	23.88	23.31	28.56	27.14	25.15	27.03	2.72	2.57	2.07	1.39	1.73	1.60
T^oC	675	885	765	760	720	720	705	695	695	693	680	687	682	675	610	440	430	420	410	410	410
$-\log_{10} fO_2$	18.5	12.3	16.0	16.1	16.5	16.6	16.3	17.2	17.2	17.3	17.7	18.0	18.1	18.2	21.2	25.0	25.8	25.5	26.0	26.0	27.0

'FeO' total iron determined as FeO

Chapter 5

FELDSPAR AND IRON TITANIUM OXIDE THERMOMETRY IN GRANITE SHEETS FROM THE SCOURIAN COMPLEX, N.W. SCOTLAND

Summary

Granite sheets in the Scourian complex of N.W. Scotland represent residual liquids formed during the evolution of the Scourian tonalites and trondhjemites. Feldspars and iron titanium oxides were analysed by electron microprobe and equilibration temperatures were determined using the methods of Buddington and Lindsley (1964) and Powell and Powell (1977b) for iron titanium oxides and Stormer (1975), Whitney and Stormer (1977), Powell and Powell (1977a) and a modification of the Powell and Powell equation for co-existing alkali feldspar and plagioclase. Temperatures are in the range 1100°C to 350°C and these are used to interpret the cooling history of these rocks.

Hypersolvus granite contains mesoperthite feldspar ($An_{12}Ab_{51}Or_{37}$) which crystallised from a melt between 1100°C and 1250°C. Two feldspar, plagioclase-mesoperthite granites give a preferred equilibration temperature of 645°C (at 10kb) and two feldspar, perthitic microcline-plagioclase granites give equilibration temperatures of 654°C. These temperatures are closure temperatures for the exchange of albite between alkali feldspar and plagioclase during cooling.

Iron titanium oxides from the same granite sheets define two cooling curves on an oxygen fugacity - temperature diagram; high temperature oxides equilibrated between 910 and 660°C and oxygen fugacity was buffered along the QFM buffer curve; low temperature oxides equilibrated between 530°C and 320°C and the oxygen fugacity was not buffered. An increase in oxygen fugacity in the temperature interval 660-530°C indicates that water was

introduced into the system; the availability of water assisted exsolution in the mesoperthite feldspars, exsolution in and equilibration between iron titanium oxides and the alteration of ferromagnesian minerals.

1. INTRODUCTION

An accurate and detailed assessment of temperature conditions is very important in the interpretation of crystallisation events in metamorphic terrains. Granitic rocks lend themselves to a study of this kind because they often contain mineral assemblages which allow at least two independant methods of estimating temperature so that a certain amount of 'cross-checking' of the assumptions inherent in the formulation of the thermometers can be carried out. Co-existing iron titanium oxide solid solutions, commonly present in 'granitic' rocks, have been calibrated by Buddington and Lindsley (1964) for temperature and oxygen fugacity at equilibration; more recently Stormer (1975) and Whitney and Stormer (1977b) have discussed the use of the distribution of $NaAlSi_3O_8$ between co-existing plagioclase and alkali feldspar as a geothermometer. They have tested their model in a number of different geological environments against other mineral thermometers and obtained meaningful results (Whitney and Stormer, 1976; 1977a; Stormer and Whitney, 1977).

The purpose of this study is to show that the application of geothermometry to slowly cooled metamorphic terrains needs careful interpretation and the results must be treated with the same caution as the radiometric 'age' of a rock. The application of more than one thermometer to variably equilibrated mineral pairs in the same rock suite yields a range of temperatures, which may or may not include the peak of metamorphism, but coupled with a detailed textural study it can yield information about the cooling history of the rock. Iron titanium oxide solutions are also valuable tools in unravelling the effects of the fluid phase during cooling. Studies in the Scourian complex

are further complicated because of the clearly igneous origin of the rocks studied, so that it is necessary to distinguish igneous from metamorphic events, if in fact the two can be separate.

O'Hara (1978) proposed that the Scourie gneisses were metamorphosed at very high temperatures and pressures (ca 1150 $\pm$ 100°C and 15 $\pm$ 3kb) on the basis of geothermometry on ternary pyroxenes and feldspars of unusual composition and of relevant experimental studies. However, O'Hara (op. cit.) also found that the application of several recent geothermometers and barometers to garnet - pyroxene assemblages yields much lower temperatures and generally lower pressures.

2. GEOLOGICAL SETTING

Granitic rocks represent a minor part of the granulite facies gneisses of the Scourian complex. Rocks containing alkali feldspar and plagioclase or a single anorthite-bearing alkali feldspar are loosely called granite in this study even though some are more strictly granodiorites. The rocks studied crop out in the area between Scourie and Badcall, Sutherland; they form sheets two to three metres wide and up to a few hundred metres long, and are intrusive into tonalitic gneiss and gabbro. They were derived by the fractional crystallisation of plagioclase from a trondhjemitic parent and represent the last stages of crystallisation of a tonalite-trondhjemite-granite suite. Deformation of the sheets has given rise to flattened lenticles of quartz and ferromagnesian minerals with a granulite facies mineralogy (bluish quartz and orthopyroxene or almandine garnet as the main ferromagnesian mineral).

3. TWO FELDSPAR THERMOMETRY

The two feldspar thermometer as originally formulated by Barth (1934, 1951, 1956, 1962, 1970) and modified (e.g. Dunham, 1971; Orville, 1962) is based upon the distribution of albite between alkali feldspar and plagioclase and applies irrespective of geological environment, i.e. of the means by which equilibrium was attained, whether in a magma, via solid diffusion or through a fluid phase. Stormer (1975) and Whitney and Stormer (1977b) presented two equations which can be used to set limits on the equilibration temperature of natural feldspars which contain only small amounts of the orthoclase molecule in plagioclase and small amounts of the anorthite molecule in alkali feldspar. For feldspars which crystallised in rapidly cooled lavas, in a disordered structural state Stormer's (1975) equation is based on margules parameters calculated by Thompson and Waldbaum (1969) for the sanidine-high albite solvus. The equation of Whitney and Stormer (1977) is based on margules parameters for the metastable low albite-maximum microcline solvus determined by Bachinski and Mueller (1971) and is more applicable to feldspars in slowly cooled plutons. It is important therefore to establish the degree of ordering of feldspar pairs at the time they reached intercrystalline equilibrium even if subsequently they have re-equilibrated internally to a more ordered structural state. For most granitic rocks, where the potassium feldspar has crystallised as orthoclase, equilibration temperatures calculated using these two equations will give upper and lower limits to the true equilibration temperature. Whitney and Stormer (1977b) suggest that feldspars in granitic plutonic rocks crystallising in the range 600 - 800^{o}C may be partially ordered and that orthoclase is the stable phase, implying an intermediate equilibration temperature. At temperatures

greater than 800°C feldspars will be disordered and the high temperature solvus is appropriate.

The assumption that only small amounts of anorthite are present in alkali feldspar and small amounts of potassium feldspar are present in plagioclase is not always valid and solutions may depart appreciably from the Henry's Law range where the activity coefficients for binary and ternary solutions are approximately the same. This is particularly so for the alkali feldspars from Scourian granites, which contain in excess of 10% anorthite. Powell and Powell (1977a) have modified the equation of Stormer (1975) to correct for small amounts of the anorthite molecule in alkali feldspar; their arguments can also be applied to small amounts of barium feldspar in alkali feldspar when anorthite is minimal (up to 2% Ba-feldspar is present in some Scourian alkali feldspars). A ternary sub-regular solution model expression is used for the activity coefficient; for low concentrations of calcium in alkali feldspar the equation reduced to that of Stormer (1975), but at high An contents there is an appreciable difference resulting in much lower equilibration temperatures. If the margules parameters of Bachinski and Mueller (1971) are used in Powell and Powell's (1977) formulation, the limiting case for the more ordered structural state with appreciable An in alkali feldspar can be derived. A more detailed discussion of the formulation of two-feldspar thermometers is given in Appendix 2.

4. ANALYTICAL PROCEDURE

Feldspar analyses were obtained using a Cambridge Microscan V (wave length dispersive) electron probe microanalyser. Operating conditions were 15.0 kV and a specimen current of 20 na. on copper. Natural microcline, jadeite, wollastonite and barite were used as standards. Point analyses were made with a beam of less than 1μm

diameter for individual lamellae in perthitic intergrowths and on plagioclase. Average analyses of mesoperthite grains were made using a scanning beam (1-2 μm wide and about 100 μm long) counting for 4 x 10 seconds. In order to obtain an average analysis of a grain three such determinations were made and the average taken. This is believed to give a close approximation to the grain composition prior to exsolution. In most cases counts were made for peak and background on the standards using the same scanning technique.

5. AN ESTIMATE OF FELDSPAR STRUCTURAL STATE

In order to make a semiquantitative estimate of the structural state of the feldspars X-ray diffraction powder patterns were made on rock powders of samples HR 82, 87, 263 and microcline from Scourian pegmatite HR 268. Measurements were made on a Philips vertical goniometer X-R-D apparatus at 40 kV and 20 μ amps, using CuKα radiation with an Ni filter.

The difference between the (131) and $(1\bar{3}1)$ peaks and the (060) and $(\bar{2}04)$ peak positions were measured and compared with quoted values for high and low potassium feldspar and albite (Table 1) in Stuart (1975) and an estimate of structural state made. All the samples contain fine or coarse perthites, but the (060) Na and K peaks are always separately resolved indicating that the structures are not coherent. From Table 1 it is concluded that the potassium feldspars are in a low or intermediate structural state and all plagioclase feldspars now have a low structural state although ordering has probably taken place during cooling (Martin, 1974).

TABLE 1. Structural state of feldspars estimated from X-ray diffraction powder patterns.

Potassium Feldspar	(131-1$\bar{3}$1)	(060)	($\bar{2}$04)	Structure
Theoretical High Sanidine	0·000	41.54	50·886	
" Maximum Microcline	-0·791	41·808	50·521	
HR 268	-0·78	41·83	50·55	maximum microcline
HR 87	-0·66	41·85	50·70	intermediate
HR 263	-0·53	41·87	50·71	intermediate
HR 82	-0·55	41·78	50·73	intermediate
		41·88	50·84	maximum microcline
Plagioclase				
Theoretical High Albite	1·994	42·198	51·469	
" Low Albite	1·118	41·525	51·134	
HR 268	0·99	42·75		low
HR 87	0·93	42·60		low
HR 263	0·94	42·48		low
HR 82	0·99	42·49	51·425	low
		42·54	51·53	low
Quartz	(100)	(101)	(112)	
Theoretical	20·85	26·66	50·21	
HR 268	20·92		50·15	
HR 87	20·92	26·675	50·18	
HR 263	20·98	26·70	50·19	
HR 82	20·90	26·71	50·20	

6. GRANITE SHEETS FROM THE SHIOS PENINSULA, SCOURIE MORE

Field Relations

Several granite sheets (up to three metres wide) cut banded tonalitic gneiss on the Shios peninsula, Scourie More (138 447). Tonalitic gneiss contains abundant ultramafic inclusions, up to three metres long and a few tens of cm wide which lie concordant with the banding in the gneiss. The granite sheets are generally concordant but sometimes cut the banding in the gneiss; they have a well-developed mineral fabric and a weak banding. Feldspars have been studied from two granite sheets; sample 67 and samples 68 and 69 were collected at the edge and centre respectively of the same sheet and sample 82 was collected from a more coarsely grained sheet nearby.

Petrography

The principal minerals are quartz, plagioclase, mesoperthite feldspar, micaceous pseudomorphs after orthopyroxene and ilmenite-magnetite intergrowths. Small, rounded grains of microcline (ca. 0.2 mm) are also found and apatite (containing fluid inclusions) and zircon are accessary minerals. Most rocks are fine-grained and inequigranular, with curved and lobate grain boundaries. Quartz-quartz grain boundaries are very irregular and internally quartz grains are granulated. The subhedral form of the pseudomorphs after orthopyroxene suggest that originally the rock had a granular texture. Most of these textural features are a function of subsolidus re-equilibration in the presence of a fluid phase.

Feldspar textures

Plagioclase is lightly sericitised along cleavage planes, occasionally shows multiple albite twinning, and contains small, rounded inclusions of quartz.

Mesoperthite intergrowths in samples HR 69 and 68 show a variety of textures. Orthoclase lamellae in plagioclase vary from thin, regularly spaced, crystallographically oriented lamellae 4 μm wide to irregular broad lamellae up to 30 μm wide, which show only a hint of regular crystallographic control over their orientation (Fig. 1). Some perthites are very irregular intergrowths of orthoclase (more rarely microcline) and plagioclase and resemble a replacement texture where orthoclase replaces plagioclase. In sample HR 82 (Fig. 3) the most common perthitic intergrowths are very irregular, broad (over 40 μm) lamellae of orthoclase, with no preferred crystall ographic orientation in a plagioclase host; more rarely thinner oriented lamellae of orthoclase in plagioclase make up the mesoperthite. The most fine-grained perthitic intergrowths (Fig. 1a) are not perfectly straight although they tend to be uniform in width and show great regularity in their spacing (about 4 μm). The lamellae may be continuous over the length of the grain (500-700 μm), they may bifurcate or taper to a point. The lamellae are uniformly developed throughout the grain and there is no significant variation in lamellar width throughout the grain. The lamellae are oriented normal to the principal (001) cleavage in plagioclase and are parallel (010).

In HR 68 and 68 there is a gradual change in texture between the finest grained mesoperthite intergrowths and coarse, irregular feldspar intergrowths, implying that the two are related: Six stages are identified (see Fig. 1):

1) Fine, regular lamellae, as described above with slight coarsening and coalescing of lamellae at grain boundaries with quartz (Fig. 1a, 1b).

2) fewer, broader lamellae which are not continuous across the grain (Fig. 1c).

FIGURE 1. Stages in the progressive coarsening of exsolution lamellae in mesoperthites. All photomicrographs are taken with crossed polars. The scale bar is 100 μm.

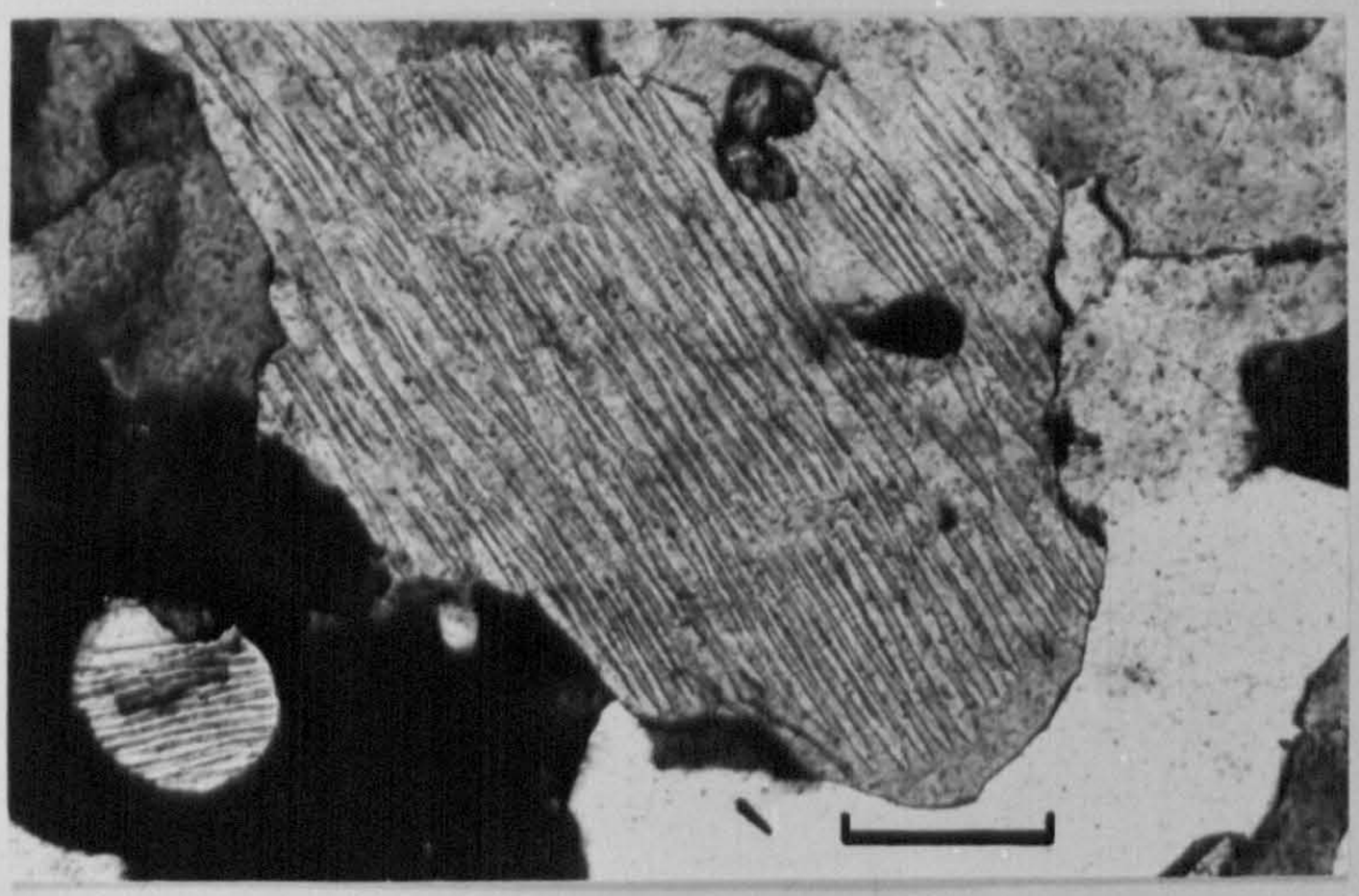

A. STAGE 1. Fine, regular lamellae of potassium feldspar in plagioclase. Note the isolated mesoperthite grain in quartz at the bottom left.

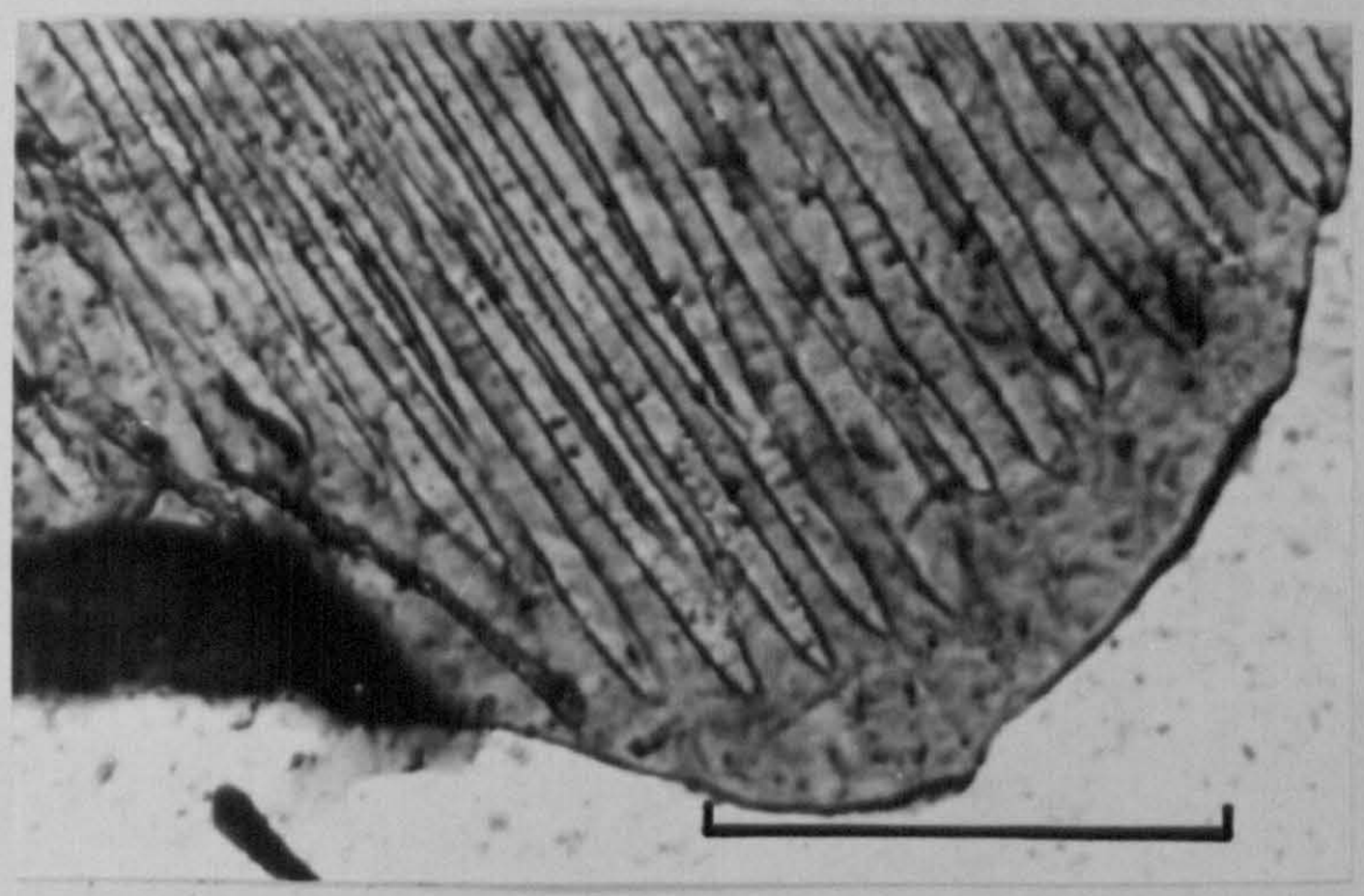

B. STAGE 1. (Detail from A). Note the slight coarsening and coalescence of lamellae at the edge of the grain. Potassium feldspar lamellae are 4 to 8 μm. wide.

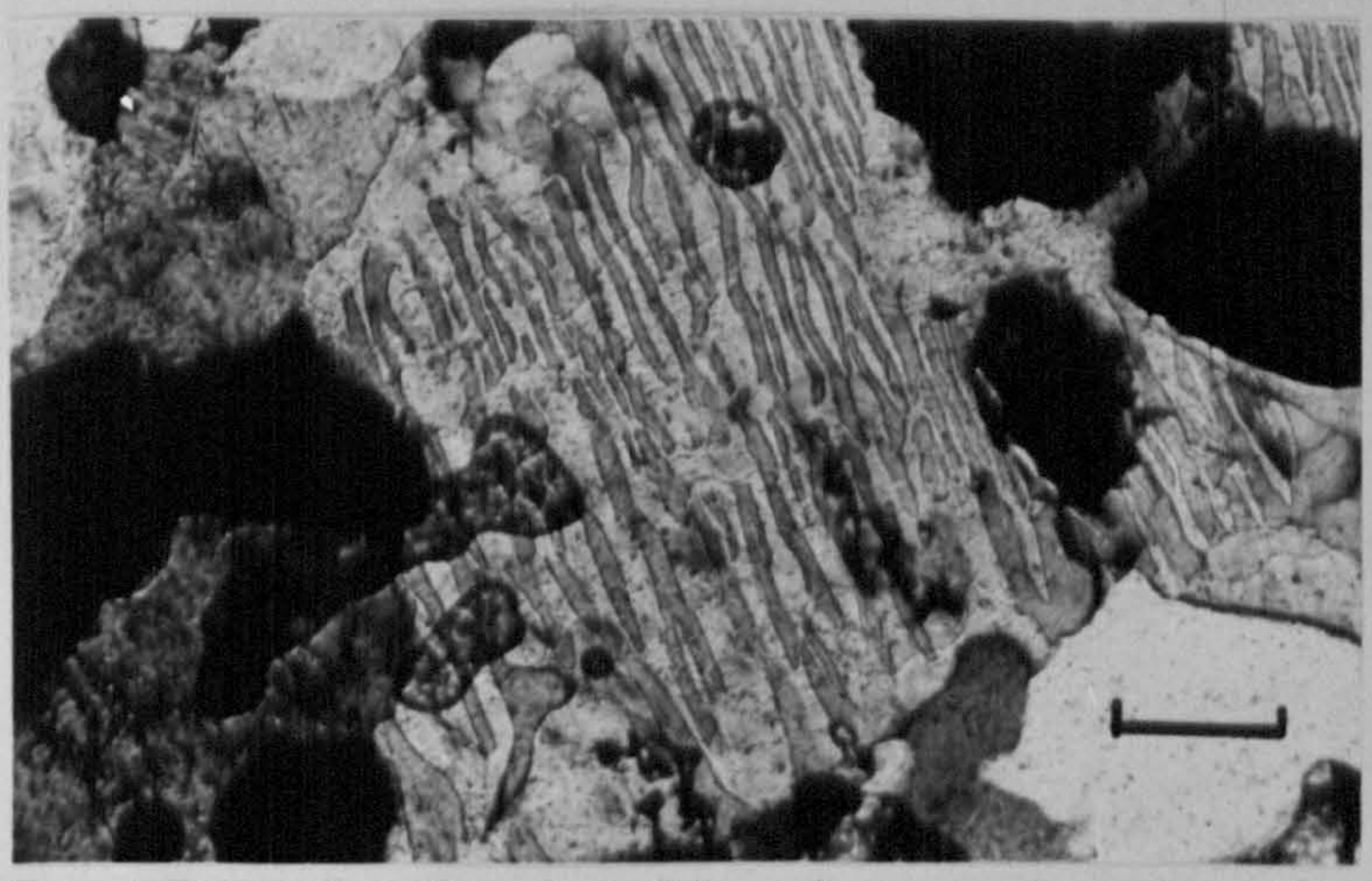

C. STAGE 2. The lamellae become broader (ca. 10 μm.) and less regular and are no longer continuous across the grain.

FIGURE 1. (continued)

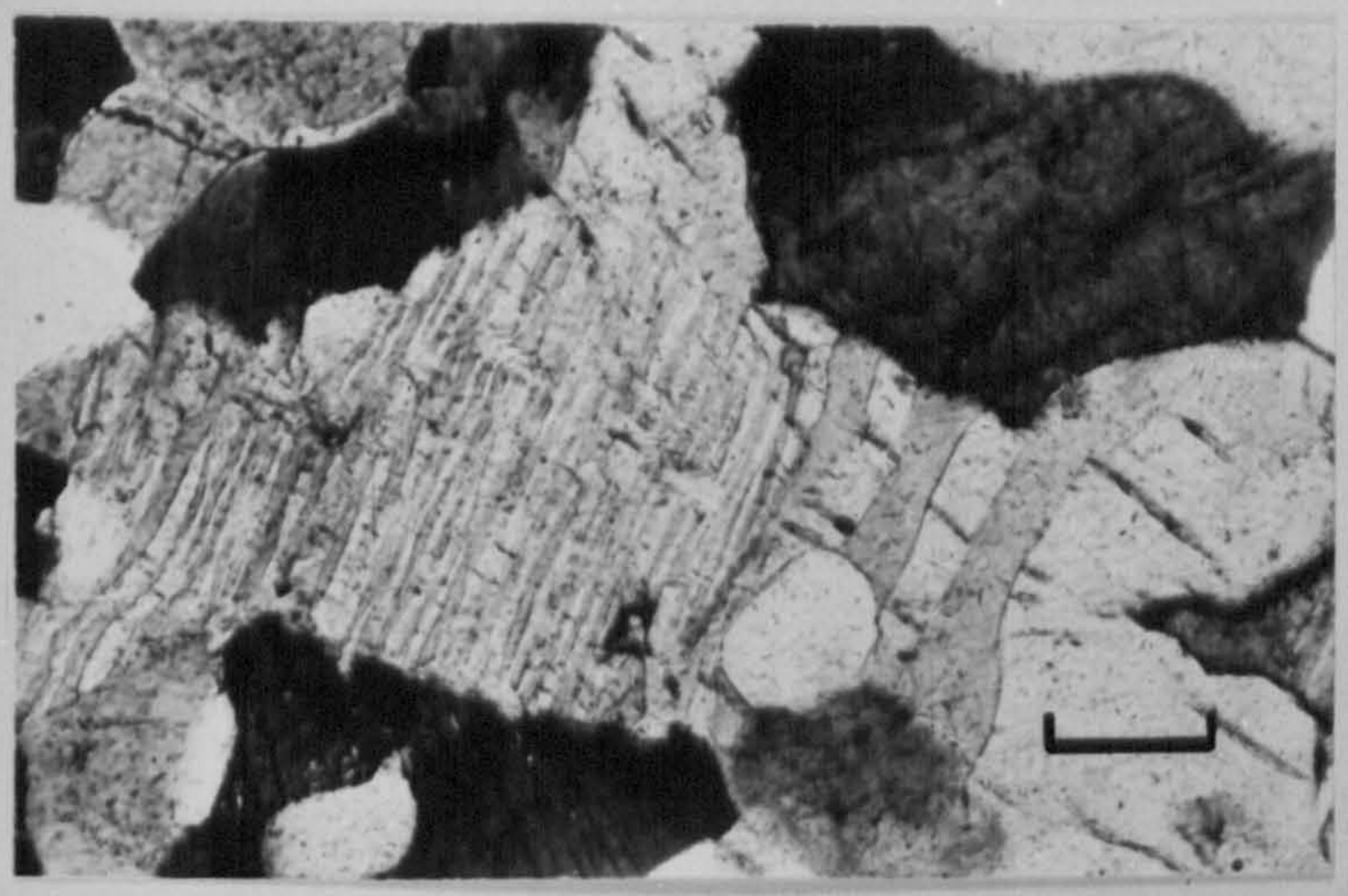

D. STAGE 3. Fine perthitic intergrowths give way to broad bands (30 μm. across) of potassium feldspar and plagioclase; there is some crystallographic control over the orientation of the lamellae.

E. STAGE 4. The lamellae become broader and less regular.

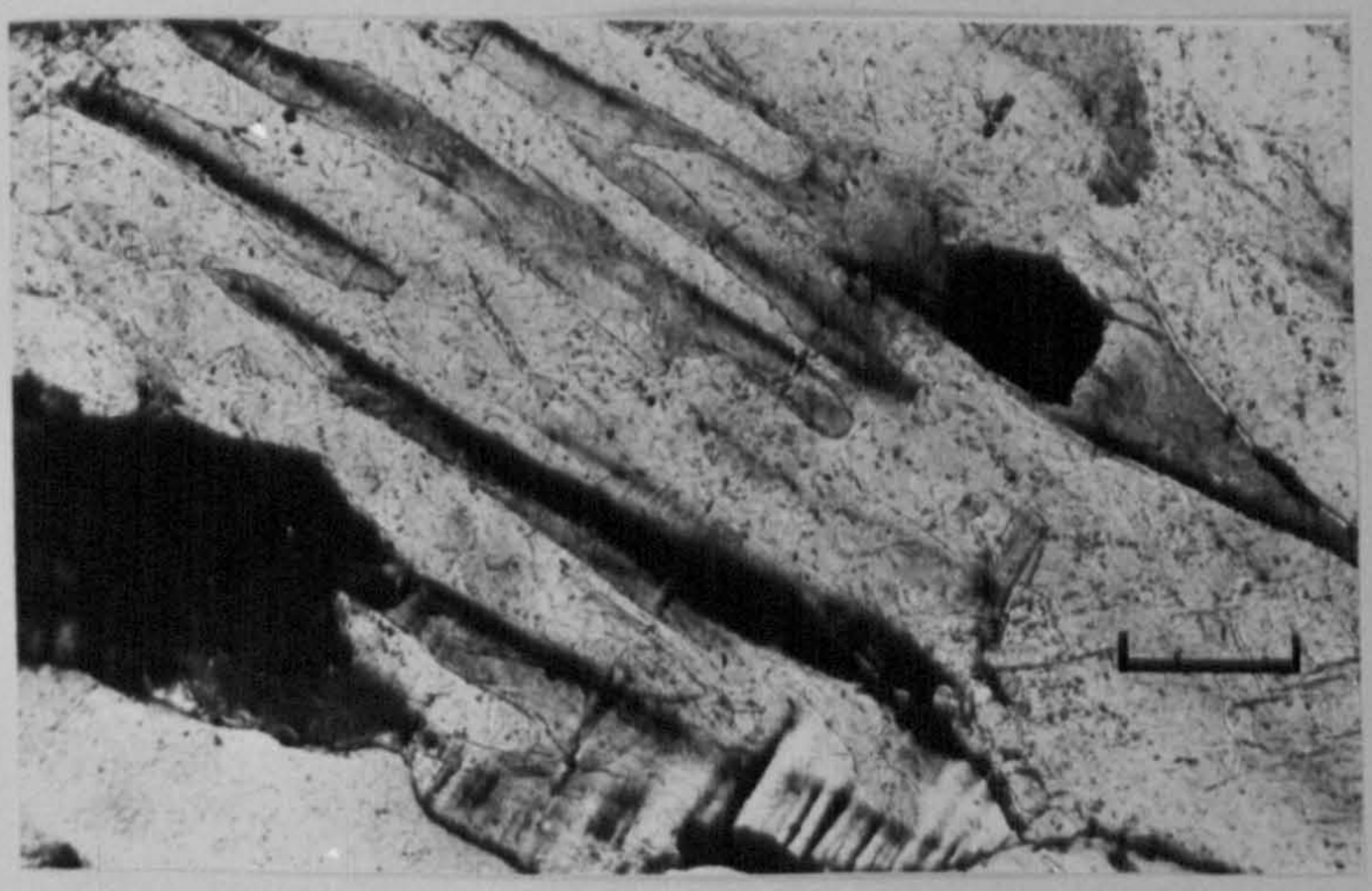

F. STAGE 5. Patchy microcline or orthoclase appears to replace plagioclase.

FIGURE 1. (continued)

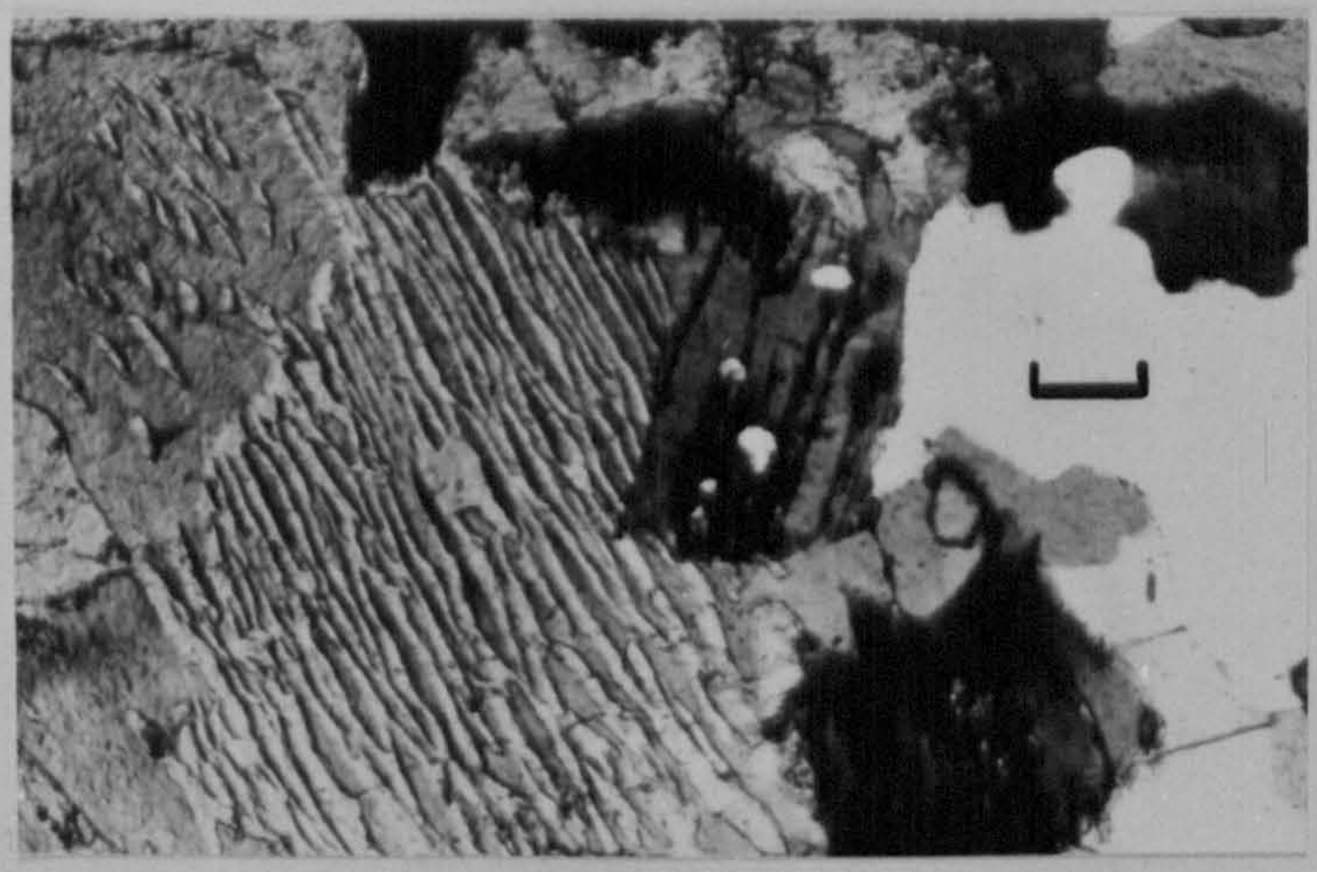

G. STAGE 6. Three-feldspar granite with plagioclase, mesoperthite and perthitic microcline; the microcline formed by granular exsolution from mesoperthite.

FIGURE 2.

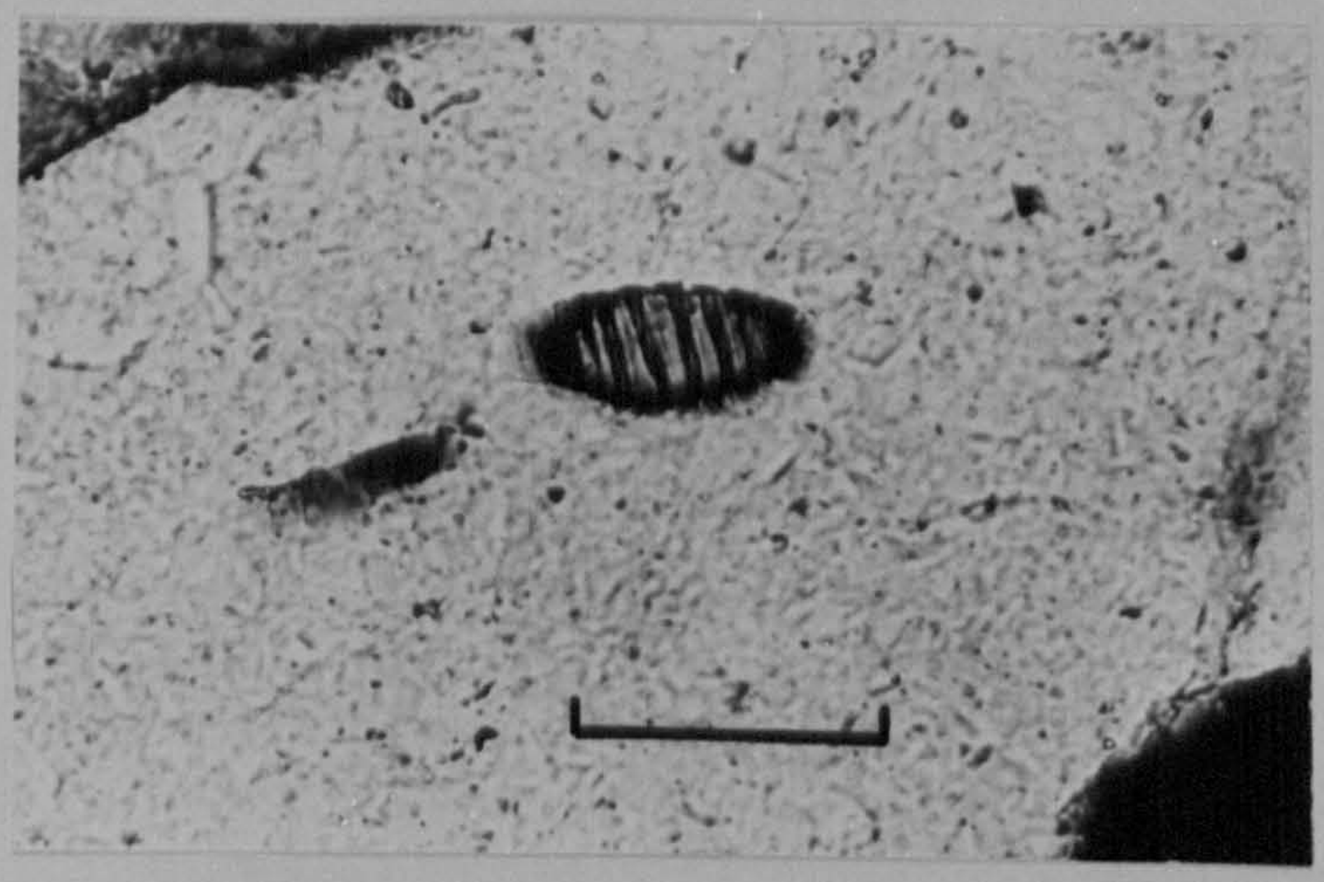

Isolated mesoperthite grain in quartz; this suggests that this is a homogeneous feldspar that has unmixed rather than plagioclase feldspar replaced by orthoclase.

FIGURE 3. Feldspar textures in granodiorite HR 82. Scale bar is 100 μm. wide. All photomicrographs are taken under crossed polars.

A. Mesoperthite grain with both fine and coarse lamellae; the fine lamellae are restricted to the centre of the grain.

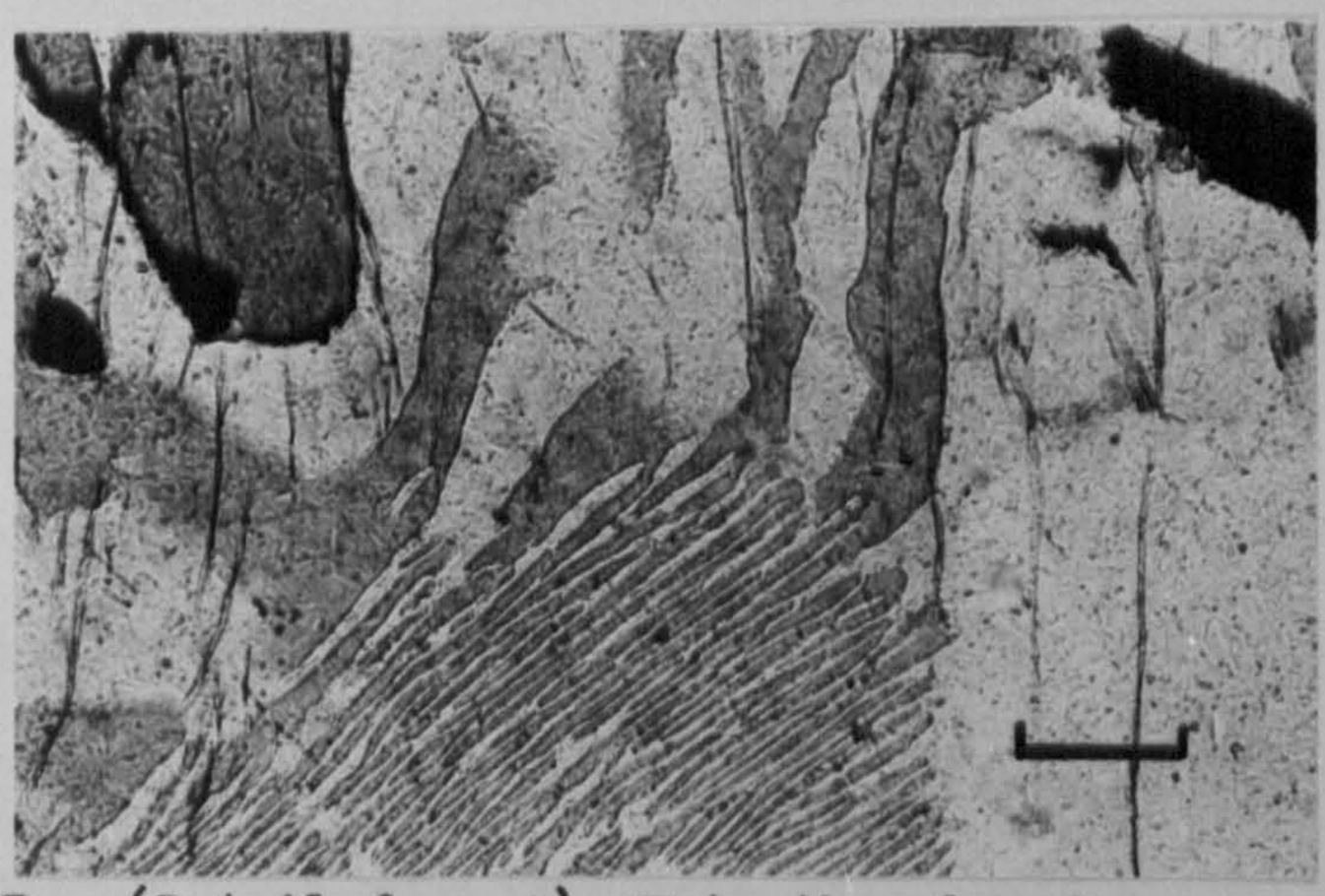

B. (Detail from A). Note the abrupt coarsening of the lamellae near the edge of the grain and the difference in orientation between the coarse and fine lamellae. The lamellae widen from ca. 7 μm. to ca. 43 μm.

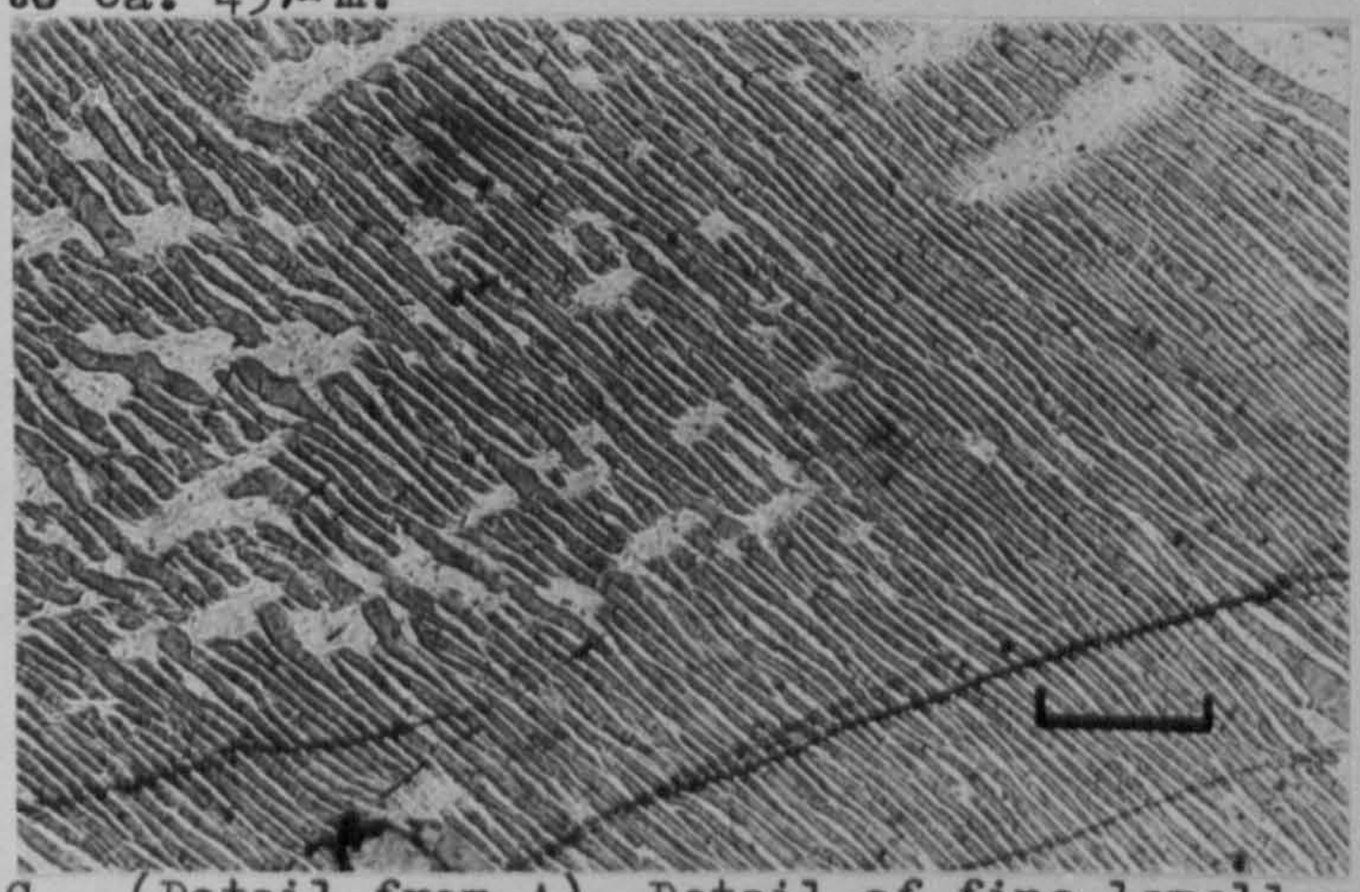

C. (Detail from A). Detail of fine lamellae.

3) lamellae become broader and fewer in number and fine perthitic intergrowths with orthoclase lamellae about 6 μm wide give way to broad bar-like intergrowths 30 μm wide (Fig. 1d).

4) irregular, broad and crudely oriented lamellae of orthoclase in plagioclase (Fig. 1e).

5) patchy intergrowth of microcline or orthoclase in plagioclase resembling replacement texture (Fig. 1f).

A similar process of coarsening lamellae can explain the very irregular coarse perthites in HR 82. One grain has a fine-grained, well-orientated, regularly-spaced, perthitic intergrowth in the centre of the grain which is replaced at the margin (the outer 0.2 to 0.5 mm) by very coarse-grained irregular perthitic intergrowths (Fig. 3a). The centre of the grain shows regularly spaced tapering lamellae ca 7 μm wide which occasionally broaden, change orientation leaving irregular patches and blebs of plagioclase host normal to the lamellae (Fig. 3c); at an irregular distance from the centre of the grain the lamellae abruptly coarsen due to the coalescing of fine lamellae into broader bands ca 40 μm wide and there is a loss of crystallographic control (Fig. 3b).

A further stage of coarsening (stage 6) is seen in samples HR 35 and 245 collected from granite sheets on Torran nan Clach Boga, near Upper Badcall. There are three feldspars in these sheets: plagioclase, perthitic microcline and mesoperthite (Fig. 1g). The lamellae in the mesoperthite vary in width from 8 to 115 μm and mesoperthite grains are in crystallographic continuity with microcline grains containing small lamellae of plagioclase (130 μm long and ca 12 μm wide). This represents a stage of granular exsolution in which new microcline grains grow at the expense of earlier mesoperthite grains. The lamellae

in microcline tend to have the same orientation as the mesoperthite lamellae and are probably relics of mesoperthite rather than the product of further exsolution from an originally homogeneous alkali feldspar.

The Origin of mesoperthites

Mesoperthites have traditionally been interpreted as the product of either exsolution or replacement; recently Lofgren and Gooley (1977) suggested that perthitic intergrowths may form as a result of simultaneous crystallisation from the melt. Heier (1955) illustrated mesoperthites from Norway which show a gradation from broad irregularly-oriented patches of potassium feldspar in plagioclase to oriented lamellae, similar to the feldspars illustrated above and he suggested that they formed by replacement. An exsolution origin is preferred for the comparable Scourian mesoperthites for the following reasons:

1) the regular orientation of the fine perthitic intergrowths closely resembles microperthite textures which are regarded as having formed by exsolution (Yund, 1975).

2) there is an adequate mechanism for the formation of coarse lamellae by the coalescing of fine lamellae within a grain to render a replacement origin unnecessary.

3) small, rounded mesoperthite grains are enclosed in quartz (Fig. 1a, 2) and cannot have been influenced by migrating fluids, implying that the 3 μm orthoclase lamellae must have exsolved from an originally homogeneous feldspar.

The subsolidus history of mesoperthites

Since the mesoperthites are believed to have formed by exsolution, they attained their present textures in the following stages:

1) Crystallises from the melt as a homogeneous feldspar ca. $An_{14}Ab_{45}Or_{41}$.

2) Coherent Spinodal decomposition; the resemblance of the fine perthitic lamellae to cryptoperthite lamellae formed by coherent spinodal decomposition suggests a similar mechanism of formation (Yund, 1975). The regular spacing of the lamellae argues for spinodal decomposition rather than heterogeneous nucleation which would allow irregular grain boundaries to form. Yund (1975) suggested that the spinodal decomposition mechanism can be tested by estimating the time necessary for the lamellae to attain their present width assuming they formed as cryptoperthite lamellae, using experimentally determined coarsening rates. Using an extrapolation of Yund's data and his equation Y-2 (Yund, 1975) it would take ca. 2.5 Ma. to form the fine lamellae observed if the rock was at 600°C. This is certainly geologically reasonable; a more detailed discussion of this method is given below.

3) A loss of coherency. The coarsening of lamellae has the effect of lowering the interfacial energy in the grain and can only procede so far before coherency will give way to domains of plagioclase and orthoclase. Unmixing is slowed down in these feldspars because of the high An content so that unmixing involves framework ordering as well as Na-K exchange.

4) Ordering and further coarsening of lamellae in the presence of a fluid phase. There is good evidence from the hydration of ferromagnesian minerals and from the opaque oxide chemistry (see below) that during cooling a hydrous fluid phase was introduced into these granites. This was probably the main coarsening agent in the perthites. Smith (1974) stated that the availability of a fluid aids the disordering of feldspars; Yund (1975) pointed out how a fluid phase promotes nucleation by dissolution and reprecipitation

and Goldsmith and Newton (1974) have shown that at high pressure the presence of a fluid phase speeded up the reaction between feldspars. The occurrence of coarse lamellae at the edge of a grain and fine in the centre (Fig. 3) can be explained in terms of the availability of a fluid phase and its inability to penetrate the centre of some grains. The presence of granular exsolution would indicate a greater amount of the fluid phase allowed the complete recrystallisation of some grains. A similar coarsening of perthitic lamellae was explained by Richardson (1968) in his study of the Glen Dessary Syenite in terms of the availability of a fluid phase.

Feldspar Chemistry

Electron probe analyses of coexisting feldspar pairs from samples HR 67, 68, 69, 82 and 35 are presented in Table 2 and the compositions are plotted in Fig. 4.

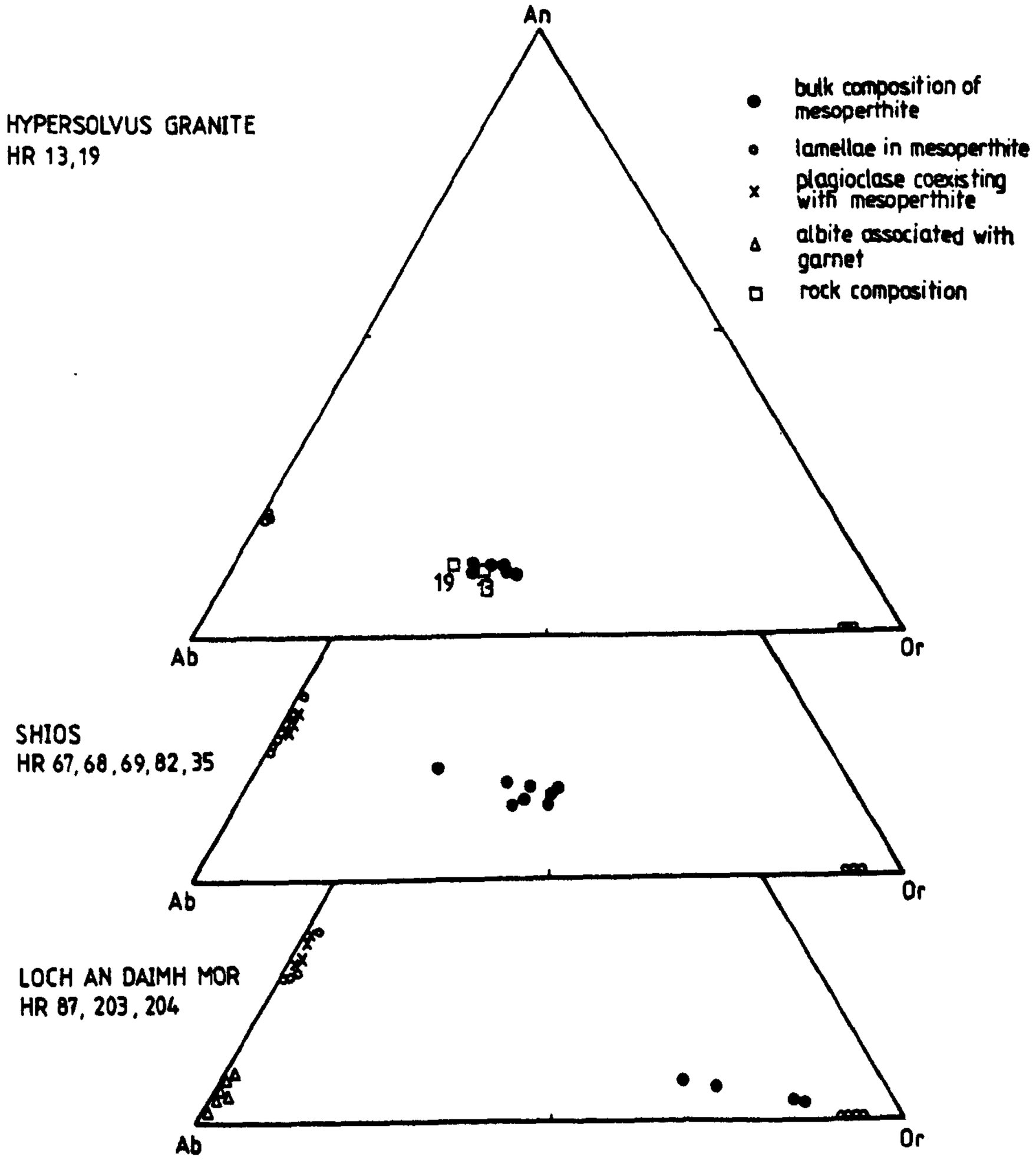

Figure 4. The composition of co-existing feldspars from granite sheets in the Scourie area.

	ANALYSIS NO.			SIO2	AL2O3	CAO	NA2O	K2O	BAO	TOTAL	AN	AB	OR	BA-FSP
1	HR68	846/9	COARSE PERTHITE (HOST)	66.26	20.33	4.14	8.61	.08		99.92	.209	.789	.002	
		846/7	(LAMELLA)	64.78	17.43	.03	1.08	15.17		98.47	.001	.096	.903	
2	HR68	1173/15	COARSE PERTHITE (HOST)	63.28	23.78	4.53	8.33	.14	.08	100.06	.223	.762	.015	
		1178/14	(LAMELLA)	64.61	18.74	.09	.86	15.21	.56	99.49	.005	.080	.906	.010
3	HR68	1173/19	COARSE PERTHITE (HOST)	62.18	23.42	4.68	8.35	.14	.01	98.97	.242	.756	.002	
		1173/20	(LAMELLA)	64.15	18.55	.06	.85	15.52	.58	99.75	.003	.076	.911	.010
4	HR68	846/1	PLAGIOCLASE	63.80	22.35	4.55	8.66	.17		99.03	.219	.771	.010	
		846/2	GRANULAR K-FELDSPAR	64.63	17.35	.02	.77	15.07		97.86	.001	.069	.930	
5	HR68	846/3	PLAGIOCLASE	62.95	21.77	4.37	8.83	.21		98.14	.212	.776	.012	
		846/4	GRANULAR K-FELDSPAR	63.47	17.61	.06	.94	15.53		97.04	.004	.084	.912	
6	HR68	846/11	PLAGIOCLASE	63.25	21.87	4.34	8.40	.13		98.11	.210	.771	.011	
		846/10	GRANULAR K-FELDSPAR	64.46	17.37	.04	.79	15.32		97.96	.002	.070	.928	
7	HR68	846/1,3,5,11	AVG PLAGIOCLASE	63.64	21.95	4.37	8.75	.16		98.26	.214	.775	.011	
		1178/16,17,18	AVG MESOPERTHITE 1	63.32	21.35	2.53	5.64	6.56	.24	99.66	.122	.494	.379	.004
8	HR68	846/1,3,5,11	AVG PLAGIOCLASE	63.01	21.95	4.37	8.75	.15		98.26	.214	.775	.010	
		1178/21,22,23	AVG MESOPERTHITE 2	63.22	21.20	2.57	5.09	7.56	.20	99.92	.123	.441	.431	.005
9	HR68	846/1,3,5,11	AVG PLAGIOCLASE	63.01	21.95	4.37	8.75	.16		98.26	.214	.775	.011	
		1178/24,25,26	AVG MESOPERTHITE 3	63.10	21.25	2.72	5.44	6.91	.26	99.66	.130	.471	.394	.005
10	HR69	974/17-24	AVG PLAGIOCLASE	62.73	24.21	5.05	8.43	.27	.06	100.69	.245	.748	.010	
		974/7-9	AVG MESOPERTHITE 1	62.26	21.76	3.15	5.36	6.83	.17	99.23	.154	.447	.397	.010
11	HR69	974/17-24	AVG PLAGIOCLASE	62.73	24.21	5.05	8.43	.27	.01	100.69	.245	.748	.006	
		974/14-16	AVG MESOPERTHITE 2	62.53	21.56	3.05	4.76	7.72	.14	99.67	.147	.465	.442	.006
12	HR69	974/17-24	AVG PLAGIOCLASE	62.73	24.21	5.05	8.43	.27	.01	100.69	.245	.748	.010	
		974/27,28	AVG MESOPERTHITE 3	62.43	21.76	3.25	5.37	6.88	.17	99.10	.162	.478	.357	.003
13	HR69	974/2	COARSE PERTHITE (HOST)	61.65	24.93	6.14	8.01	.20	.11	100.33	.294	.694	.011	
		974/1	(LAMELLA)	64.50	18.69	.05	.03	15.53	.38	100.14	.002	.074	.917	.007
14	HR69	974/4	COARSE PERTHITE (HOST)	61.49	24.55	5.97	8.77	.12	.11	100.77	.266	.725	.007	
		974/3	(LAMELLA)	64.45	18.76	.05	.04	15.63	.41	100.17	.002	.075	.917	.007

TABLE 2. Chemical analyses of coexisting feldspar pairs from granite sheets on the Shios peninsula. The numbers in the column on the left refer to temperatures in Table 3.

ANALYSIS NO.				SIO2	AL2O3	CAO	NA2O	K2O	BAO	TOTAL	AN	AB	OR	BA-FSP
15 HR69	974/6	COARSE PERTHITE	(HOST)	61.27	24.63	6.27	8.13	.21	.01	100.50	.295	.693	.012	
	974/5		(LAMELLA)	65.65	18.74	.06	.82	15.68	.48	101.34	.003	.073	.917	.007
16 HR69	974/11	COARSE PERTHITE	(HOST)	62.23	24.56	5.57	8.21	.15	.01	100.08	.271	.721	.008	
	974/11		(LAMELLA)	64.56	18.77	.07	.96	15.59	.35	100.34	.003	.086	.904	.006
17 HR69	974/12	COARSE PERTHITE	(HOST)	61.56	24.65	5.54	8.56	.19	.03	100.43	.262	.727	.011	
	974/13		(LAMELLA)	64.73	18.93	.09	.93	15.47	.29	101.45	.004	.083	.907	.005
18 HR68	974/26	FINE PERTHITE	(HOST)	61.47	24.41	6.30	7.73	.25	.06	100.63	.306	.670	.010	
	974/25		(LAMELLA)	64.57	18.36	.06	.78	15.78	.39	100.47	.003	.069	.921	.007
19 HR67	846/14	COARSE PERTHITE	(HOST)	61.65	22.63	5.27	8.34	.13		97.56	.257	.737	.006	
	846/13		(LAMELLA)	65.21	17.56	.15	.92	15.25		98.96	.008	.083	.909	
20 HR67	846/19	FINE PERTHITE	(HOST)	60.95	23.24	5.73	7.57	.16		97.66	.292	.690	.010	
	846/18		(LAMELLA)	64.45	17.32	.08	.82	15.61		98.22	.004	.074	.922	
21 HR67	846/16	PLAGIOCLASE		61.92	22.54	5.47	8.17	.15		97.06	.253	.736	.009	
	846/17	K-FELDSPAR		64.43	17.48	.07	.82	15.27		98.12	.004	.085	.910	
22 HR62	1175/23,28	AVG PLAGIOCLASE (CORE)		61.75	22.96	5.39	8.34	.24	.02	98.70	.259	.726	.014	
	1175/11-25	AVG MESOPERTHITE		62.56	20.68	2.99	5.11	7.05	.38	95.77	.144	.445	.404	.007
23 HR62	1175/22,24,27,29	AVG PLAG (RIM)		61.82	23.23	5.52	8.23	.18	.03	98.78	.266	.722	.010	
	1175/11-25	AVG MESOPERTHITE		62.56	20.68	2.99	5.11	7.05	.38	96.77	.144	.445	.404	.007
24 HR62	1175/1	COARSE PERTHITE (HOST)		61.92	23.56	5.62	8.54	.12	.03	99.69	.272	.722	.007	
	1175/2	(LAMELLA-EDGE)		63.81	18.21	.07	1.16	15.69	1.01	99.26	.003	.098	.001	.016
25 HR62	1175/1	COARSE PERTHITE (HOST)		60.92	23.56	5.82	8.54	.12	.03	98.68	.272	.722	.007	
	1175/3	(LAMELLA-CENTRE)		64.65	17.74	.07	1.07	14.96	.94	98.77	.003	.096	.003	.017
26 HR62	1175/7	COARSE PERTHITE (HOST)		61.02	23.54	5.72	8.41	.13	.01	98.82	.271	.721	.007	
	1175/6	(LAMELLA)		63.93	18.35	.09	1.09	15.26	.07	99.36	.004	.097	.003	.016
27 HR62	1175/5	COARSE PERTHITE (HOST)		61.34	23.69	5.78	8.54	.11	.06	99.58	.280	.726	.010	
	1175/4	(LAMELLA)		63.78	18.15	.08	1.17	15.16	.79	98.94	.004	.099	.307	.014
28 HR62	1175/19	COARSE PERTHITE (HOST)		61.62	23.45	5.65	8.42	.12	.01	99.29	.276	.723	.007	
	1175/18	(LAMELLA)		63.84	18.64	.07	1.08	15.33	.91	99.04	.003	.096	.004	.016

TABLE 2. continued

	ANALYSIS NO.			SIO2	AL2O3	CAO	NA2O	K2O	BAO	TOTAL	AN	AB	OR	BA-FSP
29	HR82	1175/21	COARSE PERTHITE (HOST)	61.53	22.98	5.49	8.44	.16	.00	98.00	.262	.729	.009	
		1175/22	(LAMELLA)	63.99	18.24	.30	1.11	15.07	1.32	99.49	.014	.090	.006	.018
30	HR82	1175/26	COARSE PERTHITE (HOST)	61.84	23.24	5.21	8.39	.16	.06	97.79	.254	.739	.007	
		1175/25	(LAMELLA)	63.66	18.10	.05	.90	15.35	.95	99.09	.002	.087	.094	.017
31	HR82	1175/9	FINE PERTHITE (HOST)	62.01	23.16	5.15	8.07	.16	.03	99.07	.241	.750	.009	.001
		1175/8	(LAMELLA)	64.41	18.03	.00	1.10	15.02	.37	99.58	.004	.098	.001	.017
32	HR82	1175/6	FINE PERTHITE (HOST)	61.22	23.33	5.73	8.35	.15	.05	98.06	.272	.717	.011	
		1175/10	(LAMELLA)	64.15	17.99	.12	1.06	15.00	.90	99.28	.006	.095	.003	.016
33	HR35	769/16	COARSE PERTHITE (LAMELLA)	64.20	23.71	5.33	8.58	.16	.00	101.52	.254	.740	.006	
		769/9	(HOST)	66.94	18.39	.00	.94	14.54	.45	101.25	.000	.089	.913	.009
34	HR35	769/12	COARSE PERTHITE (HOST)	62.29	22.25	5.77	8.45	.14	.00	99.50	.271	.721	.006	
		769/14	(LAMELLA)	66.23	17.02	.01	.97	14.43	.47	99.18	.001	.092	.090	.009
35	HR35	769/15	COARSE PERTHITE (LAMELLA)	62.12	23.33	5.55	8.50	.16	.00	99.43	.262	.726	.011	
		769/16	(HOST)	64.93	17.82	.08	.73	14.33	.45	98.91	.000	.069	.922	.009
36	HR35	1280/4	COARSE PERTHITE (HOST)	62.21	24.67	5.16	8.35	.17	.03	100.56	.250	.742	.010	.001
		1280/5	(LAMELLA)	64.83	19.35	.04	.95	15.91	.03	101.75	.002	.092	.905	.011
37	HR35	1280/14	COARSE PERTHITE (LAMELLA)	62.42	24.73	5.43	8.34	.21	.05	101.18	.261	.726	.012	.001
		1280/15	(HOST)	65.47	19.02	.03	.91	15.77	.05	101.83	.002	.079	.905	.011
38	HR35	1280/1	PLAGIOCLASE(CORE)	62.16	24.87	5.16	8.63	.13	.04	101.01	.240	.746	.007	.001
		1280/6-8	MESOPERTHITE 1	63.37	21.74	2.54	4.07	7.56	.33	100.01	.141	.422	.431	.010
39	HR35	1280/1	PLAGIOCLASE(CORE)	62.13	24.87	5.16	8.63	.13	.04	101.01	.246	.746	.007	.001
		1280/9-11	MESOPERTHITE 2	62.56	22.33	3.73	6.47	4.52	.14	99.80	.179	.561	.250	.012
40	HR35	1280/3	PLAGIOCLASE (RIM)	61.98	25.13	5.49	8.16	.13	.05	100.84	.271	.727	.002	.001
		1280/12,13	AVG MICROCLINE PERTHITE	63.64	20.10	1.46	3.10	11.25	.42	100.23	.076	.276	.646	.007

TABLE 2. continued

Plagioclase: co-existing with mesoperthite lies in the compositional range An_{21} to An_{27} and becomes progressively less calcic from HR 82, 67, 69 to 68 as the normative bulk composition of the rock approaches the minimum in the tetrahedron Qz-Ab-Or-An. Plagioclase is zoned in samples 35 ($An_{24.6(core)}$ to $An_{27.0(rim)}$) and sample 82 ($An_{25.9(core)}$ to $An_{26.8(rim)}$) but is homogeneous in samples 68 and 69. There is a slight difference between the composition of plagioclase grains and plagioclase lamellae in mesoperthite; most plagioclase lamellae show a range of compositions within a single thin section and they are generally more calcic than the co-existing plagioclase. Plagioclase lamellae in mesoperthite and in perthitic microcline in HR 35, the 'three feldspar granite', lie within the compositional range of the co-existing plagioclase ($An_{24.6(core)}$ to $An_{27.0(rim)}$).

Alkali feldspar: Bulk compositions of mesoperthite grains obtained by analysing the fine perthitic intergrowths with a scanning electron probe beam show that they were rich in anorthite prior to exsolution; compositions are plotted in Fig. 4 and resemble mesoperthites analysed by O'Hara (1978) from similar granite sheets in the Scourian complex, mesoperthites from mangerites and charnockites from Rogaland, S. Norway analysed by J.V. Smith (1974) and mesoperthites from quartzofeldspathic granulites in the Musgrave Ranges, Central Australia (Collerson, 1976). Broad plagioclase lamellae are poorer in An (by about 3%) and Or relative to fine lamellae and broad alkali feldspar lamellae are richer in orthoclase by 1 to 2% than the fine lamellae. Granular alkali feldspar is enriched in the orthoclase component by up to 2 mol % relative to mesoperthite lamellae in HR 68 and 35. This suggests that as mesoperthite lamellae coalesced and formed discrete grains there was continued exchange of Na and K between K-feldspar and plagioclase lamellae so that Or increased in alkali

feldspar and Ab increased in plagioclase; in this way plagioclase lamellae approach the composition of co-existing plagioclase.

Feldspar Thermometry

The composition of co-existing plagioclase and alkali feldspar is used to determine the equilibration temperature of the granite sheets. Four different methods are used, designated T_1 to T_4; the theoretical basis for these different methods is discussed above and in more detail in appendix 2. T_1 is derived from the equation of Stormer (1975) and applies to feldspars which equilibrated in a disordered structural state; T_2 is based upon the equation of Whitney and Stormer (1977) and applies to feldspars which equilibrated in an ordered structural state; both T_1 and T_2 assume that Ca in the alkali feldspar has little effect upon the equilibration temperature. T_3 is derived from the equation of Powell and Powell (1977) which applies to feldspars equilibrated in a disordered structural state and assumes that Ca in alkali feldspar has a significant effect upon the equilibration temperature; T_4 is a modification of the equation of Powell and Powell (1977) which is applicable to ordered feldspars. In view of the high Ca content of these alkali feldspars and their intermediate structural state temperatures between T_3 and T_4 are the most realistic. The distribution of $NaAlSi_3O_8$ between alkali feldspar and plagioclase is pressure dependant and all the temperatures quoted are for a pressure of 10 kb. Preliminary data on orthopyroxene-garnet pairs from adjacent gabbros suggests pressures in the range 8 to 12 kb. A difference of 2 kb makes a difference in equilibration temperature of about $25^{\circ}C$ at $700^{\circ}C$

Plagioclase and mesoperthite (homogenised using a scanning electron probe beam) yield mean equilibration temperatures between $578^{\circ}C$ (range $601 - 544^{\circ}C$) for the disordered structural state and

TABLE 3 FELDSPAR EQUILIBRATION TEMPERATURES AT 10 KB SHIOS

ANAL. NO.	ROCK	T_1	T_2	T_3	T_4
Plagioclase and rehomogenised mesoperthite					
7	HR68	918	1309	593	744
8	HR68	869	1149	586	719
9	HR68	896	1234	571	707
10	HR69	923	1238	561	687
11	HR69	882	1129	573	693
12	HR69	962	1356	544	673
22 Pl core	HR82	941	1264	595	732
23 Pl rim	HR82	948	1275	601	741
mean		917	1244	578	712
Plagioclase and granular potassium feldspar					
4	HR68	470	517	467	516
5	HR68	496	543	490	539
6	HR68	471	518	467	516
21	HR67	499	545	493	542
40	HR35	499	545	480	532
mean		487	534	480	532
Fine-grained perthite lamellae					
18	HR69	492	537	481	529
20	HR67	496	542	490	538
31	HR82	526	574	504	555
32	HR82	530	577	507	557
mean		511	558	496	545

ANAL. NO.	ROCK	T_1	T_2	T_3	T_4
Coarse-grained perthite lamellae					
1	HR68	513	561	510	560
2	HR68	491	538	476	525
3	HR68	487	534	473	522
13	HR69	498	543	487	536
14	HR69	491	537	480	529
15	HR69	496	541	484	532
16	HR69	514	560	503	552
17	HR69	506	552	495	544
19	HR67	505	551	495	544
24	HR82	534	581	511	561
25	HR82	531	578	510	560
26	HR82	533	580	512	562
27	HR82	528	575	510	559
28	HR82	531	578	510	560
29	HR82	532	579	508	559
30	HR82	510	557	490	540
33	HR35	513	560	503	529
34	HR35	524	571	513	562
35	HR35	479	525	468	517
36	HR35	502	548	488	537
37	HR35	499	545	485	534
mean		510	557	496	545

712°C (range 744 - 673°C) for the ordered structural state so that a partially ordered feldspar pair probably equilibrated at about 645°C. The equations of Whitney and Stormer (1977b) and Stormer (1975) yield substantially higher temperatures of about 920°C (Table 3); feldspars at these temperatures are not likely to be highly ordered.

Mesoperthite lamellae equilibrated between 496°C (disordered) and 545°C (ordered) and there is no difference between the fine and coarse grained lamellae. It is probable that the equilibration temperature is closer to 545°C as some orthoclase lamellae are altered to microcline. Granular alkali feldspar has equilibrated with plagioclase in the same temperature range (480 - 532°C). Temperatures base on Stormer (1976) and Whitney and Stormer's (1977) equations are broadly comparable in this instance because of the low Ca in alkali feldspar.

7. LOCH AN DAIMH MOR GRANITE SHEET

Field relations

This three metre wide granite sheet crops out in a road cutting at NC 159 435 east of Loch an Daimh Mor. Granite cuts garnetiferous gabbro and is separated into smaller sheets by screens of gabbro a few tens of cm wide. The sheet is coarse grained and foliated at its margin, with flattened grey quartz grains up to 10 by 3 mm and there is a trace of graphic texture. The centre of the sheet is fine-grained (less than 0.5 mm) and granular and contains small, rounded garnets 2 to 3 mm across, replaced in part by chlorite, which occasionally forms thin bands in the granite.

Petrography

The principal alkali feldspar is perthitic microcline with pronounced cross-hatched twinning and untwinned orthoclase perthite is less common. The perthitic lamellae tend to be parallel to the (010) twin direction in the microcline and are usually in the centre of the grain and smaller lamellae with a slightly different orientation occur near the edge. Microcline is unaltered except for rare calcite and chlorite overgrowths. Plagioclase shows multiple albite twinning (parallel (010)) and in orientations where no twinning is seen the grains show slight undulose extinction. Plagioclase is often altered to sericite and a low birefringence mica.

Grain boundaries tend to be irregular (Fig. 5a), triple junctions are rarely seen between quartz grains and plagioclase grains, and more commonly grain boundaries are curved to highly irregular and lobate. Some feldspar-feldspar grain boundaries are highly irregular and feldspars are rarely euhedral. Quartz forms the largest grains and some rounded quartz inclusions are found in the feldspars. Large quartz grains are often granulated at the margin. The rock is largely equigranular and there is a tendancy towards a clustering of aggregates of the same mineral in the coarser grained margins of the sheet.

Garnet rimmed with chlorite (Fig. 5c) is the principal ferromagnesian mineral; muscovite, calcite and epidote are rare accessories.

This granite sheet is unusual in several respects and differs from other granitic sheets described above in the following ways:

FIGURE 5. Textures in Loch an Daimh Mor granite. Scale bar is 100 μm. All photomicrographs taken under crossed polars.

A. Note the irregular grain boundaries and the presence of microcline.

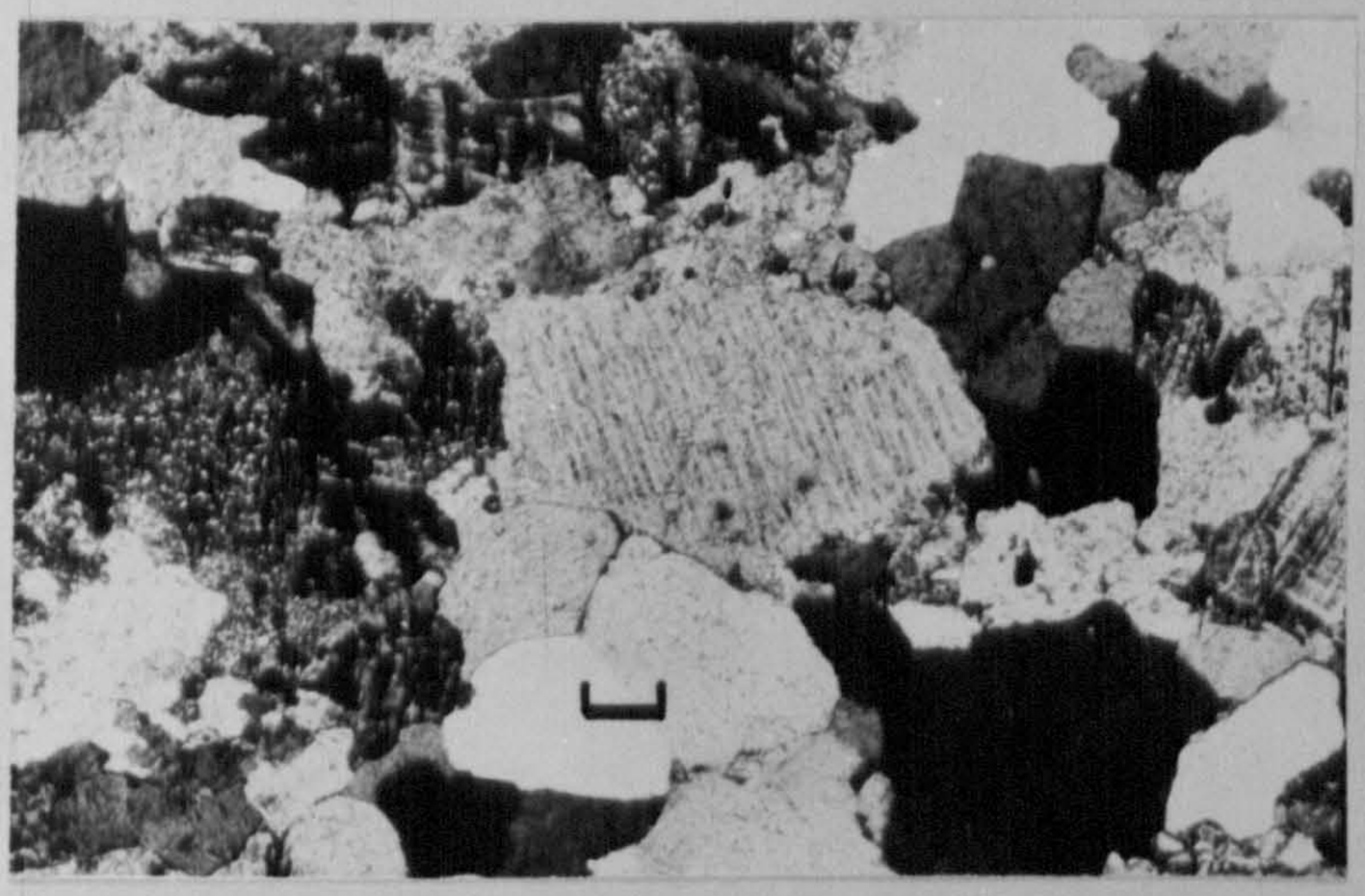

B. Untwinned, perthitic alkali feldspar; note the triple junctions between quartz grains.

C. Garnet rimmed by sericitised albite.

1) it is the most potassic of the granitic sheets analysed with over 5.0 wt % K_2O and represents the most evolved of the granitic rocks implying a very high degree of fractionation from parental trondhjemite (see Chapter 1 for a more detailed discussion). The anhydrous bulk composition plots close to the centre of the Qz-Ab-Or projection.

2) the centre of the sheet is finer grained, more granular and whiter in colour than other granite sheets.

3) microcline is the dominant alkali feldspar. Parsons (1978b) noted that microcline is found in place of orthoclase in only the most evolved members of a fractionation series.

4) garnet is the dominant ferromagnesian mineral; Cawthorn and Brown (1976, 1978) pointed out that garnet tends to concentrate in the more leucocratic members of granitoid complexes.

Feldspar Chemistry.

Mineral analyses were made on four separate samples collected from the centre of the sheet. The compositions of co-existing feldspar pairs are given in Table 4 and plotted in Fig. 4.

Plagioclase (An_{27}-An_{31}) is slightly zoned with the rim of grains slightly more calcic (by about 1% An) than the cores; and it is more calcic than plagioclase in the Shios granites. Plagioclase adjacent to garnet is much more albitic (average Ab_{95}) compared with the usual Ab_{68}, and grains enclosed within garnet are ca. Ab_{98}. These feldspars are badly sericitised and contain measurable FeO and in one case MgO indicating that either these feldspars contain some Fe^{3+} replacing Al^{3+} or the analyses include small amounts of phengitic mica.

Alkali feldspar: there is a slight difference in composition between the non-perthitic rim of microcline grains (Ab_{10}) and the

	ANALYSIS NO.		SIO2	AL2O3	CAO	NA2O	K2O	BAO	TOTAL	AN	AB	OR	BA-FSP
1	HR87	1176/1,3	AVG PLAGIOCLASE (CORE)	61.24	24.05	5.56	6.36	.30	.00	99.53	.265	.716	.017	
		1178/7-9	HOMOGENISED MICR 1	63.39	19.42	1.26	3.23	11.55	.09	99.16	.058	.281	.660	.002
2	HR87	1178/1,3	AVG PLAGIOCLASE (CORE)	61.24	24.05	5.56	8.36	.30	.00	99.53	.265	.716	.017	
		1178/12,13	HOMOGENISED MICR 2	63.92	19.29	.99	2.71	12.31	.09	99.31	.046	.238	.713	.002
3	HR87	1176/2,4	AVG PLAGIOCLASE (RIM)	61.32	23.94	5.56	8.46	.17	.01	99.53	.264	.726	.010	
		1178/6,11	MICROCLINE	64.07	18.33	.03	.74	15.91	.09	100.06	.001	.066	.931	.002
4	HR87	1179/5	PERTHITE (LAMELLA)	61.86	23.75	5.09	8.71	.29	.00	99.69	.240	.743	.016	
		1176/6	(HOST)	64.44	18.43	.03	.75	15.99	.11	99.76	.001	.066	.933	.002
5	HR87	820/10	PERTHITE (LAMELLA)	63.32	23.51	4.91	8.26	.30	.00	100.30	.242	.737	.021	
		820/9	(HOST)	65.53	18.22	.02	.76	15.76	.10	100.45	.001	.066	.931	.001
6	HR87	820/11	PERTHITE (LAMELLA)	62.59	23.89	5.64	8.76	.16	.00	100.43	.233	.752	.009	
		820/12	(HOST)	65.19	18.18	.02	.74	16.03	.09	100.24	.001	.062	.935	.002
7	HR203	1177/2,7	AVG PLAGIOCLASE (CORE)	61.03	24.67	6.39	8.05	.19	.00	99.32	.301	.669	.011	
		1177/14-16	HOMOGENISED MICR	63.51	18.32	.62	1.56	14.43	.19	98.71	.031	.139	.829	.013
8	HR203	1177/1,3,6	AVG PLAGIOCLASE (RIM)	60.80	24.22	6.62	8.06	.18	.00	99.56	.305	.681	.013	
		1177/4,9	MICROCLINE RIM	64.92	17.95	.05	1.21	15.30	.26	99.74	.001	.075	.923	.000
9	HR203	1177/12	PERTHITE (LAMELLA)	60.41	24.20	6.57	8.16	.26	.00	99.61	.300	.679	.014	
		1177/13	(HOST)	64.71	17.82	.03	.85	15.09	.19	99.56	.001	.075	.924	.013
10	HR204	1177/18,26	AVG PLAGIOCLASE (CORE)	60.63	24.63	6.27	8.14	.19	.00	99.23	.295	.694	.011	
		1177/24,25	HOMOGENISED MICR	62.77	18.31	.49	1.46	14.45	.34	97.84	.024	.131	.839	.006
11	HR204	1177/17,19	AVG PLAGIOCLASE (CORE)	60.42	24.11	6.39	7.99	.18	.00	99.06	.304	.687	.009	
		1177/21-22	AVG MICROCLINE	63.41	18.11	.03	.87	15.75	.33	98.49	.001	.077	.916	.006

TABLE 4. Chemical analyses of coexisting feldspar pairs from Loch an Dainh Mor granite sheet. The numbers in the column on the left refer to temperatures in Table 5.

perthitic centre of grains (Ab_{7-8}). The composition of plagioclase lamellae in microcline is the same as the plagioclase grains indicating that microcline is completely equilibrated with plagioclase as well as its exsolution lamellae. Barium varies between 0.08 and 0.34% wt BaO which is lower than that for potassium feldspar in nearby granite sheets and plots outside the field for granulite feldspars (Fig. 8b), Smith (1974).

Feldspar Thermometry

The bulk composition of perthitic microcline grains was estimated using a scanning electron probe beam; the range in composition suggests that either the method used is inaccurate since the breadth and infrequency of the lamellae are very different from mesoperthites analysed in this way or that the grains show several stages of albite loss to plagioclase and are 'frozen' in disequilibrium.

Equilibration temperatures were calculated using the four different equations described above T_1 to T_4. Homogenised microcline and plagioclase equilibrated in the temperature range 562 to 681°C for disordered feldspars (mean 617°C) and 616-782°C for ordered feldspars (mean 690°C). Although microcline is the dominant feldspar, it is not certain that the feldspars equilibrated in the ordered state since some orthoclase is present in these rocks, so that an average temperature ca. 654°C is probably more realistic. This is close to the temperature deduced for the Shios granite sheets. Plagioclase and microcline (not perthitic) and lamellae in microcline perthite have probably equilibrated as ordered feldspars in the range 503 - 545°C with a mean temperature of 526°C; this is also close to the alkali feldspar closure temperature in the Shios granites.

TABLE 5 FELDSPAR EQUILIBRATION TEMPERATURES LOCH AN DAIMH MOR GRANITE AT 10 kb

ANAL. NO.	ROCK	T_1	T_2	T_3	T_4
Plagioclase core - homogenised mesoperthite					
1	HR87	767	880	681	782
2	HR87	720	806	653	737
7	HR203	607	659	570	626
10	HR204	595	646	562	616
	mean	672	748	617	690
Plagioclase rim - microcline rim					
3	HR87	473	519	468	516
8	HR203	503	548	496	544
11	HR204	505	551	497	545
	mean			487	535
Perthites					
4	HR87	470	516	465	513
5	HR87	475	521	471	519
6	HR87	459	505	454	503
9	HR203	503	549	497	544
	mean			472	520

8. ONE FELDSPAR MESOPERTHITE GRANITE, SCOURIE MORE

One feldspar granites are uncommon in the trondhjemite granite suite of the Scourie Badcall area and represent a liquid composition which became isolated from the parental trondhjemite fortuitously close to the crest of the alkali feldspar solvus. Two examples are known; HR 19 is part of a composite, intrusive

trondhjemite-anorthosite-granite sheet 2 to 3 metres wide and traceable for about 200 metres on the east aide of Camas an Lochain; HR 13 is from a small granite lens in gabbro outcropping on the headland between Camas nam Buth and Camas an Lochain.

The rocks are equigranular in texture and feldspar-feldspar grain boundaries are very irregular, sericated and become granular indicating recrystallisation. Pseudomorphs after orthopyroxene form small clusters of grains and are composed of fibrous uralite, magnetite and quartz or biotite and/or chlorite, rutile and sphene. Quartz contains small needle-like inclusions of rutile and iron-titanium oxides are present.

Mesoperthite texture

Mesoperthite feldspars resemble the finely intergrown perthites described above from the Shios peninsula. The lamellae are composed of untwinned potassium feldspar and plagioclase and are long compared with their breadth (Fig. 6a, 6b); they are not perfectly straight and tend to be variable in width (3 - 10 μm) and although they are regularly spaced, potassium feldspar lamellae (probably orthoclase) become broader at the edge of the grain, but may be replaced en echelon and have pointed ends; occasionally they bifurcate. The lamellae are oriented almost normal to the main cleavage in the plagioclase lamellae and continue to the edge of the grain; more rarely there is a rim of non-perthitic plagioclase.

In HR 19 there are reddened bands parallel to the foliation up to about 1 cm wide where patchy microcline appears to have replaced plagioclase (Fig. 6c). This is interpreted as granular recrystallisation of the mesoperthite in the presence of late fluids introduced into the rock during cooling. The presence of water is also indicated by the alteration of pyroxene to chlorite and biotite.

FIGURE 6. Texture in hypersolvus granite from Scourie More. Scale bar is 100 μm. All photomicrographs taken under crossed polars.

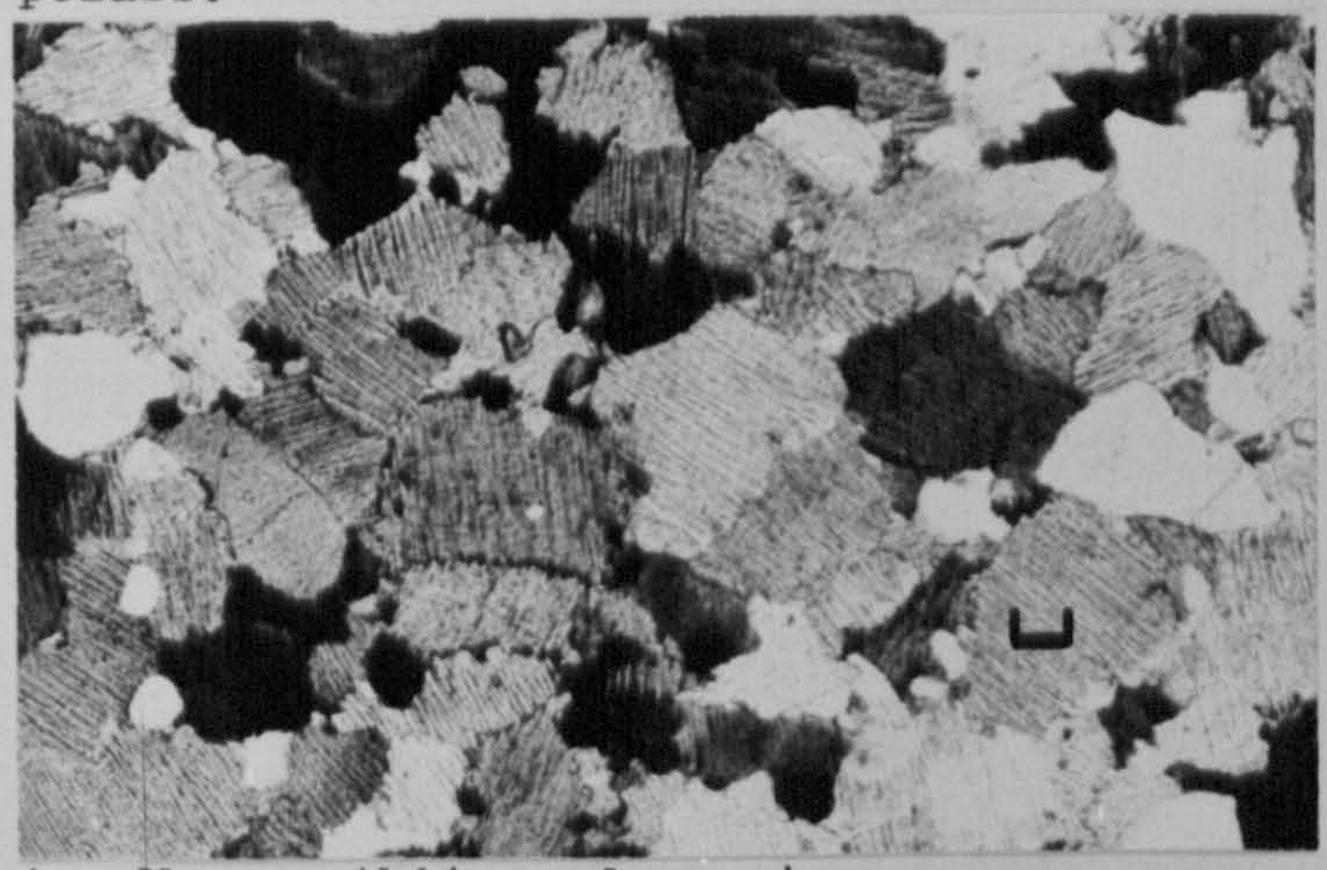

A. Mesoperthite and quartz.

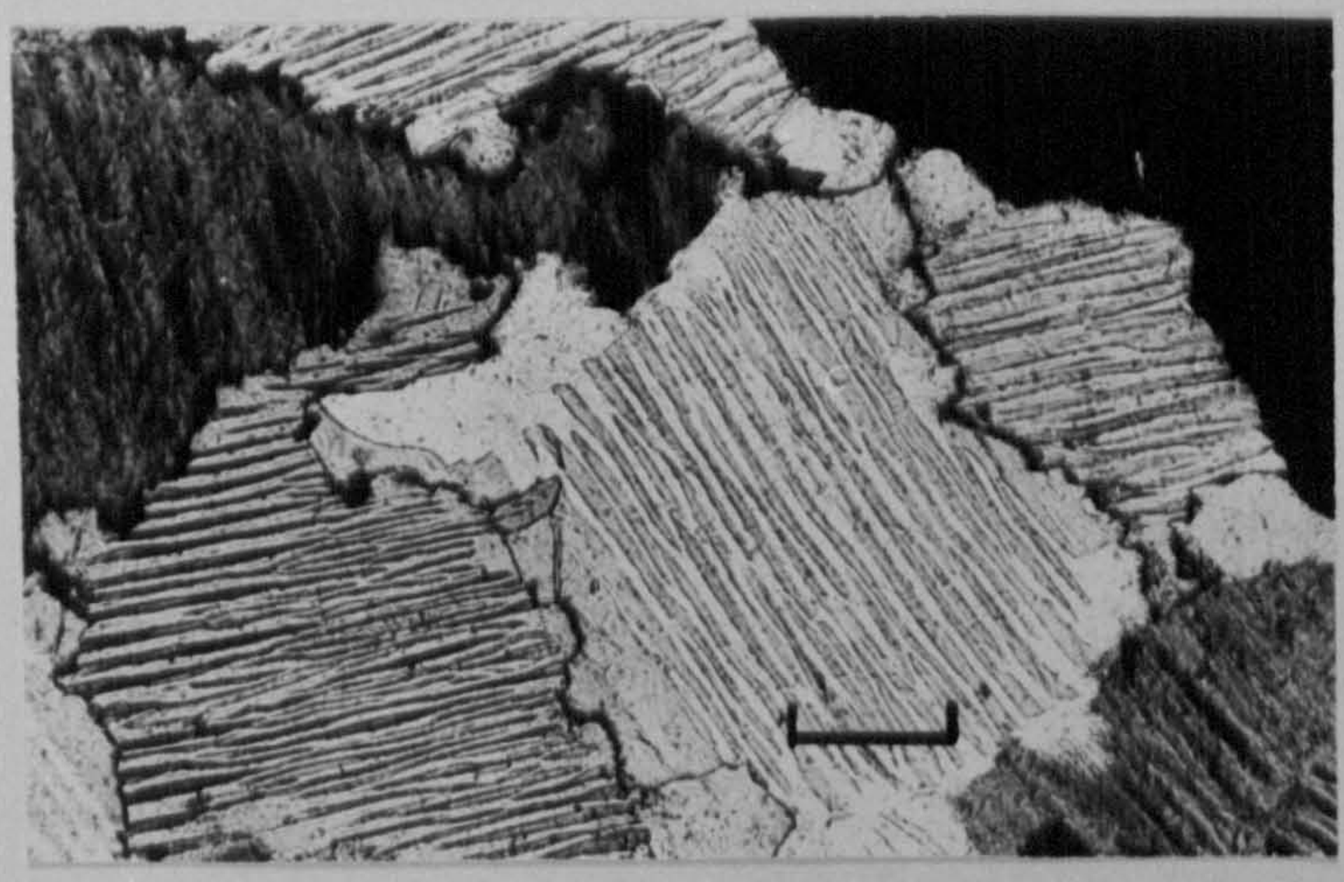

B. Lamellae of orthoclase in plagioclase; the lamellae are not perfectly straight and vary in width; they have pointed ends and are replaced 'en-echelon'.

C. Replacement of mesoperthite by plagioclase and microcline in hypersolvus granite.

Feldspar Chemistry

Analyses of six grains determined by microprobe are given in Table 6. The most important feature of the analyses is the high anorthite content An_{11-12} in HR 19 and An_{10-11} in HR 13. Barium is relatively low (ca. 0.15 wt % BaO). The feldspar analyses plot close to the normative composition of the rock in the An-Ab-Or projection as would be expected if feldspar is the only mineral in the rock with appreciable Na, K and Ca; the slight discrepancy between HR 19 rock and feldspar compositions may be due to the slight metasomatic effect (movement of K) in later recrystallisation.

Estimation of Crystallisation Temperature

A one feldspar granite is particularly useful in the estimation of crystallisation temperatures for it must have crystallised in the interval between the rock liquidus and the alkali feldspar solvus. Parsons (1978b) has shown that hypersolvus rocks have a restricted range of bulk feldspar compositions which straddle the crest of the alkali feldspar solvus. The average composition of the analysed feldspars is $(Ab_{58}Or_{42})_{88}An_{12}$ which is in the crest region of the high albite sanidine solvus. Parsons (op. cit) estimated the critical temperature of the feldspar solvus at high An contents and showed that it increases with increasing mol per cent anorthite; this is only useful, however, if the critical composition does not change with increasing An content. Parsons (1978a) also suggested that the change in critical temperature with pressure is 16^{o}/kb on the basis of solvus data of Smith and Parsons (1974) and Orville (1963). This is in good agreement with the calculations of Thompson and Waldbaum (1969) and the experimental data of Luth et al. (1974), reviewed in Luth (1974). If the effect of pressure

(a)

	ANALYSIS NO.		SIO2	AL2O3	CAO	NA2O	K2O	BAO	TOTAL	AN	AB	OR	BA-FSP
1	HR 19 1279/1-3	HOMOGENISED MESOPERTHITE	63.73	20.57	2.53	5.84	6.64	.15	99.61	.120	.502	.375	.003
	S.D.		.12	.11	.06	.31	.42	.01					
2	HR 19 1279/4-6	HOMOGENISED MESOPERTHITE	64.43	20.73	2.40	6.01	5.77	.15	99.54	.119	.530	.346	.003
	S.D.		.04	.01	.10	.52	.75	.01					
3	HR 19 1279/7-9	HOMOGENISED MESOPERTHITE	64.31	20.66	2.37	5.77	6.66	.16	100.33	.113	.496	.388	.003
	S.D.		.27	.06	.10	.06	.17	.03					
4	HR 13 1279/16-20	HOMOG. MESOPERTHITE	64.77	20.75	2.32	5.99	6.54	.14	100.54	.110	.516	.371	.002
	S.D.		.23	.12	.24	.41	.74	.02					
5	HR 13 1279/21-23	HOMOG. MESOPERTHITE	64.67	20.43	2.07	5.58	7.22	.15	100.12	.099	.485	.413	.003
	S.D.		.58	.17	.12	.37	.64	.04					
6	HR 13 1279/24-26	HOMOG. MESOPERTHITE	64.92	20.49	2.08	6.57	6.14	.11	100.31	.096	.556	.343	.002
	S.D.		.23	.37	.36	.66	.94	.02					

(b)

1	HR 13	761/1	PERTHITE (HOST)	65.85	23.13	4.40	9.11	.27	.00	102.77	.207	.815	
		769/2	(LAMELLA)	66.77	19.36	.07	.60	14.69	.24	102.00	.014	.964	.927 .005
2	HR 19	769/6	PERTHITE (HOST)	65.74	22.03	4.14	9.13	.14	.00	101.98	.199	.793	.006
		761/5	(LAMELLA)	67.11	18.35	.00	.61	14.65	.39	101.30	.008	.057	.935 .008
3	HR 19	769/7	PERTHITE (HOST)	65.46	23.08	4.60	9.25	.15	.00	102.55	.214	.778	.008
		761/6	(LAMELLA)	66.80	18.25	.03	.81	14.56	.41	100.86	.002	.077	.913 .006
4	HR 13	1279/11	PERTHITE (HOST)	64.12	22.75	3.62	9.31	.12	.00	100.11	.184	.816	.007
		1279/10	(LAMELLA)	65.53	18.57	.01	.65	15.83	.45	101.01	.000	.058	.933 .006
5	HR 13	1279/13	PERTHITE (HOST)	64.57	22.40	3.86	9.34	.09	.03	100.26	.165	.812	.005
		1279/12	(LAMELLA)	65.23	18.46	.00	.73	15.71	.33	100.47	.012	.066	.928 .006
6	HR 13	1279/14	PERTHITE (HOST)	64.46	22.58	3.69	9.49	.11	.02	100.36	.176	.819	.005
		1279/15	(LAMELLA)	65.30	18.26	.01	.76	15.69	.34	100.96	.012	.068	.925 .006
7	HR 13	1279/16	PERTHITE (HOST)	65.04	22.29	3.79	9.43	.12	.00	100.66	.181	.813	.007
		1279/17	(LAMELLA)	65.87	18.27	.03	.69	15.94	.34	101.11	.002	.061	.933 .001

Table 6. (a) Chemical analyses of homogenised mesoperthite grains from hypersolvus granites, Scourie More. Each analysis is an average of 3 scanning analyses. SD standard deviation.
(b) Chemical analyses of mesoperthite grains (host and lamella) from hypersolvus granites, Scourie More.

and An content are additive, the crest of the alkali feldspar at 10 kb (the probable load pressure during intrusion) and An_{12} will be between 1125°C and 1175°C (Fig. 7). Since the feldspar compositions are a small distance away from the crest of the

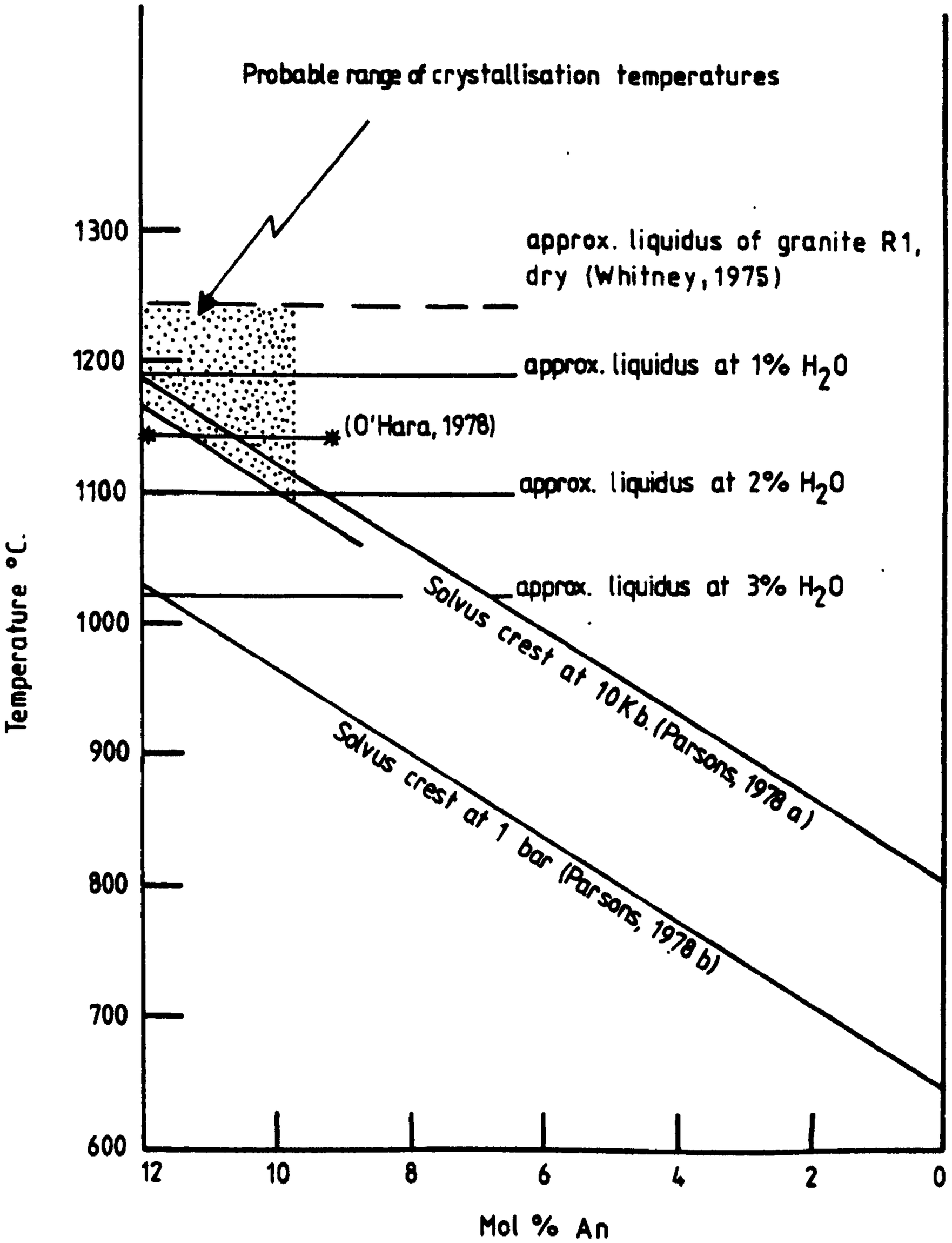

Fig. 7. The probable range of crystallisation temperatures for hypersolvus granite sheets from the Scourian complex based on the relationship between the critical temperature and both pressure and An content for the alkali feldspar solvus (after Parsons, 1978a,b). The results agree well with the study of O'Hara (1978). The maximum water content of the melt is estimated from liquidus temperatures for granite R1 in Whitney (1975).

solvus the minimum temperature limit at crystallisation is between 1100° and 1150°C. An estimate of the liquidus temperature can be made from the experimental data of Whitney (1975). Granite R 1 has a similar An content although is slightly more potassic than HR 19 and 13 and has a dry liquidus temperature of ca 1180°C at 2 kb and ca 1225°C at 8 kb; a temperature of ca 1245°C is estimated for a total pressure of 10 kb dry. This sets an upper limit on the crystallisation temperature of about 1250°C (Fig. 7).

The possible crystallisation temperature of this granite is between 1100 and 1250°C. These data can be also used to estimate the maximum percentage of water permissible in the granite liquid. Since water reduces the temperature of the liquidus, a limit may be set to the percentage of dissolved water of 2% since the alkali feldspar solvus for these rocks and the rock liquidus intersect at this water content; (this assumes that the solvus does not move when water is added).

Independant evidence for very high temperatures (ca, 1270°C at 15 kb) is given by O'Hara *et al.* (1978) who has applied the feldspar thermometer of Stormer (1975) to a two feldspar assembleage in a similar granite sheet from the north side of Scourie Bay. These temperatures are reduced to ca. 1145°C at 15 kb when the effect of Ca in alkali feldspar and K in plagioclase are taken into account. O'Hara also reports melting experiments on this sample at 15 kb; partial melting begins in the absence of water at about 1200°C and is well advanced at 1300°C. These data are in good agreement with the above one feldspar granite data.

Equilibration of perthitic lamellae

The similarity between the texture in these mesoperthites and that found in cryptoperthites, which formed by coherent

spinodal decomposition, suggests that initially they may have formed by a similar mechanism. Using the equation (Y-2) from Yund (1975):

$$\lambda = \lambda_o + kt^{1/3}$$

where λ is the wavelength of the lamellar spacing at time t (in days), λ_o is the initial wavelength at t = 0 (use 60 Å) and k is a constant (use 41.28 for 600°C) for each temperature, it is possible to estimate the length of time necessary for the lamellae to attain their present width assuming spinodal decomposition. In view of the An content of these grains this could be viewed as a minimum estimate as the ordering of the Al-Si lattice will be slower than in a pure alkali feldspar. Lamellae of 3 μm width could form in 1.05 Ma. and lamellae of 10 μm in 38.8 Ma. at 600°C both of which are acceptable values in view of the age of these rocks.

Estimates of the equilibration temperature for the perthitic lamellae fall between 430-470°C (disordered, after Powell and Powell, 1977a) and 480-520°C (ordered feldspars, after modified Powell and Powell); the potassium feldspar is mainly orthoclase so that at 10 kb the lamellae equilibrated at ca. 470°C. If margules parameters for the coherent high albite solvus are used calculated by Luth (1974) for the solvi by Tuttle and Bowen (1958) for the specimens Spencer P and Mitchell Mesa and a W_v term added for both expressions of 0.11P at 10 kb, the equilibration temperature is 330°C. This is appreciably lower than for the strain free solvus but is probably not very meaningful since the data of Tuttle and Bowen are not very reliable at low temperatures.

9. BARIUM IN FELDSPARS

Barium in alkali feldspar varies between 700 and 10,000 ppm and in coexisting plagioclase between 500 and 100 ppm (the minimum detection limit of the electron probe). There is a crude correlation between the Ba content in the host rock and Ba in homogenised alkali feldspar (Fig. 8a); in view of the variability of Ba in feldspars and the host rock (204 and 87 Loch an Daimh mor; 69 and 68 Shios) this correlation suggests that either there was an initial heterogeneity in the melt with respect to Ba (due to different proportions of crystals and liquid) or that Ba was redistributed during the reequilibration of feldspars. There is no strong correlation between purer potassium feldspar and rock composition for Ba.

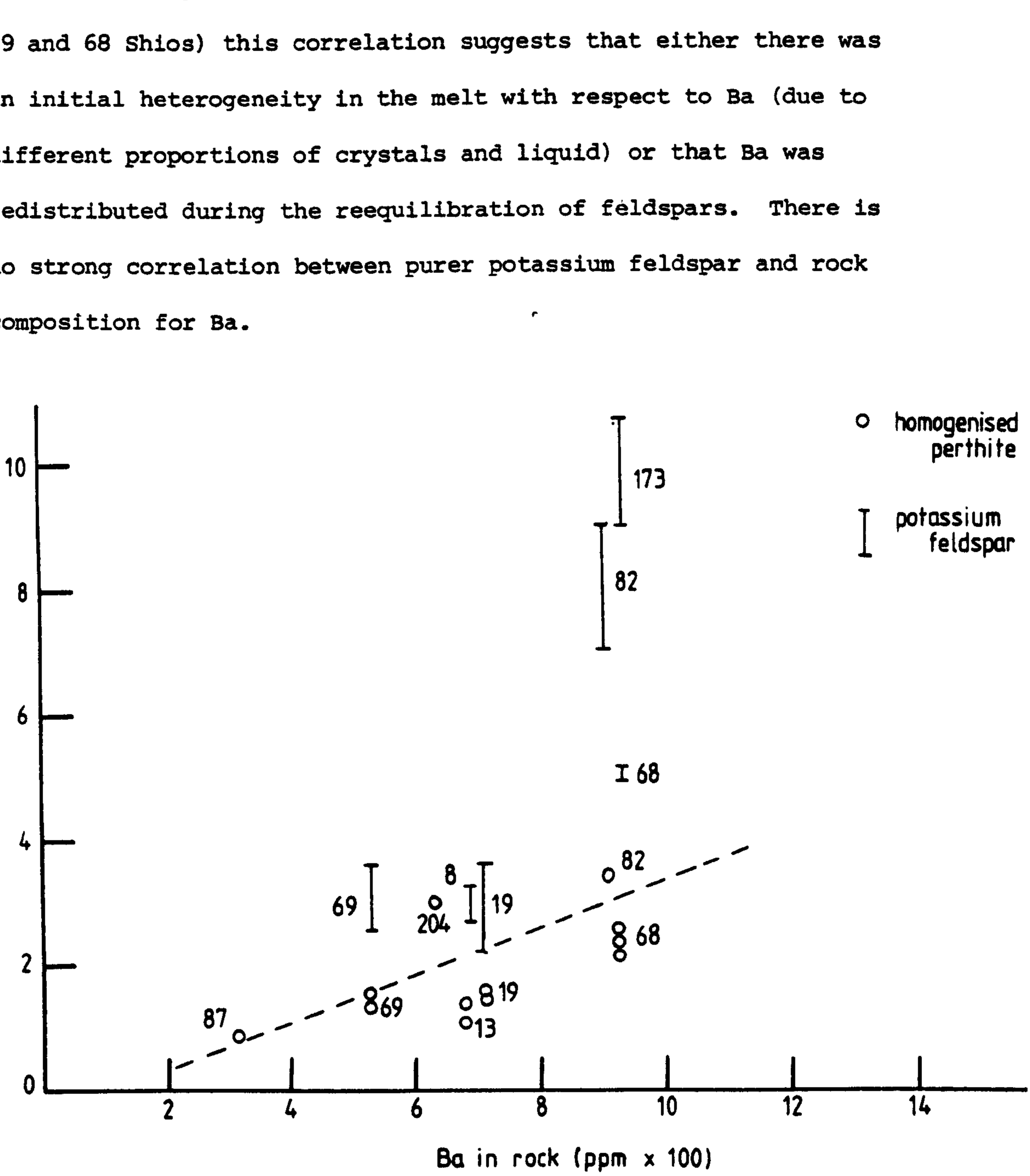

Fig. 8a. A comparison between the Ba content of feldspars from Scourian granite sheets and Ba in the host rock.

Barium substitutes on the M-site in feldspars and favours potassium feldspar over plagioclase due to the similarity in size between the K and Ba ions; consequently when mesoperthite and antiperthite unmix Ba is partitioned into the potassic phase. The highest concentration of Ba in these rocks is found in antiperthite lamellae in plagioclase in trondhjemite with granulite facies mineralogy. There is no structural control over the distribution of Ba as Ba in microcline (700-10,800 ppm) and orthoclase (2200-9100 ppm) are in the same region.

Most potassium feldspars have Ba contents closer to the amphibolite facies field of Virgo (1969) rather than his granulite facies field (Fig. 8b). Mesoperthites define a field of their own (Ba 800-3400 ppm) in view of their low orthoclase content.

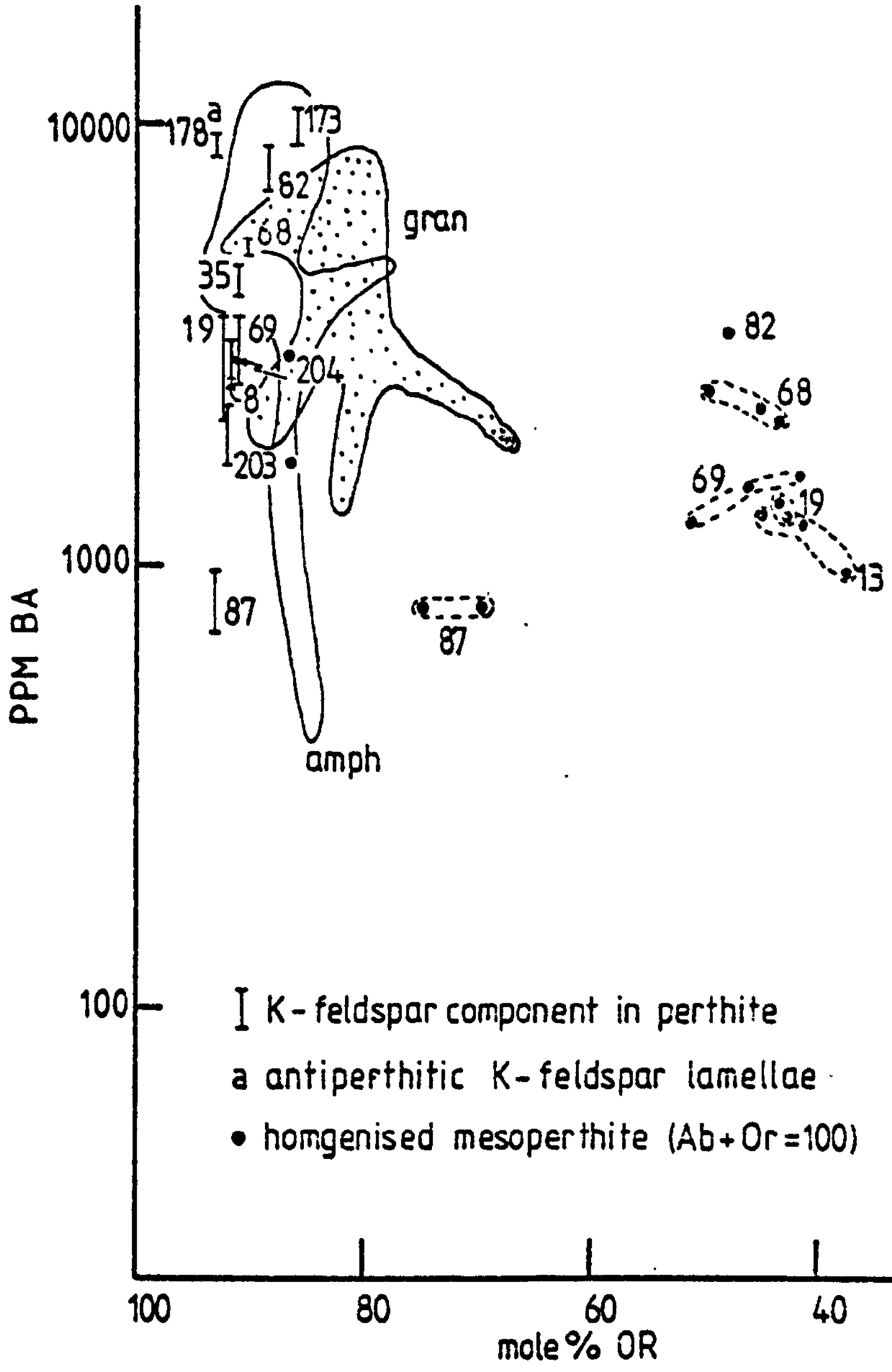

Fig. 8b Ba in Scourian granite feldspars plotted against mole per cent Or compared with the fields for granulite facies (gran) and amphibolite facies (amph) feldspars from Virgo (1969).

10. THE SIGNIFICANCE OF GARNET IN GRANITIC LIQUIDS

Small 1 to 2 mm euhedral garnets with occasional inclusions of quartz and feldspar are present in the granite sheets on Loch an Daimh Mor, North of Camas nam Buth, Scourie more and on the north side of Scourie Bay (the same granite sheet from which O'Hara (1978) obtained high feldspar temperatures). Garnet coexists with plagioclase, mesoperthite and iron-titanium oxides or with plagioclase and perthitic microcline and appears in place of orthopyroxene as the main liquidus ferromagnesian phase in these rocks as the two are never found together. Garnet in the Loch an Daimh Mor sheet is rich in almandine (63%) and contains appreciable spessartine (15%) which is unusual in view of the small amount of MnO in the host rock (0.02 - 0.12 wt % MnO). The garnets are unique in composition compared with garnets in neighbouring basic and supracrustal rocks, implying that they are not xenocrysts, but were in equilibrium in the granitic liquid (Fig. 9b); they are, however, more calcic than garnets from compositionally similar granulite facies rocks containing sillimanite (from W. Greenland) and Kyanite (from Saxony). They are more Mn rich than the majority of garnets found in silicic liquids (Green, 1977) (Fig. 9a).

Large garnets, over 1 cm across, occur in anorthositic trondhjemite in the composite granite-trondhjemite sheet E. of Camas an Lochain and are more calcic, less spessartine rich and plot closer to garnets from nearby gabbros reflecting the more calcic rock composition. These garnets are zoned with almandine rich cores and are rimmed with green biotite. They contain vermiform fluid inclusions which are probably rich in CO_2 since carbonate is an accessory associated with the breakdown of garnet.

Garnets in the Loch an Daimh Mor sheet are only slightly zoned and show both normal and reversed trends (Table 7). The most strongly zoned grain is enriched in the centre in FeO (1.2%),

	86 1 E	86 1 C	86 1 E	87 1 E	87 1 C	87 1 E	87 2 C	87 2	87 2 E
SI 02	38.74	37.81	37.87	37.96	37.40	37.51	37.69	37.76	38.01
AL203	20.74	20.76	20.70	20.77	21.25	20.26	20.75	20.80	20.73
FE O	27.94	27.78	28.19	27.66	28.62	28.36	28.24	28.43	28.17
MN O	6.51	6.73	6.58	5.93	6.45	6.23	6.67	6.49	6.71
MG O	3.55	3.41	3.58	2.66	3.16	3.45	3.50	3.41	3.43
CA O	3.31	3.03	3.13	4.82	3.46	3.65	3.13	3.30	3.19
CR203	.02	.02	.03	.05	.03	.02	.02	.03	.11
TOTAL	100.80	99.67	99.98	99.82	99.22	99.59	100.01	100.24	100.35
UNIT FORMULA									
SI	6.113	6.059	6.054	6.075	6.055	6.051	6.033	6.034	6.060
AL	3.861	3.921	3.944	3.916	3.964	3.853	3.915	3.916	3.896
FE	3.691	3.723	3.756	3.762	3.922	3.697	3.701	3.796	3.756
MN	.869	.913	.894	.853	.885	.852	.934	.870	.905
MG	.836	.834	.853	.635	.763	.734	.835	.812	.829
CA	.560	.521	.536	.827	.534	.831	.537	.565	.545
CR	.002	.003	.004	.016	.004	.003	.003	.004	.011
O	24.000	24.000	24.000	24.000	24.000	24.000	24.000	24.000	24.000
GARNET MOLECULES (RICKWOOD(1968))									
UVAROVIT	.05	.06	.1	.10	.1	.07	.06	.10	.03
PYROPE	14.42	14.16	14.57	14.70	13.14	12.66	14.21	13.61	14.19
SPESSART	15.19	15.52	15.21	13.59	15.32	14.72	15.35	14.53	15.46
GROSSULA	9.60	8.92	9.66	13.03	9.11	10.64	9.47	9.51	9.29
ALMANDIN	60.72	61.33	61.56	61.53	62.33	61.65	61.26	61.65	61.11
PERCENTAGE CATIONS ASSIGNED									
	96.96	96.21	97.64	98.34	96.64	96.27	97.89	97.95	97.47

TABLE 7. Chemical analyses of garnets from Loch an Daimh Mor granite sheet. The analyses were made on three separate grains in samples HR 88 and HR 87. E edge of grain; C centre of grain.

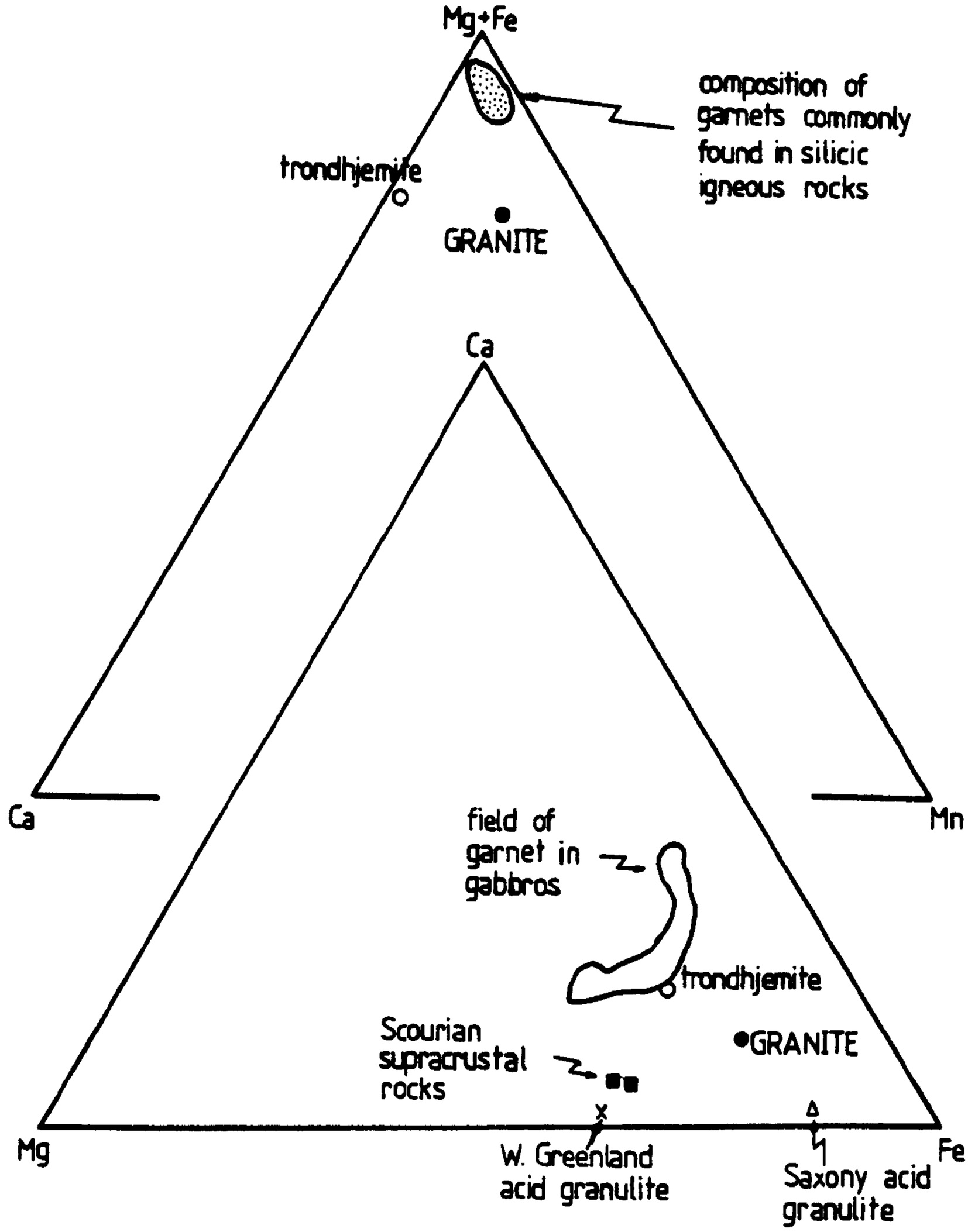

Fig. 9. The composition of garnet in acid sheets from Loch an Daimh (GRANITE) compared (a) with garnets from acid igneous rocks (Green, 1977) and (b) with garnets from the Scourian complex and other granulite facies terrains.

MnO (0.6%), MgO (0.5%) and depleted in CaO (1.8%) relative to the rim. In other grains the difference between core and rim is about 0.2% for most oxides. Most zoning is probably due to the late growth of chlorite on garnet; Green and Ringwood (1968) analysed garnets from Palaeozoic calc alkaline igneous rocks in Australia

which have reaction rims of hypersthene and cordierite, and these garnets are relatively unzoned with almandine rich (by about 2 mole %) outer rims 40 - 10 μm wide. Krogh (1977) described garnets from eclogites which show both normal and reversed zoning which he interprets as the effect of prograde and retrograde metamorphism respectively. He proposes that at a certain temperature the diffusion rate in the garnet will be high enough to homogenise the mineral and obliterate the effect of the prograde zoning; this temperature is in excess of 750°C. The small amount of zoning in the Scourian acid garnets may imply that they were held at a temperature in excess of 750°C for a long period.

Garnet in acid liquids has commonly been regarded as an indicator of high pressure; however, the evidence suggests that in this suite of rocks the bulk composition controlled the appearance of garnet. Green and Lambert (1965) squeezed dry adamellite and found that orthopyroxene is replaced by clinopyroxene and garnet at pressures of 13.75 kb at 950°C and 16.25 kb at 1100°C. Green and Ringwood (1968) proposed that garnets in rhyodacites crystallised from the melt at pressures between 9 and 18 kb. Green (1977) showed that Mn in garnet stabilises it to lower pressures, Ca content is largely a function of bulk composition but that there is some pressure effect and that the distribution coefficient for Fe and Mg between garnet and liquid is dependant upon temperature. Cawthorn and Brown (1976), however, suggested that the crystallisation of garnet is largely a function of magma composition rather than crystallisation pressure and that garnet tends to concentrate in the more leucocratic members of granitoid complexes: this is borne out by the euhedral appearance and lack of resorbtion of garnet in granitic liquids. Similarly, Wood (1975) suggested that the activity of silica controlled the appearance of garnet in the

granulite facies tonalites and gabbros of South Harris.

Garnet in the granitic rocks of the Scourian complex appears to replace orthopyroxene as the main ferromagnesian phase, in bulk compositions that are enriched in normative orthoclase and poor in normative anorthite (Fig. 10), although the two phases are never seen together or in a reaction relationship.

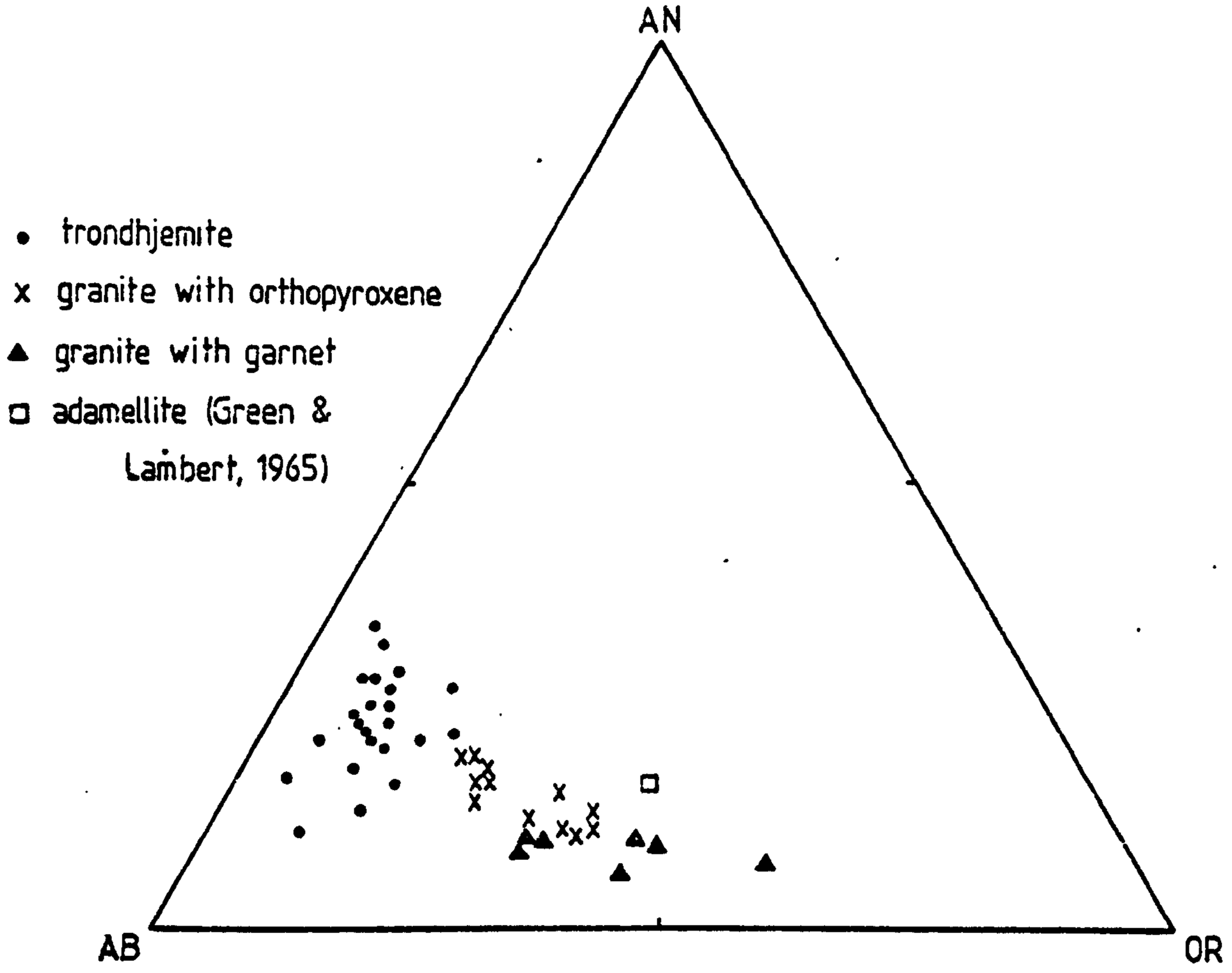

Fig. 10. The composition of Scourian granites plotted in the projection normative Ab-Or-An; note the low An content of garnet-bearing granites. The composition of the adamellite used by Green and Lambert (1964) is plotted for comparison.

Since orthopyroxene-bearing and garnet-bearing granites are the same relative age with respect to the enclosing gneiss and belong to the same fractionation series (see Chapter 1) it is unlikely that they evolved at substantially different pressures. This suggests that the appearance of garnet in these rocks is

primarily a function of rock composition and not pressure.

Compositional control over the appearance of garnet may be exerted in one of two ways: (i) during metamorphism by the composition of the coexisting phases (ii) in a magma by the composition of the melt. These two possibilities are discussed in turn below.

During metamorphism garnet forms at the expense of orthopyroxene at higher pressure according to the reaction:

$$Mg_2Si_2O_6 + CaAl_2Si_2O_8 \rightarrow \frac{1}{3}Ca_3Al_2Si_3O_{12} + \frac{2}{3}Mg_3Al_2Si_3O_{12} + SiO_2$$

in orthopyroxene anorthite in garnet quartz

Garnet and orthopyroxene do not coexist in the same rock so that it is not possible to estimate the equilibrium pressure directly. If, however, the composition of the orthopyroxene that could coexist with garnet is estimated and vice versa it is possible to set upper and lower pressure limits on the stability of the assemblages orthopyroxene-plagioclase-quartz and garnet-plagioclase-quartz. Orthopyroxene is always altered to chlorite but the original composition can be estimated by assuming that the Fe/Mg ratio is not changed substantially; this assumption is thought to be realistic in view of the similarity in composition between the estimated orthopyroxene composition and that of orthopyroxene in nearby leucotonalite. Using the composition of the minerals (Table 7) and the thermodynamic data of Newton (1978) the upper stability limit of orthopyroxene co-existing with plagioclase (An_{21}) and quartz at 850°C, is 6.8 kb (8 kb at 1150°C) and the lower stability limit of garnet co-existing with plagioclase (An_{31}) and quartz is 5.3 kb at 850°C (6 kb at 1150°C). Orthopyroxene and garnet, therefore, co-exist in granitic sheets of differing

bulk composition in the same pressure range (5.3 to 6.8 kb) because they co-exist with plagioclase of differing composition).

The pressure interval at 850°C estimated for these granite sheets is lower than that estimated for the granulite facies metamorphism (ca. 10 kb, see Chapter 8) and yet the granitic sheets are deformed and their intrusion predates the granulite facies metamorphism. This may be because the assumed garnet and orthopyroxene compositions are incorrect or because garnet and orthopyroxene are igneous minerals and the above reaction does not apply.

The small size and euhedral form of the garnets compared with the large 'spongy' garnet porphyroblasts in nearby gabbros and the low pH_2O during the crystallisation of these rocks (see above) support the suggestion that garnet and orthopyroxene may be primary igneous minerals. If this is so the appearance of garnet was controlled by the Al_2O_3 activity of the melt by the reaction

$$3Fe_2Si_2O_6 + Al_2O_3 \rightarrow 2Fe_3Al_2Si_3O_{12}$$

in orthopyroxene in melt almandine garnet

Al_2O_3 activity is higher in rocks with low normative anorthite, because a smaller amount of Al_2O_3 is used in the feldspars. The difference in Fe/Mg ratio between garnet and orthopyroxene and the absence of magnetite in some garnet-bearing granite sheets suggests that magnetite is also involved in the garnet forming reaction, in which case the presence of garnet will depend upon the activity of SiO_2, Al_2O_3 and O_2 in the melt. The pressure limits suggested above do not apply if garnet and orthopyroxene crystallised

from a melt because the thermodynamic values are different and the activity of anorthite is lower.

Garnet is usually mantled with chlorite (or green biotite), albite (Fig. 4) and is associated with magnetite. The breakdown of garnet to chlorite can be represented by the reaction:

garnet + plagioclase (An_{27}) + H_2O → chlorite + albite (An_2)
+ garnet (enriched in Ca, depleted in Mn, Mg, Fe) + magnetite

Chlorite and magnetite are poor in Mn and it seems that Mn is lost from the system during this reaction. Evidence from iron - titanium oxides indicates that Mn was mobilised in the presence of a fluid phase during retrogression.

11. IRON TITANIUM OXIDE THERMOMETRY

It was recently shown by Bowles (1976, 1977), Oliver (1978), Anderson (1968), Duchesne (1972) and Rollinson (Chapter 4) that the detailed study of iron titanium oxide intergrowths from slowly cooled rocks can yield a wealth of information about the magmatic and metamorphic temperatures and the subsequent subsolidus cooling history of a rock.

In this study detailed electron probe analyses were made on 10 separate ilmenite - magnetite grains from three different intrusive sheets collected from the Scourie - Badcall area. Samples 67, 68 and 69 come from the Shios peninsula, sample 82 from a nearby granite sheet and sample 35 from Torran nan Clach Boga, north of Upper Badcall. The feldspars in these rocks have also been analysed and are described above.

Iron - titanium oxides form intergrowths of ilmenite and magnetite which show either high temperatures (660-910°C) or low equilibration temperatures (530-320°C) on the Buddington and Lindsley thermometer (1964). High temperature grains are composed

of about equal proportions of ilmenite and magnetite and form simple bipartite grains; there may be fine lamellae of ilmenite in magnetite host and more rarely fine lamellae of magnetite in ilmenite. Low temperature grains form simple bipartite intergrowths or contain lamellae of magnetite 10 to 60 μm wide in a host of ilmenite; in low temperature grains ilmenite dominates over magnetite.

Analytical Procedure

A detailed description of the electron probe procedure used is given in Rollinson (in press); in addition to the standards quoted natural rutile (59.69% Ti, 0.33% Fe, 39.98% O) was used to determine Ti, and synthetic wollastonite (23.58% Si, 34.52% Ca, 41.59% O) for Ca and Si. Both a scanning beam and a point (less than 1 μm diameter) were used to analyse areas of grains and domains within grains respectively. It will be noted that the totals for magnetite analyses are low and are lower in the high temperature than the low temperature grains; Rollinson (in press) has suggested (see Chapter 4) that this indicates non stoichiometry in the magnetite due to late alteration to γ-maghemite. This is borne out in the present study because grains which continued to equilibrate with ilmenite to low temperatures are less susceptible to this form of late alteration. Values for FeO and Fe_2O_3, mol per cent ulvopinel and mol per cent R_2O_3 (Fe_2O_3 + Al_2O_3 + Cr_2O_3) were calculated using the method of Carmichael (1967).

Scanning analyses were made over areas containing fine lamellae in the high temperature grains in order to estimate the pre-exsolution composition of the grain. These are termed 'average grains' in Table 8a. Point analyses were made 5 to 10 μm away from the boundary separating ilmenite and magnetite lamellae in several places in the same grain along the length of the lamellae

and also normal to the length of lamellae in order to check for compositional zoning. The analysed grains and the mole fraction of ulvospinel and R_2O_3 in magnetite and ilmenite respectively are depicted in Fig. 11. Adjacent ilmenite-magnetite point analyses are used to estimate the equilibration temperature at that particular point in the grain from the Buddington and Lindsley thermometer. This assumes that whilst grains are zoned with respect to their mole fraction of ulvospinel and R_2O_3 equilibrium is preserved in small microsystems within the grain and that if iron or titanium is lost from either ilmenite or magnetite to a silicate phase then the ilmenite and magnetite will reequilibrate. This means that a variety of equilibration temperatures may be obtained for a single grain and that limits can be set on the distance which iron and titanium can diffuse at the temperature in question.

The experiments of Buddington and Lindsley (1964) were carried out in the pure system $FeO-Fe_2O_3-TiO_2$, so that any impurities in natural iron titanium oxides involve a certain amount of extrapolation in order to estimate temperature and oxygen fugacity at equilibrium. Powell and Powell (1977b) developed a method which estimates the effect of minor elements on the activities of the magnetite, ulvospinel, haematite and ilmenite components; since, however, it is not clear what components the minor elements make within the rhombohedral and spinel phases it is only possible to set limits on the activities of magnetite, ilmenite, ulvospinel and haematite. The activities of the phases are combined to give the most and least favourable alternatives which are then used with the experimental data of Buddington and Lindsley (1964) to give a maximum and minimum temperature and oxygen fugacity. The results are plotted with their estimated uncertainty in Fig. 13. The only drawback with

this method is that the mineral analysis has to be calculated to three and four oxygens for ilmenite and magnetite respectively which for microprobe analyses involves some assumptions since the calculation of Fe^{3+} depends upon the way in which the minor elements are treated. Manganese in ilmenite is the only minor element of importance and occurs up to 8.6 wt % MnO in grain 69/1, but since the spinel phase is almost pure magnetite - ulvospinel solid solution the uncertainty is small.

Ilmenite - Magnetite Chemistry

The variation in composition across grains is shown in Fig. 11. Whilst there is variation in the mole per cent of ulvospinel in the high temperature grains (44-23 mole %), the only evidence of zoning is in grain 68/2 in which the mole fraction of ulvospinel decreases towards the edge of the grain. Low temperature grains show strong zoning:

(i) a. magnetite increases in mole % ulvospinel towards ilmenite (grains 69/1, 82/1).

b. magnetite is richer in mole % ulvospinel in an ilmenite-rich environment that in an ilmenite poor environment (grain 35/2).

(ii) magnetite decreases in mole % ulvospinel along the length of a lamella towards the edge of a grain (grain 35/1) and even parallel to an ilmenite-magnetite boundary (grain 69/1).

(iii) ilmenite increases in mole per cent R_2O_3 away from magnetite (grains 69/1, 35/1)

(iv) ilmenite increases in mole % R_2O_3 towards the edge of a grain even when parallel to a magnetite lamella (grains 82/1, 35/2, 35/3) although in grain 69/1

FIGURE 11. Iron - titanium oxide grains analysed in this study; stippled areas are magnetite, unshaded areas are ilmenite. The mole percent ulvospinel in magnetite and R_2O_3 in ilmenite are shown. Scale bar is 50 μm.

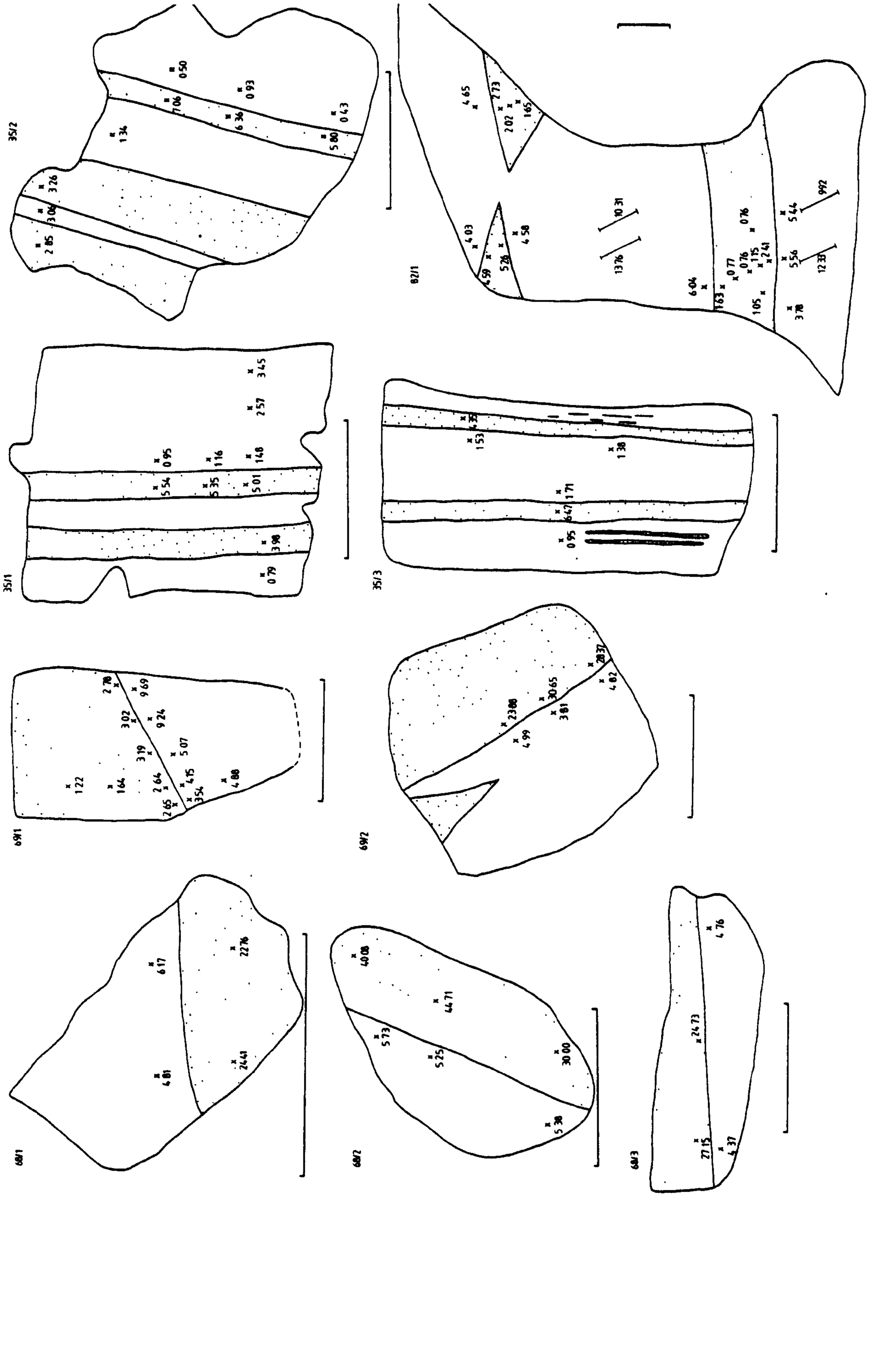

TABLE 8a Co-existing ilmenite and magnetite in samples HR 67, 68, 69 from the Shios peninula

ILMENITE

	Averaged grains			Grain-boundary pairs										Low temperature grains				
	1	2	3	4	5	6	7	8	9	10	11	12	13	14	15	16	17	18	19
Rock/Grain	68/3	68/2	69/2	68/2	68/2	67/1	68/2	69/2	69/2	69/2	68/1	68/3	68/1	68/3	69/1	69/1	69/1	69/1	69/1
Anal. No.	1152/16	1145/7,8	973/1,2,3	1145/14	1145/15	848/6	1145/9	973/8	973/9	973/12	1145/3	1152/15	1145/4	1152/17	972/19	972/21	972/24	972/13	972/26
SiO_2	0.14	0.20	-	0.14	0.12	0.06	0.17	-	-	-	0.14	0.15	0.14	0.15	-	-	-	-	-
TiO_2	46.29	47.56	49.83	49.34	49.40	47.77	49.15	49.27	49.89	49.55	48.46	50.04	49.59	49.63	46.63	47.11	48.86	49.99	49.33
Al_2O_3	0.08	0.06	0.06	0.05	0.03	0.05	0.08	0.04	0.03	0.03	0.03	0.03	0.03	0.03	0.03	0.05	0.04	0.03	0.03
Cr_2O_3	0.04	0.02	0.00	0.01	0.03	0.00	0.00	0.00	0.00	0.00	0.04	0.06	0.01	0.02	0.00	0.00	0.00	0.00	0.00
'FeO'	50.91	49.80	41.83	48.81	49.28	41.70	48.80	41.91	41.87	42.72	49.01	48.36	48.88	48.40	42.35	42.92	40.32	40.26	39.09
MnO	0.72	0.25	6.75	0.24	0.27	5.74	0.23	6.67	6.37	6.29	0.31	0.72	0.31	0.77	7.94	8.30	8.11	8.38	8.34
MgO	0.08	0.15	0.05	0.19	0.20	0.00	0.17	0.04	0.03	0.06	0.05	0.06	0.05	0.02	0.03	0.03	0.02	0.03	0.02
CaO	0.00	0.01	-	0.00	0.00	0.05	0.00	-	-	-	0.00	0.01	0.00	0.01	-	-	-	-	-
Total	98.25	97.05	98.07	98.79	99.33	95.37	98.61	97.93	98.58	98.66	98.04	99.43	99.06	99.03	96.96	98.61	97.36	98.69	96.81
FeO	40.92	42.48	37.88	43.95	43.94	37.15	43.87	37.48	38.36	38.08	43.34	44.93	44.41	43.98	33.84	33.90	35.69	36.41	35.88
Fe_2O_3	11.10	8.41	4.39	5.40	5.94	5.06	5.48	4.92	3.90	5.16	6.30	4.48	4.97	4.91	9.46	10.02	5.15	4.28	3.57
TOTAL	99.37	99.12	98.96	99.32	99.92	95.88	99.15	98.42	98.60	99.17	98.67	99.88	99.51	99.52	97.92	99.41	97.87	99.12	97.17
R_2O_3	10.82	8.19	4.30	5.25	5.73	5.09	5.38	4.82	3.81	4.99	6.17	4.37	4.81	4.76	9.24	9.69	5.07	4.15	3.54

MAGNETITE

Anal. No.	1152/13	1145/5,6	973/4,5,6	1145/13	1145/16	848/7	1145/10	973/7	973/10	973/11	1145/2	1152/14	1145/1	1152/18	972/20	972/22	972/23	972/12	972/25
SiO_2	0.15	0.14	-	0.11	0.16	0.12	0.16	-	-	-	0.17	0.17	0.16	0.14	-	-	-	-	-
TiO_2	14.73	14.63	15.77	14.81	13.20	9.28	9.80	9.30	10.07	7.84	7.31	8.82	7.88	8.02	1.02	0.94	1.07	0.89	0.89
Al_2O_3	0.13	0.30	0.12	0.13	0.17	0.16	0.15	0.16	0.15	0.15	0.12	0.16	0.14	0.12	0.23	0.27	0.24	0.25	0.24
Cr_2O_3	0.08	0.10	0.07	0.11	0.10	0.05	0.11	0.09	0.07	0.09	0.04	0.09	0.07	0.11	0.07	0.04	0.07	0.06	0.06
'FeO'	76.01	76.40	72.66	76.49	77.64	79.61	80.69	79.37	79.05	80.85	82.23	81.27	81.88	81.76	89.75	89.80	89.12	89.57	89.10
MnO	0.14	0.06	1.40	0.02	0.10	0.26	0.04	0.22	0.22	0.34	0.08	0.14	0.02	0.04	0.07	0.10	0.06	0.12	0.10
MgO	0.00	0.06	0.03	0.00	0.08	0.00	0.00	0.09	0.02	0.01	0.00	0.00	0.00	0.01	0.02	0.03	0.01	0.02	0.06
CaO	0.02	0.01	-	0.00	0.00	0.02	0.00	-	-	-	0.02	0.02	0.01	0.03	-	-	-	-	-
Total	91.25	91.70	90.05	91.66	91.46	89.51	90.95	89.22	89.59	89.28	89.98	90.66	90.16	90.24	91.17	91.18	90.57	90.90	90.38
FeO	43.21	43.28	33.85	43.51	41.91	37.75	38.98	37.46	38.34	36.21	36.44	37.93	37.06	37.12	31.20	31.10	31.07	30.69	30.76
Fe_2O_3	36.45	36.81	42.21	36.65	39.71	46.52	46.35	46.58	45.24	49.61	50.88	48.17	49.81	49.61	65.07	65.24	64.51	65.14	64.84
TOTAL	94.91	95.37	93.47	95.34	95.43	94.16	95.59	93.90	94.11	94.25	95.07	95.50	95.15	95.20	97.68	97.72	97.03	97.44	96.95
Usp	44.82	44.20	48.05	44.71	40.08	28.72	30.00	28.37	30.65	23.88	22.76	27.15	24.41	24.73	3.02	2.78	3.19	2.64	2.65
Tmax	910	829	828	787	775	711	707	707	691	684	680	667	662	664	533	530	487	457	449
Tmin	906	825	804	785	771	706	705	701	687	678	678	663	661	662	527	522	483	450	445
$-f_{O_2}$max	11.6	13.8	14.3	15.2	15.2	16.8	16.8	17.0	17.8	17.7	17.0	18.1	18.0	18.0	19.4	19.3	22.3	23.7	24.3
$-f_{O_2}$min	11.7	13.9	15.3	15.2	15.4	17.1	16.9	17.3	18.1	17.4	17.2	18.3	18.1	18.1	19.9	20.0	22.7	24.5	24.9

'FeO' total iron determined as FeO

TABLE 8b CO-EXISTING ILMENITE AND MAGNETITE IN SAMPLE HR 82 FROM THE SHIOS PENINSULA

ILMENITE

	Grain boundary pairs					
	1	2	3	4	5	6
Rock/Grain	HR 82/1	HR 82/1	HR 82/1	HR 82/1	HR 82/1	HR 82/1
Anal. No.	1144/ 3	1144/ 1	1144/19	1144/ 5	1144/18	1144/21
TiO_2	49.84	47.70	49.60	50.02	49.15	50.49
Al_2O_3	0.02	0.12	0.01	0.05	0.06	0.04
Cr_2O_3	0.00	0.00	0.00	0.01	0.00	0.00
'FeO'	44.71	41.58	45.92	44.85	45.63	44.60
MnO	4.24	4.41	3.69	4.22	3.99	4.05
MgO	0.05	0.16	0.10	0.09	0.07	0.12
Total	98.86	93.97	99.31	99.24	98.90	99.30
FeO	40.44	38.14	40.69	40.55	40.03	41.09
Fe_2O_3	4.75	3.82	5.82	4.78	6.22	3.90
TOTAL	99.34	94.35	99.90	99.72	99.52	99.69
R_2O_3	4.58	4.03	5.56	4.78	6.04	3.78

MAGNETITE

Anal. No.	1144/ 3	1144/ 2	1144/13	1144/ 6	1144/17	1144/20
TiO_2	1.79	1.56	0.81	0.93	0.56	0.36
Al_2O_3	0.22	0.21	0.28	0.25	0.42	0.76*
Cr_2O_3	0.13	0.11	0.13	0.12	0.12	0.12
'FeO'	89.64	89.61	88.99	90.37	89.54	90.20
MnO	0.05	0.09	0.01	0.02	0.03	0.02
MgO	0.00	0.06	0.14	0.03	1.05*	0.50*
Total	91.83	91.65	90.37	91.72	91.72	91.97
FeO	32.14	31.71	30.63	31.34	29.49	30.29
Fe_2O_3	63.91	64.35	64.85	65.60	66.74	66.59
TOTAL.	98.23	98.12	96.86	98.29	98.71	98.63
Usp	5.26	4.59	2.41	2.73	1.63	1.05
Tmax°C	510	488	467	463	420	400
Tmin°C	509	481	454	459	-	-
$-fO_2$max	21.9	22.8	22.2	23.3	25.4	26.8
$-fO_2$min	22.1	23.5	23.7	23.7	-	-

'FeO' total iron determined as FeO

TABLE 8c CO-EXISTING ILMENITE AND MAGNETITE IN SAMPLE BR 35, FROM TONGAN BAN CLACH BOGA

ILMENITE

Grain Boundary Pairs

	1	2	3	4	5	6	7	8	9	10	11	12
Rock/Grain	BR 35/3	BR 35/2	BR 35/2	BR 35/1	BR 35/3	BR 35/1	BR 35/5	BR 35/2	BR 35/1	BR 35/2	BR 35/2	BR 35/1
Anal. No.	1278/23	1278/19	1278/19	1278/ 3	1278/26	1278/5	1278/21	1278/14	1278/ 8	1278/11	1278/15	1278/10
TiO_2	51.19	50.19	50.19	51.61	51.18	51.97	51.67	51.63	52.03	51.86	51.63	51.51
Al_2O_3	0.03	0.04	0.04	0.05	0.03	0.05	0.06	0.05	0.03	0.04	0.04	0.24
Cr_2O_3	0.00	0.00	0.00	0.01	0.00	0.00	0.00	0.00	0.00	0.01	0.00	0.00
'FeO'	45.42	45.69	45.69	45.45	45.27	45.40	45.15	45.20	45.30	44.97	44.80	44.41
MnO	2.11	1.87	1.87	2.21	2.06	2.30	2.01	1.99	2.06	2.04	1.95	2.21
MgO	0.02	0.19	0.19	0.02	0.03	0.02	0.05	0.01	0.03	0.00	0.00	0.04
Total	98.77	97.98	97.98	99.35	98.58	99.74	98.94	98.87	99.44	98.91	98.43	98.41
FeO	43.86	42.90	42.90	44.14	43.88	44.37	44.43	44.93	44.65	44.57	44.45	44.01
Fe_2O_3	1.73	3.10	3.10	1.46	1.54	1.15	0.90	0.89	0.95	0.45	0.39	0.79
TOTAL	98.94	98.25	98.25	99.50	98.72	99.85	99.03	98.97	99.74	98.96	98.45	98.45
R_2O_3	1.71	3.06	3.06	1.48	1.53	1.16	0.95	0.93	0.96	0.50	0.43	0.44

MAGNETITE

Anal. No.	1278/22	1278/17	1278/20	1278/ 4	1278/25	1278/ 6	1278/22	1278/13	1278/ 7	1278/12	1278/16	1278/ 9
TiO_2	2.21	1.10	0.96	1.70	1.46	1.82	2.21	2.16	1.09	2.40	1.98	1.35
Al_2O_3	0.70	0.23	0.23	0.22	0.23	0.24	0.70	0.33	0.21	0.29	0.17	0.33
Cr_2O_3	0.09	0.11	0.12	0.07	0.12	0.10	0.09	0.11	0.09	0.09	0.07	0.08
'FeO'	89.04	89.68	89.51	89.62	88.70	89.69	89.04	88.99	89.90	88.85	88.61	89.59
MnO	0.05	0.02	0.01	0.02	0.03	0.04	0.05	0.04	0.04	0.08	0.04	0.04
MgO	0.00	0.00	0.00	0.00	0.00	0.00	0.00	0.02	0.01	0.04	0.00	0.02
Total	92.08	91.14	90.83	91.63	90.55	91.90	92.09	91.65	92.15	91.74	90.83	91.40
FeO	32.65	31.34	31.13	32.02	31.44	32.20	32.65	32.39	32.32	32.56	31.98	31.61
Fe_2O_3	62.66	64.83	64.88	64.01	63.63	63.90	62.66	62.90	63.99	62.56	62.97	64.43
TOTAL	98.37	97.64	97.33	98.04	96.92	98.28	98.37	97.95	98.35	98.02	97.15	97.87
Dup	6.47	3.26	2.85	5.01	4.35	5.35	6.47	6.36	5.54	7.06	5.80	3.98
T_{max}	451	443	434	422	417	412	410	408	403	376	358	347
T_{min}	449	441	433	419	415	408	405	404	400	369	352	310
$-\log O_{2max}$	26.3	25.1	25.4	27.7	27.8	28.7	29.3	29.4	29.5	32.4	33.6	33.7
$-\log O_{2min}$	26.5	25.2	25.5	28.0	27.9	29.0	29.8	29.8	29.8	33.2	34.2	37.6

'FeO' total iron determined as FeO

R_2O_3 increases across the grain.

(v) manganese in ilmenite increases towards the edge of a grain in both high and low temperature grains (grains 69/1, 69/2, 82/1) although in the lowest temperature grains this is reversed and Mn decreases towards the edge of the grain (grain 35/1).

Manganese is variable in ilmenite from 0.2 to 6.7 weight per cent in high temperature grains and from 1.9 to 8.6 wt % in low temperature grains. This is not related to the composition of the host rock as samples 69 and 82 contain the same amount of MnO (0.03 - 0.04 wt % MnO) and yet ilmenite grains contain twice as much MnO in HR69 as in HR82. Also the variation of MnO in ilmenite within a single granite sheet 0.2 - 0.8 % MnO in HR68 and 8.6% MnO in HR69 suggests that it is as a result of local exchange reactions (probably with orthopyroxene) rather than an original feature of the rock.

Electron probe scans across and X-ray images of grain 82/1 show that cracks in magnetite are enriched in MgO (ca. 17.0%) (Fig. 12); these cracks also contain Al_2O_3 (ca 11.0%) and minimal Cr, Fe and Ti. Bowles (1976) reported fine lamellae of ceylonite associated with magnetite in ilmenite-magnetite intergrowths in the gabbros of the Freetown Complex, Sierra Leone and it may be that this is an alteration product of this or spinel associated with magnetite.

Thermometry and Cooling History

Fig. 13 shows two distinct cooling curves on a temperature vs. oxygen fugacity plot for the high temperature and low temperature grains with a gap between 660°C and 530°C and a distinct difference in oxygen fugacity. The highest temperatures

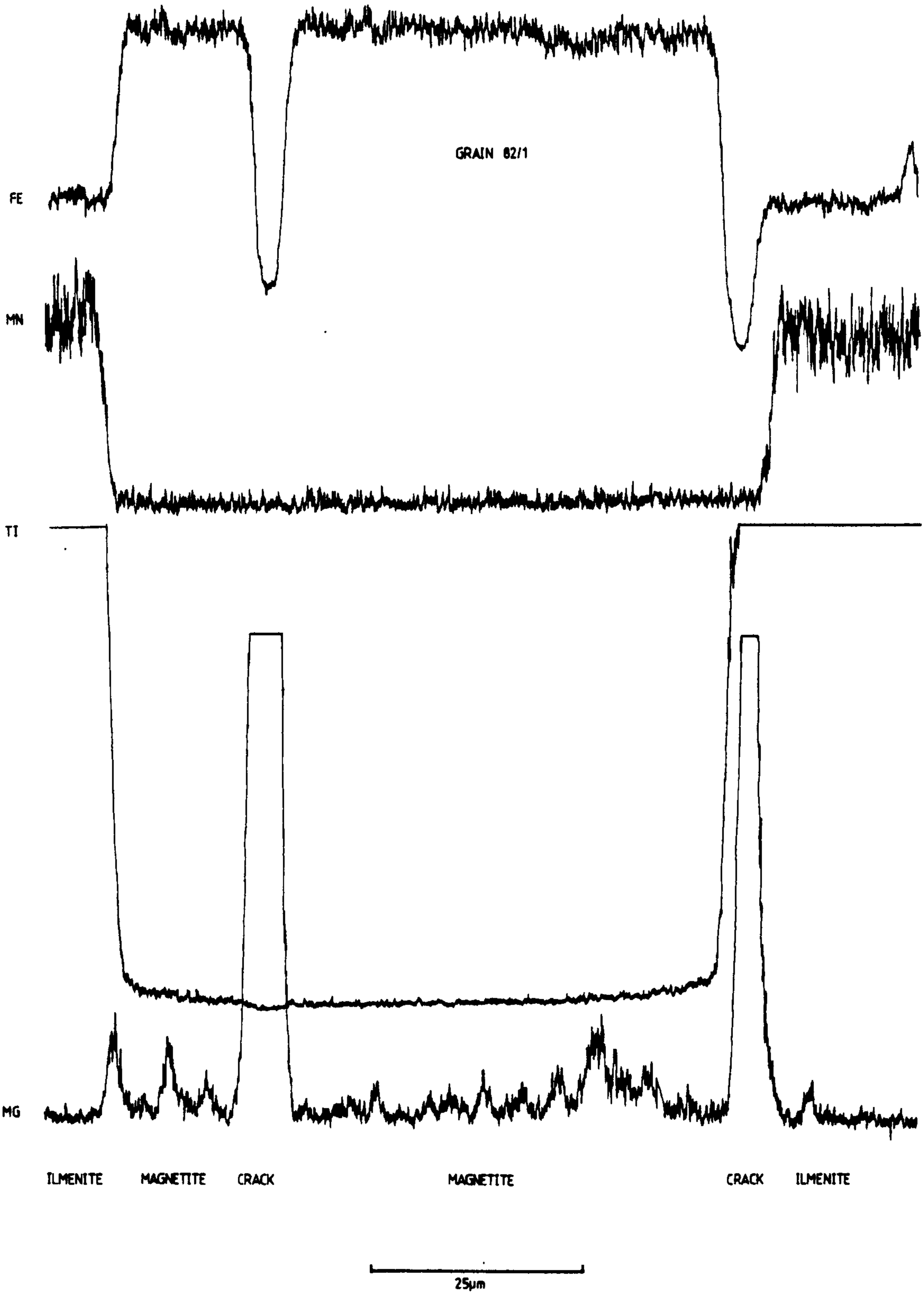

FIGURE 12. Electron probe scans across part of composite ilmenite - magnetite grain HR 82/1 to show high Mg in cracks. Note the high Ti in magnetite close to ilmenite; this zone is too broad to be due entirely to boundary effects.

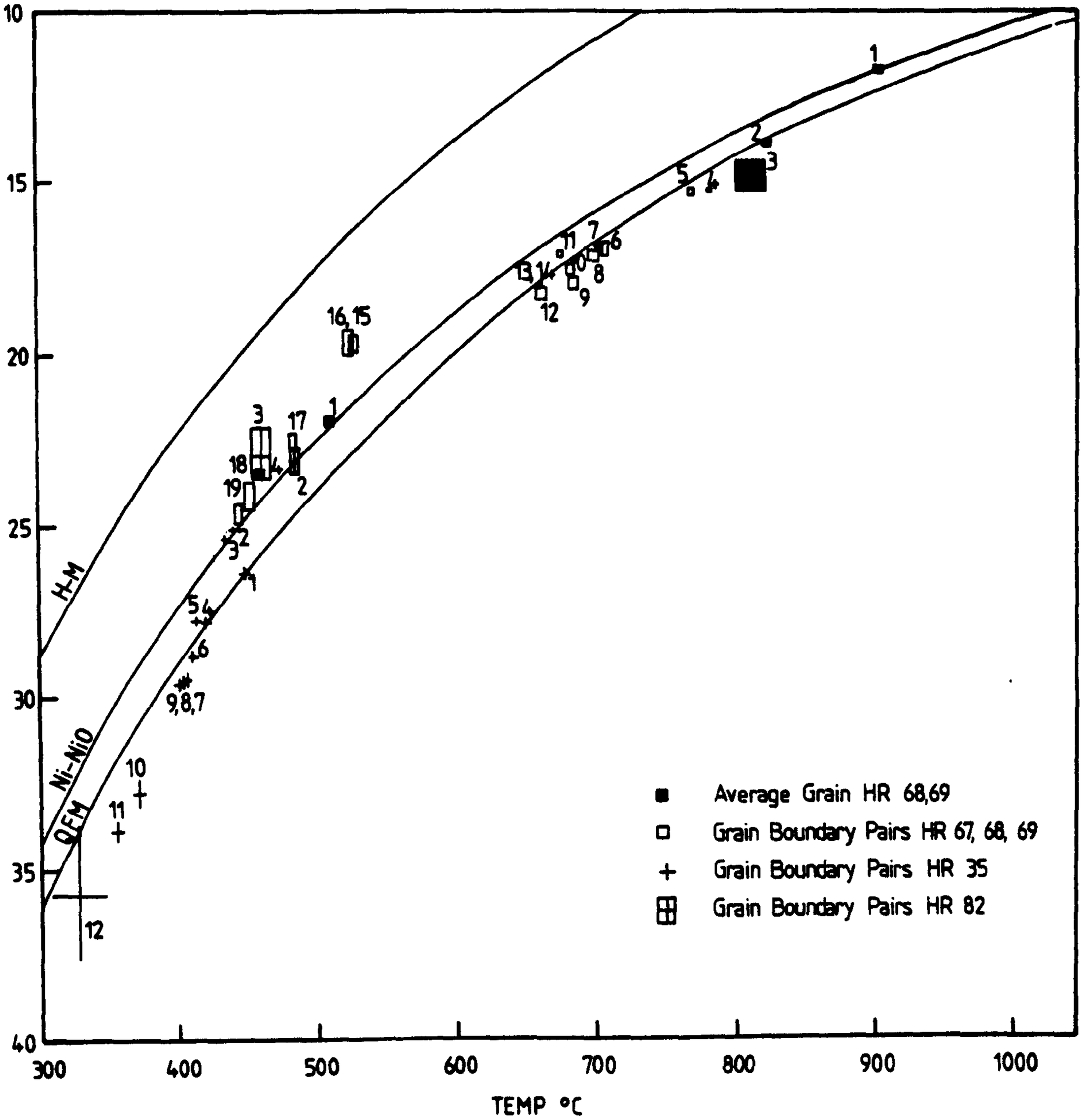

Fig. 13. Oxygen fugacity - temperature cooling curves for iron titanium oxide pairs from Scourian granites. Error bars are for the method of Powell and Powell (1977b); buffer curves are calculated for 8 kb total pressure after Eugster and Wones (1962). Sample numbers refer to analyses in Table 8. H-M haematite-magnetite buffer; Ni-NiO nickel-nickel oxide buffer; QFM quartz, fayalite, magnetite buffer.

were obtained on average grains and fall between 800°C and 910°C; these may be magmatic temperatures since they agree with

postulated magmatic temperatures between 1010°C and 820°C for trondhjemites from the same area (Rollinson, in press) but in view of the high temperatures in hypersolvus granite they may represent subsolidus temperatures. Temperatures between 780°C obtained on pairs of adjacent points across ilmenite-magnetite boundaries represent subsolidus reequilibration of ilmenite and magnetite grains in response to falling temperature. The oxygen fugacity follows a buffered path parallel to the QFM buffer curve recalculated for 8 kb (after Eugster and Wones, 1962).

The low temperature cooling curve represent continued equilibration of ilmenite-magnetite pairs under different oxygen fugacity conditions. Between 660°C and 530°C an event took place which altered the oxygen fugacity of the system. Oxygen fugacity is most likely to be controlled by dissociation of H_2O and CO_2 in these rocks and since carbonate is only a minor phase CO_2 is probably only present in small amounts so that H_2O is probably the controlling factor. The equilibrium constant K for the dissociation of H_2O is given by:

$$K = \frac{f(H_2O)}{f(H_2) . f\ O_2^{\frac{1}{2}}}$$

Since K is a constant dependant only upon temperature (Eugster, 1977) an increase in H_2O at a given temperature will be associated with an increase in O_2. There is good textural evidence in these rocks for the introduction of H_2O into the system from the extreme coarsening of mesoperthite lamellae and the alteration of orthopyroxene to biotite and chlorite. The low temperature curve cuts across oxygen buffer curves and implies that a finite amount of water was injected into the system and that ilmenite-magnetite pairs readjusted their compositions in response to the changing vapour phase and falling temperature and consumed oxygen in order

to regain equilibrium. It is important to bear in mind that the lowest temperature points on Fig. 13 involved considerable extrapolation of the Buddington and Lindsley data (1964).

Sample HR69 contains both high and low temperature oxide grains indicating that the fluid phase can be extremely localised. In general oxide grains yielding high temperatures are either enclosed in quartz grains or are associated with unaltered quartz aggregates. Low temperature grains are associated with sericitised feldspar and fine grained aggregates of quartz.

A dark patch in ilmenite grain 69/1 has the composition FeO 34.57%, TiO_2 54.24%, MnO 9.2%, Al_2O_3 0.13%, MgO 0.03%. This is too rich in titanium to be expressed as either ilmenite-haematite solid solution or as ulvospinel-magnetite solid solution and is probably a mixture of rutile and magnetite. The ilmenite with which this is associated contains 24% R_2O_3 which is mainly Fe_2O_3. The assemblage Fe_2O_3 - ilmenite in the presence of magnetite and rutile yields a minimum temperature of 520°C at an oxygen fugacity of -17.5 from the haematite ilmenite solvus of Lindh (1972). This lies on the continuation of the low temperature curve and is in agreement with the other temperatures and oxygen fugacity conditions determined.

Mechanisms of Equilibration

In the high temperature grains the presence of ilmenite lamellae in magnetite indicates that in response to falling temperatures ulvospinel has reacted to produce ilmenite:

$$6\ Fe_2TiO_4 + O_2 \rightarrow 6\ FeTiO_3 + 2\ Fe_3O_4$$

ulvospinel — ilmenite lamellae — magnetite

and magnetite lamellae in ilmenite form by the reduction of Fe_2O_3:

$$3\ Fe_2O_3 \rightarrow 2\ Fe_3O_4 + \tfrac{1}{2}\ O_2$$

haematite magnetite

The principal compositional difference between high and low temperature grains is the mole % of ulvospinel in magnetite; in high temperature grains it is greater than 20% and in low temperature grains it is 7% or less. In comparison the mole fraction of R_2O_3 in ilmenite is about the same in both high and low temperature grains. This suggests that in response to increase oxygen fugacity ulvospinel reacted to produce ilmenite and magnetite:

$$6\ Fe_2TiO_4 + O_2 \rightarrow 6\ FeTiO_3 + 2\ Fe_3O_4$$

ulvospinel ilmenite magnetite

This agrees well with the increased amount of ilmenite in composite ilmenite-magnetite intergrowths in low temperature grains.

At low temperatures reequilibration continues on a localised scale to produce zoning as discussed above. The increase in ulvospinel in magnetite close to ilmenite and the associated decrease in R_2O_3 in the ilmenite suggests the reaction:

$$2\ Fe_2O_3 + 4\ FeTiO_3 \rightarrow 4\ Fe_2TiO_4 + O_2$$

haematite ilmenite ulvospinel

in a restricted zone, which in HR 82/1 is not greater than 15 μm (Fig. 11). This is broader than any apparent zonation produced

by boundary effects between ilmenite and magnetite. The reduction in R_2O_3 and ulvospinel towards the edge of a grain may imply some loss of Fe and Ti to silicates, but may also mean that the reaction:

$$Fe_2TiO_4 + Fe_2O_3 \rightarrow Fe_3O_4 + FeTiO_3$$

ulvospinel haematite magnetite ilmenite

procedes. This reaction is temperature sensitive and may imply a gradient across the grain.

12. DISCUSSION

Feldspar and oxide temperatures are extremely variable and may be summarised as follows:-

Feldspars

1) mesoperthite feldspars in hypersolvus granites appear to indicate extremely high equilibration temperatures of the order of 1100 - 1150°C.
2) most feldspars (mesoperthites and plagioclase pairs) equilibrated at about 650°C
3) perthite lamellae in alkali feldspar equilibrated in the range 470 - 550°C.

Fe-Ti oxides

1) high temperatures of 800 - 910°C are recorded and these are comparable with those in excess of 1000°C for trondhjemites at Badcall Bay.
2) subsolidus cooling in a buffered system occurred between 800 and 660°C
3) water was introduced into the system in the temperature interval 660 - 530°C which increased the oxygen fugacity
4) reequilibration in response to falling temperature and

higher oxygen fugacity in the range 530 - 320°C.

A comparison of feldspar and oxide temperatures from quartzofeldspathic granulites was made by Bohlen and Essene (1977) in their study of the Adirondack highlands. They found that there was an excellent agreement between temperatures obtained from the Fe-Ti oxide thermometer of Buddington and Lindsley (1964) and Stormer's (1975) two feldspar thermometer, although their temperatures (790 - 610°C) do not necessarily represent the peak of metamorphism. The similar and opposite effects of the alkali feldspar structural state (microcline) and Ca in alkali feldspar on the equilibration temperature mean that a revision of the feldspar temperatures after Whitney and Stormer (1977b) and Powell and Powell (1977a) will yield similar results to those presented. Stormer and Whitney (1977) have calculated metamorphic temperatures in quartzo-feldspathic granulites from Salvador B.A., Brazil. Feldspar temperatures are in the range 915 - 480°C if they are ordered and 750-440°C if they are disordered; the preferred temperature is 750°C and this is taken as a minimum value for the peak of metamorphism. Two pyroxene temperatures are higher (760 - 900°C) and are thought to be 100°C too high. Iron titanium oxides give very low temperatures in these rocks.

Interpretation of oxide temperatures

Several mechanisms are suggested above to explain the variety of oxide temperatures in terms of continued equilibration between ilmenite and magnetite in a buffered system. A few chemical reactions can be written which proceding backwards or forwards on a variety of scales are sufficient to explain the response of oxide pairs to changing equilibrium conditions. Since oxygen is involved in most of these reactions their "frozen in"

temperature may reflect the availability of oxygen or more likely hydrogen since it is more mobile and dependant upon oxygen fugacity.

Interpretation of feldspar temperatures

Most mesoperthite - plagioclase temperatures are extremely low compared with the initial high temperature at which these rocks formed. This is interpreted as due to the exchange of albite (and minor anorthite) between alkali feldspar and plagioclase. There are several lines of evidence which point to this:

1) there is a wide variation in mole fraction of albite in alkali feldspar bulk composition from the albitic alkali feldspar in one feldspar granites, through mesoperthites to the more orthoclase rich perthites in the Loch an Daimh Mor granite (Fig. 4).

2) in the Loch an Daimh Mor granite sheet rare orthoclase is strongly perthitic (Fig. 5b) (almost a mesoperthite), whereas microcline (later) varies from perthitic to virtually non-perthitic.

3) irregular grain boundaries imply recrystallisation in most of the granite sheets.

Alkali feldspars in rocks containing no plagioclase would not lose albite and so have retained their original bulk composition. The close correspondence between the temperature at which mesoperthite and plagioclase equilibrated and the temperature at which a fluid was introduced into the system is probably meaningful and reflects the closure temperature of this exchange reaction, further equilibration only taking place within mesoperthite grains.

High temperatures in the Scourian Complex

A high temperature origin ca. 1000 - 1150°C for these granite sheets is similar to that proposed by O'Hara (1978) for the metamorphism of the Scourian complex. In view of the igneous origin of the granite sheets the temperatures are regarded as the temperature of emplacement into the complex as a melt. Such high temperatures are permissible for melts of granite to granodiorite compositions that are low in H_2O. At the high pressures at which the rocks formed the distinction between igneous and metamorphic events is blurred. However, since the granite and trondhjemite sheets show sharp intrusive contacts with the enclosing tonalitic gneiss and no evidence of remelting close to the margins, this implies that the tonalites must be extremely refractory. Trace element chemistry of the granite and parental trondhjemites precludes their derivation from the tonalites by partial melting.

The role of water during cooling of the complex

The introduction of water into Scourian granites during cooling has had an important effect upon the oxide, feldspar and ferromagnesian mineral chemistry. Oxides have equilibrated down to very low temperatures; feldspars to higher temperatures and a wide variety of textures; ferromagnesian minerals are generally partially or totally altered to hydrous silicates. Furthermore (Rollinson, Chap. 1 .) the presence of water has affected the trace element concentration on the scale of 10's of cm and reset the radiometric clocks in these granites.

Chapter 6

CONTROLS ON THE PARTITIONING OF Mn INTO ILMENITE IN THE SCOURIE GRANULITES

SUMMARY

The partitioning of Mn into ilmenite is discussed in the light of observed exchange reactions between Fe and Mn, Mg and Mn in ilmenite and the distribution of Mn between ilmenite and magnetite in Scourian granulite facies rocks, which vary in composition from ultramafic to granitic.

Mn replaces Mg in ilmenite in granulite facies gneisses of intermediate composition at low temperature in the presence of a hydrous fluid phase. Mn replaces Fe and is unusually enriched in ilmenite in granodiorite and trondhjemite either by reaction with orthopyroxene in the melt or during high temperature subsolidus exsolution of titanomagnetite. In ultrabasic rocks Mn increases in ilmenite with increasing Fe due to the formation of ilmenite from ulvospinel during cooling.

The distribution of Mn between ilmenite and magnetite shows two trends which reflect two stages in the equilibration of ilmenite and magnetite, exsolved from an originally homogeneous titanomagnetite, and shows the increased preference of Mn for ilmenite at low temperatures.

1. INTRODUCTION

In a series of studies on coexisting ilmenite and magnetite in granulite facies tonalites, trondhjemites and granodiorites (see Chapters 4, 5 and 7), ilmenite and magnetite grains were routinely analysed for the elements Fe, Ti, Mn, Mg, Al, Cr and sometimes Ca and Si. The concentrations of the minor elements Mg, Al, Cr, Si and Ca are low in ilmenite and magnetite, and as predicted by crystal chemistry, Al and Cr are concentrated in magnetite and Mn and Mg in ilmenite. Manganese is the only minor element which is present in significant amounts (up to 8.6 wt % in ilmenite) and was found to show a number of interesting relationships with other elements in the ilmenite lattice, which are used to place constraints on the partitioning of Mn into ilmenite.

The rocks used in this study vary in composition from ultramafic to granitic and analyses for coexisting ilmenite - magnetite pairs are given in Chapters 4, 5 and 7 and additional data are presented in Table 1.

Ilmenite is a rhombohedral mineral with two equivalent octahedral sites ordered into like-atom layers; substitutions for Fe^{2+} and Ti^{4+} in the ilmenite lattice are controlled by the constraints of ionic radius and charge balance. The divalent ions Mn and Mg substitute for Fe^{2+}, and Fe^{3+}-Fe^{3+} forms a coupled substitution for Fe^{2+}-Ti^{4+} in ilmenite-haematite solid solutions. Under highly oxidising conditions it is possible that the smaller Mn^{3+} ion, with the same ionic radius as Fe^{3+}, replaces Fe^{3+} in ilmenite-haematite solid solutions. The ionic radii used in this study are those of Whitaker and Muntus (1970) for octahedrally-coordinated cations in the high-spin state.

2. Mn - Mg EXCHANGE IN ILMENITE

There is an inverse correlation between Mn and Mg in ilmenite in granulite facies gneisses of intermediate composition from the Scourie area (Fig. 1). In sample HR 72 (banded tonalitic

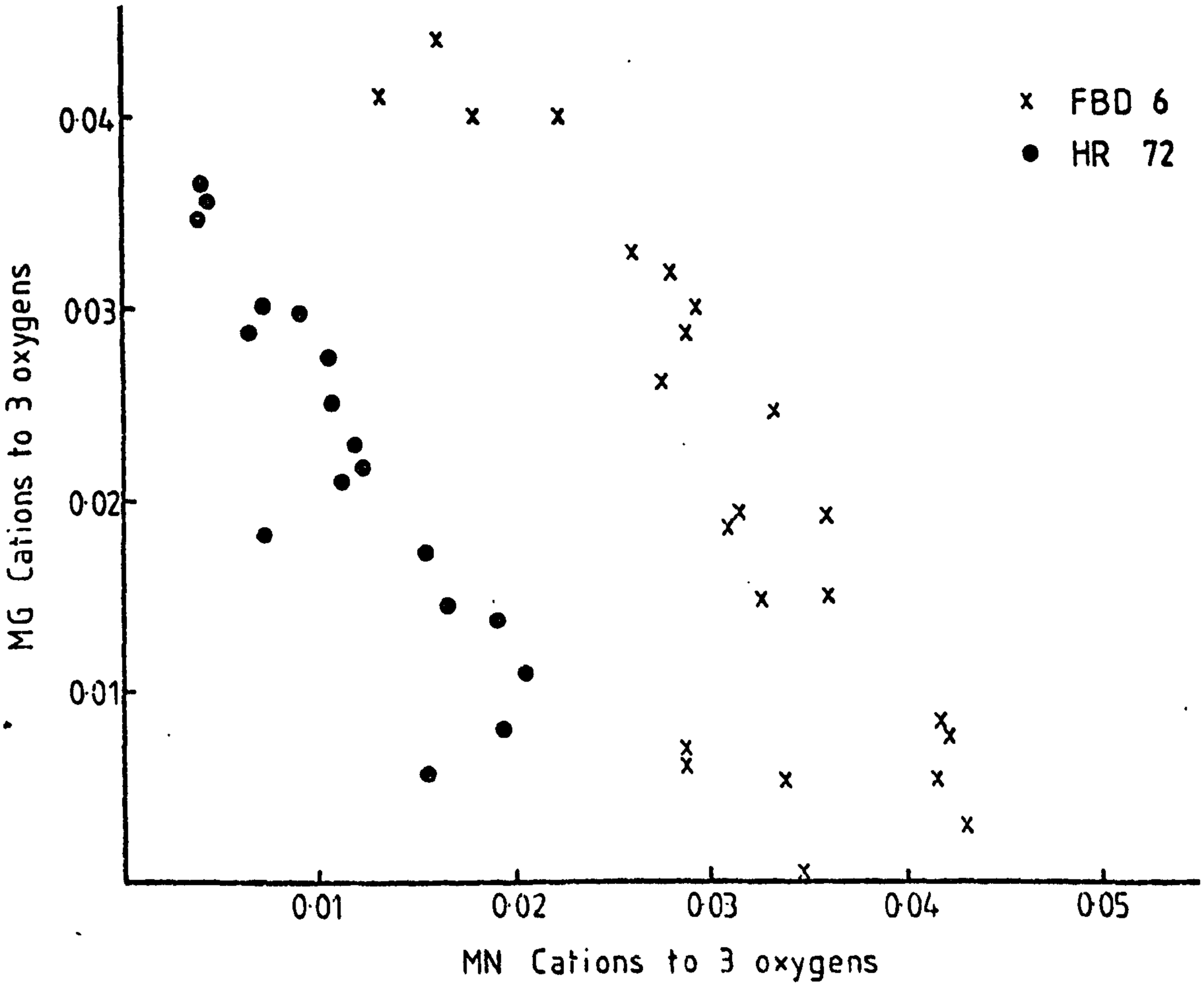

Fig. 1. Plot of Mn vs. Mg (cations to 3 oxygens) in ilmenite in samples HR 72 (tonalitic gneiss) and FBD 6 (calc-silicate rock).

gneiss) ilmenite and magnetite form lamellar intergrowths and coexist with orthopyroxene; in sample FBD 6 (a calc-silicate rock enclosed in tonalitic gneiss) ilmenite and magnetite form both lamellar and granular intergrowths and coexist with clinopyroxene. Five composite grains were studied and in every case except one the ilmenite lamellae are zoned with respect to Mn and Mg and have Mg-rich cores and Mn-rich rims. (The one composite grain that does not fit into this pattern is unusual in that it is predominantly

ilmenite). Ilmenite coexisting with clinopyroxene in the more Mg-rich rock FBD 6 contains more (Mg + Mn) than ilmenite coexisting with orthopyroxene in HR 72. The equilibration temperatures for the ilmenite-magnetite pairs on the Buddington and Lindsley (1964) thermometer are between 470 and 560°C in HR 72 and 430 and 512°C in FBD 6.

Anderson et al. (1972) suggested that the amount of Mg, substituting for Fe in ilmenite coexisting with pyroxene is dependent upon temperature. This was confirmed in an experimental study by Bishop (pers. comm.) who calibrated the exchange reactions for Fe and Mg between ilmenite and clinopyroxene, ilmenite and orthopyroxene and ilmenite and olivine. Silicate-ilmenite temperatures for the Mg-rich cores of the ilmenite grains yield slightly lower temperatures than the Buddington and Lindsley (1964) method.

Recent calorimetric work on ortho- and clinopyroxenes and olivines by Navrotsky (1978) suggests that Mg-Mn and Fe-Mn exchange reactions are less temperature-sensitive than Mg-Fe reactions between ilmenite and silicates.

The experimental study of Bishop suggests that during granulite facies metamorphism Mg was partitioned from pyroxene into ilmenite and that during cooling Mg was replaced in ilmenite by Fe and that the Mg/Fe ratio is a function of temperature and the composition of the coexisting phases; ilmenite-silicate temperatures suggest that the Fe-Mg exchange reactions closed at about 500°C. At lower temperatures Mn entered the ilmenite structure in preference to Mg and Fe and the data of Navrotsky (1978) suggest that this was controlled by factors other than temperature, since Mn-Mg and Mn-Fe exchange reactions are not very sensitive to temperature.

Mn is a larger ion than Mg^{2+} and Fe^{2+} and cannot be preferentially accepted into ilmenite on the basis of its size; similarly its crystal field stabilisation energy (CFSE) is the same as Mg (zero) and less than Fe^{2+} in an octahedral site and therefore it cannot be preferentially accommodated on the basis of its CFSE. Mn^{2+} does, however, form a hydrated ion more readily than Fe^{2+} and during retrogression of granulite facies rocks at low temperature in the presence of a hydrous fluid phase Mn^{2+} could replace Mg in ilmenite.

A discontinuity in the temperature-oxygen fugacity curve for ilmenites and magnetites in Scourian granodiorites indicates that water was introduced into the rocks between 660°C and 530°C (see Chapter 5). By analogy with sedimentary systems the Eh and pH of the fluid are the prime controls on the mobility of Mn^{2+} in metamorphic solutions and this in turn is a function of the amount of sulphide ion and CO_2 present.

In summary therefore, Mn replaces Mg in ilmenite (i) at low temperatures, probably less than 500°C, (ii) when there is a source of Mn (in coexisting silicate or magnetite) and (iii) in the presence of a hydrous fluid phase.

3. Fe - Mn EXCHANGE IN ILMENITE

Two different types of Fe-Mn exchange reactions are observed in ilmenites in the Scourie granulites.

(a) Fe-Mn exchange in trondhjemite and granodiorite. In trondhjemite and granodiorite there is up to 8.6 wt % MnO in ilmenite and there is an inverse correlation between MnO and FeO (Fig. 2a) indicating that Mn^{2+} replaces Fe^{2+} in ilmenite. A homogeneous granodiorite sheet on the Shios peninsula, Scourie More (Chapter 1, Fig. 5) with a uniform MnO content contains ilmenite grains which vary in their MnO content from 8.6 wt % (HR 69) to 0.8 wt % (HR 68) and yet the

FIGURE 2. (a) Plot of MnO (wt%) vs FeO (wt %) in ilmenite in trondhjemite and granodiorite from Scourie compared with the trend for granite to monzonite in Czamanske and Mihalik (1972). Open and filled circles represent the measured composition of the ilmenite grains; crosses represent estimated compositions prior to exsolution obtained by scanning the whole lamella with the electron probe. (b) Plot of MnO vs FeO in ilmenite in ultrabasic rock HR 42B compared with the trend of Duchesne (1972). Note the change of scale from (a).
(c) TiO_2 vs MnO in ilmenite in ultrabasic rock HR 42B. (d) Fe_2O_3 vs MnO in ilmenite in ultrabasic rock HR 42B.

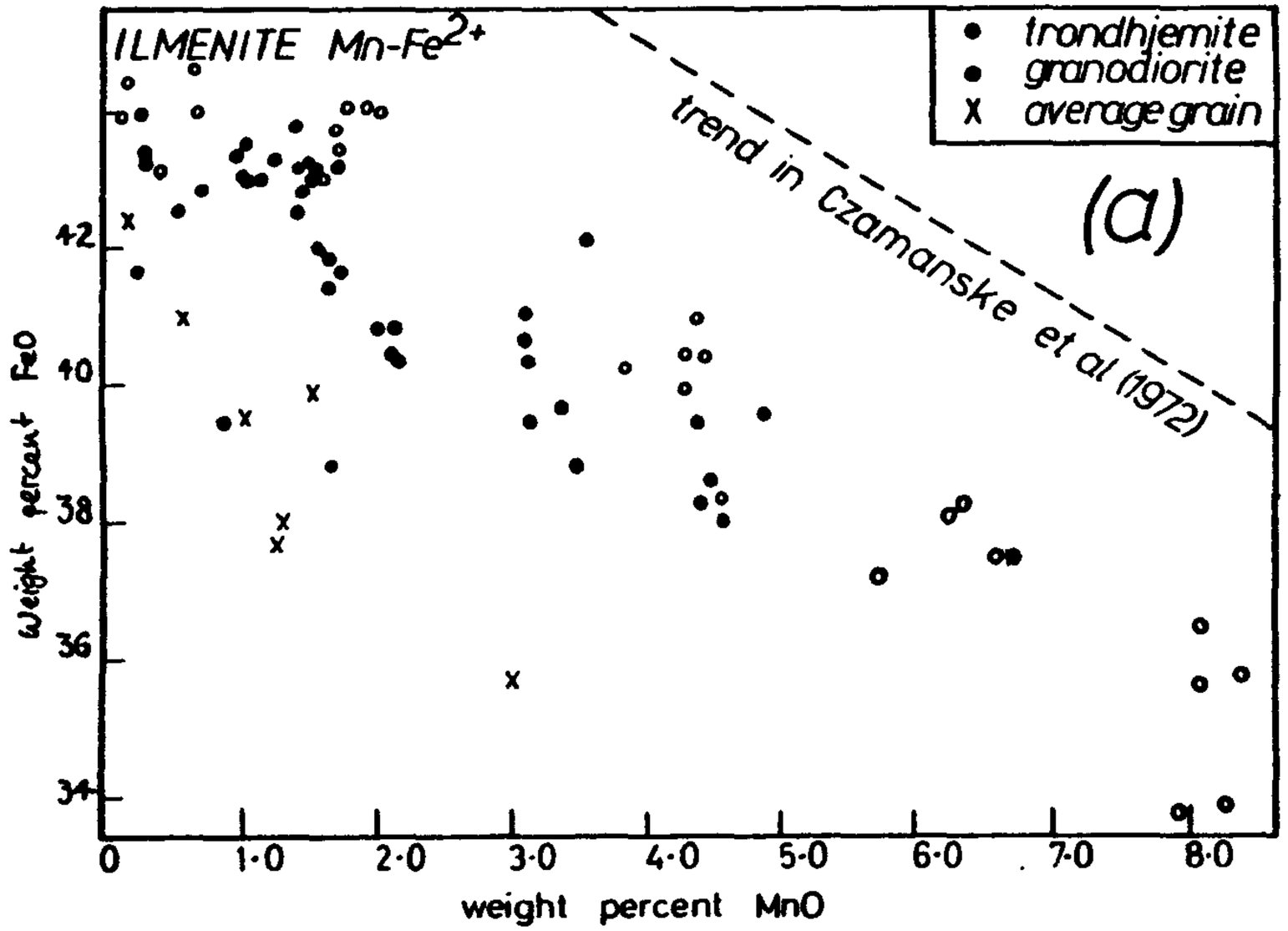
ILMENITE Mn-Fe2+
trondhjemite
granodiorite
average grain
trend in Czamanske et al (1972)
(a)
weight percent FeO
42
40
38
36
34
0
1·0
2·0
3·0
4·0
5·0
6·0
7·0
8·0
weight percent MnO

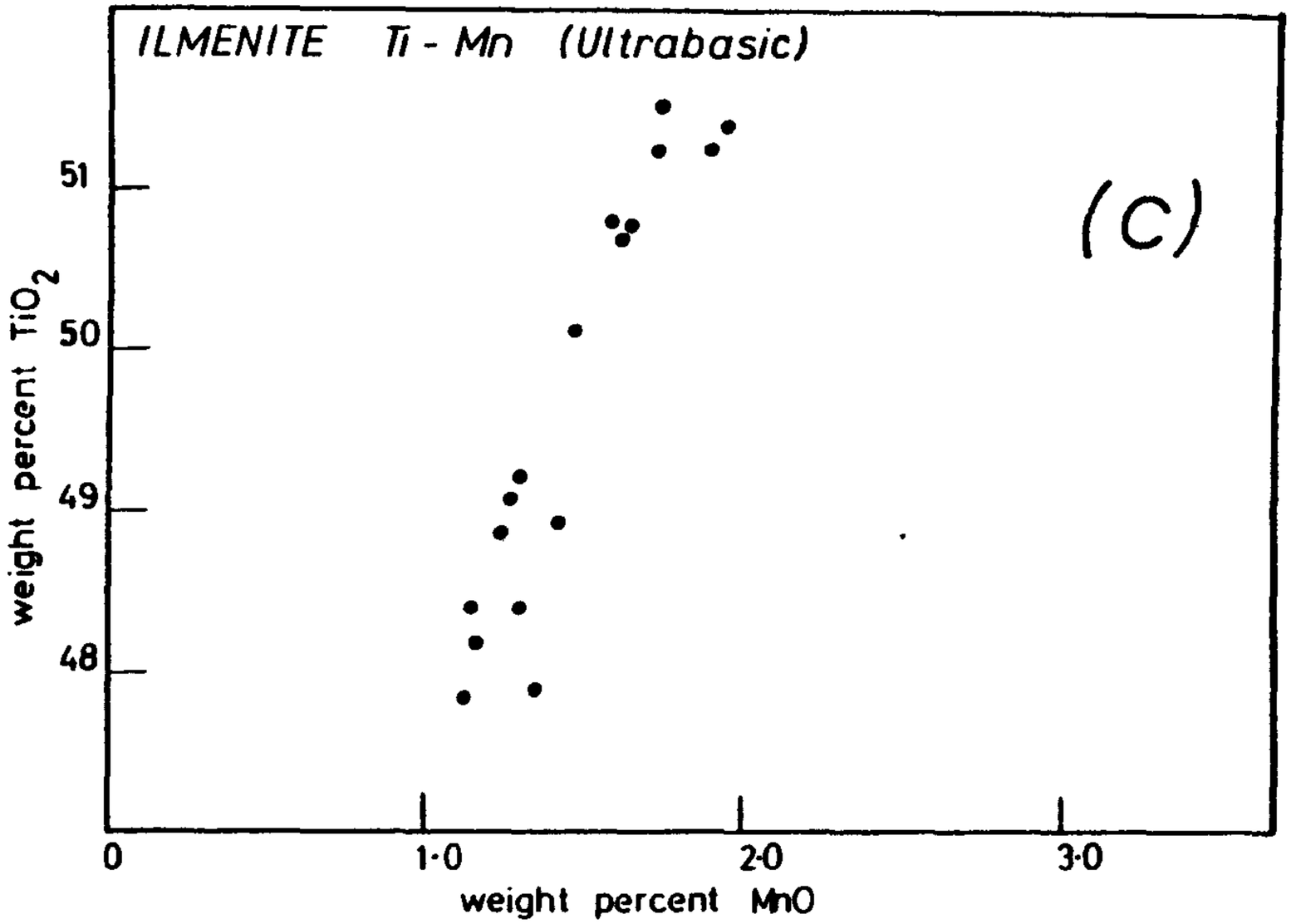
ILMENITE Ti - Mn (Ultrabasic)
(c)
weight percent TiO2
51
50
49
48
0
1·0
2·0
3·0
weight percent MnO

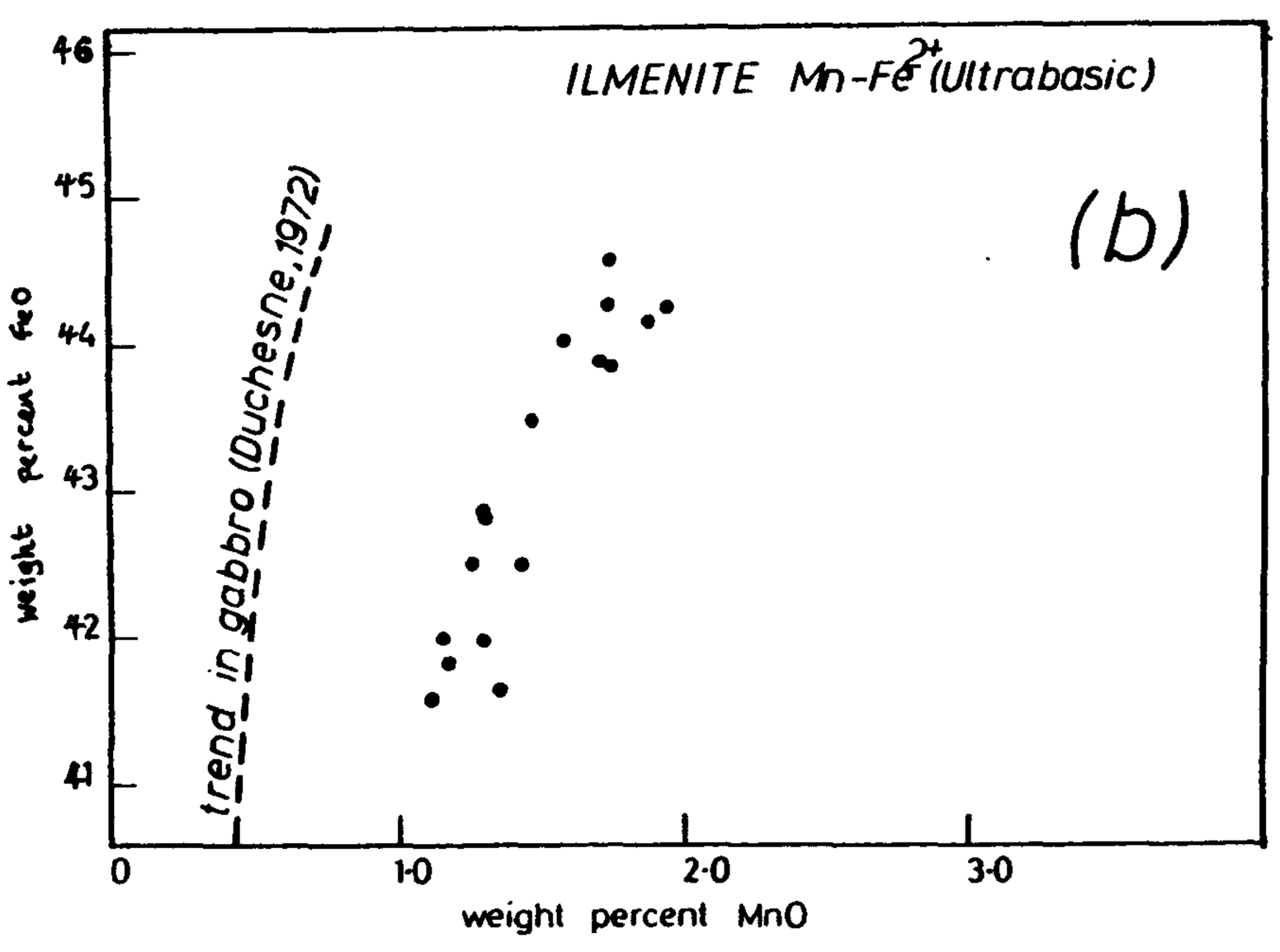
ILMENITE Mn-Fe2+ (Ultrabasic)
(b)
trend in gabbro (Duchesne, 1972)
weight percent FeO
46
45
44
43
42
41
0
1·0
2·0
3·0
weight percent MnO

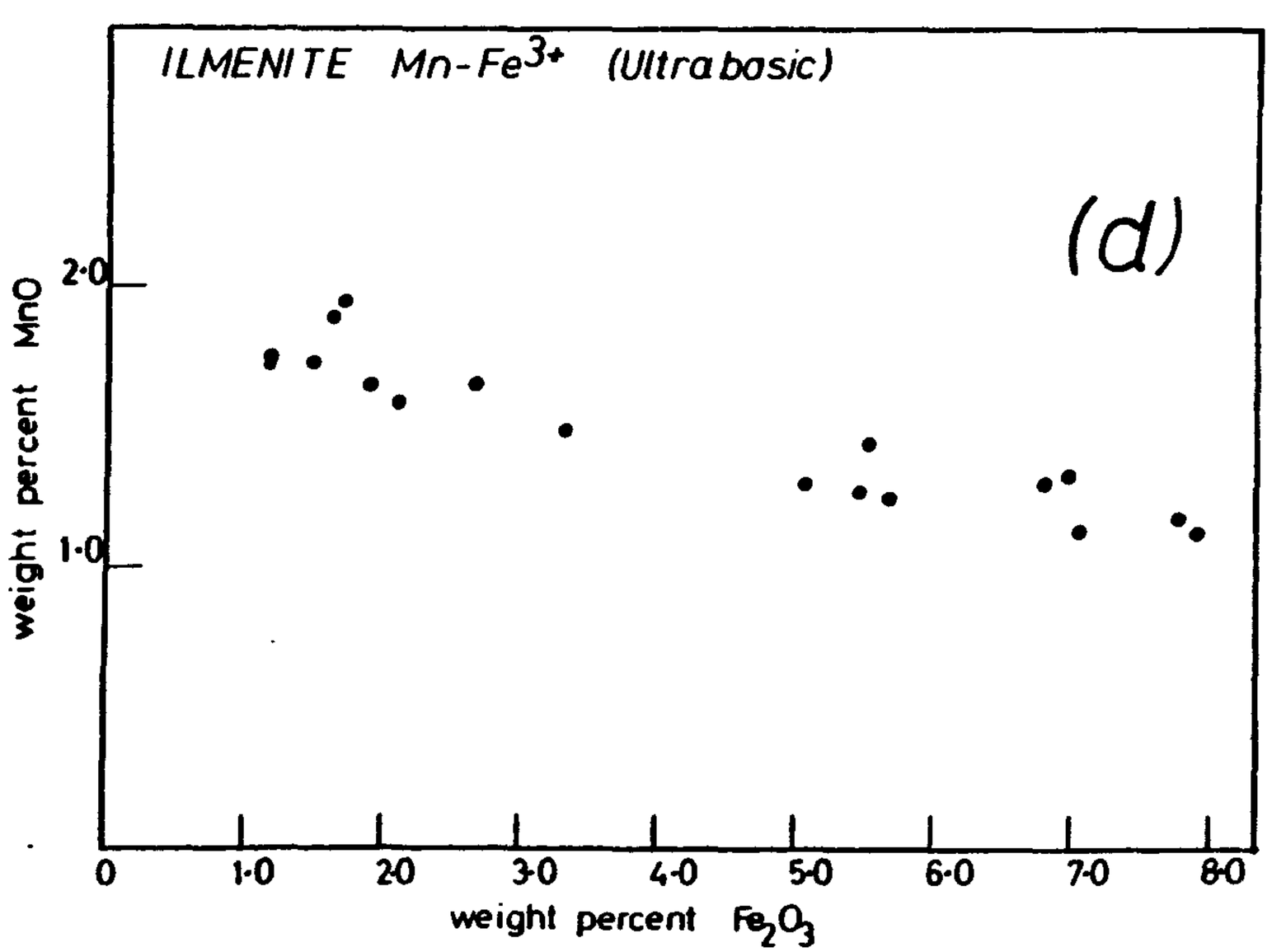
ILMENITE Mn-Fe3+ (Ultrabasic)
(d)
weight percent MnO
2·0
1·0
0
1·0
2·0
3·0
4·0
5·0
6·0
7·0
8·0
weight percent Fe2O3

two samples were collected within two meters of each other from the centre of the granodiorite sheet. Czamanske and Mihalik (1972) described Mn-rich ilmenites containing up to 30 wt % MnO from monzonitic to granitic units in the Finnmarka complex, Norway and found that in the granodiorite unit the ilmenite grains varied in MnO content from 10.8 to 19.5 wt %. They ascribed the Mn enrichment in ilmenite to the preferential oxidation of Fe^{2+} to Mn^{2+} in ilmenite during the alteration of ilmenite to rutile and sphene. Sphene and rutile are not commonly associated with ilmenite in the Scourie rocks and this mechanism is not applicable.

The heterogeneity of ilmenite grains in granodiorite is a function of localised reactions either subsolidus or between ilmenite and the melt. Several lines of evidence suggest that ilmenite was enriched in Mn at high temperatures; (i) ilmenite and magnetite in grain 69/2 (see Chapter 5) equilibrated at a high temperature (ca. 820°C), is enclosed in relatively unaltered feldspar and quartz and the ilmenite has a high MnO content (6.75 wt %), (ii) Unlike the Mg-Mn exchange reactions discussed above where Mg and Mn are mobile in a fluid at low temperatures, Fe^{2+} is not likely to be mobile in a fluid phase at low temperatures and so Fe-Mn exchange is not likely to be a function of low temperature exchange with silicates.

(b) <u>Fe-Mn exchange in an ultrabasic rock</u>. Ilmenite in an ultrabasic rock from Badcall (HR 42) shows a <u>positive</u> correlation between FeO and MnO (Fig. 2b) in contrast to the granodiorites and trondhjemites suggesting that Mn <u>follows</u> Fe into the ilmenite structure rather than replaces it; a similar trend was described by Duchesne (1972) for ilmenites in the Bjerkrem - Sogndal anorthosite-norite-mangerite body in S.W. Norway. MnO also correlates positively with TiO_2 and inversely with Fe_2O_3 (Figs. 2c and 2d) suggesting that Mn is partitioned into ilmenite from magnetite by reactions 1A and 1B

occurring together:

$$FeMnTiO_4 + Fe_2O_3 = MnTiO_3 + Fe_3O_4 \quad (1A)$$

$$Fe_2TiO_4 + Fe_2O_3 = FeTiO_3 + Fe_3O_4 \quad (1B)$$

these reactions proceed to the right with decreasing temperature.

The difference between processes (a) and (b) above is mainly a function of scale; process (b) probably operates in granodiorites and trondhjemites and accounts for the scatter in Fig. 2a but is secondary to the processes discussed below.

The enrichment of Mn in ilmenite in granodiorites and trondhjemites is not fully understood but a number of inferences can be made:

1) Mn enrichment in ilmenite is only found in acid igneous rocks (Czamanske and Mihalik, 1972; Snetsinger, 1969; Lipman, 1971) in contrast to ilmenite in basic igneous rocks which is Mg-rich (Thompson, 1976). This suggests that the composition of the melt plays an important part in controlling the distribution coefficient for Mn and Mg between ilmenite and melt.

2) Mn is not always enriched in ilmenite in acid igneous rocks.

3) The data of Carmichael (1967) for ilmenite-magnetite phenocrysts coexisting with a wide variety of silicate phenocrysts, in acid lavas quenched in the restricted temperature range 1025 - 790°C show that the Mg/Mn ratio in ilmenite is extremely variable and suggests that temperature and rock composition are not the prime controls in the positioning of Mn into ilmenite and that the coexisting solid phases are also important. A similar conclusion was reached by Thompson (1976) in an experimental study of ilmenite in tholeiitic andesite.

4) Ilmenite-magnetite pairs initially crystallised from the melt as a homogeneous titanomagnetite grain and the important distribution coefficients are for Mn between titanomagnetite and melts of

different compositions; these are not known.

There are two possible mechanisms for producing the observed enrichment of Mn in ilmenite and the heterogeneity of ilmenite grains in the Scourie rocks, neither of which is entirely satisfactory. Firstly, ilmenite was enriched in Mn by means of exchange reactions with orthopyroxene in isolated pockets of melt at a late stage in the crystallisation of the granodiorite and the heterogeneity of the ilmenite depends upon whether or not pyroxene was present in the pocket of melt. It does not explain, however, why Mn and not Mg was partitioned into ilmenite in view of the known temperature dependance of Mg and Fe partitioning between ilmenite and orthopyroxene. A second mechanism is the subsolidus partitioning of Mn from magnetite into ilmenite during the exsolution of ilmenite from titanomagnetite; the variable Mn content of ilmenite is a function of the Ti content of the titanomagnetites. If, for example, titanomagnetite with a small amount of Ti and a moderate amount of Mn exsolved into ilmenite and magnetite the Mn would be partitioned into the small amount of ilmenite formed and would give rise to a Mn-rich ilmenite. A Ti-rich titanomagnetite, however, containing the same amount of Mn would exsolve more ilmenite and so the ilmenite would not be so strongly enriched in Mn. This, however, implies that titanomagnetites with variable Ti contents crystallised from the same magma, which is unlikely, and furthermore the ratio of ilmenite to magnetite in the Mn-rich and Mn-poor composite ilmenite-magnetite grains is approximately the same.

4. THE DISTRIBUTION OF MnO BETWEEN ILMENITE AND MAGNETITE

There are two trends for the distribution of MnO between ilmenite and magnetite (Fig. 3):

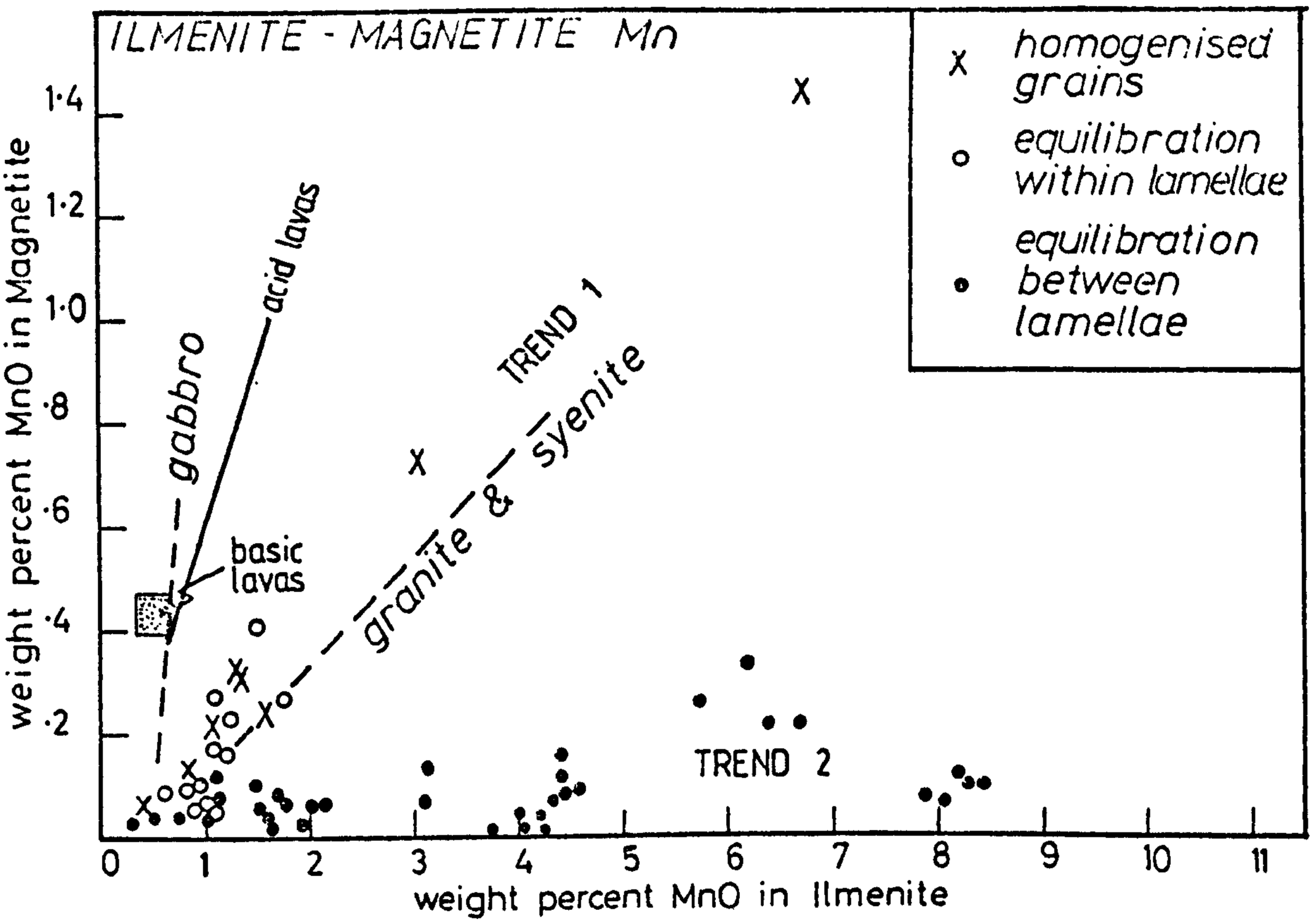

Fig. 3. The distribution of MnO between coexisting ilmenite and magnetite in Scourie granulites, compared with trends for gabbro and granite and syenite, identified by Buddington and Lindsley (1964) and in basic lavas (stippled area) after Anderson (1968) and in acid lavas (Heavy line) after Carmichael (1967). An explanation of the symbols used is given in the text and amplified in Chapter 4.

Trend 1 (Fig. 3) shows moderate enrichment of Mn in magnetite with increasing Mn in ilmenite and is defined by high temperature ilmenite-magnetite lamellae (homogenised grains, Fig. 3) whose compositions were determined by averaging the composition of host and small exsolution lamellae within wide lamellae in composite ilmenite-magnetite grains, and also defined by ilmenite-magnetite pairs where ilmenite forms small lamellae in wider magnetite lamellae and vice versa. Trend 1 is close to the trend outlined by granites and syenites in the study of Buddington and Lindsley (1964).

Trend 2 (Fig. 3) shows marked enrichment of Mn in ilmenite with little or no enrichment in magnetite and is defined by ilmenite-magnetite pairs close to the boundaries between broad lamellae.

Buddington and Lindsley (1964) studied the distribution of MnO between ilmenite and magnetite and found that gabbros and associated ores, granites and syenites and metamorphic rocks defined three different trends and they proposed that the main factor controlling the distribution of Mn between ilmenite and magnetite is temperature. This view was favoured by Dasgupta (1970) (in spite of his data which showed the contrary) and Duchesne (1972) who showed that the distribution of Mn between ilmenite and magnetite is strongly dependent upon the equilibration temperature of the oxide pair but that the temperature dependence is reduced at high temperatures (greater than 800°C). Steele et al. (1977) pointed out that the distribution of Mn between ilmenite and magnetite is not a simple indicator of temperature and that a correction for Cr in magnetite is necessary in Cr-rich magnetites (greater than 10% Cr).

There are three different mechanisms which control the apparent distribution of Mn between ilmenite and magnetite:

1) Mineral-melt distribution coefficients. Data from Carmichael (1967) and Anderson (1968) for coexisting ilmenite and magnetite pairs in acid and basic lavas, and which show magmatic equilibration temperatures (790 - 1160°C) are assumed to have minor element concentrations which are primarily a function of mineral-melt distribution coefficients. The concentrations of Mn in ilmenite-magnetite pairs in acid and basic lavas are plotted in Fig. 3. and lie close to each other and to the trend for gabbros defined by Buddington and Lindsley (1964). Irving (1978) quotes a value

of 1.7 - 1.8 for the distribution coefficient for Mn between magnetite and a basaltic liquid. Coupled with the data from Fig. 3 this suggests that in basic liquids the distribution coefficient, based on the mole fraction of Mn in the mineral and melt, is greater for ilmenite than magnetite in basic liquids (because the atomic weight of ilmenite is less than magnetite and they both contain similar amounts of MnO) and that the ratio of the distribution coefficients in acid melts is the same as in basic melts. There is, however, no information for distribution coefficients for Mn between titanomagnetite and melt.

2) Subsolidus exchange reaction between ilmenite and magnetite.

There is a positive correlation between Mn and Ti in magnetites (Duchesne, 1972; Prevot and Mergoil, 1973; Carmichael, 1967; this study, Fig. 4) indicating that Mn is in the ulvospinel

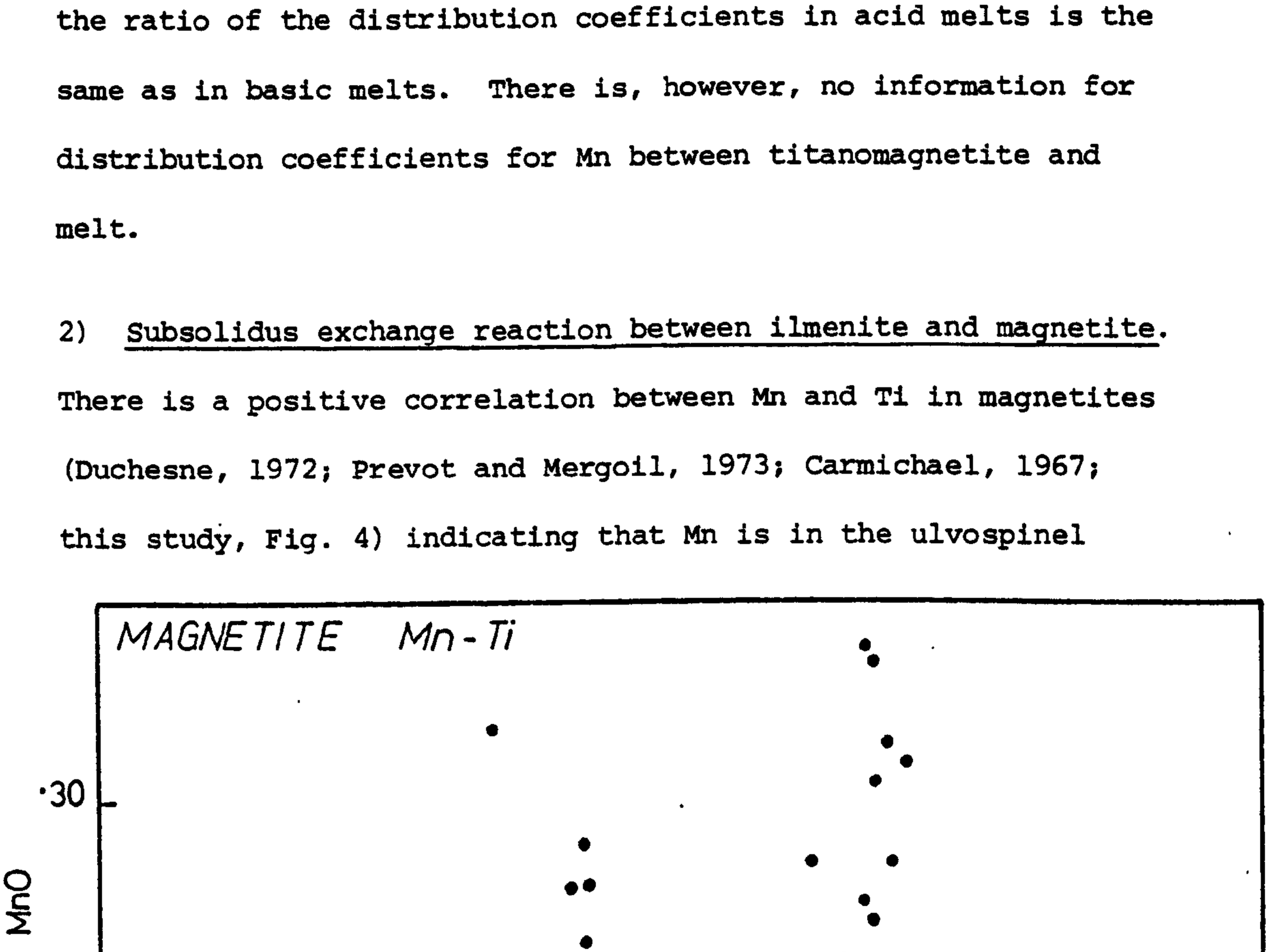

Fig. 4. Plot of MnO (wt %) vs. TiO_2 (wt %) in magnetite in Scourie granulites.

component in titanomagnetite solid solutions. This suggests that Mn is partitioned between ilmenite and magnetite by reactions (1A) above and (2) below:

$$6FeMnTiO_4 + O_2 = 6MnTiO_3 + 2Fe_3O_4 \qquad (2)$$

and is a function of temperature, fO_2 and the composition of the coexisting ilmenite and magnetite solid solutions, and not simply a function of temperature as discussed above.

3) Subsolidus exchange reactions between ilmenite and silicates.

It was shown above that Mn preferentially enters ilmenite from silicate phases during some low temperature subsolidus reactions. This may produce spuriously high, apparent-distribution coefficients for Mn between ilmenite and magnetite.

The data from Carmichael (1967) and Anderson (1968) in Fig. 3 indicate that the distribution of Mn between ilmenite and magnetite in the Scourian rocks is not a function of Mineral-melt equilibria but reflects subsolidus equilibria between ilmenite and magnetite.

The partition of Mn between ilmenite and magnetite is interpreted in terms of a three-stage model (Fig. 5):

I. Mn enters titanomagnetite from the melt.

II. Titanomagnetite exsolves ilmenite and Mn enters ilmenite in preference to magnetite.

III. Magnetite and ilmenite exsolve small lamellae of ilmenite and magnetite, respectively and Mn enters ilmenite in preference to magnetite.

Stages II and III are represented in the Scourian rocks by trends 1 and 2 respectively described above (Fig. 3) which reflect the increased preference of Mn for ilmenite at lower temperatures (cf. Pinkney and Lindsley, 1976), confirming the suggestion of Buddington and Lindsley, 1964, that

temperature is the main factor controlling the distribution of

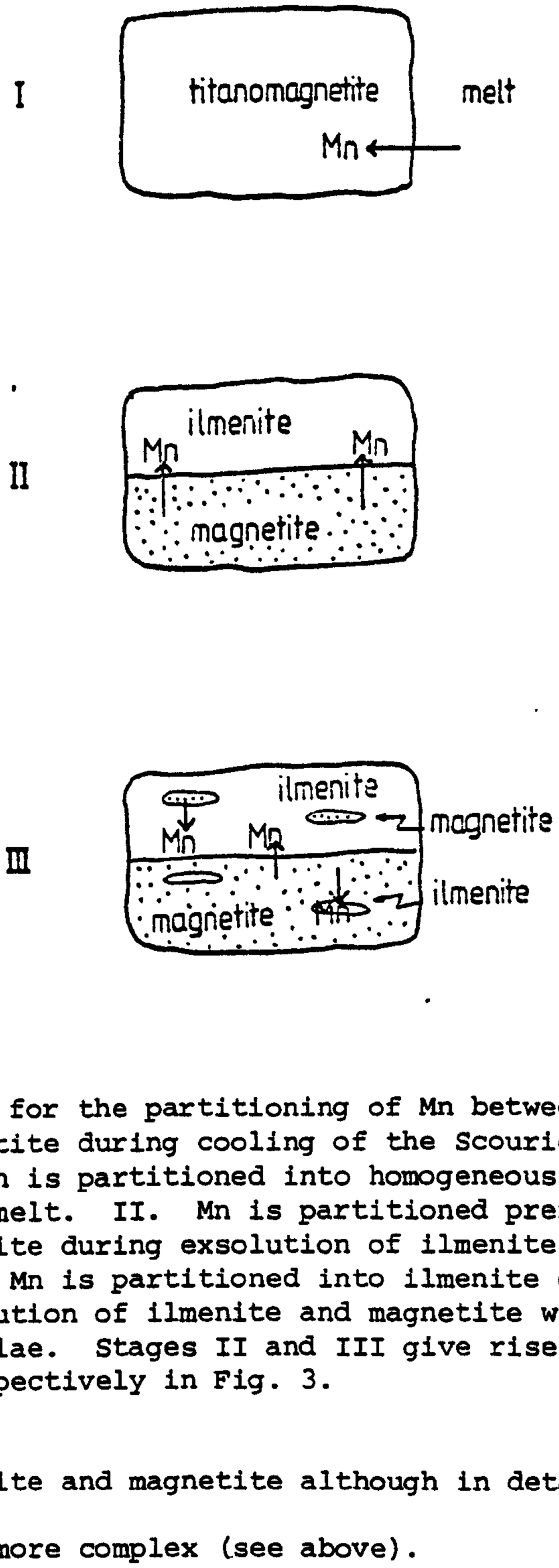

Fig. 5. Model for the partitioning of Mn between ilmenite and magnetite during cooling of the Scourie granulites. I. Mn is partitioned into homogeneous titanomagnetite from melt. II. Mn is partitioned preferentially into ilmenite during exsolution of ilmenite from titanomagnetite. III. Mn is partitioned into ilmenite during further exsolution of ilmenite and magnetite within larger lamellae. Stages II and III give rise to trends 1 and 2 respectively in Fig. 3.

Mn between ilmenite and magnetite although in detail the relationship is more complex (see above).

5. CONCLUSIONS

1. Mn replaces Mg in ilmenite at low temperatures in the presence of a hydrous fluid phase.

2. Mn replaces Fe in ilmenite (a) during the subsolidus reaction of ulvospinel to ilmenite in basic rocks and (b) either during the reaction between ilmenite and orthopyroxene in an acid

melt or during high temperature exsolution of ilmenite from titanomagnetite in acidic rocks.

3. The partitioning of Mn between ilmenite and magnetite is not a function of magmatic processes but reflects the subsolidus equilibration between ilmenite and magnetite. The two observed trends indicate two stages in the equilibration between ilmenite and magnetite during exsolution from an originally homogeneous titanomagnetite and indicate the increased preference of Mn for ilmenite at low temperatures.

	SIO2	TIO2	AL2O3	CR2O3	FEO	MNO	MGO	CAO	
SC TON 72/1/1	0.00	1.51	.27	.36	89.23	.13	.02	0.00	MAGNETITE
	0.00	49.17	0.00	0.00	47.62	.75	.37	0.00	ILMENITE
SC TON 72/1/2	0.00	1.77	.27	.31	88.66	.03	.03	0.01	MAGNETITE
	0.00	49.25	0.01	.03	47.88	.48	.66	0.01	ILMENITE
SC TON 72/1/3	0.00	1.69	.27	.32	89.09	.12	.02	0.00	MAGNETITE
	0.01	49.86	0.10	0.00	47.17	.30	.76	0.01	ILMENITE
SC TON 72/1/4	0.00	1.73	.27	.33	89.10	.13	.02	0.00	MAGNETITE
	0.01	49.60	0.00	.02	47.50	.53	.57	0.01	ILMENITE
SC TON 72/1/5	0.00	1.62	.27	.35	89.01	.13	.03	0.00	MAGNETITE
	0.01	49.30	0.01	.02	47.68	.71	.45	0.00	ILMENITE
SC TON 72/1/6	0.00	1.60	.27	.34	89.11	.03	.03	0.01	MAGNETITE
	0.00	49.43	0.00	0.00	48.36	.98	.03	0.01	ILMENITE
SC TON 72/1/7	0.00	2.99	.27	.30	88.50	.17	.02	0.00	MAGNETITE
	0.01	49.03	0.01	.12	47.72	.66	.36	0.01	ILMENITE
SC TON 72/1/8	0.00	1.34	.27	.27	88.15	.13	.03	0.01	MAGNETITE
	0.00	45.31	.04	0.00	47.47	.08	.12	0.00	ILMENITE
SC TON 72/1/9	0.00	1.32	.26	.35	88.69	0.00	.05	0.01	MAGNETITE
	0.00	50.13	.04	.11	47.12	.73	.55	0.00	ILMENITE
SC TON 72/1/10	0.00	1.20	.30	.33	87.85	0.00	.13	0.01	MAGNETITE
	0.00	49.11	.10	0.01	47.72	.07	.13	0.01	ILMENITE
SC TON 72/2/1	0.00	.27	.35	.33	88.20	.12	.06	0.01	MAGNETITE
	0.00	45.51	.05	0.01	50.64	.42	.78	0.01	ILMENITE
SC TON 72/2/2	0.00	.35	.36	.39	88.29	.01	.03	0.01	MAGNETITE
	0.01	48.85	.05	.01	47.38	.71	.15	0.01	ILMENITE
SC TON 72/2/3	0.00	1.17	.51	.39	88.92	.11	.03	0.00	MAGNETITE
	0.01	49.55	.06	.01	47.59	.51	.52	0.01	ILMENITE

TABLE 1. Chemical analyses for coexisting ilmenite and magnetite in tonalite HR 72 from Scourie more (SC TON 72) grains 1 & 2 (see fig 1.) and an ultramafic dyke from the Scourie area (SC UM 42) grains 1 to 4,(see fig. 2d). Total iron as FeO.

	SIO2	TIO2	AL2O3	CR2O3	FEO	MNO	MGO	CAO	
SC TON 72/2/4	0.00	.09	.34	.37	88.79	.13	.04	0.00	MAGNETITE
	0.00	49.11	.06	.01	47.63	.54	.60	0.01	ILMENITE
SC TON 72/2/5	0.01	.48	.36	.40	88.69	.01	.03	0.00	MAGNETITE
	0.01	45.34	.05	.01	50.33	.19	.93	0.01	ILMENITE
SC UM 42/1/1	0.04	.09	.42	.35	89.42	.02	.01	0.01	MAGNETITE
	0.00	50.82	.25	.01	45.91	1.60	.03	0.00	ILMENITE
SC UM 42/1/2	0.0	.49	.29	.33	89.34	.01	.01	0.01	MAGNETITE
	0.00	50.79	.04	.03	46.02	1.65	.06	0.01	ILMENITE
SC UM 42/1/3	0.00	.34	.52	.35	89.31	.02	.01	0.00	MAGNETITE
	0.00	50.72	.04	.02	45.72	1.63	.04	0.01	ILMENITE
SC UM 42/2/1	0.00	.60	.34	.49	91.36	.01	0.00	0.00	MAGNETITE
	0.00	51.06	0.00	.02	45.64	1.69	.02	0.01	ILMENITE
SC UM 42/2/2	0.00	.46	.31	.46	89.05	.03	0.00	0.00	MAGNETITE
	0.00	51.23	.03	.06	45.80	1.72	.03	0.00	ILMENITE
SC UM 42/2/3	0.00	.50	.33	.54	90.12	.02	.01	0.01	MAGNETITE
	0.00	51.41	.01	.03	45.80	1.95	0.01	0.00	ILMENITE
SC UM 42/3/1	0.00	.66	.30	.59	89.44	.02	.04	0.00	MAGNETITE
	0.00	48.25	.05	.05	47.51	1.43	.03	0.01	ILMENITE
SC UM 42/3/2	0.01	.52	.28	.56	89.73	.04	.03	0.00	MAGNETITE
	0.00	49.59	.04	.07	47.71	1.20	.04	0.00	ILMENITE
SC UM 42/4/1	0.01	.58	.30	.49	89.57	.02	.01	0.01	MAGNETITE
	0.01	48.53	.03	.07	46.12	1.30	.12	0.00	ILMENITE
SC UM 42/4/2	0.01	.59	.29	.53	89.33	0.00	.05	0.01	MAGNETITE
	0.00	48.20	.03	.06	47.64	1.26	.03	0.00	ILMENITE
SC UM 42/4/3	0.01	.76	.34	.55	89.75	.03	0.00	0.00	MAGNETITE
	0.01	49.41	.03	.04	48.32	1.15	.21	0.01	ILMENITE

TABLE 1. continued.

Chapter 7

MINERAL REACTIONS IN A GRANULITE FACIES CALC - SILICATE ROCK FROM SCOURIE

SUMMARY

A calc-gneiss from the type area of the granulite facies Scourian complex contains the mineral assemblage plagioclase (An_{43-46}), scapolite (Me_{63-65}, SO_4 26-30), clinopyroxene, ilmenite-magnetite, rutile and minor amounts of pyrite, chalcopyrite, carbonate, uralite, sericite, quartz and apatite.

Mineral reactions can be written which define the maximum pressure and minimum temperature of the granulite facies metamorphism and stages in the cooling history of the rock. The distribution of Na and Ca between plagioclase and scapolite, calibrated by Goldsmith and Newton (1978) yields excessively high temperatures (ca. 1200°C). This is revised using thermodynamic data from their experimental work and suggests a minimum temperature of 800°C for the granulite facies metamorphism; a maximum pressure of 11 kb for the metamorphism is obtained from the stability of plagioclase with respect to clinopyroxene and quartz.

Ilmenite-magnetite pairs equilibrated between 512° and 430°C and oxygen fugacity conditions were probably externally controlled. Ilmenite and clinopyroxene may have exchanged Fe and Mg to temperatures as low as 540°C, but at lower temperatures Mn replaces Mg in ilmenite.

1. INTRODUCTION

Calc gneisses are not uncommon in the Scourian complex; they have been described from granulite facies gneisses at Scourie (Barooah, 1970) and Assynt (Sheraton et al., 1973) and from metasedimentary belts in the Outer Hebridees (Coward et al., 1969). This sample was collected from the type granulite facies locality on Scourie More and comprises plagioclase (40%), clinopyroxene (36%), scapolite (18%), sulphides (2.3%), ilmenite-magnetite (1.3%), rutile (1.2%) and minor amounts of carbonate, uralite, sericite, quartz and apatite. Modal proportions are based on 2900 points counted in two thin sections.

Pyroxene and plagioclase form equigranular grains with straight to slightly curved grain boundaries. The clinopyroxene is clouded with small elongate opaque inclusions parallel to (100) and (001), which are prominent at the centre of some grains, whilst the margins are inclusion free; they represent exsolved magnetite from an originally Fe-rich clinopyroxene. Scapolite wraps around clinopyroxene grains, has more irregular grain boundaries and appears to replace plagioclase; it is altered to calcite and uralite and iron pyrites and chalcopyrite replace some grains along irregular cracks. Rutile forms small rounded grains; plagioclase is lightly sericitized in places. A small amount of fine-grained quartz with undulose extinction and sutured grain boundaries is associated with clinopyroxene and scapolite.

Whilst most calc-silicate rocks in the Scourian complex are thought to have been metasediments, an approximate analysis for this specimen shows that it is poor in CaO (15%) and enriched in FeO (6.5%, MgO (3.5%) and TiO_2 (1.6%) compared with the analyses given by Barooah (1970). If the oxysalt component is removed from the scapolite the rock is 94% clinopyroxene + plagioclase which is consistent with a metabasic igneous origin.

2. MINERAL CHEMISTRY

Plagioclase is slightly zoned, varying in composition from An_{46} at the core to An_{43} at the rim.

Clinopyroxene analyses (Table 2) plot on the diopside-hedenbergite join with a variable Fe-Mg ratio. The grains are quite strongly zoned with Fe-rich cores and Mg-rich rims; Fe^{2+}, Al^{IV}, Ca and Ti decrease towards the rim and Mg and Na increase.

Scapolite shows slight zoning; the grains are fairly sodic (Me_{63-65}) with 26 - 30% SO_4 in the anion site and virtually no Cl (Table 1). The analyses have been recalculated on the basis of 12 (Si + Al); W values i.e. the sum of cations on the M sites (Na + Ca + K + Fe + Ba) vary from 4.1035 to 3.9473 with a mean of 4.054; this compares well with values between 4.068 and 3.927 and a mean of 3.981 obtained by Evans et al. (1969) in their microprobe analyses. Weight per cent CO_2 has been estimated by assuming that the sum of the anions is 1.0. This appears to be valid since there is only a small amount of Ca unused when the scapolite end-members are calculated on this basis. The probability that CO_2 fills at least part of the anion site is indicated by the presence of $CaCO_3$ in the thin section associated with scapolite. Furthermore since F, Cl and SO_4 have been determined CO_3 is the only other anion likely to be found in the structure, although Goldsmith (1976) suggested that the more sodic scapolites may tolerate some OH^-. If the above assumptions are made, wt % CO_2 varies from 3.2 to 3.4% and the analysis totals are between 98.2 and 99.4%.

Ilmenite and Magnetite. Three composite ilmenite-magnetite grains have been analysed (Fig. 1 & Table 3). Two are predominantly ilmenite with both lamellar and granular intergrowths of magnetite- (lamellae up to 30 μm wide, granules up to 150 μm wide) and a third grain is predominantly magnetite with granular exsolution lamellae (ca. 70 μm wide) of magnetite. The ilmenite contains smaller exsolution lamellae (2 μm wide) of magnetite. Ilmenite is zoned with respect to Mg and Mn with Mg rich cores (MgO up to 1.2 wt %, MnO up to 0.6 wt %) and

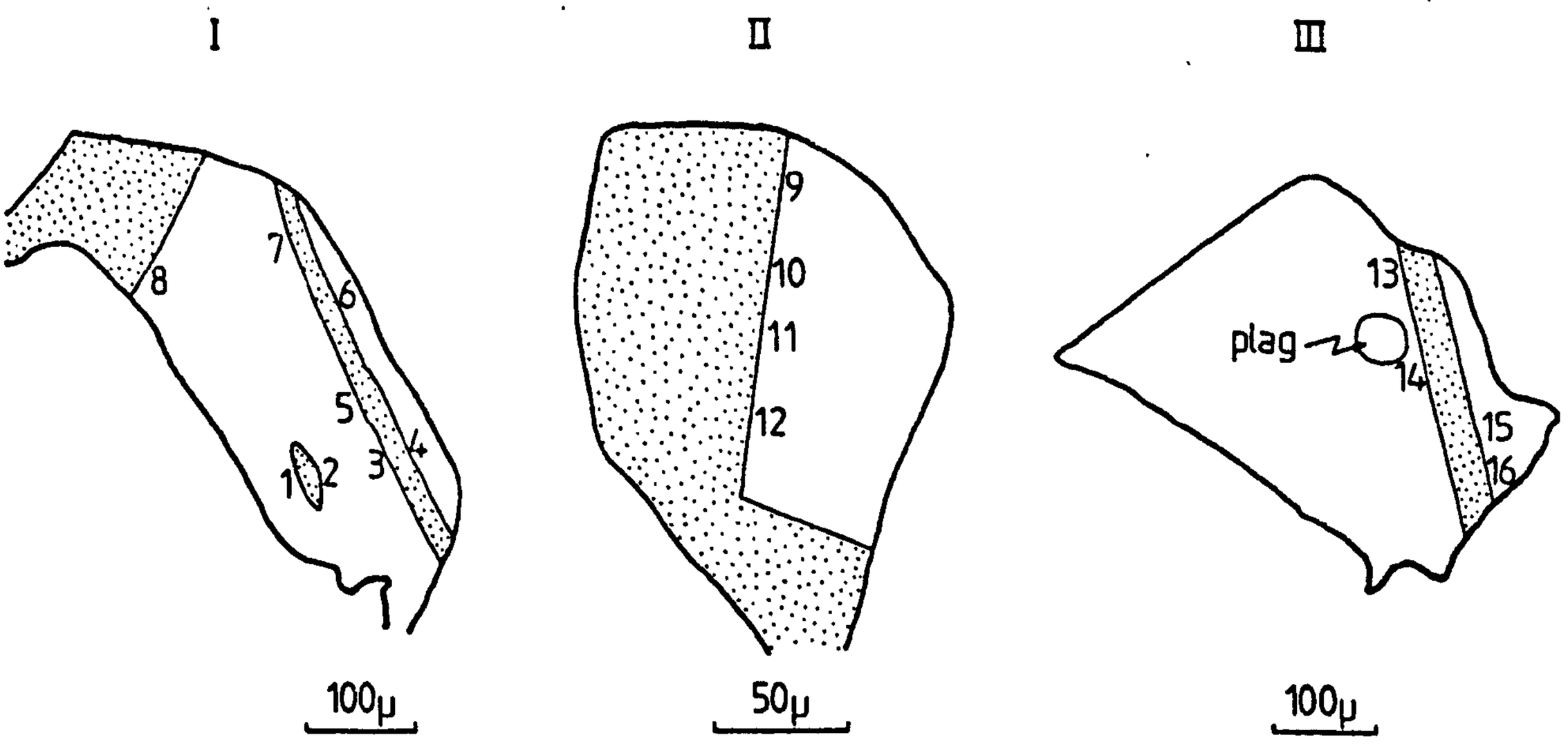

Fig. 1. Sketch of composite ilmenite grains analysed. Numbers refer to ilmenite-magnetite pairs in Table 3, and calculated T and fO_2 in Fig. 3. Magnetite stippled.

Mn-rich rims (MnO 2.0 wt %, MgO 0.1 wt %). There is an inverse correlation between Mg and Mn in ilmenite suggesting that Mn replaced originally Mg-rich ilmenite (this is discussed in more detail in Chapter 6). Clinopyroxene is the most likely source of Mn and Mg in this rock since magnetite, the only other possible source, tends to contain small amounts of Mn and Mg even at high temperatures (Pinkney, 1976). Bishop (1976) has shown that Mg will partition into ilmenite from clinopyroxene at high temperatures; this means that the high MgO content in the core of ilmenite grains is probably a relic of granulite facies metamorphism. Mn and a small amount of Fe from clinopyroxene appear to have replaced Mg in ilmenite during cooling.

Sulphides replace scapolite, clinopyroxene and overgrow ilmenite and magnetite. A possible reaction for the reduction of scapolite is:

$$6CaSO_4 + 3Fe_2Si_2O_6 \rightarrow 3FeS_2 + 3Ca_2Si_2O_6 + Fe_3O_4 + 10\ O_2 \qquad (1)$$

in scap. in cpx iron pyrites in cpx. magt

This is consistent with Fe-poor rims of the clinopyroxene. Chalcopyrite is overgrowing and overgrown by pyrite. CuO was measured in clinopyroxene but is below detection limit (0.05 wt % CuO) except in the centre of grains. Oxygen produced by the above reaction appears to have been buffered by ilmenite-magnetite equilibria.

3. PRESSURE TEMPERATURE DETERMINATIONS

Plagioclase-Scapolite

The recent experimental work of Goldsmith and Newton, summarised in their 1977 paper shows the importance of scapolites as a lower crustal mineral. They found that Ca-rich carbonate and sulphate scapolites are stable relative to the oxysalt + plagioclase. This is contrary to the ideas of early workers who regarded scapolite as a late metasomatic alteration product of plagioclase (Barth, 1952; Fyfe and Turner, 1958). Scapolite is a primary phase in granulite xenoliths in basaltic and kimberlitic pipes and is also reported in granulite facies terrains in West Africa, Western Australia, India and the Adirondacks. These occurrences are reviewed by Goldsmith (1976) and Goldsmith and Newton (1977). Lower crustal scapolites tend to be rich in CO_3^- and $SO_4^=$ and virtually free from Cl^-; this led Goldsmith and Newton to postulate that scapolite may be an important means of storing volatiles, particularly CO_2, in the lower crust.

Scapolite is not common in the Scourie area; it is mentioned as an accessory mineral in the calc-silicates described by Barooah (1970) and was found in Scourian gneisses from Assynt by Sheraton et al. (1973) who regarded it as a late retrogressive mineral.

Scapolite coexisting with plagioclase is potentially a good thermometer. Goldsmith and Newton (1977) calibrated the distribution

of Na and Ca between plagioclase and scapolite with temperature for the pure CO_3, pure SO_4 and the $\frac{1}{2}CO_3$-$\frac{1}{2}SO_4$ systems. They found that pressure has little effect on the Na-Ca distribution. Two adjacent plagioclase-scapolite pairs were analysed and have the compositions An_{45}, Me_{65} CO_3 = 0.733 and An_{46}, Me_{63} CO_3 = 0.718 (Table 1). When plotted on Figs. 9 and 10 of Goldsmith and Newton (1977) they yield temperatures of 1224°C and 1182°C respectively. These temperatures seem high in view of equilibration temperatures on pyroxene pairs, feldspar pairs and iron titanium oxide pairs from the granulites of Scourie More, which fall in the range 600°C to 1000°C. Goldsmith and Newton point out that for more sodic compositions their thermometer appears to give excessively high temperatures. A compositionally similar plagioclase-scapolite pair (An_{40}, Me_{65} CO_3 = 0.70) from a garnet granulite xenolith in an alkaline basalt pipe in New South Wales (Wilkinson, 1974) yields temperatures of 1200°C to 1300°C. In view of the presence of primary hornblende in the rock Goldsmith and Newton consider this temperature estimate unreasonable. They suggest that their experiments may not have reached equilibrium in the high Na range (the reactions were not reversed), that there is non-ideal behaviour in both the scapolite and plagioclase components in this composition range and that ordering in the scapolite at lower temperatures affects its activity.

Calcite + 3 Plagioclase = Scapolite

It is possible to estimate the equilibration temperature of more sodic scapolite - plagioclase pairs using thermodynamic data derived from the experiments of Goldsmith and Newton (1977). The reaction:

$$3CaAl_2Si_2O_8 + CaCO_3 = Ca_4Al_6Si_6O_{24}CO_3 \qquad (2)$$

plagioclase calcite scapolite

has been determined for the pure system (Goldsmith and Newton, 1978, Fig. 2) using the thermodynamic relationship:

$$\Delta H^{o} - T\Delta S^{o} + (P - 1)\Delta V^{o} = -RT\ln K \quad (3)$$

where $K = \dfrac{a_{scap}}{(a_{plag})^{3}(a_{CaCO_3})}$ (4)

the equilibration temperature of the assembleage plagioclase - scapolite - calcite can be determined if the activity of the components is known and thermodynamic data for the pure system are available. Thermodynamic data are given in Goldsmith and Newton (1977); ΔS^{o} = 9 $\pm$ 0.5 cals/^{o}C, ΔV^{o} is 1.22 cm^{3} at 25^{o}C and is smaller at high temperatures and can be ignored; ΔH^{o} can therefore be derived using an equilibration temperature of 875^{o}C in the pure system, ΔH^{o} = 10332 $\pm$ 574 cals. An ideal solution model can be used to estimate the activity of scapolite, and, although this is probably wrong, it is the most realistic assumption that can be made. Assuming the coupled substitution NaSi = AlCa, and ideal mixing on the anion site:

$$a_{scap} = (X_{M}^{Ca})^{4} \; (X_{anion}^{CO_3}) \quad (5)$$

If an activity coefficient of 1.2 is used for anorthite in plagioclase (Windom and Boettcher, 1976), and $CaCO_3$ is pure, temperatures are 949^{o}C and 915^{o}C for the two scapolite pairs, although there is an error of 130^{o}C due to uncertainty in the thermodynamic data (Fig. 2). If calcite is not a primary mineral these temperatures represent a minimum estimate of the equilibration temperature.

$CaSO_4$ + 3 Plagioclase = Scapolite

The reaction:

$$3CaAl_2Si_2O_8 + CaSO_4 = Ca_4Al_6Si_6O_{24}SO_4 \quad (6)$$

plagioclase scapolite

is dependent on both pressure and temperature; this allows a P - T line to be drawn, which limits the pressure and temperature of equilibration. From Goldsmith and Newton (1977) ΔS° = 9.03 cal/$^{\circ}$C, ΔH° = 11833 cals at reaction point 850°C, 9 kb. The activity is esimated in an analogous way to that above, a value of 1.2 is used for the activity coefficient of anorthite in plagioclase, and $CaSO_4$ is assumed pure. Two P - T lines can be drawn for the two plagioclase-scapolite pairs (Fig. 3) which in the absence of $CaSO_4$ define a lower P - T limit to this reaction.

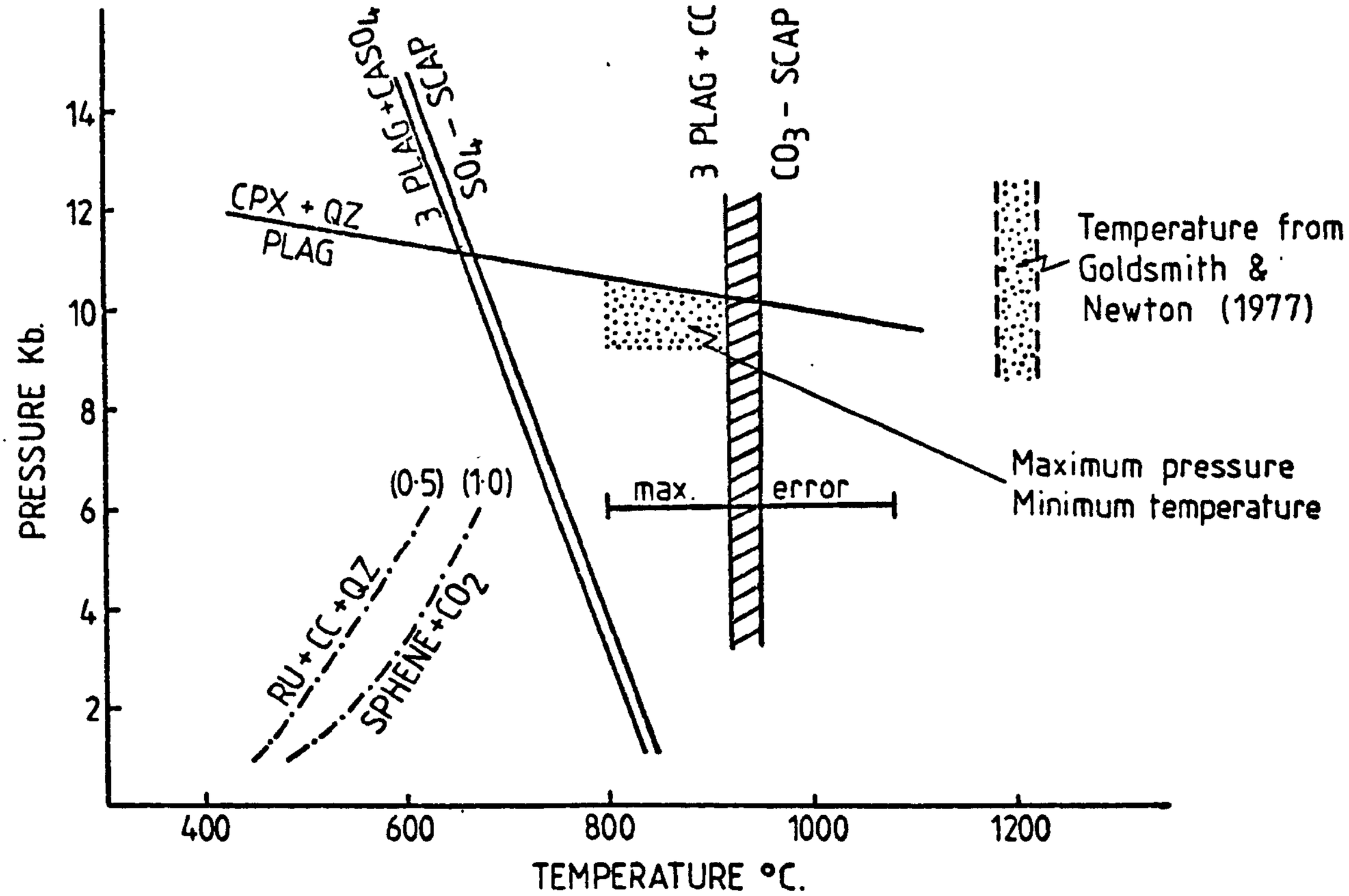

Fig. 2. Mineral reactions in calc gneiss; stability curves calculated for compositions presented in Tables 1 & 2. Stability curves for reaction Ru + cc + Qz = Sphene + Co_2 shown for XCO_2 = 1.0 and XCO_2 = 0.5.

Plagioclase = clinopyroxene + quartz

The assemblage plagioclase, clinopyroxene quartz can be used as a geobarometer using the method of Wood (1977) as discussed below (Chapter 8). The Mg/(Mg + Fe) ratio at the centre of clinopyroxene grains is 0.6 and so the activity of $CaAl_2SiO_6$ (CaTs) is probably equal to its mole fraction (Wood, 1976). The mole fraction of CaTs was obtained by the method of Cawthorn and Collerson (1974); using an activity coefficient of 1.2 for anorthite in plagioclase (Windom and Boettcher, 1976) and assuming that the quartz is pure, a P - T line can be drawn at 11 kb and 700°C and 10.3 kb and 900°C for the centre of the grains. The lines are virtually insensitive to temperature. If the quartz in this rock is primary, these lines represent the equilibration pressure for the reaction plagioclase = clinopyroxene + quartz, otherwise they represent a maximum pressure.

Ilmenite - magnetite thermometry and oxygen barometry

Equilibration temperatures and oxygen fugacities were estimated from the composition of coexisting ilmenite and magnetite grains, using the experimental data of Buddington and Lindsley (1964) and the treatment of minor elements in the $FeO-Fe_2O_3-TiO_2$ system proposed by Powell and Powell (1977b). Equilibration temperatures and oxygen fugacities from adjacent pairs of analyses at several different points within a single grain are given for three grains and these define a curve midway between the NiNiO and Haematite-Magnetite buffers at 1 atmosphere in the temperature range 510°C to 430°C (Fig. 3). Error limits are those produced by the method of Powell and Powell (1977b). The mole fraction of ulvospinel in magnetite and R_2O_3 in ilmenite (calculated after the method of Carmichael, 1967) is variable throughout the grains but tends to be the highest nearest the centre of grains and lowest at the edge,

consequently the highest equilibration temperatures are at the centre of grains. The fO_2 cooling curve is coincident with curves in the same temperature range from a Scourian pyroxenite (clinopyroxene + orthopyroxene), an orthopyroxene-bearing trondhjemite gneiss, a hornblende-bearing trondhjemite and orthopyroxene granite. This suggests that at these temperatures oxygen fugacity is externally controlled, probably by a fluid phase and that sulphide and carbonate equilibria do not control fO_2 in this rock. There appears to be no significant difference in the equilibration temperature of the different grains despite their slightly different silicate environments (cf. Bowles, 1976).

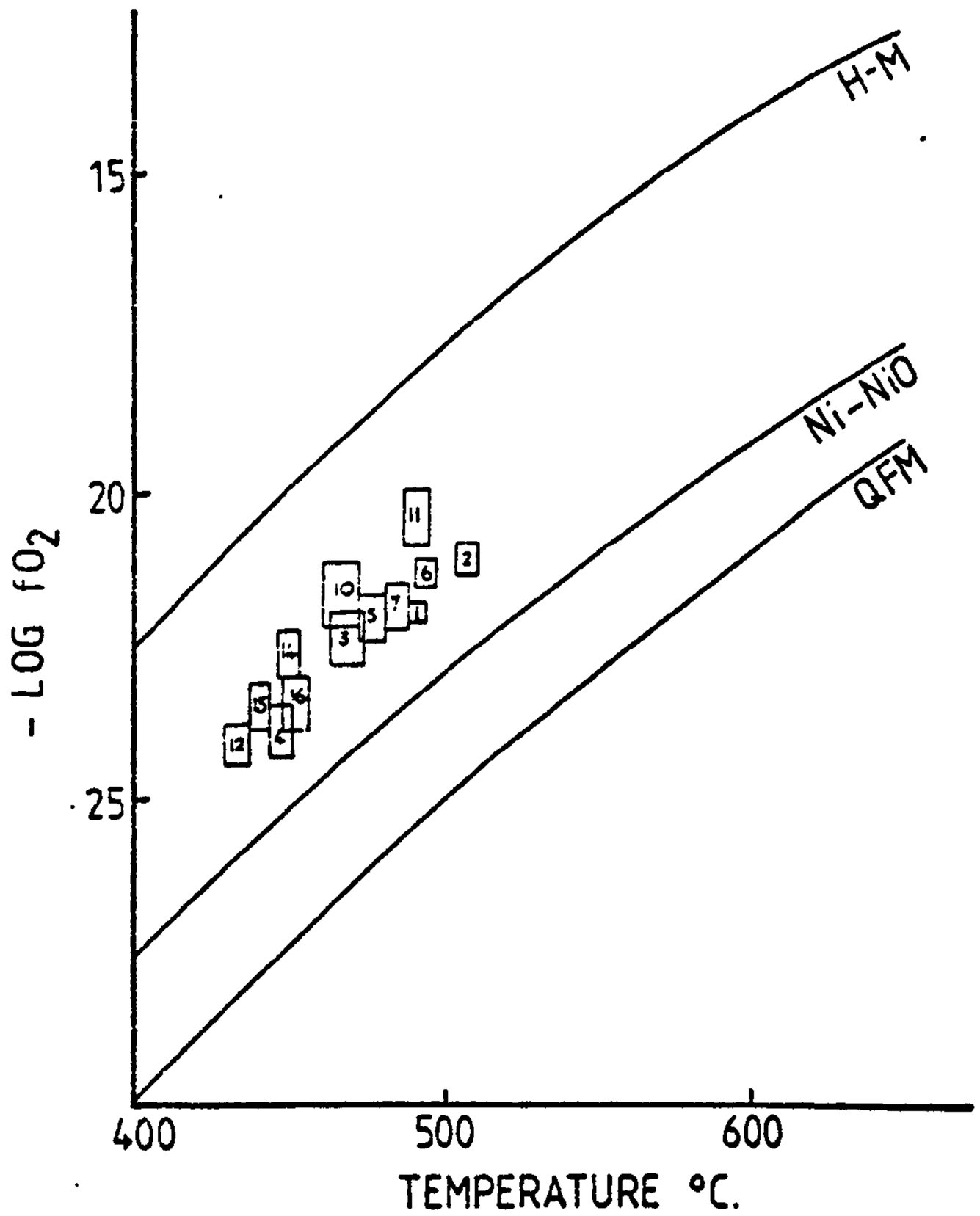

Fig. 3 Temperature vs. log fO_2 diagram for ilmenite-magnetite pairs. Numbers refer to analyses in Table 3 and points on grains in Fig. 1. Error limits after Powell and Powell (1977b). Buffer curves at 1 atmosphere pressure - HM haematite-magnetite, Ni-NiO Nickel Oxide, QFM quartz-fayalite-magnetite

Ilmenite - clinopyroxene thermometry

Temperatures based on the distribution of Fe and Mg between ilmenite and clinopyroxene using the equation of Bishop (pers. comm.) are between 450°C and 540°C for the centre of grains. These must be regarded as minimum temperatures in view of the observed Mn-Mg exchange in ilmenite; clinopyroxene - ilmenite temperatures are about 30°C lower than ilmenite - magnetite temperatures for the same part of the grain.

4. DISCUSSION

Textural evidence suggests that quartz and calcite are late minerals and grew after the granulite facies metamorphism. This means that the pressure estimate based on the assemblage clinopyroxene-plagioclase-quartz is a maximum and that temperature estimates based on the stability of scapolite are a minimum. The stability of scapolite with respect to calcite suggests a minimum temperature of 915°C, but the large error in the thermodynamic data suggests that temperatures as low as 800°C are plausible. A maximum pressure of 10 - 11 kb is suggested by the stability of plagioclase with respect to clinopyroxene and quartz. This means that a minimum temperature of 800°C and a maximum pressure of 11 kb is required for the granulite facies metamorphism at Scourie.

At lower temperatures:

(i) the stability of rutile, calcite and quartz with respect to sphene defines a minimum pressure for a given temperature, although the position of this curve depends upon the composition of the fluid phase (Hunt and Kerrick, 1977)(fig. 2).

(ii) Mg-Fe exchange between clinopyroxene and ilmenite could have closed at temperatures as low as 540°C; this is broadly consistent with the closure temperature of 590°C proposed below for Fe-Mg exchange between ortho- and clinopyroxene (see Chapter 8).

(iii) Fe-Ti exchange between ilmenite and magnetite closed in different part of composite ilmenite-magnetite grains at different temperatures between 512 and 439^{o}C, and in this temperature range oxygen fugacity was externally buffered.

(iv) Mn-Mg exchange between ilmenite and possibly clinopyroxene occurred at temperatures less than 540^{o}C.

TABLE 1. Coexisting plagioclase and scapolite

Plagioclase

	1149/2	1149/5
SiO_2	56·13	56·52
Al_2O_3	26·58	26·98
CaO	9·31	9·59
BaO	0·00	0·01
Na_2O	5·98	5·99
K_2O	0·28	0·22
TOTAL	98·28	99·31
An	45	46
Ab	53	52
Or	2	1

Scapolite

	1148/8	1148/4
SiO_2	44·81	45·27
Al_2O_3	26·39	25·43
Fe_2O_3	2·04	0·64
CaO	16·90	17·40
BaO	0·05	0·04
Na_2O	3·45	3·58
K_2O	0·09	0·08
Cl	0·03	0·02
SO_3	2·30	2·48
TOTAL	95·68	94·97
cations to Si+Al = 12000		
Si	7082	7220
Al	4918	4780
Fe	243	77
Ca	2863	2974
Ba	1	0
Na	1064	1107
K	20	16
Cl	5	5
SO_3	266	297
* CO_2	729	698
W	3947	4097
Na/Na+Ca	0·271	0·271

* CO_2 estimated see text.

TABLE 2. Clinopyroxene analyses

	edge	centre
SiO_2	50·61	48·61
TiO_2	0·44	0·60
Al_2O_3	3·81	4·47
Cr_2O_3	0·02	0·04
* Fe_2O_3	3·08	3·17
FeO	8·54	10·97
MnO	0·50	0·46
MgO	11·13	8·99
CaO	21·91	21·74
Na_2O	0·86	0·74
TOTAL	100·90	99·79
	cations to six oxygens	
Si	1·892	1·860
Al4	0·109	0·140
Al6	0·059	0·062
Fe^{2+}	0·267	0·351
Fe^{3+}	0·087	0·096
Mg	0·620	0·513
Mn	0·016	0·015
Ti	0·012	0·017
Cr	0·001	0·001
Ca	0·878	0·888
Na	0·062	0·055
X_{Ca-Ts}	0·040	0·056
Mg/Mg+Fe	0·699	0·594

* Fe_2O_3 estimated from charge balance

	SIO2	TIO2	AL2O3	CR2O3	FEO	MNO	MGO	CAO	
FBD 6 1	.08	1.32	.32	.31	92.06	.06	.02	.02	MAGNETITE
	.05	50.20	.04	.02	47.81	1.70	.52	.01	ILMENITE
FBD 6 2	.08	1.32	.32	.31	92.06	.06	.02	.02	MAGNETITE
	.04	50.14	.25	.07	48.71	1.24	.93	0.00	ILMENITE
FBD 6 3	.10	.88	.33	.31	92.04	.06	.06	.01	MAGNETITE
	.04	50.14	.35	.02	47.99	1.43	.79	.03	ILMENITE
FBD 6 4	.07	.33	.34	.28	91.83	.03	.06	.02	MAGNETITE
	.05	50.95	.05	.02	47.58	1.97	.22	.05	ILMENITE
FBD 6 5	.06	.91	.34	.30	92.07	.03	.06	.01	MAGNETITE
	.06	50.16	.02	.04	48.37	1.35	.06	0.00	ILMENITE
FBD 6 6	.06	1.04	.40	.31	91.57	.03	.04	.01	MAGNETITE
	.06	48.52	.02	.03	48.72	1.71	.40	.07	ILMENITE
FBD 6 7	.07	1.04	.32	.31	91.79	.06	.06	.01	MAGNETITE
	.04	49.52	.05	.04	48.37	2.03	.08	0.00	ILMENITE
FBD 6 8	.04	.62	.36	.30	91.43	.05	.06	.03	MAGNETITE
	.04	48.37	.03	.04	48.37	1.94	.15	.02	ILMENITE
FBD 6 9	.33	.60	.35	.42	89.56	.03	.35	.05	MAGNETITE
	.04	49.12	.03	.06	48.55	1.34	.13	.01	ILMENITE
FBD 6 10	.63	.63	.61	.41	90.14	.05	.06	0.00	MAGNETITE
	.04	45.62	.05	.03	49.64	1.35	.19	0.00	ILMENITE
FBD 6 11	.22	.60	.48	.44	90.39	.02	.05	.01	MAGNETITE
	.06	47.19	.05	.16	50.32	1.36	.14	0.00	ILMENITE
FBD 6 12	.09	.58	.35	.42	89.90	.03	.02	.01	MAGNETITE
	.17	50.23	.12	.07	47.31	1.59	.66	.05	ILMENITE
FBD 6 13	.09	.64	.35	.39	90.75	.01	.07	.08	MAGNETITE
	.06	49.64	.06	.06	47.73	1.49	.51	.02	ILMENITE
FBD 6 14	.15	.56	.39	.41	91.21	.03	.03	.01	MAGNETITE
	.06	49.13	.04	.07	48.19	1.28	.71	.02	ILMENITE
FBD 6 15	.17	.61	.39	.45	91.12	.05	.03	0.00	MAGNETITE
	.08	49.61	.04	.03	47.49	1.45	.50	.01	ILMENITE
FBD 6 16	.10	.34	.33	.36	91.11	.04	.06	.02	MAGNETITE
	.07	49.38	.06	.03	47.30	1.52	.39	.02	ILMENITE

TABLE 3. Chemical analyses of coexisting ilmenite - magnetite pairs in calc-silicate rock FBD 6. The sample numbers refer to the points on figure 3. Total iron as FeO.

Chapter 8

GARNET - PYROXENE THERMOMETRY AND BAROMETRY IN THE SCOURIE GRANULITES

SUMMARY

Coexisting garnet, ortho- and clinopyroxene and plagioclase from granulites at Scourie ranging in composition from trondhjemitic to ultramafic were analysed with the electron probe in order to test current geothermometric and geobarometric models and provide an estimate of the pressure and temperature of metamorphism of the Scourie granulites.

Seven two-pyroxene geothermometers were tested and an ideal solution model based on the diopside - enstatite miscibility gap data of Nehru and Wyllie (1974) was found to yield the most reliable results, which are also consistent with the garnet - clinopyroxene thermometer proposed by Raheim and Green (1974). Equilibration temperatures range between 590°C and 820°C and reflect the range of cooling temperatures between the peak of metamorphism (ca. 820°C) and pyroxene-blocking temperatures (ca. 590°C).

Three independent estimates of pressure were made using the methods of Wood (1974) (garnet-orthopyroxene), Wood (1977) (clinopyroxene - plagioclase - quartz) and Newton (1978) (garnet - orthopyroxene - plagioclase - quartz). Garnet - orthopyroxene pairs yield pressures which are dependant upon an accurate knowledge of equilibration temperature and are not definitive. The methods of Wood (1977) and Newton (1978) yield pressures of ca. 10 kb.

These results are discussed in the light of P - T estimates of other workers for the Scourian complex and it is concluded that higher pressures may have been operational in the Outer Hebrides reflecting an original difference in geothermal gradient and that the temperature estimate of O'Hara and Yarwood (1978) for the Scourie area

of ca. 1150 $\pm$ 100°C is an igneous temperature and that their pressure estimate of ca. 15 kb is therefore too high.

1. INTRODUCTION

An accurate estimate of the pressure and temperature of metamorphism in Archaean granulites is important for a number of reasons; firstly it provides a means of estimating the geothermal gradient during Archaean granulite facies metamorphism; secondly an accurate assessment of pressure can lead to a reliable estimate for the thickness of the Archaean crust, and thirdly an estimate of the depth at which metamorphism takes place provides a useful constraint on the suggestion that granulites represent a section of the lower crust. In 1976 Lambert commented that the lack of detailed mineralogical studies in regionally metamorphosed Archaean rocks means that it is difficult to define precisely the pressure and temperature conditions of their formation.

This study seeks to help to redress this balance and presents new chemical analyses for garnets, pyroxenes and plagioclase from a range of lithologies from the Scourie granulites and these are used to test current geothermometric and geobarometric models as applied to granulites and to obtain a consistent estimate of the pressure and temperature conditions during granulite facies metamorphism at ca. 2.7 Ma. in the Scourie area.

The rocks analysed in this study range in composition from trondhjemitic to ultramafic and a summary of mineral assemblages is presented in Table 1. These rocks have a granular texture with straight to curved grain boundaries and triple junctions; clinopyroxene grains are generally larger than orthopyroxene and show exsolution of magnetite and/or hypersthene. Garnet in gabbros shows two main parageneses: (i) as rims on opaque oxide grains or hypersthene and (ii) more commonly as large irregular porphyroblasts rimmed with plagioclase and sometimes intergrown with clinopyroxene. Some zoning is detected in clinopyroxene and garnet with respect to

TABLE 1 Mineral assemblages in rocks used in this study

No.	Rock-type	Locality	Mineral assemblage
HR 5	Garnet Gabbro	Scourie	Gt - Cpx - Opx - Plag - Opq
HR 9	Garnet Gabbro	Scourie	Gt - Cpx - Opx - Plag - Hbl - Sulph
HR 12	Ultramafic rock	Scourie	Opx - Cpx - Plag - Hbl - Opq
HR 62	Gabbro	Badcall	Gt - Cpx - Opx - Plag - Hbl - Opq - (Bi - cc - cht - sulph)
HR 181	Ultramafic rock	N. side Scourie Bay	Ol - Cpx - Opx - Opq - Spin
HR 196	Homogeneous gabbro	Badcall	Gt - Opx - Cpx - Plag - Hbl - (Bi - opq - cc - qz)
HR 199	Homogeneous gabbro	Badcall	Gt - Opx - Cpx - Plag - Opq - (Bi - hbl - qz - ap)
HR 200	Homogeneous gabbro	Badcall	Gt - Opx - Cpx - Plag - Hbl - Opq - Qz
HR 217	Gabbro	Scourie	Gt - Opx - Cpx - Plag - Hbl - Opq - Spin
HR 42 B	Ultramafic dyke	Badcall	Opx - Cpx - (opq - cc)
HR 41	Homogeneous gabbro	Badcall	Opx - Cpx - Plag (Bi - opq - Hbl)
HR 70	Tonalitic gneiss	Scourie	Opx - Cpx - Plag - (opq - sulph - ap - hbl)
FBD 5	Tonalitic gneiss	Scourie	Opx - Cpx - Plag - Qz - opq - bi
FBD 3	Tonalitic gneiss	Scourie	Opx - Cpx - Plag - Qz - Bi - Hbl - Opq
275	Supracrustal rock	N. side Scourie Bay	Gt - Opx - Plag - Qz - Bi - Opq
178	Trondhjemite	N. side Scourie Bay	Cpx - Plag - Qz - Opq

Fe, Mg, Ca, Al and equilibration temperatures and pressures are calculated for both edge and centre of some grains.

Analyses were made by electron microprobe; samples HR 5, 9, 12, 62, 181, 196, 199, 200, 217, 275 were analysed by energy dispersive electron probe at the University of Cambridge and samples HR 41, 42B, 70, 178, FBD 5 and FBD 3 by wave-length dispersive electron probe at the University of Leicester. In most rocks at least two points were analysed on each grain and usually more than one mineral pair was analysed in each rock. Generally the average of several point analyses was used in P-T calculations, except where significant zoning is detected.

A rough estimate of Fe^{3+} in pyroxenes was obtained by iteratively solving the charge balance equation $Al^{VI} + Fe^{3+} + Cr^{3+} - 2Ti^{4+} = Al^{IV} + Na^{+}$ (after Papike et al., 1974). Coexisting pyroxene pairs and garnet-clinopyroxene pairs are plotted in the quadrilateral CaMg - CaFe - Fe - Mg (Figs. 1a & 1b); pyroxenes show a limited range in composition, although garnets show a greater range.

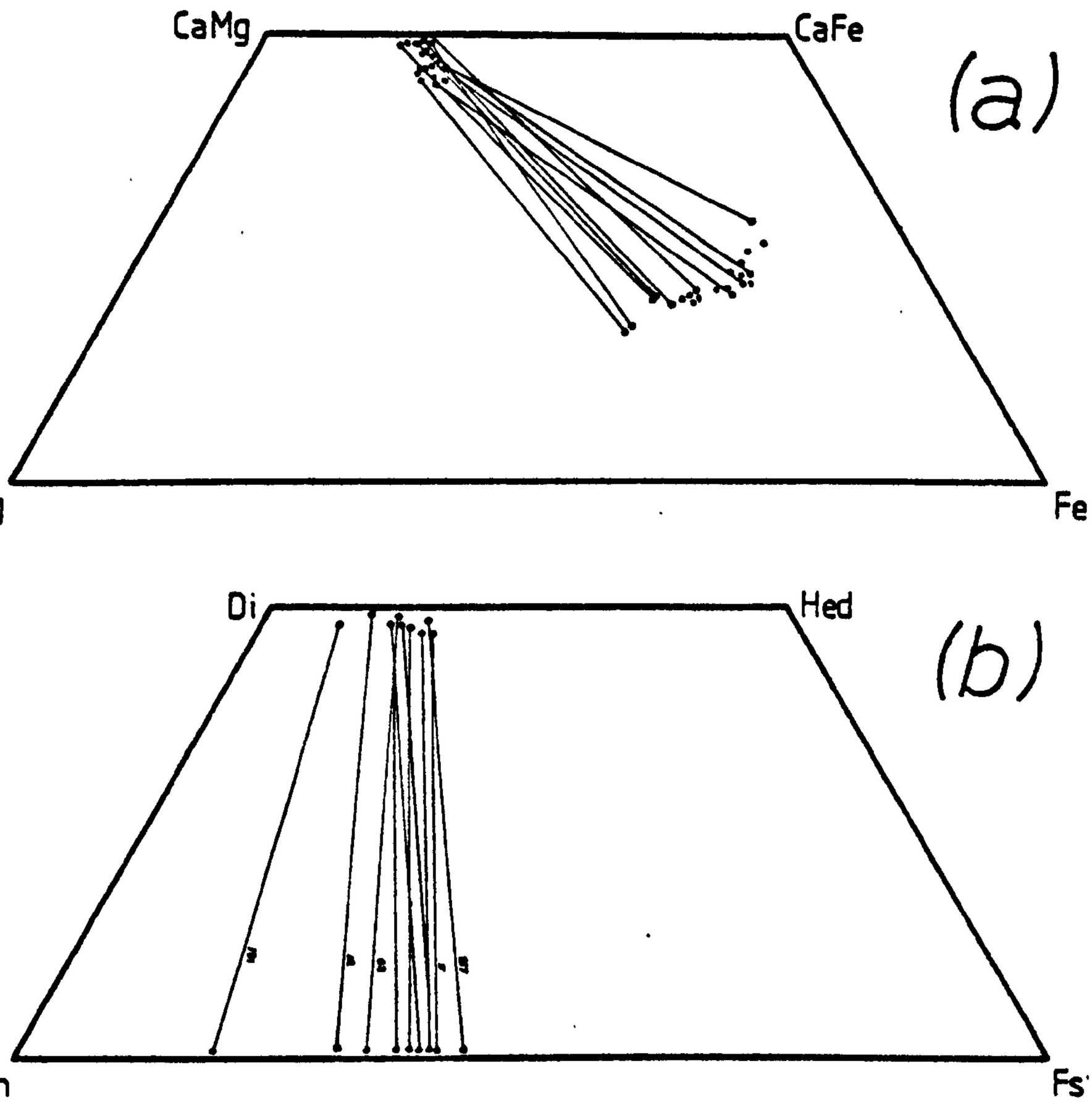

Fig. 1. (a) Compositions of coexisting clinopyroxene and garnet in gabbros at Scourie and Badcall; (b) compositions of coexisting ortho- and clinopyroxenes in ultramafic rocks, gabbros and tonalites at Scourie and Badcall; sample numbers are indicated on the tie lines.

2. THE THERMODYNAMIC APPROACH

The application of equilibrium thermodynamics to experimentally determined simple systems allows the results from such systems to be extrapolated to the more complex compositions of real rocks. The basis of the thermodynamic approach is the equilibrium relation for a balanced chemical reaction between the components of mineral phases taking part in the reaction. For example, consider the reaction:

$$Mg_2Si_2O_6 \quad = \quad Mg_2Si_2O_6 \qquad (1)$$

in orthopyroxene in clinopyroxene

the equilibration relation is:

$$-\Delta G^{\circ} = RT\ln K \qquad (2)$$

ΔG° is the standard free energy change for reaction (1) and is a linear function of pressure (P) and temperature (T); K is the equilibrium constant for reaction (1) and takes into account the compositional difference between natural mineral phases and the end members used in the reaction and is a function of composition temperature and pressure; R is the gas constant and T, the temperature is expressed in Kelvins.

For reaction (1) the equilibrium constant K may be expressed:

$$K = \frac{a^{cpx}_{Mg_2Si_2O_6}}{a^{opx}_{Mg_2Si_2O_6}} = \frac{X^{cpx}_{Mg_2Si_2O_6} \cdot \gamma^{cpx}_{Mg_2Si_2O_6}}{X^{opx}_{Mg_2Si_2O_6} \cdot \gamma^{opx}_{Mg_2Si_2O_6}} \qquad (3)$$

where $a^{cpx}_{Mg_2Si_2O_6}$ is the activity of $Mg_2Si_2O_6$ in clinopyroxene and $\gamma^{cpx}_{Mg_2Si_2O_6}$ is the activity coefficient for $Mg_2Si_2O_6$ in clinopyroxene. The problem of formulating K therefore is reduced to the problem of formulating X, the mole fraction and the activity coefficient for each component in each mineral.

A reaction constitutes a good thermometer if K varies with T, but does not vary with P and a reaction constitutes a good barometer if K varies rapidly with changing P but varies little with changing T.

3. TEMPERATURE ESTIMATES USING COEXISTING ORTHOPYROXENE AND CLINOPYROXENE

Davis and Boyd (1966) showed that the solid solution of enstatite in diopside is sensitive to temperature in the range 900 - 1400°C, is relatively insensitive to pressure and therefore

is potentially a good geothermometer. Several attempts have been made, using mixing models of varying degrees of complexity, to apply the diopside-enstatite miscibility gap to natural pyroxene compositions (Boyd, 1973; Wood and Banno, 1973; Nehru and Wyllie, 1974; Saxena and Nehru, 1976; Saxena, 1976; Wells, 1977; Powell, 1978). Two different approaches were adopted. Wood and Banno (1973) and Wells (1977) assumed an ideal solution model, i.e. they assumed that the activity coefficients in equation (3) are unity so that the activity of a component and its mole fraction are the same. Saxena (1976), Saxena and Nehru (1976) and Powell(1978) assumed a mixing model which enables the activity coefficient to be expressed as a function of composition, pressure and temperature. There are problems with both approaches and these are discussed below.

(i) Ideal solution models

Wood and Banno (1973) and Wells (1977) formulated their ideal solution models in the following way using reaction (1) above:

(a) assume ideal, two-site mixing in pyroxenes

(b) obtain an expression relating lnK to temperature from miscibility gap data in the CMS system

(c) calibrate empirically the expression for the additional effect of Fe on the position of the miscibility gap.

The problems that arise with this approach are as follows:

(1) the assumption that there is no interaction between Ca and Mg in pyroxene is incorrect in view of a miscibility gap (indicating a strong interaction between Ca and Mg) in the diopside - enstatite system.

(2) there are several different determinations of the diopside-enstatite miscibility gap (e.g. Davis and Boyd, 1966; Nehru and Wyllie, 1974; Lindsley and Dixon, 1976) and calculated temperatures are strongly dependant upon which miscibility gap is used.

(3) the values for ΔS° obtained from miscibility gap data are much higher than expected (Wood and Banno, 1973; Wells, 1977) suggesting that the model adopted is too simple.

(4) the temperature range of interest in granulites, i.e. 700 - 1000°C is the least well calibrated part of the Wood and Banno (1973) and Wells (1977) models and involves additional assumptions about the degree of ordering at low temperatures.

(5) the effect of pressure is neglected even though most experiments were carried out at 30 kb. Mori and Green (1976), Lindsley and Dixon (1976), Nehru (1976) and Howells and O'Hara (1975) showed that there is a significant pressure effect on the diopside-enstatite miscibility gap, although Mori and Green (1976) point out that it will be insignificant at temperatures below 1000°C.

In view of the formidable array of problems associated with ideal solution models it is surprising that they are capable of reproducing experimental temperatures and that they yield geologically reasonable temperatures for granulites (see below). Wood and Fraser (1974) suggested that one reason why this may be so is because activity coefficients in silicate solid solutions tend to be of the same size and magnitude and therefore cancel out in an expression such as (3).

Five equations based on ideal solution models are tested in this study and they are designated T_1 to T_5 in Table 2. T_1 is from equation (27) of Wood and Banno (1973) based on the miscibility gap data of Davis and Boyd (1966), T_2 is from equation (5) of Wells (1977) and is based on the best fit of miscibility gap data from a large number of sources (see Wells op.cit. for references) T_3 and T_4 are from Stormer and Whitney (1977) and are based on the miscibility

ANALYSIS NO.	M1MG	M1FE	M2MG	M2FE	M2CA	T1	T2	T3	T4	T5
F30 5 01 OP	.580	.376	.560	.376	.019	814.3	824.6	670.7	701.1	0.0
F30 5 01 CP	.656	.219	.048	.016	.874					
F30 3 01 OP	.575	.379	.575	.379	.022	812.9	823.9	670.1	700.6	1145.5
F30 3 01 CP	.645	.238	.048	.016	.873					
M+B OP B/1120/25	.924	.059	.896	.057	.043	1164.2	1048.4	971.7	1054.6	0.0
M+B CP	.872	.073	.122	.010	.846					
M+B OP C/900/15	.823	.085	.888	.091	.019	1071.3	973.2	866.9	916.6	1623.1
M+B CP	.732	.078	.098	.011	.773					
M+B OP C/1120/15	.935	.056	.895	.055	.047	1237.0	1132.7	1084.8	1222.3	997.3
M+B CP	.881	.072	.164	.013	.822					
M+B OP F/1000/15	.861	.060	.864	.062	.028	1154.6	1064.9	984.9	1082.3	0.0
M+B CP	.809	.061	.137	.014	.811					
M+B OP J/1010/15	.803	.083	.885	.091	.017	990.0	877.8	752.8	764.1	0.0
M+B CP	.941	.036	.046	.002	.944					
M+B OP J/350/7.5	.803	.124	.828	.126	.030	1103.2	1052.2	955.1	1054.0	942.7
M+B CP	.791	.096	.131	.016	.812					

T1 WOOD + BANNO (1973)
T2 WELLS (1977)
T3 NEHRU + WYLLIE (1974)
T4 LINDSLEY + DIXON (1976)
T5 MYSEN + BOETTCHER (1975)

TABLE 2. Calculated site occupancies and equilibration temperatures for ortho- and clino- pyroxene pairs from rocks in the Scourie area. Equilibration temperatures calculated using ideal solution models. OP orthopyroxene, CP clinopyroxene. The last two digits of the sample number refer to the points analysed and the remaining digits are the rock number.

ANALYSIS NO.	M1MG	M1FE	M2MG	M2FE	M2CA	T1	T2	T3	T4	T5
HRR 501 OP	.533	.374	.578	.402	.013	762.9	758.2	608.4	669.9	0.0
HRR 501 CP	.336	.167	.058	.029	.870					
HRR 901 OP	.548	.374	.580	.397	.014	817.6	833.5	668.5	716.5	0.0
HRR 901 CP CENTRE	.565	.279	.057	.028	.877					
HRR 911 OP	.548	.374	.580	.397	.014	966.3	1056.9	940.5	1103.4	0.0
HRR 911 CP EDGE	.530	.330	.107	.116	.697					
HRR 912 OP	.552	.370	.561	.389	.023	878.4	926.6	777.6	851.9	0.0
HRR 912 CP CENTRE	.559	.296	.093	.049	.819					
HRR 912 OP	.552	.370	.561	.389	.023	878.1	928.2	777.2	851.3	0.0
HRR 912 CP EDGE	.566	.269	.069	.041	.837					
HRR 1201 OP	.610	.306	.642	.322	.023	890.3	907.8	761.6	818.9	1097.3
HRR 1201 CP	.620	.259	.082	.027	.836					
HRR 1202 OP	.627	.294	.665	.312	.012	892.4	903.1	756.8	809.5	1166.7
HRR 1202 CP	.620	.209	.062	.027	.836					
HRR 1207 OP	.619	.287	.665	.308	.027	632.2	618.5	663.6	662.5	796.5
HRR 1208 CP	.659	.167	.046	.012	.887					
HRR 1209 OP	.625	.281	.675	.304	.012	786.3	757.5	598.8	596.2	982.1
HRR 1210 CP	.641	.168	.032	.010	.913					
HRR 6201 OP	.590	.328	.615	.342	.015	816.1	813.6	658.1	660.1	0.0
HRR 6202 CP EDGE	.632	.219	.046	.016	.850					
HRR 6202 OP	.594	.328	.615	.342	.015	866.1	799.8	643.3	660.5	0.0
HRR 6202 CP CENTRE	.607	.211	.044	.015	.864					
HRR 6204 OP	.603	.320	.625	.332	.016	820.7	815.7	660.3	681.8	1143.6
HRR 6205 CP	.643	.237	.046	.015	.892					
HRR 6206 OP	.619	.336	.631	.336	.006	817.8	810.9	655.2	675.1	0.0
HRR 6207 CP	.623	.214	.048	.017	.881					

T1 WOOD + BAINO (1973)
T2 WELLS (1977)
T3 NEHRU + WYLLIE (1974)
T4 LINDSLEY + DIXON (1976)
T5 MYSEN + BOETTCHER (1975)

TABLE 2. continued

ANALYSIS NO.	M1MG	M1FE	M2MG	M2FE	M2CA	T1	T2	T3	T4	T5
HRR 16101 OP	.757	.178	.786	.185	.020	934.8	861.8	742.3	767.7	926.5
HRR 16101 CP	.748	.149	.063	.012	.892					
HRR 16102 OP	.748	.185	.781	.193	.016	952.0	910.6	773.8	812.6	923.8
HRR 16102 CP	.730	.170	.075	.018	.888					
HRR 13601 OP	.544	.412	.546	.414	.028	828.8	858.3	709.5	756.9	0.0
HRR 13601 CP	.607	.316	.061	.032	.884					
HRR 13610 OP	.508	.401	.545	.430	.010	813.9	839.5	689.4	732.1	0.0
HRR 13611 CP	.616	.297	.052	.025	.879					
HRR 13613 OP	.532	.428	.534	.429	.024	760.1	764.8	686.3	623.4	0.0
HRR 13612 CP	.645	.266	.032	.013	.906					
HRR 19302 OP	.547	.395	.564	.407	.015	835.9	864.5	715.5	765.8	0.0
HRR 19301 CP	.625	.265	.062	.028	.881					
HRR 19302 OP	.559	.382	.576	.393	.018	860.6	869.3	654.7	681.8	0.0
HRR 19302 CP	.619	.276	.645	.020	.867					
HRR 21707 OP	.518	.404	.543	.424	.019	808.8	831.3	680.2	719.1	0.0
HRR 21701 CP	.534	.275	.051	.024	.901					
HRR 428 01 OP	.556	.386	.557	.387	.034	839.2	866.3	717.1	766.5	0.0
HRR 428 01 CP	.614	.260	.063	.026	.856					
HRR 428 02 OP	.574	.365	.591	.375	.015	778.7	773.2	615.6	627.5	0.0
HRR 428 02 CP	.624	.225	.036	.013	.891					
HRR 428 03 OP	.560	.377	.574	.366	.020	806.6	816.7	662.5	651.1	0.0
HRR 428 03 CP	.633	.234	.046	.017	.884					
HRR 428 04 OP	.563	.376	.576	.384	.021	815.8	833.5	680.6	715.4	0.0
HRR 428 04 CP	.623	.227	.052	.019	.869					
HRR 428 04 OP	.563	.376	.576	.384	.021	891.2	939.4	799.0	863.0	0.0
HRR 428 04 CP HOMOG	.536	.267	.897	.043	.803					

T1 WOOD + BANNO (1973)
T2 WELLS (1977)
T3 NEHRU + ARYLEE (1974)
T4 LINDSLEY + DIXON (1976)
T5 WYSEN + BOETTCHER (1975)

TABLE 2 Continued.

ANALYSIS NO.	M1MG	M1FE	M2MG	M2FE	M2CA	T1	T2	T3	T4	T5
HRR 428 05 OP	.555	.373	.573	.385	.021	666.2	935.7	794.8	877.1	0.0
HRR 428 05 CP	.624	.255	.691	.038	.810					
HRR 428 06 OP	.561	.352	.573	.396	.017	606.2	817.1	663.0	652.1	0.0
HRR 428 06 CP	.616	.227	.648	.418	.674					
HRR 41 01 OP	.561	.359	.569	.376	.015	600.4	803.7	648.1	670.5	1666.7
HRR 41 01 CP	.606	.238	.644	.417	.681					
HRR 41 02 OP	.573	.358	.593	.370	.019	823.2	833.8	680.5	713.3	0.0
HRR 41 02 CP	.620	.243	.653	.421	.675					
HRR 41 03 OP	.561	.375	.580	.387	.015	810.0	820.8	666.9	696.8	0.0
HRR 41 03 CP	.612	.211	.649	.417	.685					
HRR 41 04 OP	.571	.368	.591	.373	.017	759.9	747.0	587.9	591.7	0.0
HRR 41 04 CP	.637	.247	.629	.410	.906					
HRR 41 05 OP	.567	.365	.587	.378	.012	880.8	920.3	776.8	849.2	0.0
HRR 41 05 CP	.614	.260	.665	.436	.823					
HRR 41 06 OP	.575	.347	.602	.364	.613	912.5	960.9	822.8	914.4	1554.8
HRR 41 06 CP	.607	.261	.107	.046	.794					
HRR 41 07 OP	.569	.367	.589	.380	.012	856.4	864.6	736.6	792.8	0.0
HRR 41 07 CP	.632	.248	.078	.026	.840					
HRR 41 08 OP	.381	.440	.408	.471	.092	806.7	851.9	713.8	775.4	0.0
HRR 42 08 CP	.618	.222	.639	.414	.886					
HRR 41 09 OP	.573	.360	.593	.374	.012	861.0	898.4	743.8	808.2	0.0
HRR 41 09 CP	.612	.230	.074	.828	.645					
HRR 70 01 OP	.534	.363	.596	.366	.015	866.0	816.6	655.2	678.7	1261.6
HRR 70 01 CP	.651	.232	.045	.016	.874					
HRR 70 02 OP	.588	.306	.591	.368	.617	838.9	844.6	692.2	729.2	1316.0
HRR 70 02 CP	.667	.224	.053	.018	.865					

T1 WOOD + BANNO (1973)
T2 WELLS (1977)
T3 NEMEC + WYLLIE (1974)
T4 LINDSLEY + DIXON (1976)
T5 MYSEN + BOETTCHER (1975)

TABLE 2. continued

gaps of Nehru and Wyllie (1974) and Lindsley and Dixon (1976) respectively, formulated by Henry and Medaris (in Stormer and Whitney, 1977); T_5 is based on an empirical study of Al-Cr exchange between coexisting orthopyroxene in peridotite (Mysen and Boettcher, 1975) and can be expressed by the reaction:

$$CaAlAlSiO_6 + MgCrAlSiO_6 = MgAlAlSiO_6 + CaAlCrSiO_6 \quad (4)$$

in cpx in opx in opx in cpx

(ii) Non-ideal solution models

The non-ideal solution models of Saxena (1976), Saxena and Nehru (1976) and Powell (1978) are primarily concerned with the non-ideal mixing of Ca and Mg on the M_2 site in clinopyroxene; all other interactions are assumed ideal. There are a number of problems with non-ideal solution models which make them inadequate even though they are more physically realistic than ideal solution models. These are discussed below:

(1) ideal solution models assume a mixing model. This is done empirically and the choice of model is often governed by the experimental data available to calibrate it.

(2) mixing models depend upon a large number of parameters many of which are unknown, due to lack of relevant experimental information and so have to be guessed or ignored depending upon the way in which the thermodynamics are formulated.

Two non-ideal solution models are tested below and are designated T_6 and T_7. T_6 is from the equation (22) of Powell (1978) and is based on the reaction:

$$CaMgSi_2O_6 + Mg_2Si_2O_6 = CaMgSi_2O_6 + Mg_2Si_2O_6 \quad (5)$$

T_7 is from equations (13) and (22) of Saxena and Nehru (1976) who considered the diopside-enstatite miscibility gap as two solvi between

the end members orthoenstatite-'orthodiopside' and clinoenstatite-diopside.

(iii) Results and Discussion

Calculated temperatures T_1 to T_7 are presented in Tables 2 and 3 for coexisting orthopyroxene and clinopyroxene from tonalitic gneiss, gabbro and ultramafic rock from the Scourie-Badcall area and the mineral analyses are presented in Tables 7a & 7b . The main features of Tables 2 and 3 are (1) there is a great variation in the calculated temperature depending on which method is used, (2) when the same method is used there is a great variation in calculated temperature in a single thin section, and (3) when the same method is used there is a large variation in calculated temperature between the different rocks analysed. It is important to decide (a) which temperature method or methods are the most reliable and reflect the true equilibration temperature the most accurately and (b) the reasons behind the variations in temperature observed in a single rock and between rocks.

(a) Choice of method. There is a difference of at least 100°C between the different methods used on any one coexisting pyroxene pair and results diverge more markedly at lower temperatures. This is principally a function of the experimental results against which the ideal solution models are calibrated, show the greatest divergence at low temperatures, hence the greater difference between calculated temperatures using this data is at low temperatures.

One approach is to test the models using coexisting pyroxene pairs whose equilibration temperature is known. Six pyroxene pairs from the experimental study of peridotite of Mysen and Boettcher (1975) are presented in Tables 2 and 3 and are designated by the symbol M+B; the letters B, C etc. indicate the rock composition studied and these are followed by the temperature and pressure of

Table 3 Calculated equilibration temperatures for coexisting pyroxene pairs using the methods of Powell (1978) T_6 and Saxena and Nehru (1976) T_7; equilibration temperatures from the method of Nehru and Wyllie (1974) are shown for comparison.

Rock	T_6	T_7	Nehru & Wyllie
HR 5	701	740	600
HR 9 centre	717	960	681
HR 9 edge	788	ca.1500	940
HR 18101	810	860	742
HR 217	778	1050	680
HR 42B04	788	1150	799
M+B/1120/25 (B)	1080	1020	
M+B/1000/15 (F)	922		
M+B/ 950/7.5 (D)	903		
M+B/ 900/15 (C)	784	700	

the experiment. Temperatures based on Wood and Banno (1973) (T_1) are generally too high by as much as 170°C; temperatures based on Wells (1977) (T_2), Lindsley and Dixon (1976) (T_3) and Mysen and Boettcher (1975) (T_5) are erratic, and temperatures based on Powell (1978) (T_6) and Saxena and Nehru (1976) (T_7) are too low. Temperatures based on the miscibility gap data of Nehru and Wyllie (1974) as formulated in Stormer and Whitney (1977) are the closest to experimentally determined temperatures.

The equation of Mysen and Boettcher (1975) yields erratic results for two main reasons: firstly, the concentrations of Cr and Al in pyroxenes are low and therefore small analytical errors will be propagated into large temperature differences, and secondly, some pyroxenes in the Scourie-Badcall area have exsolved magnetite, into which, according to crystal field theory, Cr will be preferentially partitioned, so that subsolidus reequilibration can also cause spuriously large temperature differences.

Stormer and Whitney (1977) compared temperatures derived from the methods designated in this study T_1, T_3 and T_4 with the results of two feldspar thermometry and a preferred P-T range estimated on the basis of mineral reactions in granulites from Brazil containing sapphirine and cordierite, and suggested that temperatures based on the Wood and Banno (1973) model were ca. 100°C too high and found that the results of the Nehru and Wyllie (1974) equation were the closest to the preferred temperature range. Wood (1975) suggested that the equation of Wood and Banno (1973) probably overestimated temperatures to the order of 60°C in the temperature range 800 - 900°C; similarly Hewins (1975) in a study of granulite facies pyroxenes found that the Wood and Banno (1973) equation yields temperatures that are not too low and are probably not too high by more than 50°C. Steele et al. (1977) found that ilmenite-silicate temperatures are closer to Nehru-Wyllie temperatures than Wood-Banno temperatures and

suggest that the Nehru-Wyllie miscibility gap is to be preferred because they used an electron-probe to analyse the phases rather than X-ray powder data.

These results suggest that two-pyroxene temperatures based on an ideal solution model calibrated against the miscibility gap data of Nehru and Wyllie (1974) yield temperatures that the the most consistent with experimental and other geothermometric data. Further support for this model comes from the results of the Raheim and Green (1975) geothermometer which gives temperatures in the same range as the Nehru and Wyllie model; this is discussed in more detail below.

(b) Variation within a thin section

There are two possible causes of the large variation in equilibration temperature in a single thin section: (i) analytical error; Stormer and Whitney (1977) pointed out hat because the limbs of the diopside-enstatite miscibility gap are steep in the temperature range of interest (i.e. less than 1000°C) small uncertainties in composition can contribute to large errors in calculated temperature; (ii) disequilibrium on the scale of millimetres, which is a function of differential diffusion, in and between pyroxenes.

Analyses made using the wavelength electron probe (see above) are subject to the following errors: less than 0.1% Al_2O_3, less than 0.2% FeO, MgO, CaO, and less than 0.4% SiO_2 in clino- and ortho-pyroxenes. Analyses made on the energy dispersive probe, however, have poorer precision. In samples HR 41 and HR 42B analysed with the wavelength probe there are apparent differences in equilibration temperature of up to 150°C using the Wood and Banno (1973) equation (T_1); there are real differences in the FeO and MgO in orthopyroxene and FeO, MgO and CaO in clinopyroxene which are greater than the sensitivity limits outlined above, so that the temperature differences are a function of real chemical differences in the pyroxenes and

therefore are meaningful.

(c) Interpretation of temperature variation

In granulites from the Scourie-Badcall area two-pyroxene equilibration temperatures, as determined by the Nehru-Wyllie (1974) model, vary between 590°C and 820°C (excluding the spuriously high temperature in sample HR 901, which is probably due to an inaccuracy in the Al_2O_3 content). In view of the real variation in equilibration temperature on the scale of a thin section (see above), which is regarded as due to local disequilibrium, the variation in equilibration temperature between rocks is regarded as meaningful. Ilmenite-magnetite pairs and feldspar pairs from rocks in this area show a range of equilibration temperatures which reflect continued equilibration with cooling possibly in the presence of a fluid phase. It is probable therefore that the range of pyroxene temperatures includes the peak of metamorphism, but for the most part reflect cooling temperatures, which record the exchange of Fe and Mg between ortho- and clino-pyroxenes during cooling and exsolution in clinopyroxenes.

A bulk analysis of clinopyroxene grains containing exsolved hypersthene lamellae was obtained by using a scanning electron probe beam; this yielded, together with nearby orthopyroxene, a temperature of 799°C (T_3). The highest temperatures recorded are ca. 820°C and it is proposed that these reflect the temperature of the peak of the granulite facies metamorphism.

On the other hand, sample 196 12 (clinopyroxene) is enclosed in orthopyroxene and yields a low equilibration temperature (608°C) (T_3) suggesting that the grains continued to equilibrate because of the large amount of mutual contact. It is possible that local compositional effects may also control diffusion in pyroxenes; pyroxene pairs in HR 41 which are in textural equilibrium with

brown granulite facies hornblende show a mean temperature 110°C higher than pyroxene pairs coexisting without hornblende in the same thin section. Blocking temperatures in pyroxenes are ca. 590°C and are higher than feldspars (ca. 450°C) and ilmenite-magnetite pairs.

4. TEMPERATURE ESTIMATES USING COEXISTING CLINOPYROXENE AND GARNET

Raheim and Green (1974) showed that the distribution of Fe and Mg between garnet and clinopyroxene according to the reaction:

$$CaFeSi_2O_6 + \frac{1}{3}Mg_3Al_2Si_3O_{12} = CaMgSi_2O_6 + \frac{1}{3}Fe_3Al_2Si_3O_{12} \qquad (6)$$

clinopyroxene garnet clinopyroxene garnet

is strongly dependent upon temperature and only slightly dependent upon pressure. They calibrated the exchange reaction in basaltic compositions at 30 kb and showed that variations in bulk composition in the range $6.2 < 100\ Mg/Mg + Fe^{2+} < 93.0$ does not affect the value for the distribution coefficient K_D, where:

$$K_D = \frac{(FeO)_{gt}\ (MgO)_{cpx}}{(MgO)_{gt}\ (FeO)_{cpx}} \qquad (7)$$

Raheim and Green (1974) obtained an expression for the variation of K_D as a function of temperature and pressure so that when K_D is known and an estimate of pressure is given, it is possible to calculate temperature.

Wood (1977) reinvestigated this system and suggested that some of the pressure dependence of K_D observed by Raheim and Green (1974) is a function of non-ideality in garnet solid solutions where grossular is a significant component. Raheim and Green found that the volume change for reaction (6) (2.357 cm^3) was larger than expected; if this value is incorrect the pressure dependence of K_D

will not be as great as they suggest. Wood (1977) proposed that the 30 kb data of Raheim and Green (1974) can be extrapolated to lower pressures if the more realistic value of 1.0 cm^3 is used for the volume change in reaction (6).

Temperatures at 10 kb pressure based on the equation of Raheim and Green (1974) and a modified version using the smaller V of Wood (1977) are presented in Table 4 below for gabbros from the Scourie-Badcall area, and the relevant clinopyroxene and garnet analyses are presented in Table 8.

Table 4. Temperatures based on coexisting clinopyroxene and garnet in gabbros at Scourie and Badcall, based on Raheim and Green (1974) and a modification proposed by Wood (1977) at 10 kb pressure. Temperatures from the two pyroxene model of Nehru and Wyllie (1974) are shown for comparison.

MINERAL PAIR	RAHEIM + GREEN	WOOD	NEHRU + WYLLIE
5 01	798	754	600
5 02	706	665	
9 01	818	773	680 - 770
9 02	809	764	
9 03	810	766	
62 01	697	657	643 - 660
62 02	692	653	
196 01	686	646	608 - 709
196 02	654	616	
199 01	669	630	655 - 715
200 01	598	562	not determined
200 02	675	636	
217 01	760	717	680
217 02	777	734	

The correction suggested by Wood (1977) does not make a significant difference to rocks formed in the P - T range under discussion.

Temperatures derived from clinopyroxene - garnet pairs broadly correspond to temperatures derived from the two-pyroxene Nehru and Wyllie (1974) model and show the same range. Garnet overgrowing opaque oxide (HR 5 02) equilibrated with clinopyroxene at a lower temperature than larger irregular garnet grains. Some garnet - clinopyroxene pairs yield higher temperature at the edge of the grain than at the core (e.g. HR 196, HR 200). Garnet-clinopyroxene pairs from Badcall (HR 62, 196, 199, 200) tend to give lower temperatures than is found in similar rocks in the Scourie area (HR 5, 9, 217). The rocks at Badcall are more altered to amphibolite facies mineral assemblages than similar rocks at Scourie, suggesting that equilibration between garnet and clinopyroxene proceeded to a lower temperature in this region, although this is not apparent in two pyroxene temperatures.

In summary the results of clinopyroxene thermometry support the two propositions made above (1) that the Nehru-Wyllie model reflects the metamorphic temperatures the most accurately and (2) that there is a range of equilibration temperatures, which probably reflect cooling.

5. PRESSURE LIMITS FOR THE SCOURIE GRANULITES

The presence of garnet in basic (gabbroic) granulites in the Scourie-Badcall area indicates that these rocks formed at relatively high pressures; Newton (1978) suggests that a minimum pressure of 8 kb is necessary for the formation of garnet in basic compositions at temperatures of 700°C; O'Hara's (1977) extrapolation of the data of Green and Ringwood (1967) for the appearance of garnet in olivine normative tholeiitic compositions suggests pressures between 7 and 8 kb in the temperature range 700 - 800°C. An upper stability limit

of ca. 10 - 12 kb at 800°C is suggested by the non-appearance of garnet in quartz saturated rocks (O'Hara, 1977) or 13 kb at 800°C by the presence of spinel rather than garnet in ultrabasic compositions. The application of equilibrium thermodynamics has led to several quantitative methods for estimating pressures in granulites; these are discussed below.

6. PRESSURE ESTIMATES USING THE SOLUBILITY OF ALUMINA IN ENSTATITE

Boyd and England (1964) and MacGregor and Ringwood (1964) were the first workers to show that if the temperature of equilibration is known the pressure may be estimated from the solubility of alumina in enstatite in equilibrium with garnet. This idea was developed by Boyd (1973) in his classic determination of the late Cretaceous geotherm beneath Lesotho.

Recent discussions have centred on the experimental study of MacGregor (1974) who showed that the weight per cent of Al_2O_3 in enstatite in spinel and garnet lherzolites is a function of pressure and temperature. MacGregor (1974) produced a series of isopleths for Al_2O_3 in enstatite in equilibrium with spinel or garnet which show a strong P - T dependence and do not noticeably change in slope in passing from the field of garnet lherzolite to spinel lherzolites.

A number of workers (e.g. Wood, 1975; Presnall, 1976; Obata, 1976) showed that MacGregor's (1974) isopleths in the spinel field are incorrect and that they are not strongly pressure dependent and vary principally with temperature. Similarly plagioclase lherzolites have Al_2O_3 isopleths with a negative slope, rather than a positive one implied by the data of MacGregor (1974) (Presnall, 1976; Obata, 1976).

Wood (1974) used the experimental data of MacGregor (1974)

to calibrate the reaction:

$$Mg_2Si_2O_6 + MgAl_2SiO_6 = Mg_3Al_2Si_3O_{12} \qquad (8)$$

in orthopyroxene garnet

and showed that it was a sensitive geobarometer, applicable to naturally occurring garnet - orthopyroxene pairs, capable of reproducing experimentally known pressures to within 2 to 3 kb provided the temperature is known.

Powell (1978), however, pointed out that this method is strongly dependent upon an accurate estimation of the mole fraction of Al in the M_1 and tetrahedral sites in orthopyroxene. Because silicon is the least precisely determined element in an electron probe analysis, the error in Al in the tetrahedral site and therefore the M_1 site can be large. Wood (1974) tried to circumvent this problem by dividing Al equally between the M_1 and tetrahedral sites. Howells and O'Hara (1978) showed that the solubility of alumina in enstatite can vary according to the starting material used in the experiments and suggested that Al_2O_3 solubility in enstatite is lower than that shown by MacGregor (1974) and that therefore at temperatures of less than 1200°C the orthopyroxene garnet geobarometer reads too low.

A further, purely empirical objection to the Wood (1974) geobarometer as applied to the Scourie granulites is that it is strongly temperature dependent, so that a variation in 100°C can mean a pressure variation of up to 5 kb (see Table 5). Similarly the proposed geobarometer of Powell (1978) based on the exchange of Ca and Mg between garnet and orthopyroxene is more sensitive to temperature than pressure when applied to granulites (see Fig. 3).

Table 5. **Pressures (in kilobars) calculated for garnet-orthopyroxene pairs after Wood (1974) at temperatures from 700 to 1000°C**

ROCK	P @ 700°C	P @ 800°C	P @ 900°C	P @ 1000°C
5 01	2.3	6.7	11.1	15.4
5 02	2.6	7.0	11.4	15.8
5 03	2.7	7.2	11.6	16.0
9 01	0.9	5.1	9.2	13.4
9 02	1.0	5.2	9.4	13.5
62 01	-	2.2	6.1	10.0
62 02	0.4	4.4	8.5	12.5
196 01	5.5	10.2	15.1	19.8
196 02	-	2.0	5.9	9.8
199 01	2.5	6.9	11.3	15.8
217 01	1.0	5.2	9.4	13.7
275 01	4.4	9.0	13.5	18.1

The results of Wood's (1974) geobarometer based on reaction (8) and corrected for non-ideal interactions between Fe and Al in orthopyroxene, using his equation (12) are presented in Table 5. There is a wide pressure range, some of which may be due to slight inaccuracies in Al_2O_3 in orthopyroxene. Clearly this method is not definitive in estimating pressure in granulites and should be treated with caution.

7. A PRESSURE ESTIMATE FROM THE ASSEMBLAGE ORTHOPYROXENE - GARNET - PLAGIOCLASE - QUARTZ

Wood (1975b) showed that the reaction:

$$Mg_2Si_2O_6 + CaAl_2Si_2O_8 = \frac{2}{3}Mg_3Al_2Si_3O_{12} + \frac{1}{3}Ca_3Al_2Si_3O_{12} + SiO_2 \quad (9)$$

in opx plagioclase in garnet solid solution quartz

can be used to estimate an upper pressure limit of ca. 13 kb for the granulite facies Scourian meta-tonalites in South Harris. This estimate is based on the non-appearance of garnet in quartz normative tonalites, which indicates that these rocks were metamorphosed to the low pressure side (orthopyroxene + plagioclase) of this reaction boundary (9). Wood (1975b) calculated the composition of garnet that would coexist with orthopyroxene and plagioclase at higher pressure and showed that it would be ca. $gross_{21-24}\ pyr_{23-27}\ ald_{51-53}$ and concluded that the appearance of garnet was controlled by the activity of silica.

Newton (1978) revised the thermodynamic data relevant to this reaction and produced new activity coefficient data for the grossular and pyrope components in garnet. A revised estimate of Wood's upper pressure limit using the new data is 12.7 $\pm$ 1.77 kb at 727°C, which agrees well with the original estimate of 13 kb.

Both these calculations, however, assume the composition of a garnet not seen and therefore are subject to some uncertainty.

The assemblage orthopyroxene - garnet - plagioclase - quartz is present in HR 275, a possible supracrustal rock (Davies, 1976), collected from the north side of Scourie Bay. It has an unusual composition (55% SiO_2, 17% Al_2O_3, 10% FeO, 4% MgO, 5% CaO, 5% NaO) and may represent an intermediate lava or metasediment. The composition of the garnet and orthopyroxene are presented in Table 9. There is a significant difference in the grossular content of the

garnet from that proposed by Wood (1975b) for a tonalitic bulk composition. Orthopyroxene and garnet coexist with plagioclase An_{29}.

From the experimental data of Newton (1978) it is possible to derive the expression:

$$P = R\ T\ \ln K + 1370 + 7.03T\ /\ 0.5382 \qquad (10)$$

where K is the equilibrium constant for reaction (9). Using activity coefficients estimated from Newton (1978) for garnet and a value of 1.28 for anorthite in plagioclase from Orville (1972) and assuming that $Mg_2Si_2O_6$ in orthopyroxene is an ideal solution at 800°C, a pressure of ca. 10 kb is obtained at 800°C. If this P - T line is combined with the method of Wood (1974) based on reaction (8) the two lines intersect at 10.7 kb and 840°C. (Fig. 2). Equation (23) of Powell (1978) is a sensitive geothermometer in these bulk compositions and suggests the slightly lower temperature and pressure of 720°C and 9.8 kb. This may be regarded as the closure temperature and pressure for exchange reactions between orthopyroxene and garnet and plagioclase in HR 275; since both pressure and temperature are based on the same mineral pair, 10.7 kb and 840°C, this is one of the few reliable points we have for an Archaean geotherm for the Scourian.

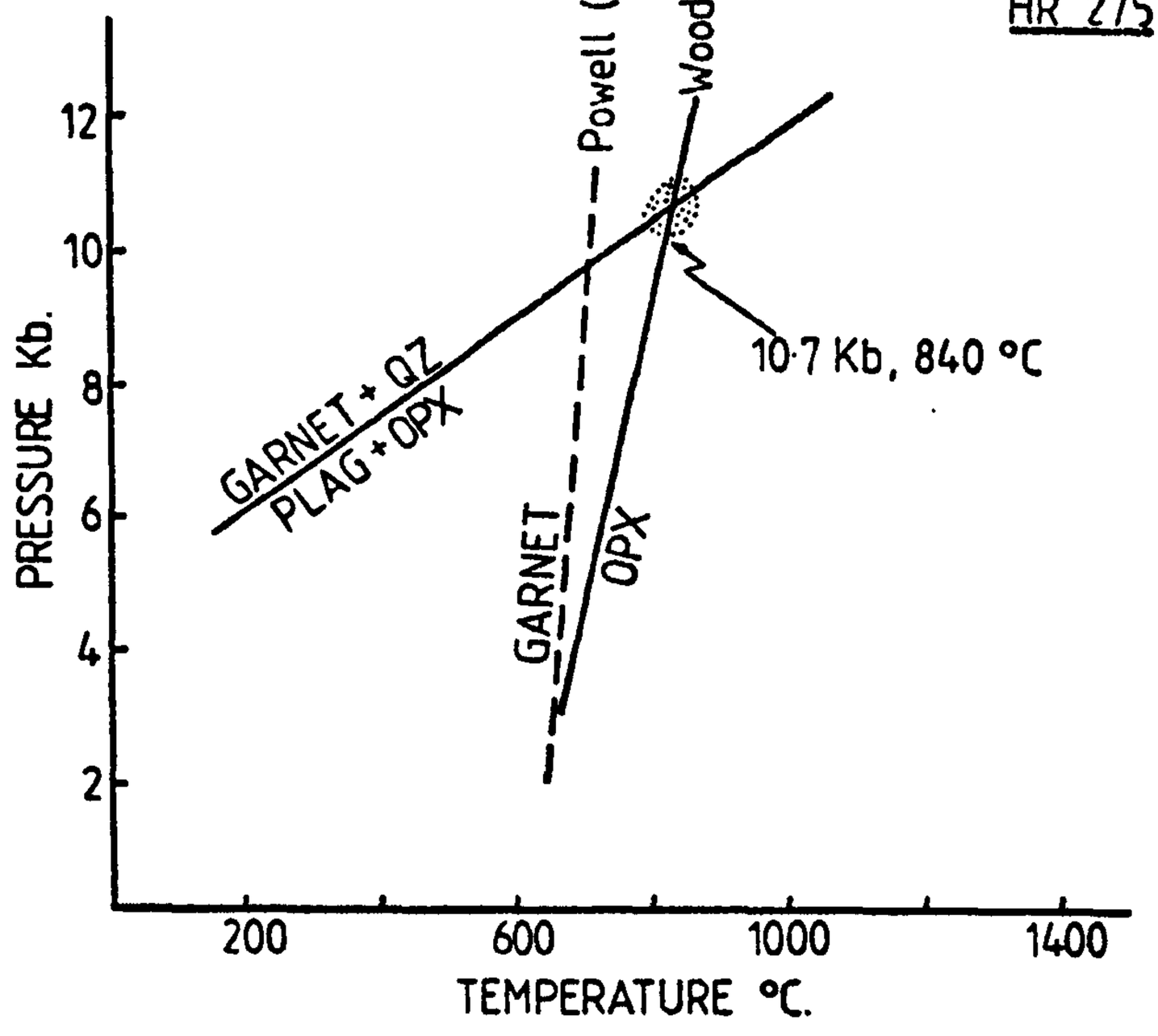

Fig. 2. Stability curves for the reactions opx + plag = gt + qz and opx = gt in sample HR 275 and the preferred P - T range.

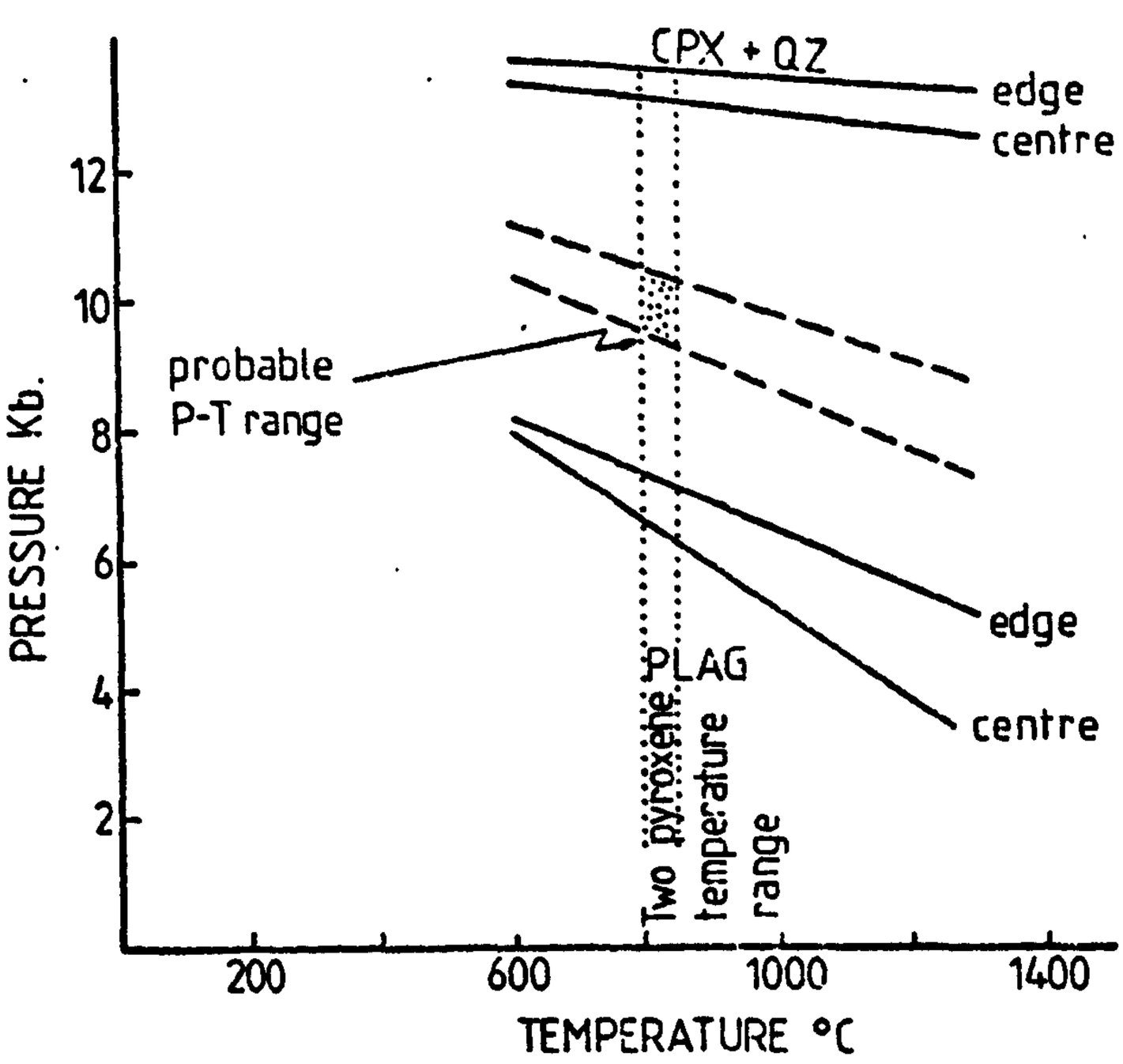

Fig. 3. Calculated P - T lines for the reaction plagioclase = clinopyroxene + quartz for tonalite (solid line) and trondhjemite (broken line) showing the position of the P - T lines for clinopyroxene and plagioclase analyses made at the centre and edge of grains. Maximum and minimum stability limits are a function of the means by which the mole fraction of $CaAl_2SiO_6$ in clinopyroxene is calculated. The probable P - T range is constrained by a temperature estimate from coexisting pyroxenes based on the Nehru - Wyllie (1974) model.

8. A PRESSURE ESTIMATE BASED ON THE ASSEMBLAGE CLINOPYROXENE - PLAGIOCLASE - QUARTZ

The assemblage clinopyroxene + plagioclase + quartz is not common in the Scourie area but is present in tonalite FBD 5 from Scourie More and in trondhjemite HR 178 from the north side of Scourie Bay. Wood (1977) showed that the reaction:

$$CaAl_2Si_2O_8 = CaAl_2Si_2O_6 + SiO_2 \qquad (11)$$

in plagioclase in cpx quartz

is sensitive to pressure and is relatively insensitive to temperature.

Following Wood (1977) values for ΔS° and ΔV° were obtained from Robie and Waldbaum (1968) and a value of ΔH° estimated from the experimental data of Hariya and Kennedy (1968) and the expression:

$$-R\ T\ \ln K = 5062 + 3.4 - (P-1)0.349$$

obtained where K is the equilibrium constant for reaction (11).

There are a number of problems when this method is applied to natural mineral assemblages:

(i) there is no unique way of calculating the mole fraction of $CaAl_2SiO_6$ (CaTs) in a clinopyroxene. The mole fraction of CaTs depends upon the order in which the other molecules are made in the recalculation scheme. In this study two limiting cases are taken: (a) jadeiite is calculated first (after Cawthorn and Collerson, 1974) and this will give a minimum value for CaTs and (b) acmite is calculated first and this will give a maximum value for CaTs.

(ii) the relationship between the mole fraction of CaTs and its activity is not fully understood. Wood (1976) studied the mixing

properties of CaTs and showed that in $CaMgSi_2O_6$ - $CaAl_2SiO_6$ solid solutions the activity of CaTs is greater than its mole fraction, and in $CaFeSi_2O_6$ - $CaAl_2SiO_6$ solid solutions the activity of CaTs is less than its mole fraction and that the two are approximately equal when the Fe/Fe+Mg ratio of the clinopyroxene is 0.6. The nature of the mixing is the subject of debate (Wood, 1976, 1978; Newton, 1978) and although this will affect the value of the activity coefficient and the way in which activity composition relations are expressed it does not affect Wood's (1976) experimentally measured activities.

(iii) Wood (1978, pers. comm.) found that the experimental results of Hariya and Kennedy (1968) are incorrect so that the activities and thermodynamic data for reaction (11) are not quite right; since, however, the two are interdependent in Wood's (1977) paper the results presented below are internally consistent.

In both FBD 5 and HR 178 the Mg/Mg+Fe ratio in clinopyroxene is greater than 0.6 so that the activity of CaTs is greater than its mole fraction. Because CaTs and plagioclase show the same size of positive deviations from ideality (see Orville (1972) for plagioclase), the ratio of the mole fraction is approximately the same as the activity ratio and it is the mole fraction ratio that is used in the following calculations.

P - T lines for reaction (11) using equation (12) are shown in Fig. 3. The maximum and minimum pressure region is well constrained in the trondhjemite HR 178 and suggests pressures in the range 9.5 to 10.5 at 800°C which is consistent with the results presented above for garnet-orthopyroxene-plagioclase-quartz equilibria.

9. DISCUSSION

The results of this study suggest that the peak of metamorphism in the Scourie granulites was at ca. 820°C and ca. 10 kb and that two-pyroxene temperatures based upon the Nehru-Wyllie experimental data for the diopside enstatite solvus are the most reliable.

O'Hara and Yarwood (1978) pointed out that pyroxene pairs will not preserve peak-of-metamorphism temperatures unless the closure temperature for pyroxene pairs is above the metamorphic temperature. The results of this study suggest that the pyroxene closure temperature is ca. 590°C and that the peak of metamorphism was at 820°C. It is possible, however, that the peak of metamorphism was higher than 820°C. Ilmenite - magnetite pairs and alkali feldspars in hypersolvus granite (see Chapters 4 and 5) suggest that these minerals equilibrated at temperatures in excess of 1000°C; it is probable, however, that these minerals reflect igneous temperatures and that the 820°C and 10 kb reflect the later granulite facies metamorphism.

TABLE 6 Estimates of the pressure and temperature of the Scourian Granulite facies metamorphism

Wood (1975b) (South Harris)	800 - 860°C	10 - 13 kb
Wood (1977) (South Harris)	825°C	13 kb
O'Hara and Yarwood (1978) (Scourie)	1150 ± 100°C	15 kb
Muecke (1969) (Scourie)	700 - 800°C	7 - 9 kb
Pride (pers. comm.) (Scourie)	916 ± 33°C	11 kb
This study (Chapter 7)	800°C (min.)	11 kb (max)
This study	820°C	10 kb

Estimates of pressure and temperature of the granulite facies metamorphism in the Scourian complex made by other workers are given in Table 6. O'Hara (in the discussion of Wood (1977)) pointed out that pressure and temperature estimates are usually derived independently from different mineral pairs and that there is no certain way of marrying the correct temperature to the appropriate pressure when a range of pressures and temperatures is apparent. This may help explain the very high P-T estimate of O'Hara and Yarwood (1978); the high pressure reported depends upon the high temperature estimate based upon two-feldspar thermometry. If the high feldspar temperatures reflect an igneous event, which predated the granulite facies metamorphism, as suggested above, the high pressure suggested is incorrect and a pressure lower than 12 kb is more appropriate.

The temperature of Pride (pers. comm.) is based upon the two pyroxene thermometer of Wells (1977) and compares well with a maximum temperature of 960°C for the Wells thermometer (T_2) in this study. The high pressure (ca. 13 kb) suggested by Wood for the Outer Hebrides is significantly greater than proposed here for the Scourie area and may reflect a real difference in the geothermal gradient between these two areas during the Scourian.

TITLE	SiO2	AL2O3	FEO	FE2O3	MGO	MNO	TIO2	CR2O3	CAO	NA2O
HRR 501 OP	51.58	3.60	24.69	0.00	19.52	.22	0.00	0.00	.32	0.00
HRR 501 CP	50.19	5.17	9.91	0.00	11.10	0.00	.65	.07	.52	.58
HRR 901 OP	51.01	3.17	24.20	0.00	19.07	.28	0.00	0.00	.35	0.00
HRR 901 CP CENTRE	49.40	5.71	9.57	0.00	10.09	0.00	.63	.13	22.53	.51
HRR 901 OP	51.01	3.17	24.20	0.00	19.07	.28	0.00	0.00	.35	0.00
HRR 901 CP EDGE	49.46	5.03	13.67	0.00	12.01	0.00	.56	.14	16.98	0.00
HRR 902 OP	51.44	3.15	24.04	0.00	20.13	.20	.15	0.00	.58	0.00
HRR 902 CP CENTRE	50.20	5.41	10.86	0.00	11.52	.16	.45	0.00	20.27	.46
HRR 902 OP	51.44	3.15	24.04	0.00	20.13	.20	.15	0.00	.58	0.00
HRR 902 CP EDGE	49.99	5.56	9.06	0.00	11.96	0.00	.59	0.00	20.74	.46
HRR 1201 OP	49.06	3.29	19.56	.48	21.07	.38	0.00	.14	.55	0.00
HRR 1201 CP	49.08	5.69	7.42	.96	12.37	.17	.34	.33	20.49	.67
HRR 1202 OP	50.06	3.02	19.17	.69	22.45	.36	0.00	.14	.30	0.00
HRR 1202 CP	49.08	5.69	7.42	.96	12.37	.17	.34	.33	20.49	.67
HRR 1207 OP	51.26	4.26	15.13	.04	23.17	.33	0.00	.13	.42	0.00
HRR 1206 CP	49.47	5.11	5.67	2.04	12.55	.16	.33	.36	21.43	.06
HRR 1209 OP	51.46	3.95	16.76	0.00	23.37	.29	0.00	.21	.29	0.00
HRR 1213 CP	49.20	5.52	6.24	1.26	11.93	0.00	.37	.42	22.47	.62
HRR 6201 OP	50.00	3.40	21.21	.43	21.41	.09	0.00	0.00	.37	0.00
HRR 6201 CP EDGE	49.16	4.39	7.34	1.24	11.91	.30	.59	0.00	21.75	.53
HRR 6202 OP	50.86	3.46	21.21	.43	21.41	.09	0.01	0.00	.37	0.00
HRR 6202 CP CENTRE	48.71	5.00	7.11	1.70	11.51	.28	.63	.17	21.73	.66
HRR 6204 OP	51.52	3.32	21.00	0.00	21.49	.04	0.00	.11	.41	0.00
HRR 6205 CP	49.26	4.06	6.95	1.33	12.15	.25	.55	.15	21.06	.53
HRR 6206 OP	51.07	2.22	21.16	0.00	22.19	.27	0.01	0.00	.19	0.00
HRR 6207 CP	49.57	5.36	7.33	1.05	11.97	.29	.63	.16	21.06	.62
HRR 18101 OP	53.03	2.74	12.06	.51	26.65	.33	0.00	.06	.52	0.06
HRR 18101 CP	51.22	3.75	5.13	.15	14.48	.13	.03	.26	22.16	.39
HRR 16102 OP	54.02	2.64	12.46	0.00	28.29	.00	0.00	.13	.43	0.00
HRR 16102 CP	50.03	3.00	5.90	0.00	14.19	.13	.08	.32	21.91	.26

TABLE 7 (a). Analyses of coexisting orthopyroxenes (OP) and clinopyroxenes (CP) used in temperature calculations.

TITLE	SIO2	AL2O3	FeO	FE2O3	MGO	MNO	TIO2	Cr2O3	CAO	NA2O
HRR 19611 OP	52.77	1.50	26.23	0.00	19.40	.36	0.00	0.00	.70	0.00
HRR 19601 CP	51.46	2.46	10.64	0.00	11.67	.15	.27	.00	21.71	.05
HRR 19610 OP	51.71	3.31	26.21	0.00	16.63	.48	0.00	0.00	.25	0.00
HRR 19611 CP	51.72	2.45	10.24	.78	11.89	.18	.17	.16	21.00	.53
HRR 19613 OP	51.05	1.45	26.86	0.00	18.74	.41	0.00	0.00	.59	0.00
HRR 19612 CP	52.10	2.46	8.96	.81	12.17	.25	.35	.22	22.69	.57
HRR 19612 OP	52.25	2.12	24.88	0.00	19.56	.45	0.00	0.00	.37	0.00
HRR 19661 CP	51.20	3.37	9.93	0.00	12.21	.21	.18	.15	21.81	.31
HRR 19662 OP	52.43	2.33	24.71	0.00	20.31	.43	0.00	0.00	.45	0.00
HRR 19662 CP	51.11	3.24	9.42	.80	11.85	.23	.45	.11	22.00	.55
HRR 21707 OP	50.33	2.80	25.68	0.00	18.47	.45	.13	0.00	.45	0.00
HRR 21701 CP	51.43	5.06	9.57	0.00	11.00	.12	.60	0.00	22.82	.29
HRR 420 01 OP	51.59	2.27	24.63	.49	19.89	.63	.22	0.00	.04	.02
HRR 420 01 CP	50.75	3.69	9.11	1.43	12.07	.25	.45	0.00	21.23	.65
HRR 428 02 OP	51.32	2.54	23.46	.28	20.72	.58	.14	0.00	.37	.01
HRR 428 02 CP	50.48	4.03	7.59	2.56	11.83	.23	.50	0.00	22.22	.72
HRR 428 03 OP	51.34	2.58	24.20	.42	20.18	.61	.07	0.00	.49	.01
HRR 428 03 CP	50.65	3.86	7.99	1.72	12.12	.23	.47	0.00	21.86	.08
HRR 428 04 OP	51.44	2.44	24.11	.45	20.29	.60	.08	0.00	.51	.01
HRR 428 04 CP	50.00	3.78	7.67	2.99	12.13	.25	.46	0.00	21.73	.72
HRR 428 04 OP	51.44	2.44	24.11	.45	20.29	.60	.08	0.00	.51	.01
HRR 428 04 CP HOMOG	50.51	3.78	9.90	2.14	12.41	.26	.62	0.00	20.01	.65
HRR 428 05 OP	51.19	2.48	24.07	1.23	20.16	.59	.11	0.00	.53	.03
HRR 428 05 CP	50.63	3.66	9.29	1.66	12.53	.23	.46	0.00	20.33	.73
HRR 428 06 OP	51.54	2.19	24.39	0.00	20.10	.60	.06	0.00	.41	.01
HRR 428 06 CP	50.05	3.84	7.90	3.44	12.14	.28	.49	0.00	22.06	.72
HRR 41 01 OP	50.77	2.91	23.24	.39	20.42	.53	.10	.01	.38	.03
HRR 41 01 CP	49.06	4.55	6.89	1.42	11.56	.24	.64	.01	21.77	.64
HRR 41 02 OP	51.32	2.76	24.13	.52	20.79	.53	.05	0.00	.47	.02
HRR 41 02 CP	49.96	4.48	8.32	1.68	11.92	.27	.45	0.00	21.56	.56

TABLE 7 (a). continued

TITLE	SIO2	AL2O3	FEO	FE2O3	MGO	MNO	TIO2	CR2O3	CAO	NA2O
HRR 41 03 OP	51.07	2.61	24.06	0.00	20.18	.54	.06	0.00	.38	0.00
HRR 41 03 CP	49.21	4.72	7.25	3.65	11.61	.24	.54	0.00	21.47	.57
HRR 41 04 OP	51.21	2.69	23.22	.49	20.06	.51	.06	.01	.43	.04
HRR 41 04 CP	50.17	4.41	6.92	2.42	11.93	.22	.47	0.00	22.56	.67
HRR 41 05 OP	50.92	2.60	23.34	.40	20.34	.52	.04	0.00	.30	.69
HRR 41 05 CP	50.29	4.11	9.21	0.00	12.29	.20	.44	.01	20.07	.67
HRR 41 06 OP	51.06	2.06	22.56	.07	20.96	.54	.05	.01	.32	.05
HRR 41 06 CP	49.29	4.15	9.50	.99	12.40	.22	.46	.01	19.19	.01
HRR 41 07 OP	51.24	2.47	23.64	.53	20.55	.55	.01	.01	.29	.02
HRR 41 07 CP	50.00	4.42	0.36	.23	12.35	.21	.49	0.00	20.75	.06
HRR 41 08 OP	44.16	2.91	29.30	0.00	14.23	.49	0.01	.01	2.16	.17
HRR 41 08 CP	49.36	4.87	7.49	1.04	11.66	.24	.60	0.00	21.92	.74
HRR 41 09 OP	51.17	2.64	23.18	.61	20.62	.54	.03	.01	.30	.05
HRR 41 09 CP	48.33	4.42	0.07	2.52	12.15	.25	.64	0.00	20.05	.61
HRR 70 01 OP	52.20	1.60	23.25	.44	21.35	.66	.04	.05	.30	0.00
HRR 70 01 CP	51.57	2.73	7.92	2.00	12.46	.32	.25	.00	21.00	.75
HRR 70 02 OP	51.93	1.59	23.36	.69	21.14	.74	.05	.04	.02	0.00
HRR 70 02 CP	51.33	2.58	7.65	1.77	12.01	.33	.23	.07	21.41	.72
FBD 5 01 OP	51.26	1.68	23.60	.43	20.42	.77	.07	0.00	.06	0.00
FBD 5 01 CP	50.09	2.76	7.46	2.45	12.49	.31	.32	.05	21.52	.72
FBD 3 01 OP	51.64	1.66	23.95	.46	20.39	.68	.07	.05	.54	.03
FBD 3 01 CP	51.17	2.65	0.11	1.88	12.35	.27	.31	.10	21.65	.72

TABLE 7 (a). continued

TITLE	SI	ALTET	ALOCT	FE2	FE3	MG	MN	TI	CR	CA	NA
HRR 501 OP	1.9206	.0794	.0884	.7725	0.0000	1.1106	.0070	0.0000	0.0000	.0126	0.0000
HRR 501 CP	2.2056	-.2056	.4732	.3640	0.0000	.7319	0.0000	.0213	.3623	.6700	.0426
HRR 901 OP	1.9361	.0639	.0779	.7602	0.0000	1.1240	.0088	0.0000	0.0000	.0140	0.0000
HRR 901 OP CENTRE	1.8784	.1216	.1344	.3043	0.0000	.6171	0.0000	.0180	.0039	.8772	.0376
HRR 901 OP	1.9361	.0639	.0779	.7602	0.0000	1.1240	.0088	0.0000	0.0000	.0140	0.0000
HRR 901 CP EDGE	1.8818	.1182	.1169	.4378	0.0000	.7626	0.0000	.0161	.0042	.6968	0.0000
HRR 902 OP	1.9343	.0657	.0739	.7560	0.0000	1.1261	.0062	.0041	0.0000	.0234	0.0000
HRR 902 OP CENTRE	1.8920	.1080	.1324	.3423	0.0000	.6471	.0051	.0128	0.0000	.6166	.0336
HRR 902 OP	1.9343	.0657	.0739	.7560	0.0000	1.1261	.0062	.0041	0.0000	.0234	0.0000
HRR 902 CP EDGE	1.8814	.1182	.1285	.3085	0.0000	.6716	0.0000	.0167	0.0000	.8366	.0356
HRR 1201 OP	1.9104	.0896	.0655	.6256	.0139	1.2527	.0124	0.0000	.0043	.0227	0.0000
HRR 1201 CP	1.8686	.1314	.1240	.2362	.0275	.7019	.0055	.0097	.0099	.8359	.0495
HRR 1202 OP	1.9209	.0791	.0554	.6654	.0196	1.2916	.0115	0.0000	.0042	.0121	0.0000
HRR 1202 CP	1.8686	.1314	.1240	.2362	.0275	.7019	.0055	.0097	.0099	.8359	.0495
HRR 1207 OP	1.9455	.0545	.0896	.5947	.0012	1.2836	.0104	0.0000	.0038	.0167	0.0000
HRR 1206 CP	1.8672	.1328	.0946	.1791	.0500	.7359	.0051	.0094	.0113	.8869	.0498
HRR 1209 OP	1.9142	.0858	.0876	.5843	0.0000	1.2971	.0091	0.0000	.0062	.0116	0.0000
HRR 1210 CP	1.8647	.1353	.1113	.1978	.0359	.6739	0.0000	.0105	.0126	.9125	.0456
HRR 6201 OP	1.9182	.0818	.0696	.6699	.0122	1.2049	.0265	0.0000	0.0000	.0150	0.0000
HRR 6201 CP EDGE	1.8725	.1275	.0970	.2343	.0357	.6775	.0097	.0169	0.0000	.8695	.0392
HRR 6202 OP	1.9182	.0818	.0696	.6699	.0122	1.2049	.0265	0.0000	0.0000	.0150	0.0000
HRR 6202 CP CENTRE	1.8485	.1515	.1060	.2258	.0510	.6510	.0090	.0188	.0051	.8636	.0400
HRR 6204 OP	1.9277	.0723	.0741	.6569	0.0000	1.2262	.0266	0.0000	.0033	.0164	0.0000
HRR 6205 CP	1.8734	.1266	.0916	.2215	.0361	.6695	.0081	.0158	.0045	.8919	.0391
HRR 6206 OP	1.9523	.0477	.0505	.6663	0.0000	1.2561	.0245	0.0000	0.0000	.0077	0.0000
HRR 6207 CP	1.8644	.1356	.1021	.2306	.0383	.6710	.0092	.0178	.0048	.8816	.0452
HRR 18101 OP	1.9341	.0659	.0497	.3623	.0137	1.5420	.0099	0.0000	.0023	.0240	0.0000
HRR 18101 CP	1.9243	.0757	.0982	.1513	.0044	.8100	.0043	.0006	.0077	.8920	.0264
HRR 18102 OP	1.9505	.0495	.0629	.3770	0.0000	1.5225	.0090	0.0000	.0036	.0164	0.0000
HRR 18102 CP	1.9270	.0730	.0876	.1867	0.0000	.8082	.0042	.0021	.0094	.8682	.0147

TABLE 7 (b). Coexisting orthopyroxene (OP) and clinopyroxene (CP) pairs used in temperature calculations. (Cations to six oxygens).

TITLE	SI	ALTET	ALOCT	FE2	FE3	MG	MN	TI	CR	CA	NA
HRR 19601 OP	1.0777	.0223	.0440	.0221	0.0000	1.0836	.0114	0.0000	0.0000	.0261	0.0000
HRR 19601 CP	1.0561	.0439	.0664	.3445	0.0000	.6612	.0047	.0077	.0023	.8641	.0164
HRR 19610 OP	1.0436	.0564	.0803	.0239	0.0000	1.0436	.0153	0.0000	0.0000	.0101	0.0000
HRR 19611 CP	1.0467	.0533	.0554	.3222	.0221	.6670	.0057	.0048	.0048	.8792	.0307
HRR 19613 OP	1.0748	.0252	.0398	.8539	0.0000	1.0617	.0132	0.0000	0.0000	.0240	0.0000
HRR 19612 CP	1.0421	.0579	.0502	.2792	.0228	.6761	.0079	.0096	.0065	.9063	.0412
HRR 19912 OP	1.0625	.0375	.0582	.7966	0.0000	1.1049	.0146	0.0000	0.0000	.0152	0.0000
HRR 19901 CP	1.0303	.0697	.0801	.3136	0.0000	.6660	.0065	.0051	.0045	.8811	.0223
HRR 19902 OP	1.0568	.0432	.0593	.7714	0.0000	1.1298	.0134	0.0000	0.0000	.0160	0.0000
HRR 19902 CP	1.0229	.0771	.0666	.2964	.0228	.6644	.0072	.0126	.0031	.8866	.0405
HRR 21707 OP	1.0449	.0551	.0740	.8222	0.0000	1.0538	.0146	.0037	0.0000	.0185	0.0000
HRR 21701 CP	1.0958	.1050	.1122	.2949	0.0000	.6371	.0036	.0167	0.0000	.9010	.0204
HRR 428 01 OP	1.0374	.0626	.0379	.7737	.0137	1.1132	.0200	.0062	0.0000	.0338	.6015
HRR 428 01 CP	1.0089	.0911	.0725	.2666	.0405	.6766	.0080	.0127	0.0000	.6556	.0474
HRR 428 02 OP	1.0360	.0640	.0490	.7401	.0079	1.1649	.0185	.0040	0.0000	.0150	.0067
HRR 428 02 CP	1.0870	.1130	.0649	.2377	.0723	.6601	.0073	.0141	0.0000	.8914	.6523
HRR 428 03 OP	1.0336	.0650	.0496	.7628	.0120	1.1335	.0195	.0020	0.0000	.0198	.0067
HRR 428 03 CP	1.0030	.0970	.0713	.2512	.0486	.6767	.0073	.0133	0.0000	.6801	.0495
HRR 428 04 OP	1.0375	.0625	.0458	.7596	.0128	1.1390	.0191	.0023	0.0000	.0206	.0067
HRR 428 04 CP	1.0684	.1116	.0538	.2456	.0640	.6747	.0079	.0125	0.0000	.8698	.8521
HRR 428 04 OP	1.0375	.0625	.0458	.7596	.0128	1.1390	.0191	.0023	0.0000	.0206	.0067
HRR 428 04 CP HOMOG	1.0925	.1075	.0595	.3103	.0614	.6930	.0069	.0175	0.0000	.0633	.0472
HRR 428 05 OP	1.0269	.0731	.0370	.7579	.0320	1.1276	.0188	.0031	0.0000	.0214	.0022
HRR 428 05 CP	1.0212	.0888	.0741	.2933	.0455	.7049	.0074	.0114	0.0000	.6102	.0534
HRR 428 06 OP	1.0581	.0419	.0554	.7690	0.0000	1.1293	.0192	.0017	0.0000	.0166	.0007
HRR 428 06 CP	1.0816	.1194	.0606	.2444	.0958	.6636	.0088	.0136	0.0000	.8742	.0516
HRR 41 01 OP	1.0291	.0809	.0488	.7340	.0203	1.1504	.0178	.0028	.0003	.0154	.0022
HRR 41 01 CP	1.0762	.1238	.0966	.2555	.0404	.6506	.0077	.0182	.0003	.0089	.0498
HRR 41 02 OP	1.0307	.0693	.0531	.7277	.0148	1.1656	.0169	.0014	0.0000	.0189	.0015
HRR 41 02 CP	1.0833	.1079	.0931	.2635	.0369	.6731	.0087	.0128	0.0000	.8753	.0426

TABLE 7 (b). continued

TITLE	SI	ALTET	ALOCT	FE2	FE3	MG	MN	TI	CR	CA	NA
HRR 41 03 OP	1.9368	.0632	.0624	.7612	0.0000	1.1406	.0173	.0017	0.0000	.0154	0.0000
HRR 41 03 CP	1.8494	.1506	.0585	.2278	.1032	.6615	.0076	.0153	0.0000	.0047	.0415
HRR 41 04 OP	1.9328	.0672	.0525	.7328	.0140	1.1621	.0163	.0017	.0003	.0174	.0025
HRR 41 04 CP	1.8795	.1205	.0743	.2168	.0683	.6661	.0070	.0132	0.0000	.0056	.0487
HRR 41 05 OP	1.9373	.0627	.0539	.7426	.0132	1.1535	.0166	.0011	0.0000	.0122	.0006
HRR 41 05 CP	1.9230	.0770	.1089	.2946	0.0000	.7016	.0065	.0127	.0003	.0226	.0497
HRR 41 06 OP	1.9244	.0756	.0515	.7116	.0246	1.1773	.0172	.0014	.0003	.0129	.0037
HRR 41 06 CP	1.9004	.0996	.0694	.3068	.0269	.7139	.0072	.0134	.0003	.0044	.0457
HRR 41 07 OP	1.9377	.0623	.0478	.7475	.0150	1.1582	.0176	.0003	.0003	.0118	.0015
HRR 41 07 CP	1.9176	.0924	.1164	.2668	.0067	.7022	.0068	.0141	0.0000	.0463	.0468
HRR 41 08 OP	1.8739	.1261	.0910	.2355	.0522	.6571	.0077	.0171	0.0000	.0081	.0513
HRR 41 09 OP	1.9333	.0667	.0511	.7340	.0173	1.1633	.0173	.0059	.0003	.0122	.0037
HRR 41 09 CP	1.8685	.1315	.0675	.2577	.0725	.6058	.0081	.0184	0.0000	.0449	.0452
HRR 70 01 OP	1.9565	.0435	.0272	.7280	.0125	1.1926	.0210	.0011	.0015	.0153	0.0000
HRR 70 01 CP	1.9305	.0695	.0516	.2478	.0565	.6963	.0101	.0078	.0024	.0044	.0544
HRR 70 02 OP	1.9530	.0470	.0235	.7346	.0156	1.1792	.0236	.0014	.0012	.0169	0.0000
HRR 70 02 CP	1.9303	.0697	.0510	.2414	.0561	.7262	.0105	.0065	.0021	.0054	.0527
FBD 5 01 OP	1.9541	.0459	.0296	.7523	.0122	1.1602	.0249	.0023	0.0000	.0188	0.0000
FBD 5 01 CP	1.9206	.0794	.0439	.2345	.0697	.7053	.0099	.0085	.0015	.0737	.0529
FBD 3 01 OP	1.9540	.0460	.0289	.7581	.0138	1.1498	.0218	.0020	.0015	.0219	.0022
FBD 3 01 CP	1.8261	.1739	.0526	.2552	.0533	.6924	.0086	.0088	.0038	.0732	.0525

TABLE 7 (b). continued

TITLE	SIO2	AL2O3	FEO	FE2O3	MGO	MNO	TIO2	CR2O3	CAO	NA2O
HR5 01 GT	39.27	21.76	24.91	0.00	7.18	.84	.08	.06	6.83	0.00
HR5 01 CP	50.03	5.26	10.62	0.00	11.43	.06	.60	.04	20.00	.61
HR5 02 GT	39.43	21.85	27.62	0.00	5.64	.41	0.00	0.00	6.72	0.00
HR5 02 CP	50.79	5.14	10.14	0.06	11.63	.20	.63	.14	20.48	.67
HR9 01 GT	39.30	21.63	23.05	0.00	8.13	.57	.16	.14	6.30	0.00
HR9 01 CP	49.78	5.43	9.19	0.00	11.64	0.00	.65	.13	20.04	.71
HR9 02 GT	39.41	21.74	23.92	0.00	8.23	.58	.08	.07	6.27	0.00
HR9 02 CP CENTRE	48.68	5.59	8.86	0.60	11.41	0.00	.60	0.00	21.56	.56
HR9 03 GT	39.41	21.74	23.92	0.00	8.23	.58	.08	.07	6.27	0.00
HR9 03 CP EDGE	49.55	5.38	9.22	0.00	12.06	0.00	.66	.18	20.83	.41
HR62 01 GT CENTRE	38.93	20.74	23.76	0.00	6.61	1.01	.16	0.00	8.93	0.00
HR62 01 CP CENTRE	47.31	5.80	7.11	1.78	11.51	.26	.63	.17	21.73	.66
HR62 02 GT EDGE	39.08	21.49	24.53	0.00	7.22	.47	0.00	0.00	7.34	0.00
HR62 02 CP EDGE	49.26	4.86	6.95	1.33	12.15	.25	.55	.15	21.66	.53
HR196 01 GT	38.79	20.72	27.52	0.00	4.52	.77	.23	0.00	8.00	0.21
HR196 01 CP EDGE	51.14	2.39	11.39	0.30	11.46	.16	.24	0.00	21.38	0.00
HR196 02 GT	38.79	20.72	27.52	0.00	4.52	.77	.23	0.00	8.00	0.21
HR196 02 CP CENTRE	51.77	2.53	10.28	0.00	11.88	.13	.30	.15	20.83	.50
HR199 01 GT	39.00	20.99	27.04	0.00	5.30	.07	.15	0.00	7.68	0.06
HR199 01 CP	51.16	3.31	9.32	.73	12.03	.21	.31	.13	21.79	.43
HR200 01 GT CENTRE	37.77	20.34	25.99	0.86	3.55	2.17	.20	0.00	9.51	0.00
HR200 01 CP	50.47	2.52	9.17	1.91	11.65	.69	.27	0.00	20.69	.67
HR200 02 GT EDGE	37.96	20.95	26.34	0.00	5.22	2.09	0.00	0.00	7.10	0.00
HR200 02 CP	50.17	2.52	9.17	1.91	11.65	.69	.27	0.00	20.69	.67
HR217 01 GT	39.46	21.16	23.47	0.00	6.11	.39	.06	0.00	7.55	0.00
HR217 01 CP	51.60	1.54	9.71	.45	11.48	.24	0.00	.15	22.07	.58
HR217 02 GT	40.21	21.45	22.26	0.00	6.41	.53	.04	0.00	7.59	0.00
HR217 02 CP	51.43	5.00	9.46	.12	11.68	.12	.68	0.00	22.02	.29

TABLE 8. Analyses of coexisting garnet (GT) and clinopyroxene (CP) used in temperature calculations (see Table 4).

TITLE	SIO2	AL2O3	FEO	FE2O3	MGO	MNO	TIO2	CR2O3	CAO	NA2O
HR5 01 OP	51.66	2.43	25.36	0.00	19.92	.24	0.00	0.00	.41	0.00
HR5 01 GT CENTRE	39.02	21.73	24.75	0.00	7.04	.87	.14	.12	6.93	0.00
HR5 02 OP	51.66	2.43	25.36	0.00	19.92	.24	0.00	0.00	.41	0.00
HR5 02 GT EDGE	39.57	21.57	25.14	0.00	7.43	.84	0.00	0.00	6.72	0.00
HR5 03 OP	51.66	2.43	25.36	0.00	19.92	.24	0.00	0.00	.41	0.00
HR5 03 GT ON OPAQUE	39.43	21.88	27.62	0.00	5.04	.41	0.00	0.00	6.72	0.00
HR9 01 OP	51.44	3.15	24.04	0.00	20.13	.20	0.00	0.00	.58	0.00
HR9 01 GT CENTRE	39.30	21.63	23.85	0.00	6.17	.57	.16	.14	6.30	0.00
HR9 02 OP	51.44	3.15	24.04	0.00	20.13	.20	0.00	0.00	.58	0.00
HR9 02 GT EDGE	39.51	21.85	23.96	0.00	6.27	.57	.16	.14	6.30	0.00
HR62 01 OP	51.16	3.36	21.20	0.00	21.70	.07	0.00	.06	.39	0.00
HR62 01 GT CENTRE	38.53	20.74	23.76	0.00	6.61	1.01	.16	0.00	6.93	0.00
HR62 02 OP	51.16	3.36	21.20	0.00	21.70	.07	0.00	.06	.39	0.00
HR62 02 GT EDGE	38.60	21.49	24.53	0.00	7.22	.47	0.00	0.00	7.34	0.00
HR196 01 OP EDGE	51.71	3.31	26.21	0.00	18.63	.48	0.00	0.00	.25	0.00
HR196 01 GT EDGE	38.31	20.87	27.57	0.00	4.56	.78	.19	0.00	8.10	0.00
HR196 02 OP CENTRE	52.77	1.56	26.23	0.00	19.40	.36	0.00	0.00	.70	0.00
HR196 02 GT CENTRE	39.06	20.77	27.62	0.00	4.66	.91	.26	0.00	6.89	0.00
HR199 01 OP	51.96	2.20	24.77	0.00	19.99	.43	0.00	0.00	.42	0.00
HR199 01 GT	39.02	20.99	27.65	0.00	5.08	.78	.15	0.00	7.68	0.00
HR217 01 OP	51.62	2.66	25.35	0.00	19.00	.42	.07	0.00	.45	0.00
HR217 01 GT	39.04	21.39	26.16	0.00	6.26	.46	.05	0.00	7.57	0.00
HR275 01 OP	50.45	2.31	26.18	0.00	19.20	.19	.06	.17	.24	.14
HR275 01 GT	38.58	22.38	26.76	0.00	7.72	1.15	.16	0.00	2.41	0.00

TABLE 9. Analyses of coexisting garnet (GT) and orthopyroxene (OP) used in pressure calculations (see Table 5).

Conclusions

CONCLUSIONS

From the results of this study I propose that:

(1) the gabbro-tonalite-trondhjemite-granodiorite-granite suite of the Scourian complex of N.W. Scotland represents highly deformed and metamorphosed plutonic igneous rocks whose formation 2900 Ma. ago represents the generation of new continental crust.

(2) tonalitic magma was derived by the partial melting of amphibolite (possibly island arc tholeiite) either at the base of a thick lava pile or in a subduction zone and that trondhjemite, granodiorite and granite evolved from tonalite by the fractional crystallisation of plagioclase and hornblende at depths of less than 60 km.

(3) layered gabbroic-ultramafic complexes enclosed in the quartzofeldspathic gneisses not directly related to the original tonalites and trondhjemites and do not represent the crystal residue generated during the fractional crystallisation of trondhjemite and granodiorite from tonalite. Amphibolites enclosed in trondhjemitic gneiss, at Gruinard Bay, are chemically similar to island arc tholeiites and may represent basaltic lavas, the majority of which were partially melted to form tonalite. The gabbros and (metavolcanic?) amphibolites are probably related, and form complimentary parts of a basic volcanic-plutonic suite; the more refractory gabbros survived partial melting.

(4) there are significant differences between amphibolite and granulite facies areas in the Scourian complex: (a) the principal magma-type in the granulite facies areas is tonalite whereas in amphibolite facies areas it is trondhjemite or granodiorite; (b) there is a bimodal distribution of rock types as plotted on an A-F-M diagram in amphibolite facies areas, whereas in granulite facies areas there is a continuum of rock

types; (c) basic rocks in granulite facies areas are represented by layered ultramafic-gabbroic complexes; in amphibolite facies areas amphibolites (possible metalavas) are more common and ultramafic rocks are relatively rare.

The differences represent different erosional levels in the complex and suggest that fractional crystallisation processes (giving rise to trondhjemite and granodiorite) are more important at higher levels in the crust.

(5) there is an increase in K_2O southwards across the complex from Scourie to Torridon, which is probably a function of the level of exposure. Alternatively the three areas studied represent three sections through different 'plutons' which by chance show the potash relationship. It would be unwise, with our present knowledge of the Scourian, to infer depths of origin in a batholithic environment from the increase in K_2O towards the south.

(6) Granulite facies metamorphism depleted originally wet tonalitic and trondhjemitic magmas in LIL elements but not K. Relatively dry granitic magmas were not depleted during granulite facies metamorphism.

(7) Both igneous and metamorphic thermal events are identifiable in the Scourie granulites. Igneous temperatures are preserved in some trondhjemites (greater than 1000^{o}C) and granites (greater than 1100^{o}C). The peak of the granulite facies metamorphism at ca. 2700 Ma. was ca. 820^{o}C and ca. 10 kb, indicating a geothermal gradient of ca. 23^{o}C/km, which is consistent with determinations from other Archaean high-grade areas (Tarney and Windley, 1977) but is higher than the average present day continental geotherm.

(8) the peak of granulite facies metamorphism in the Scourie area is different from that determined by Wood (1967) for the Outer Hebrides (ca. 825^{o}C, 13 kb) and reflects a real difference in geothermal gradient between the two areas.

(9) many temperatures obtained reflect cooling history; different mineral pairs became closed systems at different temperatures. Between 660°C and 530°C water was introduced into cooling granite sheets and the reequilibration of Rb and Sr isotopes in these rocks at 2420 Ma dated this event.

(10) the Scourian complex cooled relatively rapidly and the cooling curve (temperature vs. time) is concave upwards, as suggested by O'Hara (1977) and not concave downwards, as suggested by Dickinson and Watson (1976).

(11) the moderately high pressure origin of these rocks (ca. 10 kb) suggests that the Archaean crust was at least 35 km thick; geophysical evidence indicates that the present crustal thickness is 25 to 30 km (Bamford and Prodehl, 1977) implying an Archaean crust ca. 60 km thick.

Windley and Smith (1976) proposed that Archaean high-grade terrains are equivalent to the deep seated levels of modern granitic batholiths located along active continental margins. They based their argument principally on a comparison between the layered ultramafic-gabbro-anorthosite complexes found in Archaean terrains and Mesozoic-Cenozoic batholiths. Also Tarney (1976) recognised the chemical similarity between the Archaean quartzofeldspathic gneisses and the Palaeozoic tonalite-granodiorite plutons developed along the active continental margin of the Caledonide fold belt of Scotland. A consideration of the magmatic processes which gave rise to the quartzofeldspathic rocks which make up 80-85% of the Scourian complex and of the thermal history of the Scourian complex supports the batholith model of Tarney (1976) and Windley and Smith (1976).

The magma-types present in the Scourian complex, (tonalite, trondhjemite, granodiorite], their relative ages (gabbro and minor sediments intruded by tonalite, followed by trondhjemite and then granodiorite), their chemistry (they define a calc-alkaline trend on an A-F-M diagram) and their petrogenesis (tonalite evolved by partial melting of basalt and subsequent fractionation to trondhjemite and granodiorite) all invite comparison with Mesozoic-Cenozoic batholiths located along the western coast of North and South America.

The presence of high pressure granulites also supports the batholith model, for high pressure granulites imply an unusually thickened crust, with a higher than average geothermal gradient; Phanerozoic granulites are rare but are reported from the British Columbia Batholith (Hollister, 1975). The addition to the crust, during the Archaean, of large volumes of magma whose buoyant uprise was halted by loss of heat can account for both a thickened crust and the thermal input necessary for a high geothermal gradient and is consistent with a batholithic model for the generation of Archaean granulites. Bridgwater et al. (1974), however, suggest that the main agent of crustal thickening in the Archaean of Greenland was the piling up of thrust sheets and nappes and the injection of concordant calc-alkaline intrusions. I propose that in the case of the Scourian complex the situation was different from Greenland inasmuch as there was no earlier crust to thicken (i.e. no equivalent of the Amitsoq gneisses) and that new crust was generated by the addition of tonalitic magmas to an early (? island arc) lava pile and that the principal agent of crustal thickening was magmatic and not tectonic.

England and Richardson (1977) showed that it is possible to distinguish tectonically thickened crust from magmatically thickened crust by looking at the thermal history during erosion; tectonically

thickened crust initially increases in temperature during its rise to the surface, whereas magmatically thickened crust initially cools isobarically and shows extremes of pressure and temperature. High igneous temperatures of ca. 1100°C and lower metamorphic temperatures (ca. 800°C) in rocks of the same age suggest that the early history of the Scourian complex involved rapid cooling at possibly the same pressure and is more consistent with a magmatically thickened crust than a tectonically thickened one.

In summary, therefore, the Scourian complex was generated as new crustal material at 2900 Ma; tonalites were generated by the partial melting of amphibolite either at the base of a thickened lava pile or in a subduction zone and trondhjemite and granodiorite evolved at a slightly higher level in the crust by the fractional crystallisation of plagioclase and hornblende. Tonalitic magma was added to early basaltic crust and substantial crustal thickening took place at ca. 2900 Ma. The thick crust and thermal input from the addition of magmas gave rise to a high geothermal gradient in which granulites formed at depth and which were exposed by isostatic readjustment in response to erosion.

References

REFERENCES

ANDERSON, A.T. (1968a). The oxygen fugacity of alkali basalts and related magmas. Tristan da Cunha. Am. J. Sci. 266, 704-727.

ANDERSON, A.T. (1968b). Oxidation of the La Blache Lake titaniferous magnetite deposit, Quebec. J. Geol. 76, 528-547.

ANDERSON, A.T., BRAZIUNAS, T.F., JACOBY, J. and SMITH, J.V. (1972) Thermal and mechanical history of breccias 14306, 14063, 14270 and 14321. In, Proceedings of the third lunar science conference. (Supplement 3, Geochim. Cosmochim. Acta)1, 819-835.

ARNDT, N.T. (1977) The separation of magmas from partially molten peridotite. Ybk. Carnegie Inst. Wash. 76, 424-428.

ARTH, J.G. and BARKER, F. (1976) Rare earth partitioning between hornblende and dacitic liquid and implications for the genesis of trondhjemitic - tonalitic magmas. Geology 4, 534-536.

ARTH, J.G., BARKER, F., PETERMAN, Z.E. and FRIEDMAN, I. (1978) Geochemistry of the gabbro-diorite-tonalite-trondhjemite suite of southwest Finland and its implications for the origin of tonalitic and trondhjemitic magmas. J. Petrol. 19, 289-316.

ARTH, J.G. and HANSON, G.N. (1972) Quartz diorites derived by the partial melting of eclogite or amphibolite at mantle depths. Contrib. Mineral. Petrol. 37, 161-174.

ARTH, J.G. and HANSON, G.N. (1975) Geochemistry and origin of the

early Precambrian crust of northeastern Minnesota Geochim. Cosmochim. Acta 39, 325-362.

BAMFORD, D. and PROHDEL, C. (1977) Explosion seismology and the crust-mantle boundary. J. Geol. Soc. Lond. 134, 139-151.

BARKER, F. and ARTH, J.G. (1976) Generation of trondhjemitic-tonalitic liquids and Archaean bimodal trondhjemite-basalt suites. Geology 4, 596-600.

BARKER, F., ARTH, J.G., PETERMAN, Z.E. and FRIEDMAN, I. (1976) The 1·7- to 1·8- b.y.-old trondhjemites of southwestern Colorado and northern New Mexico: Geochemistry and depths of genesis. Geol. Soc. Am. Bull. 87, 189-198.

BAROOAH, B.C. (1970) Significance of calc-silicate rocks and meta-arkose in the Lewisian complex, southeast of Scourie. Scott. J. Geol. 6, 221-225.

BARTH, T.F.W. (1934) Polymorphic phenomena and crystal structure. Am. J. Sci. 5, 273.

BARTH, T.F.W. (1951) The feldspar geologic thermometers. Neues Jahrb. Mineral. 82, 143-154.

BARTH, T.F.W. (1952) Theoretical petrology. Wiley, New York. 387 pp.

BARTH, T.F.W. (1956) Studies in gneiss and granite. Norske Vidensk. Acad. Oslo I Mat-Naturv Klasse, 1, 263-274.

BARTH, T.F.W. (1962) The feldspar geologic thermometer. Norsk. Geol. Tidsskr. 42, 330-339.

BARTH, T.F.W. (1970) Additional data for the two-feldspar thermometer. Lithos, 1, 21-22.

BERTHELSON, A. (1960) Structural studies in the Precambrian of W. Greenland II Geology of Tovqussap Nuna. Gron. Geol. Unders. Bull. 25.

BICKLE, M.J. and NISBET, E. (1972) Oceanic affinities of some alpine mafic rocks based on their Ti-Zr-Y contents. J.Geol. Soc. Lond. 128, 267-271.

BISHOP, F.C. (1976) Partitioning of Fe^{2+} and Mg between ilmenite and some ferromagnesian silicates. Ph.D. Thesis. Univ. Chicago.

BLOXHAM, T.W., and LEWIS, A.D. (1972) Ti, Zr, Cr in some British pillow lavas and their petrogenetic affinities. Nature Phys. Sci. 273, 134-6.

BOHLEN, S.R. and ESSENE, E.J. (1977) Feldspar and oxide thermometry of granulites in the adirondack highlands. Contrib. Mineral. Petrol. 62, 153-169.

BOWES, D.R. (1978) Shield formation in early Precambrian time; the Lewisian complex. In D.R. Bowes and B.E. Leake Crustal evolution in northwestern Britain and adjacent regions. Geol. J. Spec. Issue 10.

BOWES, D.R., BAROOAH, B.C. and KHOURY, S.G. (1971) Original nature of the Archaean rocks of northwest Scotland. Spec. Pubs. Geol. Soc. Austral. 3, 77-92.

BOWLES, J.F.W. (1976) Distinct cooling histories of troctolites from the Freetown layered gabbro. Mineral. Mag. 40, 703-714.

BOWLES, J.F.W. (1977a) A method of tracing the temperature and oxygen fugacity histories of complex magnetite-ilmenite grains. Mineral. Mag. 41, 103-109.

BOWLES, J.F.W. (1977b) An estimate of the probable errors of the method of tracing the cooling history of complex magnetite-ilmenite grains and a discussion of the results produced by using different methods of treatment of the minor elements contained in these minerals when using the Buddington and Lindsley (1964) thermometer. Mineral. Mag. 41, M16-M17.

BOYD, F.R. (1973) A pyroxene geotherm. Geochim. Cosmochim. Acta. 37, 2533-2546.

BOYD, F.R. and ENGLAND, J.L. (1964) The system enstatite-pyrope. Ybk. Carnegie Inst. Wash. 63, 157-161.

BRIDGWATER, D., McGREGOR, V.R. and MYERS, J.S. (1974) A horizontal tectonic regime in the Archaean of Greenland and its implications for early crustal thickening. Precamb. Res. 1, 179-197.

BROOKS, C.K. and HART, S.R. (1974) On the significance of komatiite. Geology 2, 107-110.

BROWN, G.C. and BOWDEN, P. (1973) Experimental studies concerning the genesis of the Nigerian younger granites. Contrib. Mineral. Petrol. 40, 131-139.

BUDDINGTON, A.F. and LINDSLEY, D.H. (1964) Iron titanium oxide minerals

and synthetic equivalents. J. Petrol. 5, 310-357.

BURNHAM, C.W. and DAVIES, N.f. (1974) The role of H_2O in silicate melts II Thermodynamic and phase relations in the system $NaAlSi_3O_8$- H_2O to 10 kilobars, 700°C to 1100°C. Am. J. Sci. 274, 902-940.

CANN, J.R. (1969) Spilites from the Carlsberg ridge, Indian Ocean. J.Petrol. 10, 1-19.

CANN, J.R. (1970) Rb, Sr, Y, Zr, and Nb in some ocean floor basaltic rocks. Earth Planet. Sci. Lett. 10, 7-11.

CARMICHAEL, I.S.E. (1967) The iron titanium oxides of sialic volcanic rocks and their associated ferromagnesian silicates. Contrib. Mineral. Petrol. 14, 36-64.

CARMICHAEL, I.S.E. and NICHOLLS, J. (1967) Iron titanium oxides and oxygen fugacity in volcanic rocks. J. Geophys. Res. 72, 4665-4687.

CARMICHAEL, I.S.E., TURNER, F.J. and VERHOOGEN, J. (1974). Igneous petrology. McGraw Hill, New York. 739 pp.

CAWTHORN, R.G. (1976) Problems of electron microprobe analysis of quenched liquids. In Progress in experimental petrology; Natural Env. Res. Council 150.

CAWTHORN, R.G. and BROWN, P.A. (1976) A model for the formation and crystallisation of corrundum-normative calc-alkaline magmas through amphibole fractionation. J. Geol. 84, 467-476.

CAWTHORN, R.G. and BROWN, P.A. (1978) A model for the formation and

crystallisation of corrundum-normative calc-alkaline magmas through amphibole fractionation. A reply. J. Geol. 86, 272-275.

CAWTHORN, R.G. and COLLERSON, K.D. (1974) The recalculation of pyroxene end-member parameters and the estimation of ferrous-ferric iron content from electron microprobe analyses. Am. Mineral. 59, 1203-1208.

CAWTHORN, R.G., FORD, C.E., BIGGAR, G.M., BRAVO, M.S. and CLARKE, D.B. (1973) Determination of liquid composition in experimental samples: discrepancies between microprobe analyses and other methods. Earth Planet. Sci. Lett. 21, 1-5.

CHAPMAN, H.J. (1978) Geochronology and isotope geochemistry of Precambrian rocks from N.W.Scotland. D.Phil. thesis, Univ. Oxford.

CHAPMAN, H.J. and MOORBATH, S. (1977) Lead isotope measurements from the oldest recognised Lewisian gneisses of north-west Scotland. Nature 268, 41-42.

CHATTERJEE, N.D. and FROESE, E. (1975) The pseudobinary join Muscovite-paragonite. Am. Mineral. 60, 985-993.

COLBY, J.W. (1971) Magic IV a computer program for quantitative electron microprobe analysis. Unpubl.

COLLERSON, K.D. (1976) Composition and structural state of alkali feldspars from high grade metamorphic rocks, central Australia. Am. Mineral. 61, 200-211.

CONDIE, K.G. and HUNTER, D.R. (1976) Trace element geochemistry of Archaean granitic rocks from the Barberton region, South Africa. Earth. Planet.

Sci. Lett. 29, 389-400.

COWARD, M.P., FRANCIS, P.W., GRAHAM, R.H., MYERS, J.S. and WATSON, J.V. (1969) Remnants of an early metasedimentary assemblage in the Lewisian complex of the outer Hebrides. Proc. Geol. Ass. 80, 387-408.

CZAMANSKE, G.K. and MIHALIK, P. (1972) Oxidation during magmatic differentiation, Finnmarka complex, Oslo area, Norway: Part 1. The opaque oxides. J.Petrol. 13, 493-509.

DASGUPTA, H.C. (1970) Influence of temperature and oxygen fugacity on the fractionation of manganese between coexisting titanomagnetite and ilmenite. J. Geol. 78, 243-249.

DAVIES, F.B. (1974) A layered basic complex in the Lewisian, south of Loch Laxford, Sutherland. J. Geol. Soc. Lond. 130, 279-284.

DAVIES, F.B. (1975) Origin and ancient history of gneisses older than 2800 m.y. in the Lewisian complex. Nature 258, 589-591.

DAVIES, F.B. (1976) Early Scourian structures in the Scourie-Laxford region and their bearing on the evolution of the Laxford front. J. Geol. Soc. Lond. 132, 543-54.

DAVIES, F.B. (1977) The Archaean evolution of the Lewisian complex of Gruinard Bay. Scott. J. Geol. 13, 189-196.

DAVIES, F.B. (1978) Progressive simple shear deformation on the Laxford shear zone, Sutherland. Proc. Geol. Ass. 89, 177-196.

DAVIES, F.B. and WATSON, J.V. (1977) The early history of the type-Laxfordian complex, northwest Sutherland, Scotland. J. Geol. Soc. Lond.

133, 529-539.

DAVIS, B.T.C. and BOYD, F.R. (1966) The join $Mg_2Si_2O_6$ - $CaMgSi_2O_6$ at 30 kilobars pressure and its application to pyroxenes from kimberlites. J. Geophys. Res. 71, 3567-3576.

DEITRICH, V., EMMERMANN, R., OBERHANSLI, R. and PUCHELT, H. (1978) Geochemistry of basaltic and gabbroic rocks from the W. Mariana basin and Marianas trench. Earth Planet. Sci. Lett. 39, 127-144.

DICKENSON, B.B. and WATSON, J.V. (1976) Variations in crustal level and geothermal gradient during the evolution of the Lewisian complex of northwest Scotland. Precamb. Res. 3, 363-374.

DRAKE, M.J. and WEILL, D.F. (1975) Partitioning of Sr, Ba, Ca, Y, Eu^{2+} Eu^{3+} and other REE between plagioclase feldspar and magmatic liquid: an experimental study. Geochim. Cosmochim. Acta 39, 689-719.

DRURY, S.A. (1972) The chemistry of some granitic veins from the Lewisian of Coll and Tiree, Argyllshire, Scotland. Chem. Geol. 9, 175-193.

DRURY, S.A. (1978) REE distributions in a high grade gneiss complex in Scotland. Implications for the genesis of ancient sialic crust. Precamb. Res. 7, 239-257.

DUCHESNE, J.C. (1972) Iron titanium oxides in the Bjerkrem-Sogndal Massif, S.W. Norway. J.Petrol. 13, 57-81.

DUNHAM, A.C. (1971) The two feldspar geothermometer. Ann. Acad. Brazil cienc. 43, 627-631.

ELLIOT, R.B. (1973) The chemistry of gabbro amphibolite transitions in S.Norway. Contrib. Mineral. Petrol. 38, 71-79.

ENGEL, A.E.J. and ENGEL, C.G. (1962) Progressive metamorphism of amphibolite, northwest Adirondack mountains, New York. Mem. Geol. Soc. Am. (Buddington Volume) 37-82.

ENGLAND, P.C. and RICHARDSON, S.W. (1977) The influence of erosion upon the mineral facies of rocks from different metamorphic environments. J. Geol. Soc. Lond. 134, 201-213.

ERLANK, A.J. and KABLE, E.J.D. (1976) The significance of incompatible elements in Mid Atlantic ridge basalts for 45° N, with particular reference to Zr/Nb. Contrib. Mineral. Petrol. 54, 281-291.

EUGSTER, H.P. and WONES, D.R. (1962) Stability relations of the ferruginous biotite Annite. J.Petrol. 3, 82-125.

EVANS, B.W., SHAW, D.M. and HAUGHTON, D.R. (1969) Scapolite stoichiometry. Contrib. Mineral. Petrol. 24, 293-305.

FIELD, D. and CLOUGH, P.W.L. (1976) K/Rb ratios and metasomatism in metabasites from a Precambrian amphibolite-granulite transition zone. J. Geol. Soc. Lond. 132, 277-288.

FIELD, D. and ELLIOT, R.B. (1974) The chemistry of gabbro-amphibolite transitions in S.Norway. Trace elements. Contrib. Mineral. Petrol. 47, 63-76.

FLOYD, P.A., LEES, G.J. and ROACH, R.A. (1976) Basic intrusions in the Ordovician of North Wales - geochemical data and tectonic setting. Proc. Geol. Ass. 87, 389-400.

FLOYD, P.A. and WINCHESTER, J.A. (1975) Magma type and tectonic setting discrimination using immobile elements. Earth Planet. Sci. Lett. 27, 211-218.

FYFE, W.S. (1973) The granulite facies, partial melting and the Archaean crust. Phil Trans. R. Soc. Lond. A. 273, 457-461.

FYFE, W.S., TURNER, F.J. and VERHOOGEN, J. (1958) Metamorphic reactions and metamorphic facies. Geol. Soc. Am. Mem. 73, 259 pp.

GASTIL, R.G., KRUMMENACHER, D., DOUPONT,J. and BUSHEE, J. (1974) The batholith belt of southern California and western Mexico. Pacific Geol. 8, 73-78.

GHENT, E.D. (1976) Plagioclase-garnet-Al_2SiO_5-quartz; a potential geobarometer-geothermometer. Am. Mineral. 61, 710-714.

GILETTI, B.J., MOORBATH, S. and LAMBERT, R.ST. J., (1961) A geochronological study of the metamorphic complexes of the Scottish highlands. Q. J. Geol. Soc. Lond. 117, 233-264.

GILL,J. (1970) Geochemistry of Vitu Levu, Fiji and its evolution as an island arc. Contrib. Mineral. Petrol. 27, 179-203.

GILL, J.B. (1978) Role of trace element partition coefficients in models of andesite genesis. Geochim. Cosmochim. Acta. 42, 709-724.

GOLDSMITH, J.R. (1976) Scapolites, granulites and volatiles in the lower crust. Bull. Geol. Soc. Am. 87, 161-168.

GOLDSMITH, J.R. and NEWTON, R.C. (1974) An experimental determination of the alkali feldspar solvus. In, W.S.MacKenzie and J.Zussman (Eds) The feldspars. Manchester Univ. Press: Manchester. 337-359.

GOLDSMITH, J.R. and NEWTON, R.C. (1977) Scapolite-plagioclase stability relations at high pressures and temperatures in the system $NaAlSi_3O_8$-$CaAlSi_3O_8$-$CaCO_3$-$CaSO_4$. Am. Mineral. 62, 1063-1081.

GRAY, C.M. (1977) The geochemistry of central Australian granulites in relation to the chemical and isotopic effects of granulite facies metamorphism. Contrib. Mineral Petrol. 65, 79-89.

GREEN, D.H. and LAMBERT, I.B. (1965) Experimental crystallisation of anhydrous granite at high pressures and temperatures. J. Geophys. Res. 70, 5259-5268.

GREEN, T.H., BRUNFELT, A.O. and HEIER, K.S. (1972) Rare earth element distribution and K/Rb ratios in granulites mangerites and anorthosites, Lofoten-Vesteraalen, Norway. Geochim. Cosmochim. Acta 36, 241-257.

GREEN, T.H. (1977) Garnet in silicic liquids and its possible use as P-T indicator. Contrib. Mineral. Petrol. 65, 59-67.

GREEN, T.H. and RINGWOOD, A.E. (1967) Experimental investigation of the gabbro to eclogite transformation and its petrological implications. Geochim. Cosmochim. Acta 31, 767-833.

GREEN, T.H. and RINGWCOD, A.E. (1968) Origin of garnet phenocrysts in calc alkaline rocks. Contrib. Mineral Petrol. 18, 163-174.

GRIFFIN, W.L., HEIER, K.S., TAYLOR, P.N. and WEIGAND, P.W. (1974) General geology, age and chemistry of the Raftsund Mangerite intrusion, Lofoten Vesteraalen. Norges. Geol. Unders. 312, 1-30.

HALLBERG, J.A. and WILLIAMS,D.A.C. (1972) Archaean mafic and ultramafic rock association in the E. Goldfields region, W.Australia. Earth Planet. Sci. Lett. 15, 191-200.

HAMILTON, P.J., CARTER, S.R., EVENSEN, N.M., ONIONS,R.K. and TARNEY, J. (in press) Sm-Nd systematics of Lewisian gneisses: implications for the origin of granulites. Nature.

HANSON, G.N. (1978) The application of trace elements to the petrogenesis of igneous rocks of granitic composition. Earth Planet. Sci. Lett. 38, 26-43.

HANSON, G.N. and LANGMUIR, C.H. (1978) Modelling of major elements in mantle melt systems using trace element approaches. Geochim. Cosmochim. Acta 42, 725-741.

HARIYA, Y. and KENNEDY, G.C. (1968) Equilibrium study of anorthite under high pressure and temperature. Am. J. Sci. 260, 193-203.

HART, S.R. (1969) K, Rb, Cs contents and K/Rb ratios of fresh and altered submarine basalts. Earth Planet. Sci. Lett. 10, 17-28.

HART, S.R., BROOKS, C., KROGH, T.E., DAVIS, G.L. and NAVA, D. (1970) Ancient and modern volcanic rocks: a trace element model. Earth Planet. Sci. Lett. 10, 17-28.

HART, S.R., ERLANK, A.J. and KABLE, E.J.D. (1974) Sea floor basalt alteration: some chemical and Sr isotope effects. Contrib. Mineral. Petrol. 44, 219-230.

HART, S.R., GLASSLEY, W.E. and KARIG, D.E. (1972) Basalts and sea floor spreading behind the Mariana island arc. Earth Planet. Sci. Lett. 15, 12-18.

HART, S.R. and NALWALK, A.J. (1970) K, Rb, Cs, and Sr relationships in submarine basalts from the Peuto Rico trench. Geochim. Cosmochim. Acta 34, 145-155.

HAWKSWORTH, C.J., O'NIONS, R.K., PANKHURST, R.J., HAMILTON, P.J., and EVENSEN, N.M. (1977) A geochemical study of island arc and back arc tholeiites from the Scotia sea. Earth Planet. Sci. Lett. 36, 253-262.

HEIER, K.S. (1955) The formation of feldspar perthites in highly deformed metamorphic gneiss. Norsk. Geol. Tidsskr. 35, 87-92.

HEIER, K.S. (1973) Geochemistry of granulite facies rocks and problems of their origin. Phil. Trans. R. Soc. Lond. A. 273, 429-442.

HEITENAN, A. (1973) Origin of andesite and granite magma in the north Sierra Nevada California. Geol. Soc. Am. Bull. 84, 2111-2118.

HERRMANN, A.G. (1974) Yttrium and the Lanthanides. In, K.H.Wedepohl (Ed) Handbook of Geochemistry, Vol II-4. Springer-Verlag, Berlin.

HERRMANN, A.G., POTTS, M.J. and KNAKE, D. (1974) Geochemistry of the rare earth elements in spilites from the oceanic and continental crust. Contrib. Mineral. Petrol. 44, 1-16.

HEWINS, R. (1975) Pyroxene geothermometry of some granulite facies rocks. Contrib. Mineral. Petrol. 50, 205-209.

HEWITT, D.A. (1973) Stability of the assemblage muscovite-calcite-quartz. Am. Mineral. 58, 785-791.

HOLDAWAY, M.J. (1971) Stability of andalusite and the aluminium silicate phase diagram. Am. J. Sci. 271, 97-131.

HOLLAND, J.G. and LAMBERT, R. ST.J. (1973) Comparative major element geochemistry of the Lewisian rocks of the mainland of Scotland. In, R.G.Park and J.Tarney (Eds) The early Precambrian rocks of Scotland and related rocks of Greenland. Univ. Keele. 51-62.

HOLLAND, J.G. and LAMBERT, R. ST.J. (1975) The chemistry and origin of the Lewisian gneisses of the Scottish mainland: the Scourie and Inver assemblages and subcrustal accretion. Precamb. Res. 2, 161-188.

HOLLISTER, L.S. (1975) Granulite facies metamorphism in the coast range crystalline belt. Can. J. Earth Sci. 12, 1953-1955.

HOWELLS, S. and O'HARA, M.J. (1975) Palaeogeotherms and the diopside-enstatite solvus. Nature, Lond. 254, 406-408.

HOWELLS, S. and O'HARA, M.J. (1978) Low solubility of alumina in enstatite and uncertainties in estimated palaeogeotherms. Phil. Trans. R. Soc. Lond. A. 288, 471-486.

HUANG, W.L. and WYLLIE, P.J. (1975) Melting reactions in the system $NaAlSi_3O_8$-$KAlSi_3O_8$-SiO_2 to 35 kilobars, dry and with excess water. J.Geol. 83, 737-748.

HUMPHRIS, S.E. and THOMPSON, G. (1978) Trace element mobility during hydrothermal alteration of oceanic basalts. Geochim, Cosmochim. Acta 42, 127-136.

HUNT, J.A. and KERRICK, D.M. (1977) The stability of sphene: experimental redetermination and geologic implications. Geochim. Cosmochim. Acta 41, 279-288.

IRVINE, T.N. and BARAGAR, W.R.A. (1971) A guide to the chemical classification of the common volcanic rocks. Can. J. Earth Sci. 8, 523-48.

IRVING, A.J. (1978) A review of the experimental studies of crystal/liquid trace element partitioning. Geochim. Cosmochim. Acta 42, 743-770.

ISHIZAKA, K. and YANAGI, T. (1977) K, Rb and Sr abundances and Sr isotopic composition of Tanzawa granitic and associated gabbroic rocks, Japan: Low potash island arc plutonic complex. Earth Planet. Sci. Lett. 33, 345-352.

JAKES, P. (1969) Distribution of the granulites within the Bohemian Massif and their petrological features. Spec. Publs. Geol. Soc. Austral. 2, 269-277.

JAKES, P. and WHITE, A.J.R. (1972) Major and trace element abundances in volcanic rocks of orogenic areas. Geol. Soc Am. Bull. 83, 29-40.

JAMES, R.S. and HAMILTON, D.L. (1969) Phase relations in the system $NaAlSi_3O_8$- $KAlSi_3O_8$- $CaAl_2Si_2O_8$- SiO_2 at 1 kilobar water vapour pressure. Contrib. Mineral. Petrol. 21, 111-141.

KROGH, E.J. (1977) Evidence of Precambrian continent-continent collision in western Norway. Nature, Lond. 267, 17-19.

KUSHIRO, I. (1972) Effect of water on the composition of magmas formed at high pressures. J.Petrol. 13, 311-334.

LAGACHE, M. and WEISBROD, A. (1977) The system: two alkali feldspars - KCl - NaCl - H_2O at moderate to high temperature and low pressures. Contrib. Mineral. Petrol. 62, 77-102.

LAMBERT, I.B. and HEIER, K.S. (1969) Chemical investigations of deep seated rocks in the Australian shield. Lithos, 1, 30-53.

LAMBERT, I.B. and WYLLIE, P.J. (1974) Melting of tonalite and crystallisation of andesite liquid with excess water to 30 kilobars. J.Geol. 82, 88-97.

LAMBERT, R. ST.J. (1976) Archaean thermal regimes, crustal and upper mantle temperatures and a progressive evolutionary model for the earth. In, B.F.Windley (Ed) The Early History of the Earth, Wiley, London. 363-387.

LANGMUIR, C.H., BENDER, J.F., BENCE, A.E. and HANSON, G.N. (1977) Petrogenesis of basalts from the FAMOUS area: Mid Atlantic ridge. Earth Planet. Sci. Lett. 36, 133-156.

LEAKE, B.E. (1964) The chemical distinction between ortho and para amphibolites. J.Petrol. 5, 238-254.

LINDH, A. (1972) A hydrothermal investigation of the system FeO, Fe_2O_3, TiO_2. Lithos 5, 325-343.

LINDSLEY, D.H. and DIXON, S.A. (1976) Diopside-enstatite equilibria at 850-1400°C, 5-35 kbar. Am. J. Sci. 276, 1285-1301.

LIPMAN, P.W. (1971) Iron-titanium oxide phenocrysts in composite zoned ash flow sheets from South Nevada. J.Geol. 79, 438-456.

LOFGREN, G.E. and GOOLEY, R. (1977) Simultaneous crystallisation of feldspar intergrowths from the melt. Am. Mineral. 62, 217-228.

LUTH, W.C. (1974) Analysis of experimental data on alkali feldspar unit cell parameters and solvi. In, W.S.MacKenzie and J.Zussman (Eds) The feldspars. Manchester Univ Press: Manchester. 249-296.

LUTH, W.C., JAHNS, R.H. and TUTTLE, O.F. (1964) The granite system at pressures of 4 to 10 kilobars. J. Geophys. Res. 69, 759-773.

LUTH, W.C. and TUTTLE, O.F. (1966) The alkali feldspar solvus in the system Na_2O-K_2O-Al_2O_3-SiO_2-H_2O. Am. Mineral. 51, 1359-1373.

LUTH, W.C., MARTIN, R.F. and FENN, P.M. (1974) Peralkaline feldspar solvi. In, W.S.MacKenzie and J.Zussman (Eds) The feldspars. Manchester Univ. Press, Manchester. 297-312.

MACDONALD, G.A. (1968) Composition and origin of Hawaiian lavas. Geol. Soc. Am. Mem. 116, 477-522.

MACGREGGOR, I.D. (1974) the system $MgO-Al_2O_3-SiO_2$: solubility of Al_2O_3 in enstatite for spinel and garnet peridotite compositions. Am. Mineral. 59, 110-119.

MACGREGGOR, I.D. and RINGWOOD, A.E. (1964) The natural system enstatite pyrope. Carnegie Inst, Wash. Ybk. 63, 161-163.

MARTIN, R.F. (1974) Controls of ordering and subsolidus phase relations in the alkali feldspars. In, W.S.MacKenzie and J.Zussman (Eds) The Feldspars. Manchester Univ.Press, Manchester. 313-336.

MASON, P.K., FROST, M.T. and REED, S.J.B. (1969) N.P.L. (I.M.S.) Report No. 2.

MOORBATH, S. (1977) Ages, isotopes and the evolution of Precambrian continental crust. Chem. Geol. 20, 151-187.

MOORBATH, S., POWELL, J.L. and TAYLOR, P.N. (1975) Isotopic evidence for the age and origin of the 'grey gneiss' complex of the southern Outer Hebrides, Scotland. J. Geol. Soc. Lond. 131, 213-222.

MOORBATH, S., WELKE, H. and GALE, N.H. (1969) The significance of lead isotope studies in ancient high grade metamorphic basement complexes as exemplified by the Lewisian rocks of northwest Scotland. Earth Planet. Sci. Lett. 6, 245-256.

MORI, T. and GREEN, D.H. (1976) Subsolidus equilibria between pyroxenes in the $CaO-MgO-SiO_2$ system at high pressures and temperatures. Am. Mineral. 61, 616-625.

MORRISON, M.A. (1978) The use of 'immobile' trace elements to distinguish the palaeotectonic affinities of metabasalts: Applications to the Palaeocene basalts of Mull and Skye, N.W.Scotland. Earth Planet. Sci. Lett. 39, 407-416.

MORSE, S.A. (1970) Alkali feldspars with water at 5 kb pressure. J. Petrol. 11, 221-253.

MUECKE, G. (1969) The petrochemistry of the Scourie granulites. D.Phil. thesis. Univ. Oxford.

MYSEN, B.O. (1977) Magma genesis in peridotite upper mantle in the light of experimental data on the partitioning of trace elements between garnet peridotite minerals and partial melt. Carnegie Inst. Wash. Ybk. 76, 545-550.

MYSEN, B.O. and BOETTCHER, A.L. (1975) Melting of a hydrous mantle II. Geochemistry of crystals and liquids formed by anatexis of mantle peridotite at high pressure and high temperatures as a function of the controlled activity of water, hydrogen and carbon dioxide. J. Petrol. 16, 549-590.

MYSEN, B.O., KUSHIRO, I., NICHOLLS, I.A. and RINGWOOD, A.E. (1974) A possible mantle origin for andesitic magmas: discussion of a paper by Nicholls and Ringwood. Earth Planet. Sci. Lett. 21, 221-230.

NAVROTSKY, A. (1978) Thermodynamics of element partitioning (1) systematics of transition metals in crystalline and molten silicates and (2) defect chemistry and the Henry's Law problem. Geochim, Cosmochim. Acta 42, 887-902.

NEHRU, C.E. AND WYLLIE, P.J. (1974) Electron microprobe measurement of pyroxenes coexisting with H_2O undersaturated liquid in the join $CaMgSi_2O_6$-$Mg_2Si_2O_6$-H_2O at 30 kilobars, with applications to geothermometry. Contrib. Mineral Petrol. 48, 221-228.

NEWTON, R.C. (1978) Experimental and thermodynamic evidence for the operation of high pressures in Archaean metamorphism. In, B.F. Windley and S.M.Naqvi, Archaean geochemistry. Elsevier, Amsterdam. 221-240.

OBATA, M. (1976) The solubility of Al_2O_3 in orthopyroxenes in spinel and plagioclase peridotites and spinel pyroxenite. Am. Mineral. 61, 804-816.

O'HARA, M.J. (1977) Thermal history of excavation of Archaean gneisses from the base of the continental crust. J.Geol. Soc Lond. 134, 185-200.

O'HARA, M.J. and YARWOOD, G. (1978) High pressure - temperature point on an Archaean geotherm, implied magma genesis by crustal anatexis and consequences for garnet pyroxene thermometry and barometry. Phil. Trans. R. Soc. Lond. A. 288, 441-456.

OLIVER, G.J.H. (1978) Ilmenite-magnetite geothermometry and oxygen barometry in granulite and amphibolite facies gneisses from Doubtful Sound, Fiordland, New Zealand. Lithos 11, 147-154.

O'NIONS, R.K. and PANKHURST, R.J. (1974) Rare earth element distributions in Archaean gneisses and anorthosites, Godthab area, W.Greenland Earth Planet. Sci. Lett. 22, 328-338.

O'NIONS, R.K. and PANKHURST, R.J. (1978) Early Archaean rocks and geochemical evolution of the earth's crust. Earth Planet. Sci. Lett. 38, 211-236.

ORVILLE, P.M. (1962) Comments on the two-feldspar geothermometer. Norsk. Geol Tidssk. 42, 340-346.

ORVILLE, P.M. (1963) Alkali ion exchange between vapour and feldspar phases. Am. J. Sci. 261, 201-237.

ORVILLE, P.N. (1972) Plagioclase cation exchange equilibria with aqueous chloride solution. Results at 700°C and 200 bars in the presence of quartz. Am. J. Sci. 272, 234-272.

PAPIKE, J.J., CAMERON, K.L. and BALDWIN, K. (1974) Amphiboles and pyroxenes; characterisation of other than quadrilateral components and estimates of ferric iron from microprobe data. Geol. Soc. Am. Abs. 6, 1053-1054.

PARSONS, I. (1978a) Alkali feldspars. Which solvus ? Phys. Chem. Mineral. 2, 199-213.

PARSONS, I. (1978b) Feldspars and fluids in cooling plutons. Mineral. Mag. 42, 1-17.

PEACH, B.N., HORNE, J., GUNN, W., CLOUGH, C.T., HINXMAN, L.W. and TEALL, J.J.H. (1907) The geological structure of the N.W.Highlands of Scotland. Mem. Geol. Surv. Gt. Britain 668 pp.

PEARCE, J.A. (1975) Basalt geochemistry used to investigate past tectonic environments on Cyprus. Tectonophys. 25, 41-67.

PEARCE, J.A. (1978) Petrogenetic studies of metabasalts using immobile trace element ratios. Abs. In, W.J.Rea (Ed) Trace element studies of the origin of igneous rocks. J. Geol. Soc Lond. 135, 591-595.

PEARCE, J.A. and CANN, J.R. (1971) Ophiolite origin investigated by discriminant analysis using Ti, Zr and Y. Earth Planet. Sci. Lett. 12, 339-349.

PEARCE, J.A. and CANN, J.R. (1973) Tectonic setting of basic volcanic rocks determined using trace element analyses. Earth Planet. Sci. Lett. 19, 290-300.

PEARCE, T.H., GORMAN, B.E. and BIRKETT, T.C. (1975) The TiO_2-K_2O-P_2O_5 diagram: a method of discriminating between oceanic and non oceanic basalts. Earth Planet. Sci. Lett. 24, 419-426.

PEARCE, T.H., GORMAN, B.E. and BIRKETT, T.C. (1977) The relationship between major element chemistry and tectonic environment of basic and intermediate volcanic rocks. Earth Planet. Sci. Lett. 36, 121-32.

PETO, P. and HAMILTON, D.L. (1976) Partial fusion of basalts and andesites under vapour excess and vapour deficient conditions at 10 kb. total pressure. In, Progress in experimental petrology. Natural Environment Research council. 45-50.

PHILPOTTS, J.A., SCHNETZLER, C.C. and HART, S.R. (1969) Submarine basalts; some K, Rb, Sr, Ba, rare earth, H_2O and CO_2 data bearing on their alteration and modification by plagioclase and possible source materials. Earth Planet. Sci. Lett. 7, 293-299.

PINKNEY, L.R. and LINDSLEY, D.H. (1976) The effect of Magnesium on iron-titanium oxides. Geol. Soc. Am. Abs. 8, 1051.

PITCHER, W.S. (1978) The anatomy of a batholith. J. Geol. Soc. Lond. 135, 157-182.

PIWINSKII, A.J. (1973) Experimental studies of igneous rock series central Sierra Nevada batholith, California: Part II. Neues. Jahrb. Mineral. Monatsh. H5 193-215.

POWELL, R. (1974) A comparison of some mixing models for crystalline silicate solid solutions. Contrib. Mineral Petrol. 46, 265-274.

POWELL, R. (1978) The thermodynamics of pyroxene geotherms. Phil. Trans R. Soc. Lond. A. 288, 457-469.

POWELL, M. and POWELL, R. (1977a) Plagioclase - alkali feldspar geothermometry revisited. Mineral. Mag. 41, 253-256.

POWELL, R. and POWELL, M. (1977b) Geothermometry and oxygen barometry

using coexisting iron-titanium oxides: a reappraisal. Mineral. Mag. 41, 257-263.

PRESNALL, D.C. (1976) Alumina content of enstatite as a geobarometer for plagioclase and spinel lherzolites. Am. Mineral. 61, 582-588.

PREVOT, M. and MERGOIL, J. (1973) Crystallisation trend of titanomagnetites in an alkali basalt from Saint Clement (Massif Central, France). Mineral. Mag. 39, 474-81.

RAHEIM, A. and GREEN, D.H. (1974) Experimental determination of the temperature and pressure dependence of the Fe-Mg partition coefficient for coexisting garnet and clinopyroxene. Contrib. Mineral. Petrol. 48, 179-203.

RICHARDSON, S. (1968) The petrology of the metamorphosed syenite in Glen Dessarry, Inverness-shire. Q. J. Geol. Soc. Lond. 124, 9-51.

RICKWOOD, P.C. (1968) On recasting analyses of garnet into end-member molecules. Contrib. Mineral. Petrol. 18, 175-198.

ROBIE, R.A. and WALDBAUM, D.R. (1968) Thermodynamic properties of minerals and related substances at 298·15 (25·0°C) and one atmosphere (1·013 bars) pressure and at higher temperatures. U.S. Geol. Surv. Bull. 1259, 256 pp.

RODDICK, J.A. and HUTCHINSON, W.W. (1974) Setting of the Coast Plutonic Complex, British Columbia. Pacific Geol. 8, 91-108.

ROLLINSON, H.R. (in press) Ilmenite-magnetite geothermometry in trondhjemites from the Scourian complex of N.W. Scotland. Mineral. Mag. (This thesis, chapter 4)

SAUNDERS, A.D. and TARNEY, J. (1978) The origin and evolution of basalts from an intra-oceanic marginal basin in the East Scotia Sea: a trace

element study. Abs. In, W.J.Rea (Ed) Trace element studies of the origin of igneous rocks. J. Geol. Soc. Lond. 135, 591-595.

SAXENA, S.K. (1976) Two-pyroxene geothermometer: a model with an approximate solution. Am. Mineral. 61, 643-652.

SAXENA, S.K. and NEHRU, C.E. (1976) Enstatite-diopside solvus and geothermometry. Contrib. Mineral. Petrol. 49, 259-267.

SCHARBERT, H.G. and KURAT, G. (1974) Distribution of some elements between coexisting ferromagnesian minerals in Moldanubian granulite facies rocks, Lower Austria. Tschermacks. Mineral. Petrol. Mittr. 21, 110-134.

SECK, H.A. (1972) The influence of pressure on the alkali feldspar solvus from peraluminous and persilicic materials. Fortschr. Mineral. 49, 31-49.

SEIDEL, E. (1974) Zr contents of glaucophane bearing metabasalts of W. Crete, Greece. Contrib. Mineral. Petrol. 44, 231-236.

SHAW, D.M. (1968) A review of K-Rb fractionation trends by covariance analysis. Geochim. Cosmochim. Acta 32, 573-601.

SHERATON, J.W. (1970) The origin of the Lewisian gneisses of northwest Scotland, with particular reference to the Drumbeg area, Sutherland. Earth Planet. Sci. Lett. 8, 301-310.

SHERATON, J.W., SKINNER, A.C. and TARNEY, J. (1973) The geochemistry of the Scourian gneisses of the Assynt district. In, R.G.Park and J.Tarney (Eds.) The early Precambrian rocks of Scotland and related rocks of Greenland. Univ. Keele. 13-30.

SIPLING, P.J. and YUND, R.A. (1976) Experimental determination of the coherent solvus for sanidine-high albite. Am. Mineral. 61, 879-906.

SMITH, J.V. (1974) Feldspar Minerals II. Chemical and textural properties. Springer-Verlag, Heidelberg. 690 pp.

SMITH, P. and PARSONS, I. (1974) The alkali feldspar solvus at 1 kilobar water vapour pressure. Mineral. Mag. 39, 747-767.

SMITH, R.E. and SMITH, S.E. (1976) Comments on the use of Ti, Zr, Y, Sr, K, P. and Nb on the classification of basaltic magmas. Earth Planet. Sci. Lett. 32, 114-120.

SNETSINGER, K.C. (1969) Manganoan ilmenite from a Sierran adamellite. Am. Mineral. 54, 431-436.

STEMLE, I.M., BISHOP, F.C., SMITH, J.V. and WINDLEY, B.F. (1977) The Fiskenaesset complex, west Greenland, Part III. Gron. Geol. Unders. Bull. 124.

STEIGER, R.H. and JAGER, E. (1977) Subcommision on geochronology: convention on the use of decay constants in geo- and cosmochronology. Earth Planet. Sci. Lett. 36, 359-362.

STEINER, J.C., JAHNS, R.H. and LUTH, W.C. (1975) Crystallisation of alkali feldspar and quartz in the haplogranite system $NaAlSi_3O_8$-$KAlSi_3O_8$-H_2O at 4 kb. Geol. Soc. Am. Bull. 86, 83-98.

STERN, C.R. (1974) Melting product of olivine tholeiite basalt in subduction zones. Geology 2, 227-230.

STEWART, D.B. (1975) Lattice parameters. composition, and Al/Si order in alkali feldspars. In, P.H.Ribbe (Ed.) Feldspar Mineralogy. Mineral. Soc. Am. Short course notes. 2.

STORMER, J.C. (1975) A practical two-feldspar geothermometer. Am. Mineral. 60, 667-674.

STORMER, J.C. and WHITNEY, J.A. (1977) Two-feldspar geothermometry in granulite facies metamorphic rocks: sapphirine granulites from Brazil. Contrib. Mineral. Petrol. 65, 123-133.

STRECKEISEN, A.L. (1973) Plutonic rocks. Classification and nomenclature recommended by IUGS subcommission on the systematics of igneous rocks. Geotimes Oct. 1973, 26-30.

SUN, S.S. and HANSON, G.N. (1975) Origin of Ross Island basanitoids and limitations upon the heterogeneity of mantle sources for alkali basalts and nephelinites. Contrib. Mineral. Petrol. 52, 77-106.

SUTTON, J. and WATSON, J.V. (1951) The pre-Torridonian metamorphic history of the Loch Torridon and Scourie areas in the northwest highlands. Q. J. Geol.Soc. Lond. 106, 241-307.

TARNEY, J. (1976) Geochemistry of Archaean high-grade gneisses, with implications as to the origin and evolution of the Precambrian crust. In, B.F.Windley (Ed.) The early history of the earth. Wiley, London. 405-417.

TARNEY, J., SKINNER, A.C. and SHERATON, J.W. (1972) A geochemical comparison of major Archaean gneiss units from northwest Scotland and E, Greenland. Rept. 24th Int. Geol. Congress, Montreal. 1, 162-74.

TARNEY, J., DALZIEL, I.W.D. and DEWIT, M.J. (1976) Marginal 'Rocas Verdes' complex from S. Chile: A model for Archaean greenstone belt formation. In, B.F.Windley (Ed.) The early history of the earth. Wiley, Lond. 131-146.

TARNEY, J., WEAVER, B.L. and DRURY, S.A. (in press) Geochemistry of Archaean trondhjemitic and tonalitic gneisses from Scotland and East Greenland.

TARNEY, J. and WINDLEY, B.F. (1977) Chemistry, thermal gradients and evolution of the lower continental crust. J. Geol. Soc. Lond. 134, 153-172.

THOMPSON, J.B. (1967) Thermodynamic properties of simple solutions. In, P.H.Abelson (Ed.) Researches in geochemistry II. Wiley. 340-361.

THOMPSON, J.B. and WALDBAUM, D.R. (1969a) Analysis of the two phase region halite-sylvite in the system NaCl-KCl. Geochim. Cosmochim. Acta 33, 671-690.

THOMPSON, J.B. and WALDBAUM, D.R. (1969b) Mixing properties of sanidine crystalline solutions, III. Calculations based on two phase data. Am.Mineral. 54, 811-838.

THOMPSON, R.N. (1976) Chemistry of ilmenite crystallised within the anhydrous melting range of a tholeiitic andesite at pressures between 5 and 26 kb. Mineral. Mag. 40, 857-62.

TOWELL, D.G., WINCHESTER, J.W. and SPIRN, R.W. (1965) Rare earth distributions in some rocks and associated minerals of the batholith of Southern California. J.Geophys. Res. 10, 3485-3496.

TUTTLE, O.F. and BOWEN, N.L. (1958) Origin of granite in the light of experimental studies in the system $NaAlSi_3O_8$-$KAlSi_3O_8$-SiO_2-H_2O. Mem. Geol. Soc. Am. 74.

VALLANCE, T.G. (1974) Spilitic degradation of a tholeiitic basalt. J. Petrol. 15, 79-96.

VAN DE KAMP, P.C. (1969) Origin of amphibolites in the Beartooth mountains, Wyoming and Montana: new data and interpretation. Geol. Soc. Am. Bull. 80, 1127-1136.

VELDE, B. (1967) Si^{4+} content of natural phengites. Contrib. Mineral. Petrol. 14, 250-258.

VIRGO, D. (1969) Partitioning of sodium between coexisting K-feldspar and plagioclase from some metamorphic rocks. J.Geol. 77, 173-182.

WALDBAUM, D.R. and THOMPSON, J.B. (1969) Mixing properties of sanidine crystalline solutions: IV. Phase diagrams from equations of state. Am. Mineral. 54, 1274-1298.

WATSON, J.V. The Lewisian complex. In, A correlation of Precambrian rocks in the British Isles, Geol. Soc. Lond. Sp. Rep., 6, 15-29.

WELLS, P.R.A. (1975(Pyroxene thermometry in simple and complex systems. Contrib. Mineral. Petrol. 62, 129-139.

WHITNEY, J.A. (1975) The effect of pressure temperature and X_{H2O} on phase assemblage in four synthetic rock compositions. J. Geol. 83, 1-31.

WHITNEY, J.A. and STORMER, J.C. Geothermometry and geobarometry in epizonal granitic intrusions: a comparison of iron-titanium oxides and coexisting feldspars. Am. Mineral. 61, 751-761.

WHITNEY, J.A. and STORMER, J.C. (1977a) Two feldspar geothermometry, geobarometry in mesozonal granitic intrusions: three examples from the piedmont of Georgia. Contrib. Mineral. Petrol. 63, 51-64.

WHITNEY, J.A. and STORMER, J.C. (1977b) The distribution of $NaAlSi_3O_8$ between coexisting microcline and plagioclase and its effect on geothermometric calculations. Am. Mineral. 62, 687-691.

WHITTAKER, E.J.W. and MUNTUS, R. (1970) Ionic radii for use in geochemistry. Geochim.Cosmochim. Acta 34, 945-956.

WILKINSON, J.F.G. (1974) Garnet clinopyroxenite inclusions from diatremes in the gloucester area, New South Wales, Australia. Contrib. Mineral. Petrol. 46, 275-299.

WINCHESTER, J.A. and FLOYD, P.A. (1976) Geochemical magma type discrimination: application to altered and metamorphosed basaltic igneous rocks. Earth Planet. Sci. Lett. 28, 459-469.

WINDLEY, B.F., HERD, R.K. and BOWDEN A.A. (1973) The Fiskenaesset complex, West Greenland Part I. A preliminary study of the stratigraphy petrology and whole rock chemistry from Qeqertarssuatsiaq. Gron. Geol. Unders. Bull. 106.

WINDLEY, B.F. and SMITH, J.V. (1976) Archaean high grade complexes and modern continental margins. Nature, Lond. 260, 671-675.

WINDOM, K.E. and BOETTCHER, A.L. (1976) The effect of the reduced activity of anorthite on the reaction grossular + quartz = wollastonite: a model for plagioclase in the earth's lower crust and upper mantle. Am. Mineral. 61, 889-896.

WOOD, B.J. (1974) Solubility of alumina in orthopyroxene coexisting with garnet. Contrib. Mineral. Petrol. 46, 1-15.

WOOD, B.J. (1975a) The application of thermodynamics to some subsolidus equilibria involving solid solutions. Fortschr. Miner. 52, 21-45.

WOOD, B.J. (1975b) The influence of pressure, temperature and bulk composition on the appearance of garnet in orthogneiss - an example from South Harris. Earth Planet. Sci. Lett. 26, 299-311.

WOOD, B.J. (1976) Mixing properties in tsermakitic clinopyroxenes. Am. Mineral. 61, 599-602.

WOOD, B.J. (1977) The activity of components in clinopyroxene and garnet solid solutions and their applications to rocks. Phil. Trans. R. Soc. Lond. A. 286, 331-342.

WOOD, B.J. (1978) Experimental determination of the mixing properties of solid solutions with particular reference to garnet and clinopyroxene solutions. In, D.G,Fraser (Ed.) Thermodynamics in geology. D.Reidel, Dordrecht, Holland. 11-27.

WOOD, B.J. and BANNO, S. (1973) Garnet orthopyroxene and orthopyroxene clinopyroxene relationships in simple and complex systems. Contrib. Mineral. Petrol. 42, 109-124.

WOOD, B.J. and FRASER, D.G. (1977) Elementary thermodynamics for geologists. Oxford. 303 pp.

WYLLIE, P.J. (1977) Crustal anatexis, an experimental review. Tectonophys. 43, 41-71.

YUND, R.A. (1975) Subsolidus phase relations in the alkali feldspars with emphasis on coherent phases: and Microstructure, Kinetics and mechanisms of alkali feldspar exsolution. In, P.H.Ribbe (Ed.) Feldspar mineralogy. Mineral. Soc. Amer. Short course notes, 2.

Appendices

APPENDIX 1

ADDITIONAL DATA IN SUPPORT OF LOW K / RB RATIOS IN HIGH PRESSURE GRANULITES; TWO EXAMPLES OF GRANULITE SENSU STRICTO FROM SAXONY AND W. GREENLAND

This appendix presents new chemical data for four samples of granulite sensu stricto from Saxony and W. Greenland in order to show that (a) from the mineral chemistry that they formed at high pressures and (b) from whole rock chemistry that they have low K/Rb ratios.

Two samples of granulite sensu stricto from the Granulitgebirge, Saxony (HR 31, HR 32) and two samples of granulite ss. from Tovqussap, W. Greenland (87710 and 8772) were kindly supplied by Dr. B.F. Windley and form the basis of this study. In each case mineral analyses are presented for one of the samples and whole rock analyses for both samples.

The distribution of granulites within the Bohemian Massif was reviewed by Jakes (1969); the common occurrence of kyanite and the presence of ecologite indicates that they are of high pressure origin. Granulite ss. contains the mineral assemblage quartz - plagioclase - mesoperthite - garnet - kyanite ± sillimanite. Grain boudaries between quartz and feldspar are very irregular and are not typical of 'granulites'; garnet and kyanite form rounded subhedral grains with droplet inclusions of quartz; sillimanite overgrows kyanite on some grains. Mesoperthite is made up of coarse and fine, closely spaced lamellae of orthoclase in plagioclase. Opinion differs over the original nature of these rocks and they have been described as metasediments and acid lavas.

Granulite ss. was described from Tovqussap, W. Greenland by Berthelson (1960) who mapped a zone of granulite ss. up to 800 m wide and 7 km long discordant to the enclosing pyroxene granulites and containing inclusions of cummingtonite - cordierite schist and hypersthene - garnet - biotite schist. Samples 87710 and 8772 contain the mineral assemblage quartz - mesoperthite - plagioclase - garnet - sillimanite - biotite. Sillimanite and garnet define a weak banding. Garnet grains are small and elliptical with inclusions of quartz and are overgrown by biotite. Sillimanite (low birefringence, straight extinction, not blue in hand specimen) forms fine angular grains. Mesoperthite varies between a lamellar perthite with long, thin bifurcating lamellae of orthoclase or microcline, in a plagioclase host and a patch (microcline) perthite; microcline has also grown as a result of granular exsolution from mesoperthite.

Mineral Chemistry

The two reactions:

$$\underset{\text{plagioclase}}{CaAl_2Si_2O_8} = \underset{\text{garnet}}{Ca_3Al_2Si_3O_{12}} + \underset{\substack{\text{sillimanite}\\ \text{kyanite}}}{2Al_2SiO_5} + \underset{\text{quartz}}{SiO_2} \qquad (1)$$

$$\underset{\text{plagioclase}}{NaAlSi_3O_8} = \underset{\text{alkali feldspar}}{NaAlSi_3O_8} \qquad (2)$$

are used to obtain an estimate of the equilibration pressure and temperature for granulite ss. from Saxony and W. Greenland. Reaction 1 is sensitive to both pressure and temperature; reaction 2 is mainly sensitive to temperature so that the two reaction curves intersect at a relatively high angle and are therefore able to yield a fairly precise P-T estimate for these rocks.

The following assumptions have been made:

1. Reaction 1:

(i) ideal solution behaviour in garnet and plagioclase. Wood (1978) reported near ideal solution behaviour in Ca-Fe garnets. Wood and Fraser (1977) suggest that the activity of anorthite in plagioclase is approximately equal to its mole fraction.

(ii) all Fe in garnet is regarded as Fe^{2+}. This means that the estimated pressure is a maximum.

(iii) kyanite and quartz are assumed pure.

2. Reaction 2:

(i) Ca in alkali feldspar significantly affects the equilibration temperature, therefore ternary models are to be preferred to the binary models (see appendix 2).

(ii) The structural state of the alkali feldspar is between orthoclase and microcline so that there is a range of possible pressure and temperatures which is dependant upon the structural state of the feldspars at equilibration.

(iii) mesoperthite represents an originally homogeneous alkali feldspar whose composition can be estimated by a bulk analysis of the grain with a scanning electron probe beam.

A P-T line can be drawn for reaction 1 from the thermodynamic data of Ghent (1976) (his reaction 2) in which kyanite is the aluminosilicate phase; similarly a line can be drawn for reaction 2 using the two feldspar thermometer of Powell and Powell (1977a) and my modification of this equation (Appendix 2). The intersection of these two reactions indicates that the Saxony granulite ss. sample HR 32 equilibrated in the range 8 - 13 kb and 670 - 860°C depending upon the ordering of the feldspar (Fig. 1a); a partially ordered feldspar is likely, in which case an intermediate pressure and temperature is probable. This pressure-temperature estimate is consistent with the kyanite-sillimanite boundary of Holdaway (1971) and in good agreement with the P-T estimate of Scharbert and Kurat (1974) who estimated a pressure of 11 kb and a temperature of 760°C for granulites from the southern part of Bohemian Massif, from experimentally determined reaction curves.

Thermodynamic data for reaction 1 where sillimanite is present instead of kyanite are presented in Wood and Fraser (1977, eq. 3:22); if this is combined with P-T lines from the two feldspar thermometers described above the estimated P-T range for the Greenland granulite ss. is 4.0 - 6.8 kb and 525 - 715°C (Fig. 1b). At these temperatures alkali feldspar is likely to be ordered and so the higher end of the range is to be preferred. This is consistent with the reaction boundary of Holdaway (1971) and the presence of sillimanite; this boundary also defines a lower pressure limit of 4 kb for these rocks using the temperatures derived from Powell and Powell (1977a) although these temperature estimates appear to be a little low as they suggest the possible appearance of andalusite which is not seen. Similarly the model of Whitney and Stormer (1977) yields a P-T estimate of 1550°C and 19 kb and is clearly inappropriate.

Rock Chemistry

The high pressure Saxony granulites ss. are low in normative anorthite and in the Qz-Ab-Or projection plot close to the minimum melt composition for 500 bars pH_2O, suggesting that they may be derived from rhyolite lavas. (Fig. 2).

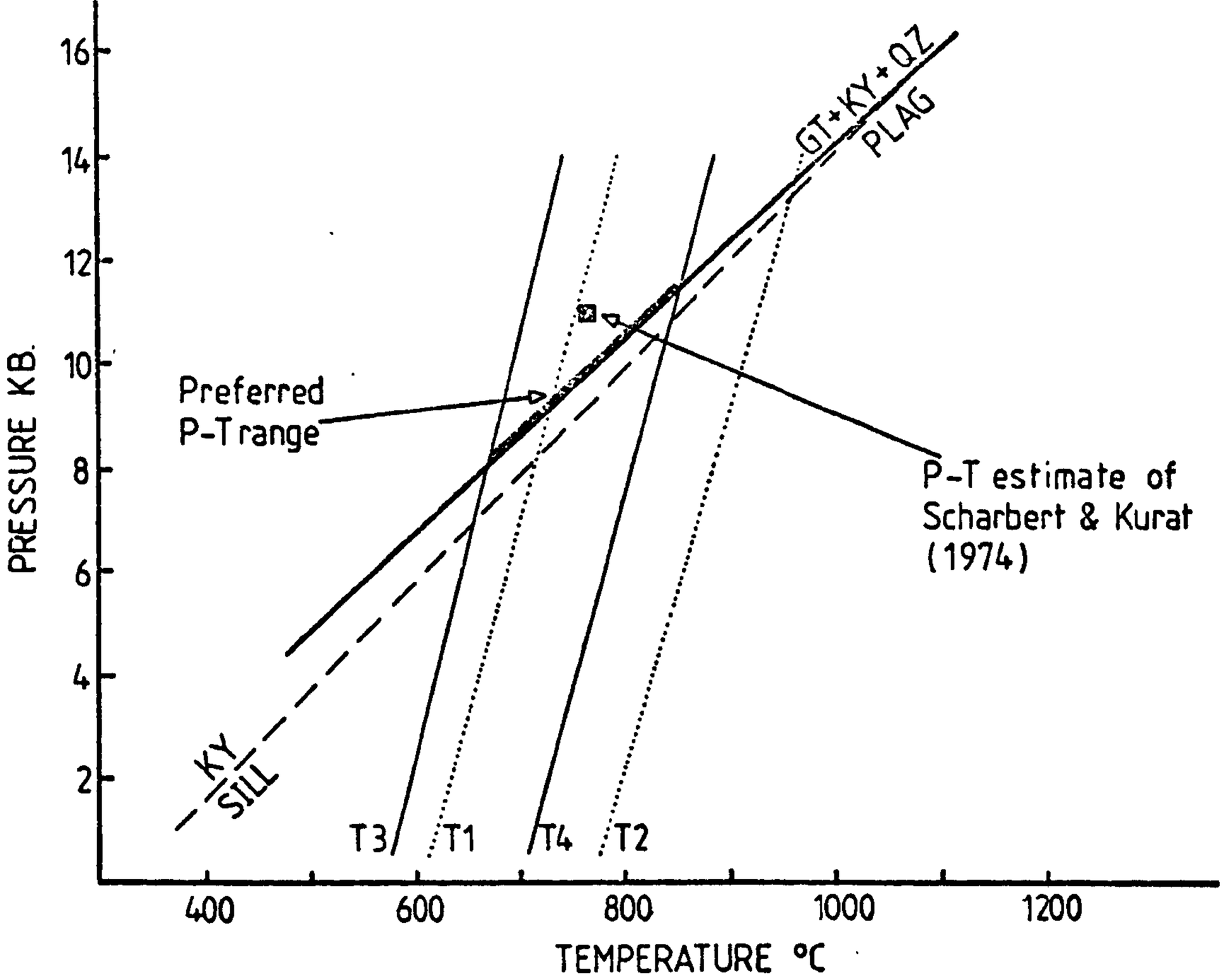

FIGURE 1 (a). Preferred P-T range for Saxony granulite ss. based on the mineral assemblages garnet-kyanite-plagioclase-quartz and plagioclase + alkali feldspar. T1 to T4 are P-T lines for feldspar pairs calculated using the equations in Appendix 2. The P-T estimate of Scharbert and Kurat(1974) for granulites from the southern Bohemian Massif is also shown.

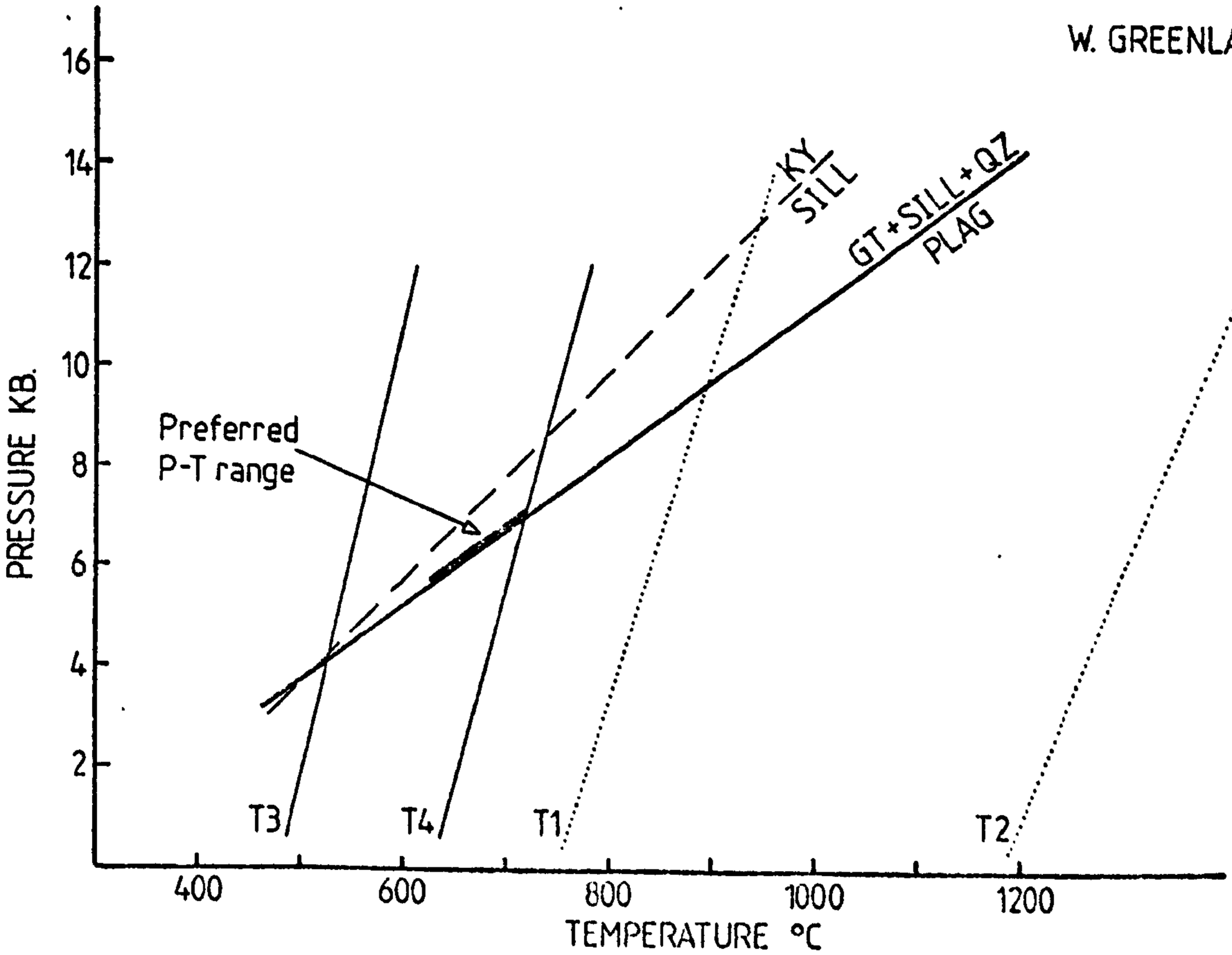

FIGURE 1 (b). Preferred P-T range for W.Greenland granulite ss. based on the mineral assemblages garnet-sillimanite-plagioclase-quartz and alkali feldspar-plagioclase. T1 to T4 as above in 1 (a).

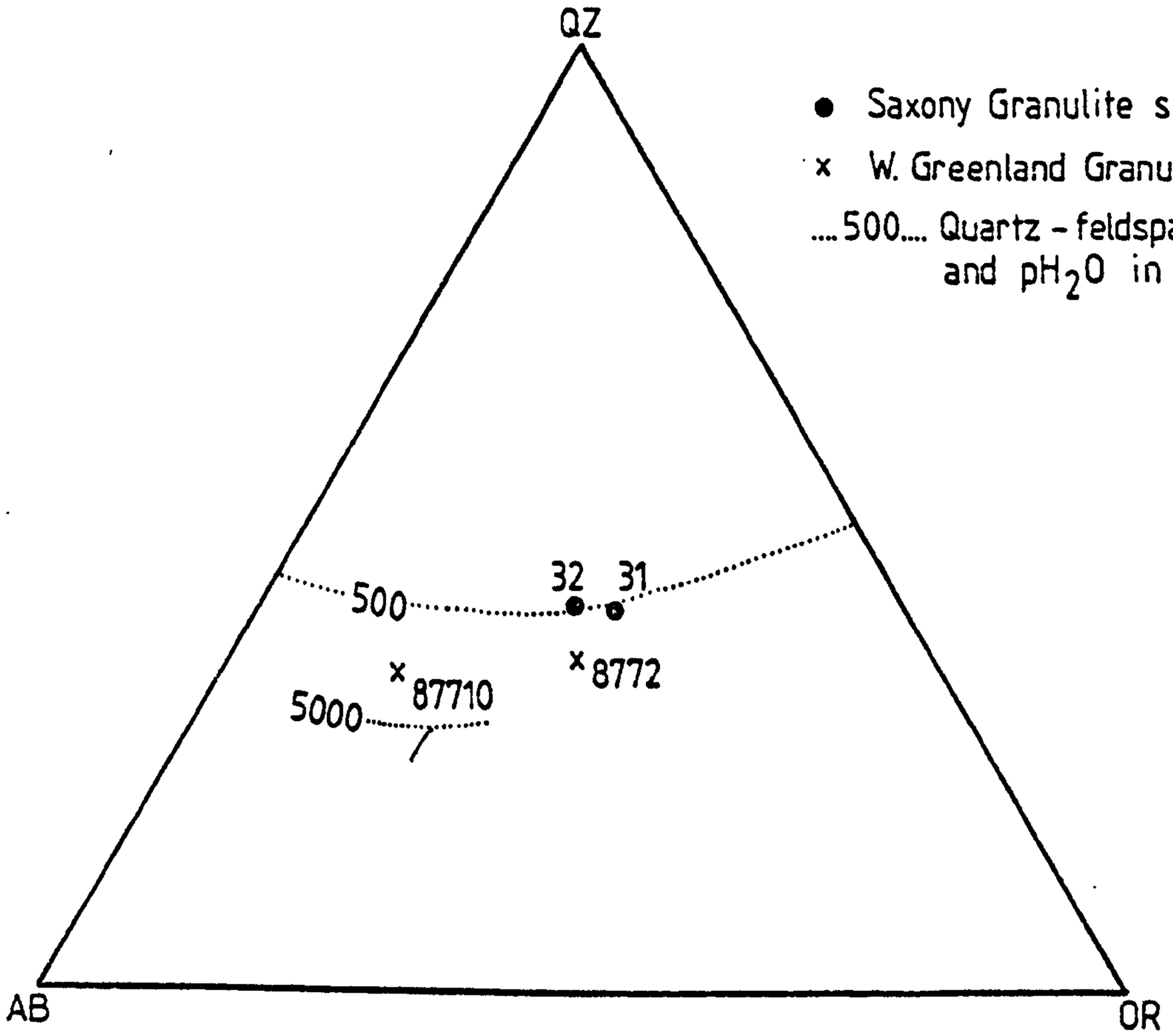

Fig. 2. Composition of Saxony granulites ss. HR 31 and HR 32 and W. Greenland granulites ss. 87710 and 8772 plotted in the projection normative Qz-Ab-Or, and compared with the water-saturated quartz-feldspar cotectic curves for 500 bars and 5000 bars.

These granulites have high concentrations of Rb (240 - 320 ppm) and have K/Rb ratios in the range 117 - 176 which is lower than Shaw's (1968) main trend of ca. 230 (for rocks with 5% K).

The W. Greenland granulites ss. are richer in normative An and plot in the field defined by trondhjemites and granites from Scourie (see Chapter 1) indicative of a high pressure magmatic origin (Fig. 2) and have K/Rb ratios in the range 279 - 550. It is interesting to note that the lower pressure granulites of W. Greenland have higher K/Rb ratios than the high pressure Saxony granulites ss.

Conclusions

1. Granulite ss. from the Granulitgebirge of Saxony equilibrated in the range 10 ± 1.5 kb and 760 ± 90°C and has K/Rb ratios in the range 117 - 176. These granulites probably represent metamorphosed rhyolites.

2. Granulite ss. from W. Greenland equilibrated in the range 6.4 ± 0.8 kb and 675 ± 50°C and has K/Rb ratios in the range 279 - 550. These granulites represent intrusive granodiorite - granite sheets which may represent a relatively high pressure melt.

3. These data are inconsistent with the thesis of Heier (1973) and Lambert and Heier (1968) who suggested that high pressure granulites are always depleted in Rb relative to K.

TABLE 1. Chemical analyses of granulite ss. from Saxony and W. Greenland.

	HR 31	HR 32	87710	8772
SiO_2	78·38	78·72	75·00	74·89
TiO_2	·13	·06	·01	·13
Al_2O_3	13·24	13·55	15·33	14·65
Fe_2O_3	2·01	1·55	·35	1·62
MgO	·16	·06	·09	·26
CaO	·72	·52	1·77	1·22
Na_2O	2·98	3·47	5·36	3·54
K_2O	5·10	4·54	2·47	4·84
P_2O_5	·13	·07	·02	·01
TOT	102·55	102·54	100·40	101·16
Y	49·6	25·4	10·7	73·8
Sr	48·	18·	117·	119·
Rb	241·	323·	37·	114·
Th	2·	0·	0·	27·
Pb	8·	3·	11·	33·
W	2·	0·	1·	3·
Ga	19·	21·	21·	19·
Zn	11·	8·	3.	18·
Ba	278·	69·	507·	488·
Ni	0·	1·	0·	2·
Cr+V	5·	0·	1·	0·
Ce	31·	15·	19·	75·
La	14·	6·	7·	39·
Zr	82·	12·	45·	166·
K/Rb	176	117	550	279

TABLE 2. Mineral analyses for garnet, sillimanite, kyanite and feldspars in granulites ss.

	GARNET				KYANITE	SILLIMANITE
	87710 (edge)	87710 (centre)	32 (centre)	32 (edge)	32	87710
SiO_2	39·05	39·13	37·87	37·71	37·76	36·98
TiO_2	·02	·03	·04	·04	·04	·01
Al_2O_3	22·24	22·31	21·83	21·25	62·35	60·81
Cr_2O_3	·01	·01	·00	·00	·02	·00
Fe_2O_3	nd	nd	nd	nd	·42	·99
FeO	25·34	24·61	36·86	36·83	nd	nd
MnO	5·12	4·74	·67	·69	·00	·00
MgO	8·25	9·08	2·94	2·98	·01	·00
CaO	.80	.85	.94	.76	.00	.00
TOT	100·83	100·76	100·60	100·26	100·59	98·82

	FELDSPARS			
	32 (plag)	32 (alk-fsp)	87710 (plag)	87710 (alk-fsp)
SiO_2	64·64	64·95	63·54	62·83
TiO_2	·02	·01	·02	·02
Al_2O_3	20·79	18·70	21·92	19·66
CaO	2·63	0·59	3·74	2·24
Na_2O	10·07	4·35	9·42	6·23
K_2O	·28	10·50	·22	6·12
TOT	98·43	99·10	98·86	97·10

nd not determined

APPENDIX 2

THE THEORETICAL BASIS FOR TWO - FELDSPAR THERMOMETRY

The two-feldspar thermometer, as proposed by Barth (1934, 1951, 1956, 1962, 1970) and modified by subsequent workers (e.g. Dunham, 1971; Orville, 1962) is based upon the distribution of albite between two coexisting feldspars (an alkali feldspar and plagioclase) and applies irrespective of the means by which equilibrium is attained whether via a magma, by solid diffusion, or in a fluid phase. Thermodynamically this means the chemical potential (μ_{ab}) of albite must be equal in both phases:

$$\mu_{ab\ AF} = \mu_{ab\ PF} \qquad (1)$$

Since most natural feldspars are ternary, the equilibria $\mu_{or,AF} = \mu_{or,PF}$ and $\mu_{an,AF} = \mu_{an,PF}$ must also apply for true equilibrium. It is assumed that because they are usually small Or in plagioclase has no effect on the plagioclase feldspar and An in the alkali feldspar has no effect upon alkali feldspar.

Chemical potential can be related to composition by means of the expressions:

$$\mu_{ab,AF} = \mu^{o}_{ab,AF} + RT\ln a_{ab,AF} \qquad (2)$$

$$\mu_{ab,PF} = \mu^{o}_{ab,PF} + RT\ln a_{ab,PF} \qquad (3)$$

where μ^{o} is the standard state, a conveniently chosen reference point and a is the activity of the component considered, R the gas constant and T in ^{o}K. Therefore from 1, 2 and 3:

$$\mu^{o}_{ab,PF} - \mu^{o}_{ab,AF} = RT\ln \frac{a_{abAF}}{a_{abPF}} \qquad (4)$$

Assuming that the standard chemical potential of the albite component is the same in both plagioclase and alkali feldspar then:

$$RT\ln \frac{a_{ab,AF}}{a_{ab,PF}} = 0 \qquad (5)$$

and

$$a_{ab,AF} = a_{ab,PF} \qquad (6)$$

If ab in plagioclase and the alkali feldspar was an ideal solution, the mole fraction of albite (X_{ab}) is equal to the activity of albite a_{ab}; but the solutions are not ideal and the non-ideality can be expressed by the activity coefficient γ, which relates activity to mole fraction X; from (6):

$$X_{ab,AF}.\gamma_{ab,AF} = X_{ab,PF}.\gamma_{ab,PF} \qquad (7)$$

The distribution coefficient by definition and from (7):

$$K_{D,ab} = \frac{X_{ab,AF}}{X_{ab,PF}} = \frac{\gamma ab,PF}{\gamma ab,AF} \qquad (8)$$

Plagioclase solution is assumed to be ideal for albite (Orville, 1972) in the range Ab_{100} - Ab_{45}. At low temperatures non-ideality may be important (Whitney and Stormer, 1977) near 500°C, at the peristerite solvus, but cannot yet be quantified:

Therefore from (8):

$$K_{D,ab} = \frac{1}{\gamma ab,AF} \qquad (9)$$

Determination of activity coefficient of albite in alkali feldspar

There are several mixing models which can be used to calculate activity coefficient of binary mixtures from coexisting minerals and they may yield widely differing results (Powell, 1974).

A subregular solution model is used after Thompson (1967) and is applicable to assymetric binary solvi:

$$RT\ln\gamma_{ab} = x_2^2 \, (W_1 + 2x_1 \, (W_2 - W_1)) \qquad 1=Or,\ 2=Ab$$

i.e.:

$$RT\ln\gamma_{ab,AF} = (1-x_{ab,AF})^2 (W_G^{Ab} + 2x_{ab,AF} (W_G^{Or} - W_G^{Ab})) \qquad (10)$$

W_G is an interaction parameter, which contributes to the excess free energy in non-ideal mixing. W_G is found to vary as a function of both pressure and temperature:

$$W_G = W_{H_{1\ bar}} - TW_S + (P-1)W_V \quad \text{(Wood \& Fraser, 1977; eq. 3.36)} \qquad (11)$$

Where the W terms are all excess terms in the mixing properties of the solid solution V excess can be determined from x-ray data.

Thompson and Waldbaum (1969b) developed a method of calculating W_G from assymetric solvus data. This, however, highlights another problem area, since there are a host of determinations of the alkali feldspar solvus and which one is chosen is to some extent arbitrary.

Derivation of W_G's from the alkali feldspar solvus

The total Gibbs energy for a non-ideal solution is given by:

$$G_{ss} = X_A\mu^o_A + X_B\mu^o_B + nRT(X_A\ln X_A + X_B\ln X_B) + X_AA_B(W_{G_A}X_B + W_{G_B}X_A) \qquad (12)$$

G^o — $Gmix = -TSmix$ additional term due to increased entropy of mixing — G_{excess} due to non-ideal mixing

(Thompson, 1967, eq. 73)

from this can be derived (Thompson, 1967, eq. 79a):

$$\mu_1 = \mu_1^o + nRT\ln X_A + X_B^2 \, (W_{GA} + 2(W_{GA} - W_{GB})X_A)$$

setting μ_{1A} equal to μ_{1B} (equilibrium in an assymetric solution)
and μ_{2A} equal to μ_{2B} (A and B phases in end members 1 and 2)
then:

$$RT\ln X_{1A} + X_{2A}^2 W_{GA} + 2X_{1A}.X_{2A}^2 (W_{G_B} - W_{G_A}) = \quad (13)$$

$$RT\ln X_{1B} + X_{2B}^2 WG_B + 2X_{1B}X_{2B}^2 (W_{G_B} - W_{G_A})$$

and a similar equation.

These equations can be solved for W_{G_A} and W_{G_B} at a known temperature and composition of coexisting phases from experimental data and the temperature and pressure dependence of $W_{G_{A,B}}$ obtained. Thompson and Waldbaum (1969b) have developed this method and used it to smooth experimentally determined data.

Alkali Feldspar Solvi

The position of the alkali feldspar solvus is dependent on the structural state and ordering of the phases and whether or not the phases are coherent. There are four possible solvi, which are all distinguishable from each other: High albite - sanidine, (curve 3) (free of strain); low albite - maximum microcline (strain free) (Curve 1); the coherent low albite - maximum microcline solvus (curve 2) and the coherent high albite - sanidine solvus (curve 4). Coherency implies there is structural continuity between lamellae of differing compositions and so there is a degree of strain in the structure due to the different size of the Na^+ and K^+ ions, and applies primarily to cryptoperthites. There is a

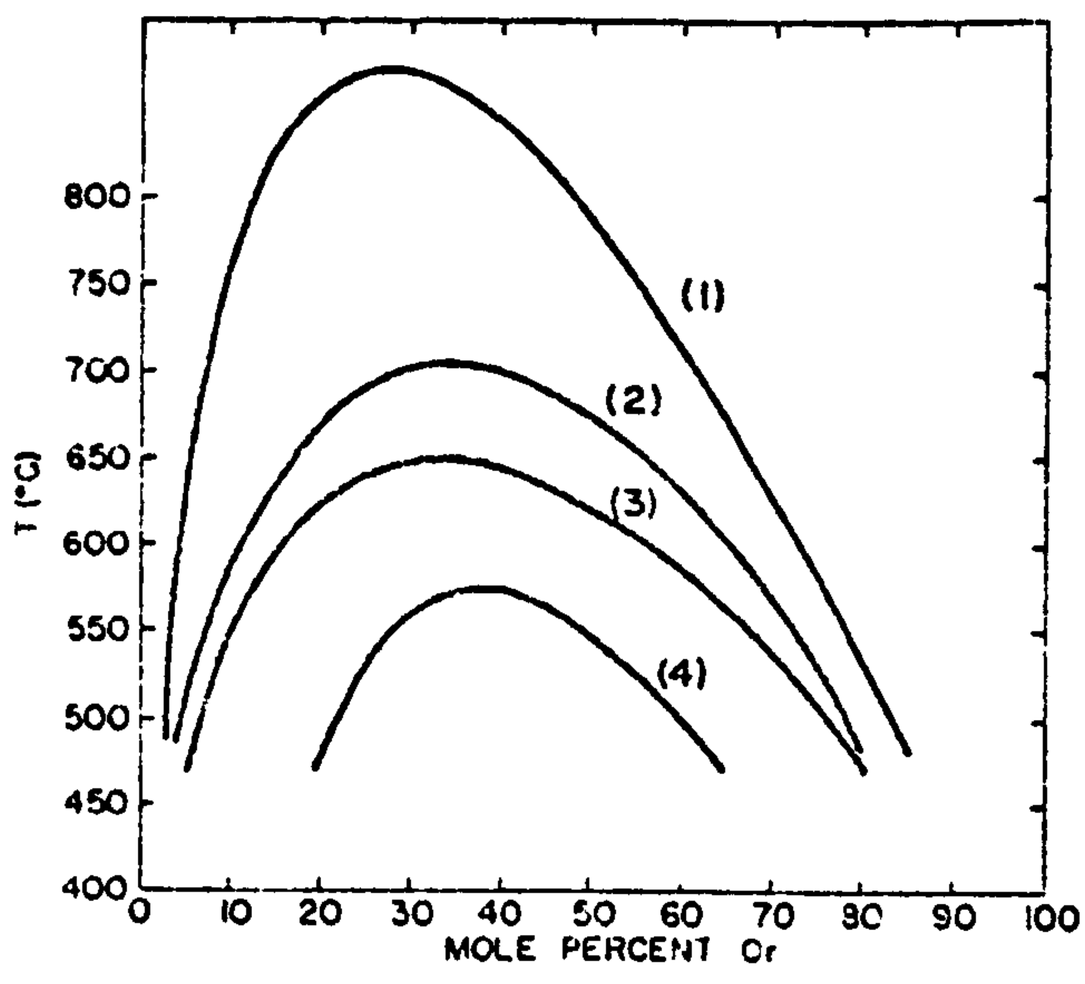

bewildering variety of determinations, particularly of the high albite - sanidine solvus, which are to some extent due to the following problems encountered in locating the solvus:

1) Achieving and demonstrating equilibrium between coexisting feldspars in the experiments (qv. Parsons, 1978; Goldsmith and Newton, 1974) ideally by 'bracketing' the solvus.
2) The identification of the phases produced in the experiment, which is dependent upon determinative curves for $(\bar{2}01)$ spacing, which can differ by as much as 0.06 N_{OR} (Parsons, 1978).
3) The accuracy of the temperature setting of the experiment.
4) The structural state of feldspars produced in experiment.
5) The possibility that non-stoichiometric feldspars are produced in the experiment.

The High Albite - Sanidine solvus was studied by Orville (1963), Luth and Tuttle (1966), Goldsmith and Newton (1974), Luth, Martin and Fenn (1974), Seck (1972), Morse (1970), Smith and Parsons (1974) and Legache and Weisbrod (1977); Thompson and Waldbaum (1969b) utilising the method outlined in Thompson and Waldbaum (1969a) and the data of Orville (1963) and Luth and Tuttle (1966) calculated isobaric solvi at a number of pressures. Luth and Tuttle (1966) and Luth and Fenn (1973) proposed that solvi determined from different starting compositions yield significantly different curves as also proposed by Morse (1970). In contrast Goldsmith and Newton (1974) and Smith and Parsons (1974) concluded that compositional factors do not noticeably affect the equilibrium position of the solvus.

There is good agreement between the bracketed solvi of Smith and Parsons (1974), Goldsmith and Newton (1974), Legache and Weisbrod (1977), and Orville (1963) and the calculated solvus of Thompson and Waldbaum (1969b) and the principal uncertainty is the lower temperature position (i.e. below 600°C) of the potassic limb. The calculated curve of Thompson and Waldbaum (1969b), based on data of Orville (1963) and Luth and Tuttle (1966), has been used in thermodynamic calculations in feldspar thermometry and is used in the calculations below.

The low albite - maximum microcline solvus lies above the high albite - sanidine curve. It was determined independently by Backinski and Muller (1971) using fused-salt-alkali ion exchange and homogenisation-unmixing techniques, in the region 600 - 900°C. Since the solvus is only stable below about 500 - 600°C, this represents the metastable extension of the ordered solvus, possibly because of the slow disordering rate.

Coherent Solvi for high albite - sanidine and low albite - maximum microcline have been determined by Sipling and Yund (1976) and Yund (1974) respectively and lie within their respective strain free solvi. The coherent low albite maximum microcline solvus has only been approximately located (Yund, 1975, p.23), whilst the coherent high albite - sanidine curve has been located using exsolution and homogenisation experiments with compositions determined from X-ray photographs and corrected for coherency strain; the inception of unmixing was checked using transmission microscopy.

Coherent solvi only apply to perthitic feldspars, and ideally to cryptoperthites, whose lamellae are by definition too small to analyse on the microprobe. It is uncertain whether more coarsely perthitic feldspars exsolve by the same mechanism as cryptoperthites (Sipling and Yund, 1976, p. 905) and therefore whether these solvi apply to geothermometric calculations.

Margules parameters

Luth (1974) has reviewed the calculated margules parameters for some of the above solvi (and a summary is given in Table 1). There is a wide and confusing variety of possible values and slightly different mathematical treatments can generate different numbers from the same data. The parameters calculated by Thompson and Waldbaum (1969b) for the high albite - sanidine

solvus are used in the thermometer proposed by Stormer (1975) and Powell and Powell (1977) since this calculated solvus is consistent with solvi determined by Smith and Parsons (1974), Goldsmith and Newton (1974) and Lagache and Weisbrod (1977). Luth et al. (1974), however, noted a systematic error in the data of Luth and Tuttle (1966) used by Thompson and Waldbaum (1969b) in their calculations and Luth (1974) suggested that the $W_{V(i)}$ terms may also be inaccurate.

In the treatment of coexisting feldspars with a low structural state the parameters of Bachinski and Muller (1971) are used after Whitney and Stormer (1976). Luth (1974) calculated margules parameters for data from Bowen and Tuttle (1958) for Spencer P and Mitchell Mesa rhyolite; these solvi have an identical critical point to that determined for the high albite coherent solvus by Sipling and Yund (1976) although the early data is imprecise at low temperatures.

Equations for the two feldspar thermometer

Stormer (1975) and Whitney and Stormer (1977) presented two equations which give limiting equilibration temperatures for natural feldspars which contain only small amounts of Or in plagioclase and small amounts of An in alkali feldspar. For feldspar which equilibrated in a disordered structural state (e.g. rapidly cooled lavas) the following equation can be used based on the margules parameters of Thompson and Waldbaum (1969b) for the sanidine-high albite solvus:

$$T^{o}K = (6326.7 - 9963.2X_{AF} + 943.3X_{AF}^{2} + 2690.2X_{AF}^{3} + (0.0925 - 0.1458X_{AF} + 0.0141X^{3})\ P) \Big/ (-1.9872 \ln K_{D} + 4.6321 - 10.815X_{AF} + 7.7345X_{AF}^{2} - 1.5512X_{AF}^{3}) \quad (14)$$

where $K_D = X_{AF}/X_{PF}$ and X_{AF} and X_{PF} are the mole fraction of albite in alkali feldspar and plagioclase respectively.

For feldspars which have equilibrated in an ordered structural state (e.g. slowly cooled plutons) the margules parameters from the Bachinski and Muller (1971), low albite - maximum microcline solvus are applicable and the equation becomes:

$$T^{o}K = (7973.1 - 16910.6X_{AF} + 9901.9X_{AF}^{2} + (0.11 - 0.22X_{AF} + 0.11X_{AF}^{2})\ P) \Big/ (-1.9872 \ln K_{D} + 6.48 - 21.58X_{AF} + 23.72X_{AF}^{2} - 8.62X_{AF}^{3})$$

For many granitic rock temperatures calculated from the above equations will set limits on the true equilibration temperature. A more precise temperature estimate can only be made if the ordering of the feldspars can be established for the time they were at intercrystalline equilibrium for most feldspars become more ordered during cooling. Whitney and Stormer (1977b) suggest that feldspars in granitic plutonic rocks crystallising slowly in the range 600-800°C may be partially ordered and that orthoclase is the stable phase implying an intermediate equilibration temperature, whilst at crystallisation temperatures greater than 800°C the feldspars are disordered and the high temperature solvus is appropriate.

Equations for ternary feldspars

The assumption that only small amounts of anorthite are present in alkali feldspar and small amounts of potassium feldspar are present in plagioclase are not always valid and solutions may depart appreciably from the Henry's Law range

so that γ(ab, ternary feldspar) $\neq \gamma$(ab, binary feldspar). Powell and Powell (1977a) modified the equation of Stormer (1976) to correct for small amounts of calcium in alkali feldspar and this equally applies for Barium in alkali feldspar when Ca is minimal. A ternary subregular solution model expression for the activity coefficient is used which reduces to:

$$RT\ln_{\gamma Na,AF} \simeq X_{OR}^2 \ (W_1 + 2X_{AB}(W_2 - W_1)) \qquad (16)$$

The difference between this expression and that used by Stormer (1975) is that $(1 - X_{AB})^2$ is replaced by X_{OR}^2. If the alkali feldspar is a binary solution these two equations will yield the same result, but if it is a ternary solution (with Ca or Ba as the other phase) X_{OR} will be less than $(1 - X_{AB})$ and since the term is squared this can make a significant difference. The equation of Powell and Powell (1977a) applicable to a high structural state is:

$$T^{\circ}K = - X_{OR}^2 \ (6330 + 0.093P + 2X_{AB}(1340 + 0.019P)) \ / \ R\ln K_D + X_{OR}^2 \ (-4.63 + 1.54X_{AB}) \qquad (17)$$

If the margules parameters of Bachinski and Muller (1971) are used it is possible to derive an equation for the limiting case where ternary feldspars equilibrated in a low structural state:

$$T^{\circ}K = -X_{OR}^2 \ (7973.1 + 0.11P - 964.6X_{AB}) \ / \ (R\ln K_D + X_{OR}^2(-6.48 + 8.62X_{OR})) \qquad (18)$$

TABLE 1 MARGULES PARAMETERS

W_G	=	$W_{E(i)}$	$-W_{S(i)}T$	$+W_{V(i)}$	Reference
High Albite					
W_G^{Ab}	=	6326.7	-4.6321T	+0.0925P	*1*
W_G^{Or}	=	7671.8	-3.8565T	+0.1121P	
Low Albite					
W_G^{Ab}	=	7973.1	-6.48T	+0.11P	*2*
W_G^{Or}	=	7490.9	-2.17T	+0.11P	
Low temperature					
W_G^{Ab}	=	2980.0	0	+0.06817P	*3*
W_G^{Or}	=	5315.7	0	+0.21230P	
High temperature					
W_G^{Ab}	=	0	+3.0306T	-0.0212P	*3*
W_G^{Or}	=	12100.0	+9.0418T	+0.24959P	
Coherent high albite - Spencer P					
W_G^{Ab}	=	10582.00	-9.866T		*3*
W_G^{Or}	=	8323.0	-5.338T		
Coherent high albite - Mitchell Mesa					
W_G^{Ab}	=	10160.0	-9.068T		*3*
W_G^{Or}	=	9818.0	-7.117T		

1 Thompson and Waldbaum (1969b)

2 Bachinski and Muller (1971)

3 Luth et al. (1974)